Phytophthora parasitica and lupin (*Lupinus angustifolius*) interactions: changes in gene expression during infection and after phosphite treatment

A thesis submitted for the degree of Doctor of Philosophy of

The

Australian National University

© Copyright by

PERNELYN SORIA TORREÑA

May 2017

All Rights Reserved

Declaration

Except where otherwise acknowledged, original data supplied are based upon my own research results, analyses, and opinions. I declare that this thesis is my own account and has not been previously submitted for a degree at any tertiary educational institution.

PERNELYN SORIA TORREÑA

May 2017

Acknowledgements

My PhD journey in Australia will not be possible without the help of so many people. I would like to express my immeasurable appreciation and sincerest gratitude to all who rendered their support in all forms.

I am so grateful to my main supervisor, Prof. Adrienne R. Hardham, who accepted me in Hardham Lab and helped me on my application to the Australian Leadership Awards (ALA) Scholarship. Her wisdom, inputs, guidance, her patience in correcting my thesis, her utmost understanding and support counts a lot. I am very thankful to my co-supervisor, Dr. Leila M. Blackman who helped me in doing laboratory techniques especially the molecular stuff which at first I felt hesitant of doing. Her effort of letting me understand the RNA-Seq part of my thesis and in correcting my chapters is so valuable. I would like to thank also my third panel member, Dr. Peter S. Solomon for his valuable thoughts and suggestions during research presentations.

I am thankful to the Statistical Consulting Unit especially to Bob Forrester and Terry Newman for the statistical analysis of my growth assay experiments.

I am truly grateful to my labmates: to Victoria Anne Ludowici who helped me carried out the growth assay experiments and analysis. To Darren Peter Cullerne for helping me during the big experiment on lupin infection assay and for the bioinformatics analysis of the RNA-Seq paper. To Weiwei Zhang, Wenjie Wu, Wil Hee, Remi Branco, and Kiki Kots, for their help, concern and humour. To Yueqi Zhang who did the bioinformatics analysis of my RNA-Seq samples. To Chelsea, George, and other students who have been in the same lab with me.

My appreciation also extends to my co-students and friends in RSB who contributed ideas during our chitchats and for their friendship: Nadia Radzman, Jason Ng, Samira Hassan, Chooi Hua, Debora Veliz, Kevin Tee, Laura Rolston, Huong Do, Nadya Farah, Jordi Gonzales and Florence Denila.

I am also grateful to the Couples for Christ Family-Canberra Chapter, the ANU Catholic Society, the St John's Chapel Choir, and the Voices for Christ Choir who

helped me in my spiritual journey while in Australia. To the ANU Filipino Association whom I felt joy in serving as treasurer and a lifetime member.

I am very much indebted to the Australian Government, who gave me a full-time ALA scholarship. To the Philippines-Australia Human Resource and Organisational Development Facility, to Ms Gina Abarquez and her staff who facilitated all scholarship matters. I am also grateful to the Philippine Rice Research Institute (PhilRice) management for allowing me a full-time study leave and to my PhilRice family in Midsayap for accepting the R&D responsibilities in my behalf. I am also thankful to my professors in the University of Southern Mindanao who helped me in my PhD scholarship applications.

My appreciation also to our housemates, friends and co-students especially to Joyacs, Graziella, Eliezer, Louie Joi, Val, Cecille, Dave, Cindy, Raul, Fay, Rey, and to all who helped me and my family.

To my family: especially to our parents, Nanay Perla and Tatay Necing who tried to cope up the advances in social media just to reach us from a distance; for their prayers and unconditional love especially for our twins. For my brother Manoy Melvin, sister Daisy Amor, my in-laws and relatives for their tireless support, ardent prayers, inspiring words, and other form of assistance. To my hubby, Renen for helping me setting-up my infection assay experiments, for always believing and trusting that I can do all things when I am in doubt of my own capability, and for the love and care he gave in good and in bad times. To our tots, Brynn and Bryle who cannot fully understand why I need to do school works at home and yet prayed that I will finish soon so I can give them more quality time.

For those whose names are not mentioned but who contributed in a way to the success of my study, thank you very much.

Lastly, I want to thank our Dear God, for all His blessings, graces, forgiveness, and love. For without Him, I can do nothing. To God be the glory, honour, and praise forever and ever.

Abstract

Phytophthora species are Oomycete pathogens that cause highly destructive diseases in a variety of agricultural and horticultural crops, and natural ecosystems. An understanding of the key biological processes that occur during development and infection of hosts is important for the development of effective *Phytophthora* control mechanisms.

An infection assay model system was developed for *P. parasitica* based on lupin (*Lupinus angustifolius*) seedlings. The progress of lesion development and colonisation of *P. parasitica* in inoculated root tissues was assessed macroscopically and using light microscopy of sectioned material. At 24 hours post inoculation (hpi), a few hyphae were observed in the epidermal and outer cortical cells in the region of the root that had been at the surface of the zoospore suspension during the inoculation period. As root infection progressed, the hyphae grew both towards the vascular tissue at the centre of the root and longitudinally along the root. At 42 hpi, *P. parasitica* hyphae developed haustoria within root cortical cells. No evidence of callose deposition, a typical plant defence response, by the lupin root cells was observed after infected roots stained with aniline blue.

Development of the model lupin-*P. parasitica* infection assay system facilitated ensuing studies of this plant-pathogen interaction, including the cellular and molecular basis of plant infection. The model assay system was used to examine levels of resistance of different lupin cultivars following inoculation with *P. parasitica* and to analyse temporal patterns of *P. parasitica* gene expression using quantitative real-time PCR (qPCR) during lupin root infection.

One crucial component of *Phytophthora* pathogenicity is the digestion of the plant cell wall to allow penetration of the plant surface and colonisation within the plant tissues. Plant cell walls are complicated structures that are composed of a wide range of complex polysaccharides (i.e. cellulose, hemicelluloses and pectins) and proteins and they constitute an effective barrier that impedes the

entry of many potential pathogens. In order to penetrate the plant cell wall, pathogens secrete a diverse array of cell wall degrading enzymes (CWDEs). The identity and timing of the expression of genes encoding *P. parasitica* CWDEs was analysed using qPCR. It is believed that pathogens secrete cascades of CWDEs during the infection process and evidence supporting this hypothesis was obtained from the lupin-*P. parasitica* data.

One management strategy used in the control of *Phytophthora* diseases is the application of the chemical phosphite. Our understanding of the mechanism(s) underlying phosphite inhibition of *Phytophthora* diseases in plants is limited. Phosphite is known to have effects on both host plants and *Phytophthora* pathogens. In the present study, RNA-Seq was used to investigate the effects of phosphite on *P. parasitica* gene expression *in vitro* and *in planta*. Phosphite treatment was found to induce extensive changes in the expression of many pathogen genes both *in vitro* and *in planta*. One of the exciting results was the discovery that there was a general tendency for phosphite to up-regulate the expression of genes that are normally expressed early in lupin infection (30-36 hpi) and to down-regulate the expression of genes that are normally expressed during late infection (54-60 hpi). This was exemplified in particular by *P. parasitica* genes encoding pectinase and cellulase CWDEs and RxLR effectors.

In conclusion, the research described in this thesis has developed a new and robust model infection assay for use in studies of plant infection by *P. parasitica* and, potentially, by other *Phytophthora* species. The research also presents the results of using this assay in transcriptomic studies of pathogen gene expression during plant infection. The results that have been obtained provide a better understanding of *Phytophthora* pathogenicity mechanisms and should aid the future development of improved methods of controlling *Phytophthora* diseases.

Table of Contents

List of Abbreviations

˚C	Degrees Celsius
µl	Microlitre (s)
µm	Micrometre (s)
µM	Micromolar (s)
AA	Auxiliary activity
AGPs	Arabinogalactan proteins
AGRF	Australian Genome Research Facility
ANOVA	Analysis of variance
ANK	Ankyrin
BCAs	Biological control agents
BSA	Bovine serum albumin
CAZyme	Carbohydrate-Active enzyme
CBEL	Cellulose binding elicitor lectin
CBM	Carbohydrate binding module
cDNA	Complementary DNA
CE	Carbohydrate esterase
CesA	Cellulose synthase
cm	Centimetre(s)
CMV	Cucumber mosaic virus
Cpa	Cyst peripheral adhesive
CRN	Crinkler

Cv or cvs	Cultivar(s)
CWDE or CWDEs	Cell wall degrading enzyme(s)
DABCO	1,4-diazabicyclo-[2,2,2]-octane
DAFWA	Department of Agriculture and Food, Western Australia
DE	Differential expression
DEPC	Diethylpyrocarbonate
DI	Disease index
DIC	Differential interference contrast microscopy
DNA	Deoxyribonucleic acid
dpi	Days post inoculation
DTT	Dithiothreitol
ED50	Effective dose 50 percent
EDTA	Ethylenediaminetetraacetic acid
ELISA	Enzyme-linked immunosorbent assay
ESTs	Expressed sequence tags
EtOH	Ethanol
FDR	False Discovery Rate
FITC	Fluorescein isothiocyanate
g	Gram(s)
g	Gravity
gDNA	Genomic deoxyribonucleic acid
GH	Glycosyl hydrolase

GIPs	Glucanase inhibitor proteins
GO	Gene ontology
GRDC	Grains Research & Development Corporation
GSTs	Glutathione S-transferases
GT	Glycosyl transferase
h	Hour(s)
H_2O_2	Hydrogen peroxide
HRGPs	Hydroxylproline-rich proteins
HG	Homogalacturonan
hpi	Hour post inoculation
HR	Hypersensitive response
IKI	Iodine/potassium iodide
JGI	Joint Genome Institute
Kb	Kilobase
l	Litre(s)
Lpv	Large peripheral vesicle
LSD	Least significant difference
MAbs	Mouse monoclonal antibodies
MAP	Mitogen-activated protein
mM	Millimolar(s)
min	Minute(s)
mg	Milligram(s)

ml	Millilitre(s)
MRM	Modified Ribeiro's medium
n	Number of samples
NCBI	National Center for Biotechnology Information
NGS	Next Generation Sequencing
NPPs	Necrosis-inducing factors
O.C.T.	Optimal cutting temperature
PBS	Phosphate buffered saline
PCD	Programmed cell death
PCR	Polymerase chain reaction
PEI	Polyethyleneimine
PIPES	Piperazine-1, 4-bis (2-ethanesulfonic acid) disodium salt
Phi	Phosphite
PL	Polysaccharide lyases
PnCcp	*Phytophthora nicotianae* complement control protein
Pp	*Phytophthora parasitica*
PPTG	*Phytophthora parasitica* INRA-310 (V2) protein
PRR	Phytophthora root rot
qPCR	Quantitative real-time polymerase chain reaction
RGI	Rhamnogalacturonan I
RGII	Rhamnogalacturonan II
RO	Reverse osmosis

ROS	Reactive oxygen species
RNA	Ribonucleic acid
RNase	Ribonuclease
RPKM	Reads Per Kilobase of transcript per Million mapped reads
RT	Reverse transcription
RT-PCR	Reverse transcription polymerase chain reaction
SAM-FITC	Sheep anti-mouse conjugated to fluorescein isothiocyanate
SAT	Systemic acquired tolerance
sdH_2O	Sterile deionized water
SNE1	Suppressor-necrosis 1
SP	Secretion signal
SA	South Australia
TAE	Tris-acetate-EDTA
TMD	Ttransmembrane domains
Vsv	Ventral surface vesicle
WA	Western Australia

CHAPTER 1
Introduction

1.1. *Phytophthora* diseases worldwide: effects on agriculture and natural ecosystems

Species in the genus *Phytophthora* cause highly destructive diseases in a variety of agricultural crops and natural ecosystems (Govers and Gijzen, 2006; Hardham and Blackman, 2010; Hüberli *et al.*, 2013; Lamour, 2013). The name, *Phytophthora* means "plant destroyer". During history, *Phytophthora* became widely known after one species, *P. infestans*, caused the late blight disease of potato and devastated Ireland's staple food supply in 1845 and 1846 (Erwin and Ribeiro, 1996; Ribeiro, 2013). Identification of *P. infestans* in 1876 (Bourke, 1991) as the causal agent of potato late blight was a major milestone in plant pathology. Currently, there are more than 150 recognised species of *Phytophthora* with additional species being identified each year (Hansen *et al.*, 2012; Kroon *et al.*, 2012; Thines, 2013; Yang *et al.*, 2017). For example, the following species were reported in 2015: *P. lilii*, *P. pseudolactucae* (Rahman *et al.*, 2015), *P. macilentosa*, *P. mississippiae*, *P. stricta* (Copes *et al.*, 2015), *P. agathidicida*, *P. cocois* (Weir *et al.*, 2015), and *P. niederhauserii* (Saurat *et al.*, 2015).

In a published book on *Phytophthora*, *Phytophthora*: a global perspective (Lamour, 2013), several important species of *Phytophthora* were featured including *P. cinnamomi* (Hee *et al.*, 2013), *P. nicotianae* (syn. *P. parasitica*) (Ludowici *et al.*, 2013), *P. infestans* (Cooke and Andersson, 2013; Halterman and Gevens, 2013), and *P. sojae* (Dorrance, 2013). These *Phytophthora* species, as well as *P. ramorum*, a persistent problem in sudden oak deaths, were among the top 10 most serious Oomycete plant pathogens in terms of scientific and economic importance (Grünwald *et al.*, 2008; Kamoun *et al.*, 2014).

P. cinnamomi is one of the most highly destructive soil-borne pathogens; it has a wide host range and a considerable impact in agricultural and natural ecosystems (Figure 1.1-a) (Weste, 2003; Cahill *et al.*, 2008). It was first described

in association with cinnamon trees in Sumatra in the 1900s (Hardham, 2005; Bishop *et al.*, 2012). *P. cinnamomi* thrives in tropical and subtropical climates, but is most prevalent in Mediterranean-type climates such as the Cape Floristic Region of South Africa, Mediterranean Europe, and the South-West Botanical Province of Western Australia (Drenth and Guest, 2004; Burgess *et al.*, 2016). .*P. cinnamomi* is the only Oomycete included in the top 100 of the world's worst invasive alien species (Lowe *et al.*, 2000). It infects nearly 5,000 species of woody plants around the world but it terms of damage and total plant species infected, nothing surpasses what is documented in Australian plant communities (Shearer *et al.*, 2004; Cahill *et al.*, 2008; Jung *et al.*, 2013). It causes extensive environmental damage and threatens biodiversity in a number of Australian national parks (Hardy *et al.*, 2001a; Hardham, 2005). Of the almost 6000 endemic plant species in the south-west Botanical Province of Western Australia (WA), more than 2000 species are susceptible to *P. cinnamomi* (Shearer *et al.*, 2004). In the Stirling Range National Park in WA, 20 taxa of plants are at risk of extinction (Cahill *et al.*, 2008). Two decades ago, annual economic losses were estimated to be over AUS$200 million in Australia (Irwin *et al.*, 1995). In the USA and other parts of the world, *P. cinnamomi,* as the causal pathogen of Phytophthora root rot (PRR), is an important disease of avocado (Kotze *et al.*, 1987; Smith *et al.*, 2010). In California, 60-75% of the avocado acreage is infested with *P. cinnamomi*, with an estimated loss of $44 million per year (Costa *et al.*, 2000). *P. cinnamomi* also causes destructive diseases in a range of plant species globally. For example, oak decline in Europe and Southern Ohio (Brasier, 1996; Nagle *et al.*, 2010), root and crown rot of pine in Brazil (Dos Santos *et al.*, 2011), heart rot of pineapple, and serious diseases of chinchona and cinnamon in Southeast Asia (Drenth and Guest, 2004; Cahill *et al.*, 2008).

P. parasitica is another important species of *Phytophthora*. It has a wide host range and is capable of infecting over 255 genera in 90 families of plants (Cline *et al.*, 2008). It is most well-known for the diseases it causes in tobacco (Figure 1.1-b), tomato, and citrus but has recently also become a major threat to potato production (Matheron and Matejka, 1990; Neher and Duniway, 1992; Taylor *et al.*, 2012; McCorkle *et al.*, 2013). In tobacco, black shank caused by *P. parasitica*

is the most destructive soil-borne disease, reducing tobacco production in the world and resulting in yearly losses of millions of dollars in revenue (Johnson *et al.*, 2002; Ren *et al.*, 2012; Bittner and Mila, 2014).

Late blight caused by *P. infestans* (Figure 1.1-c), has devastated potato production for more than a century. It remains a major threat in Europe, USA and has been identified as the most destructive potato disease in the world (Fry, 2008; Haas *et al.*, 2009; Cooke and Andersson, 2013; Halterman and Gevens, 2013). In the early 2000s, the estimated revenue loss for US growers amounted to US$210.7 million but globally the estimated loss exceeds $5 billion every year (Birch and Whisson, 2001; Guenthner *et al.*, 2001; Haas *et al.*, 2009). In South America, *P. infestans* causes blight-like symptoms on several plant hosts such as tamarillo and melon pear (Forbes *et al.*, 2013).

P. sojae (*P. megasperma* f. sp. *glycinea*) is a narrow host range soil-borne pathogen that primarily infects soybean (Erwin and Ribeiro, 1996). It causes damping-off (Figure 1.1-d) and rotting of seeds, seedlings, roots and stems (Figure 1.1-e) (Gordon *et al.*, 2007a; Gordon *et al.*, 2007b; Tyler, 2007). Replanting is still associated with lower yield and economic losses because of late planting dates (Dorrance, 2013). *P. sojae* causes $200 million in annual yield loss in the USA, with a global yearly loss of $1-2 billion (Tyler, 2007).

Another important *Phytophthora* species is *P. ramorum,* with its known host-range of over 100 plant species in more than 40 genera (Grünwald *et al.*, 2008; Grünwald *et al.*, 2012). It is an aggressive plant pathogen causing extensive damage in a variety of plant species in the USA and Europe (Brasier *et al.*, 2004; Dart and Chastagner, 2007; Frankel, 2008; Goss *et al.*, 2011). *P. ramorum* causes sudden oak death on oak trees and tanoaks (Figure 1.1-f), with devastating effects in forest and nursery environments (Grünwald *et al.*, 2012). It also causes severe damage in Australian native plant species, natural ecosystems and plant industries and is acknowledged as a plant biosecurity threat worldwide (Ireland *et al.*, 2010; Ireland *et al.*, 2012).

As mentioned above, new *Phytophthora* diseases are being reported every year. In 2015, for example, the first reports of the presence of *Phytophthora* as the

causal pathogen in different crops were documented in different parts of the world such as China (Dai *et al.*, 2015; Shao *et al.*, 2015; Yu *et al.*, 2015), France (Saurat *et al.*, 2015), Italy (Garibaldi *et al.*, 2015; Luongo *et al.*, 2015), Turkey (Türkölmez *et al.*, 2015), and Oregon, USA (Reeser *et al.*, 2015; Weiland, 2015).

Figure 1.1. (a) Death of grass trees due to *P. cinnamomi* in an open forest in Victoria, Australia (Weste, 2003); (b) *P. parasitica* causing symptoms of black shank on flue-cured tobacco (Gallup *et al.*, 2006); (c) Late blight symptoms on potato plants and tuber (inset) caused by *P. infestans* (Kirk *et al.*, 2004); (d) *P. sojae* damping-off, (e) stem rot on soybean (Tyler, 2007), and (f) *P. ramorum* canker on tanoak (Davidson *et al.*, 2003).

1.2. *Phytophthora* life cycle

Phytophthora species have both asexual and sexual phases in their life cycles (Figure 1.2) but, in general, pathogen dissemination and disease establishment depend on asexual spores (Judelson and Blanco, 2005; Robold and Hardham, 2005). During asexual sporulation, hyphae form sporangia at their apex. Multinucleate sporangia can germinate directly and form hyphae, or the cytoplasm can cleave to form uninucleate compartments which develop into biflagellate zoospores which are released through an apical pore in the sporangium. The wall-less zoospores encyst, forming walled cysts that germinate and penetrate the host plant. For most *Phytophthora* species, the motile zoospores are the major infective agents that are chemotactically and electrotactically attracted to potential infection sites on roots and leaves (Robold and Hardham, 2005; Hardham and Blackman, 2010). Zoospores and hyphae synthesise and secrete a range of pathogenicity factors including effector proteins that facilitate plant infection. Both zoospores and hyphae secrete adhesive material that attaches the pathogen cells to the plant host (Gaulin *et al*., 2002; Robold and Hardham, 2005). Hyphae also secrete a range of enzymes that degrade the plant cell wall to allow penetration of host tissues (Götesson *et al.*, 2002; Costanzo *et al*., 2006).

Most *Phytophthora* species produce another asexual spore called a chlamydospore. Chlamydospores are survival structures with thick walls generally around 1.5 μm in width and remain viable after a long period of time (Erwin and Ribeiro, 1996). In *P. cinnamomi*, for example, chlamydospores are formed at temperatures between 10°C and 30°C and can survive in host-free, conducive soils as a response to drying conditions (Weste and Marks, 1987).

Many *Phytophthora* species also undergo sexual sporulation. Sexual reproduction can be heterothallic, as in *P. parasitica,* or it can be homothallic, as in the case of *P. sojae* and *P. infestans* (Savage *et al.*, 1968; Erwin and Ribeiro, 1996; Hardham, 2005; McCarren *et al.*, 2009). Homothallic species are self-fertile and can reproduce when only one thallus is present (Cvitanich and Judelson, 2003). Heterothallic species usually require the interaction of two different thalli

(A1 and A2 mating types) (Savage *et al*., 1968) in order to cross-fertilise, however, self-fertilisation *in planta* has been reported for *P. cinnamomi* (Boccas, 1981; Crone *et al.*, 2013). During sexual sporulation, the male gametangium is an antheridium and the female structure is called an oogonium. The male and female gametangia develop which later unite and form oospores. The oospores germinate to form either a hyphal tubes or asexual sporangia (Cvitanich and Judelson, 2003; Judelson and Blanco, 2005).

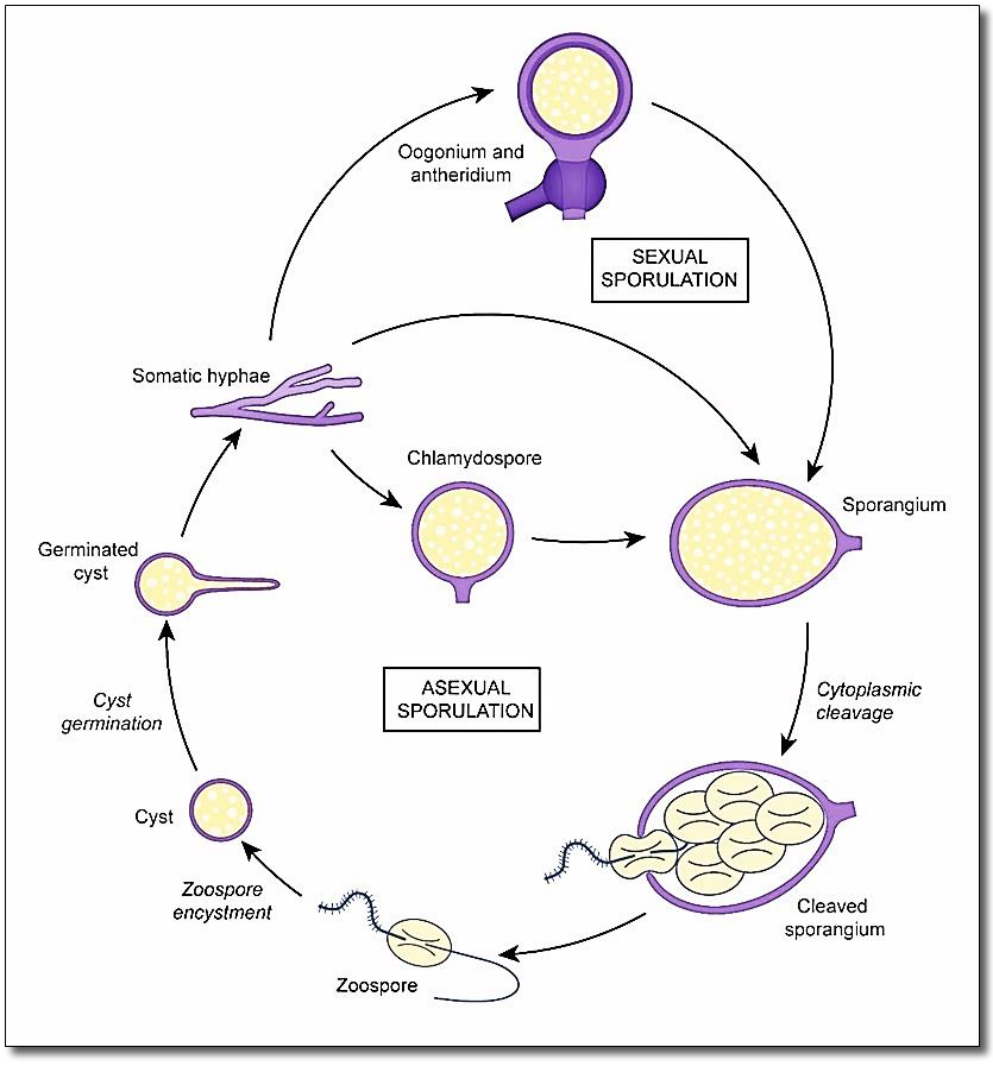

Figure 1.2. Diagram depicting the life cycle of *Phytophthora cinnamomi* (Hardham, 2005)

1.3. Plant pathogen parasitic lifestyles

Oomycete plant pathogens possess diverse parasitic lifestyles and include necrotrophs, biotrophs and hemibiotrophs (Qutob *et al.*, 2002). Almost all biotrophic and several necrotrophic pathogens cause disease in only one or a few species of plants (Kubicek *et al.*, 2014). Necrotrophs are facultative pathogens that actively kill the host during the infection process by producing toxin molecules (Qutob *et al.*, 2002; Grenville-Briggs, 2005; van Kan, 2006; Bellincampi *et al.*, 2014).

Biotrophs are obligate pathogens which infect the host plant but do not cause death of the host cells (Oliver and Ipcho, 2004; Spanu, 2012). Facultative biotrophs like *Ustilago maydis* and *Claviceps pupurea*, grow entirely biotrophically in nature but can be cultured *in vitro*. Obligate biotrophs, such as rusts, powdery and mildews, invade epidermal cells and depend on living plant tissues for their growth and reproduction are either difficult to culture *in vitro* or it will only grow to a limited extent (Hückelhoven, 2005; O'Connell and Panstruga, 2006; Catanzariti *et al.*, 2011).

Hemibiotrophs, such as *P. infestans* (Figure 1.3), and *P. parasitica* establish themselves in the host by initially evading detection and growing in living tissues at the beginning of the infection process (biotrophic phase) (Cho *et al*., 2013; Lee and Rose, 2010). Later during the infection process, these pathogens can spread rapidly and actively kill host cells in order to take up nutrients from the degraded tissues (necrotrophic phase) (Qutob *et al.*, 2002; Pais *et al.*, 2013). A secreted effector protein (SNE1) was found to suppress the action of necrosis-inducing effectors (Nep1-like proteins) during the necrotrophic phase suggesting an antagonistic act that controls the shift from biotrophic to necrotrophic phase (Lee and Rose, 2010).

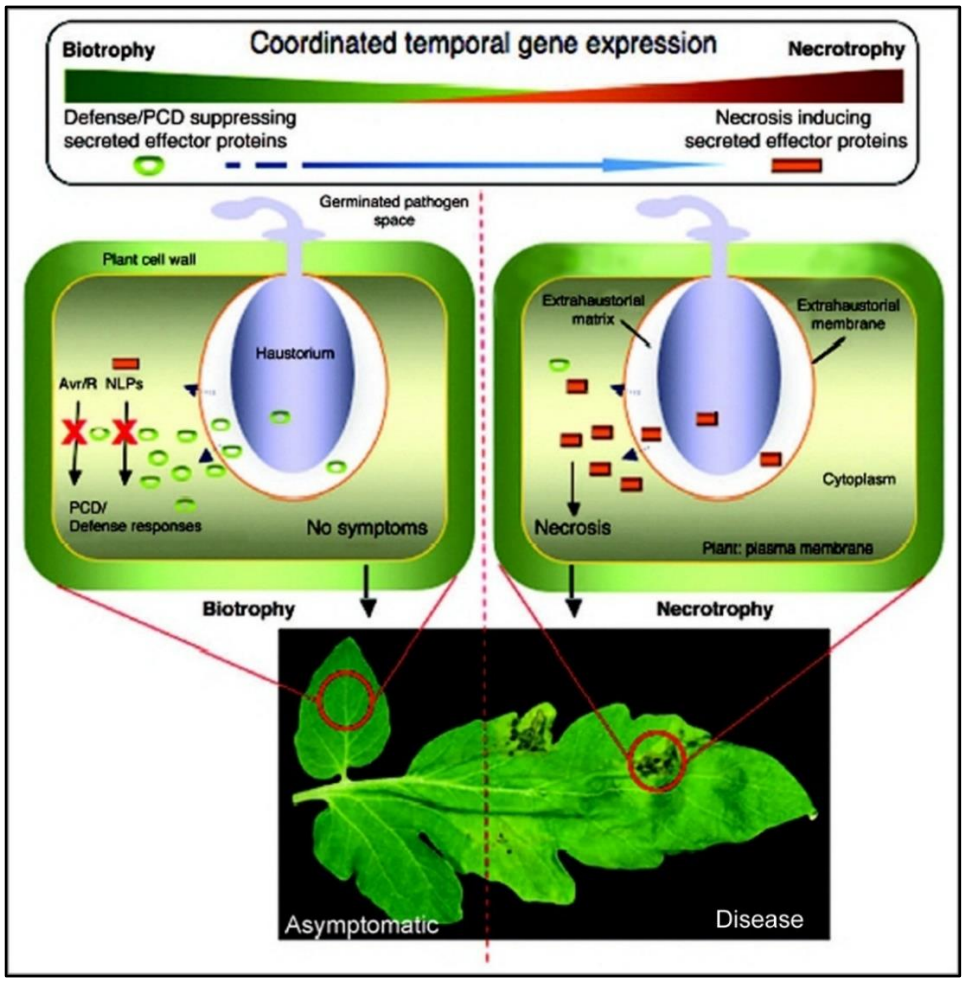

Figure 1.3. Hypothetical model that shows *P. infestans* sequential stages from biotrophy to necrotrophy (Lee and Rose, 2010).

1.4. *Phytophthora* infection strategies

1.4.1. Motility of zoospores to initiate contact with a possible host

Oomycetes and fungi often share common infection strategies (Latijnhouwers *et al.*, 2003; Haldar *et al.*, 2006; Hardham, 2007; Dodds *et al.*, 2009). However, a key difference between disease development by Oomycete and fungal pathogens centres on the role of motile Oomycete zoospores in the initiation of infection (Hardham, 2007).

The infection process in *Phytophthora* starts when the motile, biflagellate zoospores come in contact with the host (Hardham, 2001; Narayan *et al.*, 2010). *Phytophthora* zoospores are capable of swimming a great distance in water and

waterlogged soils because of the presence of two distinct flagella, the anterior flagellum and the posterior flagellum (Figure 1.4) (Hardham, 2001; Hardham, 2005; Hee *et al.*, 2013). The anterior flagellum is shorter than the posterior flagellum with two rows of opposing "tripartite flagellar hairs" called mastigonemes which play a role in forward locomotion (Carlile, 1983; Cahill *et al.*, 1996; Blackman *et al.*, 2011). The posterior flagellum is smooth and displays a "whiplash" movement that controls the zoospores as it swims (Cahill *et al.*, 1996; Hardham, 2005).

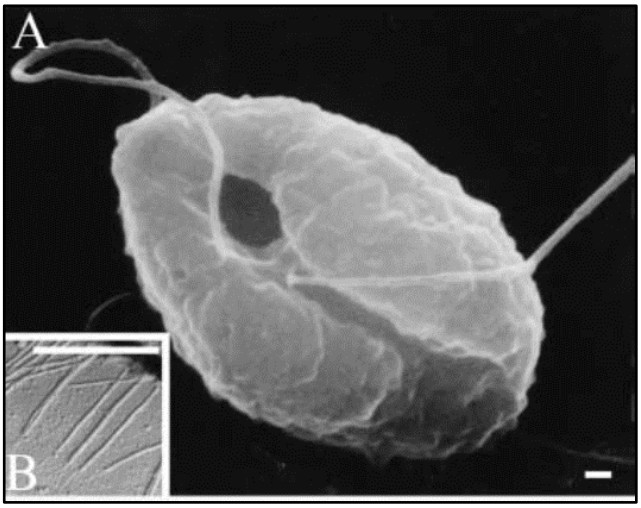

Figure 1.4. Scanning electron micrograph of a zoospore that shows two flagella emerging from the centre of the longitudinal groove on the ventral surface (A) Shadowcast image of the mastigonemes forming two opposite rows along the anterior flagellum (B). Scale bars = 1 μm (Hardham, 2001; Hardham, 2005)

Phytophthora zoospores use chemotactic and/or electrostatic signals to direct their motility towards a suitable host (Walker and van West, 2007; Hua *et al.*, 2008). In *P. sojae*, G-protein-coupled receptors with a phosphatidylinositol phosphate kinase domain control zoospore development, virulence and chemotaxis (Hua *et al.*, 2008; Wang *et al.*, 2010; Yang *et al.*, 2013a). Zoospores encyst when they reach the surface of the host. During encystment, the flagella are detached and adhesins are released from small vesicles that underlie the ridges of the groove on the ventral surface (Hardham and Gubler, 1990; Hardham, 2001). The stable adhesion of spores to the host surface facilitates

spore anchorage and invasion of the host cells (Hardham and Mitchell, 1998; Robold and Hardham, 2005). A major adhesive protein found in *P. cinnamomi* is called PcVsv1 and contains 47 copies of the thrombospondin type 1 repeat, a motif also found in adhesive proteins in malarial parasites (Robold and Hardham, 2005). Another adhesive protein that has been identified in *P. parasitica*, is a protein containing a Sushi domain (or complement control) motif (PnCcp) (Škalamera and Hardham, 2006; Zhang *et al.*, 2013). Immunocytochemical studies indicate that PnCcp is stored in the large peripheral vesicles as a shell of material surrounding a core of PnLpv proteins (Zhang *et al.*, 2013).

1.4.2. Spore germination and host penetration

After zoospore encystment, *Phytophthora* cysts germinate in 20-30 min and the germ tube emerges from a site adjacent to a cluster of small vesicles (Hardham, 2001). Zoospores orient their ventral surface towards the plant before settling and adhering to the root surface (Hardham, 2001; Hardham, 2005). Germination of cysts generally occurs from the side of the cell facing the root and the germ tube often forms an appressorium-like swelling from which a hypha grows and penetrates the host tissue intercellularly and sometimes intracellularly (Tippett *et al.*, 1976; Ho and Zentmyer, 1977; Hosseini *et al.*, 2015). Proteomic analysis has revealed that there is a greater range of proteins in *P. pisi* and *P. sojae* germinating cysts than in hyphae, a feature that may be involved in host specificity. These proteins include serine proteases, membrane transporters and a berberine-like protein (Hosseini *et al.*, 2015).

As for other plant pathogens, host penetration by *Phytophthora* involves the production and secretion of wide array of cell wall degrading enzymes (CWDEs) that breakdown the plant cell wall (Hardham, 2005). CWDEs include pectinases, cellulases, and hemicellulases. Pectinases are often the first CWDEs secreted by plant pathogens including *Phytophthora* species (Blackman *et al.*, 2014). RNA-Seq analysis of *P. parasitica*-infected lupin roots revealed that the infection transcriptomes included more than 60% of the genes encoding *P. parasitica* CWDEs (Blackman *et al.*, 2015).

1.4.3. Host cell colonisation and nutrient acquisition

After host penetration, *Phytophthora* hyphae may grow both intercellularly and intracellularly within the root cortex (Tippett *et al.*, 1976; Benhamou and Côté, 1992; Enkerli *et al.*, 1997b). Intracellular hyphae may be observed 48 h after inoculation and have a similar diameter to that of intercellular hyphae (Malajczuk *et al.*, 1977; Hardham, 2001). In some cases, intracellular structures that resemble small globular or finger-like projections develop and are called haustoria. Haustoria are specialised infection structures that form in non-necrotic host cells (Enkerli *et al.*, 1997b; Bozkurt *et al.*, 2011). During haustorium formation, the host cell walls are breached and the haustorial cell is closely associated with the plant plasma membrane. Susceptible hosts are colonised quickly and within 2–3 days, sporangia may develop on the root surface (Hardham, 2005). The accumulation of electron-dense material in the plant cell wall may occur after the development of haustoria as in the case of *P. infestans* (Hohl and Suter, 1976). The number of haustoria formed depends on the level of compatibility of the plant-pathogen interaction. Fewer haustoria are formed in resistant plants compared to susceptible plants (Hohl and Suter, 1976; Hardham, 2001).

1.4.4. Sporulation

In 2-3 days after invasion, *Phytophthora* species are able to sporulate: chlamydospores are formed in cortical cells and sporangia on the root surface (Tippett *et al.*, 1976; Ho and Zentmyer, 1977). In laboratory conditions, sporulation of *P. cinnamomi* is induced when mycelium is transferred from nutrient broth to a mineral salts solution devoid of nutrients (Narayan *et al.*, 2010). The formation of different vesicles occurs during sporulation. After transfer to mineral salts solution, dorsal vesicles form within 30 min, large peripheral and ventral vesicles form after 5 h and sporangia are first observed after 7.5 h (Dearnaley *et al.*, 1996). Functional analysis of *P. sojae* revealed that the *PsTatD4* gene is a key regulator during infection and is needed for sporulation and production of zoospores (Chen *et al.*, 2014). Other genes that are expressed

during sporulation include *PnMas2* in *P. parasitica*, and *Cdc14* and *M90* in *P. infestans* (Ah-Fong and Judelson, 2003; Cvitanich and Judelson, 2003; Blackman *et al.*, 2011).

1.5. Management of *Phytophthora* diseases

Integrated disease management combines ecologically and economically effective strategies to manage and protect crops from damage (Jones, 2001; Maloy, 2005; Khokhar and Gupta, 2014). Management methods differ substantially from one disease to another depending on the host, the pathogen, the environmental conditions, and many other factors (Agrios, 1997). Like other important disease-causing agents, *Phytophthora* is best managed using an integrated approach. Although these management practices have been developed independently, a more effective result is obtained if they are combined than if used alone. Disease management has been classified into two categories: preventive (prophylaxis) and curative (therapy or treatment). Preventive management strategies are those applied before the plant is infected while curative management strategies are applied after the plant is infected (Maloy, 2005).

1.5.1. Breeding for host resistance

Most plant pathogens including *Phytophthora* species are rapidly evolving and can breakdown plant resistance, resulting in disease spread. Disease development can be influenced by several factors, including weather conditions, disease pressure and pathogen genetic stability (McDonald and Linde, 2002; Zimnoch-Guzowska *et al.*, 2003; Vasudevan *et al.*, 2014). The search for plant resistance genes started a long time ago. After the great potato famine in Ireland in the 1840s, much research effort was focused on the discovery of late blight resistant potato cultivars (Allen and Friend, 1983; Zimnoch-Guzowska *et al.*, 2003; Nowicki *et al.*, 2012). Race-specific and hypersensitive response genes derived from wild species of potato were mapped, cloned and incorporated into

potato cultivars. The presence of these genes, however, is not a guarantee of total protection as new and more virulent strains of *P. infestans* arise and will breakdown resistance (Evers *et al.*, 2006; Vleeshouwers *et al.*, 2011; Nowicki *et al.*, 2012).

In the screening of resistance against *P. cinnamomi* in elite radiata pine (*Pinus radiata*) families, genetically controlled traits were observed to be heritable in both glasshouse and field conditions (Butcher *et al.*, 1984). Glasshouse screening of resistant eucalypt plants showed increased phenylalanine ammonia-lyase, phenolics, and lignin concentration as compared to susceptible plants (Cahill *et al.*, 1993). In avocado and citrus, grafting of tolerant rootstocks was effective in controlling *P. cinnamomi* and *P. parasitica*, respectively (Coffey, 1987; Matheron *et al.*, 1998; Douhan *et al.*, 2004). In addition to screening for resistance in glasshouse trials, application of molecular plant pathology techniques such as quantitative real-time polymerase chain reaction (qPCR), have accelerated the evaluation of plant varieties for resistance to *Phytophthora* diseases (Gordon *et al.*, 2007a; Gordon *et al.*, 2007b; Bnejdi *et al.*, 2009; Catal *et al.*, 2013).

1.5.2. Cultural practices

Cultural practices for the management of diseases helps in the reduction of initial inoculum levels and the rate of disease dissemination (Ogle and Dale, 1997). The cultural management of PRR of avocado includes planting of seedlings on mounds, irrigation management, mulching and incorporation of organic materials (Thurston, 1990). In forests, mining sites and national parks, restriction of vehicle movement, prevention of movement of infested water to disease-free areas, removal of diseased plants and installation of physical root barriers are among the cultural management strategies aimed at limiting the spread of *P. cinnamomi* (Hardy *et al.*, 2001a; Dunstan *et al.*, 2010).

Crop and cultivar rotation have been implemented as management strategies for PRR of lupins and avocado (Coffey, 1987; Lindbeck and Nikandrow, 2002). Cultivar rotation also reduced black shank disease incidence in tobacco and minimized the continuous shift of *P. parasitica* races (Sullivan *et al.*, 2005;

Mammellaa *et al.*, 2011). Similarly, the addition of lime before planting, amendment of calcium and gypsum in deficient soils, incorporating a fallow period, and proper soil drainage were found to be beneficial in controlling PRR (Kotze *et al.*, 1987; Messenger *et al.*, 2000; Jung and Blaschke, 2004; Serrano *et al.*, 2013).

1.5.3. Biological control

Biological control uses another kind of living organism (pathogens, predators, and parasitoids), excluding man, to control pests and diseases (Cook and Baker, 1983; Baker, 1987; Pearson and Callaway, 2003; Maloy, 2005). It aims to reduce inoculum and the potential of a microorganism to infect a host, with a long term and sustainable effect in the agricultural ecosystem (Baker, 1987; Lo, 1998; Vigo *et al.*, 2000). The mechanisms involved in the suppression of pathogens by biological control agents (BCAs) may be through microbial competition, antibiosis, production of pathogenicity enzymes, induced resistance, and mycoparasitism (Mitchell, 1973; Elad, 1996; Lo, 1998; Godfrey *et al.*, 2000; Cao and Forrer, 2001; Ren *et al.*, 2012). Pathogen suppression by BCAs may involve only one mechanism or may be a result of the combine action of many processes (Lo, 1998). Table 1.1 summarises the kinds of microorganisms used as BCAs against *Phytophthora* species.

Although in many cases the use of BCAs against disease pathogens has been effective, there are cases in which it was not a success (Gubler *et al.*, 2005). For instance, the use of non-pathogenic *P. parasitica* var. *nicotianae* isolates as BCAs did not totally control the damping-off caused by *P. parasitica* (Holmes and Benson, 1994). One cause of failure in the use of BCAs is the inability of the beneficial pathogen to grow and colonise faster than the disease-causing pathogen (Zinati, 2015).

Table 1.1. Summary of some biological control agents used to control *Phytophthora* species and diseases.

Biological control agents	*Phytophthora* species	Reference
Myrothecium roridum	*P. cinnamomi*	(Gees and Coffey, 1989)
Penicillium funiculosum	*P. cinnamomi*	(Fang and Tsao, 1995a)
Pythium nunn	*P. cinnamomi*	(Fang and Tsao, 1995b)
Gliocladium virens	*P. cinnamomi*	(Costa *et al.*, 2000)
Trichoderma harzianum		
Fungi	*P. cinnamomi*	(Aryantha and Guest, 2006)
Trichoderma sp.		
Gliocladium penicillioides		
Fusarium sp.		
Actinomycetes		
Streptomyces sp.		
Fluorescent pseudomonads		
Pseudomonas sp.		
Endospore-forming bacteria		
Bacillus sp.		
Penicillium funiculosum	*P. cinnamomi*	(Fang and Tsao, 1995a)
Pythium nunn	*P. cinnamomi*	(Fang and Tsao, 1995b)
Bacillus subtilis	*P. ramorum*	(Elliott *et al.*, 2009)
Streptomyces lydicus		
T. atroviride		
T. virens		
Trichoderma species	*P. ramorum*	(Widmer, 2014)
T. aspellum		
Nonpathogenic fungi	*P. parasitica*	(Cartwright and Spurr, 1998)
binucleate *Rhizoctonia*		
Fusarium sp.		
Arbuscular mycorrhizal fungi	*P. parasitica*	(Trotta *et al.*, 1996; Cordier *et al.*, 1998; Pozo *et al.*, 1999; Vigo *et al.*, 2000)
Glomus mosseae		
Paenibacillus polymyxa C5	*P. parasitica*	(Ren *et al.*, 2012)
Bacillus cereus	*P. parasitica*	(Handelsman *et al.*, 1991)
Streptomyces species	*P. infestans*	(Cao and Forrer, 2001)
Bacteria	*P. infestans*	(Daayf *et al.*, 2003)
Arbuscular mycorrhizal fungi	*P. infestans*	(O'Herlihy *et al.*, 2003)
Pseudomonas koreensis	*P. infestans*	(Hultberg *et al.*, 2010)
Rhizobacteria	*P. infestans*	(An *et al.*, 2010)
Burkholderia gladioli		
Miamiensis avidus		
Acinetobacter quenomosp		
Bacillus cereus		
Actinomycetes	*P. sojae*	(Filonow and Lockwood, 1985)
Actinoplanes missouriensis		
A. utahensis		
Amorphosporangium auranticolor		
Micromonospora sp.		
Fungus		
Hyphochytrium catenoides		
Streptomyces species	*P. sojae*	(Xiao *et al.*, 2002)
Pseudomonas aureofaciens	*P. sojae*	(Godfrey *et al.*, 2000)

1.5.4. Chemical method

Phytophthora belongs to the group of eukaryotic microbes known as Oomycetes (Randall *et al.*, 2005). Many aspects of the development and pathogenicity of *Phytophthora* and other Oomycetes are similar to those of fungi, but the Oomycetes are phylogenetically quite distinct from true fungi (Latijnhouwers *et al.*, 2003; Kamoun *et al.*, 2014). This distinct phylogeny is associated with a range of biochemical differences between the two groups of organisms and means that Oomycetes are not inhibited by many of the fungicides used to control fungal diseases (Hardham, 2001; Hardham, 2007; Hee *et al.*, 2013). Oomycetes are not fungi but the word "fungicide" in the literature and in this thesis may encompass chemicals used to kill Oomycete pathogens. These chemicals may also be referred to as anti-Oomycete substances.

There are chemicals that inhibit *Phytophthora* growth and infection of host plants but the number of these chemicals is limited. The most frequently used are metalaxyl and phosphite, and in both cases resistance to these chemicals has already emerged (Marks and Smith, 1992; Garbelotto *et al.*, 2009; Burra *et al.*, 2014). The chemical phosphite (phosphonate) has been used for decades for the control of *Phytophthora* in different host plants (Zentmyer, 1979; Smillie *et al.*, 1989; Hardy *et al.*, 2001a; Shearer and Crane, 2009; Anderson *et al.*, 2012; Akinsanmi and Drenth, 2013). Studies on phosphite have focused on the effective concentration *in vitro* and *in planta*, the means of application, and the mode of action (Smillie *et al.*, 1989; Jackson *et al.*, 2000; Tynan *et al.*, 2001; Wilkinson *et al.*, 2001c; Shearer *et al.*, 2006; Gentile *et al.*, 2009; Wong *et al.*, 2009; King *et al.*, 2010; Machinandiarena *et al.*, 2012).

Despite the fact that phosphite has been shown to be effective against *Phytophthora* diseases, problems such as phytotoxicity, growth deformities, and decreased reproductive capacity were observed in some species of plants (Hardy *et al.*, 2001a; Hardy *et al.*, 2001b; Barrett *et al.*, 2004; Solla *et al.*, 2009; Pilbeam *et al.*, 2011). Phosphite application is now an integral part in the management of *Phytophthora* diseases, however, there is still an urgent need to fully understand the mode of action of phosphite during plant infection.

1.6. Project aims

The research described in this thesis had four main aims. These were:

(1) To develop a new, robust plant infection assay for *P. parasitica.* This was achieved through the development of a qPCR-based assay that used the roots of young lupin (*Lupinus angustifolius*) seedlings as the host plant material (Chapter 2).

(2) To use the newly-developed qPCR infection assay to test the susceptibility or resistance of different lupin cultivars to *P. parasitica* (Chapter 3).

(3) To use the lupin-*P. parasitica* assay system to investigate the infection transcriptomes during the first 60 h of disease development (Chapter 4). Analysis of the infection transcriptomes focused especially on the patterns of expression of *P. parasitica* genes encoding cell wall degrading enzymes during lupin root infection.

(4) To determine the effects of phosphite treatment on *Phytophthora* growth, pathogenicity and gene expression (Chapter 5).

In the majority of the research, *P. parasitica* was used as the pathogenic species under investigation. However, another broad host range species, *P. cinnamomi*, was also used in initial experiments that examined the effects of phosphite on *Phytophthora* growth. The effects of phosphite on *P. cinnamomi* have been studied extensively and the initial experiments using *P. cinnamomi* allowed the experimental methodology to be checked prior to its application to studies of *P. parasitica*. As described in this thesis, the four main research aims were successfully completed and the resultant information should make a valuable contribution to the understanding of *Phytophthora* pathogenicity mechanisms and to the future development of improved methods of controlling *Phytophthora* diseases.

CHAPTER 2

Development of a model assay for plant infection by *Phytophthora parasitica*

2.1. Introduction

2.1.1. The importance of lupins in agriculture

There are more than 300 species of *Lupinus* but only five (*L. albus*, *L. angustifolius*, *L. luteus*, *L. mutabilis*, and *L. cosentenii*) are currently cultivated. Lupin is one of the many legumes associated with nitrogen-fixing bacteria; it produces seeds that contain high levels of protein and is used for animal feed and as a human food source globally (Kettel *et al.*, 2003). Human consumption of lupins is encouraged because medical studies have provided evidence of their beneficial contributions to combating high blood sugar, heart disease and obesity (https://www.agric.wa.gov.au/crops/grains/lupins).

Lupin is an economically important legume crop in Australia and other parts of the world (Yang *et al.*, 2013b). Because cultivars of *L. angustifolius*, or narrow-leafed lupin, are resistant to many of the diseases that infect white lupins (*L. albus*) this species is now widely domesticated. Lupin has been a vital component of the wheat:lupin rotation in WA farming systems for over 40 years and WA has become the world's top lupin producer. It is responsible for about 80% of world production and is the only major lupin exporter. Dr Gladstones of the University of WA released the first fully domesticated lupin cultivars adapted to WA conditions in 1960-1970 and with the help of the WA Department of Agriculture (now Department of Agriculture and Food, WA or DAFWA) has promoted the wheat:lupin rotation practice (French, 2008).

2.1.2. Lupin diseases

Lupin species are susceptible to a wide range of fungal and viral diseases (Thomas, 2008). Among fungal pathogens, anthracnose caused by *Colletotrichum lupini*, previously called *C. gloeosporiodes* or *C. acutatum* (Thomas

and Sweetingham, 2004; Bennett *et al.*, 2013), is considered a serious disease of lupins worldwide (Yang *et al.*, 2004; Tivoli *et al.*, 2006). In Australia, an outbreak of anthracnose occurred in WA on *L. angustifolius*, *L. albus*, *L. luteus* and *L. mutabilis* in 1994 and reoccurred in 1996 on *L. angustifolius*, and *L. albus.* A major eradication campaign to destroy infected crops was established but due to the scale of the outbreak in WA, eradication was impossible. Thus, restrictions to seed and machinery movement between states and districts were implemented to prevent further spread of the pathogen (Kaiser *et al.*, 2000).

Other fungal diseases of lupins include Phomopsis stem blight caused by *Diaporthe torxica* (Cowley *et al.*, 2008), root rots caused by *Fusarium oxysporum* f. sp. *lupini* (Mohamed and Mazen, 2012) and *Pleiochaeta setosa* (Cowling *et al.*, 1997), Rhizoctonia bare patch and hypocotyl rot caused by *Rhizoctonia solani*, and Sclerotinia collar rot caused by *Sclerotinia sclerotiorum* (Thomas, 2008). Cucumber mosaic virus (CMV) is also a damaging viral disease of lupins. In 1986 in WA, CMV was widespread in breeders' selections of narrow-leafed lupins, lupin cultivar collections and wild *L. angustifolius* lines. CMV is capable of causing almost a 100% yield loss if lupins are infected at an early stage of growth (http://www.depi.vic.gov.au/agriculture-and-food).

2.1.3. *Phytophthora* diseases of lupins

As described in Chapter 1, the genus *Phytophthora* includes a large number of plant pathogens that are renowned for their destructive economic and ecological impacts on agricultural and natural ecosystems (Hardham and Blackman, 2010; Hüberli *et al.*, 2013). *P. parasitica*, the species studied in the research described in this thesis, has one of the broadest host ranges of any *Phytophthora* species, infecting plants in over 100 genera (Erwin and Ribeiro, 1996). Lupin has also been shown to be susceptible to *Phytophthora* species, including *P. parasitica*. Seedlings of *L. angustifolius*, *L. luteus*, and *L. albus* wilted and died when seeds were sown in soil taken from fields previously cropped with soybean infected by *P. megasperma* var. *sojae* (Jones and Johnson, 1960). *P. megasperma* var. *sojae* was isolated from the lupin plant material. The fact that *Phytophthora* species

caused root and basal stem rot disease of lupin in New South Wales (NSW) was first documented in 1993, and in 1999 it was shown that *Phytophthora* species could severely affect *L. angustifolius* cv. Wonga (Nikandrow *et al.*, 2001). In studies conducted by Eshraghi *et al.* (2011b) and Allardyce *et al*. (2012), *P. cinnamomi* isolates successfully infected a number of *L. angustifolius* cultivars. *P. parasitica* infection of *L. albus* and *L. luteus* was documented in the early 1900s in Italy and the USA as reported in Erwin and Ribeiro (1996).

The principal aim of the work reported in this chapter was to develop a model plant infection system for *P. parasitica*. In the past, tobacco has been the host species most often used to study *P. parasitica* pathogenicity mechanisms, although tomato and citrus have also been used (Blaker and Hewitt, 1987; Graham, 1995; Grote *et al.*, 2002). Recently, it has been shown that *Arabidopsis* is susceptible to *P. parasitica* (Meng *et al.*, 2014) and, because of the extensive genomic and transcriptomic information available, *Arabidopsis* will be suitable for some investigations of *P. parasitica*-plant interactions, especially those that focus on plant defences against *P. parasitica* infections.

In addition to developing a model system for studies of *P. parasitica* disease development, it was clear from the literature that a reliable assay system for assessing diseases of lupin and other legumes would also be of considerable value. There has been little uniformity in the procedures used to screen food legumes such as pea, lentil, chickpea, faba bean and lupin or to score their germplasm and breeding lines for disease resistance (Tivoli *et al.*, 2006). For example, a range of inoculation methods for foliar pathogens have been utilised. Thomas and Sweetingham (2004) spray inoculated *C. lupini* var. *setosum* spore suspension (10^5 spores/ml + 0.1% Tween 20) on 14-day old lupin plants. For Phomopsis blight, 28-day old *L. angustifolius* were inoculated with a suspension of 1×10^6 conidia/ml (Williamson *et al.*, 1991). Yang *et al.* (1996) using an artist's airbrush sprayed a conidial suspension (flow rate of 13 ml/min) of *P. setosa* onto 21-day old lupin plants. Each of these inoculation techniques has its own merits and limitations. None is really suitable for investigations of lupin infection by the soil borne pathogen, *P. parasitica*. The present study aimed to develop a lupin-*P.*

parasitica infection assay system that incorporated suitable scoring parameters and pathogen quantification, that was simple and quick, but which provided reliable and sensitive results.

2.2. Materials and Methods

2.2.1. *Phytophthora* culture

P. parasitica H1111 (ATCC MYA-141) was used in the infection assays. Axenic cultures of the isolate were maintained on 10% V8 agar plates (Appendix I) sealed with Parafilm and stored in the dark at 25˚C. Stock plates were subcultured weekly by taking a 3 mm^2 piece of agar and mycelium from the edge of a colony growing on V8 agar and placing it at the centre of a new plate of V8 agar, hyphal side down, sealing the plate with Parafilm and placing it in the dark in a 25˚C incubator (Watson Victor Ltd, Australia). After 4 days, an 85 mm diameter disc of sterile, moist Miracloth (Calbiochem®, Darmstadt, Germany) was placed onto the surface of a new V8 agar plate and seven 3 mm^2 pieces of mycelia were placed evenly on the Miracloth. Plates were sealed with Parafilm and incubated at 25˚C in the dark. After 7 days, the Miracloth with adherent mycelia was carefully removed and placed in 100 x 20 mm Tissue Culture Dishes (Greiner Bio-One CELLSTAR®) with 5% of V8 broth. Plates were incubated in the light at 23˚C.

2.2.2. Zoospore production and quantification

After the *P. parasitica* cultures on Miracloth had been growing in V8 broth for 3-5 weeks they were used for zoospore production. The cultures were first observed under low magnification on a microscope to check for the presence of sufficient numbers of sporangia. If sporangia were present, the V8 broth was removed and the Miracloth disc was rinsed in cold, sterile reverse osmosis (RO) water four times before 40 ml of cold sterile RO water was added to the Petri dish. The plates were placed at 4˚C for 12 min and then on a light box at about

15˚C for 75 min. Released *P. parasitica* zoospores from the culture plates were transferred to a sterile conical flask.

The zoospore concentration was determined by transferring a 100 µl aliquot of zoospore suspension to a 1.5 ml Eppendorf tube to which 10 µl 0.2% iodine/potassium iodide (IKI) solution was added (Appendix I). The numbers of zoospores in known volumes were counted using a haemacytometer (Laboroptik GmbH, Friedrichsdorf, Germany).

2.2.3. Plant material

Seeds of lupin, *L. angustifolius* cv Gungurru, came from the NSW Department of Primary Industries, Wagga Wagga Agricultural Institute, NSW and the DAFWA. No sterilisation of seeds was used in initial assays but to ensure that there was no surface contamination in subsequent experiments, seeds were sterilised according to the procedure described by Sun *et al.* (2014) except that 10% hydrogen peroxide (H_2O_2) was used instead of 5%. Barampuram *et al.* (2014) found that the use of H_2O_2 in cotton seed sterilisation was superior than the use of chlorine gas or commercial bleach. Lupin seed germination and viability was not adversely affected by the sterilisation procedure.

Initially, perlite was used as the seed germination medium because only a few perlite particles adhered to the roots and those that did were easily removed. However, it was found that both the *Phytophthora*-inoculated and mock-inoculated seedlings became necrotic starting at the root apex. Necrosis increased during the period 24-96 h after removing the seedlings from the perlite. Some of the mock-inoculated seedlings were more necrotic than those inoculated with *P. parasitica* (Figure 2.1).

In subsequent assays, vermiculite was used as the seed germination medium. Although more vermiculite particles adhered to the roots compared to perlite, they could be gently removed with a soft camel-hair brush dipped in deionized water. Seedlings grown in vermiculite appeared healthy and devoid of any necrosis. Lupin seeds were sown in plastic pots (21.5 cm wide and 19 cm high). Initially, the seeds were sown in three layers with about 4 cm of vermiculite

between the layers. It was noticed, however, that seeds in the uppermost layer germinated poorly, if at all, probably because of inadequate hydration. Thus, in subsequent experiments, seeds were sown only in one layer about 10 cm from the base of the pot and covered with another layer of 8 cm vermiculite. RO water was sprinkled evenly until all vermiculite was totally soaked with water. The pot was covered with plastic wrap and aluminium foil (Figure 2.2a & b), and placed at 23˚C.

Figure 2.1. Uninfected (left) and *P. paraisitica*-inoculated (right) lupin seedlings showing necrosis when seeds were germinated in perlite medium.

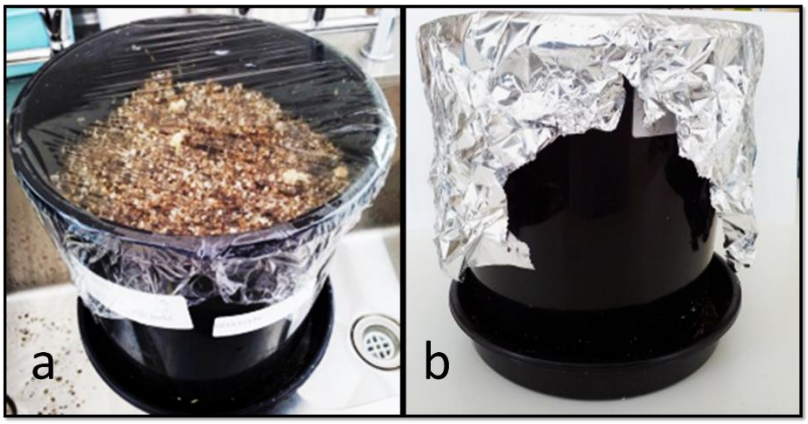

Figure 2.2. Lupin seeds were sown in pots containing vermiculite, watered to saturation and covered with plastic wrap (a). The pots were then covered with aluminium foil (b) and incubated at 23˚C.

In a series of experiments, it was established that to obtain seedlings with roots of an optimal length for the infection assay, it was best to harvest the *L. angustifolius* cv Gungurru seedlings 43-45 h after sowing the seeds. The seedlings were carefully removed from the vermiculite, washed and those with roots of the correct length selected (Figure 2.3). The optimal root length was 2.25-2.75 cm. If roots were shorter than 2.25 cm the required length of the root was not fully immersed in the zoospore suspension. If they were too long, contact of the tip of the root made the root orient obliquely rather than vertically in the zoospore suspension.

Figure 2.3. Washed lupin seedlings that have been sorted according to root length. They were placed on wet blotting paper to maintain their hydration.

2.2.4. Root inoculation and sample collection

Early infection assays used 28 seedlings (four rows of seven seedlings) arranged in the centre of a grid from a pipette tip box (12.5 cm x 10 cm x 9.5 cm; LxWxH) (Figure 2.4a). However, in order to be able to adjust the height of the grid above the inoculation solution, in later assays, three or four semi-rigid plastic grids from tip boxes were secured together with four nuts and bolts (Figure 2.4b). The height of the grid platform could be adjusted according to the position of the nuts on the bolts. Twenty-four lupin seedlings were arranged evenly across these plastic grids to allow zoospores in the inoculation suspension to swim in between

the roots and with the aim to reduce preferential access to the outer roots. The grids were placed in boxes containing sterile RO water while the seedlings were being arranged in the grids. When all the grids to be used in the experiment were ready, they were transferred to another set of plastic boxes containing 200 or 100 ml of zoospore suspension such that the root apex was immersed to a depth of approximately 20 mm or 10 mm, respectively, in the inoculum. A range of zoospore concentrations was tested as detailed below. In the initial experiments, three inoculation times (10 min, 20 min and 30 min) and different sample collection times that ranged from 8-96 hours post-inoculation (hpi) were tested. Root samples were collected by cutting the root just below the hypocotyl. After inoculation, the seedlings were randomly placed in 150 x 15 mm Petri dishes lined with three layers of moistened blotting paper. Each plate contained six to twelve seedlings which were supported by a sterilised applicator stick. The Petri dishes were sealed with Nescofilm, placed in a vertical position in a plastic container with a foil-covered lid and incubated at 23˚C in the dark. For infection assays used for DNA extraction, samples were taken at 12 hpi and every 6 hours thereafter until 60 hpi. Uninoculated roots were also collected and served as untreated controls.

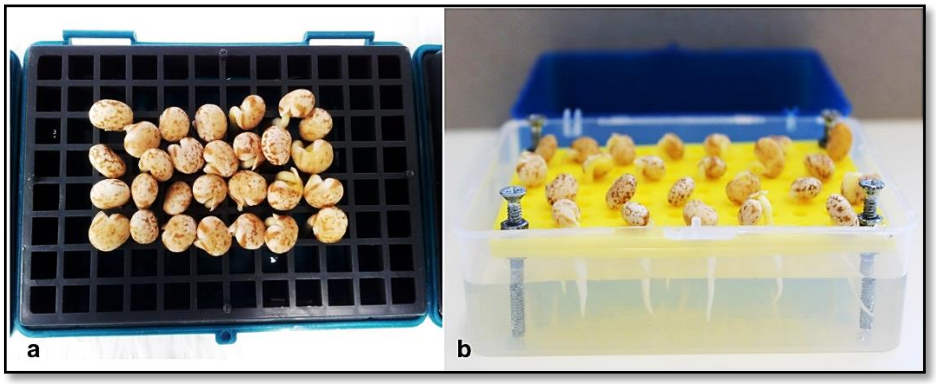

Figure 2.4. Lupin seedlings arranged (a) in the centre of a grid from a pipette tip box and (b) with even spacing in a grid whose height above the base of the inoculation box could be adjusted according to the position of the nuts on the bolts. In the case illustrated in (b), the inoculation box contained 200 ml of inoculum zoospore suspension.

2.2.5. Maintaining seedlings in a vertical position after inoculation

After inoculation, the lupin seedlings were transferred to moistened blotting paper in sealed Petri dishes. If the lupin seedlings were placed in a horizontal position, directed extension of the roots was lost and the roots curled (not shown). In order to hold the seedlings in place when the Petri dishes were placed in a vertical position, a sterilised applicator stick was inserted into two small holes drilled into the sides of the Petri dish and the seedlings carefully inserted under the stick (Figure 2.5). Using this set-up, the roots grew relatively straight during the time course of the experiment. Care was taken to maintain a high humidity within the Petri dishes containing the seedlings. Initially, 10 ml of sterile RO water was added to the layers of blotting paper. After 24 h, if the blotting paper had become dry, 5 ml of sterile RO water was added.

Figure 2.5. Lupin seedlings supported by an applicator stick to allow vertical positioning of the Petri dish.

2.2.6. Disease development

2.2.6.1. Lesion development

The progress of root infection was assessed by noting the percentage of roots that displayed visible lesions at each sample time point.

2.2.6.2. Root colonisation, haustorium development and callose deposition

Three roots were collected at each time point and placed in 100% methanol for at least overnight before cutting. In order to develop a sectioning protocol, the root samples were embedded in different kinds and percentage of agarose to find a set-up that could support the samples and allow them to be sectioned thinly and longitudinally. After a series of trials, roots were subsequently cut into segments about 5 mm in length, embedded in 3% agarose (UltraPure™ Agarose, Invitrogen) in water and sectioned with a vibratome (1000 Plus Sectioning System, Intracel Ltd, Royston, UK) at a section thickness of 150-200 µm. To obtain uniform sections, vibratome parameters were set to a low cutting speed and maximum amplitude. Sections were stained in lactophenol trypan as described in Takemoto *et al.* (2003) and viewed using a Zeiss (Germany) Axioplan microscope.

Lupin roots were also examined for callose deposition. Preliminary trials used uninfected lupin roots that were punctured with a syringe needle. Punctured roots were sampled at different times (1 h, 5 h, and 48 h). Roots without a puncture served as controls. Root segments (5 mm) were fixed overnight in 100% ethanol (EtOH). The next day, samples were rehydrated with 70% EtOH for 2 h, 50% EtOH for another 2 h and finally deionized water overnight. Vibratome sections of the root segments were cut as described above. The sections were stained in a solution of 0.01% aniline blue (BioScientific Pty Ltd, NSW) with 0.005% Tinopal LPW (Ciba-Geigy, Sydney), a fluorescent brightening agent, for 45 min. Sections were then washed with 0.01% aniline blue to remove excess Tinopal LPW and mounted on slides with 70% glycerol and 30% staining solution (0.01% aniline blue). The stained sections were examined using an epifluorescence Zeiss (Germany) Axioplan microscope using a 40x objective lens.

When no callose deposition was observed in the punctured and EtOH-fixed roots sampled at 1-48 h, unfixed fresh hand-sections from roots sampled at 54 h after puncturing were stained with a purified aniline blue fluorochrome (Biosupplies Australia, Pty Ltd, VIC) without Tinopal LPW and examined. White-yellow fluorescence was observed in the vascular bundle of the punctured sample.

Aniline blue from Biosupplies was used on the next batch of samples. It was prepared from a stock solution of 0.1 mg/ml in sterile RO water by diluting an aliquot 1:3 with sterile RO water. All stained samples and unused aniline blue stocks were stored in 4˚C in the dark.

Samples infected with *P. parasitica* were taken at different times (8 hpi, 24 hpi, 30 hpi, 48 hpi, and 54 hpi) and stained with aniline blue. *P. parasitica* hyphae were also stained in aniline blue for 30 min and examined.

2.2.6.3. Lupin Infection Assay – determining pathogen load

Measurement of the ratio of host to pathogen genomic DNA (gDNA) using quantitative real-time PCR (qPCR) has been extensively used to determine the level of host infection (Lees *et al.*, 2012) and this approach was applied to the current study of the infection of lupin by *P. parasitica*.

Root material from four biological replicates for mock-inoculated and inoculated samples was ground to a powder in liquid nitrogen. A small portion of the powder was removed for gDNA extraction as described by Dudler (1990). Mock-inoculated roots were collected at 0 h. Inoculated roots were collected at 12 hpi, 18 hpi, 24 hpi, 30 hpi, 36 hpi, 42 hpi, 48 hpi, 54 hpi and 60 hpi. At each time point, 12 roots were collected and three roots placed into each of four Eppendorf tubes. The concentration of isolated DNA was determined using an Eppendorf Biophotometer (Hamburg, Germany) and ranged from 264-4024 ng/µl. DNA quality was assessed by measuring the ratio of the absorbance at $A_{260}/A_{280\ nm}$. DNA integrity was evaluated by running samples on an agarose electrophoresis gel. DNA samples were stored at -20˚C.

Pathogen load was determined by calculating the ratio of *P. parasitica*:lupin gDNA in each sample from data obtained using a Rotor-Gene 3000 Real Time Thermal Cycler. The qPCR conditions included four technical replicates with approximately 300 ng of gDNA, 150 nM of primers against the *P. parasitica* gene *WS41* (National Center for Biotechnology Information (NCBI) accession number

CF891677) and the lupin nitrilase 4A gene (*NIT4A*; NCBI accession number DQ241759), and QuantiTect SYBR Green Master mix (Qiagen). All primer pairs used in the study are listed in Appendix II. All reactions were run in a total volume of 15 µl using a 72-well rotor. Cycling conditions were an initial step of 95°C for 5 min followed by 35 cycles at 95°C for 10 s, 20 s at 59°C and 30 s at 72°C, with data acquired at 65°C. The data were analysed using the comparative quantification function of the Rotorgene v2.0.3 software (Qiagen Pty Ltd, Hilden, Germany).

2.3. Results

2.3.1. Inoculum density and inoculation duration

The first infection assay used a zoospore concentration of 500 zoospores/ml, an inoculation time of 20 min and 200 ml of zoospore suspension. After 24 hpi, inoculated seedlings and mock-inoculated seedlings showed necrotic lesions due to the perlite germination medium. Vermiculite was used as planting medium for subsequent assays.

The next assay used a zoospore concentration of 1000 zoospores/ml, inoculation times of 10 min, 20 min and 30 min and 100 ml of zoospore suspension. Using 100 ml, the apical 10 mm of the roots was immersed in the zoospore suspension. When the lupin roots were immersed in the zoospore suspension for 20 min or 30 min, small necrotic lesions were observed about 24 hpi. When the roots were immersed for only 10 min, lesions were not observed at 24 hpi. By 48 hpi, all seedlings inoculated for 10, 20 or 30 min showed necrotic lesions on the roots. The infection assay was repeated twice using only two inoculation times (10 and 20 min) and with lower zoospore concentrations of 250 and 200 zoospores/ml. It was observed that both 10- and 20-min inoculation times showed similar frequencies of necrotic lesions at 48 hpi. From this result, it was decided to adopt the 10-min inoculation time in subsequent experiments because it was demonstrated that 10 min was a sufficient time for the zoospores to swim chemotactically and reach the roots to establish infection.

Having chosen a 10-min inoculation period, the next experiments investigated the effect of varying the numbers of zoospores in the inoculum through variation in zoospore concentration and inoculum volume. One of the challenges in this aspect of infection assay development was that extensive dilution of zoospores after their release from sporangia can induce them to encyst. This would mean that the effective inoculum concentration was lower than expected from the haemacytometer counts prior to dilution. To avoid this potential problem, zoospores can be released directly into a large volume of water but in that case, it is difficult to determine zoospore concentration through haemacytometer counts. Low number of zoospores could be concentrated by centrifugation prior to counting but this runs the risk of underestimating the zoospore concentration because of adhesion of the cells to the walls of the centrifuge tube. After a number of experiments in which the volume into which the zoospores were released and the extent to which they had to be subsequently diluted were varied, the results indicated that a good strategy was to release zoospores into a volume of 500 ml and dilute them to a final concentration of 1000 zoospores/ml.

Using this method to produce the zoospore inoculum suspensions, a series of experiments in which zoospore concentration was varied within the range of 200-1000 zoospore/ml and an inoculum volume of 100 or 200 ml was used. These experiments led to the conclusion that immersion of the apical 20 mm of the lupin roots into 200 ml of a zoospore suspension at a density of 1000 zoospore/ml for 10 min constituted a suitable inoculation strategy. A number of infection assays were then conducted using these parameters and progress of disease development was monitored by examining lesion development, colonisation of root tissues and the increase in pathogen biomass over a 60-h time course.

2.3.2. Lesion development

Using the infection assay described above, necrotic lesions were observed to form on the lupin roots by about 30 hpi. Initially a discoloration of the roots appeared at a position corresponding to that at the surface of the zoospore

suspension during inoculation. At 48 hpi, more than 50% of the roots were necrotic. To quantify necrotic lesion development, samples were collected at 12 hpi and at 6-h intervals thereafter for a total of 60 h. Lesions were first visible at 30 hpi (Figure 2.6). As the lesions continued to develop, the infected area became dark brown, shrunken and soft. By 60 hpi, almost all the roots displayed necrotic lesions, they had stopped elongating and most were at an advanced stage of necrosis.

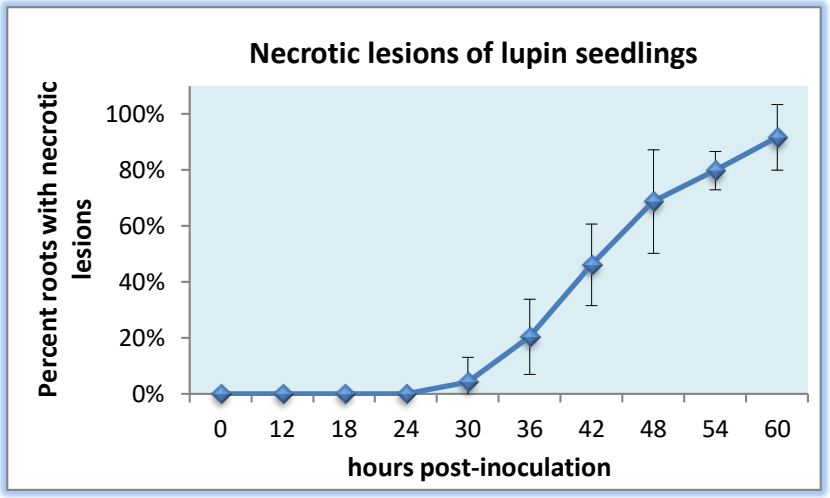

Figure 2.6. The development of necrotic lesions in lupin roots inoculated with 1000 zoospore/ml in 200 ml of suspension for 10 min. Error bars represent the standard error of the mean (n=24).

2.3.3. Microscopic examination of root colonisation by *P. parasitica*

In order to observe the progress of colonisation of root tissues by *P. parasitica* after inoculation, the roots were sectioned and stained with lactophenol trypan blue for observation using light microscopy. At 12-18 hpi, no hyphae were found in the sections but at 24 hpi, a few hyphae were observed in the epidermal and outer cortical cells in the region of the root that would have been close to the surface of the inoculum suspension (Figure 2.7). At 42 hpi, hyphae had reached the root endodermis. As the time course progressed, hyphae also grew longitudinally along the root. The infected roots continued to elongate until about 48 hpi and during this time, no hyphae were observed in the apical meristem or root cap. However, after root elongation stopped, hyphae invaded the root tip and were seen in the apical meristem and root cap at 60 hpi.

During early root infection, the *P. parasitica* hyphae developed haustoria within the cortical cells. The *P. parasitica* haustoria are short, peg-like protrusions from the hyphae (Figure 2.7). As infection progressed, haustoria were also seen within the vascular bundle.

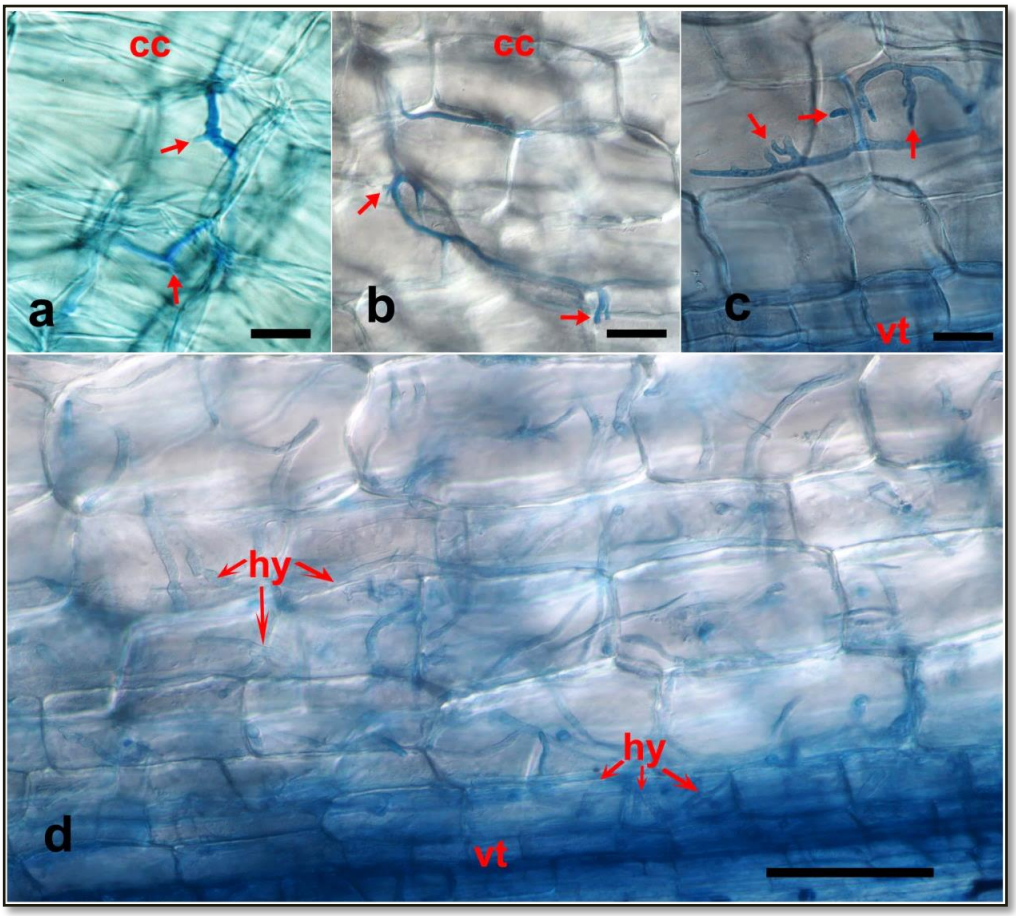

Figure 2.7. *P. parasitica* hyphae and haustoria in lupin roots stained with lactophenol trypan blue, 24 (a), 36 (b), 42 (c) and 60 (d) hpi. haustoria (red arrows), hyphae (hy), cortical cells (cc), and vascular tissues (vt). Bar represents 130 µm (a), 100 µm (b), 90 µm (c) and 80 µm (d).

2.3.4. Microscopic examination of callose deposition

Callose, a β-1,3 glucan polymer, is produced by plants in response to pathogen attack and wounding (Østergaard *et al.*, 2002; Luna *et al.*, 2011; Ellinger and Voigt, 2014). A preliminary trial for callose localisation was made by wounding the lupin roots with a needle. It was expected that callose deposits in the plant

tissues in response to wounding would be stained by the aniline blue to give a brilliant white-yellow fluorescence. However, no callose staining was observed in any of the wounded root samples.

The experiments were repeated using fresh hand-sections of wounded roots (54 h after wounding) that were not fixed in EtOH. The sections were stained with an aniline blue solution that lacked Tinopal LPW. Microscopic examination showed bright white-yellow fluorescence along the vascular bundles and in punctate spots in cell walls. These latter structures are likely to be plasmodesmata.

Vibratome sections of unfixed *P. parasitica*-inoculated lupin roots were then cut and stained immediately with aniline blue. No aniline blue fluorescence was observed in uninoculated roots or in inoculated roots 8 hpi. White-yellow fluorescence was visible in the vascular tissue of inoculated roots from 24-54 hpi. It was initially thought that aniline blue staining was indicating callose that had been deposited in response to the invading pathogen, however, when the sections were examined in detail it appeared that the material stained was in *P. parasitica* hyphae and not in the host cells (Figure 2.8).

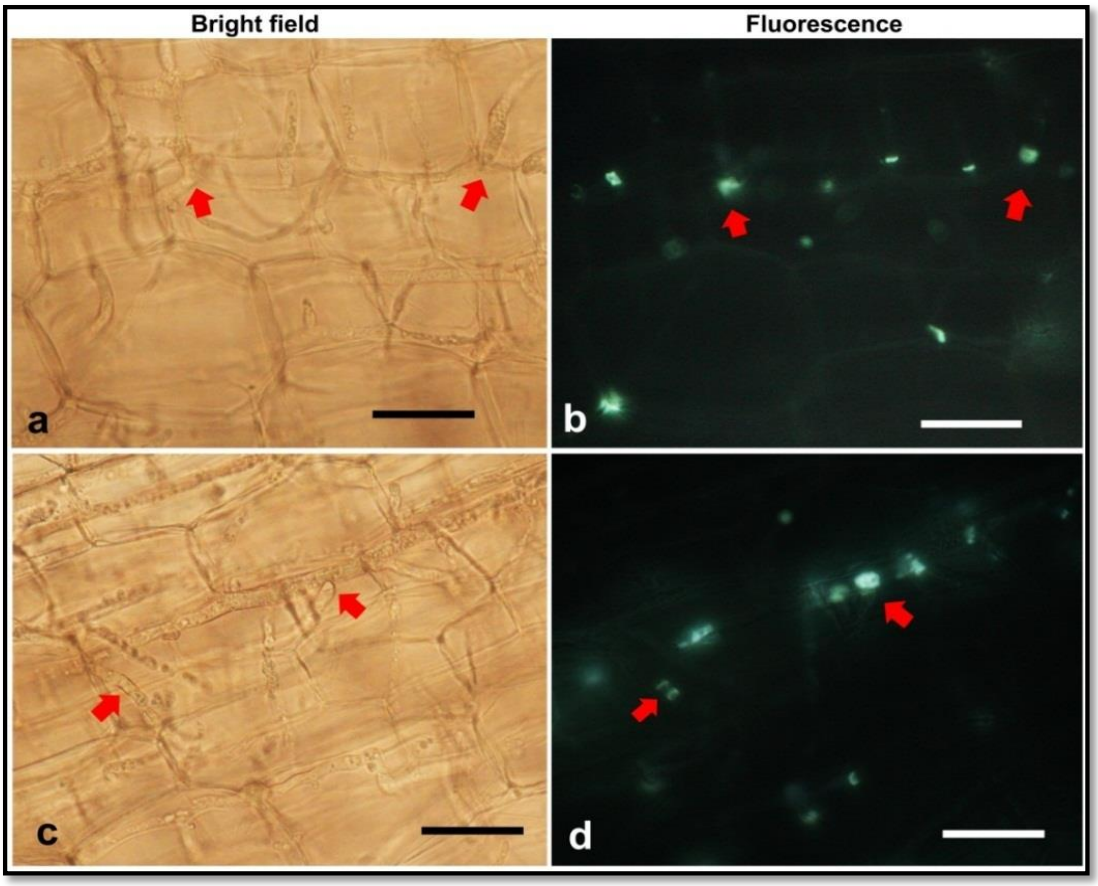

Figure 2.8. Bright field (a, c) and fluorescence (b, d) images of *P. parasitica* hyphae (red arrows) within infected lupin roots stained with aniline blue at 48 hpi (a and b), and 54 hpi (c and d). Bar represents 30 µm.

To further investigate these results, axenic cultures of *P. parasitica* were stained with aniline blue. The aniline blue stained hyphal and sporangial walls and structures that appeared to be hyphal cross-walls (Figure 2.9).

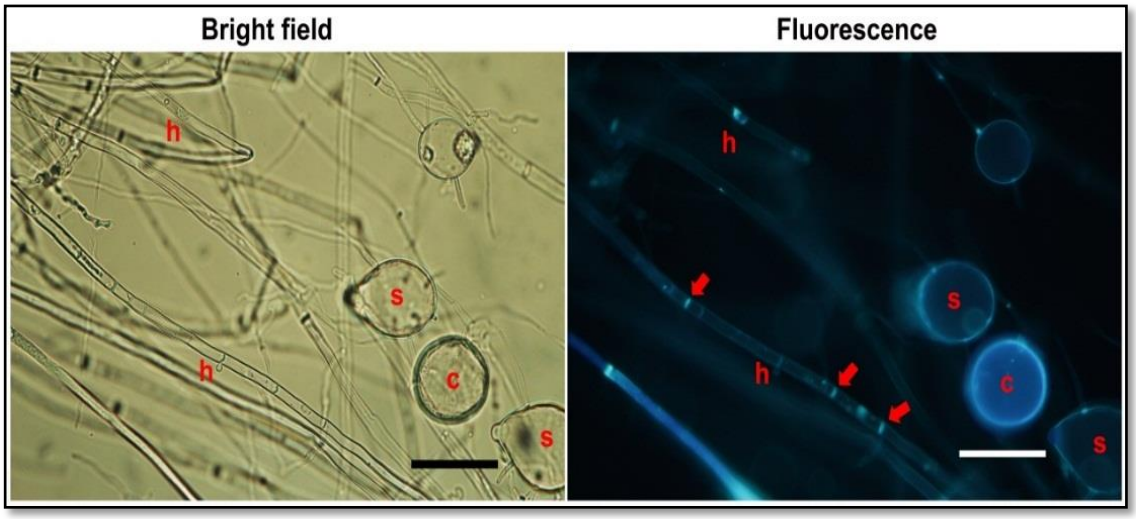

Figure 2.9. Aniline blue-staining of sporulating cultures of *P. parasitica* showing fluorescence of hyphae (h), sporangia (s), a chlamydospore (c), and hyphal cross-walls (red arrows). Bar represents 40 µm.

2.3.5. Quantification of disease development using qPCR

In order to quantitatively assess root colonisation in the infection assay, a qPCR assay was developed to determine the ratio of *P. parasitica* DNA to lupin DNA in the samples. This was done by measuring the abundance of two single-copy genes in the infected plant material. The target genes chosen were *P. parasitica WS41* and the *L. angustifolius* nitrilase 4A gene, *NIT4A*. In the mock-inoculated and 12-30 hpi samples, the *P. parasitica WS41* gene was not detectable (Figure 2.10). Calculation of the ratio of the two genes in samples from the later time points revealed a steady increase in the amount of *P. parasitica* present in the infected roots between 36-60 hpi.

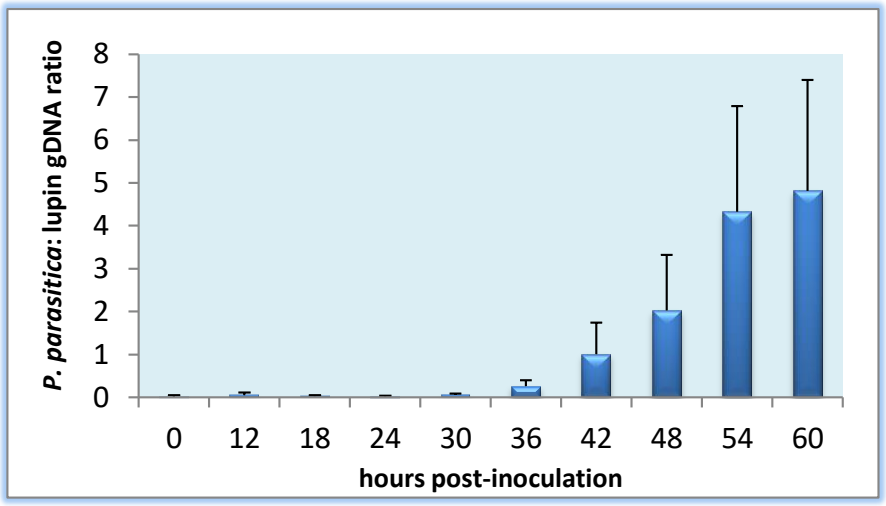

Figure 2.10. The ratio of *P. parasitica* to lupin DNA in four biological replicates at each time point through the infection assay. Error bars indicate standard deviation of the mean.

2.4. Discussion

2.4.1. Infection assays for *P. parasitica*

In the current study, narrow-leafed lupin, *L. angustifolius*, was used in the infection assay. There were a number of reasons for this choice. Tobacco, the species most commonly used, has tiny seeds and its seedlings are very small and delicate. Although in one study, 7-day old seedlings were inoculated in the wells of a microtitre plate and the effects of potential disease control chemicals assessed using microscopic examination, in general tobacco seedlings require growth for at least 2 weeks before they can be used in an infection assay (Handelsman *et al.*, 1991). Usually they are grown for longer than this. Lupin seeds, by contrast are large and germinate quickly. In less than 48 h, the lupin seedling roots were 2-2.5 cm in length and were suitable for inoculation in the assay system developed. Because of the size and robust nature of the lupin roots and seedlings, it was also possible to set up the assay so that individual roots were infected and handled rather than inoculating clusters of about 50 young tobacco seedlings (Blackman and Hardham, 2008). One problem with placing groups of small tobacco seedlings in a zoospore suspension is that the zoospores will not have free access to all parts of the surface of each tobacco seedling.

Another problem is that both shoots and roots may be infected, and thus this set-up cannot be used for investigations of shoot- or root-specific responses.

One of the aspects of many of the infection assays used to study plant infection by *P. parasitica* that is of major concern is the likely differences between the level of inoculum used in the laboratory assays with that believed to occur in the field (both agricultural or natural systems). While oospores and chlamydospores are propagules that survive during adverse conditions, as studied in particular for *P. cinnamomi* (Greenhalgh, 1978; Hwang and Ko, 1978; Goodwin *et al.*, 1990; Yang *et al.*, 2013a), the infective propagule that initiates most *Phytophthora* infections in the field is the motile zoospores (Hardham and Blackman, 2010). There is evidence that initiation of disease through hyphal growth is limited to situations in which infected and uninfected plant tissues, especially roots, are in close proximity (Hardham and Shan, 2009). Under favourable conditions, chlamydospores germinate to form one or two sporangia which, in turn, can produce and release zoospores. As discussed in Chapter 1, zoospores, can be disseminated over long distances in moving water and, over short distances, can actively move towards potential hosts. Thus, assays that use zoospores as the inoculum may be better predictors of plant susceptibility or resistance in the field than those that use hyphae as the inoculum.

Many of the infection assays that have been reported for *P. parasitica* and other *Phytophthora* species do use zoospores for plant inoculation, however, often the concentrations of zoospores are higher than those likely to occur in natural soil situations. Typically, less than three or four infective *Phytophthora* propagules per gram (g) of dry soil have been detected (Malajczuk *et al.*, 1975; Greenhalgh, 1978; Kellam and Coffey, 1985; Goodwin *et al.*, 1990). If these propagules consisted of chlamydospores or sporangia, they might each give rise to 50-100 zoospores. If, for the purposes of this estimation, 1 g of soil is equated to 1 ml of water, then a zoospore concentration similar to those existing in natural soils would be less than about 400 zoospores per ml. Zoospore concentrations used in laboratory-based assays are typically of the order of 10^4 to 10^5 zoospore per ml (Hinch *et al.*, 1985; Dolan *et al.*, 1986; Handelsman *et al.*, 1991; Van Jaarsveld

et al., 2003; Galiana *et al.*, 2008; Wang *et al.*, 2011; Allardyce *et al.*, 2012; Hosseini *et al.*, 2012; McCorkle *et al.*, 2013) and higher (Kenerly *et al.*, 1984; Blaker and Hewitt, 1987; MacDonald *et al.*, 1990) (Appendix Table 2.2). The lupin root infection assay developed in the current study employed *P. parasitica* zoospore concentrations of 500-1000/ml, and thus more closely resembles the situation in the natural environment than achieved by many previous assays. This is important because there is evidence that artificially high concentrations of zoospores can establish disease in plants that are normally resistant (Eye *et al.*, 1978; Attard *et al.*, 2010; Granke and Hausbeck, 2010). This effect is likely to be associated with effects on plant defence gene regulation. Another benefit of the lupin assay system is that it is rapid, requiring only 2 days to prepare the plant material and 2.5 days to complete the observations and sample collection.

Regarding the issue of inoculum concentration, it should be mentioned that during inoculation, the motile zoospores, which remain viable for many hours, will use chemotaxis, electrotaxis, autotaxis and/or autoaggregation to move to and settle on the surface of a potential host (Walker and van West, 2007; Galiana *et al*., 2008; Yang *et al*., 2013). *Phytophthora* zoospores are attracted to plant roots and plant root exudates, often primarily targeting the zone of cell elongation, the major region for the release of diffusible exudates (Dandurand and Menge, 1994). The operation of this phenomenon in the current, and in many other infection assays, means that, with time, the local zoospore concentration at the plant surface will increase from the initial value. In the current assay, if all zoospores in the 200 ml in which the roots are suspended were to become concentrated evenly around the 24 immersed roots, there would be on average about 8,000 zoospores per root. Even though it seems unlikely that all zoospores would achieve this relocation, the concentrating effect will be substantial. In addition, *Phytophthora* zoospores exhibit negative geotaxis and swim quickly to the surface of the liquid. The 10-minute inoculation period used in the current assay was sufficient to allow the zoospores to visibley concentrate just below the liquid surface. The implication is that there is likely to be a local zoospore concentration of considerably more than 1000 zoospores/ml around the root at the level of the liquid surface. This prediction is supported by the observation

that lesion development was usually initiated in the region of the root that had been at the surface of the zoospore suspension during the inoculation period.

A final aspect of the infection assay that should be mentioned is that of the duration of inoculation. In the present study, a number of experiments were carried out in order to determine a suitable inoculation time (at a given inoculum density). A 10-min period in the suspension of 1 x 10^3 zoospores/ml was found to be sufficient for effective lupin root inoculation. Although there was a 5-second inoculation period with 1 x 10^5 zoospores/ml used in the study of Wang *et al.* (2011), to my knowledge, all other infection assays have used longer inoculation periods. Periods of 20-30 min are common (Kenerly *et al.*, 1984; Hinch *et al.*, 1985; Hosseini *et al.*, 2012), although periods from 1 h to 3 days have also been used (Hanchey and Wheeler, 1971). A short inoculation period has the advantage of providing a well-defined start to the infection process.

Infection assays are a vital component of in-depth studies of host-pathogen interaction. Ideally, laboratory-based assays should be relatively quick and simple, cost-effective and reproducible. Over the last 40 years or more, a number of different methods have been used to monitor the infection of plants by *P. parasitica*. Because *P. parasitica* has a broad host range, a variety of host plants have been used including tomato (Blaker and Hewitt, 1987), citrus (Graham, 1995), tobacco (Colas *et al.*, 1998) and, recently, *Arabidopsis* (Wang *et al.*, 2011; Larroque *et al.*, 2013) (see Appendix Table 2.1).

Even when the same host plant is employed, infection assays have used different plant tissues and different forms of inoculation. For example, studies that aimed to screen tobacco for resistance to *P. parasitica* have used seedlings, leaves, stems or roots. Tobacco seedlings were used to determine virulence levels of different races of *P. parasitica* var. *nicotianae* in causing the black shank disease and to evaluate different tobacco cultivars for resistance to *P. parasitica* (McIntyre and Taylor, 1976; Van Jaarsveld *et al.*, 2003). On the other hand, a detached leaf assay to evaluate tobacco resistance to *P. parasitica* was used by Tedford *et al.* (1990). In a study that aimed to identify new resistance loci in tobacco cultivars,

McCorkle *et al.* (2013) found different levels of resistance or susceptibility depending on the plant tissues – roots, stems or leaves – that were inoculated.

With respect to the form of inoculation, two main types of *P. parasitica* inoculum have been used in tobacco infection assays, namely hyphae (mycelial plugs) and zoospores, with the level of inoculum varying widely. Plugs of mycelia may be placed on wounded or unwounded tobacco plant tissues (Tedford *et al.*, 1990; Way *et al.*, 2000; Van Jaarsveld *et al.*, 2003; Anderson *et al.*, 2012; Cho *et al.*, 2013). Seedlings or roots may be placed in suspensions of zoospores (Blaker and Hewitt, 1987; Handelsman *et al.*, 1991; Colas *et al.*, 1998; Grote *et al.*, 2002; Van Jaarsveld *et al.*, 2003; Wang *et al.*, 2011), zoospores suspension may be sprayed onto the plant (McIntyre and Taylor, 1976) or aliquots of zoospores may be applied to the leaf surface (McCorkle *et al.*, 2013).

The inoculation techniques used in assays aimed at studying *P. parasitica*-tobacco interactions each have their own benefits and limitations. For example, spraying seedlings with zoospore suspensions did not distinguish stem from leaf resistance and was thus not a good method for evaluating tobacco field performance although it did help to identify highly susceptible cultivars (McIntyre and Taylor, 1976). The detached leaf assay used by Tedford *et al.* (1990) was not effective in detecting race-specific resistance but the non-destructive nature of this technique allows it to be used in combination with detached-leaf screening techniques for other pathogens. Van Jaarsveld *et al.* (2003) had difficulty in identifying seedlings with low or moderate resistance to infection following inoculation of 3-week old seedlings with a zoospore suspension but, interestingly, they found a strong correlation between the results of the seedling and adult plant assays.

2.4.2. Assessment of the progress of infection

Evaluation of disease development requires the selection of parameters by which the progress of infection will be assessed (Infantino *et al.*, 2006). In the present

study, these parameters included (i) macroscopic symptoms of lesion development (frequency and area) and inhibition of root elongation, (ii) microscopic evidence of root colonisation and haustorium formation and (iii) molecular measurement of pathogen DNA relative to plant DNA.

In terms of macroscopic symptoms, in the present study necrotic lesions appeared on inoculated lupin roots at about 30 hpi and root elongation ceased after about 48 hpi. These results are similar to those observed for lupin roots (cv Wonga) inoculated with a 20-µl aliquot of 1 x 10^5 *P. cinnamomi* zoospores per ml (Allardyce *et al.*, 2012). In both cases, with time the dark-brown and water-soaked lesions extended from the initial point of inoculation until they encompassed the entire root. As mentioned above, in the present study the main point of inoculation corresponded to the region of the root at the level of the surface of the inoculation liquid. Water-soaked lesions were also visible on pea roots inoculated with 1.2 x 10^5 *P. pisi* zoospores/ml by 20 hpi (Hosseini *et al.*, 2012) and 3-5 days post inoculation on Arabidopsis leaves (Wang *et al.*, 2011).

The number of haustoria observed in the sectioned lupin roots in the present study was limited. At 24 hpi, haustoria were seen in cortical cells and later within the vascular bundles. In soybean roots inoculated with *P. sojae*, haustoria were first seen at 4 hpi in root cortical cells and by 10 hpi they occurred throughout the root tissues (Enkerli *et al.*, 1997b). Haustoria also form in compatible interactions between *P. parasitica* and *Arabidopsis* leaves and roots (Attard *et al.*, 2010; Wang *et al.*, 2011). In *Arabidopsis* roots, maximum numbers of haustoria were seen 10 hpi (Attard et al., 2010). In the current study, *P. parasitica* hyphae grew into the lupin root epidermal and cortical cells by 24 hpi, reached the endodermis by 42 hpi, and had invaded the entire root system by 60 hpi.

2.4.3. Quantification of *P. parasitica* DNA during infection

Traditionally, visual examination of infected plants and/or pathogen isolation and culture were widely used to diagnose plant diseases (Llorente *et al.*, 2010). However, these methods have a number of problems. Disease diagnosis based

on the appearance of infected plants is often not reliable because plants may exhibit similar symptoms although infected by different pathogens (Lees *et al.*, 2012). In addition, estimations of the extent of pathogen colonisation through microscopic examination are laborious and often not accurate. Regional differences in the degree of pathogen growth within the plant tissues or variability in assessments by different investigators contribute to inaccuracies in quantitation of pathogen presence (Engelbrecht *et al.*, 2013).

One approach to address these problems has been the development of immunodiagnostic assays to identify and, in some cases, quantify pathogens in infected plant or soil samples. Both polyclonal and monoclonal antibodies have been used in a range of immunodiagnostic assays for species of *Phytophthora*, including *P. parasitica* (Gautam *et al.*, 1999; Hardham, 2005). Immunodiagnostic assays for *Phytophthora* species are commercially available and are especially useful for use in the field, whether it be in the context of an agricultural or natural ecosystem. Unfortunately, these commercial kits can suffer from problems associated with the extent of cross-reactivity of the antibodies with different organisms. For example, the *Phytophthora* detection kit marketed by Agri-Diagnostics Associates (Cinnaminson, NJ) recognised some, but not all species of *Phytophthora* (Ali-Shtayeh *et al.*, 1991; Benson, 1991; Pscheidt *et al.*, 1992; Werres *et al.*, 1997), and was, thus, of limited value.

Over the last 15 years, the other approach to pathogen identification and disease diagnosis that has been developed is based on amplification of selected gene sequences by PCR. One of the strengths of this approach is that the level of specificity of the assay can be controlled through careful selection of the sequence of the primers used. For example, primers can be designed to be species-specific or to react with all species in a genus. The design of primers with the desired level of specificity is being increasingly simplified as more and more pathogen genomes are sequenced. At the simplest level, conventional PCR can be used to amplify sequences from the pathogen DNA, however, this method does not always detect low levels of pathogen DNA, such as those occurring during latent infections and, most importantly, conventional PCR does not facilitate

accurate quantitation of the amount of pathogen present in the samples (Engelbrecht *et al.*, 2013; Lan *et al.*, 2013).

In contrast, qPCR allows sensitive and specific detection of the pathogen (Lees *et al.*, 2012; Nath *et al.*, 2014). Compared to conventional PCR, qPCR is more rapid and reliable, often has greater sensitivity and can accurately measure the amount of pathogen material in a sample quantitatively (Chen *et al.*, 2012; Gangneux *et al.*, 2014). Early recognition and accurate quantification of a pathogen in host tissues or in soil is an important step in determining disease resistance (Eshraghi *et al.*, 2011b); it is fundamental to plant breeding programs, basic research and successful disease management (Llorente *et al.*, 2010; Nath *et al.*, 2014). In recent years, qPCR assays have been used to quantify a range of fungal pathogens such as *Fusarium* spp. (Nicolaisen *et al.*, 2009), *Botrytis cinerea* (Sanzani *et al.*, 2012), and *Colletotrichum lindemuthianum* (Chen *et al.*, 2013b), and Oomycete pathogens such as *Aphanomyces euteiches* (Gangneux *et al.*, 2014), *P. sojae* (Bienapfl *et al.*, 2011; Catal *et al.*, 2013), *P. ramorum* (Gagnon *et al.*, 2014), *P. pisi* (Hosseini *et al.*, 2012), and *P. colocasiae* (Nath *et al.*, 2014).

In some cases, qPCR assays have been used to compare the rate and extent of plant colonisation between different plant species or different races of pathogen. For example, qPCR was used to measure levels of *P. cinnamomi* in resistant (the non-host *A. thaliana*) and susceptible (*L. angustifolius*) plants (Eshraghi *et al.*, 2011b). The assay allowed the precise measurement of pathogen biomass even in the presence of considerable host cell necrosis. Similarly, a qPCR assay was used to distinguish between *P. ramorum* lineages isolated on different continents (Gagnon *et al.*, 2014).

In the present study, a qPCR-based assay was developed to quantify the extent of infection of *P. parasitica* in lupin roots. The assay detected significant amounts of *P. parasitica* 36 hpi, 6 h after the first necrotic lesions became visible at 30 hpi. This timing of pathogen detection by the qPCR assay relative to visual symptoms is in contrast to that reported during the infection of potato leaf and tuber tissues by *P. infestans* (Llorente *et al.*, 2010; Lees *et al.*, 2012). In the *P. infestans* studies, qPCR detected pathogen DNA 24 hpi while the first symptoms of the disease were

not observed until 48-72 hpi. One possible factor that contributed to the timing of detection of significant levels of *P. parasitica* DNA in the current study is the fact that although only the apical 20 mm of the root was inoculated, the entire root was collected for DNA extraction. The rationale for this sampling procedure was that it allowed the progressive increase of *P. parasitica* biomass within the lupin root tissues to be determined over the whole time-course. This would not have been possible if only segments of the root around the inoculation site had been collected. The results suggest that parameters of tissue collection should depend on the aim of the experiment.

QPCR is a valuable molecular tool that can be used not only for diagnosis of lupin pathogens but also within the lupin industry for the detection of lupin-specific DNA as a marker for the presence of allergenic ingredients in food products (Galan *et al.*, 2010; Demmel *et al.*, 2012). It is also used for breeding programs aimed at the identification of lupin cultivars that are resistant to or tolerant of *Phytophthora* or other pathogens. The accurate quantitative measurement of pathogen colonisation of lupin plants is also important because it contributes to the development of a better understanding of lupin-pathogen interactions. The development of the qPCR-based assay described in this chapter, demonstrates that this assay format could be used to screen selected lupin cultivars for their susceptibility to *P. parasitica* or other lupin diseases. In addition, the results of the study demonstrate that lupin is an excellent model plant host for studies of *P. parasitica* diseases.

2.4.4. Lupin defence responses

Plants have evolved a range of chemical and physical defence mechanisms to protect themselves from pathogens and to prevent pathogen entry and colonisation (Luna *et al.*, 2011; Voigt, 2014). Plant defence mechanisms include the formation of physical and chemical barriers such as reinforcement of the cell wall, including deposition of callose and cross-linking of wall proteins, at the infection site, production of reactive oxygen species (ROS) such as hydrogen peroxide and nitric acid, biosynthesis and accumulation of pathogenesis-related

compounds and secondary metabolites, and the hypersensitive response (HR) (Grenville-Briggs, 2005; Fu *et al.*, 2011; Luna *et al.*, 2011; Zhao and Dixon, 2014). HR is a form of programmed cell death that can occur at the single cell level and that can effectively limit pathogen spread (Kamoun *et al.*, 1999).

Several studies have described plant defence responses that occur during plant-*P. parasitica* interactions. Successful defence of tobacco plants against attack by *P. parasitica* includes ethylene signalling, callose deposition, ROS accumulation and induce systemic acquire resistance and HR (Ibáñez *et al.*, 2010; Anderson *et al.*, 2012; Cho *et al.*, 2013; Chang *et al.*, 2015). Similar responses have been observed in interactions with *P. infestans* (Eschen-Lippold *et al.*, 2012; Furuichi *et al.*, 2014).

In the present study, although the interaction was a compatible one, the inoculated lupin roots were stained with aniline blue to determine if any callose deposition did occur as part of the plant defence response. Callose is an amorphous, high–molecular weight 1,3-β-glucan cell wall polymer that is involved in many essential biological processes, e.g., cell division, microsporogenesis, pollen germination, fertilization and seed germination (Beffa and Meins Jr, 1996). Plants produce callose during their development and as a response to biotic and abiotic stresses like pathogen attack and wounding (Østergaard *et al.*, 2002; Luna *et al.*, 2011; Ellinger and Voigt, 2014). Callose has been suggested to play a role in defence by strengthening the plant cell wall at attempted sites of pathogen penetration and by providing a medium in which toxic compounds can be deposited (Donofrio and Delaney, 2001). Callose also promotes host defence by blocking nutrient transfer from host to pathogen. Together, these attributes allow callose deposition to delay the progress of pathogen ingress and to give the host plant time to activate other defence mechanisms (Kováts *et al.*, 1991). The formation of callose as a defence response normally indicates a resistant reaction of the host to pathogen invasion (Hückelhoven, 2007). This is illustrated in the case of *P. infestans*-potato interactions. When resistant potato cultivars were inoculated, the number of thick callose encasements around the pathogen cells were eight times more

frequent than in susceptible cultivars (Hächler and Hohl, 1984). Similarly, during the invasion of root tissues by *P. cinnamomi*, wall papillae that contained callose were produced in the resistant *Zea mays* but not in the susceptible *L. angustifolius* (Hinch and Clarke, 1982). In the present study, no callose deposition within the lupin cells was observed in the lupin tissues colonised by *P. parasitica*. This is thus likely to be due to the fact that the cultivar of lupin used was susceptible to *P. parasitica*.

In contrast to the situation in true fungi, cell walls of Oomycetes consist largely of 1,3-β-glucans, 1,6-β-glucans and 1,4-β glucans (cellulose). Cellulose forms wall microfibrils in Oomycetes while chitin forms the main cell wall microfibrillar component in fungi (Latijnhouwers *et al.*, 2003; Grenville-Briggs *et al.*, 2008; Mélida *et al.*, 2013). It is thus possible that the white-yellow fluorescence observed in the sections of the infected lupin roots in the current study, is due to the interaction of aniline blue with the 1,3-β-glucans in the *P. parasitica* cell walls. The staining of the *P. parasitica* hyphae and sporangia *in vitro* demonstrates that aniline does react with components in the walls of these cells. However, the pattern of aniline blue staining of the sections of infected lupin roots suggest that diffuse aggregates of material within the hyphal cells is being labelled. Apart from the fact that the material occurs within the hyphae, its identity is not known at this stage.

It is often thought that one of the major differences between the Oomycetes and the true fungi is that the vegetative cells of the Oomycetes generally consist of coenocytic hyphae (hyphae without septa, i.e., without cross-walls) (Tyler, 2002; Rossman and Palm, 2006). But, these hyphal cross-walls or 'false septa' have also been noticed in *P. infestans* and *P. parasitica* (Gooday and Hunsley, 1971; Hohl and Suter, 1976). The wall-like deposits or 'false septa' in *P. infestans* are more frequent under parasitic than saprophytic conditions. They are often observed at the border between normal and degenerate cytoplasm, at sites of host cell wall penetration, and at the narrow necks of sporangia, oogonia and chlamydospores. They are formed as a result of localised mechanical or physiological stress conditions (Hohl and Suter, 1976). Apart from *Phytophthora* species, cross-walls or septa have also been observed in other Oomycetes. Septa are frequently found

in mycelia of Oomycetes such as *Peronospora tabacina*, *Pseudoperonospora cubensis* and *P. humuli* (Kortekamp, 2005). Also, the zoosporangial cross-walls in the Oomycete *Saprolegnia ferax*, contain membrane that is entrapped in callose (Levina *et al.*, 2000).

2.4.5. Concluding Remarks

The development of the robust infection assay for *P. parasitica* using lupin seedlings that is described in the current chapter is an important advance for future studies of *P. parasitica* pathogenicity and plant resistance, in particular for assessement of levels of resistance or susceptibility of different lupin cultivars. Through careful investigations of the parameters involved, optimal conditions for the assay were determined. The most important parameters assessed included the concentration of zoospores in the inoculation liquid, the length of the root tip immersed in the inoculation liquid and the time in which the root was in the inoculation solution. Design of the assay system also included development of (i) a simple grid system to streamline the inoculation process, (ii) suitable ways of handling and incubating the inoculated seedlings, and (iii) methods of quantifying disease development within the lupin roots, in particular a qPCR-based assay that measures pathogen load within the infected plant tissues. The resulting assay system can be used to screen the susceptibility of other lupin cultivars to *P. parasitica*, as is the focus of the next chapter, and could form the basis for similar assay systems for other *Phytophthora* species or other host plants.

CHAPTER 3

Screening for resistance to *P. parasitica* in *Lupinus angustifolius* cultivars

3.1. Introduction

3.1.1. Narrow-leafed lupin (*L. angustifolius*)

Narrow-leafed lupin, also known as Australian sweet lupin or blue lupin (*L. angustifolius*), is the most important lupin species in WA, comprising over 95% of all lupin grain production (www.ogtr.gov.au). WA has become the world's top lupin producer and exporter with the majority of material exported as animal feed to the European Union, Japan and Korea (www.agric.wa.gov.au/crops/grains/lupins). Uniwhite was the first fully domesticated Australian-bred cultivar of narrow-leafed lupin and was released in 1967 (Gladstones, 1994). However, this cultivar matures late in the season and did not perform well in wheat-belt areas. The expansion of lupin cropping into the areas that are currently used only succeeded after the early flowering Unicrop cultivar was released in 1973 (French, 2008). Preliminary cultivar development focused on early flowering and resistance to grey leaf spot (*Stemphylium botryosum*) which threatened the lupin industry in the 1970s. Subsequent lupin breeding at the DAFWA aimed at improving environmental adaption, yield potential and disease resistance (Buirchell and Sweetingham, 2006). Breeding for disease and pest resistance was also considered to be important in order to reduce crop losses due to pathogens. Innate resistance of the crop is a valuable trait because it allows growers to reduce the need for other control methods, especially chemical application (Johnson, 1992).

The major foliar necrotrophic diseases of narrow-leafed lupins and other lupin species are brown leaf spot (*P. setosa*) (Reeves *et al.*, 1984; Cowling *et al.*, 1997), Phomopsis stem blight and pod blight (*D. torxica*) (Cowley et al., 2008), and anthracnose (*C. lupini*) (Cowling *et al.*, 1987; Yang *et al.*, 1996; Bennett *et al.*, 2013). Of these, anthracnose is the most devastating, making it the focus of breeding for resistance in different breeding programs worldwide (Tivoli *et al.*,

2006). At the species level, *L. angustifolius* is regarded as being more resistant than *L. luteus*, *L. mutabilis*, and *L. albus* to anthracnose disease (Cowling *et al.*, 1999).

Choice of a variety to be planted in any particular area depends on location and disease risk. While a range of *L. angustifolius* cultivars are available to WA growers, the recommended varieties for 2014 are PBA Barlockф, PBA Gunyidiф and Jenabillupф. Agronomic features should be taken into consideration when choosing a cultivar to be planted, with particular priority to the range of disease resistance and the adaptability in specific environments (Pritchard, 2014). The putative susceptibility or resistance of *L. angustifolius* cultivars guided the choice of cultivars selected for testing in the current study.

3.1.2. Phytophthora root rot of lupins

The cause of lupin sudden death was identified as a root rot caused by the soil-borne Oomycete pathogen, *Phytophthora*. Hence, the disease was known as Phytophthora root rot (PRR) of lupins. PRR had not been reported as a disease of lupins in Australia until it was first observed in NSW in 1993 when large areas of apparently healthy lupin crops unexpectedly died (Nikandrow *et al.*, 2001). The species of *Phytophthora* responsible was not determined. Symptoms included wilting, yellowing of leaves and sudden death of lupin plants within days during pod filling, with a dark brown sunken lesion extending from the base up the stem. Infected plants had a necrotic taproot when pulled from the soil. The pattern of disease distribution varied from single scattered plants to large areas of the crop, often in low-lying areas of the paddock. Infected lupin plants had unfilled pods or produced small seeds (Matthews *et al.*, 2014).

There are two critical requirements that trigger PRR disease development (Lindbeck and Nikandrow, 2002). Firstly, soil temperatures must be above around 15˚C. This is the reason why there is no disease occurrence during the cooler winter months. However, as soon as temperatures rise, infection occurs, with the taproot rotting and the lupin plants wilting and dying. Secondly, a period of flooding or waterlogging allows high levels of inoculum to build up in

the soil. Experiments have shown that healthy narrow-leafed lupins survive flooding for at least 8 days without *Phytophthora* but will die in a short period in the presence of *Phytophthora* (Lindbeck and Nikandrow, 2002).

3.1.3. Use of lupin for *Phytophthora* detection

In the 1950s, isolation from soil using apple fruit as selective medium led to the frequent isolation of different *Phytophthora* species (Newhook, 1959). Baiting with apple was performed by making a hole (5.08-6.35 cm) with a wood drill in the apple fruit. The hole was filled with wet soil from *Phytophthora*-infested areas, then sealed with petroleum jelly and incubated for 2-3 weeks for symptom appearance. Although the use of the apple technique has revealed a highly significant relationship between the occurrence of *Phytophthora* and plant disease, the percentages of samples from which *Phytophthora* was isolated were not always as high as expected based on symptom expression (Newhook, 1959). Later, *L. angustifolius* seedlings were adopted as a convenient host plant for infection studies with *P. cinnamomi*. Lupin seedlings were found to be more efficient and effective when used as selective baits in soil isolation tests for *P. cinnamomi* and other *Phytophthora* species as compared to other plant materials including, for example, apple (Chee and Newhook, 1965). The lupin-baiting technique for *P. cinnamomi* was also used in native forest areas of NSW and WA (Pratt *et al.*, 1973; Blowes *et al.*, 1982) and *L. angustifolius* cultivars have been used as a model host test plant for *P. cinnamomi* in a number of studies (Smillie *et al.*, 1989; Eshraghi *et al.*, 2011b; Allardyce *et al.*, 2012). Although tobacco is used most often as a test plant for studies of *P. parasitica* diseases, in the current study, the susceptibility or resistance of different *L. angustifolius* cultivars to *P. parasitica* was investigated.

3.2. Materials and Methods

3.2.1. *P. parasitica* culture

See Section 2.2.1.

3.2.2. Zoospore production and quantification

See Section 2.2.2.

3.2.3. Plant material

This present study used four *L. angustifolius* cultivars namely, Gungurru, Jenabillup, Jindalee and Wonga to study their susceptibility to *P. parasitica*.

Gungurru is an early maturing cultivar which originated as an F_4-derived selection from a cross made in 1975 between an F_4 forbear of cv. Illyarrie and P22750 (CPI 67921), a wild-type from Spain (Gladstones, 1989). Gungurru when first released in 1988 was regarded as the first cultivar resistant to *Phomopsis* (Mayfield et al., 2008).

JindaleeΦ was released in 2000 by the NSW Department of Primary Industries (DPI). Jindalee is a late flowering and maturing cultivar suited to SA conditions and high rainfall areas of NSW, but not recommended in WA (French, 2008; Matthews *et al.*, 2014; Ware, 2014).

JenabillupΦ was released in 2007 by the DAFWA. Jenabillup has been used in SA trials for 7 years with a consistently 1% higher yield than Mandelup across all SA sites (Ware, 2014). It has resistance to black pod syndrome which is a problem in cool, higher-rainfall areas of southern WA (Matthews *et al.*, 2014).

WongaΦ is an early flowering, high yielding lupin variety released in 1996 in NSW. It is suited to most areas and remains the best option for lupin growers requiring a high level of resistance to anthracnose (Matthews *et al.*, 2014; Ware, 2014).

Early infection assays only used two *L. angustifolius* cultivars, Gungurru (Wagga Wagga, NSW), and Wonga (Cleanseeds Pty Ltd, Bungendore, NSW and Jamie Tidy of Naracoorte Seeds Pty, Ltd, Naracoorte SA). Subsequent assays added the two cultivars, Jenabillup and Jindalee (Baker Seeds Co., Rutherglen, Victoria). Mandelup cultivar was excluded in the study due to poor germination of seeds after 48 h from sowing. Seeds were surface sterilised following the procedures outlined in Section 2.2.3. Seeds of the Wonga cultivar were planted 3 h ahead of

the other three cultivars because they germinated and grew more slowly and needed at least 46 h to attain a 2.25-2.75 cm root length. The other three cultivars were removed from the vermiculite growth medium and sorted after 43 to 44 h. Germinated seedlings were washed and those with roots 2.25-2.75 cm in length were selected for use in the infection assays.

3.2.4. Root inoculation and sample collection

Based on the results of the infection assays described in Chapter 2, a 10-min inoculation time was adopted. The zoospore suspension level was reduced to 50 ml to make sure that the zoospores were concentrated on the apical region of the roots. Twenty to twenty-four lupin seedlings were arranged randomly and evenly in plastic grids suspended over boxes containing 50 ml sdH_2O, and then transferred to 50 ml zoospore suspension. The seeds of each cultivar were marked with a different colour for identification purposes (Figure 3.1).

Zoospore concentrations ranging from 100-2000 zoospores/ml were used in the assays and samples were collected between 8-72 hpi. The inocula were prepared either by adding the appropriate volume of zoospores to sdH_2O previously placed in each inoculation box or by preparing 500 ml zoospore suspension at the required final concentration in a 1000 ml conical flask and then pouring 50 ml into each inoculation box. After inoculation, a Sharpie marker pen was used to gently mark each root at about 5 mm from the apex, the level of the zoospore suspension. Any negative effects of this procedure were carefully examined but none was observed. The next steps, as described in Sections 2.2.4 and 2.2.5 were followed except that root samples were cut 5-10 mm above the Sharpie pen mark. For the comparison of Gungurru versus Wonga, and Gungurru versus Jenabillup, a total of 100 seedlings were used per cultivar for the six time points examined.

Figure 3.1. Four lupin cultivars with identification marks on the seed coat. Colour coding: pink - Jenabillup, black - Jindalee, green - Wonga, no mark – Gungurru.

3.2.5. Disease development

3.2.5.1. Disease incidence and severity

Disease incidence (DI) was assessed by noting the percentage of roots that displayed visible lesions at each sample time point. Disease incidence is defined as the percentage (0 to 100) of diseased entities within a sampling unit. Incidence is a quantal measure (i.e. a plant is affected or it is not affected) (Seem, 1984). Disease severity (DS) was also estimated for all samples except for the initial assays using Gungurru and Wonga cultivars. Disease severity is defined as the area of plant tissue affected by disease (James, 1974).

Percent disease incidence was computed following the formula:

$$DI = \frac{\text{no. of lupin roots with visible lesions}}{\text{total no. of lupin roots sampled}} \times 100$$

The formula used in computing disease severity was:

$$DS = \frac{n(0) + n(1) + n(3) + n(5) + n(7) + n(9)}{tn}$$

Where: n(0), n(1), n(3), n(5), n(7), and n(9) = number of seedlings showing a reaction of a particular level from a scale of 0, 1, 3, 5, 7, and 9, respectively (see Figure 3.2). tn = total number of seedlings scored

The arbitrary disease scale (Figure 3.2) used in disease severity computation was based with some modification on a scheme devised on the Standard System for the Evaluation of Bean Germplasm (Schoonhoven and Pastor-Corrales, 1987).

The first infection assay with Gungurru and Wonga cultivars using 1000 and 5000 zoospores/ml noted the data on disease incidence only. Succeeding infection assays gathered both disease incidence and disease severity data.

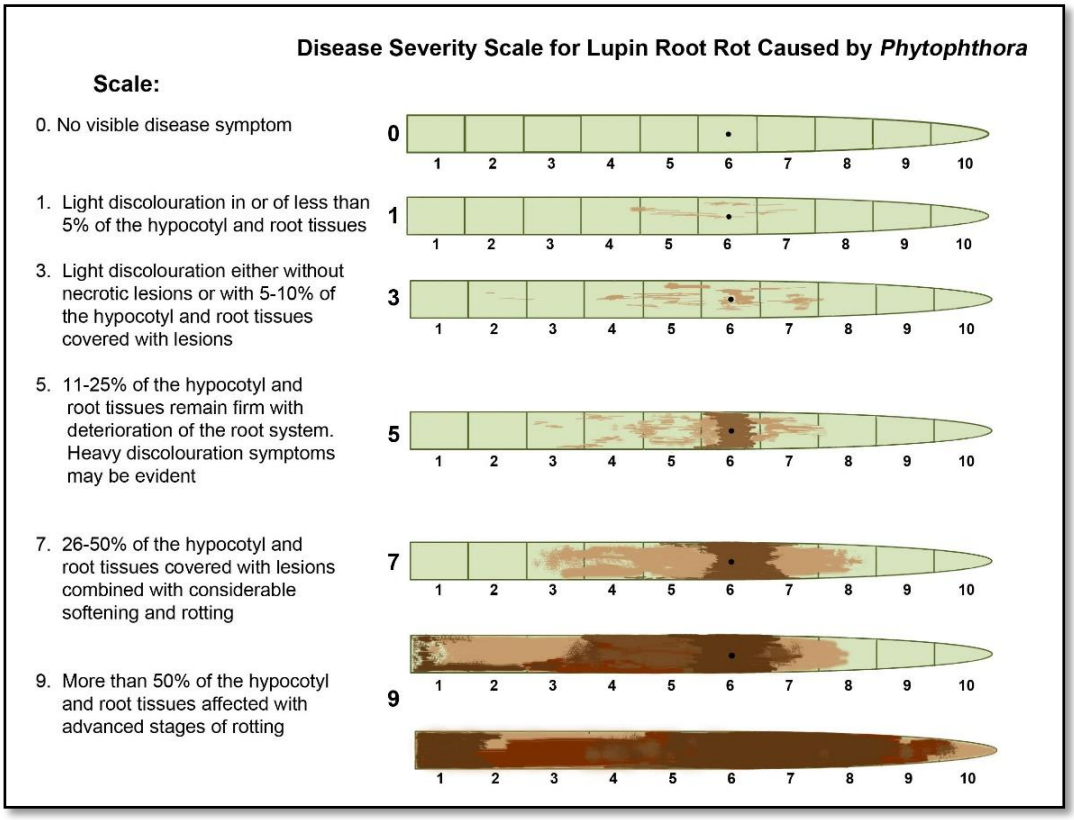

Figure 3.2. Disease severity scale used to assess the extent of disease development of infected lupin roots. Black mark on segment 6 indicates the level of the zoospore suspension during inoculation. Each segment is approximately 5 mm in length.

3.2.5.2. Statistical Analyses

When only one value for disease incidence per treatment (arising from the percentage of the 12 lupin seedlings in one Petri dish that had lesions), a statistical analysis of the disease incidence parameter could not be performed. When seedlings in two or more Petri dishes were assessed (with 24 or more lupin seedlings), statistical analysis was performed. For disease severity, statistical analyses calculating the standard errors of the mean and the significance of differences could be performed since measurement of lesion development was based on individual seedlings in each Petri dish. One-way or two-way analysis of variance (ANOVA) was performed followed by the Bonferroni post-test or

Newman-Keuls Multiple Comparison Test using GraphPad Prism version 5.00 for Windows (GraphPad Software, La Jolla California USA). Where the results were statistically significant, this is indicated on the graphs with asterisks according to the scheme shown in Table 3.1.

Table 3.1. Scheme used to describe levels of statistical significance of the P values (www.graphpad.com).

P value	Wording	Summary
< 0.001	Extremely significant	***
0.001 to 0.01	Very significant	**
0.01 to 0.05	Significant	*
> 0.05	Not significant	ns

3.2.5.3. Root colonisation, haustorium development and callose deposition

Three roots from Gungurru, Jenabillup and Wonga cultivars were inoculated by suspending them in 50 ml of a suspension of 1000 zoospores/ml for 10 minutes as described above. The roots were collected at 24 hpi, 30 hpi and 48 hpi and placed in 100% methanol before processing for microscopic examination using a Zeiss (Germany) Axioplan microscope. For the microscopic examination procedures, see Section 2.2.6.2. A Colonisation Scale (Figure 3.3) was used to estimate the abundance of *P. parasitica* hyphae in lupin tissues. The assessment produced qualitative rather than quantitative data.

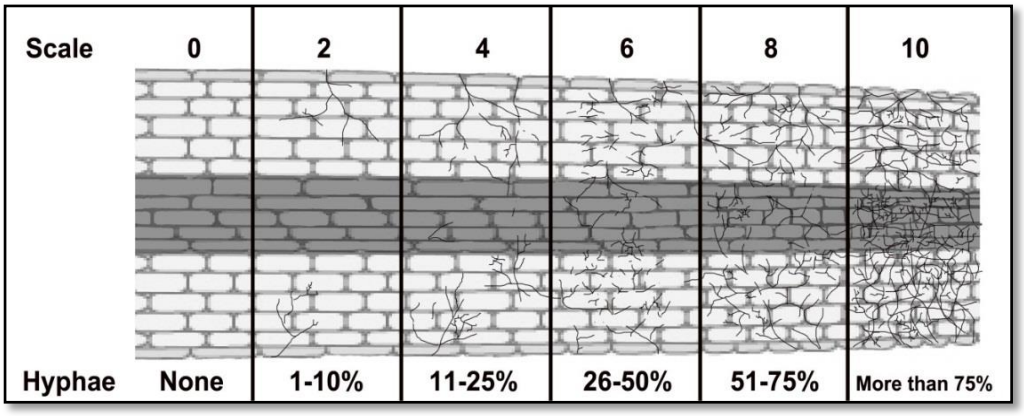

Figure 3.3. Colonisation Scale used to assess the abundance of *P. parasitica* hyphae in lupin roots.

3.2.5.4. Determining pathogen load

See Section 2.2.6.3.

3.3. Results

3.3.1. Time course of lesion development

Gungurru and Wonga

Gungurru and Wonga cultivars inoculated with *P. parasitica* concentrations of 1000 and 5000 zoospores/ml showed visible lesions 24 hpi (Figure 3.4 A & B). When 5000 zoospores/ml was used, Gungurru showed 87% disease incidence compared to Wonga which had 65% at 24 hpi. However, differences were not significant ($P > 0.05$) for either zoospore concentration and any sampling times.

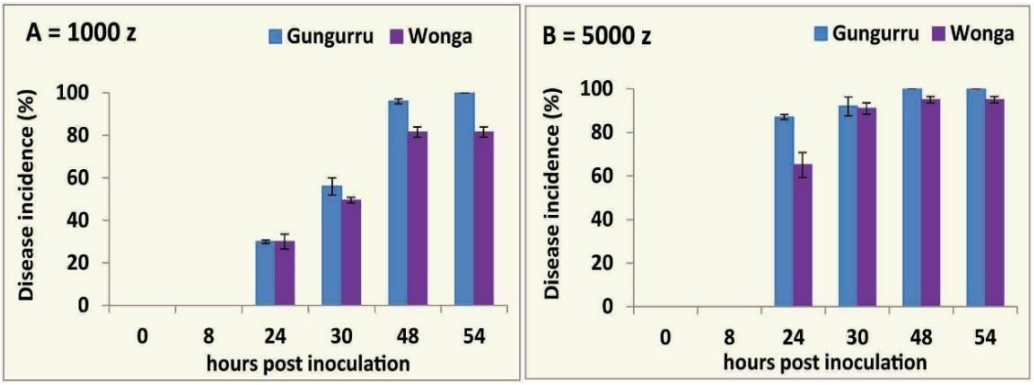

Figure 3.4. Disease incidence: the development of necrotic lesions in lupin roots of Gungurru and Wonga cultivars inoculated with 1000 zoospores/ml (A), and 5000 zoospores/ml (B) in 50 ml of suspension for 10 min. z = zoospores per ml. Error bars represent standard error of the mean (n=24). In no case was the value for Gungurru significantly different to that for Wonga.

More than 50% of the roots were necrotic for both cultivars when inoculated with 1000 zoospores/ml at 24 hpi (Figure 3.5). Wonga showed a lower frequency of disease incidence compared to Gungurru at 24 hpi to 48 hpi but the differences were not statistically ($P > 0.05$) significant at 500 zoospores/ml concentration. At 1000 zoospores/ml concentration, Gungurru showed significantly higher disease incidence at 24 hpi to 30 hpi ($P < 0.01$ and $P < 0.05$, respectively) but not at 48 hpi ($P > 0.05$). Low disease severity was observed at both zoospore concentrations and in both cultivars but the values were not significantly ($P > 0.05$) different at any sampling time.

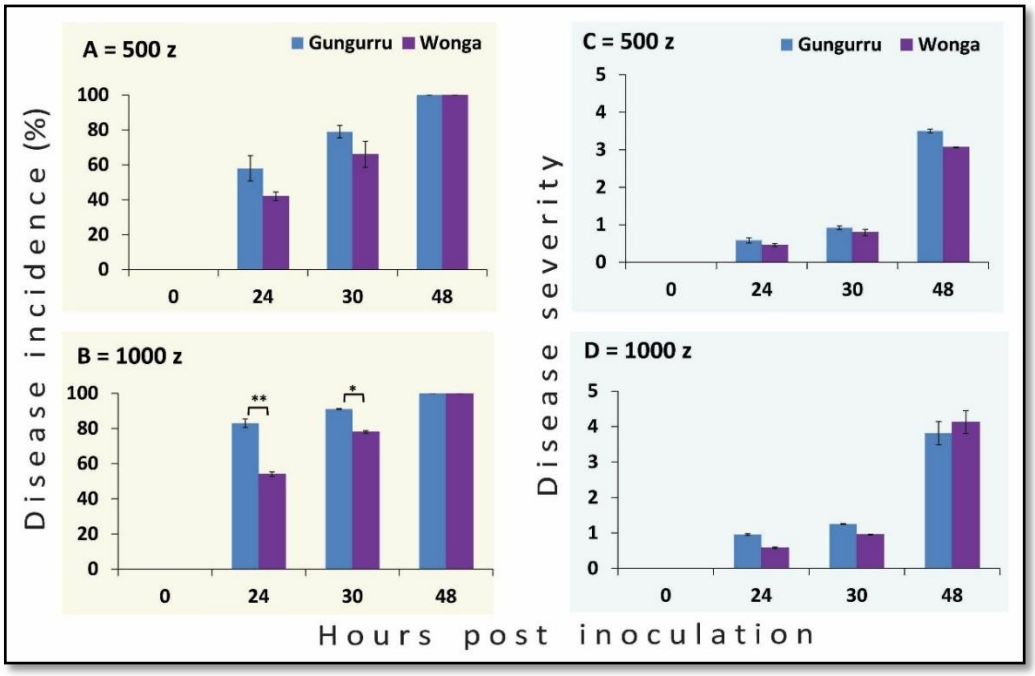

Figure 3.5. Percent disease incidence (A & B) and disease severity (C & D) of Gungurru and Wonga cultivars inoculated with 500 (A & C) and 1000 (B & D) zoospores/ml in 50 ml of suspension for 10 min. z = zoospores per ml. Error bars represent standard errors of the mean (n=24). For disease incidence at 500 zoospores/ml and for disease severity, in no case was the value for Gungurru significantly different to that for Wonga. For disease incidence at 1000 zoospores/ml, asterisks indicate statistically significant differences between pairwise comparisons. *, p = < 0.05; **, p = <0.01.

Four cultivars (Gungurru, Jenabillup, Jindalee and Wonga)

The first infection assay incorporating the four lupin cultivars used zoospore concentrations of 250 and 500 zoospores/ml with one Petri dish of 12 seedlings. Because there was only one value for disease incidence, no statistical analyses were possible but the results (Figure 3.6) indicated that Jenabillup and Wonga cultivars were slower to develop lesions (disease incidence) at 250 zoospores per ml, and that Jenabillup was also slower that the other three cultivars at 500 zoospores per ml. In terms of disease severity, development of disease again appeared to be slower in Jenabillup and Wonga but there were no significant (P>0.05) differences between the four cultivars. By 48 hpi, almost all the roots

displayed necrotic lesions. Infected roots turned brown to dark brown, shrunken and soft.

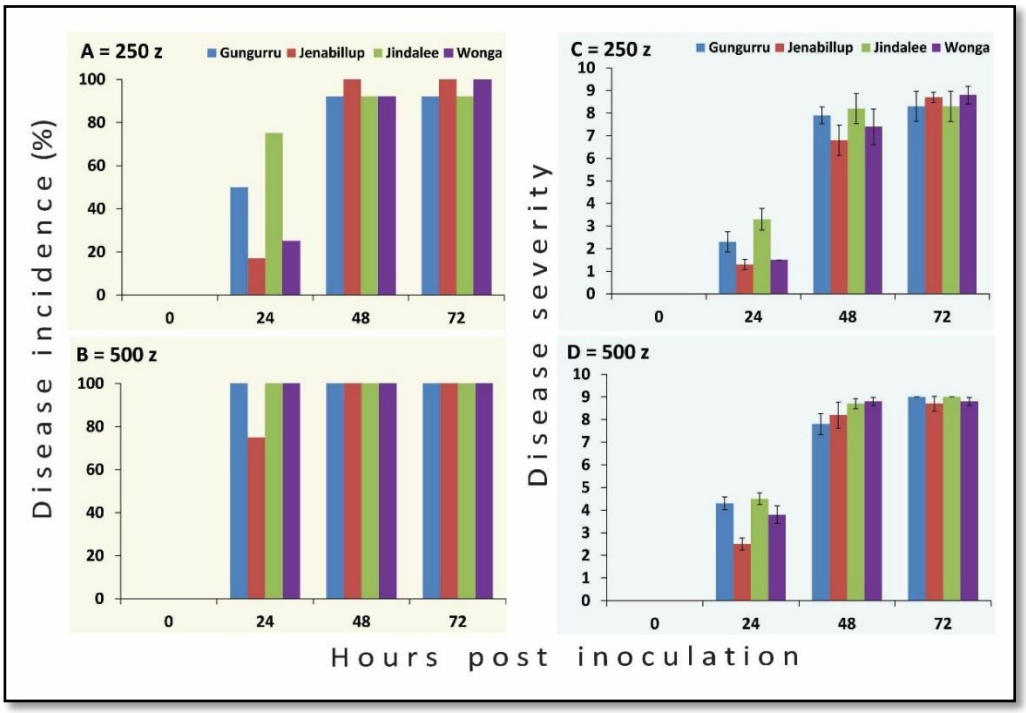

Figure 3.6. Percent disease incidence (A & B) and disease severity (C & D) in the four cultivars inoculated with 250 (A & C) and 500 (B & D) zoospores/ml in 50 ml of suspension for 10 min. z = zoospores per ml. For disease severity, error bars represent standard errors of the mean (n=12). At no time were the values for the four cultivars significantly different.

In the second infection assay, 100 and 250 zoospores/ml were used. Jenabillup and Wonga cultivars again showed slower disease incidence than Jindalee or Gungurru at both zoospore concentrations. Jindalee showed the fastest rate of lesion appearance of the four cultivars (Figure 3.7 A & B). In terms of disease severity (Figure 3.7 C & D), the extent of disease development in Jenabillup was significantly ($P<0.05$) less than that in Jindalee at 24 hpi, in Jindalee and Wonga at 30 hpi, and in Jindalee, Wonga and Gungurru at 48 hpi and 54 hpi. At 72 hpi, no significant difference was observed among the cultivars.

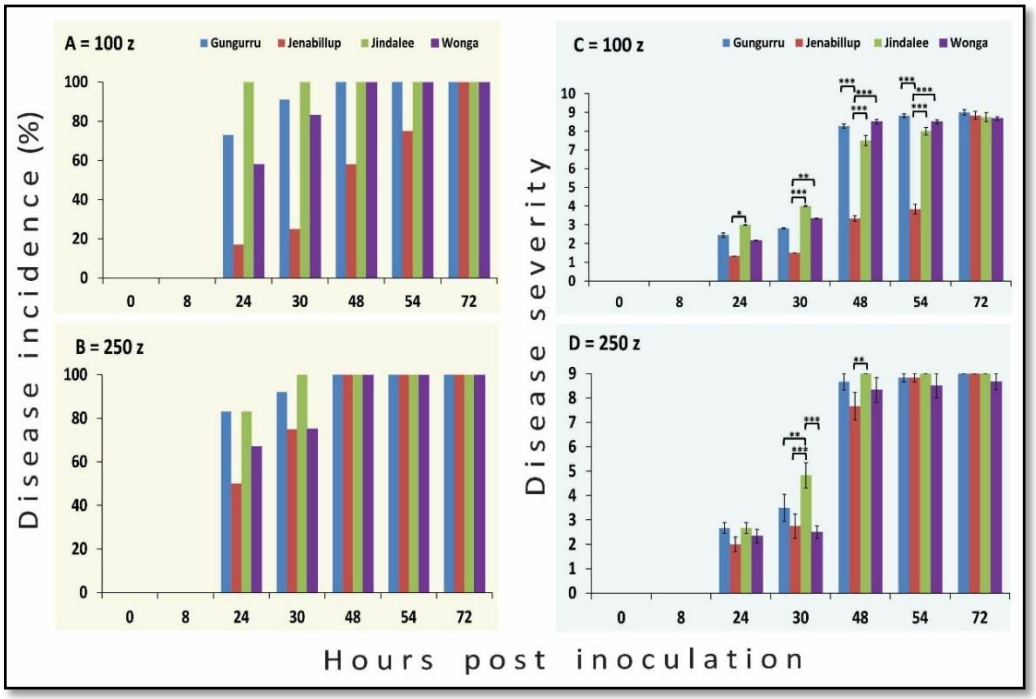

Figure 3.7. Percent disease incidence (A & B) and disease severity (C & D) of the four cultivars inoculated with 100 (A & C) and 250 (B & D) zoospores/ml in 50 ml of suspension for 10 min. z = zoospores per ml. For disease severity, error bars represent standard errors of the mean (n=12). Asterisks indicate statistically significant differences between pairwise comparisons. *, p = 0.01-0.05; **, p = 0.001-0.01; ***, p = <0.001.

Because inoculation with the low concentration of 100 zoospores/ml was sufficient to result in lupin root infection and reveal statistically significant differences in *P. parasitica* disease development in the four cultivars, the assay was repeated using this zoospore concentration. In the experiment, four Petri dishes of 12 seedlings were used, allowing statistical analysis of disease incidence of the four values to be conducted. As in the previous experiment, at 24 hpi and 30 hpi, disease incidence was highest in Jindalee although the difference was only significant compared to Jenabillup at 30 hpi (Figure 3.8). However, in this infection assay, the Wonga cultivar showed the highest disease incidence from 48 hpi to 72 hpi, although the only statistical significance was when compared to Gungurru and Jenabillup at 48 hpi. Again, Jenabillup showed the lowest percent disease incidence at 24 hpi and 30 hpi but this was significant only in comparison with Jindalee at 30 hpi. In terms of disease severity, no

significant difference between cultivars was observed at early time points (8 hpi to 30 hpi) although, as before, disease development appeared to be slower in Jenabillup. The slower rate of symptom development in Jenabillup was significantly different only at 48 hpi and then only in comparison with Wonga. Wonga showed significantly greater severity of disease compared to one or two of the other cultivars at 48 hpi, 54 hpi and 72 hpi.

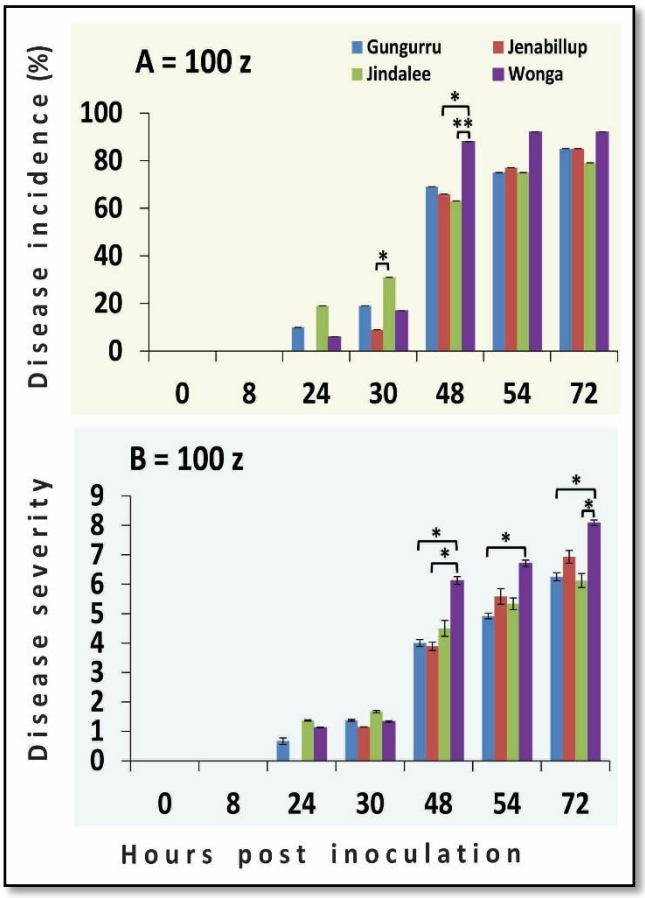

Figure 3.8. Disease incidence and severity in the four lupin cultivars inoculated with 100 zoospores/ml in 50 ml of suspension for 10 min. z = zoospores per ml. Error bars represent standard errors of the mean (n=48). Asterisks indicate statistically significant differences between pairwise comparisons. *, p = 0.01-0.05; **, p = 0.001-0.01.

Because of the limited statistical differences in the parameters measuring disease development in the four cultivars at the low zoospores concentrations (100 or 250 zoospores per ml), the effect of zoospore concentration on infection

was re-examined in an assay using only the Gungurru cultivar. Zoospore concentrations used were 125, 250, 500, 1000, and 2000 zoospores/ml. The results revealed highly significant differences in the rate and extent of disease development depending on the concentration of zoospores in the inoculation suspension (Figure 3.9) (Appendix GraphPad Output 3.1).

A striking difference between the results of this experiment and those of the previous two experiments was the much lower infection rates obtained at the low zoospore concentrations (125 and 250 zoospores/ml) (Appendix GraphPad Output 3.2). In the late time points, values for disease incidence of less than 20% in this experiment compare to values of 80% to 100% in the previous experiments. Values for disease severity of less than 1 in this experiment compare to values between 4 and 9 in the previous experiments.

The second point noted from the results of the assessment of the effect of zoospore concentration was that at 2000 zoospores/ml, 100% of the seedlings had developed lesions by 24 hpi and this result was significantly different from all other treatments. From 48 hpi onwards, the disease incidence values for 1000 and 2000 zoospores/ml were not significantly different. Disease incidence at 500 zoospore/ml was significantly less than at 2000 zoospores/ml throughout the experiment (i.e. 24-72 hpi). The extent of disease development, as measured by the disease severity index, was significantly higher at 1000 and 2000 zoospores/ml than at the three lower zoospore concentrations throughout the experiment. Together the results of this experiment suggested that a concentration of 1000 zoospores/ml would be most suitable for use in the comparison of the three lupin cultivars, Gungurru, Jenabillup, and Wonga, inoculated with *P. parasitica*.

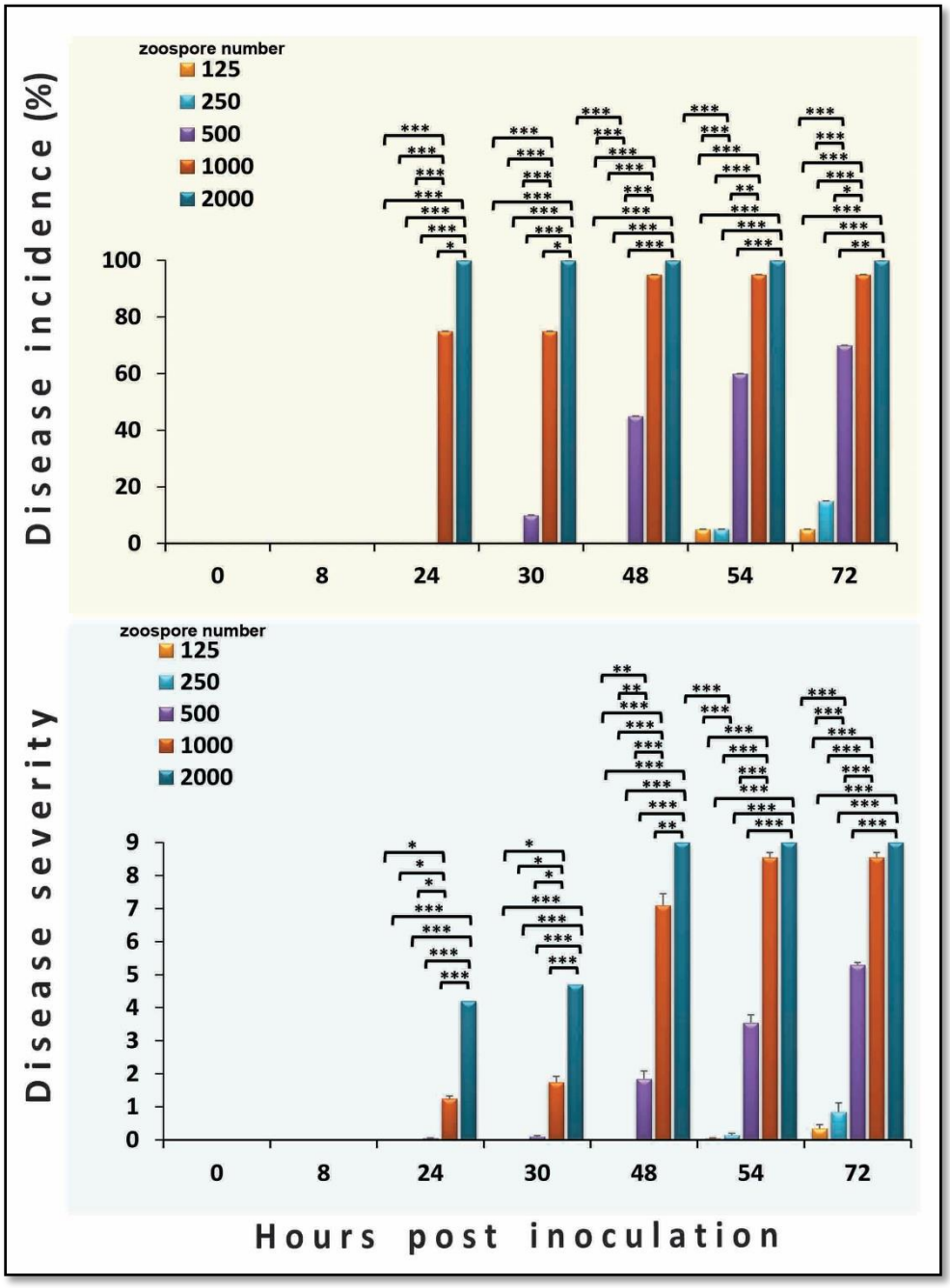

Figure 3.9. Disease incidence and severity in the Gungurru cultivar inoculated with different zoospore concentrations for 10 min. Error bars represent standard errors of the mean (n=24). Asterisks indicate statistically significant differences between pairwise comparisons. *, p = 0.01-0.05; **, p = 0.001-0.01; ***, p = <0.001.

Gungurru versus Wonga

At 12 h after inoculation with 1000 zoospores/ml, lesions were visible on the roots of both Gungurru and Wonga cultivars (Fig. 3.10). At 42 hpi, both cultivars had more than 50% of their root tissues at an advanced stage of rotting. Statistical analysis indicated that disease incidence and symptom severity on the two cultivars over the 60-h time course were not significantly different ($P > 0.05$).

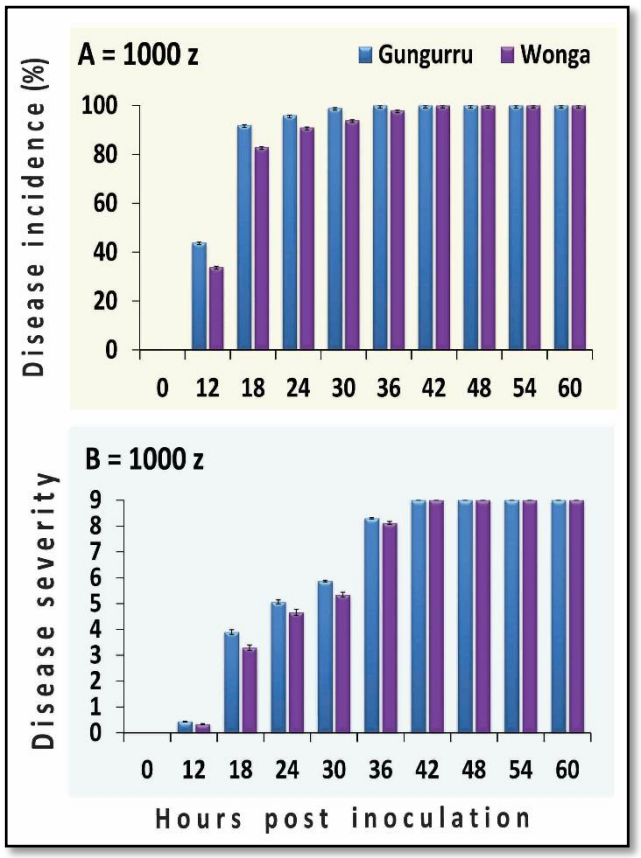

Figure 3.10. Disease incidence (A) and disease severity (B) on Gungurru and Wonga cultivars inoculated with 1000 zoospores/ml for 10 min. z = zoospores per ml. Error bars represent standard errors of the mean (n=100). There were no significant differences between the results for the two cultivars at any time.

Gungurru versus Jenabillup

Visual observations of seedlings in an experiment in which Gungurru and Jenabillup were compared revealed clear differences in the rate of disease development between these two lupin cultivars. Lesions were first visible on

Gungurru at 18 hpi but not on Jenabillup until 24 hpi (Figure 3.11) and the disease incidence and disease severity increased more rapidly in Gungurru than in Jenabillup. Statistical analysis of the results showed that disease incidence in the two cultivars was significantly different at 24 hpi, 30 hpi and 36 hpi (Appendix GraphPad Output 3.3). Disease severity was significantly different at 30 hpi, 36 hpi, 42 hpi and 48 hpi (Appendix GraphPad Output 3.4).

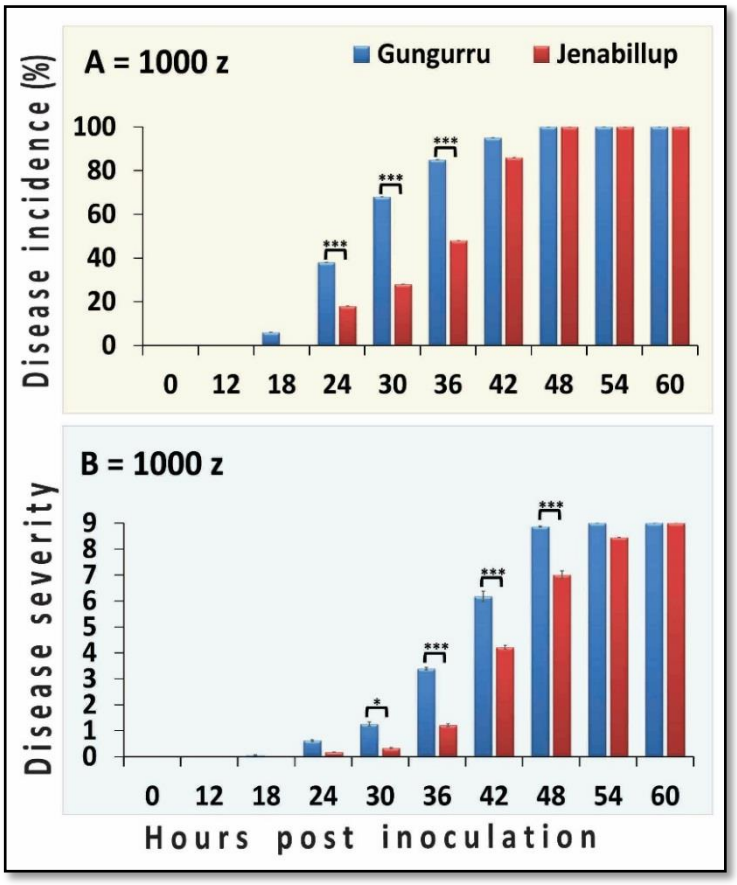

Figure 3.11. Percent disease incidence (A) and severity (B) of lesions on Gungurru and Jenabillup cultivars inoculated with 1000 zoospores/ml for 10 min. z = zoospores per ml. Error bars represent standard errors of the mean (n=100). Asterisks indicate statistically significant differences between pairwise comparisons. *, p = 0.01-0.05; ***, p = <0.001.

3.3.2. Microscopic analysis of the time course of root colonisation by *P. parasitica*

The apical region of infected roots from 5-10 mm above the pen mark to the root tip was collected and cut into three or four segments approximately 5 mm in length. The mark indicated the level of the inoculum surface. The segments were numbered 1 to 4 as shown in the diagram in Table 3.2. A vibratome was used to cut longitudinal sections 150-200 µm in thickness through each root segment. The sections were stained with trypan blue and examined microscopically to determine the distribution of hyphae and haustoria in the root sections. A colonisation score (Figure 3.3) was assigned to each section and an average value calculated from scores for all sections of each segment.

At 24 hpi, *P. parasitica* hyphae had penetrated the root epidermal cells and had begun to grow into the root cortex in the three cultivars, Jenabillup, Gungurru and Wonga, in at least the first segment of the root which includes the location on the root where the zoospores concentrate at the surface of the inoculum suspension (Table 3.2). Only a few hyphae had progressed through the cortical cell layer to reach the vascular bundle.

As indicated by the colonisation scores (see Figure 3.3), at all sampling times, hyphae were more abundant in the first root segment than in segments 2, 3 or 4 (Table 3.2). Examination of the samples suggested that in most cases the hyphae initially grew across the root from the epidermis to the vascular tissue before beginning to grow longitudinally along the root. In the samples collected this meant that, with time, increasing numbers of hyphae were present in segments closer to the root apex. By 48 hpi in all three cultivars, the most apical segment was heavily colonised. In Wonga, this situation was reached at 30 hpi. Haustoria were visible in the cortical cells in segment 1 in both Gungurru and Wonga at 24 hpi but were not observed in Jenabillup until 30 hpi (Figure 3.12). At 30 and 48 hpi, haustoria were observed in all root segments in all three cultivars. In many cases, the haustoria were formed in cortical cells although on rare occasions they were seen within the vascular bundle (Figure 3.12).

Table 3.2. Summary of the mean abundance of hyphae and presence of haustoria in the three cultivars, Gungurru, Jenabillup and Wonga during the first 48 h after inoculation of the root tip with *P. parasitica* zoospores. Microscopic observations were made in three or four segments of the infected lupin roots. The diagram shows the positions of the segments along the root. The dotted outline shows roots cut into three segments. The solid outline shows roots cut into four segments. The values shown for each root segment, sample time and cultivar are the average of values from different sections. (ha) indicates the presence of haustoria.

Cultivar (hpi)					Description
Gungurru					
24 hpi	3 (ha)	2 (ha)	0		Hyphae in the epidermal and cortical cells. Haustoria were observed in cortical cells in the first and second segments.
30 hpi	7 (ha)	6 (ha)	3 (ha)		Most of the hyphae were concentrated in the vascular bundles. Haustoria were observed in all segments.
48 hpi	10 (ha)	10 (ha)	10 (ha)	10 (ha)	Hyphae and haustoria were observed in all segments.
Jenabillup					
24 hpi	1	0	0		Sparse hyphae in epidermal cells and across the root cortex in the first segment only. No haustoria were observed.
30 hpi	3 (ha)	2 (ha)	2 (ha)		Sparse hyphae and haustoria in the root cortex up to the vascular bundle in all segments.
48 hpi	8 (ha)	3 (ha)	8 (ha)		Abundant hyphae and scattered haustoria were observed in all segments.
Wonga					
24 hpi	5 (ha)	2	0		Relatively abundant hyphae with scattered haustoria were observed across the cortical cell layer up to the vascular bundle in first segment. Sparse hyphae present in the second segment.
30 hpi	10 (ha)	10 (ha)	10 (ha)		Most of the hyphae were concentrated in the vascular bundle in all segments.
48 hpi	10 (ha)	9 (ha)	10 (ha)		Hyphae and haustoria were observed in all segments.

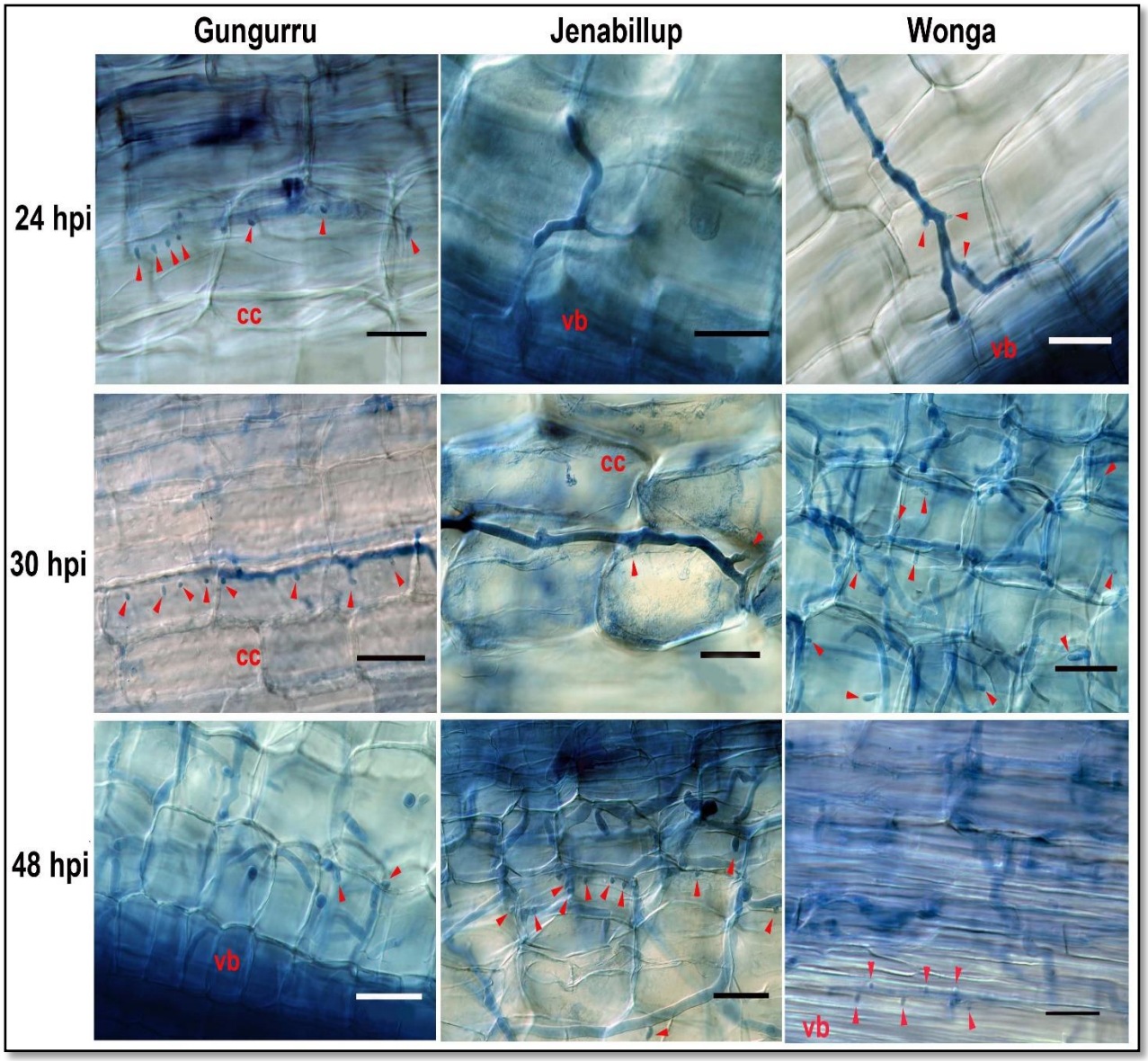

Figure 3.12. *P. parasitica* hyphae and haustoria in lupin roots stained with lactophenol trypan blue at 24, 30 and 48 hpi. Haustoria (red arrowheads), cortical cells (cc), and vascular bundle (vb). Bar represents 40 µm.

3.3.3. Microscopic examination of callose deposition

Cultivars Gungurru and Wonga were examined for signs of callose deposition during the infection time course. As described in Section 2.3.4, aniline blue stained *P. parasitica* hyphal cross-walls. However, in these samples aniline blue fluorescence was also observed around some haustoria (Figure 3.13).

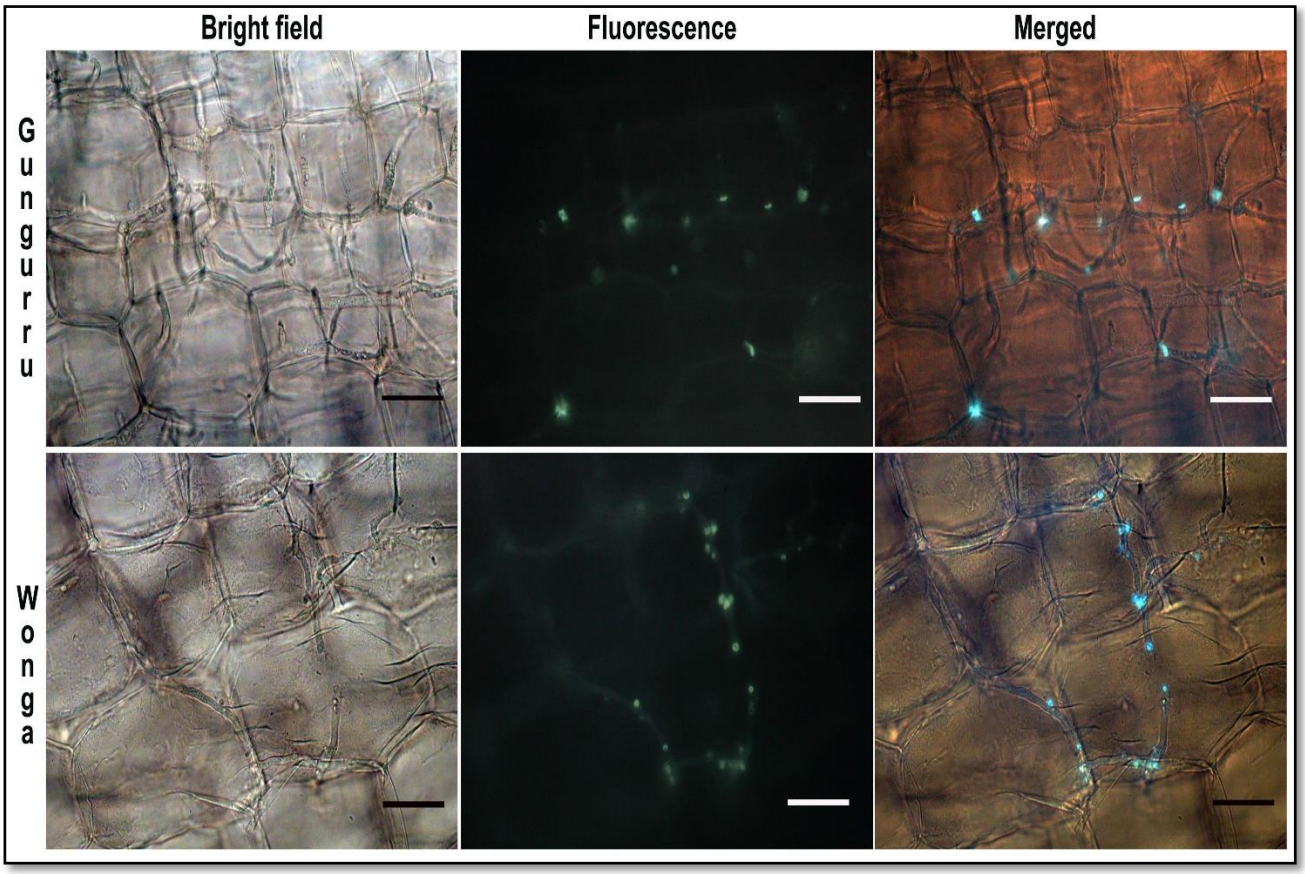

Figure 3.13. Bright field and fluorescence images of vibratome sections of lupin roots infected by *P. parasitica*. Fluorescence due to aniline blue is seen at the sites of hyphal cross-walls (red arrowheads) and haustoria (green arrowheads). Gungurru cultivar: 48 hpi; Wonga cultivar: 30 hpi). Bar represents 40 µm.

3.3.4. qPCR quantification of *P. parasitica* development in three lupin cultivars

The ratio of *P. parasitica* DNA to lupin DNA was quantitatively assessed during the infection of Gungurru, Jenabillup and Wonga lupin cultivars. The target genes were *P. parasitica WS41* and *L. angustifolius LaNIT4A* as described in Section

2.3.5. The *P. parasitica WS41* gene was first detected at 12 hpi, 24 hpi and 30 hpi in Jenabillup, Wonga and Gungurru, respectively. The highest ratio of *WS41:LaNIT4A* genes occurred at 42 hpi, 48 hpi and 54 hpi in Wonga, Jenabillup and Gungurru, respectively. However, the differences in the ratio of pathogen to plant DNA were generally not significantly different when comparing values during the later stages of infection (i.e. 42 -60 hpi) (Figure 3.14). Pairwise comparison between the three cultivars showed no difference of the ratio of *WS41:LaNIT4A* genes at the early time points from 12 to 36 hpi, however, from 42 to 60 hpi, significant differences were present between the three cultivars (Figure 3.14). These results indicated that the ratio of *P. parasitica* to lupin DNA in Jenabillup was significantly higher than that in Gungurru and Wonga at 48 hpi, 54 hpi and 60 hpi.

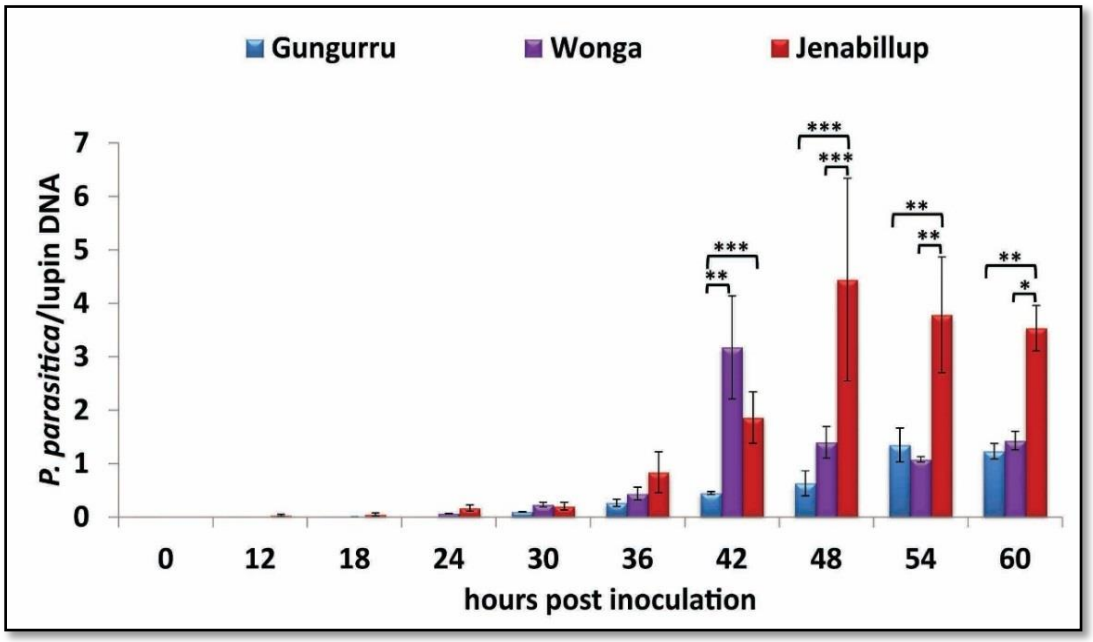

Figure 3.14. Summary of the ratio of *P. parasitica* to lupin DNA in the three lupin cultivars, Gungurru (A), Jenabillup (B), and Wonga (C). Error bars represent standard errors of the mean (n=3). Asterisks indicate statistically significant differences between pairwise comparisons. *, p = 0.01-0.05; **, p = 0.001-0.01; ***, p = <0.001.

3.4. Discussion

3.4.1. Reaction of lupin cultivars to *Phytophthora* infection

One of the most important factors to consider when choosing a cultivar of a crop species to plant at a given location, in addition to its performance under the local environmental conditions and the quality and quantity of its yield, is its resistance to potential pathogens (Brown and Caligari, 2008). After the introduction of lupins in agriculture in Australia, over 23 different cultivars had been tested by 2008 but only eight of the 23 cultivars were still recommended for use (French, 2008). In general, the main reason for the discontinuation of a cultivar centred on its susceptibility to certain pests or diseases (French, 2008). Of the four lupin cultivars used in this study, Jenabillup, Jindalee, and Wonga are among the eight cultivars still recommended for planting in Australia (Table 3.3) (French, 2008). The fourth cultivar, Gungurru, one of the earliest lupin cultivars released in Australia, is no longer deemed suitable (French, 2008).

Widespread infection of lupin crops in NSW by an unidentified species of *Phytophthora* was first observed in 1993 (Nikandrow *et al.*, 2001) and in 2013, PRR of lupins was listed as one of the diseases of pulse crops in the Southern region of NSW. In 2013, wet winter conditions in July and August favoured *Phytophthora* infection in some districts, especially in low-lying paddocks or paddocks with a hardpan that promoted waterlogging (Lindbeck *et al.*, 2014). It has been shown that *Phytophthora* species only require a short period of waterlogging (8 h) to successfully infect lupin roots (Lindbeck *et al.*, 2014) but overall the information on *Phytophthora* infections of lupins in the field in Australia is limited. It is clear that further studies of *Phytophthora* infection of lupins are needed. It will be important to identify which *Phytophthora* species is/are responsible for PRR of lupins in Australia and to determine the level of resistance or susceptibility of lupin cultivars to the range of fungal and Oomycete diseases potentially present in lupin growing regions. For this, a robust and reliable screening assay is needed and the development of one such assay was an aim of the work described in this chapter.

Lupins have been used for baiting of *Phytophthora* species from infected plant and soil samples for over 50 years (e.g. Chee and Newhook, 1965; Greenhalgh, 1978). While predominantly used in the isolation of *P. cinnamomi*, studies have also shown the infection of lupin seedlings by other *Phytophthora* species, including *P. parasitica* (e.g. Pratt and Heather, 1972; Hargreaves and Duncan, 1978). The results obtained in the present study indicate that all four lupin cultivars tested are susceptible to *P. parasitica* even when the zoospore concentration is low (i.e. 100 zoospores/ml) and exposure short (i.e. only 10 minutes in duration).

As is typically the case for most, if not all, plants, an individual lupin cultivar may be resistant to some diseases but susceptible to others (Table 3.4). In Australia, no single lupin cultivar shows resistance to all the diseases that pose a threat to the lupin industry. The Australian *L. angustifolius* cv Wonga has been found to have a high level of tolerance to anthracnose disease (Tivoli *et al.*, 2006; Buirchell, 2008) and remains the best option presently available to SA growers who want high levels of anthracnose resistance (Jeisman, 2014). However, the Wonga cultivar was severely infected by an unidentified species of *Phytophthora* (DAR 75401) in a field trial at Temora, NSW in 1999 and since then similar infections in lupin cv Wonga crops have been observed across southern NSW (Nikandrow *et al.*, 2001). My assays indicate that, even at low inoculum concentrations, this cultivar is rapidly infected by *P. parasitica*. Together, these results suggest that the Wonga cultivar should not be used in areas likely to be infested with *Phytophthora*.

Identification of the species of *Phytophthora* causing root rot disease of lupin in NSW will be an important contribution to the Australian lupin industry. Based on morphological characteristics, the isolate taken from infected lupin fields in NSW had some features of sporangia, oogonia, oospores and antheridia in common with *P. vignae*, *P. erythroseptica* and *P. megasperma* but the differences to these and other *Phytophthora* species were sufficient to suggest that the NSW isolate may not be a well-known species (Nikandrow *et al.*, 2001). In Spain, a similar disease on lupin was caused by *P. erythroseptica* (Trapero-Casas *et al.*, 2000) and in Italy and the USA, lupin root rot has been reported to be associated

with *P. parasitica* (Erwin and Ribeiro, 1996). Because examination of the morphological characteristics of the NSW isolate have not led to a conclusive identification, it may be useful to employ antibody (e.g. Gabor *et al*., 1993; Gautam *et al*., 1999) or DNA-based diagnostic assays (e.g. Bilodeau *et al.,* 2014) to determine what *Phytophthora* species is/are causing the problem.

As discussed in the previous chapter, for a laboratory-based plant disease assay to be of value and widely applicable, it is important that the assay employs a level of inoculum that is similar to that typical found in field situations (Hinch *et al.*, 1985; Dolan *et al.*, 1986; Handelsman *et al.*, 1991; Van Jaarsveld *et al.*, 2003; Galiana *et al.*, 2008; Wang *et al.*, 2011; Allardyce *et al.*, 2012; Hosseini *et al.*, 2012; McCorkle *et al.*, 2013). To address this goal, a range of zoospore concentrations was used in the infection assays for the four lupin cultivars selected for assessment in the current study. The aim was to determine (i) the lowest zoospore concentration that reliably resulted in the establishment of disease during the 60-h time course of the infection assay and (ii) a zoospore concentration that was suitable for revealing differences in the susceptibility or resistance of the four lupin cultivars to *P. parasitica* infection. Inoculation time and total inoculum volume used in the assays were kept constant. While initial experiments suggested that zoospore concentrations as low 100-250 zoospores/ml led to high levels of infection by 48 hpi in the four cultivars, it became apparent that the reproducibility of the assays was not good at these low zoospore concentrations. Re-assessment of the effect of different zoospore concentrations in the inoculum using the Gungurru cultivar clearly showed that the speed and/or severity of disease development correlated directly with the concentration of spores used during the inoculation. A similar effect has been reported previously from studies of soybean, tobacco and safflower (Eye *et al.*, 1978; Kannwischer and Mitchell, 1981; Singh and Chand, 1982). My results indicated that a concentration of 1000-2000 *P. parasitica* zoospores/ml was the most suitable level of inoculum in the assay I developed. It is necessary, of course, to be aware that when inoculating with low concentrations of inoculum, susceptible cultivars may fail to produce disease symptoms and that when the

inoculum level is increased, even resistant cultivars may produce a susceptible response to the pathogen being tested (Eye *et al.*, 1978).

Nevertheless, one of the key outcomes of the current study was that the inoculum levels used allowed differences in the rate of infection of the four cultivars to be distinguished. The Jenabillup cultivar consistently showed a statistically significant slower rate of disease development than Gungurru or Wonga cultivars. The Jenabillup cultivar has been previously selected for its resistance to black pod syndrome (French, 2008) caused by bean yellow mosaic virus (Kehoe *et al.*, 2014) but extrapolating from the current study, it may be that this cultivar also has better resistance or tolerance to *Phytophthora* diseases. It would be of value to determine in future research if this characteristic of the Jenabillup cultivar when inoculated with *P. parasitica* also applies to other *Phytophthora* and *Pythium* species.

Table 3.3. Agronomic features of narrow-leafed lupin cultivars (except cv Gungurru) still recommended for planting in Australia (sources: www.grdc.com.au, www.seednet.com.au, and www.dpi.nsw.gov.au)

Cultivar	Year of release	Flowering	Height	Early vigour	Lodging	Pod loss shatter-ring	Seed alkaloids	Seed colour	Seed size	Protein content
*Gungurru	1988	early	short	medium	MR	R	low	brown	medium	medium
*Jenabillup℗	2007	early	medium	medium	MR-MS	MR#	low	light brown	medium-large	medium
*Jindalee℗	2000	late	tall	medium	MR	R	medium	brown	medium-large	medium
Mandelup℗	2004	very early	tall	fast	MS	MR	low-medium	brown	medium-large	medium
PBA Barlock℗	2013	mid	medium	medium	MR	R	low-medium	brown	medium	medium
PBA Gunyidi℗	2011	early	medium	fast	MR-MS	R	low-medium	light brown	medium	medium
*Wonga℗	1996	early	medium	medium	MR-MS	MS	low	brown	medium	medium

R= Resistant; MR= Moderately Resistant; MS= Moderately Susceptible; S= Susceptible; VS= Very Susceptible; #= Limited observations; * = Cultivars used in the study; ℗ =Plant Breeder's Rights

Table 3.4. Disease and stress symptoms of narrow-leafed lupin cultivars (sources: www.grdc.com.au, www.seednet.com.au, and www.dpi.nsw.gov.au)

Cultivar	Grey leaf spot	Brown leaf spot	Pleiochaeta root rot	Anthracnose	CMV seed	Phomopsis on stem	BYMV	Drought tolerance	Premature wilting
*Gungurru	MS-MR	MS	S	MS	MS	MR	-	S	MR
*Jenabillup[Φ]	R	MR	R	MS	MR	MS-MR	MR	R	-
*Jindalee[Φ]	R	MR	MR	MS	MS	R	-	MS	MR
Mandelup[Φ]	R	MS	R	MR	MR	MR-R	MS	-	-
PBA Barlock[Φ]	R	MS	R	R	MR-R	MR	MS	-	-
PBA Gunyidi[Φ]	S	MS	R	MR-R	MR-R	R	MS-MR	-	-
*Wonga[Φ]	MS	MS-MR	S	R	R	MR	MS	MS	MR

R= Resistant; MR= Moderately Resistant; MS= Moderately Susceptible; S= Susceptible; VS= Very Susceptible; CMV= Cucumber Mosaic Virus; - = No information; * = Cultivars used in the study; Φ =Plant Breeder's Rights

3.4.2. Pathogen colonisation and symptom development in lupin cultivars

The results from macroscopic observations of disease incidence and severity in the lupin cultivars tested in this study showed that the Jenabillup cultivar displayed a slower rate of disease development compared to Gungurru and Wonga cultivars. Microscopic examination of the distribution of pathogen cells in the lupin roots also showed that at early times post inoculation, there were fewer *P. parasitica* hyphae in the epidermal cells, and hyphae invaded the root cortex more slowly in Jenabillup compared to Gungurru and Wonga cultivars. As discussed above, these results suggested that Jenabillup was more resistant to *P. parasitica* than Gungurru or Wonga cultivars, although by 48 hpi the differences in disease incidence or severity were not statistically significant and differences in the extent of root colonisation in the three cultivars were also not apparent.

It was thus surprising to find that the ratio of *P. parasitica* to lupin DNA in the Jenabillup cultivar at 48-60 hpi was significantly higher than in the apparently more susceptible cultivars, Gungurru and Wonga. In general, measurement of the amount of pathogen DNA relative to plant DNA by qPCR shows a correlation with visual assessments of disease symptoms, with both criteria reflecting the extent of tissue colonisation by the pathogen (Knight *et al.*, 2012; Engelbrecht *et al.*, 2013). However, the results of the qPCR assays in the current study showed that this was not the case when comparing the three lupin cultivars, Gungurru, Wonga and Jenabillup. A lack of correlation between disease symptoms and pathogen growth has also been described during the interaction of tomato and virulent *Xanthomonas campestris* pv *vesicatoria* (*Xcv*) (Block *et al.*, 2005). During this plant-bacterial interaction, so-called systemic acquired tolerance (SAT) led to reduced tissue damage in response to the virulent race of *Xcv* but with no effect on the pathogen growth. SAT is associated with rapid pathogenesis-related gene expression that leads to suppressed symptom development (Block *et al.*, 2005).

3.4.3. Localisation of β-1,3-glucans during lupin root infection by *P. parasitica*

In the current study, the two cultivars Gungurru and Wonga were stained with aniline blue to investigate potential differences in callose deposition as part of a defence response during *P. parasitica* infection. Yellow-green fluorescence indicative of reaction of aniline blue with β-1,3-glucans, including callose, was observed around haustoria and in hyphal cross-walls in both Gungurru and Wonga samples. Fluorescence of haustoria was more prominent in Wonga than in Gungurru cultivar. Callose is a an abundant component of cell wall appositions that are formed by plant cells in response to attempted penetration by fungal and Oomycete hyphae (Underwood, 2012). They are usually formed more rapidly and frequently in non-host or resistant plants than in susceptible plants. Often in susceptible plants, the callosic wall appositions are found as a collar at the base of the haustoria (Hohl and Suter, 1976). Callose deposition in wall appositions around haustoria has also been reported in potato infected by *P. infestans* and in soybean infected by *P. sojae* (Enkerli *et al.*, 1997a; Bozkurt *et al.*, 2011).

3.4.4. Laboratory-based assays compared to field results

Testing of a large number of candidate cultivars for identification of sources of disease resistance under field conditions may be difficult because of the costs and risks associated with field trials. *In vitro* screening for disease resistance is preferred because it is rapid, effective and has in many instances been shown to be a good alternative to field tests (Utkhede, 1986; Vleeshouwers *et al.*, 1999). Many plant species have been evaluated for their resistance or susceptibility to *Phytophthora* species using controlled, laboratory conditions. A high correlation between laboratory and field results has been observed. These studies include experiments on *P. megasperma* f. sp. *glycinea* in soybeans (Irwin and Langdon, 1982), *P. infestans* on potato (Vleeshouwers *et al*., 1999), *P. colocasiae* on taro (Brooks, 2008), and *P cactorum* on apple (Utkhede, 1986).

Laboratory-based infection assays have been used to screen lupin species and cultivars against a number of prominent necrotrophic diseases such as

anthracnose, Phomopsis blight and brown spot (Williamson *et al.*, 1991; Yang *et al.*, 1996; Yang and Sweetingham, 1998). However, although lupin plants have been used as bait material for *Phytophthora* species (Pratt *et al.*, 1973; Blowes *et al.*, 1982; Reid, 2006), to the best of my knowledge there has been no report of the development or use of a systematic laboratory-based infection assay to screen lupin cultivars against *Phytophthora* species. The infection assay developed in the current study can be used to assess relative levels of resistance (or tolerance) of lupin species and cultivars to different species of *Phytophthora* in laboratory conditions. Its application in the assessment of the vulnerability of lupins to soil-borne diseases could make an important contribution to the lupin industry in Australia. It should, for example, allow the determination of whether or not field resistance exhibited by newly released lupin cultivars, such as PBA Barlock$^{\Phi}$ and Jenabillup$^{\Phi}$, is specific to a certain species of *Phytophthora*. The results of this study may influence future strategies adopted for breeding lupin for resistance to *Phytophthora* root rot disease in Australia.

As in other screening techniques, successful development and application of the *P. parasitica*-lupin infection assay depends on careful consideration and control of several parameters. The following are suggested refinements associated with some parameters that may help attain a reproducible and sensitive laboratory-based assay.

Age of the plant. Different lupin cultivars may have different germination times. For example, the Wonga cultivar needs to be planted 3 h ahead of Jindalee, Jenabillup and Gungurru cultivars to obtain seedlings with uniform root lengths. However, seed storage time also influences germination rate. For example, old Gungurru seeds germinate more slowly and a 1-h time difference in sowing time between Gungurru and Wonga cultivars is enough.

Inoculum concentration. In this study, the zoospore concentration of 1000/ml in 50 ml of water constituted a good inoculum with which to infect the lupin roots. This concentration and total volume was equivalent to an average of approximately 200 spores per root and closely resembled inoculum levels

typically occurring in the natural environment (Kellam and Coffey, 1985; Goodwin *et al.*, 1990). It is important to determine the appropriate inoculum concentration because susceptible cultivars may fail to produce symptoms at low inoculum concentration while resistant cultivars may be susceptible if too high inoculum concentration is used (Eye *et al.*, 1978).

In a laboratory test to determine the relative levels of resistance of soybeans to *P. megasperma* f. sp. *glycinea*, it was found that both seedling age and inoculum concentration had profound effects on the level of resistance observed. These parameters must be carefully controlled to allow expression of resistance or susceptibility of the test plants to correlate with that observed in field conditions (Irwin and Langdon, 1982).

Sampling time. Appropriate selection of time intervals for sampling will let the researcher observe the gradual reaction of the host plant towards the pathogen both macroscopically and microscopically.

Number of replicates. Expression of disease symptom varies from plant to plant even when the utmost care is employed to keep all parameters and procedures as consistent as possible. Thus, sufficient number of replicates must be used to allow potential differences in of levels of resistance or susceptibility between species and cultivars to be statistically significant (Tivoli *et al.*, 2006).

Maintaining moisture during and after inoculation. Seedlings collected from their germination medium must be kept in moist conditions, for example, by covering with moistened paper towels. After inoculation, filter paper on which the seedlings are placed must be kept saturated throughout the experiment. Most pathogens need adequate moisture to grow, survive and reproduce. The laboratory assay for *P. infestans* resistance in various potato species showed that detached leaves incubated in covered trays at high relative humidity were more susceptible than detached leaves kept in open trays or leaves on intact plants (Vleeshouwers *et al.*, 1999). The incubation conditions rather than detachment itself appeared to influence the resistance expression. These limitations should

be considered when deciding on the appropriate incubation method (Vleeshouwers *et al.*, 1999).

3.4.5. Concluding Remarks

The Australian lupin breeding program began more than 40 years ago. A breeding program jointly funded by Grains Research & Development Corporation (GRDC) and the DAFWA has produced a number of new narrow-leaf lupin varieties with improved yield and enhanced resistance to pest and diseases over previously available varieties (http://www.grdc.com.au). However, there remains a great deal of research to be done to fully understand PRR of lupins. The species of *Phytophthora* causing this disease remains to be identified (Lindbeck and Nikandrow, 2002). It is important that whenever possible, pathogens that are present are identified correctly to allow appropriate management to take place before sowing the next lupin crop. Above ground symptoms such as poor emergence, uneven and stunted growth, yellowing of plants and wilting or death under water stress, particularly at flowering and grain fill, can indicate the presence of root disorders. However, these above ground symptoms are rarely diagnostic as many biotic and abiotic disorders will have similar above ground expression (Thomas *et al.*, 2010).

After establishing and testing the model infection assay for *P. parasitica* disease on lupin roots and observing changes at a macroscopic level, the next goal of the study was to investigate molecular and cellular aspects of the infection process. To do this, data on the expression of a selection of putative pathogenicity genes during the first 60 h of disease development were obtained. The analysis focused on the expression of *P. parasitica* genes encoding CWDEs, key factors in plant infection.

CHAPTER 4

Expression of *P. parasitica* cell wall degrading enzymes during infection of lupin roots

4.1. Introduction

4.1.1 The structure of the plant cell wall

Plant cell walls are complicated macromolecular structures that enclose and protect the cell, and they are essential components of defence against pathogens. Plant cell walls are composed of carbohydrates, proteins and aromatic compounds (Caffall and Mohnen, 2009). There are two types of cell walls in vascular plants, the primary wall and the secondary wall (Bringmann *et al.*, 2012). The primary cell wall is formed during cell division and consists of cellulose microfibrils (9-25%) crosslinked to hemicelluloses (25-50%) and embedded in a matrix of pectins (10-35%); proteins (10%) are also present (Carpita and Gibeaut, 1993; Reiter, 2002) (Figure 4.1). Cellulose microfibrils regulate the direction of cell expansion and help maintain cell shape (Bringmann *et al.*, 2012). Secondary cell walls are deposited after cell growth has ceased on the inside of the primary cell wall and confer mechanical stability to specialised cell types such as xylem elements and sclerenchyma cells. These latter walls typically contain cellulose (35-50%) and hemicellulose (20-50%) embedded in lignin (7-20%) with small amounts of pectin and proteins (Pauly and Keegstra, 2008; Vogel, 2008). The plant cell wall is a dynamic structure which varies according to tissue type and developmental stage (Somerville *et al.*, 2004).

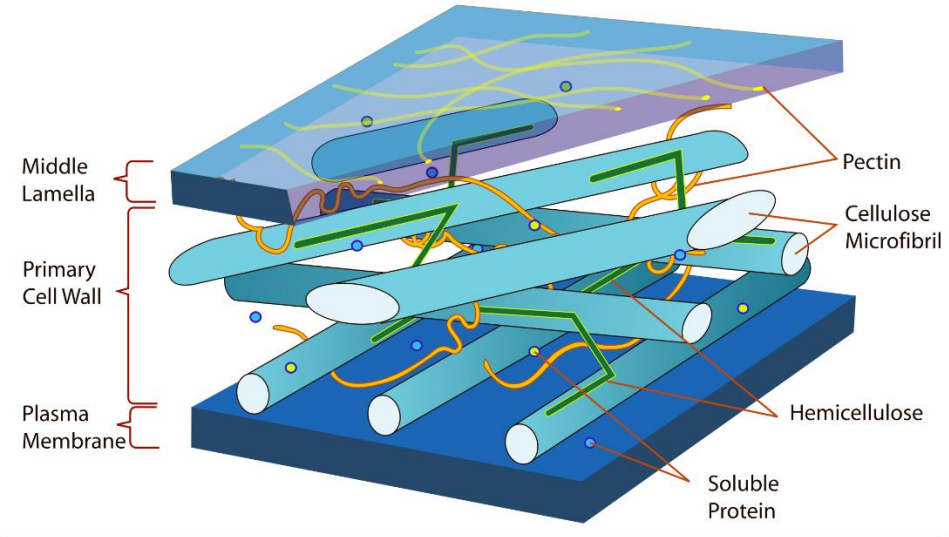

Figure 4.1. A diagram of a plant cell wall showing the three main groups of polysaccharides: cellulose, hemicellulose and pectins, as well as soluble proteins (from Carpita and Gibeaut, 1993).

4.1.2. Plant cell wall components

4.1.2.1. Cellulose

Cellulose consists of long chains of β-1,4-linked-D-glucose residues that assemble into paracrystalline microfibrils (O'Sullivan, 1997; Reiter, 2002; Brouwer *et al.*, 2014). Cellulose microfibrils are synthesised on the plasma membrane by rosettes of cellulose synthase (CesA) enzymes that (Reiter, 2002; Caffall and Mohnen, 2009).

4.1.2.2. Hemicellulose

Hemicellulose molecules are complicated structures which have backbone chains consisting of β-1,4-linked pyranosyl residues (D-glucose, D-xylose and D-mannose) and many side chains often containing D-xylose, D-galactose, L-fructose, L-arabinose and D-glucuronic acid residues (Sun *et al.*, 2012 ; Brouwer *et al.*, 2014). The hemicelluloses that contain these side branches are xyloglucans, glucuronoxylans, glucuronoarabinoxylanss, galactomannans and galactoglucomannans, respectively (Somerville *et al.*, 2004; Scheller and Ulvskov,

2010) . Residues within the backbone and side chains can be modified by methyl and acetyl esterification, and the addition of ferulic acid residues (Somerville *et al.*, 2004; Scheller and Ulvskov, 2010; Gille and Pauly, 2012). Xylans constitute a major hemicellulosic component of monocot plant walls and a minor component of dicot walls (Varner and Lin, 1989). Xylan consists of linear chains of β-1,4-D-xylose residues and can be found as arabinoxylan, glucuronoarabinoxylan, glucuronoxylan or unsubstituted xylan (Caffall and Mohnen, 2009). Xyloglucan is a neutral polysaccharide that possess a cellulose-like backbone, but differs from cellulose in that 60-75% of the glucose residues carry α-xylose and bear short side-chains (Fry, 1989; Popper and Fry, 2008). Bonding of hemicelluloses to cellulose increases cell wall strength (Cosgrove, 2005; Scheller and Ulvskov, 2010). They also link to pectin molecules providing further complexity (Cosgrove, 2005; Caffall and Mohnen, 2009).

4.1.2.3. Pectins

Pectins are cell wall polysaccharides that are most prominent in the middle lamella (Prade *et al.*, 1999; Caffall and Mohnen, 2009; Brouwer *et al.*, 2014). The three major structural classes of pectins are homogalacturonan (HG), rhamnogalacturonan I (RGI), and rhamnogalacturonan II (RGII) (Ridley *et al.*, 2001). HG is a polymer of α-1,4-linked-D-galacturonic acid and is believed to affect the adhesion and integrity of tissues (Prade *et al.*, 1999; Lionetti *et al.*, 2012). HG is an essential source of biologically active oligogalacturonides that function as signalling molecules in plant development and defence (Willats *et al.*, 1999; Willats *et al.*, 2001). Oligogalacturonides act as endogenous elicitors which inducer the expression of various genes including those encoding pathogenesis-related proteins, proteinase inhibitors and enzymes involved in phytoalexin production (Bowles, 1990). Carbons in HG galacturonic acid residues can also be methyl esterified and the acetylation of oxygen in both HG and RGI can also occur (Ridley *et al.*, 2001; Somerville *et al.*, 2004; Caffall and Mohnen, 2009). RGI has a backbone of alternating galacturonic acid and rhamnose residues and numerous side chains and forms highly complex molecules (Petersen *et al.*, 1997; Somerville *et al.*, 2004). RGII has a backbone of seven to nine α-1,4-linked-D-

galacturonic acid residues and is highly substituted with side chains containing 12 different carbohydrate residues linked by many different types of linkages (Vincken *et al.*, 2003; Somerville *et al.*, 2004; Pabst *et al.*, 2013). RGII occurs in primary cell walls as a dimer cross-linked by borate di-ester bonds (O'Neill *et al.*, 2001; Caffall and Mohnen, 2009). HG is covalently linked to RGI and RGII (Cosgrove, 2005; Popper and Fry, 2008; Caffall and Mohnen, 2009; Lionetti *et al.*, 2012).

4.1.2.4. Other Cell Wall Components

Other important components of the plant cell wall include glycoproteins and β-1,3-glucans (callose). There are five plant cell wall protein classes; extensins, glycine-rich proteins, proline-rich proteins, solanaceous lectins and arabinogalactan proteins (Showalter, 1993). Cell wall proteins are many functions. For example, extensins are involved in the assembly of the cell wall (Cannon *et al.*, 2008), whereas arabinogalactan proteins are important for development and recognition of microbes by the plant (Nguema-Ona *et al.*, 2013). Glycoproteins found in plant cell walls are either hydroxylproline-rich (HRGPs) or arabinogalactan proteins (AGPs) and many are essential for wall assembly and interaction with microbes (Velasquez *et al.*, 2011; Nguema-Ona *et al.*, 2013). For example, the genome of Arabidopsis potentially contains 500 cell wall proteins (Jamet *et al.*, 2006). β-1,3-glucans are found in various plant tissues including the newly formed cell wall (Brown and Lemmon, 2009), sieve plates and plasmodesmata (Levy and Epel, 2009). Importantly, the deposition of β-1,3-glucans in plants is associated with the basal defence response, resulting in the formation of cell wall appositions and the slowing of pathogen colonisation (Enkerli *et al.*, 1997a; Underwood, 2012). β-1,3-glucans are also found in the walls of many microbes including Oomycete species; in the Oomycetes they also occur as intracellular nutrient stores of carbohydrates (Clavaud *et al.*, 2009).

4.1.3. The plant cell wall as a barrier to potential pathogens

The wide range of complex cell wall polysaccharides and proteins that are extensively cross-linked, constitute a strong and effective barrier that impedes the ingress of potential pathogens (Vorwerk *et al.*, 2004; Cantu *et al.*, 2008). The plant cell wall is constantly modified during growth and development and in response to environmental signals (Hématy *et al.*, 2009). Pathogens confront the plant cell wall defensive structure before encountering the intracellular plant defences and in some interactions use mechanical force to invade a host (Hückelhoven, 2007). The dynamic response of plants to pathogen attack is seen through the deposition of β-1,3-glucan callose rich cell wall appositions (i.e. papillae) at sites of attempted pathogen penetration (Lu *et al.*, 2012; Ellinger *et al.*, 2013), structural changes to cell wall polysaccharides, biosynthesis of phenolic compounds and production of lignin-like polymers to strengthen the wall (Vorwerk *et al.*, 2004; Hückelhoven, 2007; Zhao and Dixon, 2011; Zhao and Dixon, 2014).

4.1.4. Enzymes involved in plant cell wall degradation

Modification or degradation of plant cell walls needs huge numbers of extremely specific enzymes. Protein motifs conferring carbohydrate catalytic activity have been classified into sequence-related families of Carbohydrate-Active enzyme (CAZyme) modules (http://www.cazy.org/, Cantarel *et al.*., 2009). Often a protein will contain more than one module allowing specific target recognition (Henrissat and Davies, 2000; Lombard *et al.*, 2010; Aspeborg *et al.*, 2012; Horn *et al.*, 2012; Levasseur *et al.*, 2013). These modules fall into six families, glycosyl hydrolases (GHs), polysaccharide lyases (PLs), carbohydrate esterases (CEs), glycosyl transferases (GTs), auxiliary activities (AAs) and carbohydrate binding modules (CBMs), but only a subset of CAZymes are CWDE. *P. parasitica* contains 750 CAZyme modules but has only 431 predicted CWDE (Blackman *et al.*, 2014). Some of these are involved in the degradation of starch and simple sugars but were included in this thesis (Chapter 5) as some have been identified as pathogenicity factors. Of the six families, GTs have been further classified into 47 different families based on PSI-BLAST sequence analysis and substrate/product

stereochemistry (Ünligil and Rini, 2000). GTs that function on the biosynthesis was identified as one of the most closely related orthologs corresponding to the up-regulated genes in the mycelium of *P. cinnamomi* treated with 40 µg/ml phosphite (King *et al.*, 2010).

4.1.5. The role of pathogen CWDE in plant invasion

The complexity of the plant cell wall is reflected by the number and diversity of CWDE produced by pathogens with most plant pathogens secreting a diverse array of CWDE (Hématy *et al.*, 2009; Kubicek *et al.*, 2014). The estimate of the number and types of CWDE in different pathogens varies, with the genome analysis of fungi and Oomycetes revealing that hemibiotrophs and necrotrophs have more CWDE than biotrophs (Battaglia *et al.*, 2011; O'Connell *et al.*, 2012; Zerillo *et al.*, 2013; Zhao *et al.*, 2013). Necrotrophs secrete toxins and have a large repertoire of CWDE and acquire nutrients from dead cells (Kemen and Jones, 2012; Zhao *et al.*, 2013). In contrast, biotrophs appear to have fewer CWDE and seem to operate by stealth to minimize the damage in the host cell wall this limiting the induction of plant defence responses (Hématy *et al.*, 2009). Hemibiotrophs, such as those found in the *Phytophthora* family, have both biotrophic and nectrotrophic stages, and also have a wide arsenal of CWDE (Blackman *et al.*, 2014; Brouwer *et al.*, 2014). In an extension of this correlation, symbionts, such as *Laccaria bicolor* and *Tuber melanosporum*, have less CWDE (Martin *et al.*, 2010; Veneault-Fourrey *et al.*, 2014). For example, *P. parasitica* contains 431 predicted CWDE (Blackman *et al.*, 2014), but the saprophyte, *Rhizopus oryzae*, contains 105 and the biotroph *Ustilago maydis* has 117 CWDE (Battaglia *et al.*, 2011).

During plant infection, plant pathogens produce a diverse range of CWDE including cellulases, hemicellulases and pectinases. These enzymes facilitate invasion into the host tissues. CWDE of pathogens and other microorganisms function during plant penetration and in the release of nutrients for pathogen use (Garbe and Collin, 2012; Zhang and Kan, 2013). Microbial pathogens produce a range of pectinases, most notably polygalacturonases, pectin and pectate lyases and pectin esterases targeted against the homogalacturonan, as well as

rhamnogalacturonases that target RGI. The degradation of pectins in the middle lamella between adjacent cells leads to tissue maceration. They are often the first CWDE to be secreted by invading plant pathogens, thereby implicating an important role in pathogenesis (Cooper, 1983).

4.1.6. *Phytophthora* CWDE

4.1.6.1. Pectinases

There are 28 CAZyme families (18 GHs, three CEs and seven PLs) that aid in pectin degradation according the functions assigned by the CAZyme database. Eighteen of these families (12 GHs, three CEs and three PLs) are found in the *P. parasitica* genome (Figure 4.2). This includes 108 proteins specific for pectins and another 100 which have the potential to degrade pectin and other substrates (Blackman *et al.*, 2014). Some pectinases in *Phytophthora* form large families and include polygalacturonases from the GH28 family (Götesson *et al.*, 2002; Blackman *et al.*, 2014; Brouwer *et al.*, 2014) and pectin methyl esterases from the CE8 family (Blackman *et al.*, 2014; Brouwer *et al.*, 2014). It is believed that these large multigene families reflect the need for a range of substrate specificities within an overall enzyme class (Götesson *et al.*, 2002) and appears to vary with the specificity of the interaction between pathogen and host plant (Esquerré-Tugayé *et al.*, 2000). A large polygalacturonase gene family might have developed to aid the pathogen in successful colonisation of hosts that differ in cell wall structure and composition and to counteract the polygalacturonase-inhibiting proteins and other defence mechanisms in different hosts (Cook *et al.*, 1999) . Other families involved in the degradation of the back bone chains of pectins are the PL families which can act at the terminal residues and/or break linkages internally, CEs involved in the removal of acetyl groups, and the RGI acting GH78 and GH105 which degrade at termini and internal linkages respectively. Several families are also involved in the RGI side chains degradation and these are shown in Figure 4.2.

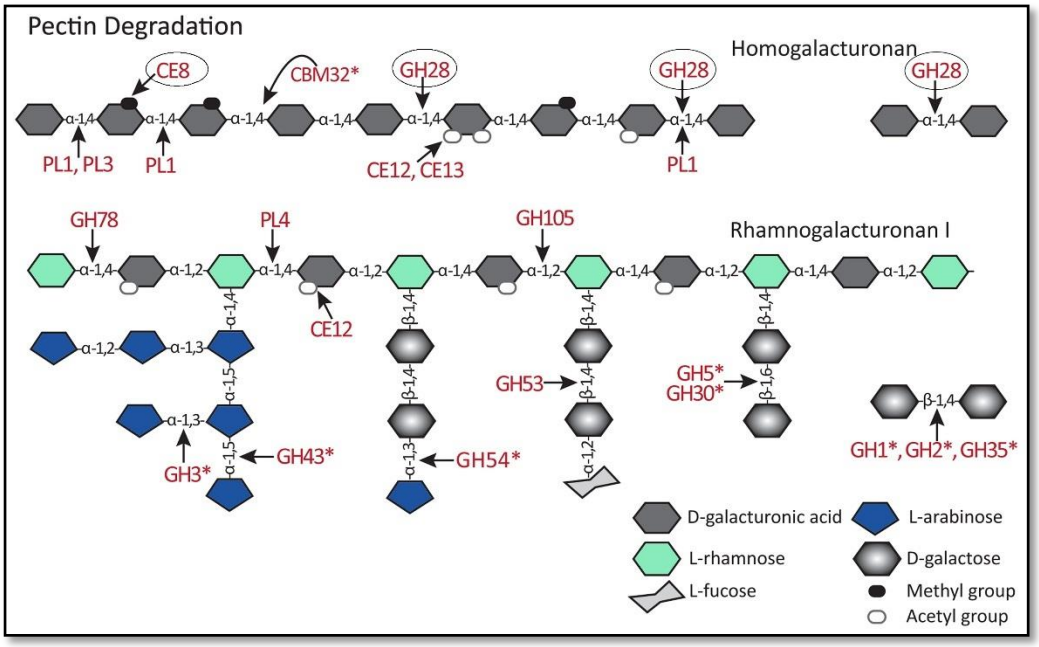

Figure 4.2. Diagrammatic representation of the pectins, HG and RGI, showing putative degradation sites for predicted *P. parasitica* pectinases (Blackman *et al.*, 2014). GH28 and CE8 families are circled. * indicates enzyme families involved in the degradation of other substrates; GH: glycoside hydrolase; CBM: carbohydrate binding module; PL: polysaccharide lyase; CE: carbohydrate esterase.

4.1.6.2. Cellulases

Enzymes that degrade cellulose belong to four groups of cellobiohydrolases, endo- and exo-β-1,4-glucanases, and β-glucosidases and in *P. parasitica* come from eight GH families (Figure 4.3). For example, *P. parasitica* contains seven proteins belonging to the GH6 family and 15 proteins from the GH12 family of endo-β-1,4-glucanases (Blackman *et al.*, 2014). Those from the GH12 family also have the potential to target hemicellulose. The four AA families also target cellulose and help in the breakdown of cellulose by probably by altering the oxidative environment (Levasseur *et al.*, 2013). CBMs do not have catalytic activity but act to target and concentrate enzyme activity and may also have some disruptive activity (Boraston *et al.*, 2004). In *Phytophthora*, most CBMs are

cellulose targeting and come from the CBM1 and CBM63 families (Blackman *et al.*, 2014; Brouwer *et al.*, 2014).

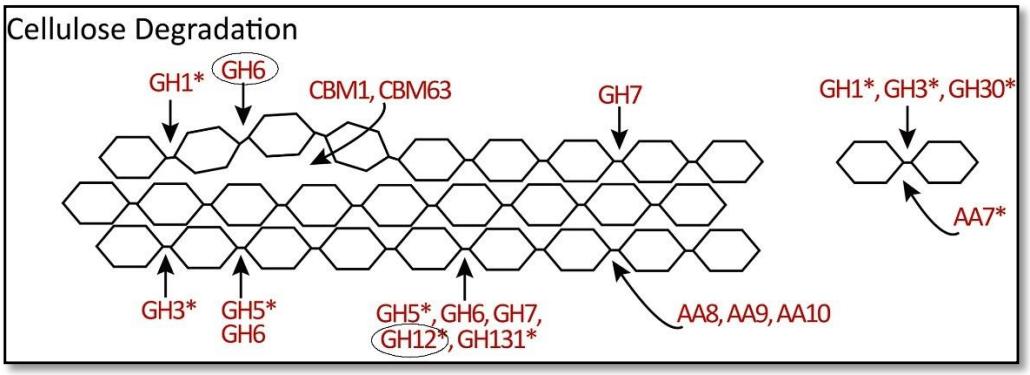

Figure 4.3. Diagrammatic illustration of cellulose showing putative target sites for predicted *P. parasitica* CWDE involved in cellulose degradation (Blackman *et al.*, 2014). The expression of two genes from GH6 and GH12 families (circled) were evaluated through qPCR. GH: glycoside hydrolase; CBM: carbohydrate binding module; AA: auxiliary activity; * indicates families that also target other substrates.

4.1.6.3. Hemicellulases

Hemicellulose degradation requires production of various diverse enzymes some of which also act in the degradation of cellulose and pectins (Sun *et al.*, 2012). Proteins from 12 GH and five CE families aside from non-catalytic CBMs are possibly involved in the degradation of hemicellulose (Figure 4.4) (Blackman *et al.*, 2014). One group of specific hemicellulases are four β-1,4-xylanases of the GH10 family that act on β-1,4-xylans linkages found in xylans, glucuronoxylans and glucuronoarabinoxylans. Another group includes proteins from CE2, 3, 4 and 5 families involved in deacetylation and CE1 that act on the removal of ferulic acid.

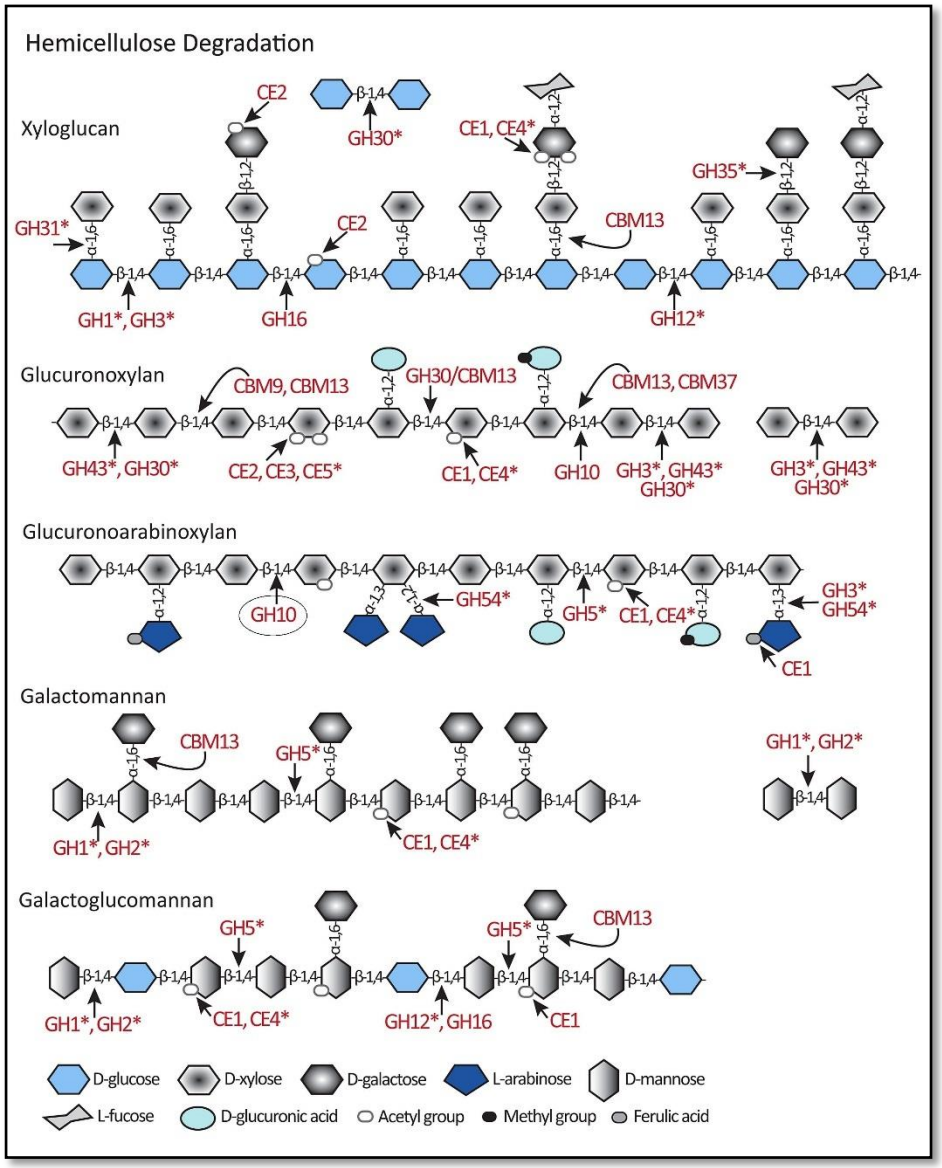

Figure 4.4. Diagrammatic illustration of hemicellulosic polysaccharides showing putative sites for *P. parasitica* CWDE that act in the degradation of hemicellulose degradation (Blackman *et al.*, 2014). The expression of four GH10 genes (circled) that act on β-1,4-xylans were analysed by qPCR. * indicates enzyme families involved in the degradation of other substrates; CE: carbohydrate esterase; GH: glycoside hydrolase; CBM: carbohydrate binding module; AA: auxiliary activity.

4.1.6.4. Other CWDE

Other CWDE are involved in the degradation of β-1,3-glucan (callose) and glycoproteins. For example, callase also known as β-1,3-glucanase and chitinase are induced in parts of plants infected with pathogens such as bacteria, viruses and fungi (Meins and Ahl, 1989). β-1,3-glucanases and chitinases usually act in synergy and are considered to play an important role in plant defence mechanisms against fungal pathogens, and involve in plant resistance against different *Phytophthora* species (Jongedijk *et al.*, 1995; Giannakis *et al.*, 1998; Pozo *et al.*, 1999).

Several glycoproteins have been identified in *Phytophthora* species with enzymes that are involved in various functions. For example, *P. megasperma* f. sp. g*lycinea*, an extracellular invertase identified as mannanglycoprotein was found to inhibit the phytoalexin glyceollin in soybean (Ziegler and Pontzen, 1982). A gene coding for α-galactosidase was correlated to a stress response to potato infected with *P. infestans* (Evers *et al.*, 2006), and *P. palmivora* adhesion and appressorium production was inhibited by a α-mannosidase or α-glucosidase (Bircher and Hohl, 1997). In *P. parasitica*, the cellulose binding elicitor lectin (CBEL) glycoprotein function in the deposition of cell wall, adhesion of cellulose substrates, induction of necrosis and defence responses in the host plant (Gaulin *et al.*, 2002; Khatib *et al.*, 2004).

4.1.7. Methods for the study of the role of CWDEs during infection

4.1.7.1. Immunolocalisation of proteins

Immunohistochemistry (also known as immunolocalisation) is a powerful approach to study the cellular and subcellular locations of antigens of interest (Avci *et al.*, 2012). The establishment of the localisation of enzyme subunits at the subcellular and tissue levels is an important aspect in the understanding of the regulation of metabolism in plants (Smith *et al.*, 1994). Although studies using *in situ* hybridisation and reporter-gene expression can provide substantial insight in the expression, regulation and function of genes, complementary protein-localisation are essential to detect the fate of proteins (Smith *et al.*, 1994).

Localisation of antibodies against specific antigens can recognise homologous proteins across many species but they also can be isolate, species or genus specific. For example, four monoclonal antibodies (Zg-1, Zt-1, Cpa-1, and Cpa-2) were localised in *P. cinnamomi* but not to other *Phytophthora* species. The antibodies, Zg-1 and Zt-1, specifically react with the flagellum and groove region of the zoospores of *P. cinnamomi*. Cpw-1, is genus-specific, that binds to the cysts of all six *Phytophthora* species but not to *Pythium* species (Hardham *et al.*, 1986). Further study on lectin and antibody labelling of *P. cinnamomi* surface components revealed that the zoospore surface is subdivided into three distinct molecular domains. Dramatic changes were observed during encysment with the secretion of material rich in N-acetyl-D-galactosamine binding the cells to any adjacent structure. Immunolabelling demonstrates that this material is localised in the small peripheral vesicles and is secreted after encystment. The binding of a monoclonal antibody to the flagella triggered encystment which suggests that specific receptors may be localised (Hardham, 1989).

Immunolabeling and transmission electron microscopic techniques have also been used to examine the chemical nature of wall appositions in roots inoculated with *P. sojae* (Enkerli *et al.*, 1997a). β-1,3-glucan, xyloglucan, and arabinogalactan proteins were found in all wall appositions irrespective of inoculation duration when appositions were developed or whether plants had resistant or susceptible reaction to *P. sojae*. β-1,3-glucan was also localised in walls and plasmodesmata of the host cells.

4.1.7.2. Gene expression analysis

The analysis of gene expression has been used to provide clues to the possible function of genes. The analysis of CWDE expression in various substrates has been used to determine possible regulatory mechanisms. For example, qPCR revealed that a *P. parasitica* polygalacturonase from the GH28 family was induced by pectin but suppressed by glucose in liquid culture (Yan and Liou, 2005) and that this gene is also highly expressed during the infection of tomato leaves (Yan and Liou, 2005). Expressed sequence tags (ESTs) have been used to identify genes that are expressed at particular development stages and were

used to identify a polygalacturonase from *P. infestans* during infection stages (Torto-Alalibo *et al.*, 2002). Using a different method, namely differential display reverse transcriptase-PCR, phosphite treatment of *P. cinnamomi* in culture induces the expression of a putative proteophosphoglycan (Wong *et al.*, 2009). Studies using microarrays have been extensively used to examine the transcriptome of a large number of pathogens during infection and *in vivo* culture and include a number of *Phytophthora* studies. For example, the analysis of the transcriptome of *P. parasitica* during the infection of Arabidopsis revealed a number of effectors and CWDE that altered their expression during development and infection (Attard *et al.*, 2014). *P. infestans* has also been used to show large changes of the transcriptome during development (Judelson *et al.*, 2008). The gene expression for a number of genes from phosphite-treated mycelium of *P. cinnamomi* have been analysed through microarray and were validated through qPCR (King *et al.*, 2010). The use of these techniques to study the transcriptome have been limited by the lack of sequenced genomes and low through-put (Wang *et al.*, 2009b). More recently, the development of high through-put next generation sequencing techniques has resulted in the sequencing of many genomes and more importantly has enabled the analysis of whole transcriptomes (Mortazavi *et al.*, 2008; Nagalakshmi *et al.*, 2008).

The experiments described in this chapter used two methods to study *P. parasitica* CWDEs during the infection of lupin. The first approach was to use qPCR to determine the expression of *P. parasitica* CWDEs during disease development using the model system that had been developed (as described in Chapter 2). These experiments focused in particular on GH28 polygalacturonases, CE8 pectin methyl esterases, GH6 and GH12 cellulases, and GH10 xylanases. The second approach was to use immunocytochemical labelling to localise CWDEs in *P. parasitica*. These investigations revealed temporal patterns of CWDE gene expression and localised CWDEs in germinated cysts. The study provided important information on the timing of pathogenicity gene expression which was used when designing the experimental approach for the subsequent analysis of the effects of phosphite on *Phytophthora* in culture and during infection (Chapter 5).

4.2. Materials and Methods

4.2.1. *P. parasitica* culture and zoospore production

P. parasitica was cultured as described in section 2.2.1. Zoospores were released from cultures grown in V8 broth and zoospores per ml was estimated as described in section 2.2.2.

4.2.2. Plant material, inoculation and sample collection

Plant material was prepared as outlined in section 2.2.3. Inoculation of lupin roots and collection of samples were described in section 2.2.4. A number of conditions were varied in 14 different infection assays as described in Chapter 2, to ensure that the subsequent procedures were adequate to obtain reproducible results. In this experiment, the inoculum concentration of 1000 zoospores/ml was taken from the original 500 ml suspension in a 1000 ml conical flask and then pouring 50 ml into each inoculation box. After inoculation, a Sharpie marker pen was used to gently mark each root at about 5 mm from the apex, the level of the zoospore suspension.

4.2.3. RNA extraction

Total RNA was isolated from *P. parasitica*-infected lupin roots following the method used by (Narayan *et al.*, 2010) using TRIzol® Reagent (Invitrogen) or with a Qiagen Plant RNeasy Plant Mini kit following the manufacturer's instructions. Three biological replicates with three roots in each replicate were taken at each sampling time. Lupin roots were placed in 2 ml Eppendorf tubes and frozen immediately in liquid nitrogen and stored at -80˚C until use. Between 150-200 mg of frozen roots were ground in liquid nitrogen using mortar and pestle. The resulting powder was added to 1 ml TRIzol® in a 2 ml Eppendorf tube. Tubes were mixed thoroughly and vortexed immediately to completely homogenize the samples and to prevent RNA degradation. The samples were

incubated for 15 min room temperature and then mixed with 200 µl chloroform each, and left at 4˚C for 20 min. The tubes were centrifuged at 12,000 *g* for 15 min at 4˚C. The supernatant of each was transferred to new 2 ml Eppendorf tubes containing 600 µl of buffer-saturated phenol solution (Sigma, pH 4.3-4.5) whilst being careful not to disrupt the interface between the upper and middle phase. The tubes were then mixed by inversion and incubated for 15 min at room temperature. Chloroform was added and the samples treated as described above. The phenol/chloroform extraction was repeated if the interface was large. The supernatants were transferred to new 1.5 ml Eppendorf tubes and 600 µl of isopropanol was added to precipitate the RNA. Samples were incubated at -20˚C for a minimum of 30 min to aid RNA precipitation. The tubes were incubated for 15 min room temperature and centrifuged at 12,000 *g* for 15 min to limit the presence of salts. The supernatant from each tube was discarded and 600 µl of 80% ethanol was added, left for 2 min and centrifuged at 12,000 *g* for 10 min at room temperature. The pellets were allowed to dry in rack with lids open in a biosafety cabinet. Air dried pellets were resuspended in 50 µl diethylpyrocarbonate (DEPC)-treated water (Sambrook and Russell, 2001). Samples were kept on ice as much as possible and RNA was stored at -80°C until use. All procedures used were designed to limit RNA nuclease activity and included the use of DEPC-treated solutions and barrier tips.

4.2.4. Assessing RNA quality and quantity

RNA concentration was determined at 260 nm using an Eppendorf BioPhotometer (Eppendorf, Hamburg, Germany). The $A_{260\ nm}/A_{280\ n}$ was also noted and gave an indication of protein contamination. To ascertain the integrity of RNA, samples were tested by agarose gel electrophoresis on a 2% agarose gel made using Tris-acetate-EDTA (TAE), DEPC-treated water, agarose (UltraPure™ Agarose, Invitrogen) to which RedSafe™ (iNtRON Biotechnology, USA) was added. All chemicals used were exclusively for RNA extractions. The electrophoresis equipment was soaked in 10% hydrogen peroxide and rinsed with DEPC-treated water prior to use and wiped with RNase AWAY (Invitrogen) to limit the action of RNase. RNA samples (1 µl) were run on agarose gels with

10 µl of RNA loading dye (95% formamide, 0.025% bromophenol blue, 0.025% xylene cyanol FF, 5 mM EDTA pH 8.0) and 5 µl of a 1 Kb DNA plus ladder (Invitrogen) and/or 10 µl RNA ladder (New England BioLabs, Inc.). The gels were electrophoresed at 100 V until the dye front had migrated two thirds of the length of the gel. Gels were photographed with a Gel Doc™ XR+ system (Bio-Rad Laboratories Pty., Ltd.,USA).

4.2.5. DNase treatment of RNA and cDNA synthesis

To ensure that all contaminating gDNA was removed from the RNA before complementary DNA (cDNA) production, total RNA samples (10 µg) were treated with 4 µl of RQ1 RNase-free deoxyribonuclease (DNase) (Promega), according to manufacturer's instructions incubated at 37˚C for 90 min followed by inactivation at 65˚C for 10 min. Where the total RNA had been isolated using the RNeasy kit, gDNA was removed by on-column DNase digestion as described by the manufacturer. cDNA was synthesised from 2.5µg of DNase-treated total RNA using 1 µl of 10 mM of dNTP mix (dATP, dCTP, dGTP, dTTP) (Invitrogen) and 1 µl Oligo $(dT)_{12\text{-}18}$ (Invitrogen). The final volume was made up to 12.5 µl with DEPC-treated water. The samples were then incubated at 65˚C for 5 min, then 25˚C for 10 min and immediately chilled on ice. Two microliters of 0.1 M dithiothreitol (DTT), 4 µl of 5x First Strand Buffer (250 mM Tris-HCl, pH 8.3, 375 mM KCl, 15 mM $MgCl_2$) and 0.5 µl of RNase inhibitor (RNasin, Promega) were added to the samples and incubated 42˚C for 2 min. cDNA was made with reverse transcriptase (1 µl of Superscript II RT, Invitrogen) at 42˚C for 50 min and the reaction was then inactivated by heating samples to 70˚C for 15 min. Negative controls containing total RNA (-RT) were included to test for contaminating gDNA and these reactions were treated in the same way except the exclusion of Oligo (dT)12-18, dNTP mix, RNasin, and Superscript II RT.

4.2.6. Assessing cDNA quality

To assess the quality of the cDNA and check for the presence of gDNA, PCR was used with primers raised against the 40S ribosomal protein S3A (*WS021*,

GenBank accession CF891675) (Shan *et al.*, 2004) (Appendix II). The cDNA samples were diluted one in ten. A PCR supermix was made containing 0.4 mM primers and 2x PCR Master Mix (Promega). Ten µl of mastermix was then added to 2 µl of either the cDNA samples or –RT controls diluted 1 in 10. The samples were then amplified according to the conditions in Table 4.1.

Table 4.1. Polymerase chain reaction conditions involved in the assessment of cDNA. Asterisks indicate steps that were repeated 35 times.

Step	Temperature	Time
Initial denaturation	94°C	2 min
Denaturation	94°C	30 s*
Annealing	60°C	30 s*
Elongation	72°C	30 s*
Final extension	72°C	5 min

After the PCR was performed, the quality of cDNA and –RT controls was tested by agarose gel electrophoresis on a 1.5% agarose gel made using 1x TAE. PCR reactions (12 µl) were run on agarose gels in loading buffer (0.05% bromophenol blue, 0.05% xylene cyanol FF, 5% glycerol). A size standard consisting of 5 µl of 1 Kb DNA Plus Ladder (Invitrogen) was included on each gel. The gel was electrophoresed and visualized as described earlier in Section 4.2.6.

4.2.7. Primer design for selected *P. parasitica* CWDEs

The relative expression of selected *P. parasitica* CWDE genes was analysed by qPCR. cDNA was prepared from RNA samples extracted using both RNA isolated methods. In initial experiments, samples from a number of preliminary infection assays where the total RNA was extracted with TRIzol® (Section 2.2.4) were

used and cDNA from these samples used to test primers. Data presented in results section of this chapter came from RNA samples extracted using the RNeasy kit and these samples were subsequently used for RNA-Seq analysis (Blackman *et al.*, 2015). A number of putative CWDE were first identified in the assembled scaffolds of *P. parasitica* INRA-310 (http://www.broadinstitute.org/annotation/genome/Phytophthora_parasitica /MultiHome.html) by Basic Local Alignment Search Tool (BLAST, Altschul *et al..*, 1997) analysis using known CWDE prior to the annotation of this genome. CWDE primers were designed by Dr Leila Blackman using Oligoexplorer v1.1.2 and were assessed using Netprimer v3 (http://www.premierbiosoft.com/netprimer/index.html). *WS041* (GenBank accession CF891677) was used as the normalising gene as it has been shown to be a constitutively expressed gene (Yan and Liou, 2006) and these primers were designed by Dr Weixing Shan (Shan *et al.*, 2004). The cDNA samples were diluted, one in ten in nuclease-free water. The master mix for each gene to be analysed contained 150 nM of primers and QuantiTect SYBR Green Master mix (Qiagen). All primer pairs used are listed in Appendix II. A minimum of three biological replicates and four technical replicates were included for each experiment. Reactions were done and levels of expression were analysed as described in Section 2.2.6.3. Gene expression levels were calculated relative to the expression in a single 3 h germinated cyst cDNA using the comparative quantification function of the RotorGene software (Qiagen). A melt curve was performed at the end of each run to check for primer-dimer formation and to ensure that there was only one amplification product. The expression of 11 CWDE genes were analysed. These were five pectinases, four hemicellulases, and two cellulases and came from six CAZyme families namely CE8 (2), GH6 (1), GH12 (1), GH10 (4), and GH28 (3) (Table 4.2). The putative targeting sites for these *P. parasitica* families are shown in Figures 4.2, 4.3 and 4.4.

Table 4.2. Cell wall degrading enzyme (CWDE) genes used in the qPCR with their predicted substrate and CAZyme family. PPTG: *P. parasitica* transcript accession numbers from *P. parasitia* INRA-310 V2.

Accession Number	CWDE annotation	Predicted substrate	CAZyme family
PPTG_15162	endopolygalacturonase	pectin	GH28
PPTG_17704	polygalacturonase	pectin	GH28
PPTG_15179	polygalacturonase	pectin	GH28
PPTG_05287	pectin methyl esterase	pectin	CE8
PPTG_10338	pectin methyl esterase	pectin	CE8
PPTG_00140	β-1,4-glucanase	cellulose	GH6
PPTG_19377	β-1,4-glucanase	cellulose	GH12
PPTG_17850	β-1,4-xylanase	hemicellulose	GH10
PPTG_17851	β-1,4-xylanase	hemicellulose	GH10
PPTG_17240	β-1,4-xylanase	hemicellulose	GH10
PPTG_07666	β-1,4-xylanase	hemicellulose	GH10

4.2.8. Immunofluorescence localisation of CWDE

4.2.8.1. Germinated cyst production and fixation

P. parasitica zoospores were released following the procedures outlined in Section 2.2.2. In order to obtain germinated cysts, 13 ml of zoospore suspension was placed in a sterile 50 ml Falcon tube and vortexed for 30 s five times with approximately 3 s intervals to produce cysts. Filter-sterilised clarified V8 juice was added to give a final concentration of 5% and the cysts allowed to germinate and grow at 23˚C for 3 h. Cyst germination was monitored using a Zeiss Axioplan microscope, and cysts were counted as being germinated when the germ tube was visible at using a 40x objective lens. After 3 h of incubation, germinated cysts were fixed in an equal volume of 8% formaldehyde in 100 mM piperazine-1,4-bis (2-ethanesulfonic acid) disodium salt (PIPES) at pH 6.5 for 30 min at room

temperature, and then collected by centrifugation at 1500 *g* for 5 min. The fixative was removed and pellet was resuspended in 3 ml of 100 mM PIPES for 5 min and washed twice and finally resuspended in 3 ml RO water. Multi-well microscope slides (MP Biomedicals, Aurora, Ohio, USA) were cleaned with 100% ethanol and then freshly treated with 0.1% polyethyleneimine (PEI, Sigma) for 1 min and rinsed in RO water and air-dried before use. Germinated cysts suspension (12 µl) were placed on the multi-well slides, dried at 37°C and rinsed in phosphate buffered saline (PBS) solution (Appendix I) twice for 3 min.

4.2.8.2. Immunolocalisation of *P. parasitica* CWDE

The predicted sequences of 13 *P. parasitica* polygalacturonase proteins from the GH28 family were aligned (Figure 4.5) and conserved regions within these proteins were identified. Mouse monoclonal antibodies (MAbs) were raised against a synthetic polypeptide, GLTGSADQIY (Figure 4.5) (Abmart, Inc., www.ab-mart.com). Six MAbs (ascites fluid) were tested by immunofluoresence localisation on *P. parasitica* 3 h germinated cysts diluted at 1 in 1000 in PBS containing 1% bovine serum albumin (BSA) and 0.1 % fish scale gelatin (Sigma). The secondary antibody used was a sheep anti-mouse conjugated to fluorescein isothiocyanate (SAM-FITC; Jackson ImmunoResearch Laboratories Inc) diluted at 1 in 150 with the same buffer. An aliquot of 12 µl of primary antibody was pipetted into each well and the slides were incubated at 37˚C for 60 min in 12 cm square dishes lined with moist blotting paper. The slides were then rinsed in PBS (2 x 2 min) in Coplin jars. Excess liquid was removed with strips of blotting paper and 12 µl of secondary antibody was pipetted onto each well and the slides were incubated at 37˚C for 45 min. After rinsing in PBS (2 x 3 min) and once with RO water, slides were mounted in Mowiol mounting medium containing 1,4-diazabicyclo-[2,2,2]-octane (DABCO) as a fluorescence anti-fade agent (Harlow and Lane, 1988). Controls of cysts labelled with secondary antibodies were included in each experiment. Samples were observed using a Zeiss (Germany) Axioplan epifluorescence microscope with a 40x objective lens. Fluorescence and differential interference contrast (DIC) optics images were collected using either a black and white Princeton Instruments MicroMax Camera (Tucson, AZ, USA) or a colour Canon EOS Rebel T3i (Canon Inc., New York, USA) camera. All

immunofluoresence localisation experiments also included a secondary antibody control, which was treated and photographed using the same conditions.

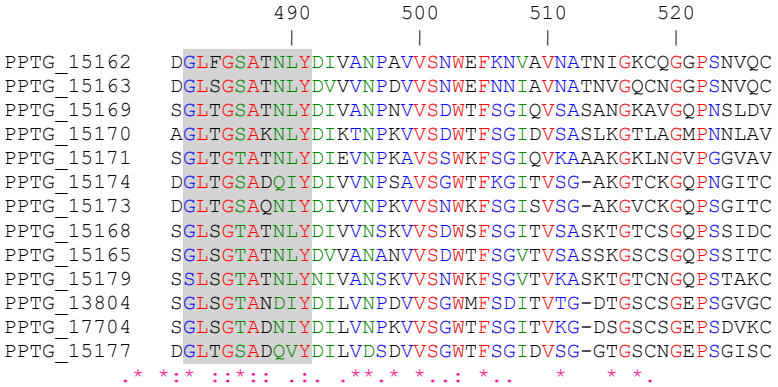

Figure 4.5. Multiple sequence alignment in the C terminal region of 13 GH28 polygalacturonase proteins with the region chosen for the production of antibodies shaded.

4.3. Results

4.3.1. Expression of CWDE during infection.

The development of lesions and the pathogen load, as indicated by the qPCR (see sections 2.3.2 and 2.3.5), were used in a number of preliminary infection assays to estimate the appropriate sampling times which would allow the expression profile of selected CWDEs to be determined. cDNA was produced from samples of infected lupin roots taken at 0, 12,18, 24, 30, 36, 40, 48, 54 and 60 hpi and the expression profile of a selection of CWDE genes were determined. Analysis of pathogen load using the cultivar Gungurru from several experiments, showed that *P. parasitica* gDNA was not detected in 12-18 hpi samples (see section 2.3.5) but could sometimes be detected at 24 hpi (see section 3.3.4). Thus, the expression of representative CWDE genes was determined by qPCR in samples taken between 24 and 60 hpi. These expression analyses were used to determine if the RNA isolated from these samples was suitable for RNA-Seq analysis and to determine the appropriate infection time for a detailed study of the effect of phosphite on the expression of *P. parasitica* CWDE during infection presented in Chapter 5.

4.3.1.1. Expression of pectinases

The expression of five pectinases was evaluated in this study; two were pectin methyl esterases from the CE8 family (PPTG_05287 and PPTG_10338) and three were GH28 polygalacturonases (PPTG_15162, PPTG_17704 and PPTG_15179). Both CE8 genes were expressed during early infection; PPTG_10338 was expressed to the highest level at 24 hpi while PPTG_05287 expression peaked at 30 hpi (Figure 4.6). There was little expression of either CE8s during late infection (54-60 hpi).

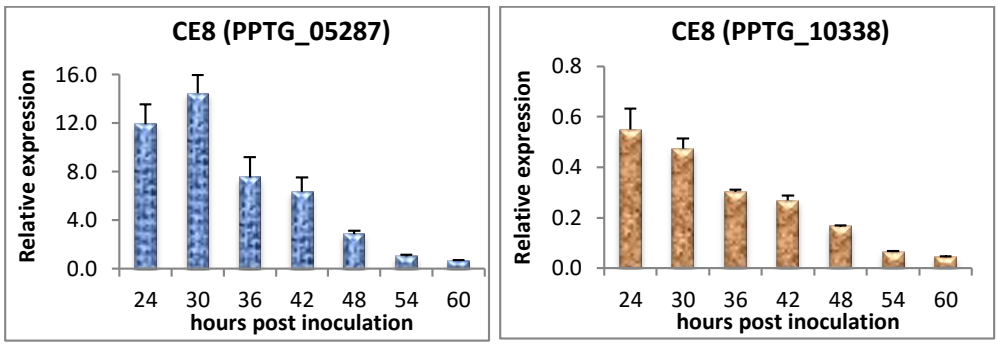

Figure 4.6. Expression profiles of two PME genes from the CE8 family during lupin root infection. Relative expression levels with respect to *WS041* expression are shown. Error bars represent standard deviation of three biological replicates.

The three PG genes analysed by qPCR showed two different expression profiles. The two PG genes from the GH28 family (PPTG_15162 and PPTG_17704) were induced as early as 24 hpi while transcripts of PPTG_15179 were not detected until 42 hpi (Figure 4.7). However, the expression of this latter gene was relatively low compared to the expression of *WS041* and confirmation of the expression profile of PPTG_15179 required RNA-Seq analysis (Section 4.4.2).

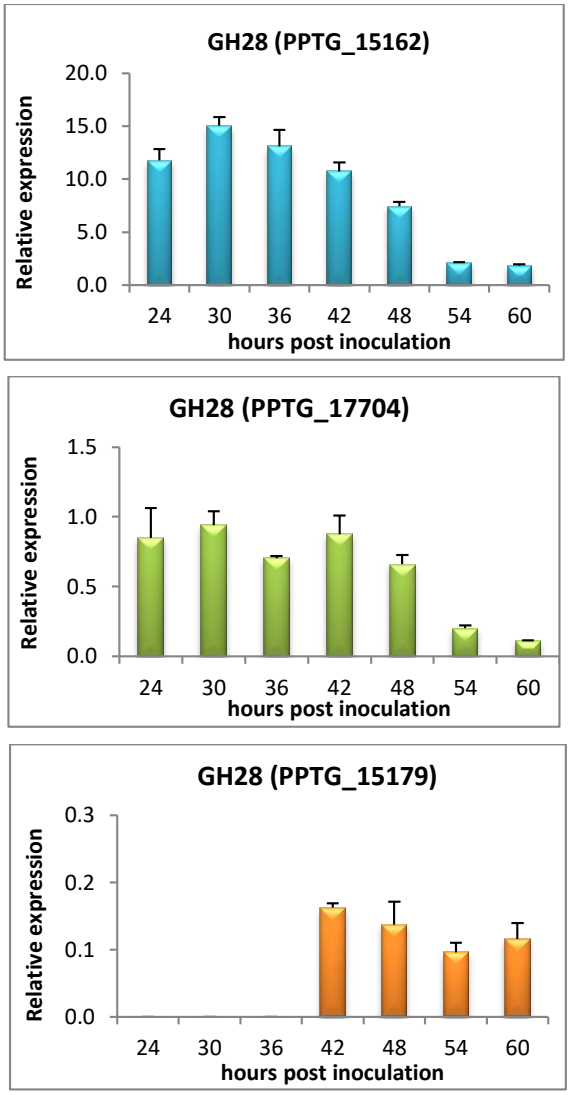

Figure 4.7. Expression profiles of three polygalacturonase genes from GH28 family during lupin root infection. Expression levels are given relative to *WS041*expression. Error bars represent standard deviation (n = 3).

4.3.1.2. Expression of xylanases

The expression profile of all four GH10 family members was determined (Figure 4.8). Three genes (PPTG_07666, 17851, and 17240) were expressed early at 24 hpi and while GH10 gene (PPTG_17850) was induced later at 36 hpi. There was a considerable variation in the peak in expression with PPTG_07666 showing relatively even expression of across all time points, while PPTG_17851 expression was induced at 36 hpi and decreased thereafter. Only one GH10 (PPTG_17240) showed a peak in expression during early infection and this was at 30 hpi.

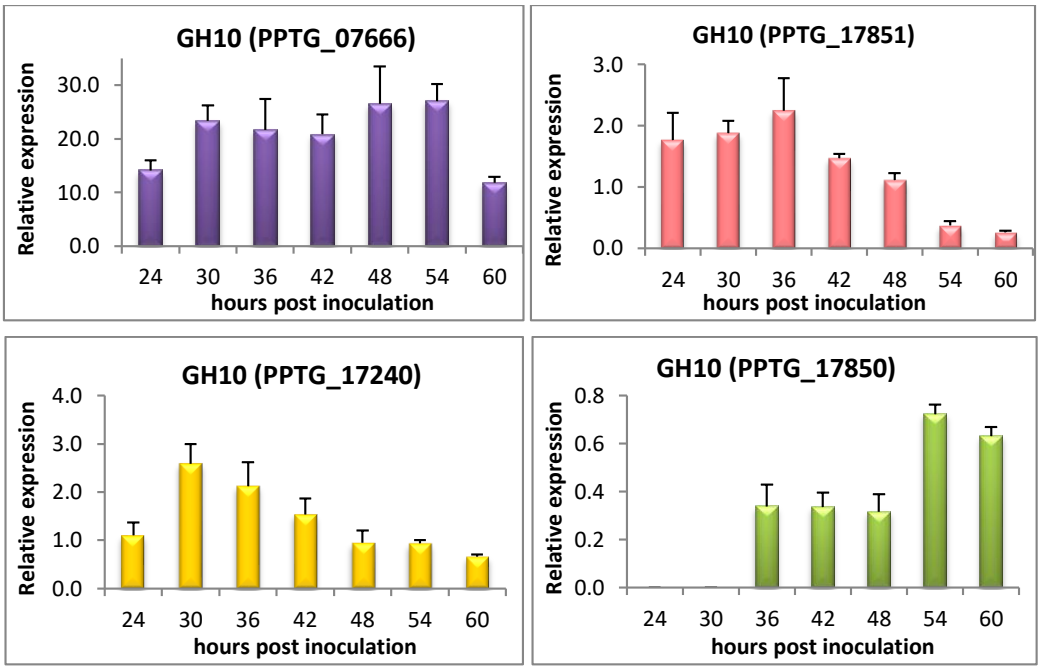

Figure 4.8. Expression profiles of four xylanase genes (GH10 family) during the infection of lupin roots. Expression levels were determined relative to *WS041* expression. Error bars represent standard deviation based on three biological replicates.

4.3.1.3. Expression of cellulases

The two β-1,4-glucanases subjected to qPCR analysis showed that these were expressed later than the pectinases and xylanases. Expression of PPTG_00140 was first detected at 36 hpi while low levels of PPTG_19377 transcripts could be detected earlier at 24hpi. Highest expression of both genes was at 48 hpi (Figure 4.9).

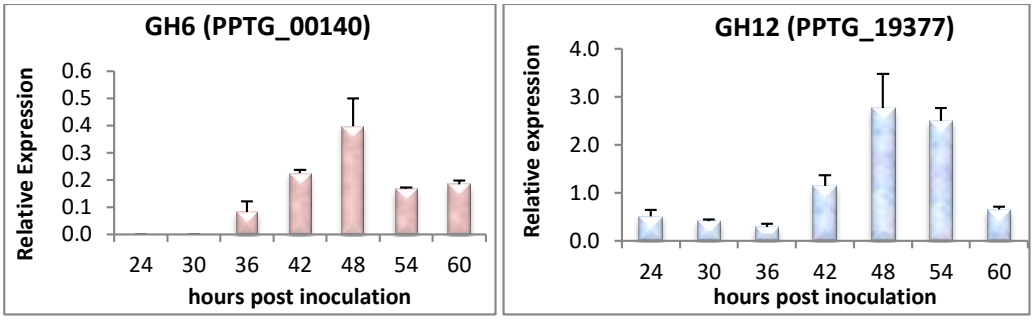

Figure 4.9. Expression pattern of the cellulases, PPTG_00140 (GH6) and PPTG_19377 (GH12) during lupin root infection. Relative expression levels in relation to *WS041*expression are shown. Error bars represent standard deviation (n = 3).

4.3.2. Immunolocalisation of polygalacturonases in *P. parasitica*

Six MAbs that were raised against a conserved region of *P. parasitica* polygalacturonases were tested on 3 h germinated cysts and revealed that two out of six MAbs labelled the tips of germinated cysts and sites of hyphal branching (Figure 4.5). However, no labelling was observed on hyphae in infected lupin roots (K. Kots, unpublished results), and these antibodies were deemed to be unsuitable for the detection of *P. parasitica* polygalacturonases *in planta*.

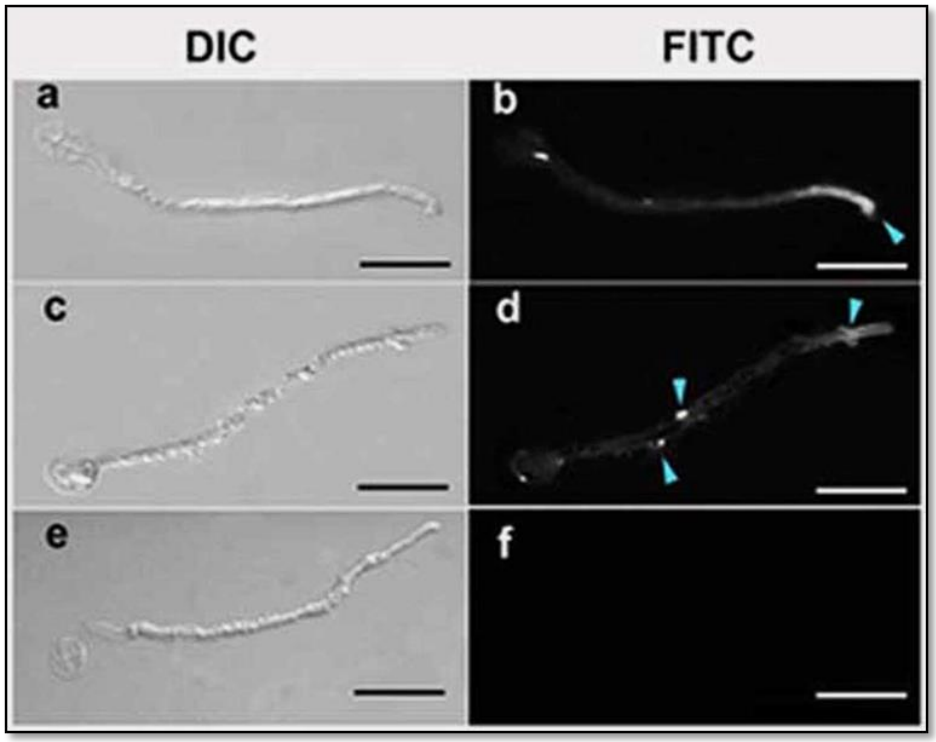

Figure 4.5. Micrographs taken using differential interference contrast (DIC) or showing fluorescein isothiocyanate (FITC) fluorescence after labelling with MAbs against polygalacturonases. The anti-polygalacturonase MAbs localised to the tips of germinated cysts and to branch points (b and d, with blue arrow heads). In a control (e and f) in which the primary Mab was omitted, there was no labelling. Bar represents 80 µm.

4.4. Discussion

4.4.1. Cascade of CWDE expression

Analysis of the expression pattern of 11 *P. parastica* genes, from one CE family and four GH families, that degrade the three main types of cell wall polysaccharides show that there is a cascade of pathogen expression during lupin root infection. In general, the first genes whose expression is induced act on pectins are induced. Expression of hemicellulose genes and then cellulose genes follows as infection continues. Some early biochemical studies on pathogen cell wall degradation during plant infection suggested a similar chronological order pectinases, hemicellulases and cellulases enzyme activity (Jones *et al.*, 1972;

Cooper and Wood, 1975; Martinez *et al.*, 1991). To gain more information on the expression of *P. parasitica* CWDE genes during infection, the RNA samples prepared for the qPCR analysis described in this chapter were also used for an RNA-Seq transcriptome experiment (Blackman *et al.*, 2015). The results of this latter study provide further evidence of the cascades of CWDE gene expression and encompassed a wide range of enzymes that target the major categories of plant cell wall polysaccharides. The RNA-Seq study also presented information on the relative timing of gene expression for proteins that target a single wall carbohydrate (Blackman *et al.*, 2015). Together, the qPCR and RNA-Seq studies provide evidence consistent with the suggestion made by Deising *et al.* (1995) that pathogens release cascades of CWDEs during plant infection. The early expression of pectin methyl esterases during lupin infection supports the hypothesis that de-esterification by CE8 proteins is required for the consequent degradation of homogalacturonan by GH28 proteins (de Vries and Visser, 2001). However, the relative importance of each gene cannot be determined by qPCR alone where primer design, amplification efficiency, quality of cDNA and efficiency of the reverse transcriptase reaction influence the levels of gene expression that are measured (Nolan *et al.*, 2006).

The roles of pectinases in plant infection have been elucidated in many biotrophic and necrotrophic pathogens (Reignault *et al.*, 2008). Biotrophic pathogens typically show only limited pectin-degradation, while necrotrophic pathogens possess a diverse range of pectin-degrading enzymes that are used to extensively degrade cell walls and initiate tissue maceration (Sprockett, 2009). During early infection (penetration), pathogenic bacteria and fungi released pectinases and plants respond to the aggressive degradation of pectin by producing polygalacturonase inhibiting proteins, a response that indicates a specific biochemical interaction at the pectin degradation level (Prade *et al.*, 1999). It is believed that the degradation of the pectin matrix is likely to facilitate access to other wall components by other CWDEs. However, this is not the case with the biotroph leaf pathogen, *Cymadothea trifolii* which locally degrades the pectin matrix but not cellulose or xyloglucan in the cell walls (Simon *et al.*, 2005). In necrotrophic pathogens, pectin degradation by enzymes is important to

achieve a successful infection. The action of pectin degrading enzymes is required to extensively breakdown the cell wall matrix and to uncover the range of cell wall polymers to the action of other CWDEs (Pogorelko *et al.*, 2013; Lionetti, 2015).

Production of pectin degrading enzymes has been studied in detail in the hemibiotrophic leaf blotch pathogen, *Mycosphaerella graminicola*, comparing the situations during plant infection and *in vitro* growth (Douaiher *et al.*, 2007; Reignault *et al.*, 2008). Correlation tests and principal component analysis showed a significant correlation between the *in vitro* production of xylanase and pectinase and *in planta* pathogenicity components. The results suggested that these CWDEs are key determinants of pathogenicity in *M. graminicola*. Furthermore, pectinases from hemibiotrophs can also have biological activities as in the case of elicitor activity of the endopolygalacturonase from *Colletotrichum lindemuthianum* (Boudart *et al.*, 2003).

4.4.2. Cascade of CWDE confirmed by RNA-Seq

The qPCR results obtained during my study are consistent with the results reported from the RNA-Seq experiment of the *P. parasitica*-lupin interaction by Blackman *et al.* (2015). A comparison of the results for the 11 CWDE genes is shown in Table 4.3. The expression peaks of each gene were classified as early (<36 hpi), middle (42-48 hpi) or late (54-60 hpi). There were similar results observed in both RNA-Seq and qPCR. For example, seven out of the 11 genes were expressed early during lupin infection and two PME genes (PPTG_10338 and PPTG_05287) were expressed and peaked early at 30 hpi both in RNA-Seq and qPCR. Differences were also observed, for example, two genes (PPTG_18589 and PPTG_15179) shown by the qPCR analysis to be expressed had no expression according to the RNA-Seq data. The qPCR results indicated that PPTG_15179 was expressed during mid-infection and PPTG_18589 was expressed late at 60 hpi. In addition, two genes (PPTG_07666 and 17850) were expressed during mid-infection at 48 hpi in RNA-Seq but were expressed later in qPCR at 54 hpi.

The degradation of cell wall components in lupin roots during a hemibiotrophic interaction was analysed and the expression of CWDE genes during the *P. parasitica*-host interaction was summarised and categorised as those expressed early or late (Blackman *et al.*, 2015). Those that were expressed early were CWDEs that (a) are involved in the degradation of pectin backbones, (b) remove methyl modifications from pectin, (c) break down the main chain of hemicellulose at random, (d) act on the main chains in RGI, (e) are responsible in cellulose degradation, and (f) are endo-acting CWDEs that degrade the cellulose and the hemicellulose backbone. CWDEs that were expressed late include those that (a) remove the acetyl groups from pectins and hemicellulose, (b) remove side chains from RGI and hemicellulose, (c) are in GHs and CBM1 families and that are responsible for cellulose degradation, (d) are exo-acting CWDEs that degrade cellulose and hemicellulose backbone, (e) are β-1,3-glucanase genes, and (f) are enzymes that degrade glycoproteins.

Table 4.3. Summary of RNA-Seq and qPCR data of the 11 CWDE genes examined in in the current study. The putative function, CAZyme family, *P. parasitica* accession numbers, the expression pattern (early, mid and late infection), RNA-Seq normalised reads per kilobase (NRPK) mapped to multiple locations (30 hpi to 60 hpi) and qPCR data (24hpi to 60 hpi) are shown. The colours of the cells are based on the level of expression of the gene (i.e. the darker the colour, the higher the expression).

Function	CAZyme family	Accession number	Expression pattern	RNA_Seq hours post inoculation (hpi)						qPCR hours post inoculation (hpi)						
				30 hpi	36 hpi	42 hpi	48 hpi	54 hpi	60 hpi	24 hpi	30 hpi	36 hpi	42 hpi	48 hpi	54 hpi	60 hpi
pectin methyl esterase (removes methyl groups from HG)	CE8	PPTG_10338	Early	183.78	103.81	144.30	56.58	15.65	10.91	0.55	0.47	0.30	0.27	0.17	0.06	0.05
pectin methyl esterase (removes methyl groups from HG)	CE8	PPTG_05287	Early	175.03	114.88	35.01	22.18	6.23	4.60	11.95	14.48	7.54	6.35	2.90	1.03	0.70
β-1,4-glucanase acting on cellulose	GH6	PPTG_00140	Late	0.00	0.00	0.70	1.74	3.96	2.55	0.00	0.00	0.08	0.22	0.40	0.17	0.18
β-1,4-glucanase acting on cellulose and hemicellulose	GH12	PPTG_19377	Mid	0.00	5.82	39.10	166.18	110.76	18.03	0.50	0.41	0.28	1.14	2.76	2.49	0.65
β-1,4-xylanase acts on β-1,4-xylans of xylans, glucuronoxylans and glucuronoarabinoxylans (hemicellulose)	GH10	PPTG_17240	Early	177.55	204.90	113.44	88.31	45.39	28.38	1.11	2.58	2.12	1.53	0.95	0.93	0.66
β-1,4-xylanase acts on β-1,4-xylans of xylans, glucuronoxylans and glucuronoarabinoxylans (hemicellulose)	GH10	PPTG_07666	Mid	27.04	36.59	35.64	53.32	38.02	12.47	14.12	23.37	21.69	20.82	26.59	27.05	11.83
β-1,4-xylanase acts on β-1,4-xylans of xylans, glucuronoxylans and glucuronoarabinoxylans (hemicellulose)	GH10	PPTG_17851	Early	45.09	47.31	28.69	24.55	6.22	4.84	1.76	1.88	2.25	1.47	1.11	0.38	0.26
β-1,4-xylanase acts on β-1,4-xylans of xylans, glucuronoxylans and glucuronoarabinoxylans (hemicellulose)	GH10	PPTG_17850	Mid	0.00	2.61	2.01	4.70	4.28	2.67	0.00	0.00	0.34	0.33	0.32	0.72	0.63
polygalacturonase (breaks α-1,4-GA linkages in HG)	GH28	PPTG_15162	Early	21.26	37.63	22.52	19.46	4.78	2.78	11.77	15.05	13.10	10.73	7.43	2.09	1.84
polygalacturonase (breaks α-1,4-GA linkages in HG)	GH28	PPTG_17704	Early	32.08	37.09	33.71	27.01	6.22	4.15	0.85	0.94	0.71	0.88	0.66	0.20	0.11
polygalacturonase (breaks α-1,4-GA linkages in HG)	GH28	PPTG_15179	—	0.00	0.00	0.00	0.00	0.00	0.00	0.00	0.00	0.00	0.16	0.14	0.10	0.12

4.4.3. Localisation of CWDEs

The current study used an immunocytochemistry technique to investigate the localisation of *P. parasitica* CDWEs. The results revealed that two PnPG6 MAbs localised to the tips of germinated cysts and to sites of hyphal branching. Localisation of proteins may occur differently in various systems (Simon *et al*., 2005). For instance, *P. infestans* CesA proteins were localised to the plasma membrane of growing hyphal tips and cysts and to infection vesicles in appressoria but were not localised in sporangia or zoospores (Grenville-Briggs *et al.*, 2008). These observations were taken as evidence that cellulose plays a key role in the appressorial cell wall. The cyst germination-specific acidic repeat proteins of *P. infestans* are rapidly produced during cyst germination and appressoria formation and are localised at the surface of the germlings (Görnhardt *et al.*, 2000).

Antibodies raised against a purified glycoprotein were localised on the cell surface of *P. parasitica* hyphae and on the flagellum surface in the wall-less zoospores (Séjalon-Delmas *et al.*, 1997). Some fungal pathogens showed evidence that certain enzymes are localised specifically in hyphal tips while other enzymes are localised in different parts of the cell. For example, immunogold labelling in *Aspergillus niger* showed glucoamylase localised only at the tips of growing hyphae (Wösten *et al.*, 1991). Intracellular localisation of *Neurospora* invertase showed that (a) conidial invertase was distributed evenly on the periphery of the cell, (b) after the conidial cell wall peripheral activity, pronounced invertase activity was observed in growing hyphal tips, (c) in early log-phase, hyphae has a strong enzyme activity in the cell wall and during late log-phase, activities are concentrated in the plasma membrane and on the points of new hyphal branches formation, and (d) strong fluorescence at developing branching points of hyphae in early stationary phase (Chung and Trevithick, 1970). In the current study, antibodies against polygalacturonases, while localising to the walls of germinated cysts, failed to react on sections of infected material. One possible explanation for this is that the binding of polygalacturonases to HG may inhibit the binding of the antibodies. Masking of antibody labelling and the enzymatic removal of specific cell wall components to

allow antibody access have been successfully used to gain insights into the structure of plant cell walls (Marcus *et al.*, 2008; Hervé *et al.*, 2010; Kim and Daniel, 2012a; Kim and Daniel, 2012b). A similar strategy may improve labelling in infected material by the polygalacturonase MAbs.

4.4.4. Concluding Remarks

P. parasitica causes disease in a wide range of plants, and is a suitable model in understanding Oomycete plant pathogens. Although tobacco (Wi *et al.*, 2012; Cho *et al.*, 2013; McCorkle *et al.*, 2013), tomato (Blaker and Hewitt, 1987; Grote *et al.*, 2002) and Arabidopsis (Wang *et al.*, 2011; Larroque *et al.*, 2013) have been used to study *P. parasitica*, the investigation reported in this chapter demonstrates the value of the lupin seedlings as a model *P. parastica* infection assay system. Using the lupin assay, temporal patterns of CWDE gene expression during the first 60 h of disease development were determined using qPCR. Among a range of important outcomes, the experiments described in this chapter revealed that of the 11 genes analysed by qPCR, all were expressed at 48 hpi. This result provided valuable information for the establishment of an experimental strategy with which to study the effects of phosphite on the infection transcriptome as described in the next chapter of this thesis.

CHAPTER 5

The effects of phosphite on *Phytophthora* growth, development and gene expression

5.1. Introduction

5.1.1. The use of phosphite to control *Phytophthora* diseases

Phosphite is a salt of phosphonic acid (H_3PO_3), an analogue or reduced form of phosphate, and a systemically mobile chemical that is translocated in both the xylem and phloem (Jackson *et al.*, 2000; King *et al.*, 2010; Eshraghi *et al.*, 2011a). Phosphite, also referred to as phosphonate, contains a carbon-phosphorus bond that is found in phosphonic acid and Fosetyl-Al (aluminum tris-*O*-ethyl phosphonate). The term phosphite is used in the recent literature to refer to the phosphonic acid salts used to control *Phytophthora* (Hardy *et al.*, 2001a; Stasikowski *et al.*, 2014). Phosphite is effective against *P. palmivora* in durian (Bunyanupappong, 1990), *P. ramorum* that causes sudden oak death (Garbelotto *et al.*, 2009), and *P. cinnamomi* diseases such as chestnut ink disease (Gentile *et al.*, 2009), and root and heart rot of pineapple (Anderson *et al.*, 2012). In Australia, phosphite has been extensively used as a fungicide in situations where *Phytophthora* damage is extensive and a wide range of plant species are being infected (Hardy *et al.*, 2001a; Cahill *et al.*, 2008; Pilbeam *et al.*, 2011).

Researchers have explored the use of different phosphite application methods to achieve the optimum disease control. In a study conducted between 1986 and 1988 in South Australia, *P. cambivora* in almond and cherry trees was inhibited by phosphite when applied as either soil drench, foliar spray or by trunk injection (Wicks and Hall, 1990). The foliar application of phosphite slowed the colonisation of *P. cinnamomi* on five Western Australian native plant species (Wilkinson *et al.*, 2001b). The effects of phosphite application methods on *P. cinnamomi*-threatened communities showed more effectiveness when phosphite was applied as a stem injection or spray rather than aerial application (Crane and Shearer, 2014). The long-term effect of phosphite depends on both the type of plant treated and the time of the year plants are inoculated with *P. cinnamomi*

(Wilkinson *et al.*, 2001b). The diverse responses of *Phytophthora* species to phosphite treatment highlights the need to evaluate the efficacy at the species level (Crane and Shearer, 2014).

5.1.2. Mode of action of phosphite

The exact mechanism of phosphite control of *Phytophthora* is not fully understood. However, phosphite has been shown to act both directly and indirectly on *Phytophthora* (Fenn and Coffey, 1985; Smillie *et al.*, 1989; Wong *et al.*, 2009). Direct adverse effects of phosphite on *P. cinnamomi* include inhibition of mycelial growth, oospore development, sporangia formation, release of zoospores and production of chlamydospores (Coffey and Joseph, 1985; Wong, 2006). Phosphite also causes hyphal swelling, hyphal branch distortion, and the lysis of sporangia, zoospores and chlamydospores (Wong et al., 2009). At high concentrations, phosphite acts directly on *P. cinnamomi* to inhibit its growth before it can establish an association with the host (Jackson *et al.*, 2000).

The indirect mode of action of phosphite involves stimulating natural host defence mechanisms (Guest, 1984; Smillie *et al.*, 1989). The significance of phosphite treatment is that it induces a strong and rapid defence in infected host plants (Guest and Bompeix, 1990). Drenching plant roots in phosphite can provide protection against *P. cinnamomi*, *P. nicotianae* and *P. palmivora* as evidenced by a decrease in lesion growth (Smillie *et al.*, 1989). Treatment of *P. parasitica*-inoculated tobacco with phosphite leads to phytoalexin accumulation, as seen by an increase in phenylalanine ammonia lyase activity, and ethylene production (Nemestothy and Guest, 1990). At low concentrations in the roots of *Eucalyptus marginata*, phosphite acts in conjunction with *P. cinnamomi* and stimulates a significant increase in two enzymes involved in the production of lignin, 4-coumarate coenzyme A ligase and cinnamyl alcohol dehydrogenase, resulting in decreased lesion development (Jackson *et al.*, 2000). The broad effects of phosphite on plant defence and plant metabolism in potato leaves infected with *P. infestans* suggest that phosphite triggers a hypersensitive response resulting in resistance (Lim *et al.*, 2013). However, despite the induction of some enzymes involved in plant defence and the observation of

morphological changes in *Phytophthora*, many aspects of phosphite control are yet to be resolved.

5.1.3. Sensitivity of *Phytophthora* isolates to phosphite

One issue in the control of *Phytophthora* by phosphite is the high variability of phosphite sensitivity within and between *Phytophthora* species (Coffey and Bower, 1984; Wilkinson *et al.*, 2001b). Most *in vitro* assays that measure sensitivity of *Phytophthora* to phosphite treatment have involved the determination of the dose at which the pathogen's growth is inhibited by 50%. This is known as the effective dose$_{50}$, ED50. The *in vitro* sensitivity of isolates of *Phytophthora* species to phosphite has been reported to range from 5 to 224 µg/ml (Coffey and Bower, 1984). In that study, the most sensitive species were *P. citricola*, *P. citrophthora* and *P. cinnamomi* and the most tolerant was *P. megasperma* f. sp. *medicaginis*. A *P. infestans* isolate from potato had the highest ED50 value of 224 µg/ml. Growth of isolates of *P. cinnamomi* were inhibited by 11.3% to 38.5% in the presence of 5 µg/ml as compared to 27.9% to 58.8% inhibition of *P. parasitica* isolates with 10 µg/ml phosphite (Coffey and Bower, 1984). In another study, the differences in ED50 of five *Phytophthora* species to phosphite ranged from 5-10 µg/ml for *P. cinnamomi*, 13 µg/ml for *P. parasitica*, 27 µg/ml for *P. citricola*, 24 µg/ml for *P. palmivora* and 49 µg/ml for *P. capsici* (Wong, 2006).

5.1.4. Transcriptome analysis

It has long been recognised that knowledge of gene expression will be fundamental to understanding molecular mechanisms underlying cell development and function. Early studies of gene expression used RNA blots to assess levels of mRNA transcripts but this method involves a gene-by-gene analysis and quantitative data on relative expression levels from RNA blots are imprecise. Improvements to the quantification of gene transcript levels came with the development of microarrays (Wan *et al.*, 2002; Pirrung and Southern, 2014) and qPCR (Wilhelm *et al.*, 2003; Gachon *et al.*, 2004). In cDNA microarrays,

a matrix of oligonucleotides represents a selection of known genes, and transcripts present in a sample are identified by hybridisation to the oligonucleotide probes on a solid state support. Relative transcript abundance can be determined through the assessment of target-probe hybridisation through measurement of fluorescence or chemiluminescence intensity but is dependent on a known genome and hampered by technical issues such as background hybridisation and problems in the comparison between experiments (Wang *et al.*, 2009b). Despite this, a successful application of this approach to studies of *P. parasitica* is given in Attard *et al.* (2014). Differential gene expression during host penetration by *P. parasitica* showed changes in CWDEs and other proteins involved in pathogenicity such as RxLR effectors (Attard *et al.*, 2014) and elicitins and elicitin-like proteins, crinkling and necrosis proteins, and toxins (Torto-Alalibo *et al.*, 2003; Kebdani *et al.*, 2010; Jupe *et al.*, 2013; Attard *et al.*, 2014). For example, in *P. cinnamomi*, the putative crinkler effector (*CRN1*) was the highest expressed gene *in planta* (Meyer *et al.*, 2016).

The expressed sequence tags (ESTs) approach has been widely used to assess complements of transcripts in cDNA samples from various *Phytophthora* species, including *P. parasitica* (Shan and Hardham, 2004; Škalamera *et al.*, 2004; Panabières *et al.*, 2005; Le Berre *et al.*, 2008; Kebdani *et al.*, 2010). Another strategy has been the measurement of transcript abundance by qPCR but this requires prior knowledge of the gene sequence. The latter approach allows the comparison of relative transcript abundance of a selected gene to be made between different cDNA samples. However, comparison of expression levels of two or more genes is not possible due to variations in amplification efficiencies unless absolute transcript levels are determined through the use of standard curves for each gene of interest.

The recent development of Next Generation Sequencing (NGS) has had a major impact on many aspects of molecular genetics research, and in particular, genome and transcriptome sequencing. The method involves the parallel sequencing of DNA fragments such that millions of sequence reads are obtained concurrently, and at considerably reduced cost. In terms of transcriptome profiling, the best method currently available is that of RNA-Seq (Wang *et al.*,

2009). RNA-Seq analysis quantifies the abundance of transcripts in a sample by mapping sequence read data to an existing or constructed reference genome or transcriptome for the organism(s) in question. The approach has a number of important advantages over qPCR and microarray techniques (Ozsolak and Milos, 2010). It does not require prior knowledge of gene sequences as the information can be used to assemble a genome *de novo*; it has a much greater dynamic range than either qPCR or microarrays; it can yield information on alternative splicing and it provides a far more accurate measurement of levels of transcripts and their isoforms than other methods (Wang *et al.*, 2009b).

The number of studies that use RNA-Seq to analyse *Phytophthora* transcriptomes is expanding (Zuluaga *et al.*, 2016). The RNA-Seq approach has been used to compare transcript profiles of *P. phaseoli* growing *in vitro* with those during infection of its host, lima bean (Kunjeti *et al.*, 2012); *P. capsici* mycelia, zoospores and germinated cysts *in vitro* (Chen *et al.*, 2013a); *P. ramorum* during infection of its host, tanoak (Hayden *et al.*, 2014), and *P. parasitica* on the expression of genes encoding CWDEs during infection in lupin (Blackman *et al.*, 2015). RNA-Seq data have been used to study mitochondrial transfer mRNAs in *P. sojae* (Hafez *et al.*, 2013). RNA-Seq has also been applied to studies of plant defence during infection by *Phytophthora* (Legavre *et al.*, 2015; Serrazina *et al.*, 2015; Shen *et al.*, 2016; Zuluaga *et al.*, 2016). These studies include the interaction between potato and *P. infestans* (Gao *et al.*, 2013; Massa *et al.*, 2013; Ali *et al.*, 2014; Zuluaga *et al.*, 2016), the expression of effectors (RxLR and crinkler) during the pre-infection stages of *P. capsici* (Chen *et al.*, 2013a), and the interaction between raspberry (*Rubus idaeus*) and an unidentified *Phytophthora* species (Ward *et al.*, 2012).

The research described in this chapter aimed to determine the effects of phosphite on *Phytophthora* growth and development at a cellular and molecular level. Because the effects of phosphite have been studied extensively in *P. cinnamomi*, this species was included in preliminary experiments in order to help establish the design and parameters for the experimental regime to be used for phosphite treatment of *P. parasitica*. In the main experiments, samples of *P. parasitica* mycelia grown *in vitro* in the presence or absence of phosphite and of *P. parasitica*-infected lupin roots with or without phosphite pre-treatment were

prepared, and RNA isolated and submitted for RNA-Seq. The analysis of the resultant transcriptomic data focused on the effects of phosphite on patterns of expression of *P. parasitica* genes for CWDEs as a complement to the earlier qPCR studies of CWDE expression in *P. parasitica* described in Chapter 5.

5.2. Materials and Methods

5.2.1. *Phytophthora* isolates and culture

Two isolates of *P. cinnamomi* var. *cinnamomi,* 1248 and H1000 (DAR 52646, ATCC 200982), were used in the growth assays described in this Chapter. *P. cinnamomi* isolate 1248 was obtained from Dr Wayne Reeve (Murdoch University, WA). *P. parasitica* H1111 (ATCC MYA-141) was as described in Section 2.2.1.

In general, the culturing of *P. cinnamomi* isolates was the same as that described for *P. parasitica* (Section 2.2.1) apart for zoospore production. For *P. cinnamomi*, after growth on V8 agar for 5 days, the Miracloth discs with adherent hyphae were transferred to a 250 ml Erlenmeyer flask containing 100 ml V8 broth (Appendix I). The flasks were gently shaken (2-3.5 *g*) in the light at 23˚C overnight. The next day, the Miracloth discs with mycelia were washed four times in sterile mineral salts solution (Appendix I), and then left gently shaking in this solution for 24 h. The mycelia were transferred to Petri dishes and checked for the presence of sporangia. Release of *P. cinnamomi* zoospores was done as for *P. parasitica* as previously described (Robold and Hardham, 1998).

5.2.2. Effect of phosphite on *P. cinnamomi* growth

5.2.2.1. Preparation of phosphite solution

The phosphite used was phosphorous acid (H_3PO_3, Sigma-Aldrich, St Louis, USA). A 10% stock solution was prepared with sterile RO water. The pH of the solution was adjusted to 6.3 with 10 M potassium hydroxide as described in King *et al.* (2010). The stock solution was filter sterilised through a 0.2 µm Minisart filter (Sartorius Stedim, Albany, New York) and stored in the dark at 4˚C.

5.2.2.2. Mycelial growth assay

Growth assays were carried out on agar in 9 cm Petri plates containing 25 ml of modified Ribeiro's medium (MRM) (Ribeiro *et al.*, 1975; Fenn and Coffey, 1984) (Appendix I) containing the desired phosphite concentration. Plates with no phosphite served as untreated controls. Petri plates were inoculated with a 6-mm diameter inoculum plug taken from the growing edge of a *P. cinnamomi* colony on MRM, placing the plug of hyphae side down in the centre of the agar in the plate.

Colony radial growth was measured every 24 h by marking the edge of the colony with four measurements of the radius along x and y axes until the colony reached the edge of one of the plates in the experiment (Fig. 5.1). Each of these four measurements are based on different hyphal samples and can be considered as biological rather than technical replicates. There were thus 24 biological replicates for each phosphite concentration. For *P. cinnamomi* isolate 1248, 13 different levels of phosphite (3, 5, 9, 10, 15, 20, 25, 27, 30, 60, 72, 243, and 729 µg/ml), each with six replicate plates, were used and compared to growth on control plates lacking phosphite. The levels of phosphite used was based on log 3 and extra phosphite levels were added to the levels used to determine the ED50 in similar studies (Wong, 2006; Ludowici, 2013). Treatments with 0 and 729 µg/ml where included and showed either no inhibition or complete inhibition of growth, respectively. This assay protocol was also used for isolate H1000, but with a lower concentration range as preliminary experiments showed the H1000 isolate was more sensitive to phosphite. Thus, phosphite concentration levels was based on log 1.5 (1.5, 2.2, 3.3, 3.8, 4.2, 5.0, 6.3, 7.5, 11.3, 17.0, 25.6, 38.4, and 57.6 µg/ml). Plates were randomly distributed on shelves and incubated at 23˚C. At the end of the experiment, all plates were imaged on a flatbed scanner (Figure 5.1) and images were analysed using Adobe Photoshop CS5 (Version 12.04, USA). Daily growth of colonies was analysed using ImageJ software (Version 1.44, USA). Each of the four measurements from each plate can be considered to be a biological replicate resulting in 24 biological replicates for each phosphite concentration.

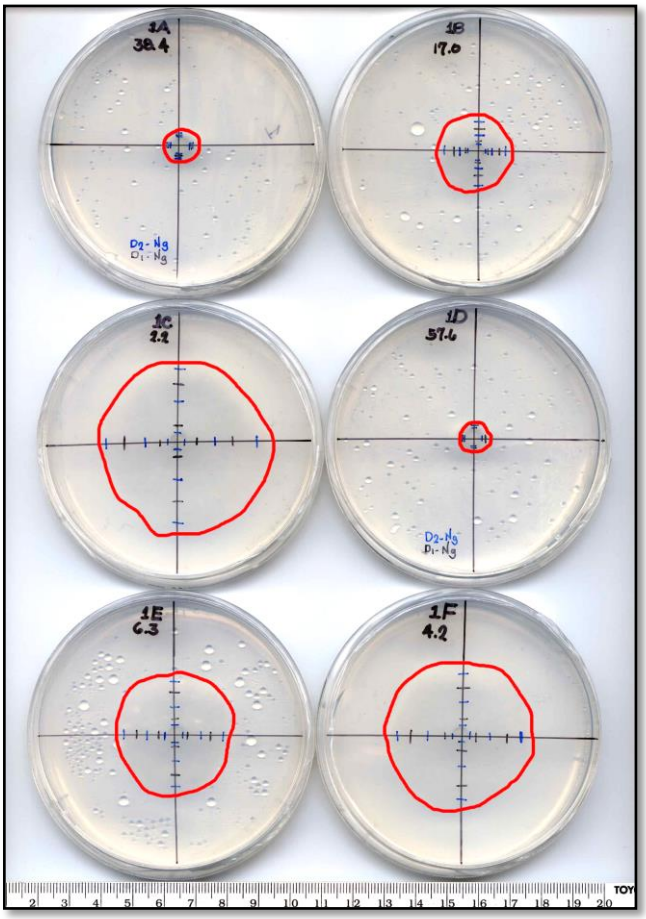

Figure 5.1. A scan showing Petri plates from each of six phosphite concentrations (38.4, 17.0, 2.2, 57.6, 6.3 and 4.2 µg/ml, as indicated on each plate) are shown at the end of an experiment. The short black or blue marks along the intersecting axes show the position of the edge of the colony of *P. cinnamomi* H1000 each day over a 4-day period. The outer edge of the colony is circled in red.

ED50 for a chemical inhibitor is defined as the concentration that reduces growth of an organism by 50% compared to that of untreated samples. ED50 of the radial mycelial growth was estimated using a simple linear regression analysis (Darakis *et al.*, 1997) in GenStat v.13 (VSN International, 2010). Genstat v. 13 was used to calculate the inflexion point (µ) of the curve (Equation 5.1). This was then back-transformed. The back-transformed inflexion point represents the ED50 for the data (Ludowici, 2013). The mean comparison of the radial growth on the

last day of observation was subjected to Student-Newman-Keuls test (GenStat Release 16.2, VSN International Ltd.).

Equation 5.1: The equation for a logistic curve used by Genstat v. 13 to fit the data.

Where:

$$y_i = \frac{\alpha + \gamma + \varepsilon_i}{1 + EXP\,(-\beta * (x_i - \mu)}$$

γ is the response variable (radial growth)

β is the slope parameter; α is one asymptote, x_i is the explanatory variable (phosphite concentration), μ is the point of inflexion for the explanatory variable, ε_i is the error term

5.2.3. Effect of phosphite on *Phytophthora* development

In preliminary experiments *P. cinnamomi* isolate 1248 was found to sporulate poorly, thus experiments investigating the effect of phosphite on *Phytophthora* morphology were conducted using *P. cinnamomi* H1000 and *P. parasitica* H1111 isolates.

5.2.3.1. Growth conditions of *Phytophthora* isolates in phosphite

After growing *P. cinnamomi* H1000 on Miracloth discs on nutrient agar for 5 days, the disks and mycelia were transferred to a 250 ml Erlenmeyer flask containing 100 ml V8 broth and 2.5 µg/ml phosphite. *P. cinnamomi* was cultured in the flasks as in Section 5.2.1. The mycelia were transferred to Petri dishes and checked for the presence of sporangia. Zoospores were released if sporangia were present and the method is described in Section 2.2.2. Hyphae, sporangia, and zoospores were fixed and stained as outlined below in Section 5.2.3.2. *P. parasitica* was grown on Miracloth discs on V8 agar for 5-7 days, the discs were transferred to a 250 ml Erlenmeyer flask added with 100 ml V8 broth and 50

µg/ml phosphite. After 3 weeks, the isolates were examined for the presence of sporangia. Zoospores were released as in Section 2.2.2.

5.2.3.2. Fixation, cryosectioning and microscopy

Tufts of hyphae were collected and fixed in 4% formaldehyde in 100 mM PIPES at pH 6.8 for 1 h. Fixed hyphae were rinsed in 100 mM PIPES with three changes for about 5 min each and once in sterile RO water. Hyphae samples were then embedded in Tissue-Tek ® optimal cutting temperature (O.C.T.) compound (Sakura®, ProSciTech) in cryomoulds (10 mm x 10 mm x 5 mm, Tissue-Tek ® Biopsy, ProSciTech) and frozen in liquid nitrogen. Sections of frozen hyphae, 12 µm thick were cut at -22˚C with a Reichert Jung 2800 Frigocut E Cryostat (Cambridge Instruments GmbH, Heidelberger, Germany). Samples were stored at -20˚C.

Zoospores were fixed in a final concentration of 4% formaldehyde in 100 mM PIPES buffer (pH 6.8) by mixing equal volumes of zoospore suspension and double-strength formaldehyde fixative in a 15 ml centrifuge tube for 30 min at room temperature. Cells were pelleted by centrifugation at 1500 *g* for 5 min. The fixative was removed and the pellet was resuspended in 3 ml of 100 mM PIPES for 5 min and washed twice. Mounting the cryosections of hyphae or 12 µl aliquots of zoospore suspension of on multi-well slides were outlined in Section 4.2.7.1. For morphological examination, hyphae and zoospores were fixed as described above. Hyphae were then stained with lactophenol trypan blue as described in Takemoto *et al.* (2003). The diameter of the hyphal fragments was measured using ImageJ software (Version 1.48, USA). The number of sporangia, chlamydospores and zoospores was determined from 15 fields of view in three replicates using a 40x objective lens.

5.2.3.3. Immunofluorescence labelling of vesicle components

Zoospores and hyphal cryosections were immunolabelled with mouse monoclonal antibodies (MAbs) raised against proteins from ventral surface vesicles (Vsv), and large peripheral vesicles (Lpv) and will be referred to as anti-

PcVsv1 (Robold and Hardham, 2005) and anti-PcLpv1 (Hardham *et al.*, 1986), respectively. The MAbs were hybridoma culture supernatants and were used undiluted. The secondary antibody used was sheep anti-mouse conjugated to fluorescein isothiocyanate (SAM-FITC; Jackson ImmunoResearch Laboratories Inc.) diluted 1 in 1000. Succeeding steps were described in Section 4.2.8.2. The effects of phosphite treatment were assessed quantitatively by counting the number of hyphal fragments from 12 field of views using a 40x objective lens containing immunolabelled vesicles in cryosections of mycelia or by counting the number of zoospores that contained immunolabelled vesicles.

5.2.4. Effect of phosphite on *P. parasitica* gene expression *in vitro* and during infection of lupin roots

5.2.4.1. Preliminary infection assay

A preliminary infection assay was done to determine the appropriate phosphite concentration to use in a full-scale experiment. A previous study by Ludowici (2013) had shown that the ED50 for *P. parasitica* H1111 on corn meal agar was 50.88 µg/ml. Thus, phosphite concentrations of 50 µg/ml and 100 µg/ml were initially tested. Twenty lupin seedlings were arranged randomly and evenly in plastic grids suspended over plastic boxes containing sterile RO water or phosphite solution for 1 hour. After treatment, the grids of seedlings were transferred to boxes containing sterile RO water for 10 min then to boxes containing 50 ml of a zoospore suspension at 1000 zoospores/ml. Lupin root inoculation and sample collection is described in Section 2.2.4. Roots were marked with waterproof ink at the point of the meniscus and hence the point of the highest concentration of zoospores. Assessment of the percent infection of phosphite-treated and untreated lupin seedlings and disease severity was based on the scale presented in Section 3.2.5.1.

5.2.4.2. Infection assay for RNA-Seq

The effect of phosphite pre-treatment on the degree of infection of the lupin roots by *P. parasitica* was assessed quantitatively by using the qPCR assay to determine the ratio of *P. parasitica*:lupin DNA in three biological replicates as outlined in Section 2.2.6.3. The infection assay used for the RNA-Seq transcriptome analysis followed the same procedure as described in Section 5.2.3.3 using 50 µg/ml phosphite. Some seedlings were treated with either 50 µg/ml phosphite or water but were not inoculated with *P. parasitica*. A previous RNA-Seq study had indicated that lupin roots at 48 hpi that had been infected with 1000 zoospores/ml generated between 4 and 13 million reads that mapped to the *P. parasitica* genome (Blackman *et al.*, 2015) a number similar to that reported in other plant pathogen RNA-Seq studies (e.g. Chen *et al.,* 2013; Ailloud *et al.,* 2016; Haddadi *et al.*, 2016). Four replicates were taken at 48 hpi with three roots in each replicate.

5.2.4.3. Treatment of *P. parasitica* mycelia with phosphite

Three biological replicates each consisting of four flasks of *P. parasitica* mycelia growing in sterilised MRM were prepared for each experimental sample. After growth at 23˚C for 9 days, cultures in 12 flasks were treated with 50µg/ml phosphite and cultures in another 12 flasks served as untreated controls. After 24 h, hyphae from each flask were harvested using a Büchner funnel lined with moistened filter paper. A small amount of sterile RO water was added to gather the hyphae at the centre of the funnel, before removal of liquid under vacuum (Diaphragm vacuum pump, Vacuubrand, Germany). Tufts of hyphae were placed in a 2 ml Eppendorf tube and weighed as quickly as possible, frozen in liquid nitrogen and stored at -80˚C. gDNA was isolated as described in Section 2.2.6.3.

5.2.4.4. RNA extraction and sequencing

Total RNA was extracted as described in Section 4.2.3. Assessment of RNA quality and quantity is outlined in Section 4.2.4. Approximately 10 µg of total RNA from three biological replicates of each treatment was sent to the Australian

Genome Research Facility (AGRF) for RNA quality analysis, library production and sequencing. These samples were total RNA isolated from (a) *P. parasitica* grown *in vitro* in liquid culture, (b) phosphite-treated *P. parasitica* grown *in vitro* in liquid culture, (c) lupin seedlings infected with *P. parasitica*, (d) lupin seedlings pre-treated with 50 µg/ml phosphite and infected with *P. parasitica*, (e) untreated lupin seedlings and (f) lupin seedlings treated with 50 µg/ml phosphite. Libraries were prepared using standard Illumina protocols (http://www.illumina.com/techniques/sequencing). Libraries produced from *P. parasitica* grown *in vitro* were multiplexed and run in one lane, whereas the lupin samples were divided into two lanes. The data were generated with the Illumina CASAVA pipeline version 1.8.2 by AGRF and consisted of 50 bp single end reads.

5.2.4.5. RNA-Seq analysis

Transcriptome analysis of the RNA-Seq data was performed in CLC Genomic Workbench 7.5.1 by Yueqi Zhang. Adaptors were removed by the CLC program and the read data analysed for quality and, if necessary, trimmed using quality scores. Reads were then mapped to the *P. parasitica* genome (phytophthora_parasitica_inra-310_2_supercontigs.fasta) downloaded from Broad Institute *Phytophthora parasitica* INRA-310 which had been annotated with the predicted transcripts (phytophthora_parasitica_inra-310_2_transcripts.gtf). CLC default mapping parameters were used and included mismatch cost at 2, insertion cost at 3, deletion cost at 3, length fraction and similarity fraction at 0.8. Read count analysis generated data that was multiple locations (reads matched more than one gene) and reads that mapped to more 10 locations (the default settings) were excluded. Expression values were given by the mean Reads Per Kilobase of transcript per Million mapped reads (RPKM) of three biological replicates. Differential expression (DE) between pairs of experimental data were determined using the Empirical Analysis of DGE (EDGE) component of CLC. EDGE performs the Exact Test and is based on the assumption that the count data follows a negative binomial distribution and accounts

biological variance (http://www.clcsupport.com). False Discovery Rate (FDR) corrected p-values were used to determine the significance of DE ($p < 0.05$).

A gene was considered to be expressed if the mean RPKM for the three biological replicates was >1. Where the RPKM value was <1 in one treatment and >1 in another treatment, a FDR >0.05 was taken into consideration (i.e. no significant difference between treatments). Only genes which were highly differentially expressed were included (fold change ≥ 2, FDR of $p \leq 0.05$, RPKM ≥ 2). These parameters were based on those found in the literature (Mortazavi *et al.*, 2008; Zenoni *et al.*, 2010; Gavery and Roberts, 2012; dos Santos Castro *et al.*, 2014). Reads mapping to alternative splice variants were omitted (322 from 20823 leaving 20501 predicted transcripts). Genes that had reads mapping to 61 predicted *P. parasitica* transcripts in mock-inoculated lupins were excluded from the analysis (Appendix Table 5.1). The analysis of the lupin transcriptome was omitted as the genome was not available at the time of the writing of this thesis and thus only the *P. parasitica* transcriptomes of the *in vitro* culture and during the infection of lupin with and without phosphite pre-treatment were included.

In this study, five *P. parasitica* genes previously shown to be constitutively expressed in qPCR and RNA-Seq studies (Yan and Liou, 2006; Blackman *et al.*, 2015), were used to assess the variation between treatments and biological replicates. These genes were the 40S ribosomal protein S3A (PPTG_07764, WS021), ubiquitin-conjugating enzyme (PPTG_08273), peptidyl prolyl isomerase 2 (PPTG_02092), WS041 (PPTG_09948) and phospholipase (PPTG_08636).

The top 20 *P. parasitica* transcripts according RPKM values and fold change were determined for each treatment (FDR of $p \leq 0.05$, DE ≥2-fold change, expression >200 RPKM). To identify proteins that may be important components of the effect of phosphite on *P. parasitica*, genes that were down-regulated or up-regulated in the presence of phosphite *in vitro* and also during infection were identified. In this analysis, only genes with a RPKM ≥5 in at least one treatment were considered and a DE ≥2-fold change with an FDR of <0.05.

While the *P. parasitica* genome has been annotated, additional information for some proteins was obtained by Blast2GO analysis (https://www.blast2go.com)

(Conesa *et al.*, 2005) and FungiDB (http://fungidb.org/fungidb/). Protein sequence alignments were done using CLUSTALW (https://npsa-prabi.ibcp.fr/cgi-bin/npsa_automat.pl? page=npsa_clustalw.html). Six groups of genes were subjected to a more detailed analysis and were the CWDEs, secreted effectors, elicitins, protease and glucanase inhibitors and kinases (Blackman *et al.*, 2015). Effectors were first identified by keyword search of the *P. parasitica* genome V2 and additional effectors identified using blast2GO. *Phytophthora* genes that were identified as differentially as being expressed in previous phosphite studies were also analysed (Wong *et al.*, 2009; King *et al.*, 2010). Gene Ontology (http://geneontology.org/) terms were obtained from FungiDB and classified into groups according to the hierarchy determined by Amigo1 (http://amigo1.geneontology.org/cgi-bin/amigo/go.cgi) (Carbon *et al.*, 2009). Some proteins annotated as hypothetical but which had GO terms were further analysed for known motifs by BLASTp of the NCBI non-redundant protein database (Altschul *et al.*, 1997; https://www.ncbi.nlm.nih.gov/). This analysis, along with the Pathways and Interactions component of FungiBD was used to determine broad functional groups for individual *P. parasitica* proteins. Down- and up-regulated *P. parasitica* genes *in vitro* and *in planta* in the absence and presence of phosphite pre-treatment were analysed and presented in scatterplots using REVIGO Web server (http://revigo.irb.hr/). REVIGO summarised the data and presented a list of GO terms that are highly redundant; it also has cluster algorithms based on semantic similarity (Supek *et al.*, 2011).

5.3. Results

5.3.1. Effect of phosphite on the growth of *P. cinnamomi* hyphae

5.3.1.1. *P. cinnamomi* 1248 ED50 determination

P. cinnamomi 1248 colony growth was measured every 24 h for 8 days. In the absence of phosphite, the radius of the colony grew on average 2.55 cm during the experiment (Figure 5.2). Addition of 3 µg/ml phosphite did not significantly inhibit hyphal growth but inhibition occurred above this concentration (Table 5.1). Phosphite concentrations of 243 µg/ml and 729 µg/ml completely inhibited

the mycelial growth (Figure 5.2). A logistic curve was fitted to the mean growth measurements using the log (Phosphite + 1) as the explanatory variable (Figure 5.3). The estimate of the log (dose) gives an ED50 value of 3.90 with a back transformed value of 46.70. This means that the ED50 of isolate 1248 is 46.70 µg/ml.

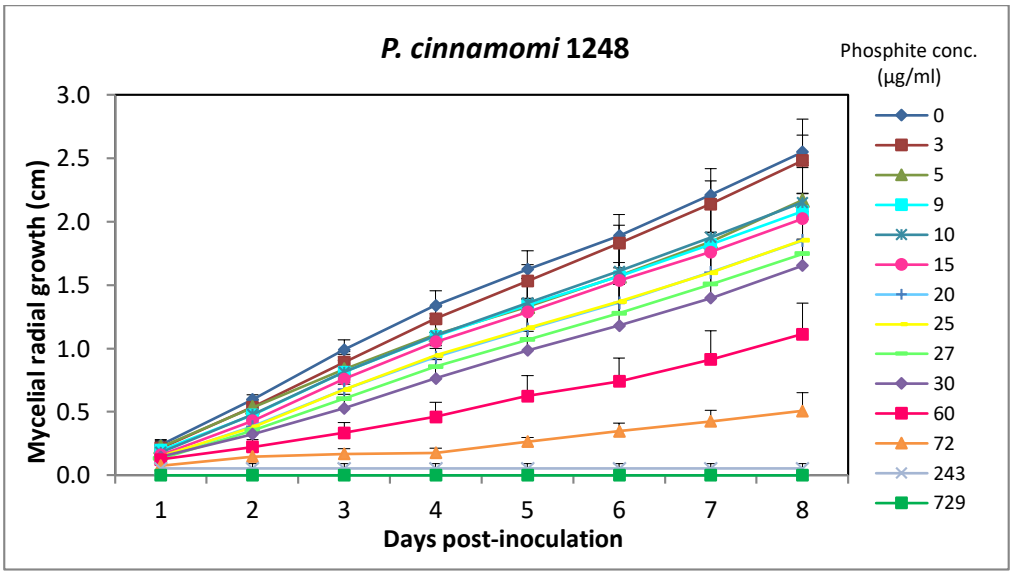

Figure 5.2. Average colony radius of *P. cinnamomi* 1248 growing on modified Ribeiro's medium with different phosphite concentrations. Error bars represent the standard error of the mean (n= 24).

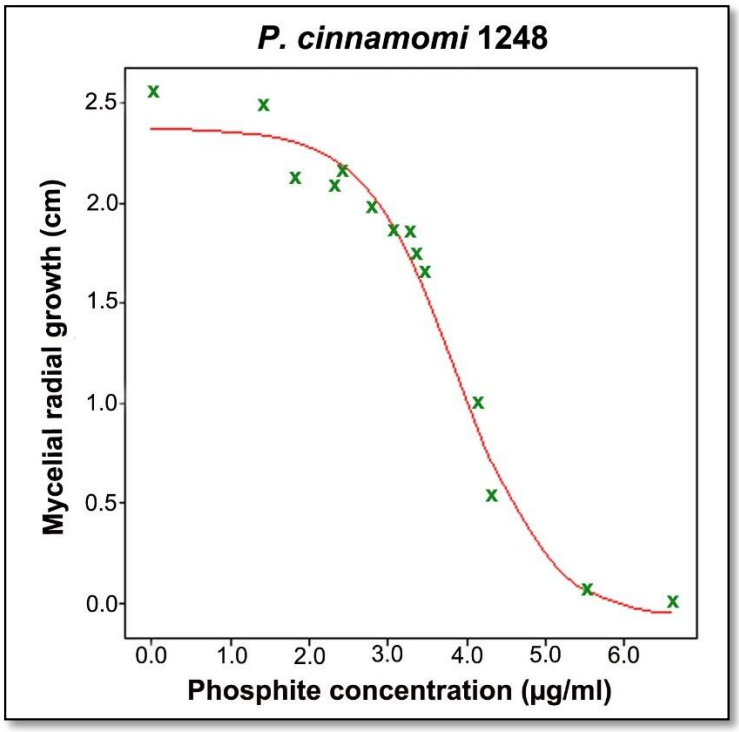

Figure 5.3. Relationship between the radial growth of *P. cinnamomi* 1248 mycelia on modified Ribeiro's medium with different phosphite concentrations. A curve (red line) is fitted to the observations (green crosses).

Table 5.1. Statistical comparison of the means of radial growth of *P. cinnamomi* 1248 at different phosphite concentrations.

Phosphite concentration (µg/ml)	Means of mycelial radial growth (cm)
0	2.55[a]
3	2.48[a]
5	1.98[bcd]
9	2.08[bc]
10	2.15[b]
15	1.97[bcd]
20	1.85[bcd]
25	1.85[bcd]
27	1.75[cd]
30	1.66[d]
60	1.00[e]
72	0.53[f]
243	0.05[g]
729	0.00[g]

Means with the same letters show no significant difference at the 0.05 level using the Student-Newman-Keuls multiple range test.

5.3.1.2. Determination of the ED50 on *P. cinnamomi* H1000

Initially, the same range of phosphite concentrations (3-729 µg/ml) was used to determine the ED50 of both *P. cinnamomi* isolates. However, the H1000 isolate grew faster and was more sensitive to phosphite than the 1248 isolate (Figure 5.4). Mycelial growth on MRM without phosphite reached the edge of the agar 4 days post inoculation (dpi). At phosphite concentrations of 27 µg/ml or higher, almost no mycelial growth was observed (results not shown). It was not possible to determine the ED50 from this experiment. The growth assay was repeated using a lower range of phosphite concentrations, namely 0-57.6 µg/ml (Figure 5.5). The average mycelial growth on MRM without phosphite was 3.40 cm over 8 days and differed significantly from growth on phosphite-containing medium. The highest phosphite concentration of 57.6 µg/ml did not completely inhibit the growth of *P. cinnamomi* H1000 and a growth mean at 57.6 µg/ml was not significantly different to that at 38.4 µg/ml phosphite (Table 5.2). In general, phosphite treatment significantly ($P<0.01$) inhibited the mycelial growth of *P. cinnamomi* H1000 on the final day of measurement (day 4). After fitting the logistic curve to the growth data (Figure 5.6), the estimate of the log (dose) gave an ED50 value of 1.26 for the log concentration and the back-transformed value is exp (1.26) – 1 which is 2.54 and hence the ED50 for *P. cinnamomi* H1000 is 2.50 µg/ml.

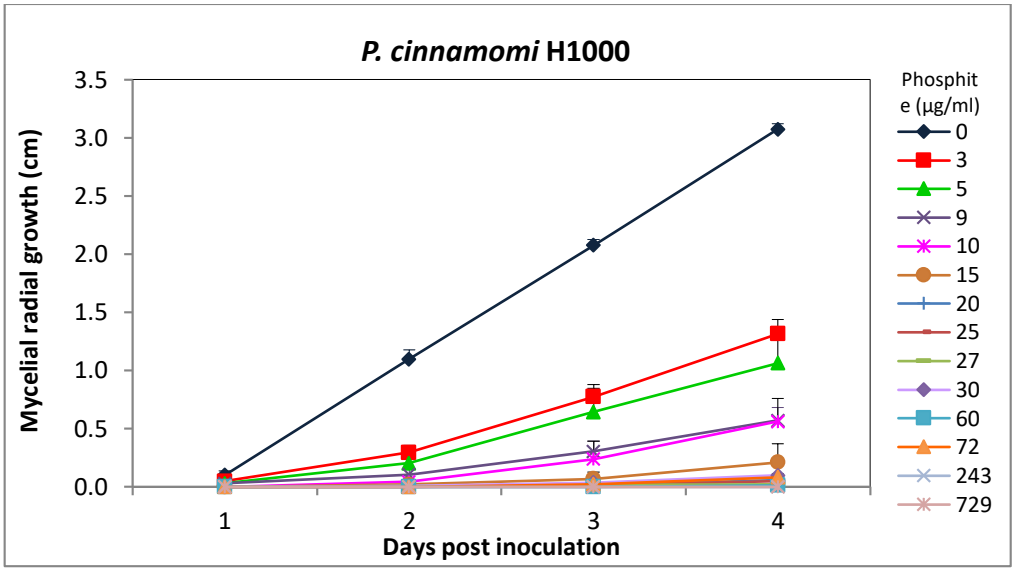

Figure 5.4. Average colony radius of *P. cinnamomi* H1000 growing on modified Ribeiro's medium at 0-729 µg/ml phosphite. Error bars show the standard error of the mean (n=24).

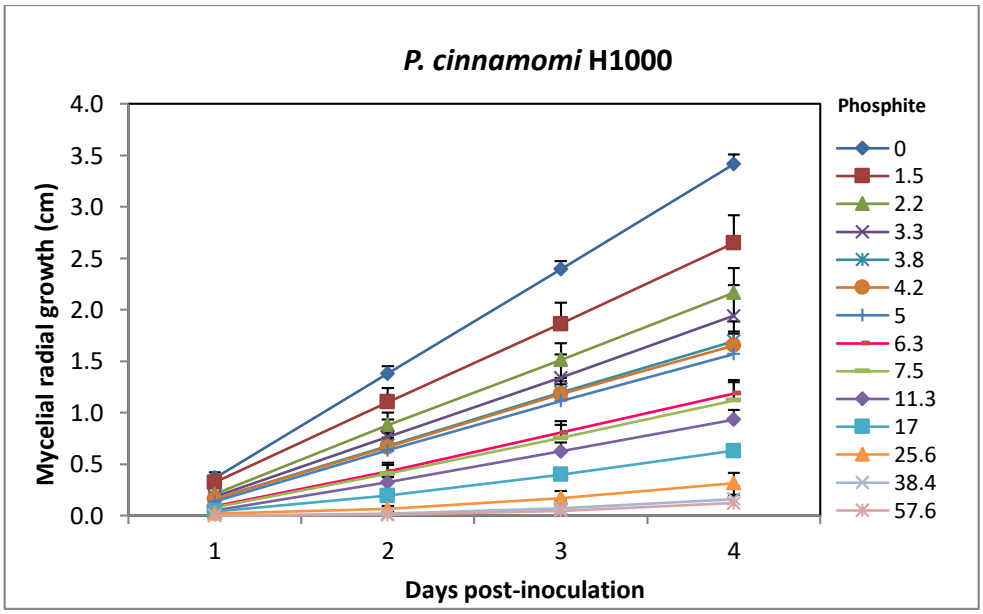

Figure 5.5. Average colony radius of *P. cinnamomi* H1000 growing on modified Ribeiro's medium with 0-57.6 µg/ml phosphite. Error bars represent the standard error of the mean (n=24).

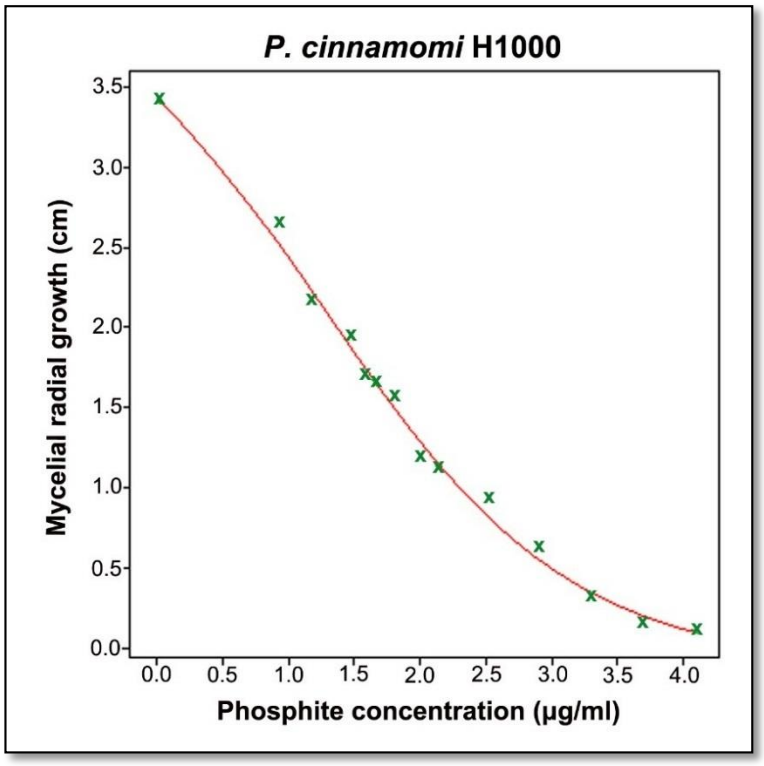

Figure 5.6. Fitted and observed relationship of mycelial radial growth of *P. cinnamomi* H1000 grown on modified Ribeiro's medium in the presence of different phosphite concentrations.

Table 5.2. Statistical analysis of the means of *P. cinnamomi* H1000 radial growth at phosphite concentrations between 0-57.6 µg/ml.

Phosphite concentrations (µg/ml)	Means of mycelial radial growth (cm)
0.0	3.41[a]
1.5	2.65[b]
2.2	2.17[c]
3.3	1.94[d]
3.8	1.70[e]
4.2	1.66[e]
5.0	1.57[e]
6.3	1.19[f]
7.5	1.12[f]
11.3	0.93[g]
17.0	0.63[h]
25.6	0.32[i]
38.4	0.16[j]
57.6	0.12[j]

Means with the same letters show no significant difference at the 0.05 level using the Student-Newman-Keuls multiple range test.

5.3.2. Effect of phosphite on *Phytophthora* morphology

The addition of phosphite to the cultures of *P. cinnamomi* H1000 and *P. parasitica* H1111 produced dramatic changes to the morphology, number and size of sporangia, chlamydospores and hyphae.

5.3.2.1. *P. cinnamomi* H1000 morphology

There was a marked difference in the number and the size of sporangia and chlamydospores produced in *P. cinnamomi* cultures with and without 2.5 µg/ml phosphite. Sporangia produced *in vitro* without phosphite were mostly ovoid or ellipsoid with inconspicuous apical thickening, tapered or rounded at the base, and terminally borne as previously described (Erwin and Ribeiro, 1996) (Figure 5.7a), while those produced in phosphite were obturbinate (Figure 5.7b). In *P. cinnamomi* cultures without phosphite, sporangia had an average dimension of 63.8 x 36.8 µm (length-breadth ratio = 1.7). In contrast, the six sporangia found in phosphite cultures were approximately half the size and had a length-breadth ratio of 1.4 (Table 5.3). Chlamydospores were observed in the presence and absence of phosphite. In the absence of phosphite, chlamydospores had an average diameter of 42.0 µm, whereas in the presence of phosphite they had an average diameter of 22.0 µm (Table 5.3). Chlamydospores were globular in shape and often occurred in botryose clusters in both cultures (Figure 5.7c & d). The cytoplasm from phosphite-treated chlamydospores appeared to be plasmolysed (Figure 5.7d). Phosphite treatment resulted in swollen hyphae with short branches (Figure 5.7f) compared to those from untreated cultures (Figure 5.7e). The mean diameter of hyphae from phosphite cultures was 8.8 µm while from untreated cultures it was 6.0 µm (Table 5.3).

5.3.2.2. *P. parasitica* morphology

The shape of sporangia from *P. parasitica* cultures not treated with phosphite varied from ellipsoid, obpyriform to ovoid (Figure 5.7g) and had average dimensions of 70.0 x 44.5 µm (length-breadth ratio of 1.6) (Table 5.3). In contrast, far fewer sporangia were found in phosphite-treated *P. parasitica*

cultures and these were marginally smaller than those from the untreated cultures at 65.0 x 36.8 µm (length-breadth ratio of 1.8) (Table 5.3). These sporangia were ellipsoid, limoniform and turbinate and were plasmolysed (Figure 5.7h). Chlamydospores in non-treated cultures had a mean of diameter of 48.0 µm (Figure 5.7i, Table 5.3) compared to those from phosphite cultures with an average diameter of 42.3 µm (Table 5.3) and these latter were also plasmolysed (Figure 5.7j). Hyphae from untreated cultures had a smaller diameter (Figure 5.7k, Table 5.3) than those from the phosphite cultures and these were also short-branched (Figure 5.7l, Table 5.3).

Table 5.3. Measurement of the length and breadth of sporangia, of the diameter of chlamydospores and of the diameter of hyphae of *P. cinnamomi* H1000 and *P. parasitica* H1111 isolates, with (+) and without (-) phosphite (Phi).

Species	Treatment	Parameters	Sporangia	Chlamydospores	Hyphae
***P. cinnamomi* H1000**	-Phi	Mean (µm)	63.8 x 36.8	42.0	8.8
		Range (µm)	54.0-76.0 x 30.0-45.0	38.0-46.0	5.0-7.0
		Number	335	34	690
	+2.5 µg/ml Phi	Mean (µm)	26.0 x 18.0	22.0	6.0
		Range (µm)	22.0-30.0 x 12.0-24.0	14.0-26.0	7.0-11.0
		Number	6	14	10
***P. parasitica* H1111**	-Phi	Mean (µm)	70.0 x 44.5	48.0	4.5
		Range (µm)	60.0-84.0 x 40.0-50.0	35.0-71.0	4.0-5.0
		Number	322	19	10
	+50 µg/ml Phi	Mean (µm)	65.0 x 36.8	42.3	5.5
		Range (µm)	64.0-67.0 x 33.0-42.0	40.0-44.0	5.0-6.0
		Number	13	19	10

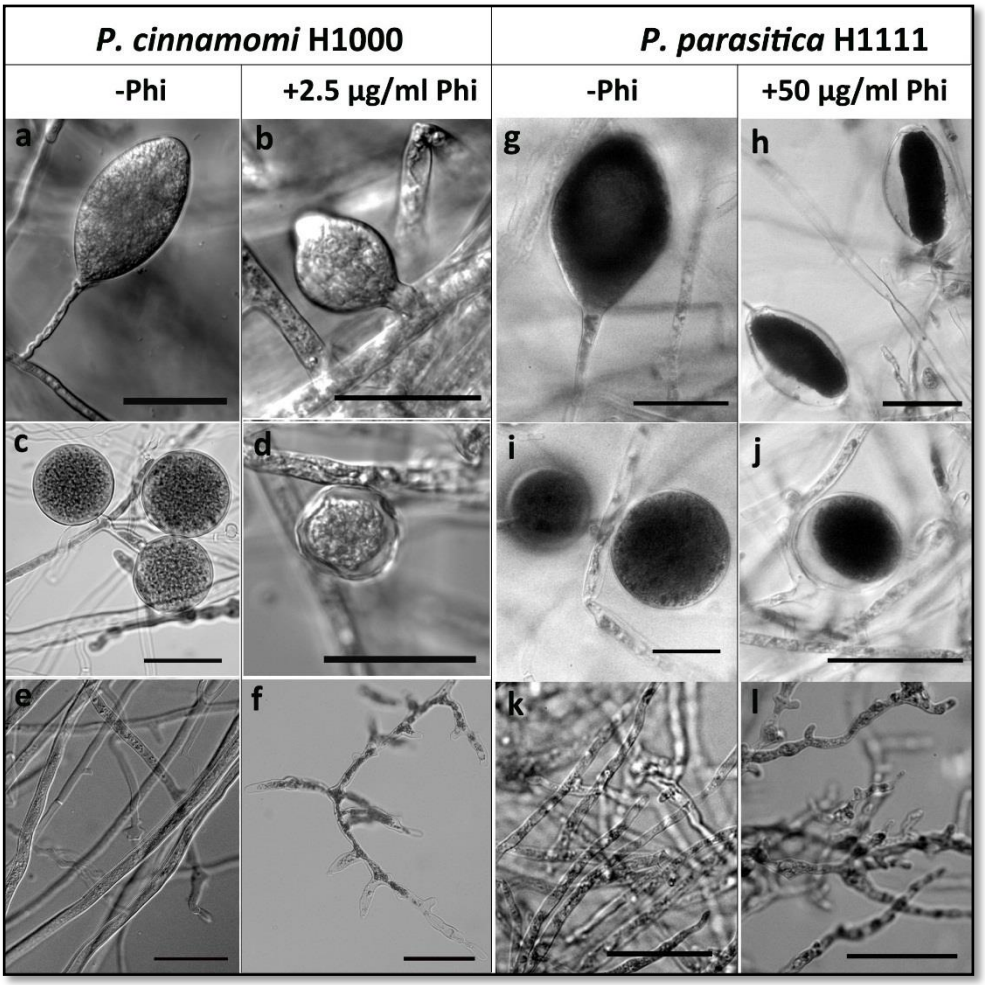

Figure 5.7. Microscopic examination of *P. cinnamomi* H1000 (a-f) and *P. parasitica* H1111 (g-l) isolates in untreated and phosphite-treated cultures. Untreated samples: sporangia (a and g), chlamydospores are spherical in shape (c and i), hyphae are straight with occasional branches (e and k). The cytoplasm of sporangia (h) and chlamydospores (d, j) was plasmolysed in cultures treated with phosphite, and the hyphae are distorted and swollen (f and l). Scale bars represent 40 µm.

5.3.3. Effects of phosphite on *Phytophthora* asexual sporulation and zoospore development

The decrease in the number of sporangia produced by *P. cinnamomi* and *P. parasitica in vitro* treated with phosphite may be related to a change in development and this was investigated by immunofluorescence localisation of

proteins produced during sporulation. Many of the components that are needed for the structure and function of *Phytophthora* zoospores are synthesised during sporulation and accumulate within the multinucleate sporangia and the timing of the appearance of some of these have been well characterised (Hardham et al., 1986). Anti-PcLpv1 and anti-PcVsv1 antibodies were used to examine the effect of phosphite on development. Because the *P. cinnamomi* isolate 1248 produced very few sporangia under any conditions, the immunocytochemical labelling studies were conducted on *P. cinnamomi* H1000 and *P. parasitica* H1111 isolates. A striking result from this study was that phosphite-treated cultures of both isolates did not produce zoospores, despite the presence of sporangia albeit in lower numbers (Section 5.3.2.2). Analysis of zoospores produced from cultures lacking phosphite was still carried out, providing controls for culturing conditions and immunofluorescence localisation.

In untreated hyphae from *P. cinnamomi*, 90% of the 397 hyphal fragments observed contained large peripheral vesicles labelled with the PcLpv1 antibody (Figure 5.8, Figure 5.9a-b). In contrast, in cultures treated with 2.5 µg/ml phosphite, only 16% of hyphal fragments (n = 440) were labelled with the anti-PcLpv1 antibody (Figure 5.9c-d). The anti-PcVsv1 antibody labelled 91% of hyphal fragments (n = 347) in untreated cultures (Figure 5.8, Figure 12a-b) and only 6% hyphal fragments (n = 450) in phosphite-treated cultures (Figure 5.11c-d). 92% of zoospores (n = 563) contained large peripheral vesicles labelled with anti-PcLpv1 antibodies (Figure 5.8, Figure 5.10). Almost all (98%) of the 402 zoospores examined were labelled by anti-PcVsv1 antibodies (Figure 5.8, Figure 5.12). Pairwise comparison revealed a highly significant ($p = <0.001$) difference between labelled hyphae from untreated and phosphite-treated samples.

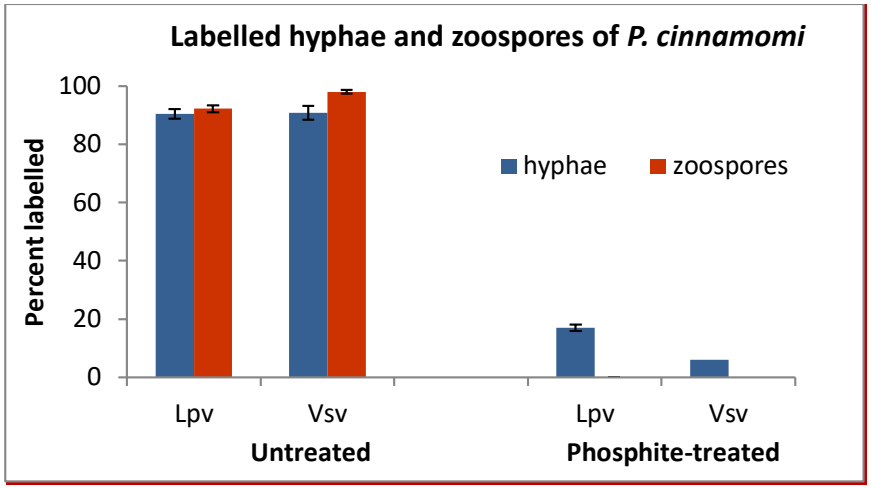

Figure 5.8. Immunofluorescence labelling of *P. cinnamomi* H1000 hyphae and zoospores with anti-PcVsv1 and anti-PcLpv1 antibodies in untreated and 2.50 µg/ml phosphite-treated samples. Error bars represent standard errors of the mean (n = 12 fields of view).

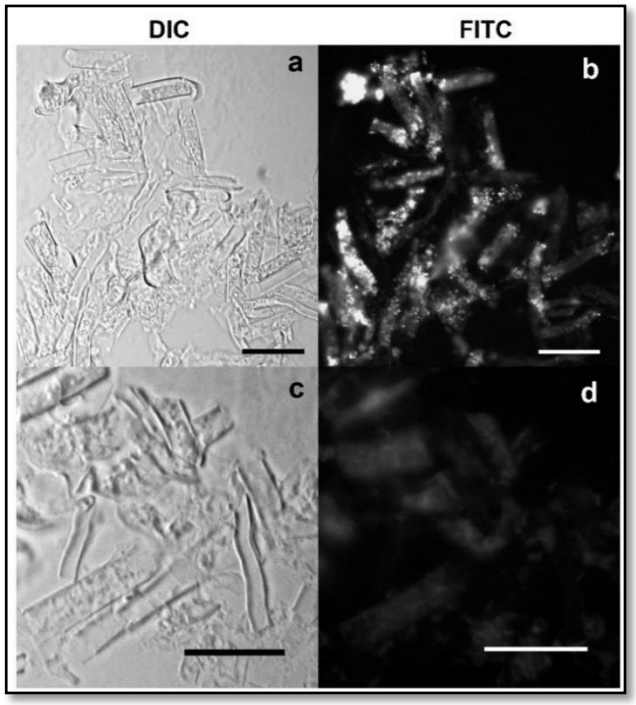

Figure 5.9. *P. cinnamomi* H1000 hyphae seen with differential interference contrast (DIC) (a & c) and fluorescence (FITC) (b & d) microscopy. Immunofluorescence labelling of proteins in large peripheral vesicles by the PcLpv1 antibody showed the abundance of vesicles in untreated hyphae (b) and their sparcity in 2.50 µg/ml phosphite-treated hyphae (d). Scale bar represents 20 µm.

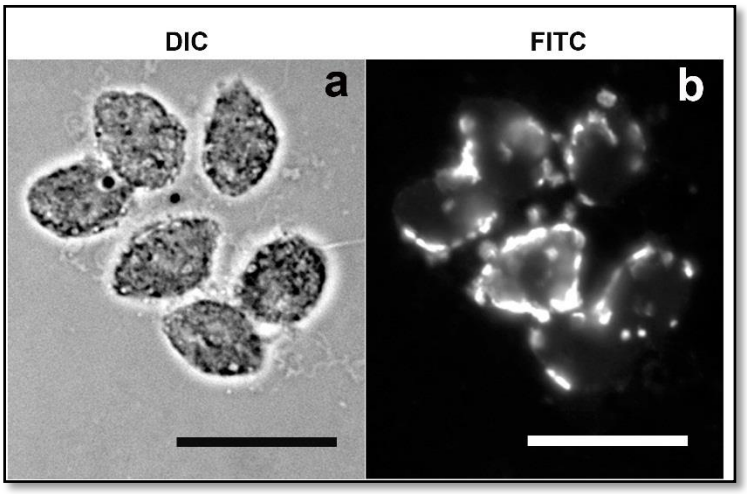

Figure 5.10. *P. cinnamomi* zoospores released by cultures growing without phosphite treatment as seen (a) using differential interference contrast (DIC) and (b) after labelling with the PcLpv1 antibody (FITC). Scale bar represents 20 µm.

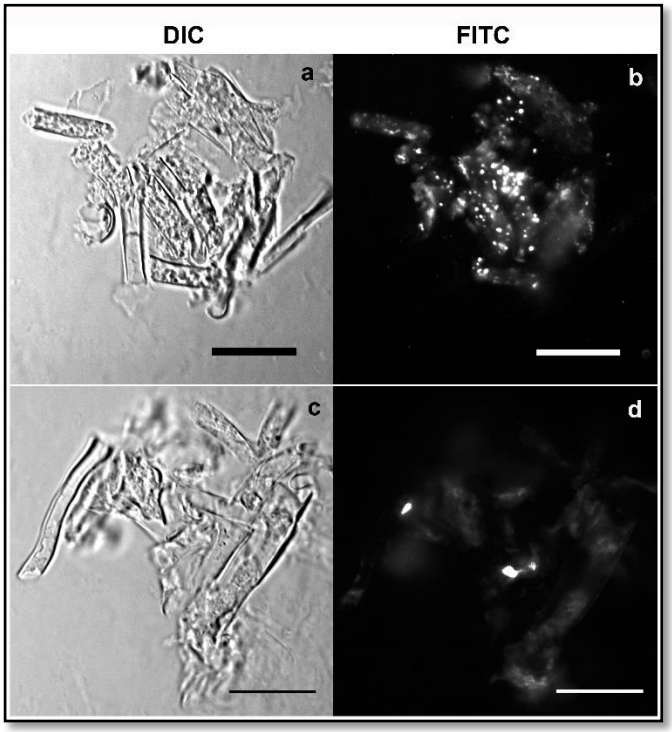

Figure 5.11. *P. cinnamomi* H1000 imaged using differential interference contrast (DIC) (a and c) and immunofluorescence (FITC) (b and d) microscopy. Labelling of ventral vesicles with PcVsv1 antibody in most hyphal fragments from the untreated sample (b) and with less labelling in samples treated with 2.50 µg/ml phosphite (d). Scale bar represents 20 µm.

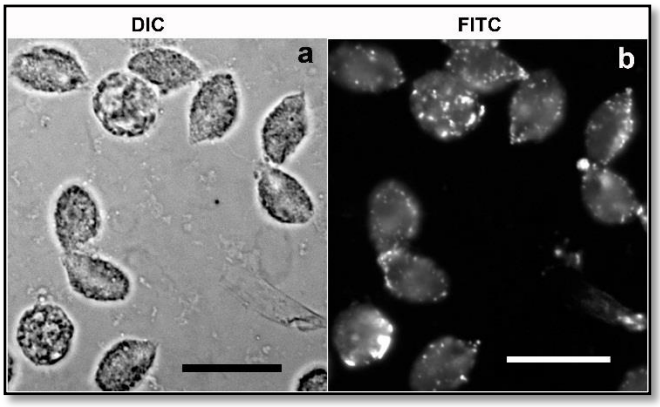

Figure 5.12. Control, untreated *P. cinnamomi* H1000 zoospores viewed using differential interference contrast (DIC) (a) and fluorescence (b) microscopy. The ventral vesicles of zoospores are labelled with the PcVsv1 antibody (b). Scale bar = 20 µm.

In untreated *P. parasitica* cultures, 91% of 618 hyphal fragments contained vesicles labelled with anti-PcLpv1 antibodies (Figure 5.13, Figure 5.14a-b) and 26% of 608 hyphal fragments treated with 50 µg/ml phosphite were labelled (Figure 5.14c-d). Immunofluorescence labelling showed 89% of hyphal fragments (n = 464) from untreated control samples were labelled with the antibodies raised against Vsv (Figure 5.16a-b) and in phosphite-treated hyphae (n=536) this was 7% (Figure 5.16c-d). Statistical analysis of the hyphal samples indicate a highly significant difference ($p = <0.001$) in vesicle abundance between *P. parasitica* samples in the absence or presence of 50 µg/ml phosphite. In the absence of phosphite, 100% of the zoospores were labelled by anti-PcLpv1 and anti-PcVsv1 antibodies (Figure 5.15, Figure 5.17). No zoospores were released in phosphite-treated samples.

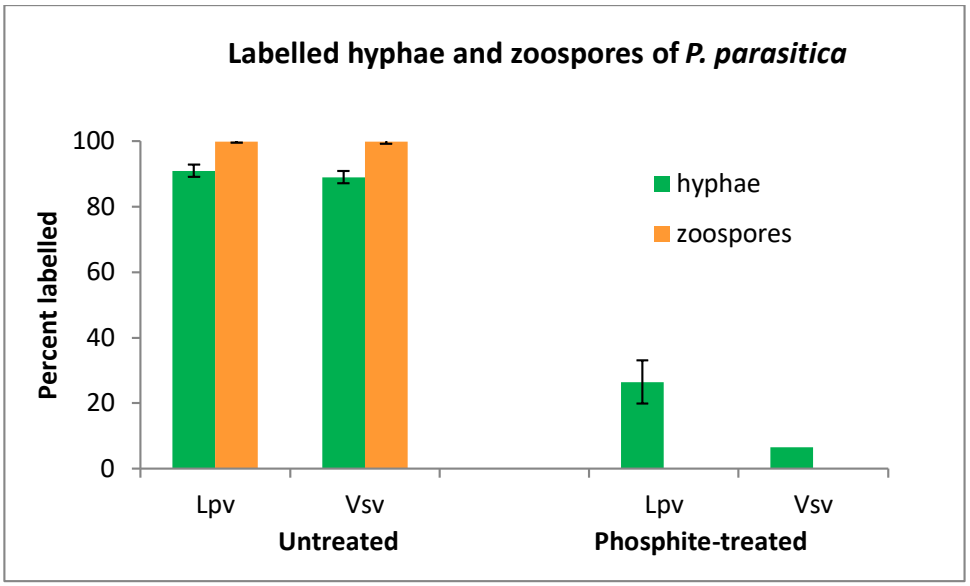

Figure 5.13. Immunofluorescence labelling of *P. parasitica* H1111 hyphae and zoospores with Lpv and Vsv in untreated and samples treated with 50 µg/ml phosphite. Error bars indicate standard errors of the mean (n=12 fields of view).

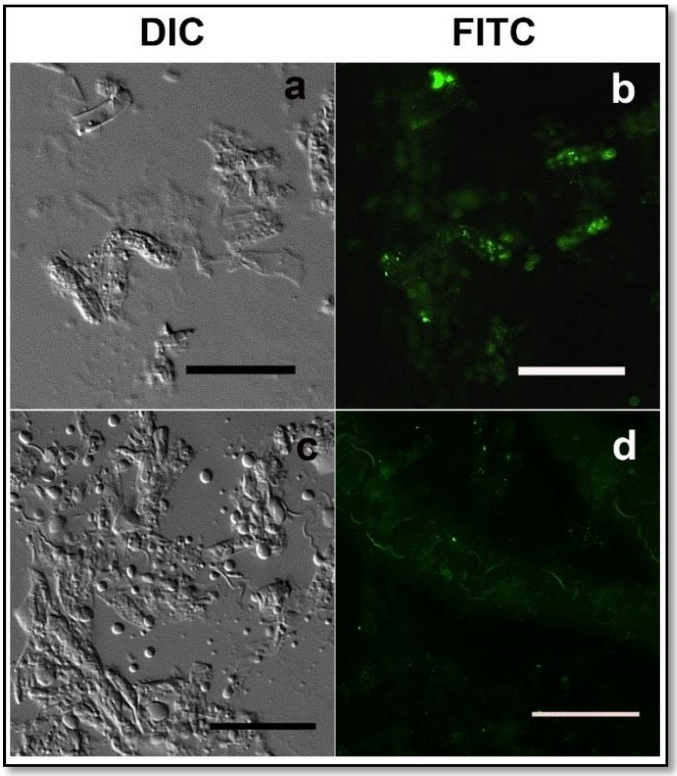

Figure 5.14. *P. parasitica* H1111 hyphae images using differential interference contrast (DIC) optics (a and c) and fluorescence (FITC) (b and d) microscopy. Immunofluorescence labelling of proteins in large peripheral vesicles with antibody PcLpv1 on untreated hyphae (b) and hyphae treated with 50 µg/ml phosphite (d). Scale bars represent 20 µm.

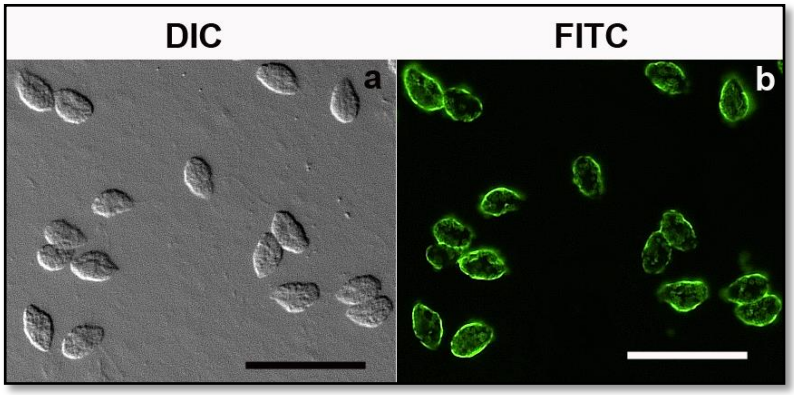

Figure 5.15. Untreated *P. parasitica* H1111 zoospores images using differential interference contrast (DIC) and fluorescence (FITC) microscopy. Immunofluorescence labelling of proteins in large peripheral vesicles with the PcLpv1 antibody (b). Scale bars represent 20 µm.

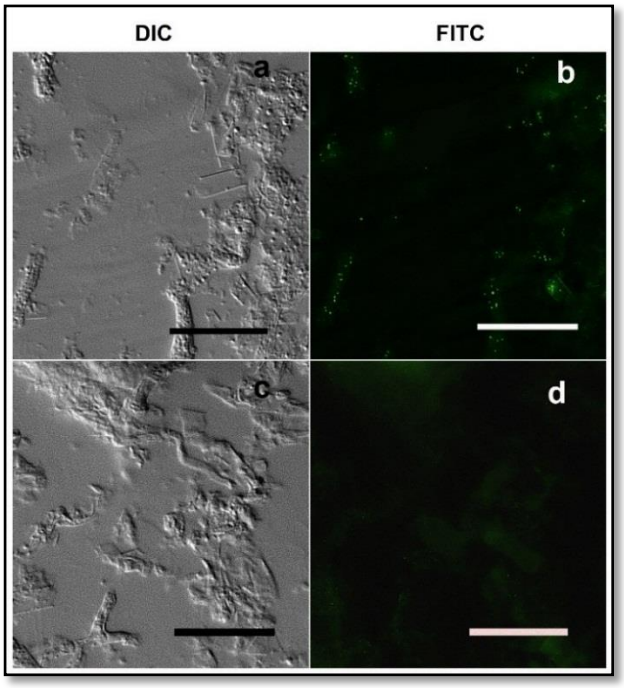

Figure 5.16. *P. parasitica* H1111 hyphae images using differential interference contrast (DIC) (a and c) and fluorescence (FITC) (b and d) microscopy. Immunofluorescence labelling of proteins in ventral vesicles with anti-PcVsv1 antibody (b) shows the presence of these vesicles in untreated hyphal fragments (b) and few in hyphal fragments treated with 50 µg/ml phosphite (d). Scale bars represent 20 µm.

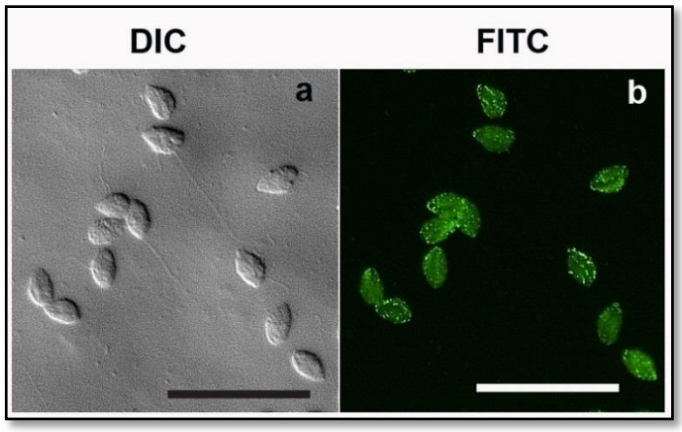

Figure 5.17. *P. parasitica* H1111 zoospores released from control hyphae imaged using DIC (a) and fluorescence (FITC) (b) microscopy. Immunofluorescence labelling of proteins in ventral vesicles with the anti-PcVsv1 antibody (b). Scale bars = 20 µm.

5.3.4. The effects of phosphite on the infection of lupin by *P. parasitica*

5.3.4.1. Lesion development and root colonisation

Uninoculated seedlings, with or without phosphite treatment remained healthy throughout the infection assay (Figure 5.18a). All seedlings inoculated with *P. parasitica* but not treated with phosphite, showed signs of infection 48 hpi (Figure 5.18b). At this time, between 5% and 100% of the length of the roots showed signs of necrosis with a disease severity between 3-9 based on the arbitrary scale presented in Figure 3.2 (Section 3.2.5.1). The most severely affected area coincided with the site of the surface of the zoospore suspension during inoculation (Figure 5.18b). In seedlings treated with 50 µg/ml phosphite for 1 h prior to inoculation, only 40% of seedlings inoculated with *P. parasitica* showed signs of infection at 48 hpi, with a disease severity between 1-5 along 1% to 25% of the root length (Figure 5.18c). In seedlings treated with 100 µg/ml phosphite for 1 h prior to inoculation, only 10% showed signs of infection, with only 5% of the length of the root being necrotic (Figure 5.18d). This preliminary experiment confirmed that pre-treatment of the lupin roots with 50 µg/ml phosphite for 1 h prior to inoculation and a post-inoculation time of 48 h were suitable parameter for the assay for the RNA-Seq study.

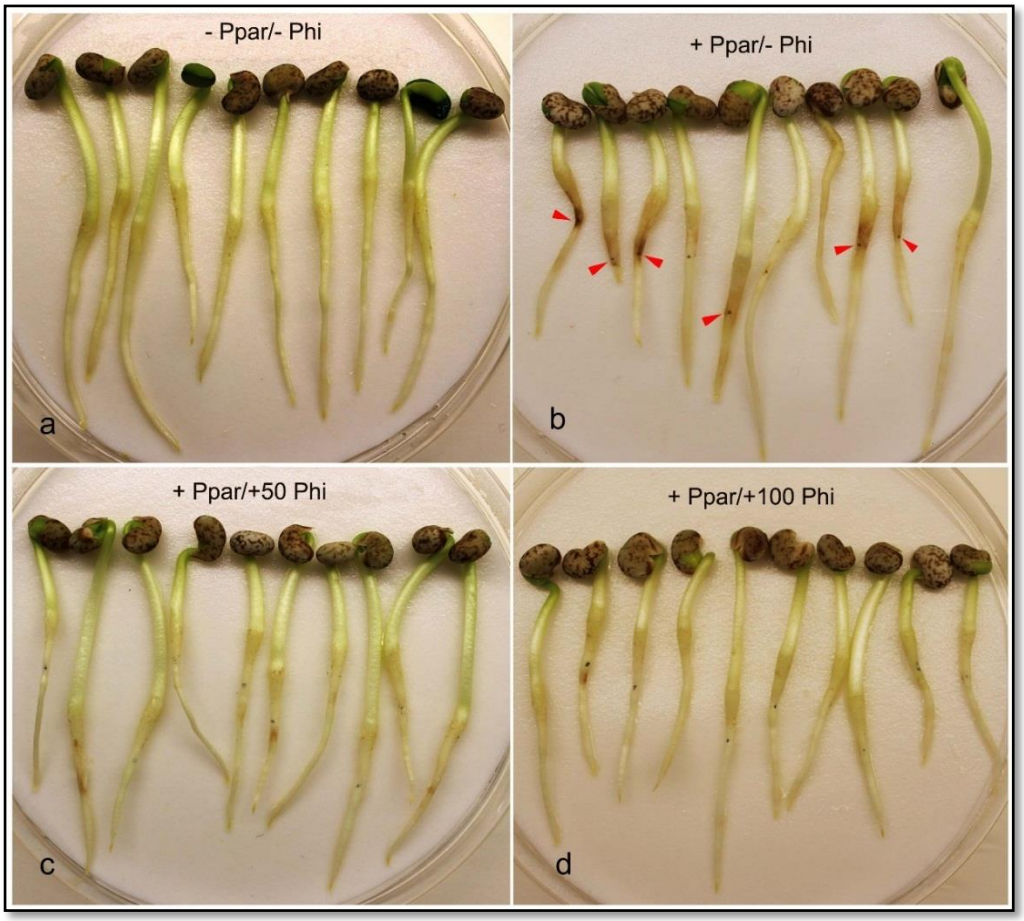

Figure 5.18. Lupin infection assay in untreated samples and samples inoculated with *P. parasitic* 48 hpi. (a) Seedlings that were not inoculated and not treated with phosphite (- Ppar/- Phi). (b) Seedlings that were inoculated with *P. parasitica* zoospores but not treated with phosphite (+ Ppar/- Phi), black marks on the roots show the level of inoculum surface and coincide with the highest zoospore concentration during inoculation (red arrow heads). (c) Seedlings that were inoculated after treatment with 50 µg/ml phosphite (+ Ppar/+50 Phi). (d) Seedlings that were inoculated after treatment with 100 µg/ml phosphite (+ Ppar/+100 Phi).

Pathogen load, as determined by qPCR, revealed that the ratio of *P. parasitica*:lupin DNA at 48 hpi was 6.1 in control samples, i.e. in the absence of phosphite pre-treatment (Figure 5.19). In contrast, the ratio of *P. parasitica*:lupin DNA at 48 hpi was 0.2 in seedlings that had been pre-treated with 50 µg/ml phosphite. No *P. parasitica* DNA was detected in seedlings treated with the

higher phosphite concentration or in the mock-inoculated seedlings. These results indicated that treatment of lupin roots with 50 µg/ml phosphite for 1 h inhibited *P. parasitica* growth and confirmed that 48 hpi was a suitable infection time for the transcriptome analysis by RNA-Seq.

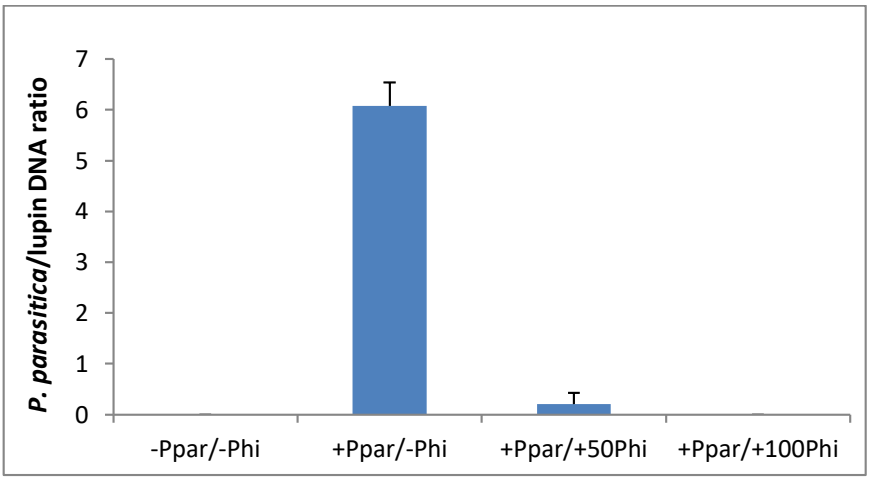

Figure 5.19. The ratio of *P. parasitica* to lupin DNA in three biological replicates at 48 hpi. -Ppar/-Phi: uninoculated and not treated with phosphite; +Ppar/-Phi: inoculated with *P. parasitica* but not treated with phosphite; +Ppar/+50Phi: inoculated after treatment with 50 µg/ml phosphite; +Ppar/+100Phi: inoculated after treatment with 100 µg/ml phosphite. Error bars represent standard error of the mean (n = 3).

The infection assay was repeated in order to prepare samples for RNA-Seq analysis. qPCR determination of pathogen load showed that the *P. parasitica*:lupin DNA ratio was 1.2 in inoculated samples that were not treated with phosphite and 0.4 in samples that were treated with 50 µg/ml phosphite (Figure 5.20). The concentration of total RNA varied between 0.63 and 3.40 µg/ml and the quality of RNA, as determined by the $A_{260}/A_{280\ nm}$ ratio, was deemed to be suitable for RNA-Seq (Table 5.4). The quality of RNA was confirmed by gel electrophoresis (Figures 5.21). Three of the four biological replicates with good quality total RNA and similar ratios of *P. parasitica*:lupin DNA were submitted for RNA-Seq.

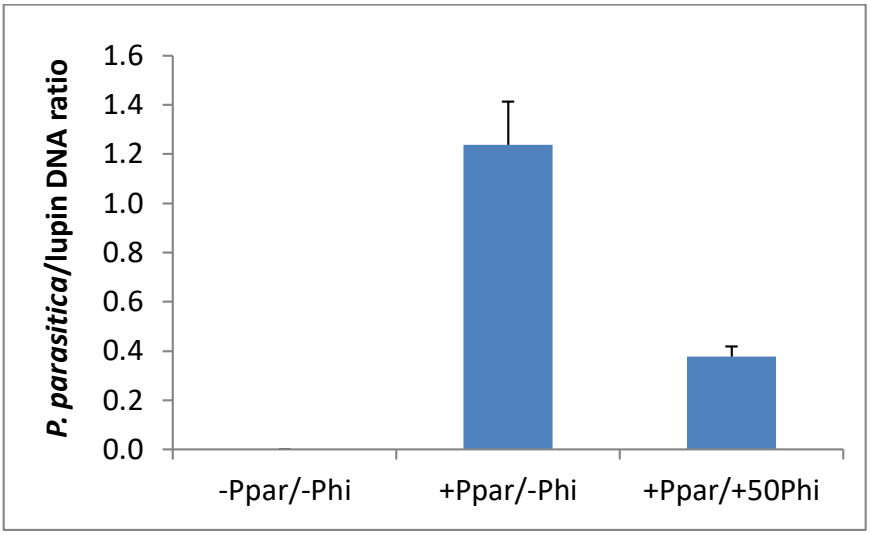

Figure 5.20. The ratio of *P. parasitica*:lupin DNA in four biological replicates at 48 hpi. Error bars indicate standard deviation of the mean (n=4).

Table 5.4. Total RNA concentration and quality as assessed by $A_{260}/A_{280\ nm}$ ratio. The replicate numbers from each treatment are shown (e. g. 9A, B and C).

Sample	Description	Concentration (µg/µl)	$A_{260}/A_{280\ nm}$
9A	*P. parasitica* mycelia	2.11	1.96
9B	*P. parasitica* mycelia	2.68	1.92
9C	*P. parasitica* mycelia	2.61	1.95
10A	*P. parasitica* mycelia + phosphite	1.93	1.95
10B	*P. parasitica* mycelia + phosphite	3.33	1.96
10C	*P. parasitica* mycelia + phosphite	3.40	1.96
11A	Mock-inoculated lupin	1.33	1.91
11B	Mock-inoculated lupin	0.83	1.91
11C	Mock-inoculated lupin	1.04	1.95
12A	Mock-inoculated lupin + phosphite	1.05	1.90
12B	Mock-inoculated lupin + phosphite	0.70	1.96
12C	Mock-inoculated lupin + phosphite	0.79	1.92
13A	*P. parasitica* inoculated lupin	1.05	1.90
13B	*P. parasitica* inoculated lupin	0.79	1.92
13C	*P. parasitica* inoculated lupin	0.74	1.96
14A	*P. parasitica* inoculated lupin + phosphite	1.04	1.94
14B	*P. parasitica* inoculated lupin + phosphite	0.70	1.94
14C	*P. parasitica* inoculated lupin + phosphite	0.63	1.88

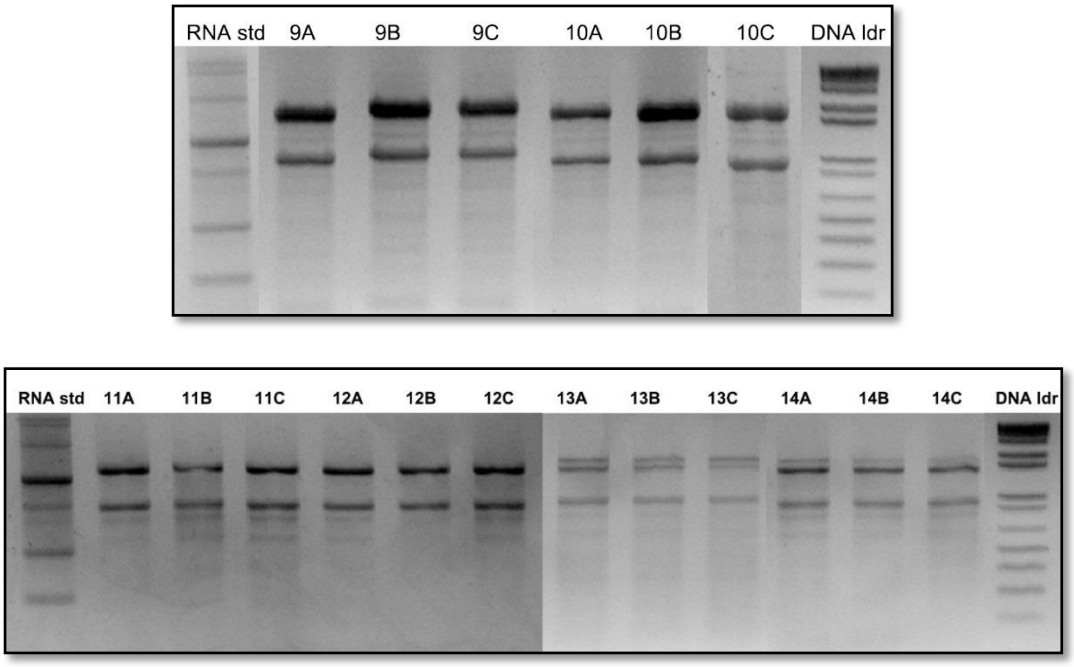

Figure 5.21. Agarose gels indicating the quality of total RNA used for RNA-Seq analysis. *P. parasitica* hyphae without phosphite (9A-C), *P. parasitica* hyphae with phosphite (10A-C) grown *in vitro*, mock inoculated lupin (11A-C), mock inoculated phosphite-treated lupin (12A-C), *P. parasitica*-inoculated lupin (13A-C), and *P. parasitica*-inoculated phosphite-treated lupin -(14A-C). RNA std = RNA standard, DNA ldr = DNA ladder.

5.3.5. Transcriptome analysis

5.3.5.1. RNA-Seq Overview

Analysis of the quality of the sequence data using CLC software showed that the data from the *in vitro* transcriptome (9A, B, C and 10A, B, C) did not require trimming. The quality of sequence data from the *in planta* lupin-infected samples was lower and six or seven bases were removed from the 5' end from all sequences (13A, B, C and 14A, B, C). The number of sequence reads generated and mapped to *P. parasitica* predicted transcripts is shown in Table 5.5. The number of reads mapping to *P. parasitica* slightly increased (0.2%-1.0%) after trimming of 13A, B, C and 14A, B, C sequence data sets. The number of reads mapping to the *P. parasitica* genome ranges from 28,595,188 to 4,434,267. There is considerable variation in the number of reads used for expression studies

reported in the literature with a figure of 10 million often quoted as the optimum (Robles *et al.*, 2012; Hart *et al.*, 2013; Liu *et al.*, 2014). However, this number is dependent on the number of genes and the number of biological replicates. In the current analysis, the number of reads mapping to *P. parasitica* was deemed to be sufficient to gain an insight into gene expression after phosphite treatment.

Table 5.5. Number of single-end reads generated and subsequently mapped to predicted transcripts from *P. parasitica*. NA: not trimmed

Sample Name	Total number of reads	Mapped reads to *P. parasitica*	*P. parasitica* mapped reads after trimming	After trimming (% increase)
9A	30,031,714	18,548,209	NA	
9B	28,560,656	23,646,824	NA	
9C	32,133,371	26,472,798	NA	
10A	32,110,990	27,622,223	NA	
10B	33,461,705	28,595,188	NA	
10C	31,850,389	27,495,928	NA	
13A	61,262,093	17,586,586	17,633,406	0.3
13B	62,129,958	7,162,732	7,234,859	1.0
13C	61,273,896	24,604,024	24,662,739	0.2
14A	59,501,481	6,917,075	6,950,011	0.5
14B	63,582,557	5,217,855	5,251,283	0.6
14C	59,341,574	4,434,267	4,465,356	0.7

The expression of five genes thought to be constitutively expressed, and which have been used as normalising genes for qPCR (Yan and Liou, 2006), were analysed to verify the computational procedures used to generate the RNA-Seq data. All five *P. parasitica* genes were not differentially expressed during *in vitro* culture or *in planta* in infected lupin roots 48 hpi with or without phosphite pre-treatment (Table 5.6, Figure 5.22). However, there was variation in expression of three normalising genes when a comparison was made between experiments. PPTG_07764 (>2.3-fold increase), PPTG_02092 (>4.5-fold increase) and PPTG_09948 (>4.6-fold increase) were more highly expressed *in planta* than in *in vitro*. These three genes have been previously identified as suitable normalisation genes for studies of the *P. parasitica*-tomato interaction (Yan and Liou, 2006) and their expression does not vary over time during the infection of lupin with *P. parasitica* (Blackman *et al.*, 2015). Given that the expression of the

five normalisation genes did not vary within an experiment, the method used to generate the data was deemed suitable.

Table 5.6. Expression of normalising genes. Normalising genes were not differentially expressed as seen by a fold change <2.

In vitro					
Gene ID	**Putative gene function**	**Pp RPKM**	**Pp+Phi RPKM**	**Fold change**	**FDR p-value**
PPTG_07764	WS021: 40S ribosomal protein S3A	2770	2634	-1.07	0.77
PPTG_08273	ubiquitin-conjugating enzyme	683	719	1.04	1.00
PPTG_02092	peptidyl prolyl isomerase 2	117	126	1.06	0.82
PPTG_09948	WS041	65	87	1.31	0.01*
PPTG_08636	phospholipase	37	45	1.18	0.11
Infected lupin					
Gene ID	**Putative gene function**	**Lupin+ Pp RPKM**	**Lupin+Pp+ Phi RPKM**	**Fold change**	**FDR p-value**
PPTG_07764	WS021: 40S ribosomal protein S3A	4697	6118	1.36	0.04*
PPTG_08273	ubiquitin-conjugating enzyme	505	600	1.24	0.2
PPTG_02092	peptidyl prolyl isomerase 2	451	513	1.19	0.38
PPTG_09948	WS041	196	306	1.64	0.00*
PPTG_08636	phospholipase	50	54	1.14	0.6

* indicates a significant EDGE False Discovery Rate (FDR) p-value

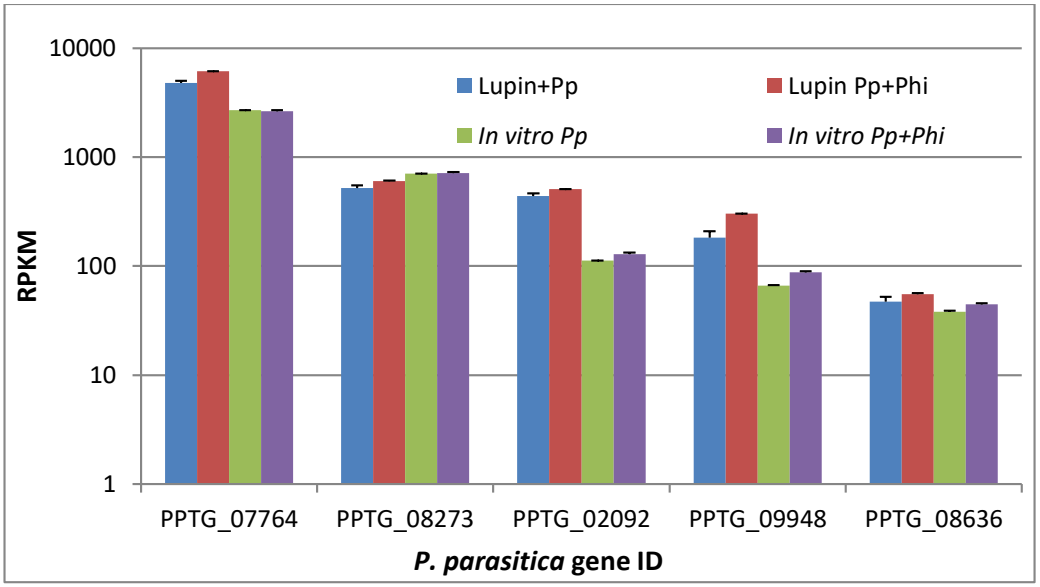

Figure 5.22. Expression of five normalising genes (Yan and Liou, 2006) during *in vitro* culture with and without phosphite (*In vitro Pp + Phi, In vitro Pp*), and in planta in inoculated lupin roots with or without phosphite pre-treatment (Lupin + Pp, Lupin Pp +Phi) presented as reads per kilobase of transcript per million mapped reads (RPKM). Error bars show the standard deviation of three biological replicates.

5.3.5.2. Gene expression during *in vitro* culture of *P. parasitica*

A total of 12,298 genes from 20,497 predicted transcripts were expressed in either untreated or/and phosphite-treated mycelia where expression is indicated by an RPKM >1 and 11,353 of these had >2 RPKM. The top 20 most highly expressed genes according to the RPKM values for *P. parasitica* grown *in vitro* with no phosphite are shown in Table 5.7; six of these genes had secretion signals. Highly expressed genes encoding proteins associated with ribosomes and other general transcription and translation activities such as elongation factors were excluded. Genes that mapped to the *P. parasitica* genome in mock-inoculated lupin samples were also omitted. These are typically highly conserved genes and included genes encoding calmodulin (PPTG_13130), actin (PPTG_15348) and S-adenosylmethionine synthase (PPTG_09226, PPTG_20306). None of these genes was differentially expressed.

All but one of the top 20 genes were more highly expressed in the absence of phosphite than in its presence. The exception was PPTG_12179. Only two genes were differentially expressed (fold change >2, FDR <0.05), one was an uncharacterised protein (PPTG_05202) and the other was an enolase (PPTG_13544). The most highly expressed gene encoded a secreted uncharacterised protein with eight transmembrane domains (PPTG_13069). The most abundant GO terms were associated with oxidoreductase activity (three proteins) and pathogenesis (two proteins). The top 20 included four highly expressed genes for proteins predicted to play a role in pathogenesis. These were the elicitins (PPTG_09075, PPTG_09080 and PPTG_19862), a cellulose binding protein (CBM1: PPTG_13482). In addition, a mucin-like protein (PPTG_01865) was also highly expressed (ranked 28th) but was also not differentially expressed in the presence of absence of phosphite (results not shown).

Tables 5.8 shows the top 20 differentially expressed, down-regulated genes *in vitro*, resulting from a comparison of expression levels in the absence versus the presence of phosphite. The results include only genes that had a minimum RPKM of 200. Seven of these genes were hypothetical proteins and only two (PPTG_02997 and PPTG_18662) were predicted to be secreted. Two genes encoded proteins associated with glycolysis, a glucokinase (PPTG_18927) and an enolase (PPTG_13544).

Table 5.7. The top 20 most highly expressed *P. parasitica* genes *in vitro* without phosphite (Pp-Phi) according to RPKM values. Within this cohort, differentially expressed transcripts with a fold change >2 (FDR <0.05) with respect to phosphite-treated cultures (Pp+Phi) are indicated with grey shading. Predicted functions, predicted GO terms, IDs and other features are shown. * putative function assigned by the presence of domains found during NCBI BLASTp analysis.

Gene ID	Putative gene function	RPKM Pp-Phi	RPKM Pp+Phi	Fold change	SP, TM	GO MF Terms	GO MF IDs	GO BP Terms	GO BP IDs	GO CCTerms	GO CC ID
PPTG_13069	hypothetical protein	5230	4249	-1.2	Yes, 8	-	-	-	-	-	-
PPTG_09075	Elicitin (INF1)	4262	3016	-1.4	Yes, 0	-	-	pathogenesis	0006952, 0009405	extracellular region	0005576
PPTG_09080	elicitin-like protein*	3617	3180	-1.2	Yes, 0	-	-	pathogenesis	0006952 0009405	extracellular region	0005576
PPTG_00145	alcohol dehydrogenase	3577	1821	-1.99	No, 0	oxidoreductase activity	0016491, 0016747	oxidation-reduction	0055114	-	-
PPTG_12179	proteolipid membrane potential modulator*	3558	3660	1.0	No, 1	-	-	-	-	integral component of membrane	0016021
PPTG_18851	hypothetical protein	3149	2989	-1.1	No, 0	-	-	-	-	-	-
PPTG_01100	glyceraldehyde-3-phosphate dehydrogenase	3080	1644	-1.9	No, 0	oxidoreductase activity	0016620	oxidation-reduction	0055114	-	-
PPTG_13482	CBM1	3014	1996	-1.5	No, 0	carbohydrate binding	0030248, 0004553, 0005515	carbohydrate metabolism	0007596, 0005975, 0006508	extracellular region	0005576
PPTG_13397	hypothetical protein	2763	2658	-1.1	No, 0	-	-	protein binding	0005515, 0016887	-	-
PPTG_04100	hypothetical protein	2574	1581	-1.7	No, 0	-	-	-	-	-	-
PPTG_19862	elicitin-like INF6	2494	1888	-1.3	Yes, 0	-	-	pathogenesis	0006952, 0009405	extracellular region	0005576
PPTG_03504	aquaporin	2457	1817	-1.4	No, 6	transporter activity	0005215	transmembrane transport	0055085, 0006810, 0006833	membrane	0016021, 0016020
PPTG_01657	hypothetical protein	2384	2361	-1.0	No, 0	-	-	-	-	-	-
PPTG_00562	hypothetical protein	2314	2165	-1.1	No, 0	-	-	-	-	-	-
PPTG_17723	hypothetical protein	2074	1944	-1.1	Yes, 0	-	-	-	-	-	-
PPTG_05202	hypothetical protein	2032	1000	-2.1	No, 1	-	-	-	-	-	-
PPTG_00531	hypothetical protein	1969	3122	1.6	Yes, 0	-	-	-	-	-	-
PPTG_13544	enolase	1966	716	-2.8	No, 0	lyase activity	0000287, 0004634	glycolysis	0006096	protein complex	0000015
PPTG_01099	hypothetical protein	1893	1040	-1.8	No, 0	oxidoreductase activity	0016620	oxidation-reduction	0055114	-	-
PPTG_12173	AN1-zinc finger-like*	1830	1489	-1.2	No, 0	DNA binding	0003677, 0008270	-	-	-	-

SP: secretion signal peptide, TM: transmembrane domain, GO: gene ontology, Phi: phosphite, MF: Molecular Function, BP: Biological Process; CC: Cellular Component

Table 5.8. The top 20 down-regulated differentially expressed *P. parasitica* genes *in vitro* in the presence of phosphite. Predicted functions, GO terms and other features are listed. The fold change shows the difference of expression comparing cultures grown in the presence (Pp+Phi) or the absence (Pp - Phi) of phosphite. * indicates that the putative function was assigned by the presence of domains found during NCBI BLASTp analysis.

Gene ID	Putative gene function	RPKM Pp-Phi	RPKM Pp+Phi	Fold change	SP, TM	GO MF Terms	GO MF IDs	GO BP Term	GO BP IDs	GO CC Terms	GO CC IDs
PPTG_12957	ankyrin repeat containing protein*	252	29	-8.8	No, 0	protein binding	0005515				
PPTG_14660	Myb-like DNA-binding protein*	249	33	-7.7	No, 0	DNA binding	0003677	-	-	-	-
PPTG_02888	hypothetical protein	673	107	-6.4	No, 0	-	-	-	-	-	-
PPTG_13950	LRR/ ribonuclease inhibitor-like protein*	746	141	-5.4	No, 0	-	-	-	-	-	-
PPTG_00485	alcohol dehydrogenase	262	57	-4.6	No, 0	oxidoreductase activity	0016491, 0016747, 0008270	oxidation-reduction process	0055114		
PPTG_02460	putative DNA-binding protein*	430	101	-4.4	No, 0	DNA binding	0003677	-	-	-	-
PPTG_02997	hypothetical protein	231	64	-3.7	Yes, 0	-	-	-	-	-	-
PPTG_12674	hypothetical protein	239	70	-3.5	No, 0	-	-	-	-	-	-
PPTG_01643	hypothetical protein	385	117	-3.4	No, 0	-	-	-	-	-	-
PPTG_01998	arrestin-like protein*	641	196	-3.3	No, 0	-	-	-	-	-	-
PPTG_15050	copine-like protein	726	222	-3.3	No, 0	protein binding	0005515	-	-	-	-
PPTG_18662	hypothetical protein	289	89	-3.3	Yes, 1	-	-	-	-	-	-
PPTG_10372	protein kinase	1402	433	-3.3	No, 0	protein kinase activity	0005524, 0004672, 0016772	protein phosphorylation	0006468	-	-
PPTG_18927	glucokinase	424	132	-3.3	No, 0	kinase activity	0005524, 0004340	cellular metabolic process, glycolysis	0051156, 0006096	-	-
PPTG_13569	pyruvate, phosphate dikinase	297	94	-3.2	No, 0	kinase activity	0005524, 0003824, 0016301, 0050242, 0016772	phosphorylation	0016310	-	-
PPTG_10026	ankyrin repeat containing protein*	224	74	-3.1	No, 0	protein binding	0006810	transport	0005515	integral to membrane	0016021
PPTG_19600	hypothetical protein	457	157	-3.0	No, 0	-	-	-	-	-	-
PPTG_16625	phosphatidylinositol-binding protein *	242	87	-2.8	No, 0	phospholipid binding, protein binding	0005543, 0005515	-	-	-	-
PPTG_14053	hypothetical protein	539	195	-2.8	No, 0	-	-	-	-	-	-
PPTG_13544	enolase	1966	716	-2.8	No, 0	lyase activity	0000287, 0004634	glycolysis	0006096	macromolecular complex	0000015

SP: secretion signal peptide, TM: transmembrane domain, GO: gene ontology, Phi: phosphite, , MF: Molecular Function, BP: Biological Process; CC: Cellular Component

The list of the top 20 most highly expressed *P. parasitica* genes *in vitro* in the presence of phosphite (Table 5.9) contained 16 genes which were also highly expressed in the absence of phosphite (Table 5.7). The four genes in the top 20 in the presence of phosphite but not in its absence were uncharacterised proteins, one of which contained a secretion signal and was the only gene of the 20 that was differentially up-regulated in the presence of phosphite (PPTG_17414). The four genes in the top 20 in the absence of phosphite but not in its presence included the enolase (PPTG_13544) and a zinc finger DNA binding protein (PPTG_12173).

The top 20 genes that were differentially expressed and up-regulated in the presence of phosphite are shown in Table 5.10. The down-regulated (Table 5.8) or up-regulated (Table 5.10) differentially expressed genes in the presence of phosphite came from different GO groups. There was down-regulation of genes for DNA-binding proteins and ankyrin repeat containing proteins (Table 5.10). Also, an up-regulation of genes encoding proteins involved in gluconeogenesis and other metabolic pathways and an increase in those associated with oxidation and reduction (Table 5.10). Of particular interest is the down-regulation of two genes containing ankyrin repeats (PPTG_12957, PPTG_10026).

Of the 12,298 predicted transcripts expressed *in vitro* (with RPKM >1 in either treatment), 118 transcripts were only expressed in the absence of phosphite and 49 were only expressed in the presence of 50 µg/ml phosphite. These genes were expressed at low levels but showed a significant difference (FDR $p<0.05$) between treatments (Appendix Table 5.2).

Table 5.9. The top 20 most highly expressed *P. parasitica* genes *in vitro* in the presence of phosphite (Pp+Phi) according to RPKM. Within this cohort, transcripts that are differentially expressed >2 are shaded grey. The fold change shows the difference of expression in modified Ribeiro's medium in the presence of phosphite compared to the expression in the absence of phosphite (Pp-Phi). Predicted functions, predicted GO terms and IDs, and other features are shown. * indicates that the putative function was assigned by the presence of domains found during NCBI BLASTp analysis.

Gene ID	Putative gene function	RPKM MRM	RPKM MRM+Phi	Fold change	SP, TM	GO MF Terms	GO MF IDs	GO BP Term	GO BP IDs	GO CC Terms	GO CC ID
PPTG_13069	hypothetical protein	5230	4249	-1.2	Yes, 8	-	-	-	-		
PPTG_12179	proteolipid membrane potential modulator*	3558	3660	1.0	No, 1		-	-	-	integral membrane component	0016021
PPTG_09080	elicitin-like protein*	3617	3180	-1.2	Yes, 0	-	-	pathogenesis	0006952 0009405	extracellular region	0005576
PPTG_00531	hypothetical protein	1969	3122	1.6	Yes, 0	-	-	-	-		
PPTG_09075	elicitin	4262	3016	-1.4	Yes	-	-	pathogenesis	0006952, 0009405	extracellular region	0005576
PPTG_18851	hypothetical protein	3149	2989	-1.1	No, 0	-	-	-	-	-	-
PPTG_17401	hypothetical protein	1749	2669	1.5	No, 0	-	-	-	-		
PPTG_13397	hypothetical protein	2763	2658	-1.1	No, 0	-	-	protein binding	0005515, 0016887	-	-
PPTG_00532	hypothetical protein	1574	2573	1.6	Yes, 0	-	-	-	-		
PPTG_01657	hypothetical protein	2384	2361	-1.0	No, 0	-	-	-	-	-	-
PPTG_00562	hypothetical protein	2314	2165	-1.1	No, 0	-	-	-	-	-	-
PPTG_13482	CBM1	3014	1996	-1.5	No, 0	carbohydrate binding	0030248, 0004553, 0005515	carbohydrate metabolic process	0007596, 0005975, 0006508	extracellular region	0005576
PPTG_00206	hypothetical protein	1705	1960	1.1	No, 1	-	-	-	-	-	-
PPTG_17723	hypothetical protein	2074	1944	-1.1	Yes, 0	-	-	-	-	-	-
PPTG_19862	elicitin-like INF6	2494	1888	-1.3	Yes, 0	-	-	pathogenesis	0006952, 0009405	extracellular region	0005576
PPTG_00145	alcohol dehydrogenase	3577	1821	-1.99	No, 0	oxidoreductase activity	0016491, 0016747	oxidation-reduction	0055114	-	-
PPTG_03504	aquaporin	2457	1817	-1.4	No, 6	transporter activity	0005215	transmembrane transport	0055085, 0006810, 0006833	membrane	0016021, 0016020
PPTG_01100	glyceraldehyde-3-phosphate dehydrogenase	3080	1644	-1.9	No, 0	oxidoreductase activity	0016620	oxidation-reduction	0055114	-	-
PPTG_04100	hypothetical protein	2574	1581	-1.7	No, 0	-	-	-	-	-	-
PPTG_17414	hypothetical protein	694	1540	2.2	Yes, 1	-	-	-	-		

SP: secretion signal peptide, TM: transmembrane domain, GO: gene ontology, MF: Molecular Function, BP: Biological Process; CC: Cellular Component

Table 5.10. The top 20 differentially expressed *P. parasitica* genes up-regulated *in vitro* in the presence of phosphite (Pp+Phi) compared to gene expression in the absence of phosphite and arranged according to fold change. Predicted functions and other features are shown. GO terms have been annotated to higher level terms according to Amigo1 and the specific GO IDs are shown. * indicates that the putative function was assigned by the presence of domains found during NCBI BLASTp analysis.

Gene ID	Putative gene function	RPKM Pp-Phi	RPKM Pp+Phi	Fold change	SP, TM	GO MF Terms	GO MF IDs	GO BP Term	GO BP IDs	GO CC Terms	GO CC ID
PPTG_08582	12-oxophytodienoate reductase	56	279	4.9	No, 0	FMN binding, oxidoreductase	0010181, 0016491	oxidation-reduction	0055114	-	-
PPTG_06756	short chain dehydrogenase	50	220	4.4	No, 0	oxidoreductase	0016491	metabolic process	0008152	-	-
PPTG_17416	hypothetical protein	110	477	4.3	Yes, 1	-	-	-	-	-	-
PPTG_02909	hypothetical protein	124	521	4.1	Yes, 0	-	-	-	-	-	-
PPTG_00530	hypothetical protein	218	853	3.9	No, 0	-	-	-	-	-	-
PPTG_00533	hypothetical protein	97	385	3.9	No, 0	-	-	-	-	-	-
PPTG_13885	dihydrodipicolinate reductase	56	207	3.6	No, 0	4-hydroxy-tetrahydro-dipicolinate reductase	0008839, 0030170	lysine biosynthesis via diaminopimelate	0009089, 0055114		
PPTG_08080	mitochondrial Carrier (MC) family	74	265	3.5	No, 0	-	-	-	-	-	-
PPTG_11770	hypothetical protein	70	240	3.4	No, 4	-	-	-	-	-	-
PPTG_16840	hypothetical protein	206	712	3.4	Yes, 1	-	-	-	-	-	-
PPTG_02177	phosphoenolpyruvate carboxykinase (ATP)	348	1151	3.3	No, 0	phosphoenolpyruvate carboxykinase	0005524, 0004612	gluconeogenesis	0006094	-	-
PPTG_02179	phosphoenolpyruvate carboxykinase (ATP)	138	446	3.2	No, 0	phosphoenolpyruvate carboxykinase	0005524, 0004612	gluconeogenesis	0006094	-	-
PPTG_11045	acyl-CoA dehydrogenase	68	218	3.2	No, 0	acyl-CoA dehydrogenase	0003995, 0050660	oxidation-reduction	0055114		
PPTG_01952	acyl-CoA desaturase	119	345	2.9	No, 3	-	-	lipid metabolism	0006629	-	-
PPTG_06067	ATP-binding Cassette (ABC) superfamily	72	213	2.9	No, 12	ATPase activity	0005524, 0016887	-	-	membrane	0016020
PPTG_06758	short chain dehydrogenase	287	813	2.8	No, 0	oxidoreductase	0016491	metabolic process	0008152	-	-
PPTG_01358	glyceraldehyde-3-phosphate dehydrogenase	192	520	2.7	No, 0	oxidoreductase	0016620	oxidation-reduction	0055114		
PPTG_13824	hypothetical protein	358	975	2.7	No, 0	-	-	-	-	-	-
PPTG_08484	Zinc finger (ZZ)-like protein*	201	540	2.6	No, 0	protein and zinc ion binding	0005515, 0008270	-	-	-	-
PPTG_04797	pyridine nucleotide-disulphide oxidoreductase	278	737	2.6	Yes, 0	FAD binding, oxidoreductase	0050660, 0016491	oxidation-reduction	0055114	-	-

SP: secretion signal peptide, TM: transmembrane domain, GO: gene ontology, MF: Molecular Function, BP: Biological Process; CC: Cellular Component

The genes only expressed *in vitro* in the absence of phosphite included 10 CWDE genes from PL1 (PPTG_12896, PPTG_12896), PL3 (PPTG_03562), CE1 (PPTG_00806), GH3 (PPTG_05877, PPTG_14483), GH17 (PPTG_17185), GH30 (PPTG_14859), GH53 (PPTG_19164) and AA8 (PPTG_04148) families, a catalase/peroxidase (PPTG_02738), two effectors (RxLR-type: PPTG_03150; CRN-like: PPTG_03762) and five protein kinases. The only expressed genes in the presence of phosphite included a catalase (PPTG_06866), four CWDE (GH28: PPTG_15173; GH81: PPTG_10140, PPTG_10161; PL1: PPTG_09460) and sporangia-induced protein (PPTG_04166). This latter gene was similar to genes annotated as encoding sporangia-induced proteins from other Oomycetes, for example, PITG_07288 from *P. infestans*, but the function of these proteins is unknown.

There are 786 transcripts with a two-fold change in expression level in the presence versus the absence of phosphite (fold change >2; FDR P<0.05, RPKM >1 (Appendix Table 5.3). Three of these were genes that mapped to *P. parasitica* in mock-inoculated lupin (Appendix Table 5.1). In the presence of phosphite, 300 of the transcripts were differentially up-regulated while 486 were down-regulated (Appendix Table 5.3). Four groups of proteins known to contribute to pathogenesis were differentially expressed and these included those encoding CWDEs, effectors, secreted proteases and proteins involved in ROS scavenging. Of the 36 CWDE genes differentially expressed, 28 were down-regulated and nine were up-regulated *in vitro* in the presence of phosphite. Twelve effectors were differentially expressed and 10 of these were down regulated in the presence of phosphite. Seven families of ROS scavengers (catalase, catalase/peroxidase, peroxiredoxin, alternative oxidase, glutathione S-transferase, ferredoxin and a thioredoxin-like protein) were differentially expressed, with 12 of the 13 genes up-regulated with phosphite treatment. Seven secreted serine proteases were differentially expressed, with six up-regulated with phosphite treatment. The expression of these four groups of proteins will be analysed in later sections (Section 5.4.4). Differentially up-regulated genes in phosphite cultures also included six HSP genes and a gene for a homolog to flagella associated protein putative from *Albugo laibachii* (CCA18224.1; Kemen *et al.*, 2011) .

5.3.5.3. Gene expression of *P. parasitica in planta* during lupin infection

During the infection of lupin, 13,384 *P. parasitica* genes were expressed if an RPKM >1 cut-off was applied and 12,230 genes were expressed if an RPKM ≥2 cut-off were applied, with the RPKM value meeting the cut-off criterion in one or both treatments (i.e. untreated and phosphite-treated inoculated lupin). This equates to a 9% greater number of genes expressed *in planta* if RPKM >1 and a 7% greater number if RPKM ≥2 when compared to the number of genes expressed in the *in vitro* study. There are 2,056 genes that were differentially expressed between infected lupins with and without phosphite pre-treatment (RPKM >1). Of these, 922 were up-regulated in the phosphite-pre-treated roots and 1,134 were down-regulated (Appendix Table 5.3). The number of genes that were specifically expressed in inoculated lupins in the presence or absence of phosphite pre-treatment was 568, with 150 containing secretion signals, (Appendix Table 5.3) compared to 167 in the *in vitro* study with 67 having secretion signals (Appendix Table 5.2). There were 293 predicted transcripts specifically expressed (EDGE $p < 0.05$) in lupins inoculated with *P. parasitica* and 275 specifically expressed in phosphite-treated inoculated lupins, although most of these were expressed at low levels. Members of a number of developmentally important gene families were expressed only in inoculated lupin roots in the absence of phosphite pre-treatment or vice versa. For example, seven *P. parasitica* dynein genes and two Myb-like DNA binding protein genes were expressed in untreated inoculated lupin roots and not in phosphite-treated, inoculated roots. Other treatment-specific gene expression included genes encoding 24 CWDEs and 20 effectors. Of the effectors, 18 were expressed in phosphite-treated roots but not in inoculated non-treated roots.

The two lists of the top 20 *P. parasitica* genes in terms of expression level in both phosphite-treated and untreated lupin roots had a number of genes in common. Most of the highly expressed genes were predicted to encode ribosomal components, and were generally not differentially expressed and were excluded from further analysis. Four genes included in these lists were differentially expressed when comparing phosphite-treated and untreated roots (Tables 5.11 and 5.12). A putative ribonuclease P protein component (PPTG_14499), which

functions in the maturation of tRNAs (Hartmann and Hartmann, 2003), exhibited a 7.5-fold down-regulation in the phosphite-treated roots (Table 5.11). A glyceraldehyde-3-phosphate dehydrogenase gene (PPTG_01100) was up-regulated in phosphite-treated roots (2.1-fold change) whereas another highly expressed glyceraldehyde-3-phosphate dehydrogenase (PPTG_01101) did not show differential expression. One highly expressed gene encoding a hypothetical protein was down-regulated (PPTG_02299) in the phosphite-treated roots and one was up-regulated (PPTG_20358) (Table 5.12). These proteins had no secretion signals or transmembrane domains (TMD). A gene for ketol-acid reductoisomerase was also differentially up-regulated 3.1-fold in phosphite (PPTG_15943). The function of this protein is in the biosynthesis of branched chain amino acids (Tyagi *et al.*, 2005). The expression level of the remaining genes expressed in both treatments was not affected by the addition of phosphite. This includes one CWDE (PPTG_01939: exo-β-1,3-glucanase, Blackman *et al.*, 2014), an annexin (PPTG_13120), a proteolipid membrane potential modulator protein (PPTG_12179, most highly expressed gene in both treatments), a phospholipase (PPTG_10444), a mitochondrial substrate carrier protein (PPTG_04703) and four hypothetical proteins (Table 5.11 and 5.12). One other *P. parasitica* CWDE from the CBM1 family of cellulose-binding proteins that have no catalytic activity (PPTG_06045) was also highly expressed and showed a 1.9-fold down-regulation in phosphite-treated lupins. Perhaps the most exciting finding of this analysis was that an elicitin gene (PPTG_15237) had a more than four-fold down-regulation in the presence of phosphite. The types of GO terms in the two lists of the top 20 expressed genes were different to those enriched in the *in vitro* study, with an increase in terms associated with phospholipid binding and a decrease in terms associated with oxidoreductase activity (Table 5.11 and 5.12).

Table 5.11. The top 20 most highly expressed *P. parasitica* genes *in planta* in the absence of phosphite treatment. Predicted functions, GO terms and other features are shown. Within this cohort, genes showing a significant differential expression (>2 fold change) in the presence compared to the absence of phosphite are shown (grey shading). * indicates that the putative function was assigned during NCBI BLASTp analysis.

Gene ID	Putative gene function	RPKM Lupin +Pp	RPKM Lupin +Pp+Phi	Fold change	SP, TM	GO MF Terms	GO MF IDs	GO BP Term	GO BP IDs	GO CC Terms	GO CC ID
PPTG_12179	proteolipid membrane potential modulator*	11069	11672	1.1	No, 1	-	-	-	-	integral to membrane	0016021
PPTG_14499	ribonuclease P protein component*	9351	1272	-7.5	No, 0	-	-	-	-	-	-
PPTG_05454	hypothetical protein	8184	4742	-1.7	No, 0	-	-	-	-	-	-
PPTG_15237	elicitin-like protein	6073	1417	-4.1	Yes, 0	-	-	pathogenesis	0006952, 0009405	extracellular region	0005576
PPTG_18851	hypothetical protein	3305	1942	-1.6	No, 0	-	-	-	-	-	
PPTG_04100	hypothetical protein	3099	2263	-1.3	No, 0	-	-	-	-	-	-
PPTG_02299	hypothetical protein	2752	1294	-2.0	Yes, 0	-	-	-	-	-	-
PPTG_06045	CBM1	2475	1230	-1.9	Yes, 0	-	-	-	-	-	-
PPTG_03934	annexin family	2446	1245	-1.9	No, 0	phospholipid binding	0005509, 0005544	-	-	-	-
PPTG_05455	hypothetical protein	2187	1236	-1.7	No, 0	-	-	-	-	-	-
PPTG_01939	GH5/CBM43	2051	1588	-1.2	Yes, 1	hydrolase activity	0004553	carbohydrate metabolic process	0005975	-	-
PPTG_13120	annexin family	1940	1924	1.0	No, 0	phospholipid binding	0005509, 0005544	-	-	-	-
PPTG_04703	mitochondrial substrate carrier protein ancA	1899	2421	1.3	No, 3	-	-	-	-	-	-
PPTG_01101	glyceraldehyde-3-phosphate dehydrogenase	1870	1732	-1.0	No, 0	oxidoreductase activity	0051287, 0050661, 0016620	oxidation-reduction	0006006, 0055114	-	-
PPTG_10444	phospholipase D	1840	1597	-1.1	No, 0	catalytic activity	0003824	metabolic process	0008152	-	-
PPTG_11591	small cysteine-rich protein*	1730	1504	-1.1	Yes, 0	-	-	-	-	-	-
PPTG_16923	glutathione transferase	1530	1285	-1.1	No, 0	protein binding	0005515		-	-	-
PPTG_13397	hypothetical protein	1515	1445	-1.0	No, 0	protein binding	0005515		-	-	-
PPTG_19007	hypothetical protein	1508	1315	-1.1	Yes, 1	-	-	-	-	-	-
PPTG_01100	glyceraldehyde-3-phosphate dehydrogenase	1493	2980	2.1	No, 0	oxidoreductase activity	0016620	oxidation-reduction process	0055114	-	-

SP: secretion signal, TM: transmembrane domain, GO: gene ontology; GO: gene ontology, MF: Molecular Function, BP: Biological Process; CC: Cellular Component Phi: phosphite

Table 5.12. The top 20 expressed *P. parasitica* genes *in planta* in the presence of phosphite. Predicted functions, GO terms and other features are shown. Within this cohort, genes showing a significant differential expression (>2 fold change) based on the comparison between cultures grown in the presence or absence of phosphite are shaded grey. * putative function assigned by domains found during NCBI BLASTp analysis.

Gene ID	Putative gene function	RPKM Lupin +Pp	RPKM Lupin + Pp+Phi	Fold change	SP, TM	GO MF Terms	GO MF IDs	GO BP Term	GO BP IDs	GO CC Terms	GO CC ID
PPTG_12179	proteolipid membrane potential modulator*	11069	11671	1.1	No, 1	-	-	-	-	integral to membrane	0016021
PPTG_05454	hypothetical protein	8184	4742	-1.7	No, 0	-	-	-	-	-	-
PPTG_01100	glyceraldehyde-3-phosphate dehydrogenase	1493	2980	2.1	No, 0	oxidoreductase activity	0016620	oxidation-reduction	0055114	-	-
PPTG_04703	mitochondrial substrate carrier protein ancA	1899	2421	1.3	No, 3	-	-	-	-	-	-
PPTG_04100	hypothetical protein	3099	2263	-1.3	No, 0	-	-	-	-	-	-
PPTG_01676	guanine nucleotide-binding protein subunit	1269	2022	1.7	No, 0	protein binding	0005515	-	-	-	-
PPTG_18851	hypothetical protein	3304.8	1942	-1.6	No, 0	-	-	-	-	-	-
PPTG_13120	annexin family	1940	1924	1.0	No, 0	phospholipid binding	0005509, 0005544	-	-	-	-
PPTG_01466	translation initiation factor eIF-5A	1275	1825	1.5	No, 0	protein binding, translation activity	0003723, 0043022, 0003746	translational elongation regulation	0008612, 0045901, 0045905, 0006452	-	-
PPTG_20358	hypothetical protein	250	1764	7.3	No, 0	oxidoreductase activity	0016620	oxidation-reduction	0055114		-
PPTG_02398	elongation factor 1-gamma	1206	1763	1.5	No, 0	protein binding, translation activity	0005515, 0003746	translational elongation	0006414	translation complex	0005853
PPTG_01101	glyceraldehyde-3-phosphate dehydrogenase	1870	1732	-1.0	No, 0	oxidoreductase activity,	0051287, 0050661, 0016620	glucose metabolism, oxidation-reduction	0006006, 0055114	-	-
PPTG_01700	transcription factor BTF3-like protein	1102	1660	1.6	No, 0	-	-	-	-	-	-
PPTG_10444	phospholipase D	1840	1597	-1.1	No, 0	catalytic activity	0003824	metabolic process	0008152		-
PPTG_01939	GH5/CBM43	2051	1588	-1.2	Yes, 1	hydrolase activity	0004553	carbohydrate metabolism	0005975	-	-
PPTG_07300	hypothetical protein	1387	1553	1.2	No, 0	-	-	-	-	-	-
PPTG_11591	small cysteine-rich protein*	1730	1504	-1.1	Yes, 0	-	-	-	-	-	-
PPTG_13397	hypothetical protein	1515	1445	-1.00	No, 0	protein binding	0005515	-	-	-	-
PPTG_15943	ketol-acid reductoisomerase	482	1440	3.1	No, 0	ketol-acid reductoisomerase activity	0004455	amino acid biosynthesis, oxidation-reduction	0009082, 0008652, 0055114		-
PPTG_15237	elicitin-like protein	6073	1417	-4.1	Yes, 0			pathogenesis	0006952, 0009405	extracellular region	0005576

SP: secretion signal peptide, TM: transmembrane domain, GO: gene ontology; Phi: phosphite, GO gene ontology MF: Molecular Function, BP: Biological Process; CC: Cellular Component

Analysis of the most highly differentially expressed genes that are more highly expressed in *P. parasitica*-inoculated lupins with no phosphite pre-treatment than with phosphite pre-treatment revealed a greater number of secreted proteins in the top 20 compared to that *in vitro* (Tables 5.8, 5.10, 5.13, 5.14). Ten proteins from this group of differentially expressed genes had classical secretion signals and five had multiple TMDs (Table 5.13). Three families of *P. parasitica* proteins involved in pathogenesis had representatives that were down-regulated in phosphite-pre-treated roots compared to untreated roots. Two secreted cysteine proteases (PPTG_11311, PPTG_11313) were identified and their gene expression was significantly reduced in lupins treated with phosphite, with fold changes of 84 and 77, respectively. Both of these predicted genes, plus another cysteine protease (PPTG_13332) were more highly expressed *in planta* than *in vitro*. Other genes with significant reduction in expression in the presence of phosphite include two elicitin proteins (PPTG_05402 and PPTG_14235) which had a 24- and 30-fold change in expression, respectively. These were different from those effectors differentially or highly expressed *in vitro* (Tables 5.7, 5.8, 5.9, 5.10). The third pathogenesis protein was a mucin-like protein (PPTG_17896) which had a 7.6-fold difference in expression. In addition, there were four transporter proteins (PPTG_09412, PPTG_09490, and PPTG_09489, PPTG_00290) with lower expression in phosphite-treated inoculated roots (Table 5.13).

Of the top differentially expressed *P. parasitica* genes up-regulated in inoculated lupins treated with 50 µg/ml phosphite, five have classical secretion signals and the majority were hypothetical proteins (Table 5.14). Of importance is the induction of GH81 (PPTG_16828) which is a CWDE capable of degrading β-1,3-glucans (callose). Also of interest is the induction of two genes encoding mannitol dehydrogenase (PPTG_06282 and PPTG_06284). This enzyme functions in the synthesis of mannitol that can be used by pathogens to limit ROS-induced resistance (Meena *et al.*, 2015). In contrast to the inoculated lupins not treated with phosphite, in which two elicitins were down-regulated, a secreted effector (PPTG_00121) was highly induced in phosphite-treated infected lupins (6.2-fold).

Table 5.13. The top 20 significantly differentially expressed down-regulated *P. parasitica* (Pp) genes *in planta* in the presence of phosphite. Predicted functions and other features are shown. The fold change shows the results of a comparison in infected lupins in the presence versus the absence of phosphite. * indicates that the putative function was assigned by the presence of domains found during NCBI BLASTp analysis.

Gene ID	Putative gene function	RPKM Lupin +Pp	RPKM Lupin + Pp+Phi	Fold change	SP, TM	GO MF Terms	GO MF IDs	GO BP Term	GO BP IDs	GO CC Terms	GO CC ID
PPTG_11311	cysteine protease C01A	522	5	-84.2	Yes, 0	cysteine-type peptidase	0008234	proteolysis	0006508	-	-
PPTG_09412	major facilitator superfamily transporter	206	3	-77.1	No, 10	substrate-specific transmembrane transporter activity	0022891,	transmembrane transport	0055085	integral to membrane	0016021
PPTG_11313	cysteine protease C01A	296	4	-63.3	Yes, 0	cysteine-type peptidase	0008234	proteolysis	0006508	-	-
PPTG_09490	major facilitator superfamily transporter	296	5	-57.6	No, 12	-	-	transmembrane transport	0055085	integral to membrane	0016021
PPTG_09489	major facilitator superfamily transporter	333	6	-55.1	No, 11	-	-	transmembrane transport	0055085	integral to membrane	0016021
PPTG_05402	elicitin	920	28	-30.3	Yes, 0	-	-	pathogenesis	0006952, 0009405	extracellular region	0005576
PPTG_09295	hypothetical protein	328	10	-29.9	Yes, 1	-	-	-	-	-	-
PPTG_11488	amino acid/auxin permease family	445	16	-27.3	No, 11	-	-	-	-	-	-
PPTG_14235	elicitin-like protein	281	11	-24.5	Yes, 0	-	-	pathogenesis	0006952, 0009405	extracellular region	0005576
PPTG_02460	endonuclease*	1404	87	-16.4	No, 0	DNA binding	0003677	-	-	-	-
PPTG_09335	hypothetical protein	202	14	-14.3	No, 0	-	-	-	-	-	-
PPTG_13387 (PPTG_23200)	hypothetical protein	289	20	-14.2	Yes, 0	phosphatase activity	0016791	metabolism	0008152	-	-
PPTG_03200	hypothetical protein	772	68	-11.0	Yes, 0	-	-	-	-	-	-
PPTG_17697	choline/carnitine O-acyltransferase	422	42	-9.5	No, 0	transferase activity	0016746	-	-	-	-
PPTG_19456	alkaline phosphatase	312	32	-9.4	Yes, 0	phosphatase activity	0016791	metabolism	0008152	-	-
PPTG_00290	ATP-binding Cassette (ABC) superfamily	202	21	-9.0	No, 10	ATPase activity, transmembrane transport	0005524, 0042626	transport	0006810	integral to membrane	0016021
PPTG_03132	Glu/Leu/Phe/Val dehydrogenase family protein	399	49	-7.9	No, 0	glutamate dehydrogenase activity	0004352	oxidation-reduction	0019551, 0055114	-	-
PPTG_17896	mucin-like*	257	32	-7.6	Yes, 1	-	-	-	-	-	-
PPTG_08040	acetyl-coenzyme A synthetase	348	48	-6.9	Yes, 0	AMP binding, acetate-CoA ligase activity	0016208, 0003987	acetyl-CoA biosynthetic	0019427	-	-
PPTG_00486 (PPTG_20750)	alcohol dehydrogenase	910	126	-6.9	No, 0	oxidoreductase activity	0016491, 0016747, 0008270	oxidation-reduction	0055114	-	-

SP: secretion signal peptide, TM: transmembrane domain, gene ontology; Phi: phosphite, GO gene ontolog,y, MF: Molecular Function, BP: Biological Process; CC: Cellular Component

Table 5.14. The top 20 most highly differentially expressed up-regulated *P. parasitica* (Pp) genes *in planta* in the presence of phosphite. The fold change shows the difference of expression *in planta* from a comparison of expression in presence versus the absence of phosphite. No Cellular Component terms were detected. * indicates that the putative function was assigned by the presence of domains found during NCBI BLASTp analysis.

Gene ID	Putative gene function	RPKM Lupin +Pp	RPKM Lupin + Pp+Phi	Fold change	SP, TM	GO MF Terms	GO MF IDs	GO BP Term	GO BP IDs
PPTG_16830	hypothetical protein	7	460	66.7	No, 0	-	-	-	-
PPTG_05254	hypothetical protein	8	317	42.5	No, 0	-	-	-	-
PPTG_16828	GH81	6	215	38.7	No, 1	β-1,3-glucanase activity	0052861, 0052862	cell wall catabolism	0016998
PPTG_16304	hypothetical protein	12	327	27.1	No, 0	-	-	-	-
PPTG_05252	hypothetical protein	14	277	20.2	No, 0	-	-	-	-
PPTG_16831	hypothetical protein	14	260	19.6	No, 0	-	-	-	-
PPTG_05764	hypothetical protein	18	215	12.7	No, 0	-	-	-	-
PPTG_16306	hypothetical protein	47	523	11.5	No, 0	-	-	-	-
PPTG_06282	cinnamyl alcohol dehydrogenase*	22	206	9.9	No, 0	oxidoreductase activity	0016491, 0016747, 0008270	oxidation-reduction process	0055114
PPTG_20358	glyceraldehyde-3-phosphate dehydrogenase	250	1764	7.3	No, 0	oxidoreductase activity	0016620	oxidation-reduction	0055114
PPTG_00562	hypothetical protein	37	236	6.5	No, 0	-	-	-	-
PPTG_00121	RxLR effector	140	842	6.2	Yes, 0	-	-	-	-
PPTG_18913	hypothetical protein	53	301	5.8	No, 4	-	-	-	-
PPTG_06284	mannitol dehydrogenase	103	543	5.5	No, 0	oxidoreductase activity	0016491, 0016747, 0008270	oxidation-reduction	0055114
PPTG_19079	hypothetical protein	51	244	4.9	Yes, 0	-	-	-	-
PPTG_03643	hypothetical protein	50	235	4.9	No, 0	-	-	-	-
PPTG_20214	hypothetical protein	210	964	4.8	Yes, 0	-	-	-	-
PPTG_03915	hypothetical protein	119	505	4.4	Yes, 0	-	-	-	-
PPTG_01905	hypothetical protein	65	272	4.4	No, 0	-	-	-	-
PPTG_03096	hypothetical protein	69	227	3.4	Yes, 0	-	-	-	-

SP: secretion signal peptide, TM: transmembrane domain, GO: gene ontology; Phi: phosphite, MF: Molecular Function, BP: Biological Process; CC: Cellular Component

5.3.5.4. Phosphite induces changes in Gene Ontology (GO) terms for *P. parasitica* genes *in vitro* and *in planta*

In order to investigate if there were specific pathways that were affected by the addition of phosphite, the global pattern of GO terms was investigated. REVIGO was used to cluster and visualise the proportion of specific GO terms assigned to Molecular Function, Biological Process and Cellular Component GO terms. Of the top 200 DE *P. parasitica* genes *in vitro*, only 79 proteins had GO terms. This includes 60 Biological Process, four Cellular Component and 146 Molecular Function terms associated with down-regulated genes (note that many proteins have two or more GO terms). Most of the GO terms were only involved in one or two of the three functions. However, there are a few proteins like the aquaporins (PPTG_03679 and PPTG_03680) and ATP-binding Cassette (ABC) superfamily (PPTG_03183) that have GO terms in all three GO categories, with six and eight GO terms, respectively.

Of the proteins encoded by up-regulated genes, 105 proteins had GO terms with 107 Biological Process, nine Cellular Component and 195 Molecular Function terms. Scatter-plot analysis showed that many different types of proteins were enriched in phosphite-treated cultures as indicated by the number and uniform size and the distribution of coloured circles where similar GO terms are grouped together. Proteins associated with cell wall macromolecule catabolism, response to stress and with pathogenesis were enriched (Figure 5.23a). Proteins associated with response to oxidative stress and carbohydrate metabolism were both enriched and depleted in phosphite-treated cultures. There was an increase in Cellular Component GO terms associated with membrane proteins (Figure 5.23b). Terms associated with the Molecular Function subgroups pectate lyase and DNA-binding were depleted in the presence of phosphite, while catalase-associated terms were enriched (Figure 5.23b).

More GO terms were assigned to down-regulated genes than to the up-regulated genes in *P. parasitica*-infected lupins with and without phosphite. Down-regulated genes had 103 Biological Process, 39 Cellular Component and 156 Molecular Functions terms while up-regulated genes had 40 Biological Process, 14 Cellular Component and 85 Molecular Functions terms (Figure 5.24).

Like the analysis of *P. parasitica* grown *in vitro* with and without phosphite, there was a wide distribution in the types of pathways that were enriched in up- and down-regulated genes. Down-regulated terms included those associated with pathogenesis and cell adhesion. There was an enrichment of terms associated with CWDE including pectinesterase, β-1,3-glucanase, pectate lyase and polygalacturonase (GH28). However, often the same GO terms were in both up-regulated and down-regulated data sets. This includes terms for the response to oxidative stress, transport (water and cation), protein polymerisation and lipid metabolism (Figure 5.24a).

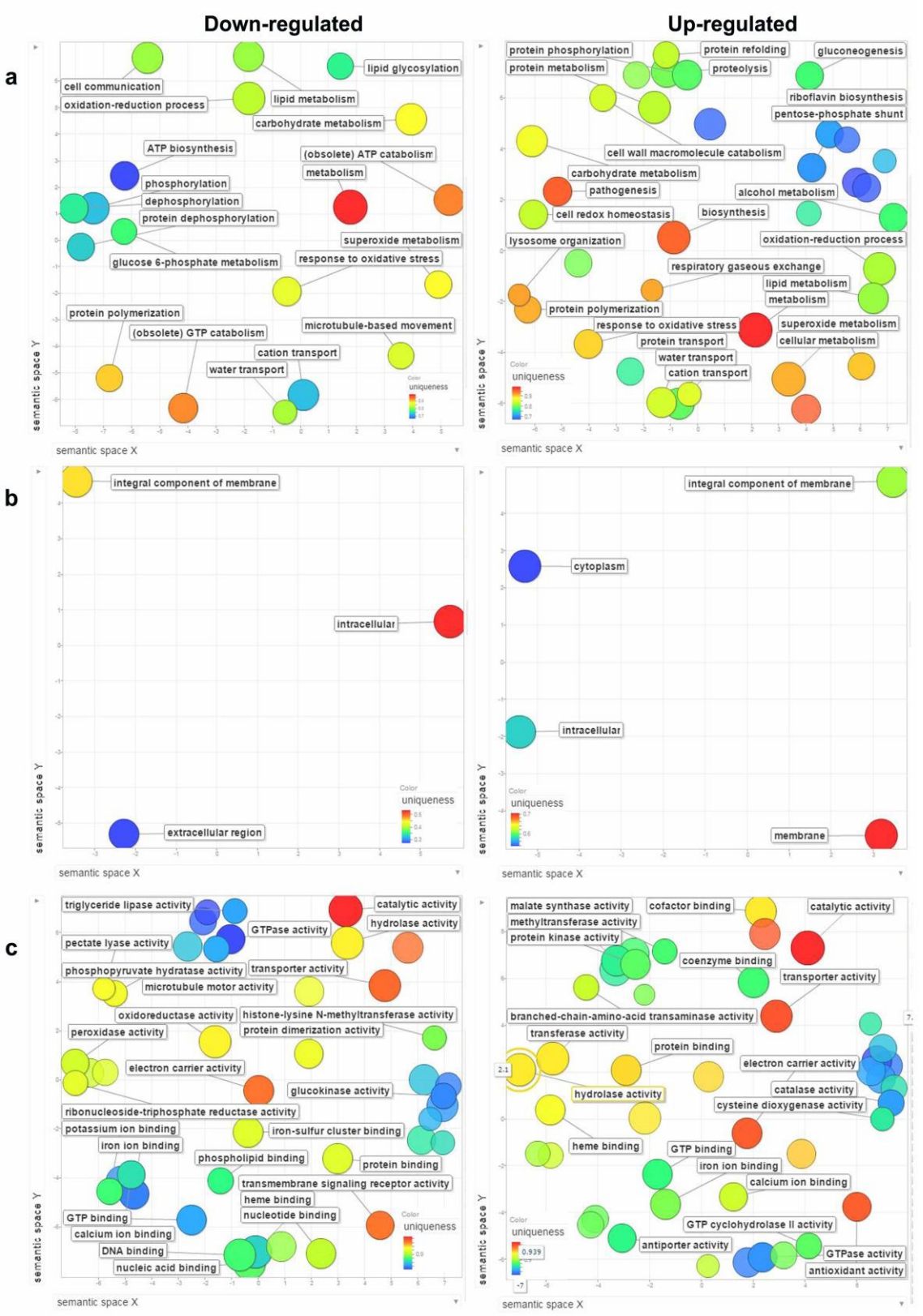

Figure 5.23. The results of a comparison of gene expression in phosphite-treated versus untreated *in vitro* samples. Differentially expressed *P. parasitica* genes were subjected to GO enrichment analysis and summarised in scatterplots using the REVIGO web server. GO terms were summarised according to Biological Process (a), Cellular Component (b), and Molecular Function (c) subgroups. Adjoining circles are most closely related and sizes are proportional to the frequency of the GO terms in Tables 5.9 & 5.10.

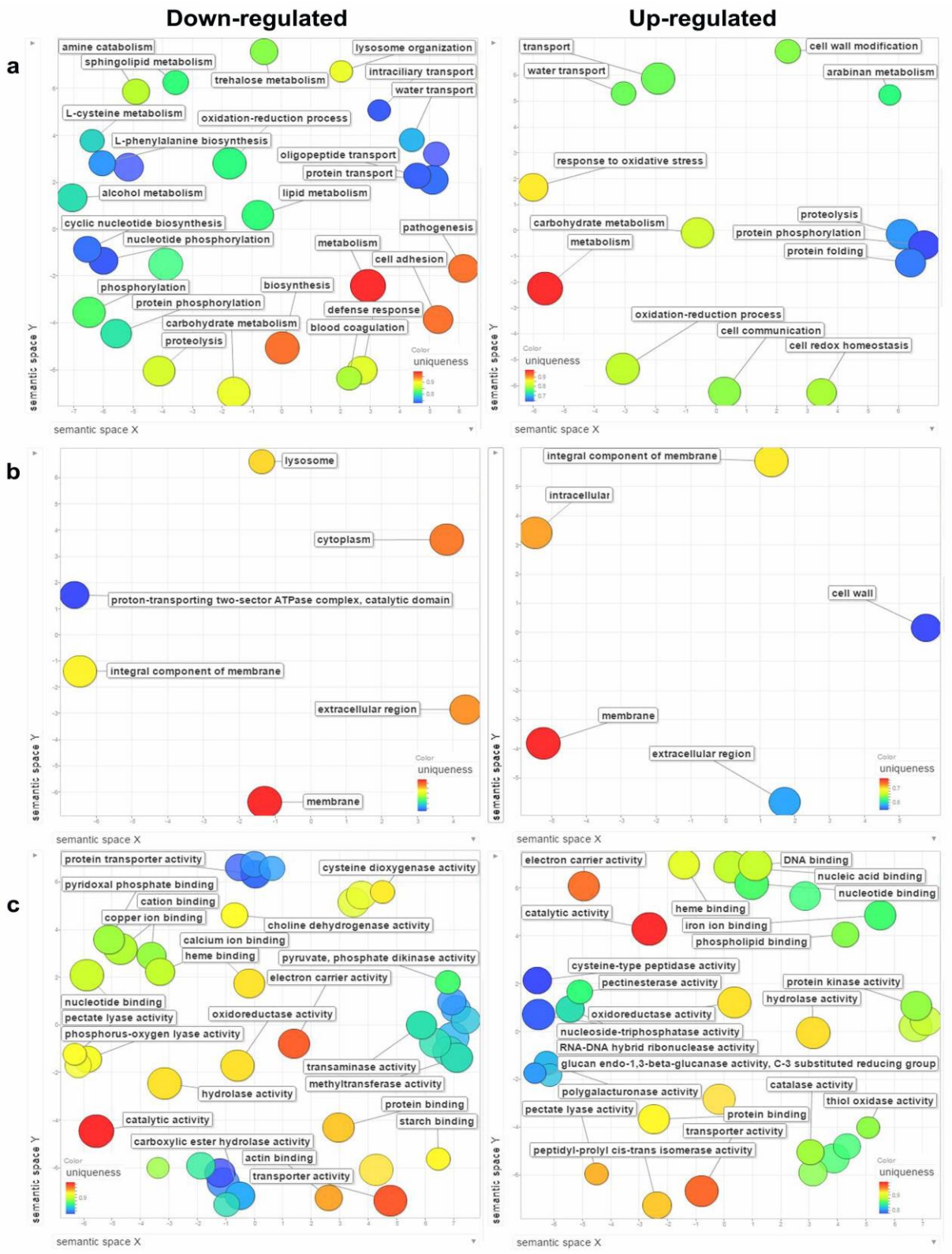

Figure 5.24. Differentially expressed *P. parasitica* genes in infected lupins (no phosphite and with phosphite) were subjected to GO enrichment analysis and summarised in scatterplots using the REVIGO web server. Summarised GO terms according to Biological Process (a), Cellular Component (b), and Molecular Function (c). Adjoining circles are most closely related and sizes are proportional to the frequency of the GO terms in Tables 5.11 & 5.12.

5.3.5.5. The effect of phosphite on the *P. parasitica* transcriptome

In order to narrow down metabolic pathways potentially affected by phosphite, an analysis focusing on identifying genes that were up-regulated or down-regulated both *in vitro* and *in planta* was employed. For this analysis, only transcripts with an RPKM ≥ 5 (FDR $p<0.05$, fold change ≥ 2) were considered. Blast2Go and NCBI BLASTp programs were used for this analysis. Phosphite treatment resulted in the down-regulation of 67 genes (Table 5.15) and the up-regulation of 54 genes (Table 5.16). Many of these genes encoded hypothetical proteins, including 44% down-regulated genes and 30% up-regulated genes. Four CWDE genes were down-regulated and these included two that act on cellulose (PPTG_05834 and PPTG_03846), a cellulose-binding protein (PPTG_00922) and one that degrades callose, (the GH17, PPTG_07724) (Table 5.15). Only one CWDE (PPTG_16828; GH81) was up-regulated and this one also acted on callose (Table 5.15). The tantalizing appearance of specific groups of genes up- or down-regulated following phosphite treatment, prompted further analysis to identify specific families or pathways.

5.3.5.6. Identification of specific families affected by phosphite

Initial analysis used the distribution of GO enrichment analysis and REVIGO visualisation to identify potential pathways in common with both experiments. There were 22 Biological Process GO terms, eight Cellular Components and 60 Molecular Function terms associated with 32 out of 66 down-regulated genes. Of the 54 up-regulated genes, only 30 had GO terms and these were 31 Biological Process, 12 Cellular Component and 61 Molecular Function terms. Following analysis, GO terms with related functions were clustered together (Figure 5.25). Most frequently represented GO terms were similar in both up- and down-regulated data sets although some terms were represented by different genes. This analysis highlighted the diversity of genes that were affected by phosphite but it did not indicate any specific families that were enriched which may be a function of the fact that not all genes of interest could be assigned GO terms.

In a different strategy, the function of all proteins encoded by genes whose expression was up- or down-regulated was analysed manually and, where

possible, functions were assigned to more general categories than that of the REVIGO analysis. Genes that were down-regulated encoded proteins that could be placed into 14 broad functional categories containing 66 proteins (Table 5.17). Of these, two were associated with oxidative stress and six were associated with transcription/translation.

There were 29 proteins that were uncharacterised and seven of which had secretion signals (Table 5.15). Proteins encoded by the 54 up-regulated genes were grouped into 16 different functional categories (Table 5.18). Two proteins were associated with pathogenesis (CWDE and secreted cysteine protease) and 11 were associated with oxidative stress. Eight proteins associated with transmembrane transport and one involved in turgor pressure regulator were also up-regulated (Table 5.18). Twenty-one proteins were uncharacterised, with two having a secretion signal and four with TMD (Table 5.16).

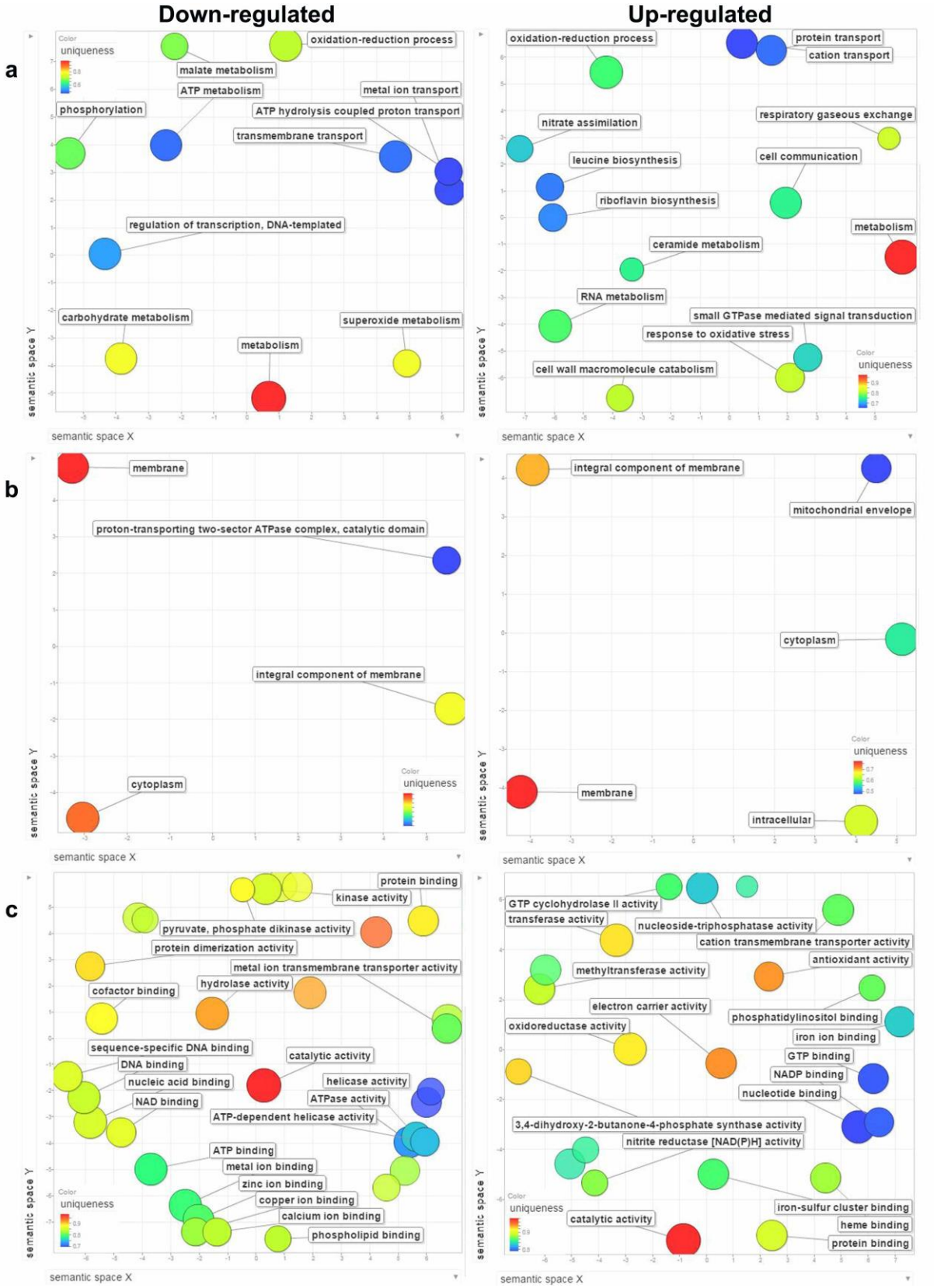

Figure 5.25. GO enrichment analysis on down-regulated and up-regulated *P. parasitica* genes in phosphite-treated mycelia and infected lupins shown in scatterplots using the REVIGO web server. Summarised GO terms according to Biological Processes (a), and Molecular Functions (b). Adjoining circles are most closely related and sizes are proportional to the frequency of the GO terms in Tables 5.15 and 5.16.

Table 5.15: *P. parasitica* genes down-regulated in the presence of phoshite according to a comparison of samples grown in modified Ribeiro's medium versus those grown in infected lupins. Data show predicted GO terms and IDs, and gene expression levels. * indicates that the putative function was assigned by the presence of domains found during NCBI BLASTp analysis.

									In vitro			***In planta***		
Gene ID	**Putative gene function**	**SP, TM**	**GO MF terms**	**GO MF ID**	**GO BP terms**	**GO BP ID**	**GO CC terms**	**GO CC ID**	**RPKM**	**RPKM + Phi**	**Fold change**	**RPKM infected lupin**	**RPKM infected lupin+ Phi**	**Fold change**
PPTG_00019	amino acid/auxin permease	No, 11	-	-	-	-	-	-	4	1	-3.7	511	129	-3.8
PPTG_00249	glycine-rich protein*	Yes, 0	-	-	-	-	-	-	3	1	-3.8	105	8	-13.3
PPTG_00364	hypothetical protein	No, 0	-	-	-	-	-	-	3	2	-2.2	6	1	-4.6
PPTG_00442	hypothetical protein	Yes, 0	metal ion binding	0046872	oxidation-reduction	0055114 0006801	-	-	24	5	-5.0	6	2	-3.1
PPTG_00922	GH78	Yes, 0	catalytic activity	0003824	-	-	-	-	2	1	-2.2	8	2	-4.1
PPTG_01190	hypothetical protein	Yes, 0	-	-	-	-	-	-	2	0	-6.4	5	2	-3.0
PPTG_01239	RNA helicase-like protein*	No, 0	ATP-dependent helicase activity,	0005524 0004386 0003676	-	-	-	-	21	9	-2.3	9	4	-2.1
PPTG_01546	hypothetical protein	No, 1	-	-	-	-	-	-	59	21	-2.9	90	23	-3.7
PPTG_02017	hypothetical protein	No, 0	-	-	-	-	-	-	333	127	-2.7	34	10	-3.4
PPTG_02053	protease inhibitor EpiC3	Yes, 0	-	-	-	-	-	-	3	1	-2.8	5	2	-3.0
PPTG_02544	zinc -ironpermease (ZIP) family	Yes, 7	metal ion transmembrane transporter	0005507 0046873 0016491	metal ion transport	0030001 0055114 0055085	membrane	0016020	55	27	-2.0	4	0	-11.0
PPTG_03113	hypothetical protein	Yes, 0	-	-	-	-	-	-	3	1	-2.0	45	7	-6.1
PPTG_03299	phosphatidylinositol-binding protein (pleckstrin)*	No, 0	-	-	-	-	-	-	381	168	-2.3	128	50	-2.4
PPTG_03448	zonadhesin-like protein	Yes, 0	-	-	-	-	-	-	11	5	-2.3	18	5	-3.3
PPTG_03815	glycine amidinotransferase	No, 0	hydrolase activity, (carbon-nitrogen)	0016813	-	-	-	0005737	390	164	-2.4	283	56	-4.8
PPTG_03846	GH5	No, 1	hydrolase activity (glycosyl)	0004553	carbo-hydrate metabo-lism	0005975	-	-	76	35	-2.2	136	37	-3.5
PPTG_04043	copine	No, 0	protein binding	0005515	-	-	-	-	137	69	-2.0	117	53	-2.1
PPTG_04387	Zinc-finger protein (CCCH type) *	No, 0	metal ion binding	0046872	-	-	-	-	59	9	-7.1	9	4	-2.3
PPTG_04510	MtN3-like protein	Yes, 6	-	-	-	-	-	-	8	1	-6.0	14	4	-3.1

Table 5.15. Cont.

PPTG_05068	bZIP DNA-binding protein*	Yes, 0	transcription factor activity	0046983 0003700	trans-cription regulation	0006355	-	-	97	16	-6.2	16	4	-4.2
PPTG_05678	hypothetical protein	Yes, 0	-	-	-	-	-	-	7	2	-2.9	4	2	-2.2
PPTG_05834	CBM1	Yes, 0	cellulose binding	0030248 0004553	carbo-hydrate metabo-lism	0005975	extracellular region	0005576	4	2	-2.2	90	9	-9.2
PPTG_05917	WD40 protein binding protein*	No, 0	protein binding	0005515	-	-	-	-	2	1	-2.2	9	3	-3.5
PPTG_05959	Myb-like DNA-binding protein	No, 0	DNA binding, chromatin binding	0003677 0003682	-	-	-	-	179	89	-2.0	40	16	-2.3
PPTG_05960	Myb-like DNA-binding protein	No, 0	DNA binding, chromatin binding	0003677 0003682	-	-	-	-	54	13	-4.2	12	3	-3.2
PPTG_06395	hypothetical protein	Yes, 1	-	-	-	-	-	-	4	1	-6.5	7	3	-2.4
PPTG_07195	hypothetical protein	No, 0	DNA binding	0003677	-	-	-	-	35	17	-2.0	3	1	-5.3
PPTG_07644	hypothetical protein	No, 0	-	-	-	-	-	-	32	7	-4.9	24	7	-3.3
PPTG_07645	ATP-binding Cassette (ABC) superfamily	No, 4	ATPase activity	0005524 0016887	-	-	membrane	0016020	58	14	-4.2	69	25	-2.6
PPTG_07724	GH17	Yes, 0	hydrolase activity (glycosyl)	0004553	carbo-hydrate metabo-lism	0005975	-	-	22	10	-2.1	187	44	-4.1
PPTG_08362	hypothetical protein	No, 0	protein binding	0005515	-	-	-	-	17	4	-4.3	13	6	-2.0
PPTG_08779	hypothetical protein	Yes, 0	-	-	-	-	-	-	412	156	-2.7	14	2	-8.4
PPTG_08856	hypothetical protein	No, 2	-	-	-	-	-	-	44	12	-3.8	60	15	-3.9
PPTG_08940	hypothetical protein	No, 0	-	-	-	-	-	-	18	5	-3.9	9	1	-7.6
PPTG_08977 (PPTG_22440)	ATP-binding cassette (ABC) lipid export transporter*	No, 8	ATPase activity	0005524 0016887	-	-	-	-	23	6	-3.8	7	3	-2.4
PPTG_08990	hypothetical protein	No, 0	-	-	-	-	-	-	254	122	-2.1	27	12	-2.1
PPTG_09370	hypothetical protein	No, 0	-	-	-	-	-	-	415	195	-2.2	234	83	-2.7
PPTG_09533	amino Acid/Auxin Permease (AAAP) family	No, 7	-	-	-	-	-	-	4	2	-2.1	85	2	-33.9
PPTG_09535	amino acid/auxin permease-like protein	No, 3	-	-	-	-	-	-	6	2	-2.8	129	3	-39.7

Table 5.15. Cont.

PPTG_09825	pyoverdine/dityrosine biosynthesis protein*	No, 0					-	-	26	10	-2.7	4	1	-2.7
PPTG_12023	D-isomer specific 2-hydroxyacid dehydrogenase	No, 0	oxidoreductase activity	0051287 0016616	oxidation-reduction	0055114	-	-	189	93	-2.1	15	6	-2.5
PPTG_12025	D-isomer specific 2-hydroxyacid dehydrogenase	No, 0	oxidoreductase activity	0051287 0016616	oxidation-reduction	0055114	-	-	38	18	-2.1	4	1	-2.3
PPTG_12638	hypothetical protein	No, 0	-	-	-	-	-	-	18	3	-7.2	17	8	-2.1
PPTG_13106	hypothetical protein	No, 0	-	-	-	-	-	-	24	10	-2.5	5	2	-2.0
PPTG_13307	hypothetical protein	No, 0	-	-	-	-	-	-	4	2	-2.1	34	16	-2.0
PPTG_13312	major facilitator superfamily transporter	No, 10	-	-	-	-	-	-	234	99	-2.4	85	32	-2.5
PPTG_13492	phosphatidylinositol-binding protein (pleckstrin)*	No, 0			-	-	-	-	109	52	-2.1	34	13	-2.6
PPTG_13504	hypothetical protein	No, 0	-	-	-	-	-	-	11	4	-2.6	6	2	-2.4
PPTG_13569	pyruvate, phosphate dikinase	No, 0	pyruvate, phosphate dikinase activity	0005524 0016301 0050242	pyruvate metabo-lism	0016310 0006090	-	-	297	93	-3.2	51	1	-69.4
PPTG_13951	ribonuclease inhibitor-like protein*	No, 0	-	-	-	-	-	-	32	11	-2.9	44	10	-4.0
PPTG_15267	hypothetical protein	No, 2	-	-	-	-	-	-	20	8	-2.5	15	7	-2.0
PPTG_15307	hypothetical protein	No, 0	-	-	-	-	-	-	19	9	-2.2	11	5	-2.1
PPTG_16848	chromosome segregation protein*	No, 0	protein binding	0005515	-	-	-	-	14	6	-2.5	12	6	-2.0
PPTG_17233	hypothetical protein	No, 0	ATPase activity	0005524 0016887	-	-	-	-	45	11	-4.2	41	15	-2.6
PPTG_17418	hypothetical protein	No, 1	transferase activity (glycosyl groups)	0016757	-	-	-	-	9	4	-2.3	4	1	-4.2

Table 5.15. Cont.

PPTG_17883	annexin family	No, 0	calcium-dependent phospholipid binding	0005509 0005544	-	-	-	-	671	297	-2.3	998	449	-2.1
PPTG_17884	annexin family	No, 0	calcium-dependent phospholipid binding	0005509 0005544	-	-	-	-	640	309	-2.1	1370	643	-2.0
PPTG_18451	inorganic phosphate transporter	No, 10	transmembrane transporter activity	0022857	trans-membrane transport	0055085	integral membrane	0016021	19	5	-4.0	47	8	-5.7
PPTG_18452	hypothetical protein	No, 6	transmembrane transporter activity	0022857	trans-membrane transport	0055085	integral membrane	0016021	5	1	-3.7	15	3	-5.2
PPTG_19000	hypothetical protein	No, 0	-	-	-	-	-	-	54	27	-2.0	76	19	-3.9
PPTG_19253	hypothetical protein	No, 0	-	-	-	-	-	-	141	58	-2.5	23	10	-2.2
PPTG_19369	NADP-dependent malic enzyme	No, 0	malate dehydrogenase	0051287 0004471	malate metabo-lism, oxidation-reduction	0006108 0055114	-	-	44	22	-2.1	4	2	-2.1
PPTG_19816	putative methyl transferase*	No, 0	protein binding	0005515	-	-	-	-	8	3	-2.6	3	1	-3.3
PPTG_20308	hypothetical protein	No, 0	-	-	-	-	-	-	28	6	-4.6	23	7	-3.3
PPTG_20376	hypothetical protein	Yes, 0	protein binding	0005515	-	-	-	-	2	1	-3.5	13	4	-3.6
PPTG_20451	ATP synthase subunit	No, 0	proton-transporting ATPase activity	0005524 0016820 0046961	ATP metabolic process	0046034 0015986 0015992	membrane	0016020	30	14	-2.3	122	16	-7.8

SP: secretion signal peptide, TM: transmembrane domain, GO: gene ontology, MF: Molecular Function, BP: Biological Process; CC: Cellular Component

Table 5.16. *P. parasitica* genes up-regulated in modified Ribeiro's medium plus phosphite and phosphite-treated infected lupins. showing predicted GO terms and IDs, and RPKM expression. * indicates that the putative function was assigned by the presence of domains found during NCBI BLASTp analysis.

									In vitro			*In planta*		
Gene ID	**Putative gene function**	**SP, TM**	**GO MF terms**	**GO MF ID**	**GO BP terms**	**GO BP ID**	**GO CC terms**	**GO CC ID**	**RPKM**	**RPKM + Phi**	**Fold change**	**RPKM infected lupin**	**RPKM infected lupin+ Phi**	**Fold change**
PPTG_00205	hypothetical protein	No, 2	-	-	-	-	-	-	150	322	2.1	1	3	2.9
PPTG_00530	hypothetical protein	No, 0	-	-	-	-	-	-	218	853	3.9	1	14	15.2
PPTG_00533	hypothetical protein	No, 0	-	-	-	-	-	-	97	385	3.9	1	5	10.5
PPTG_00627	phosphoinositide binding protein*	No, 0	phosphatidyl inositol binding	0035091	-	-	-	-	22	50	2.2	18	64	3.8
PPTG_02036	riboflavin biosynthesis protein	No, 0	3,4-dihydroxy-2-butanone-4-phosphate synthase	0008686 0003935	riboflavin biosynthesis	0009231	-	-	24	59	2.4	12	33	2.9
PPTG_02739	glutathione S-transferase	No, 0	protein binding	0005515	-	-	-	-	1	3	2.3	27	82	3.2
PPTG_02909	hypothetical protein	Yes, 0	-	-	-	-	-	-	124	521	4.1	7	19	2.6
PPTG_03018	ADP-ribosylation factor family protein	No, 0	GTP binding	0005525	GTPase mediated signal transduction	0006886 0007264	intracellular	0005622	1	12	12.6	21	86	4.3
PPTG_03046	hypothetical protein	No, 0	-	-	-	-	-	-	165	397	2.4	3	7	2.3
PPTG_04800	pyridine nucleotide-disulphide oxidoreductase	Yes, 0	oxido-reductase activity	0050660 0016491	oxidation-reduction	0055114	-	-	10	20	2.0	19	42	2.3
PPTG_05180	ornithine decarboxylase	No, 0	catalytic activity	0003824	-	-	-	-	26	71	2.7	12	25	2.1
PPTG_05254	hypothetical protein	No, 0	-	-	-	-	-	-	84	209	2.5	8	317	42.5
PPTG_05683	ankyrin-like protein*	No, 0	-	-	-	-	-	-	10	23	2.2	1	16	19.0
PPTG_06067	ATP-binding Cassette (ABC) superfamily	No, 12	ATPase activity	0005524 0016887	-	-	membrane	0016020	72	213	2.9	16	100	6.5
PPTG_06069	ATP-binding Cassette (ABC) superfamily	No, 12	ATPase activity	0005524 0016887	-	-	membrane	0016020	5	41	9.0	2	9	5.1
PPTG_06247	hypothetical protein	No, 1	-	-	-	-	-	-	8	17	2.1	7	117	18.4
PPTG_06299	mannitol dehydrogenase	Yes, 0	oxidoreductase activity	0016491 0008270	oxidation-reduction	0055114	-	-	25	54	2.2	128	332	2.7

Table 5.16. Cont.

PPTG_06664	catalase	No, 0	catalase activity	0004096 0020037	response to oxidative stress	0055114 0006979	-	-	9	22	2.3	2	12	6.1
PPTG_06756	short chain dehydrogenase	No, 0	oxidoreductase activity	0016491	metabolic process	0008152	-	-	50	220	4.4	2	5	2.3
PPTG_06758	short chain dehydrogenase	No, 0	oxidoreductase activity	0016491	metabolic process	0008152	-	-	287	813	2.8	14	33	2.5
PPTG_06866	catalase	No, 0	catalase activity	0004096 0020037	response to oxidative stress	0055114 0006979	-	-	1	2	3.1	4	28	7.8
PPTG_06907	hypothetical protein	No, 0	-	-	-	-	-	-	1	3	4.2	1	9	16.3
PPTG_07051	cytochrome c	No, 0	electron carrier activity	0009055 0020037 0005506	-	-	-	-	305	688	2.2	364	774	2.2
PPTG_07498	3-isopropylmalate dehydrogenase	No, 0	oxidoreductase activity	0003862	oxidation-reduction	0009098 0055114	cytoplasm	0005737	23	47	2.0	76	160	2.2
PPTG_08198	mitochondrial tricarboxylate carrier	No, 0	cation transmembrane transporter	0008324	transmembrane transport	0006812 0055085	membrane	0016020	9	20	2.2	12	24	2.1
PPTG_08423	PLAC8 family protein	No, 1	-	-	-	-	-	-	2	5	2.6	1	15	15.3
PPTG_08574	12-oxophytodienoate reductase	No, 0	oxidoreductase activity	0010181 0016491	oxidation-reduction	0055114	-	-	7	36	4.8	6	16	2.8
PPTG_08582	12-oxophytodienoate reductase	No, 0	oxidoreductase activity	0010181 0016491	oxidation-reduction	0055114	-	-	56	279	4.9	46	99	2.3
PPTG_09715	very-long-chain 3-oxoacyl-CoA synthase	No, 7	-	-	-	-	integral membrane	0016021	4	12	2.9	3	8	2.5
PPTG_10003	maltose O-acetyltransferase	No, 0	transferase activity	0016407	-	-	-	-	2	6	2.6	12	27	2.3
PPTG_10149	cleavage induced serine protease S33	Yes, 0	-	-	-	-	-	-	57	132	2.3	7	18	2.7
PPTG_10399	mannitol dehydrogenase	No, 0	transferase activity,	0016491 0016747 0008270	oxidation-reduction	0055114	-	-	2	5	2.2	2	8	3.7
PPTG_10400	hypothetical protein	No, 0	catalytic activity	0003824			-	-	15	31	2.0	40	175	4.6
PPTG_11416	peroxiredoxin-2	No, 0	peroxiredoxin activity	0051920	oxidation-reduction	0055114	-	-	91	214	2.3	53	157	3.1

Table 5.16. Cont.

PPTG_11417	peroxiredoxin-2	No, 0	peroxiredoxin activity	0051920	oxidation-reduction	0055114	-	-	255	571	2.2	126	384	3.2
PPTG_11615	hypothetical protein	No, 0	-	-	-	-	-	-	7	15	2.0	2	33	24.8
PPTG_11850	drug/metabolite transporter	No, 10	-	-	-	-	membrane	0016020	103	243	2.3	18	44	2.6
PPTG_11865	alkaline phytoceramidase	No, 7	hydrolase activity, (carbon-nitrogen)	0016811	ceramide metabolism	0006672	integral membrane	0016021	14	41	2.9	13	28	2.2
PPTG_13824	hypoxia induced protein*	No, 0	-	-	-	-	-	-	358	975	2.7	25	139	5.9
PPTG_13825	protein kinase (cell cycle control protein*)	No, 2	-	-	-	-	membrane	0016020	64	132	2.0	4	21	5.2
PPTG_14491	hypothetical protein	No, 0	-	-	-	-	-	-	1	3	2.1	2	5	2.5
PPTG_15061	major facilitator superfamily transporter	No, 9	substrate-specific transmembrane transporter activity	0022891	transmembrane transport	0055085	integral membrane	0016021	8	30	3.7	4	35	9.5
PPTG_15850	ATP-binding Cassette superfamily protein	No, 0	-	-	-	-	-	-	5	23	4.3	8	18	2.2
PPTG_16126	SPRYRanBP-like protein*	No, 0	protein binding	0005515	-	-	-	-	19	51	2.7	47	95	2.1
PPTG_16828	GH81	No, 1	endo-β-1,3-glucanase activity	0052861 0052862	cell wall catabolism	0016998	-	-	1	8	5.8	6	214	38.7
PPTG_16830	hypothetical protein	No, 0	-	-	-	-	-	-	15	43	2.9	7	460	66.7
PPTG_16831	hypothetical protein	No, 0	-	-	-	-	-	-	3	17	5.6	14	260	19.6
PPTG_16833	hypothetical protein	No, 0	-	-	-	-	-	-	1	2	4.2	1	41	45.9
PPTG_16900	nitrite reductase [NAD(P)H]	No, 0	nitrite reductase	0051537 0050661 0050660 0020037 0008942	nitrate assimilation	0042128 0055114	-	-	49	106	2.2	13	48	3.8
PPTG_18782	alternative oxidase	No, 1	alternative oxidase activity	0009916	oxidation-reduction	0055114	-		11	53	4.6	4	20	5.2

Table 5.16. Cont.

PPTG_18786	S-adenosylmethionine-dependent methyltransferase*	No, 0	methyltransferase activity	0008168	metabolic process	0008152	-	-	628	1320	2.1	9	38	4.3
PPTG_18913	hypothetical protein	No, 4	-	-	-	-	-	-	16	43	2.7	53	301	5.7
PPTG_18914	hypothetical protein	Yes, 3	-	-	-	-	-	-	10	29	2.8	30	141	4.9
PPTG_19128	mitochondrial carrier	Yes, 0	-	-	-	-	-	-	41	98	2.4	37	135	3.8

SP: secretion signal peptide, TM: transmembrane domain, GO: gene ontology, MF: Molecular Function, BP: Biological Process; CC: Cellular Component

Table 5.17. Grouping of down-regulated genes with similar functions. The annotation was checked manually as outlined in the methods and according to available literature.

Functional category	No.	Gene ID	Specific function
hypothetical protein	29	PPTG_00364, PPTG_00442, PPTG_01190, PPTG_01546, PPTG_02017, PPTG_03113, PPTG_05678, PPTG_06395, PPTG_07195, PPTG_07644, PPTG_08362, PPTG_08779, PPTG_08856, PPTG_08940, PPTG_08990, PPTG_09370, PPTG_12638, PPTG_13106, PPTG_13307, PPTG_13504, PPTG_15267, PPTG_15307, PPTG_17233, PPTG_17418, PPTG_18452, PPTG_19000, PPTG_19253, PPTG_20308, PPTG_20376	
adhesion	1	PPTG_03448	zonadhesin-like protein
amino acid biosynthesis/ metabolism	2	PPTG_03815	glycine amidinotransferase, (Pang *et al.*, 2015)
		PPTG_13569	pyruvate, phosphate dikinase (FungiDB)
ATP synthesis	1	PPTG_20451	ATP synthase subunit
cell cycle	1	PPTG_16848	chromosome segregation protein
pathogenesis	6	PPTG_05834	CBM1 (Blackman *et al.,* 2014)
		PPTG_07724	GH17 (Blackman *et al.,* 2014)
		PPTG_03846	(Blackman *et al.,* 2014)
		PPTG_00922	GH78 (Blackman *et al.,* 2014)
		PPTG_02053	protease inhibitor EpiC3 (Tian *et al.*, 2007)
		PPTG_00249	Secreted glycine-rich protein (putative virulence protein), (Raffaele *et al.*, 2010)
lipid-associated protein	2	PPTG_17883, PPTG_17884	annexin
phenylalanine metabolism	2	PPTG_12023, PPTG_12025	D-isomer specific 2-hydroxyacid dehydrogenase(Fujii *et al.*, 2011)
response to oxidative stress	2	PPTG_19369	NADP-dependent malic enzyme, (Valderrama *et al.*, 2006)
		PPTG_13951	ribonuclease inhibitor-like protein, (Dickson *et al.*, 2005)
signal transduction	4	PPTG_13492, PPTG_03299	phosphatidylinositol-binding protein (pleckstrin) (DOWLER *et al.*, 2000)
		PPTG_04043	Copine: calcium-dependent membrane-binding protein, (Zou *et al.*, 2016)
		PPTG_05917	WD40 protein binding protein (FungiDB)
stress response	1	PPTG_09825	pyruvate, phosphate dikinase (FungiDB)
transcription/ translation regulation	6	PPTG_05068	bZIP DNA-binding protein
		PPTG_05959, PPTG_05960	Myb-like DNA-binding protein
		PPTG_19816	methyl transferase
		PPTG_01239	RNA helicase-like protein, (Jarmoskaite and Russell, 2014)
		PPTG_04387	Zinc-finger protein (CCCH type)
transmembrane transport	8	PPTG_00019, PPTG_09533, PPTG_09535	amino acid/auxin permease
		PPTG_08977 (PPTG_22440),	ATP-binding cassette (ABC) lipid export transporter, (Schneider and Hunke, 1998)
		PPTG_07645	ATP-binding Cassette (ABC) superfamily, (Schneider and Hunke, 1998).
		PPTG_18451	inorganic phosphate transporter
		PPTG_13312	major facilitator superfamily transporter
		PPTG_02544	zinc-iron permease (ZIP) family (FungiDB)
vesicle-trafficking	1	PPTG_04510	MtN3-like protein

Table 5.18. Grouping of proteins with similar functions encoded by up-regulated genes. The annotation was checked manually as outlined in the methods and according to available literature.

Functional category	No.	Gene ID	Specific function
hypothetical protein	16	PPTG_00205, PPTG_00530, PPTG_00533, PPTG_02909, PPTG_03046, PPTG_05254, PPTG_06247, PPTG_06907, PPTG_11615, PPTG_14491, PPTG_10400, PPTG_16830, PPTG_16831, PPTG_16833, PPTG_18913/PPTG_18914 (PPTG_24384)	-
amino acid biosynthesis	1	PPTG_07498	3-isopropylmalate dehydrogenase (FungiDB)
ATP synthesis	1	PPTG_07051	cytochrome C
cell/carbon metabolism	2	PPTG_02036	riboflavin biosynthesis protein
		PPTG_10003	maltose O-acetyltransferase (Montánchez *et al.*, 2014)
cell cycle	2	PPTG_13825	protein kinase (cell cycle control protein)
		PPTG_16126	SPRY RanBP-like protein (Sacco *et al.*, 2009)
cytoskeleton	1	PPTG_03018	ADP-ribosylation factor family protein
fatty acid biosynthesis	1	PPTG_09715	very-long-chain 3-oxoacyl-CoA synthase (FungiDB)
lipoxygenase pathway	2	PPTG_08574, PPTG_08582	12-oxophytodienoate reductase (FungiDB)
polyamine biosynthesis	1	PPTG_05180	ornithine decarboxylase, (Ramos-Molina *et al.*, 2013)
pathogenesis	2	PPTG_16828	CWDE (GH81)
		PPTG_10149	cleavage induced serine protease S33
protein-protein interaction	1	PPTG_05683	ankyrin-like protein, (Mosavi *et al.*, 2004)
response to oxidative stress	11	PPTG_06664, PPTG_06866	catalase (Mittler *et al.*, 2004)
		PPTG_02739	glutathione S-transferase
		PPTG_16900	nitrite reductase; (Corpas *et al.*, 2015)
		PPTG_11416, PPTG_11417	peroxiredoxin-2, (Mittler *et al.*, 2004)
		PPTG_04800	pyridine nucleotide-disulphide oxidoreductase (Budachetri and Karim, 2015)
		PPTG_18786	S-adenosylmethionine-dependent methyltransferase, (Chatterjee *et al.*, 2015)
		PPTG_10399, PPTG_06299	mannitol dehydrogenase, (Patel and Williamson, 2016)
		PPTG_18782	alternative oxidase, (Mittler *et al.*, 2004)
signal transduction	3	PPTG_00627	phosphoinositide binding protein, (DOWLER *et al.*, 2000)
		PPTG_06756, PPTG_06758	short chain dehydrogenase, (Kavanagh *et al.*, 2008)
stress response	1	PPTG_13824	hypoxia induced protein, (Gracey *et al.*, 2001)
transmembrane transport	8	PPTG_06067, PPTG_06069, PPTG_15850	ATP-binding Cassette (ABC) superfamily (Schneider and Hunke, 1998)
		PPTG_11850	drug/metabolite transporter
		PPTG_15061	major facilitator superfamily transporter
		PPTG_08423	Placenta-specific gene 8 protein (PLAC8), (Song *et al.*, 2011; Jiang *et al.*, 2013)
		PPTG_19128, PPTG_08198	mitochondrial carrier (Picault *et al.*, 2004)
turgor pressure regulation	1	PPTG_11865	alkaline phytoceramidase(Chen *et al.*, 2015)

The number of genes associated with broad functional categories are shown in Table 5.19. From this analysis, it was possible to determine several functional groups which were up- or down-regulated following phosphite treatment. Of special note was that there were more pathogenesis-related genes down-regulated in response to phosphite than were up-regulated and there were more genes associated with reactive oxygen stress that were up-regulated than were down-regulated. The pathogenesis genes that were down-regulated included four CWDEs. Given the immunofluorescence results showing a decrease in Vsv labelling and the plasmolysis of cells in phosphite-treated hyphae (Sections 5.4.4), the identification of a down-regulated adhesive and an up-regulated turgor pressure regulator was of particular interest. Some of these groups are described in the following sections.

Table 5.19. Summary of the broad functional categories of proteins that were encoded by genes which were up- and down-regulated in response to phosphite treatment of mycelia and lupin roots prior to infection.

Down-regulated		**Up-regulated**	
Functional category	**Number**	**Functional category**	**Number**
hypothetical protein	29	hypothetical protein	16
adhesion	1		
amino acid biosynthesis/ metabolism	2	amino acid biosynthesis	1
ATP synthesis	1	ATP synthesis	1
		cell/ carbon metabolism	2
cell cycle	1	cell cycle	2
		cytoskeleton	1
		fatty acid biosynthesis	1
lipid-associated protein	2		
		lipoxygenase pathway	2
pathogenesis	6	pathogenesis	2
phenylalanine metabolism	2		
		polyamine biosynthesis	1
		protein-protein interaction	1
response to oxidative stress	2	response to oxidative stress	11
signal transduction	4	signal transduction	3
stress response	1	stress response	1
transcription/ translation regulation	6		
transmembrane transport	8	transmembrane transport	8
		turgor pressure regulation	1
vesicle-trafficking	1		

5.3.5.7. The effect of phosphite on specific gene families

5.3.5.7.1. CWDEs

There were 147 CWDE genes from a total of 431 putative CWDE genes (Blackman *et al*., 2014) that were differentially expressed both *in vitro* and *in planta* but only nine of these were differentially expressed in both situations. In *P. parasitica*-infected lupin roots, 128 CWDE genes were significantly differentially expressed between treatments (FDR $P<0.05$, RPKM ≥2, fold change ≥2) with an equal number being up- and down-regulated (Table 5.20) and the highest number of CWDEs acting on pectins (Table 5.20, Figure 5.26a). More CWDEs acting on pectins were up-regulated in phosphite-treated lupin roots infected with *P. parasitica* than were down-regulated (Figure 5.26b). By contrast, more CWDEs acting on cellulose and hemicellulose were down regulated. On the other hand, only 28 CWDEs were differentially expressed in the *in vitro* experiment and more enzymes acted on callose than on any other cell wall component (Table 5.21, Figure 5.27a). Only six of the 28 CWDEs were up-regulated with phosphite treatment. *In vitro*, more enzymes acting on callose and pectins were down-regulated following phosphite treatment than in controls (Figure 5.27b). Of the CWDEs in the *P. parasitica* genome, 25% act specifically on pectins (Blackman *et al.*, 2015), and during the infection of lupin in the current study, 33% of the differentially expressed genes were pectinases. This contrasts with the *in vitro* study where only 21% of differentially expressed genes were pectinases but 32% were β-1,3-glucanases acting on callose. The three most highly and differentially expressed CWDEs down-regulated following phosphite treatment in roots were two CBM1 genes (PPTG_05833 and PPTG_13482) and an amylase involved in starch degradation (PPTG_01216) (Table 5.20). This is different to the *in vitro* experiment in which the top three down-regulated CWDEs act on callose (PPTG_12454, PPTG_14787, PPTG_12451; Table 5.21).

Some similarities were observed in the types and number of CWDEs that were differentially expressed in *P. parasitica*-infected lupins compared to the *in vitro* samples. Of the nine *P. parasitica* CWDEs in common in both experiments (Tables 5.20, 5.21), four genes are more highly expressed during infection and are down-regulated in phosphite-treated samples in both *in vitro* and *in planta*

experiments. These were genes for a pectinase (PPTG_00922: GH78, a β-1,3-glucanase; PPTG_07724: GH17), and two proteins whose substrate was cellulose (PPTG_03846: GH5; PPTG_05834: CBM1). However, there was no consistency in the up- or down-regulation of enzymes acting on specific substrates. For example, a pectinase (PPTG_08053: CE12) and a GH3 acting on hemicellulose/cellulose and arabinogalactan proteins (PPTG_14483: GH3) were up-regulated in phosphite-treated *P. parasitica*-infected lupin and down-regulated *in vitro* in the presence of phosphite.

Table 5.20. Differentially expressed cell wall degrading enzyme transcripts in phosphite-treated (50 μg/ml) and inoculated lupins (FDR p<005; >2-fold change). Main enzyme activities as predicted by Blackman *et al.* (2014) and predicted targets are shown. HG: homogalacturonan; HC: hemicellulose; C: cellulose; RGI: rhamnogalacturonan 1; AGP: arabinogalactan protein; CA: callose. *the gene maps to *P. parasitica* genome in mock inoculated lupin.

Gene ID	Domain	Putative gene function	Lupin +Pp RPKM	Lupin +Pp+Phi RPKM	Fold change
PPTG_03142	AA10	copper-dependent monooxygenase (C)	1	3	2.7
PPTG_03081	AA10	copper-dependent monooxygenase (C)	13	28	2.3
PPTG_15949	AA7	cellobiose (C)	4	23	5.9
PPTG_15948	AA7	cellobiose (C)	3	15	5.6
PPTG_19661	AA7	cellobiose (C)	13	57	4.6
PPTG_15947	AA7	cellobiose (C)	5	21	4.1
PPTG_15796	AA7	chitooligosaccharides (AGP)	1	3	2.0
PPTG_04148	AA8	iron reductase (C)	4	16	4.2
PPTG_05659	AA8	iron reductase (C)	9	2	-5.1
PPTG_19098	CBM1	binds to β-1,4-glucans (C)	283	132	-2.1
PPTG_10047	CBM1	binds to β-1,4-glucans (C)	122	55	-2.1
PPTG_13482	CBM1	binds to β-1,4-glucans (C)	753	316	-2.3
PPTG_05833	CBM1	binds to β-1,4-glucans (C)	545	216	-2.4
PPTG_04643	CBM1	binds to β-1,4-glucans (C)	54	8	-6.3
PPTG_17441	CBM1	binds to β-1,4-glucans (C)	31	3	-9.1
PPTG_05834	CBM1	binds to β-1,4-glucans (C)	90	9	-9.2
PPTG_00479	CBM1	binds to β-1,4-glucans (C)	5	0	-12.5
PPTG_09699	CBM13	binds to hemicellulose (HC)	29	9	-3.1
PPTG_15107	CBM13	binds to hemicellulose (HC)	3	0	-5.7
PPTG_20351	CBM13	binds to hemicellulose (HC)	5	0	-14.5
PPTG_10596	CBM40	removal of sialic residues (AGP)	2	0	-4.5
PPTG_12541	CBM63	binds to β-1,4-glucans (C)	3	13	4.3
PPTG_19415	CBM63	binds to β-1,4-glucans (C)	5	12	2.7
PPTG_18397	CBM63	binds to β-1,4-glucans (C)	5	3	-2.1
PPTG_00806	CE1	feruloyl esterase (HC)	4	2	-2.1
PPTG_14690	CE12	pectin acetyl esterase (HG, RG1)	2	6	4.3
PPTG_10440	CE12	pectin acetyl esterase (HG, RG1)	16	44	2.9
PPTG_16477	CE12	pectin acetyl esterase (HG, RG1)	4	9	2.4
PPTG_08053	CE12	pectin acetyl esterase (HG, RG1)	3	6	2.3
PPTG_10136	CE13	pectin acetyl esterase (HG)	1	4	4.9
PPTG_10125	CE13	pectin acetyl esterase (HG)	99	33	-2.9

Table 5.20. Cont.

PPTG_10126	CE13	pectin acetyl esterase (HG)	30	2	-12.4
PPTG_19215	CE5	acetyl xylan esterase (HC)	4	1	-3.0
PPTG_19214	CE5	acetyl xylan esterase (HC)	51	6	-7.6
PPTG_07182	CE5	acetyl xylan esterase (HC)	21	1	-15.2
PPTG_07616	CE8	pectin methyl esterase (HG)	1	7	6.6
PPTG_10338	CE8	pectin methyl esterase (HG)	8	39	4.9
PPTG_05287	CE8	pectin methyl esterase (HG)	2	8	3.6
PPTG_06239	CE8	pectin methyl esterase (HG)	20	61	3.2
PPTG_09705	CE8	pectin methyl esterase (HG)	3	7	2.9
PPTG_12007	GH1	β-glucosidase (C, HC)	6	2	-2.6
PPTG_05794	GH1	β-glucosidase (C, HC)	26	8	-3.1
PPTG_12052	GH1	β-glucosidase (C, HC)	6	2	-3.7
PPTG_12011	GH1	β-glucosidase (C, HC)	91	20	-4.5
PPTG_12009	GH1	β-glucosidase (C, HC)	71	14	-4.8
PPTG_04933	GH1	β-glucosidase (C, HC)	5	1	-5.1
PPTG_12010	GH1	β-glucosidase (C, HC)	49	8	-5.7
PPTG_17851	GH10	β-1,4-xylanase (HC)	3	9	3.0
PPTG_17240	GH10	β-1,4-xylanase (HC)	14	31	2.3
PPTG_07904	GH105	rhamnogalacturonyl hydrolase (RG1)	5	27	5.9
PPTG_05922	GH109	α- N-acetylgalactosaminidase (AGP)	161	61	-2.5
PPTG_11504	GH12	β-1,4-glucanase (C, HC)	1	5	5.6
PPTG_16566	GH12	β-1,4-glucanase (C, HC)	7	19	2.8
PPTG_19378	GH12	β-1,4-glucanase (C, HC)	55	18	-2.8
PPTG_02681	GH13/CBM25	Amylase (starch)	34	5	-6.7
PPTG_10230	GH131	β-1,4-glucanase (C, HC)	1	3	5.3
PPTG_10232	GH131	β-1,4-glucanase (C, HC)	14	30	2.2
PPTG_00797	GH131	β-1,4-glucanase (C, HC)	8	17	2.2
PPTG_12466	GH16	β-1,3-glucanase (CA)	1	3	4.3
PPTG_12473	GH16	β-1,3-glucanase (CA)	25	10	-2.5
PPTG_12474	GH16	β-1,3-glucanase (CA)	3	1	-2.9
PPTG_00165	GH16	β-1,3-glucanase (CA)	4	1	-3.4
PPTG_12471	GH16	β-1,3-glucanase (CA)	93	25	-3.6
PPTG_12468	GH16	β-1,3-glucanase (CA)	10	2	-6.6
PPTG_17201	GH17	β-1,3-glucanase (CA)	9	28	3.5
PPTG_05079	GH17	β-1,3-glucanase (CA)	43	19	-2.2
PPTG_11267	GH17	β-1,3-glucanase (CA)	101	37	-2.6
PPTG_07724	GH17	β-1,3-glucanase (CA)	187	44	-4.1
PPTG_15171	GH28	Polygalacturonase (HG)	3	20	8.0
PPTG_15164*	GH28	polygalacturonase (HG)	1	8	6.4
PPTG_15162	GH28	polygalacturonase (HG)	2	10	5.3
PPTG_15172	GH28	Polygalacturonase (HG)	8	29	3.7
PPTG_17704	GH28	polygalacturonase (HG)	3	11	3.5
PPTG_15169	GH28	polygalacturonase (HG)	2	4	2.7
PPTG_15170	GH28	polygalacturonase (HG)	2	5	2.5
PPTG_14483	GH3	β-1,4-glucanase; α-arabinanase (C, HC, AGP)	3	9	3.5
PPTG_14613	GH3	β-1,4-xylanase (HC)	1	3	2.6
PPTG_19675	GH3	β-1,4-glucanase; α-arabinanase (C, HC, AGP)	13	29	2.3
PPTG_05877	GH3	β-1,4-glucanase; α-arabinanase (C, HC, AGP)	15	7	-2.1
PPTG_14386	GH3	β-1,4- xylanase (HC)	18	7	-2.4
PPTG_00397	GH3	β-1,4-glucanase; α-arabinanase (C, HC, AGP)	4	1	-3.8

Table 5.20. Cont.

PPTG_14482	GH3	β-1,4-glucanase; α-arabinanase (C, HC, AGP)	21	4	-4.6
PPTG_14391	GH3	β-1,4-glucanase; α-arabinanase (C, HC, AGP)	6	1	-6.1
PPTG_18120	GH30	β-1,6-galactanase (RG1, AGP)	13	30	2.5
PPTG_16010	GH30	β-1,6-galactanase (RG1, AGP)	45	100	2.3
PPTG_14860	GH30	β-1,6-galactanase (RG1, AGP)	45	97	2.3
PPTG_14859	GH30	β-1,6-galactanase (RG1, AGP)	3	7	2.1
PPTG_07665	GH30	β-1,4-glucanase (C)	161	55	-2.8
PPTG_09216	GH30	β-1,4-glucanase (C)	61	4	-14.5
PPTG_08511	GH30/CBM13	β-1,4-xylosidase (HC)	32	12	-2.6
PPTG_09365	GH31	α-glucosidase (starch)	64	13	-4.6
PPTG_01216	GH31/CBM25	α-glucosidase (starch)	468	77	-5.8
PPTG_09925	GH32	Invertase (sucrose)	5	11	2.2
PPTG_09929	GH32	Invertase (sucrose)	7	13	2.1
PPTG_18624	GH37	α, α-trehalase	20	7	-2.6
PPTG_17405	GH43	β-xylosidase, β-1,3-galactosidase, α-arabinanase (HC, RG1, AGP)	2	6	3.1
PPTG_15711	GH43	β-xylosidase, β-1,3-galactosidase, α-arabinanase (HC, RG1, AGP)	8	20	2.6
PPTG_15714	GH43	β-xylosidase, β-1,3-galactosidase, α-arabinanase (HC, RG1, AGP)	8	3	-2.8
PPTG_17406	GH43	β-xylosidase, β-1,3-galactosidase, α-arabinanase (HC, RG1, AGP)	8	1	-5.0
PPTG_05786	GH5	endo-β-1,4-glucanase (C)	7	14	2.0
PPTG_16240	GH5	exo-β-1,3-glucosidase (CA)	5	2	-2.5
PPTG_03846	GH5	endo-β-1,4-glucanase (C)	136	37	-3.5
PPTG_16244	GH5	exo-β-1,3-glucosidase (CA)	7	1	-8.3
PPTG_01940	GH5/CBM43	exo-β-1,3-glucansase (CA)	12	41	3.4
PPTG_19167	GH53	β-1,4-galactanase(RG1)	300	74	-3.8
PPTG_19168	GH53	β-1,4-galactanase(RG1)	46	6	-7.3
PPTG_18202	GH54	α-L-arabinofuranosidase (RG1, AGP)	3	15	6.3
PPTG_00142	GH6	β-1,4-glucanase (C)	5	18	4.1
PPTG_07017	GH7	β-1,4-glucanase (C)	3	10	4.1
PPTG_00925	GH78	α-rhamnosidase (RG1)	4	2	-2.3
PPTG_03793	GH78	α-rhamnosidase (RG1)	31	8	-3.7
PPTG_00922	GH78	α-rhamnosidase (RG1)	8	2	-4.3
PPTG_00926	GH78	α-rhamnosidase (RG1)	15	3	-4.7
PPTG_16828	GH81	endo-β-1,3-glucanase (CA)	6	214	38.7
PPTG_10161	GH81	endo-β-1,3-glucanase (CA)	1	2	3.1
PPTG_11777	GH89	β-N-acetylglucosaminidase (AGP)	24	7	-3.4
PPTG_15708	PL1	pectate lyase/pectin lyase (HG)	1	6	4.8
PPTG_12899	PL1	pectate lyase/pectin lyase (HG)	2	6	3.9
PPTG_12902	PL1	pectate lyase/pectin lyase (HG)	1	2	3.4
PPTG_15712	PL1	pectate lyase/pectin lyase (HG)	17	4	-4.5
PPTG_07181	PL3	pectate lyase (HG)	0	2	7.3
PPTG_05840	PL3	pectate lyase (HG)	1	4	4.8
PPTG_19418	PL3	pectate lyase (HG)	5	15	3.26
PPTG_11095	PL3	pectate lyase (HG)	6	0	-19.2
PPTG_11096	PL3	pectate lyase (HG)	14	1	-25.1
PPTG_05074	PL4	rhamnogalacturonan lyase (RG1)	9	42	4.6
PPTG_05072	PL4	rhamnogalacturonan lyase (RG1)	2	7	3.9
PPTG_05103	PL4	rhamnogalacturonan lyase (RG1)	2	8	3.5

Table 5.21. Differentially expressed cell wall degrading enzyme transcripts in phosphite-treated (50 µg/ml) *P. parasitica* mycelia. (FDR p<005; >2-fold change). Predicted main enzyme activities as suggested by Blackman *et al.* (2014) are shown with targets in brackets. HG: homogalacturonan; RGI: rhamnogalacturonan 1; AGP: arabinogalactan protein, HC: hemicellulose; C: cellulose; CA: callose.

Gene ID	Domain	Putative gene function	Mean Pp RPKM	Mean Pp+Phi RPKM	Fold change
PPTG_05834	CBM1	β-1,4-glucans (C)	4	2	-2.22
PPTG_14659	CBM40	terminal sialic residues (AGP)	15	3	-5.10
PPTG_18395	CBM63	β-1,4-glucans (C)	6	2	-2.43
PPTG_08053	CE12	pectin acetyl esterase (HG, RGI)	2	1	-2.39
PPTG_17240	GH10	β-1,4-xylanase acts (HC)	18	8	-2.17
PPTG_05922	GH109	α-N-acetylgalactosaminidase(AGP)	13	43	3.23
PPTG_12454	GH16	β-1,3-glucanase (CA)	174	66	-2.66
PPTG_12451	GH16	β-1,3-glucanase (CA)	525	198	-2.70
PPTG_07724	GH17	β-1,3-glucanase (CA)	22	10	-2.09
PPTG_02889	GH17	β-1,3-glucanase (CA)	38	16	-2.31
PPTG_02886	GH17	β-1,3-glucanase (CA)	32	11	-3.04
PPTG_15937	GH3	β-1,4-glucanase; αarabinanase (C, HC, AGP)	3	1	-2.86
PPTG_14483	GH3	β-1,4-glucanase,αarabinanase (C, HC,AGP)	5	1	-7.03
PPTG_09210	GH30	β-1,4-glucosidase (C, HC)	4	13	3.16
PPTG_09211	GH30	β-1,4-glucosidase (C)	5	2	-2.69
PPTG_08507	GH30/CBM13	β-1,4-xylosidase (CH)	2	5	2.21
PPTG_03687	GH31	α-glucosidase (starch)	2	6	2.60
PPTG_09926	GH32	invertase (sucrose)	10	4	-2.39
PPTG_01483	GH5	β-1,3-glucosidase (CA)	14	35	2.48
PPTG_03846	GH5	β-1,4-glucanase (C)	76	35	-2.23
PPTG_18794	GH53	β-1,4-galactanase (RGI)	5	2	-2.20
PPTG_14787	GH72	β-1,3-glucanase (CA)	362	164	-2.25
PPTG_09844	GH72	β-1,3-glucanase (CA)	16	6	-2.50
PPTG_00922	GH78	α-rhamnosidase (RGI)	2	1	-2.24
PPTG_16828	GH81	β-1,3-glucanase (CA)	1	8	5.83
PPTG_17499	PL1	pectate lyase/pectin lyase (HG)	52	17	-3.04
PPTG_17505	PL1	pectate lyase/pectin lyase (HG)	3	1	-3.63
PPTG_03562	PL3	pectate lyase (HG)	2	1	-3.44

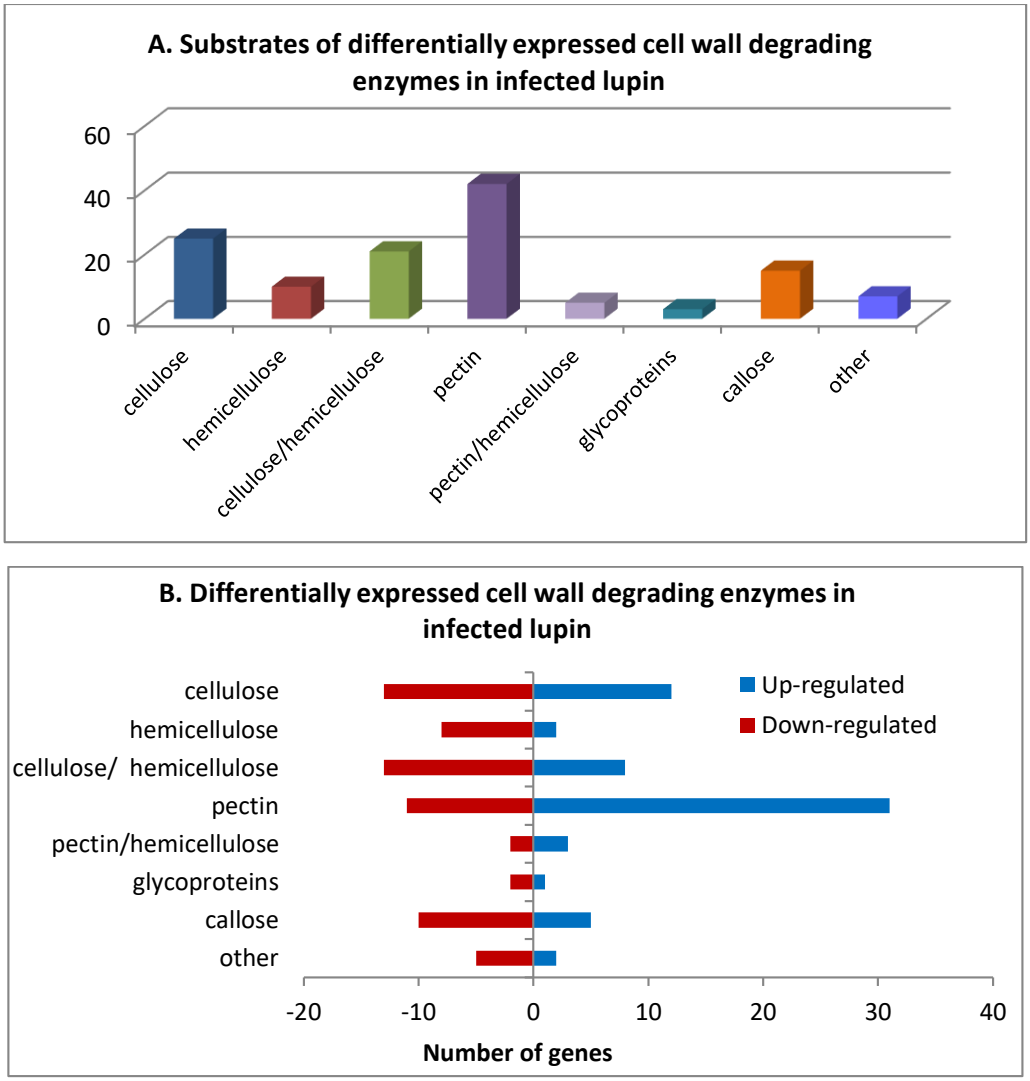

Figure 5.26. Summary of the differentially expressed cell wall degrading enzyme genes based on substrate (A) and the up- or down-regulation of the differentially expressed cell wall degrading enzymes according to their substrates (B) in phosphite-treated (50 µg/ml) *P. parasitica*-infected lupins. FDR <005. Only the main predicted substrates were included.

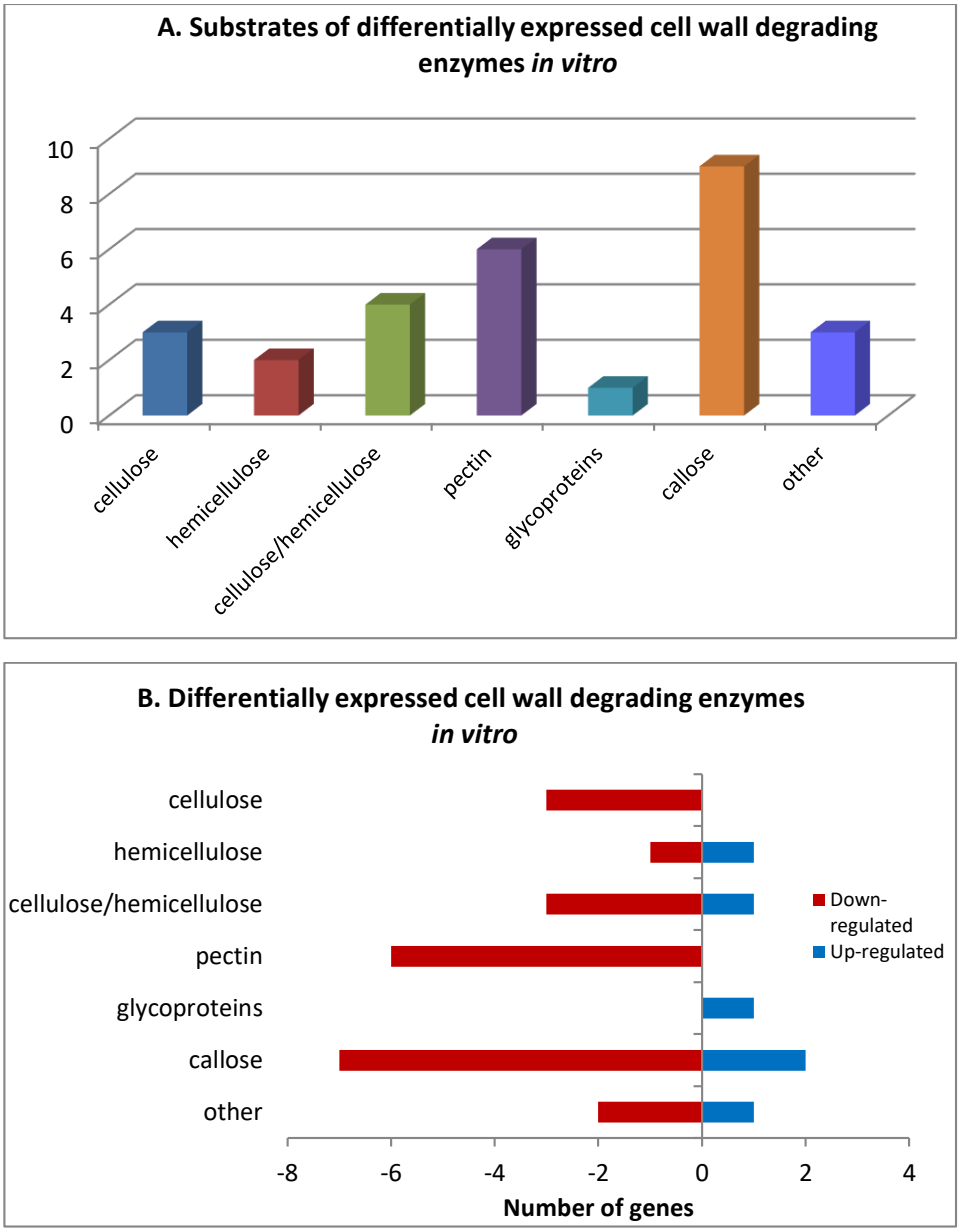

Figure 5.27. Summary of the differentially expressed cell wall degrading enzyme genes based on substrate (A) and the up- or down-regulation of the differentially expressed cell wall degrading enzymes according to substrates (B) in phosphite-treated (50 µg/ml) *P. parasitica* grown *in vitro*. FDR <005.

5.3.5.7.2. Effectors

Effectors are pathogen encoded proteins that promote infection and these fall into two categories: cytoplasmic and apoplastic (Hardham and Cahill, 2010). A total of 283 putative RxLR cytoplasmic effectors were identified in the *P. parasitica* genome by homology and domain searches (Blackman and Hardham,

unpublished results). Of these, 126 were expressed *in planta* and 41 were expressed *in vitro* (>1 RPKM) and there were many more RxLR-type effectors differentially expressed *in planta* than *in vitro* (RPKM ≥2, fold change ≥2, FDR P<0.05). In *P. parasitica*-infected lupins, a total of 50 effectors were significantly differentially expressed when comparing the effect of phosphite, with only four being down-regulated in roots pre-treated with phosphite (Table 5.22). The two most highly expressed RxLR genes that were up-regulated following phosphite treatment were PPTG_20214 and PPTG_00121. The four RxLR genes that were down-regulated in phosphite-treated roots had low expression. Only nine effector genes (FDR P<0.05, RPKM ≥2, fold change ≥2) were differentially expressed in *P. parasitica* mycelia *in vitro*; two were up-regulated and seven were down-regulated with the addition of phosphite (Table 5.23). The expression of all genes was low (38 or less RPKM). Only two differentially expressed genes were common to both data sets implying that different growth conditions affect the number and identity of RxLR that are expressed and indicating that high RxLR expression requires the presence of plant tissue.

The expression of another group of cytoplasmic effectors, crinkler (CRN)-type effectors was also analysed (Appendix Table 5.4). CRN genes are usually expressed during late infection in contrast to the early expression of RxLR effectors (Jupe et al., 2013; Blackman and Hardham unpublished results). Of the 30 CRN-like effectors identified by homology and domain searches, 29 were expressed *in planta* (Appendix Table 5.4) but only two (PPTG_17744 and PPTG_11553) were differentially expressed, albeit at low levels of expression. The two most highly expressed CRN genes, PPTG_08911 and PPTG_07145, had a minimum RPKM >250 and in phosphite-treated roots showed a down regulation of 1.2 and 1.3-fold, respectively. *In vitro*, 26 of the 30 putative CRN genes were expressed but none was differentially expressed. These results suggest that, in contrast to the situation with the RxLRs, CRN expression does not require the presence of plant tissue.

Table 5.22. Differentially expressed effector genes in phosphite-treated (50 µg/ml) *P. parasitica*-infected lupins versus *in vitro* cultures. (DE>2 exp<P0.05.)

Gene ID	Putative gene function	Lupin+Pp RPKM	Lupin+Pp+ Phi RPKM	Fold change	P-value
PPTG_03195	secreted effector peptide	4	0	-7.5	0.00
PPTG_08852	secreted RxLR effector peptide	2	0	-6.8	0.00
PPTG_05602	secreted RxLR effector peptide	19	6	-2.7	0.00
PPTG_18797	secreted RxLR effector peptide	18	8	-2.1	0.00
PPTG_10602	secreted effector peptide	4	8	2.0	0.02
PPTG_14414	secreted RxLR effector peptide	10	19	2.1	0.00
PPTG_01871	secreted RxLR effector peptide	61	124	2.1	0.00
PPTG_00504	secreted effector protein	3	6	2.3	0.00
PPTG_03526	secreted RxLR effector peptide	21	46	2.3	0.00
PPTG_03526	secreted RxLR effector peptide	21	46	2.3	0.00
PPTG_19111	secreted RxLR effector peptide	105	238	2.4	0.00
PPTG_20405	secreted RxLR effector peptide	11	25	2.5	0.00
PPTG_06733	secreted RxLR effector peptide	5	11	2.5	0.00
PPTG_03535	secreted RxLR effector peptide	32	81	2.7	0.00
PPTG_03663	secreted RxLR effector peptide	2	5	2.7	0.01
PPTG_04554	secreted RxLR effector peptide	2	6	2.7	0.00
PPTG_15973	secreted RxLR effector peptide	2	5	2.8	0.01
PPTG_18519	secreted RxLR effector peptide	2	5	3.0	0.01
PPTG_06622	secreted RxLR effector peptide	13	36	3.0	0.00
PPTG_19337	secreted RxLR effector peptide	7	19	3.0	0.00
PPTG_07169	secreted RxLR effector peptide	130	378	3.0	0.00
PPTG_00341	secreted effector peptide	1	2	3.1	0.02
PPTG_17847	secreted RxLR effector peptide	7	20	3.2	0.00
PPTG_20416	PexRD2 secreted RxLR effector peptide	37	123	3.5	0.00
PPTG_12399	secreted RxLR effector peptide	1	3	3.5	0.00
PPTG_03525	secreted RxLR effector peptide	8	27	3.5	0.00
PPTG_03525	secreted RxLR effector peptide	8	27	3.5	0.00
PPTG_15926	secreted RxLR effector peptide	2	7	3.8	0.00
PPTG_13212	secreted RxLR effector peptide	1	3	4.6	0.00
PPTG_08202	secreted RxLR effector peptide	11	48	4.6	0.00
PPTG_15620	secreted RxLR effector peptide	2	10	4.6	0.00
PPTG_20214	secreted effector	210	964	4.8	0.00
PPTG_15589	effector	5	21	4.8	0.00
PPTG_05634	secreted RxLR effector peptide	30	139	4.8	0.00
PPTG_08789	secreted RxLR effector peptide	1	6	5.2	0.00
PPTG_01492	secreted RxLR effector peptide	3	16	5.3	0.00
PPTG_15977	secreted RxLR effector peptide	11	56	5.3	0.00
PPTG_15549	secreted RxLR effector peptide	0	2	5.8	0.00
PPTG_17017	secreted RxLR effector peptide	7	40	5.8	0.00
PPTG_20226	secreted effector	1	6	6.0	0.00
PPTG_00121	secreted RxLR effector peptide	140	842	6.2	0.00
PPTG_12798	secreted RxLR effector peptide	13	104	8.5	0.00
PPTG_12414	secreted RxLR effector peptide	1	8	8.6	0.00
PPTG_15333	secreted effector peptide	0	4	9.3	0.00
PPTG_08176	secreted RxLR effector peptide	1	12	9.8	0.00
PPTG_20019	secreted RxLR effector peptide	5	45	10.2	0.00
PPTG_17749	secreted RxLR effector peptide	1	9	10.6	0.00
PPTG_03477	secreted effector peptide	0	2	12.0	0.00
PPTG_04235	secreted RxLR effector peptide	1	11	12.2	0.00
PPTG_19047	secreted RxLR effector peptide	0	5	13.3	0.00

Table 5.23. Differentially expressed effector genes *in vitro* in the presence or absence of phosphite (50 µg/ml). (DE>2 exp<P0.05.) Mean RPKM are shown for b) modified Ribeiro's medium control cultures (Pp) and phosphite treatment (Pp+Phi).

Gene ID	Putative gene function	Pp RPKM	Pp+Phi RPKM	Fold change	P-value
PPTG_08943	secreted RxLR effector peptide	2	5	2.2	0.00
PPTG_15549	secreted RxLR effector peptide	2	5	2.5	0.00
PPTG_15594	secreted effector peptide	38	17	-2.3	0.00
PPTG_00342	secreted effector peptide	3	1	-2.4	0.05
PPTG_18382	RXLR effector family protein	5	2	-2.5	0.00
PPTG_20319	secreted effector	10	4	-2. 9	0.00
PPTG_03195	secreted effector peptide	4	1	-4.3	0.00
PPTG_01912	secreted RxLR effector peptide	9	1	-7.2	0.00
PPTG_03190	secreted effector peptide	5	1	-7.2	0.00

5.3.5.7.3. Elicitins

Apoplastic effectors include CWDEs (see Section 5.3.5.5.2), elicitins and secreted enzyme inhibitors (Hardham and Cahill, 2010). Homology searches identified 67 elicitins that were expressed at RPKM levels >2 *in vitro*, 55 were expressed during infection of lupin roots, and 28 were differentially expressed either *in vitro* or *in planta* (Table 5.24). There were 21 elicitins that were expressed during infection of lupin roots and not *in vitro* and only three that were specifically expressed *in vitro* (RPKM >2). Of the three most highly expressed elicitins, two were not expressed *in vitro* (PPTG_05402 and PPTG_15237) and one was more highly expressed *in vitro* (PPTG_09075) than *in planta*. The latter gene encodes an INF1 protein which interacts with a group of kinases implicated in the detection of pathogens and results in cell death (Kamoun *et al.*, 1998; Bos *et al.*, 2006; Huang *et al.*, 2013). These three *P. parasitica* genes show between 2.5- and 30-fold decrease in expression in phosphite-treated lupin roots.

Table 5.24. Expression of *P. parasitica* elicitin genes during *in vitro* and 48 hpi infected lupin roots with and without phosphite (> 2 RPKM). Shaded regions indicate genes that are differentially expressed *in vitro* and/or *in planta* (fold change >2, >2 RPKM, *FDR p<0.05).

Gene ID	Putative gene function	*In vitro*			*In planta*		
		RPKM MRM	RPKM MRM + Phi	Fold change	RPKM infected lupin	RPKM infected lupin+Phi	Fold change
PPTG_06202	NPP1-like protein	2	2	-1.0	-	-	-
PPTG_07659	NPP1-like protein	-	-	-	0.4	2	4.3*
PPTG_07664	NPP1-like protein	6	4	-1.4*	20	28	1.3
PPTG_07671	NPP1-like protein	-	-	-	3	20	6.4*
PPTG_08017	NPP1-like protein	-	-	-	22	21	1.0
PPTG_08893	NPP1-like protein	-	-	-	2	5	2.4*
PPTG_11475	NPP1-like protein	-	-	-	2	1	-1.3
PPTG_11479	NPP1-like protein	-	-	-	5	3	-1.7
PPTG_13736	NPP1-like protein	-	-	-	4	0.2	-21.1*
PPTG_15224	NPP1-like protein	-	-	-	3	6	2.3*
PPTG_15231	NPP1-like protein	5	3	-1.5	51	19	-2.6*
PPTG_15234	NPP1-like protein	2	2	-1.1	-	-	-
PPTG_16647	NPP1-like protein	-	-	-	2	2	-1.2
PPTG_16851	NPP1-like protein	-	-	-	20	90	4.6*
PPTG_17125	NPP1-like protein	1	1	1.3	5	1	2.6*
PPTG_17049	NPP1-like protein	2	2	-1.1	1	1.2	1.2
PPTG_19330	NPP1-like protein	-	-	-	2	18	10.2*
PPTG_19331	NPP1-like protein	-	-	-	6	27	4.4*
PPTG_01904	suppressor-necrosis 1-like	1.4	1.1	-1.3	28	107	4.0*
PPTG_12252	suppressor-necrosis 1-like	-	-	-	10	38	3.8*
PPTG_09075	INF1-like elicitin	4262	3013	-1.4*	1460	559	-2.5*
PPTG_19861	INF1-like elicitin	-	-	-	1.2	3	2.8
PPTG_05266	elicitin-like mating protein M25	1.76	1.0	-1.7*	6.7	3.9	-1.7
PPTG_07733	elicitin-like protein	713	675	-1.1	562.6	742.4	1.4
PPTG_08950	elicitin-like protein	2.00	2.6	1.2	1.0	0.5	-1.9
PPTG_09073	β-elicitin cryptogein	4.9	4.3	-1.2	17.5	46	2.8*
PPTG_09074	highly acidic elicitin 20	4.4	5.6	1.3	1.2	0.4	-2.8
PPTG_09077	elicitin INF2A-like protein	285	233	-1.2	26	22	-1.1
PPTG_09079	elicitin INF2A-like protein	59	65	1.1	1.3	2.6	2.0
PPTG_09080	elicitin-like protein	3617	3178	-1.15	1221	1142	-1.0
PPTG_12289	elicitin-like protein	50	52	1.0	52	42	-1.2
PPTG_12304	GPI-anchored serine-rich elicitin	189	187	-1.0	229	166	-1.3
PPTG_12305	GPI-anchored serine-rich elicitin	5.71	5.6	-1.0	7.6	3.3	-2.3*
PPTG_12308	elicitin-like protein	10.32	9.6	-1.1	8.2	3.2	-2.5*
PPTG_12446	elicitin-like protein	17.9	15	-1.2	0.8	1.5	2.0
PPTG_12447	GPI-anchored elicitin	0.9	1	1.3	3.8	2.4	-1.6
PPTG_14235	elicitin-like protein	1.1	1.8	1.6	281	11	-24.5*
PPTG_16233	transglutaminase elicitor	32.6	24.7	-1.3*	28	10	-2.6*
PPTG_16234	transglutaminase elicitor	17.3	11.5	-1.5*	3230	121	-2.6*
PPTG_16236	transglutaminase elicitor M81D	12.3	8.1	-1.5*	91.0	148	1.7*
PPTG_16623	elicitin-like protein	1.3	0.9	-1.4	2.2	1	-2.2
PPTG_17779	elicitin-like protein	27.1	18.8	-1.5*	586	342	-1.6*
PPTG_19615	elicitor-like transglutaminase M81-like protein	2.7	2.0	-1.4	6.3	17	2.9*
PPTG_19674	transglutaminase elicitor M81C	1.1	0.2	-4.9*	6.1	23	4.0*
PPTG_19862	elicitin-like INF6	2494	1888	-1.3	961	540	-1.7*

Table 5.24. Cont.

PPTG_19863	elicitin INF2A-like protein	6.6	8.1	1.2	-	-	-
PPTG_19868	elicitin INF2A-like protein	1205	1223	1.0	1049	1200	1.2
PPTG_19869	elicitin-like protein	-	-	-	0.5	1.6	4.4
PPTG_16237	transglutaminase elicitor	-	-	-	1.2	4.5	4.0*
PPTG_16235	transglutaminase elicitor-like	-	-	-	11.8	24	2.2*
PPTG_15238	elicitin-like protein	-	-	-	90	6	-14.6*
PPTG_15237	elicitin-like protein	-	-	-	6073	1417	-4.1*
PPTG_10656	elicitor-like transglutaminase	-	-	-	2	2	1.0
PPTG_05402	elicitin	-	-	-	920	28	-30.3*
PPTG_03836	secretory protein OPEL	136	143	1.0	702	343	-2.0*

5.3.5.7.4. Protease and glucanase inhibitors

Protease and glucanase inhibitors are expressed by pathogens to counter plant pathogenesis-related proteins (Damasceno *et al.*, 2008; Hardham and Cahill, 2010; Martins *et al.*, 2014). Homology and keyword searches identified 25 putative protease inhibitors and seven glucanase inhibitor proteins in the *P. parasitica* genome (Table 5.25). As a comparison, the expression of three serine proteases was also analysed. Of the seven glucanase inhibitors only two were expressed *in vitro* and there was no change in expression in the presence of phosphite. In contrast, expression of five glucanase inhibitor genes was up-regulated in phosphite-treated lupins. Four cysteine protease inhibitors from the EpiC family (Tian *et al.*, 2007) were identified and three of these were either expressed at low levels or when highly expressed showed no differential expression between control and phosphite treatments. However, two EpiC genes (PPTG_03489, PPTG_18856) were highly expressed *in vitro* suggesting that their expression, unlike that of the glucanase inhibitors, is not dependent on the presence of plant material. Members of two serine protease inhibitor families were more likely to be expressed in the infected material than *in vitro*. These genes encoded kazal-type (Tian *et al.*, 2004) and Epi-like inhibitors (Tian *et al.*, 2007). *P. parasitica* kazal-type inhibitors were up-regulated in phosphite-treated infected lupins (5 of 7 genes were expressed). The presence of plant tissue also increased the number of Epi serine protease inhibitors that were expressed. Of the 18 identified, seven were expressed *in vitro* and 12 were expressed in infected lupins. Of the highly expressed Epi genes (PPTG_04341, PPTG_02600, PPTG_18856), only two were differentially expressed and these

were down-regulated in lupin roots pre-treated with phosphite (PPTG_04341, PPTG_02600). Of the three serine proteases examined, only two were expressed and there was no difference between phosphite and non-phosphite-treated samples. This last result is in contrast with the expression of cysteine proteases, two of which were identified earlier as being differentially down-regulated in phosphite-treated roots (Table 5.13).

Table 5.25. Expression of protease and glucanase inhibitors during *in vitro* culture and 48 hpi infected lupin roots with and without phosphite (> 1 RPKM). Shaded regions indicate genes that are differentially expressed *in vitro* and/or *in planta* (fold change >2, >2 RPKM, *FDR p<0.05).

Gene ID	Putative gene function	*In vitro*			*In planta*		
		RPKM MRM	RPKM MRM +Phi	Fold change	RPKM infected lupin	RPKM infected lupin+Phi	Fold change
PPTG_00200	glucanase inhibitor	-	-	-	-	-	-
PPTG_10494	glucanase inhibitor	-	-	-	1.0	8.8	10.4
PPTG_10495	glucanase inhibitor	-	-	-	1.4	6.8	5.3
PPTG_13057	glucanase inhibitor	3.5	4.6	1.3	15.4	68.4	4.6
PPTG_13062	glucanase inhibitor	-	-	-	-	-	-
PPTG_13156	glucanase inhibitor	-	-	-	2.7	13.5	5.2
PPTG_10490	glucanase inhibitor	0.9	1.5	1.6	4.8	16.0	3.5
PPTG_02600	protease Epi6-like inhibitor	-	-	-	46.9	21.9	-2.1
PPTG_02604	protease Epi6-like inhibitor	1.6	1.2	-1.4	18.3	12.7	-1.4
PPTG_03903	protease inhibitor Epi10	-	-	-	2.9	14.4	5.4
PPTG_04341	protease inhibitor Epi11	8.8	6.2	-1.4	160.1	4.8	-31.8
PPTG_17203	protease inhibitor Epi3	-	-	-	-	-	-
PPTG_17204	protease inhibitor Epi3	-	-	-	1.6	2.6	1.7
PPTG_03904	protease inhibitor Epi4	-	-	-	1.7	3.7	2.4
PPTG_07575	protease inhibitor Epi9	-	-	-	0.8	4.5	7.8
PPTG_16800	protease inhibitor Epi9	1.7	0.8	-2.1	14.6	14.3	1.0
PPTG_03108	protease inhibitor Epi-like	-	-	-	-	-	-
PPTG_03112	protease inhibitor Epi-like	-	-	-	-	-	-
PPTG_04342	protease inhibitor Epi-like	-	-	-	-	-	-
PPTG_11977	protease inhibitor Epi-like	-	-	-	-	-	-
PPTG_16178	protease inhibitor Epi-like	2.3	3.8	1.7	-	-	-
PPTG_03489	protease inhibitor EpiC1	82.2	82.1	-1.0	0.3	5.3	23.3
PPTG_06012	protease inhibitor EpiC1	-	-	-	-	-	-
PPTG_02053	protease inhibitor EpiC3	3.1	1.1	-2.8	5.2	1.7	-3.0
PPTG_18856	protease inhibitor EpiC4	196.7	206.3	1.0	133.5	94.6	-1.3
PPTG_05773	kazal serine protease inhibitor	44.6	54.2	1.2	3.6	19.8	5.6
PPTG_02598	kazal-type serine protease inhibitor	-	-	-	-	-	-

Table 5.25. Cont.

PPTG_03106	kazal-type serine protease inhibitor	4.1	2.4	-1.7	2.7	17.8	6.8
PPTG_03107	kazal-type serine protease inhibitor	3.9	2.2	-1.8	6.8	42.1	6.4
PPTG_03912	kazal-type serine protease inhibitor	-	-	-	1.5	3.7	2.3
PPTG_00356	kazal-type serine protease inhibitor	-	-	-	-	-	-
PPTG_03914	kazal-type serine protease inhibitor	-	-	-	3.2	16.6	5.5
PPTG_10492	serine protease family S01A	-	-	-	-	-	-
PPTG_13061	serine protease family S01A	3.2	1.7	-1.9	-	-	-
PPTG_14057	serine protease family S01A	-	-	-	8.8	9.1	1.1

5.3.5.7.5. Kinases

Early analysis had noted that three *P. parasitica* kinases were down-regulated in media containing phosphite (Table 5.8) and down-regulation of kinase expression has been reported to occur during the culture of *P. cinnamomi* in phosphite containing media (King *et al.*, 2010). The expression of a number of kinases was thus examined to determine if this down-regulation affected other *P. parasitica* kinases. In lupin infected with *P. parasitica*, the expression of 44 of 580 kinases was significantly different (FDR $P<0.05$, RPKM ≥2, fold change ≥2) in the presence or absence of phosphite. There are 14 kinase transcripts that are significantly up-regulated in phosphite-treated and infected lupin while 30 transcripts are significantly down-regulated (Table 5.26). The most highly up-regulated transcript is a mitogen-activated protein kinase kinase kinase (PPTG_15944) and most down-regulated is a pyruvate, phosphate dikinase (PPTG_13569). In *P. parasitica* mycelia grown *in vitro* with phosphite (Table 5.27), 26 kinase transcripts (FDR $P<0.05$, RPKM ≥2, and have a fold change ≥2) are expressed; eight are up-regulated and 18 are down-regulated. A cAMP-dependent protein kinase catalytic subunit alpha (PPTG_01989) is the most down-regulated transcript in the presence of phosphite *in vitro*. In addition to the differentially expressed kinases shown in Table 5.26, the expression of 19 proteins annotated as mitogen-activated protein kinases was examined (PPTG_0030, 00387, 00690, 01294, 01522, 02555, 04181, 06091, 06823, 08766, 09480, 10920, 11268, 12708, 12887, 16938, 18028, 18861, 19371) (results not shown). All of these kinases were either expressed at low levels or were not differentially expressed in the phosphite-treated samples.

Table 5.26. Differentially expressed *P. parasitica* kinases in infected lupin roots in the presence or absence of phosphite. DE>2-fold change, p <0.05.

Gene ID	Putative gene function	Lupin+Pp RPKM	Lupin +Pp+Phi RPKM	Fold change
PPTG_11612	calcium-dependent protein kinase	4	10	3
PPTG_11728	calcium/calmodulin-dependent protein kinase kinase	3	1	-3
PPTG_05149	cAMP-dependent protein kinase catalytic subunit	7	1	-5
PPTG_00169	cAMP-dependent protein kinase regulatory subunit	152	71	-2
PPTG_10718	casein kinase	1	5	5
PPTG_16821	cGMP-dependent protein kinase	0	2	7
PPTG_10603	creatine kinase	62	9	-7
PPTG_02311	creatine kinase B-type	384	142	-3
PPTG_12385	cyclin-dependent kinase, F-box domain protein	14	6	-2
PPTG_04756	dynein light chain/pantothenate kinase	5	1	-4
PPTG_09861	galactokinase	68	22	-3
PPTG_09865	galactokinase	21	6	-3
PPTG_02874	glycerol kinase 1	159	59	-3
PPTG_06660	mitogen-activated protein kinase	1	5	4
PPTG_15944	mitogen-activated protein kinase kinase kinase	0	2	8
PPTG_14187	mps one binder kinase activator-like	2	12	7
PPTG_09659	phosphatidylinositol 4-phosphate 5-kinase	3	1	-3
PPTG_13731	phosphatidylinositol kinase (PIK-H1)	11	5	-2
PPTG_02179	phosphoenolpyruvate carboxykinase (ATP)	65	17	-4
PPTG_02177	phosphoenolpyruvate carboxykinase (ATP)	176	44	-4
PPTG_15082	phosphoglycerate kinase, chloroplastic	45	204	5
PPTG_13825	protein kinase	4	21	5
PPTG_14637	protein kinase	3	11	4
PPTG_11363	protein kinase	2	6	3
PPTG_16186	protein kinase	1	2	2
PPTG_06258	protein kinase	1	2	2
PPTG_11454	protein kinase	1	2	2
PPTG_10360	protein kinase	8	4	-2
PPTG_15493	protein kinase	64	29	-2
PPTG_02748	protein kinase	35	16	-2
PPTG_10877	protein kinase	3	1	-3
PPTG_08811	protein kinase	33	12	-3
PPTG_16200	protein kinase	5	2	-3
PPTG_08125	protein kinase	37	12	-3
PPTG_09410	protein kinase	7	2	-3
PPTG_19122	protein kinase	4	1	-3
PPTG_16201	protein kinase	46	12	-3
PPTG_05416	protein kinase	15	4	-4
PPTG_00068	protein kinase	13	3	-4
PPTG_04227	protein kinase	4	1	-5
PPTG_14638	protein kinase	68	10	-7
PPTG_03708	pyruvate kinase	254	519	2
PPTG_13569	pyruvate, phosphate dikinase	51	1	-69
PPTG_10728	xylulose kinase	27	12	-2

Table 5.27. Differentially expressed kinases in *P. parasitica*-grown *in vitro* in the presence or absence of phosphite (50 µg/ml). DE>2-fold change p <0.05.

Gene ID	Putative gene function	Pp RPKM	Pp+Phi RPKM	Fold change
PPTG_06861	APS kinase/ATP sulfurlyase/pyrophosphatase fusion protein	43	88	2
PPTG_18558	bifunctional aspartokinase/homoserine dehydrogenase	14	32	2
PPTG_00044	calcium/calmodulin-dependent protein kinase II	499	200	-3
PPTG_20062	cAMP-dependent protein kinase catalytic subunit alpha	134	22	-6
PPTG_01989	cAMP-dependent protein kinase catalytic subunit alpha	116	17	-7
PPTG_07402	dual specificity protein kinase	6	16	3
PPTG_13894	dual specificity tyrosine-phosphorylation-regulated kinase	117	56	-2
PPTG_18886	fructokinase	76	25	-3
PPTG_18933	glucokinase	13	6	-2
PPTG_18927	glucokinase	424	132	-3
PPTG_06091	mitogen-activated protein kinase kinase kinase	3	1	-3
PPTG_13077	phosphatidylinositol-4-phosphate-5-kinase	52	17	-3
PPTG_02177	phosphoenolpyruvate carboxykinase (ATP)	348	1151	3
PPTG_02179	phosphoenolpyruvate carboxykinase (ATP)	138	446	3
PPTG_03936	protein kinase	24	69	3
PPTG_01769	protein kinase	2	5	2
PPTG_13825	protein kinase	64	132	2
PPTG_11455	protein kinase	4	2	-2
PPTG_04024	protein kinase	511	235	-2
PPTG_08001	protein kinase	597	270	-2
PPTG_11276	protein kinase	2	1	-2
PPTG_12563	protein kinase	34	12	-3
PPTG_10372	protein kinase	1402	433	-3
PPTG_03708	pyruvate kinase	177	52	-3
PPTG_13569	pyruvate, phosphate dikinase	297	93	-3
PPTG_13215	serine/threonine protein kinase	175	85	-2

5.3.5.7.6. Expression of stage specific genes

The analysis of Vsv and Lpv labelling and the malformation of hyphal walls (Section 5.2.3.3) plus any differential expression of genes that are linked to development may indicate that phosphite has a role in delaying development and/or the inhibition of the synthesis of wall components. *In vitro*, the expression of the gene encoding Vsv (PPTG_16264) was below the cut-off levels applied and in infected lupins its expression was down-regulated (Table 5.28). The genes encoding the large Lpv proteins (Marshall *et al.*, 2001) have not yet been assembled correctly in any of the *Phytophthora* genomes sequenced to date (L. M. Blackman, pers. comm.). In the current study, the expression of four transcripts encoding regions of the *Lpv* genes were analysed (PPTG_11464, PPTG_11465, PPTG_11858, and PPTG_11859). Two of these *Lpv* genes (PPTG_11464, PPTG_11465) were up-regulated in the presence of phosphite *in*

vitro but were down-regulated in infected lupin with phosphite but the levels of expression were very low under all conditions and no conclusions could be drawn from this analysis (Table 5.28). The gene encoding the complement control module protein, PnCcp, (PPTG_01661) which is highly expressed in zoospores and during late sporulation (Zhang *et al.*, 2013), was not expressed *in planta* or *in vitro*. In addition, the expression of four *P. parasitica* genes which have been shown to be more highly expressed in mycelia than in zoospores was also analysed (Attard *et al.*, 2014).

The effect of phosphite on the expression of genes encoding proteins involved in the biosynthesis of wall components was also investigated (Table 5.29). Four of the nine genes were identified as cellulose synthases and five were callose synthases. None of these genes showed any statistically significant difference in expression between controls and phosphite treatments. Interestingly, most genes in this group were more highly expressed *in vitro* than in infected roots.

Table 5.28. Expression of *P. parasitica* stage-specific genes during *in vitro* culture and 48 hpi infected lupin roots with and without phosphite (>1RPKM). Genes that are differentially expressed *in vitro* and/or *in planta* are shown in grey (fold change >2, >2 RPKM, *FDR p<0.05). Lpv: large peripheral vesicle protein; Vsv: ventral surface vesicle protein.

Gene ID	Putative gene function	*In vitro*			*In planta*		
		RPKM MRM	RPKM MRM + Phi	Fold change	RPKM infected lupin	RPKM MRM	Fold change
PPTG_10800	haustorium-specific membrane protein	-	-	-	4.7	15	3.4*
PPTG_10805	haustorium-specific membrane protein	-	-	-	-	-	-
PPTG_11465	Lpv (partial)	4.5	15	3.2*	18	9	-1.8
PPTG_11464	Lpv (partial)	0.7	2	3.5*	2	1	-1.6
PPTG_11858	Lpv (partial)	-	-	-	-	-	-
PPTG_11859	Lpv (partial)	-	-	-	-	-	-
PPTG_16264	Vsv	-	-	-	13	1	-11.3*
PPTG_01661	complement control module protein (Ccp)	-	-	-	-	-	-
PPTG_14111	cleavage induced protein kinase	19	19	-1.0	11	11	1.0
PPTG_18272	hypothetical protein	136	185	1.3	299	170	-1.7
PPTG_02489	hypothetical protein	577	500	-1.2	214	283	1.4
PPTG_10841	dihydroflavonol-4-reductase	150	143	-1.1	137	116	-1.1
PPTG_01439	sporangia-induced phosphatidyl inositol kinase	43	39	-1.1	4	3	-1.6

Table 5.29. Expression of genes encoding proteins involved in the biosynthesis of wall components.

Gene ID	Putative gene function	*In vitro*			*In planta*		
		RPKM MRM	RPKM MRM + Phi	Fold change	RPKM infected lupin	RPKM infected lupin+Phi	Fold change
PPTG_12937	cellulose synthase 2	519	415	-1.3*	190	128	-1.4*
PPTG_12938	cellulose synthase subunit	709	498	-1.5*	161	99	-1.6*
PPTG_16268	cellulose synthase 4	144	159	1.1	74	61	-1.2
PPTG_17902	cellulose synthase subunit	1725	1392	-1.3*	497	366	-1.3
PPTG_08579	callose synthase	304	216	-1.4*	147	118	-1.2
PPTG_13182	callose synthase	171	102	-1.7*	91	77	-1.1
PPTG_13258	callose synthase	25	31	1.2	32	21	-1.4
PPTG_14740	callose synthase	143	121	-1.2	80	56	-1.4*
PPTG_16032	callose synthase	35	40	1.1	84	80	-1.0

5.3.5.7.7. Oxidative stress

The annotated *P. parasitica* genome was searched for proteins involved in the production, scavenging and protection from ROS and 55 proteins were identified (Table 5.30). This examination identified a nitrite reductase involved in ROS production; ROS scavengers from the catalase, superoxide dismutase (SOD), glutaredoxin, glutathione S-transferase, peroxiredoxin, thioredoxin, cytochrome c peroxidase, copper amine oxidase, glutathione peroxidase, glutathione reductase and aldo/keto reductase families; and alternative oxidase and mannitol dehydrogenase proteins involved in protection from oxidative stress. Of these genes, 46 were expressed *in vitro* and 48 were expressed *in planta*. Nineteen genes were differentially expressed *in vitro* and 17 of these were up-regulated in the presence of phosphite (FDR $P<0.05$, RPKM >2, fold change >2). This pattern was mirrored in infected lupins with 24 differentially expressed genes, 19 of which were up-regulated in phosphite-treated lupins and four were down-regulated. The single nitrite reductase identified (PPTG_16900) was up-regulated after phosphite treatments both *in planta* and *in vitro*, as were one alternative oxidase (PPTG_18782) and two mannitol dehydrogenases (PPTG_10399, PPTG_06299). The other up-regulated genes were ROS scavengers and these proteins are among the major ROS-scavenging enzymes in plants as reported by Mittler *et al.* (2004). The most highly expressed genes were also the ROS scavengers.

Table 5.30. Expression of *P. parasitica* genes involved in response to oxidative stress during *in vitro* culture and 48 hpi infected lupin roots with and without phosphite. Shaded genes indicated differential expression *in vitro* and/or *in planta*. SOD: superoxide dismutase

Gene ID	Putative gene function	*In vitro*			*In planta*		
		RPKM MRM	RPKM MRM +Phi	Fold change	RPKM infected lupin	RPKM infected lupin+Phi	Fold change
PPTG_05928	aldo/keto reductase	-	-	-	-	-	-
PPTG_03745	aldo/keto reductase	-	-	-	-	-	-
PPTG_05144	aldo/keto reductase	23	26	1.1	-	-	-
PPTG_05977	aldo/keto reductase	12	13	1.1	25	16	-1.5
PPTG_12087	aldo/keto reductase	36	42	1.2	86	104	1.3
PPTG_18907	aldo/keto reductase	20	26	1.3	16	53	3.5
PPTG_20209	aldo/keto reductase	2	3	1.3	16	53	3.5
PPTG_20207	aldo/keto reductase	-	-	-	0	3	15.6
PPTG_18782	alternative oxidase	11	53	4.6	4	20	5.2
PPTG_18784	alternative oxidase	467	813	1.7	35	103	3.0
PPTG_06664	catalase	9	22	2.3	2	12	6.1
PPTG_06866	catalase	1	2	3.1	4	28	7.8
PPTG_06713	catalase	7	18	2.6	184	117	-1.5
PPTG_02738	catalase-peroxidase	14	1	-20.2	18	41	2.4
PPTG_04280	catalase-peroxidase	-	-	-	18	64	3.7
PPTG_13290	copper amine oxidase	4	5	1.1	-	-	-
PPTG_13573	copper amine oxidase	4	6	1.5	45	21	-2.0
PPTG_06915	copper/zinc SOD	114	127	1.1	256	367	1.5
PPTG_08286	cytochrome c peroxidase	169	323	1.9	509	831	1.7
PPTG_03514	glutaredoxin			-	2	1	-1.3
PPTG_03675	glutaredoxin	36	43	1.2	41	50	1.3
PPTG_04665	glutaredoxin	540	583	1.1	628	803	1.3
PPTG_05502	glutaredoxin	26	34	1.3	21	28	1.4
PPTG_11418	glutaredoxin	109	169	1.5	30	191	6.6
PPTG_00103	glutathione peroxidase	14	16	1.2	27	29	1.1
PPTG_00108	glutathione peroxidase	198	229	1.1	199	240	1.3
PPTG_00110	glutathione peroxidase	1594	1491	-1.1	223	205	-1.0
PPTG_00111	glutathione peroxidase	-	-	-	-	-	-
PPTG_13883	glutathione peroxidase	12	13	1.1	43	46	1.1
PPTG_18033	glutathione reductase	25	31	1.2	27	35	1.3
PPTG_09787	glutathione reductase	85	190	2.2	186	239	1.3
PPTG_16143	glutathione S-transferase	3	3	-1.1	5	3	-1.4
PPTG_03314	glutathione S-transferase	17	20	1.2	12	3	-4.3
PPTG_07010	glutathione S-transferase	-	-	-	2	9	4.0
PPTG_16147	glutathione S-transferase	11	18	1.7	114	137	1.3
PPTG_02739	glutathione S-transferase	1	3	2.3	27	82	3.2
PPTG_16142	glutathione S-transferase	61	145	2.4	30	20	-1.4
PPTG_07011	glutathione S-transferase	265	647	2.4	338	443	1.4
PPTG_20135	glutathione S-transferase	-	-	-	-	-	-
PPTG_10597	glutathione S-transferase	1	9	7.2	-	-	-
PPTG_20307	glutathione S-transferase	5	6	1.3	4	6	1.6
PPTG_02418	glutathione S-transferase	-	-	-	6	7	1.3
PPTG_03313	glutathione S-transferase	28	31	1.1	17	20	1.2
PPTG_02671	glutathione S-transferase	30	46	1.5	179	119	-1.4
PPTG_04112	manganese SOD	696	799	1.2	312	572	1.8
PPTG_04295	manganese SOD	364	422	1.2	21	63	2.9
PPTG_10399	mannitol dehydrogenase	2	5	2.2	2	8	3.7

Table 5.30. Cont.

PPTG_06299	mannitol dehydrogenase	25	54	2.2	128	332	2.7
PPTG_16900	nitrite reductase NADPH	49	106	2.2	13	48	3.8
PPTG_11416	peroxiredoxin-2	91	214	2.3	53	157	3.1
PPTG_11417	peroxiredoxin-2	255	571	2.2	126	384	3.2
PPTG_11404	peroxiredoxin-2	49	61	1.2	272	309	1.2
PPTG_10386	peroxiredoxin-4	59	80	1.3	83	85	1.1
PPTG_08045	thioredoxin	474	402	-1.2	49	125	2.6
PPTG_08056	thioredoxin	124	93	-1.4	505	454	-1.1

5.3.5.7.8. Comparison to other studies on changes in genes expression in response to phosphite *in vitro*.

Table 5.31 shows the comparison of the up- or down-regulation of transcripts in *P. cinnamomi* mycelium treated with 40 µg/ml phosphite in the microarray experiment of King *et al.* (2010) and *P. parasitica* mycelia treated with 50 µg/ml phosphite from the present study. Of the 43 phosphite-regulated transcripts (16 up-regulated; 27 down-regulated) in *P. cinnamomi*, 17 had homologues in *P. parasitica* but only four of the 17 genes were statistically significant with fold change values of 2.7-12.7. Two transcripts were up-regulated and one was down-regulated in both *P. parasitica* and *P. cinnamomi* mycelia treated with phosphite. One of the four genes was up-regulated in *P. cinnamomi* but was down-regulated in *P. parasitica*. ADP-ribosylation factor family protein (PPTG_03018) was the most highly up-regulated transcript and the most down-regulated transcript is a hypothetical protein (PPTG_13186). The two down-regulated *P. parasitica* genes (PPTG_02019 and PPTG_13186) had unknown function. Also, there are two genes are up-regulated in *P. parasitica* but are down-regulated in *P. cinnamomi* and these genes function in biosynthesis (PPTG_09874) and transport (PPTG_18781). In the previous study of Wong *et al.* (2009) using *P. cinnamomi* with 5 µg phosphite/ml, CP29 (GenBank accession no. EU170013) shows homology to *P. parasitica* transcript, PPTG_05823 (hypothetical protein). This transcript is up-regulated in the presence of 50 µg phosphite/ml *in vitro* with a fold change value of 1.30.

Table 5.31. Comparison of genes expressed in *P. cinnamomi* and *P. parasitica* mycelia treated with phosphite in minimal media (King *et. al*, 2010).

***Pc* GenBank No.**	***Pp* Gene ID**	**Closest putative ortholog protein ID[a]/Accession no.[b] (NCBI)**	***Pp* RPKM**	***Pp* RPKM + Phi**	**Fold change**
FJ492976[u]	PPTG_03018[u]	*Ps* ADP-ribosylation factor protein (158029)[a]	1	12	12.7*
FJ492978[u]	PPTG_16422[u]	*Ps* hypothetical protein (135523)[a]	7	30	4.2*
FJ492981[u]	PPTG_02019[d]	*Ps* hypothetical protein (138129)[a]	154	58	-2.7*
FJ492993[d]	PPTG_13186[d]	*Ps* hypothetical protein (143057)[a]	4	1	-5.1*

Pp Phytophthora parasitica, Pc Phytophthora cinnamomi, Ps Phytophthora sojae, [u]-up-regulated transcripts, [d]- down-regulated transcripts with the addition of phosphite in the minimal media, *-significant fold change

5.4. Discussion

Phosphite is known to inhibit growth of *Phytophthora* directly and to act indirectly through the induction of defence responses in the host during *Phytophthora* attack (Eshraghi *et al.*, 2011a; Machinandiarena *et al.*, 2012). However, the understanding of the cellular and molecular basis of the phosphite effects is still extremely limited. The current study analysed the effects of phosphite on *P. parasitica* gene expression *in vitro* and *in planta*, the latter experiments exploiting the *P. parasitica*-lupin infection assay system that was developed in the first part of this thesis project as described in Chapter 2 and 3. The new information on the differential expression of *P. parasitica* genes in the presence or absence of phosphite treatment *in vitro* and *in planta* will make a valuable contributon to the understanding of phosphite mechanisms that operate during host-*Phytophthora* interactions at the transcriptome level.

5.4.1. Effects of phosphite on the growth of different *Phytophthora* isolates

The variations in mycelial growth and sensitivity of *Phytophthora* species to phosphite have been attributed to the amount of phosphite taken up by the mycelium (Fenn and Coffey, 1984; Griffith *et al.*, 1993; Darakis *et al.*, 1997), the difference in susceptibility during metabolism (Niere *et al.*, 1994), and the ability of the pathogen to reduce intracellular levels of phosphite (Dunstan *et al.*, 1990). Different isolates of a single species may display different phosphite sensitivities

and the *in vitro* sensitivity of an isolate may differ from the sensitivity *in vivo*. It has been reported that >1.0 mg/ml of Fosetyl-Al can totally inhibit mycelial growth of *Phytophthora* species (Smith, 1979; Farih *et al.*, 1981). Consistent with this, Fosetyl-Al completely inhibits mycelial growth of *P. cinnamomi* with an ED50 of 54 µg/ml (Fenn and Coffey, 1984).

The use of different culture media also contributes to variations in the calculated ED50 values. For *P. parasitica*, phosphite ED50 values were reported to be as low as 25.44 µg/ml on Erwin and Katznelson modified synthetic agar medium (Ludowici, 2013) and as high as 320 µg/ml on corn meal agar (Nemestothy and Guest, 1990). Phosphite was found to be 5.8 and 14.2 times more inhibitory to two *P. capsici* isolates than to Fosetyl-Al *in vitro,* with an ED50 of 4 µg/ml on Ribeiro's modified synthetic media (Fenn and Coffey, 1984). The use of MRM for 71 Australian *P. cinnamomi* isolates resulted in calculations of phosphite sensitivity with ED50 values ranging from 4-148 µg/ml (Wilkinson *et al.*, 2001c; Wong, 2006).

In the current study, using the same MRM, *P. cinnamomi* H1000 isolate was more sensitive to phosphite treatment than the 1248 isolate, with an ED50 of 2.5 µg/ml for isolate H1000 and an ED50 of 46.7 µg/ml for the 1248 isolate. Generally, the determination of the ED50 of a fungicide is based on the radial growth of the pathogen measured over a number of days or on the final day of a trial. The current study measured the daily radial growth due to the non-destructive nature of sampling and the ED50 was computed from the values measured on the final day of the trial. Although this method is simple, it can also be deceiving and may not provide an accurate measurement since high phosphite level may not affect radial expansion of the colony but can cause a decrease in mycelium density (Wilkinson *et al.*, 2001c). The use of 50 µg/ml phosphite, the ED50 value determined by Ludowici (2013) for the *P. parasitica* isolate used in the current study resulted in morphological changes, restriction of mycelial growth and changes to developmentally expressed proteins. Thus 50 µg/ml phosphite was used to gain an understanding of the phosphite-induced changes to the *P. parasitica* transcriptome *in vitro* and during infection of a model species, lupin.

5.4.2. Effects of phosphite on *Phytophthora* cell morphology

The morphology of *P. cinnamomi* has been described in detail (Ho and Zentmyer, 1977; Hardham, 2005). In the current study, hyphae of *P. cinnamomi* H1000 not treated with phosphite developed normally, forming hyphal swellings that are typical of *P. cinnamomi* isolates (Ho and Zentmyer, 1977). In phosphite-treated cultures, in addition to hyphal swellings, there were distorted and stunted branches on many hyphae (Figure 5.7). Treatment of *P. cinnamomi* with 40µg/ml phosphite has also been reported to cause degradation of hyphal walls and release of cytoplasm (King *et al*., 2010).

In vitro studies have shown that phosphite inhibits oospore and sporangia development and reduces zoospore production in *Phytophthora* species (Wilkinson *et al.*, 2001a; Wilkinson *et al.*, 2001c; Wong, 2006; Dalio *et al.*, 2014) and a similar phenomenon was observed in the current study. Phosphite treatment of *P. cinnamomi* H1000 and *P. parasitica* H1111 isolates led to the production of low numbers of sporangia and chlamydospores and the absence of zoospore release. The reduction in the number of chlamydospores noted in this study contrasts with the results of McCarren (2006) where phosphite treatment induced the production of chlamydospores of *P. cinnamomi* and had no effect on the production of oospores at low concentrations (0 and 80 µg/ml). Total inhibition of oospore production was only observed at 100 µg/ml phosphite concentration (McCarren *et al.*, 2009).

5.4.3. Vesicle production in *Phytophthora* treated with phosphite

Phytophthora zoospores contain three distinct types of peripheral vesicles (dorsal, ventral and large peripheral vesicles) which are synthesised during sporulation (Dearnaley *et al.*, 1996; Marshall *et al.*, 2001). These vesicles are believed to play important roles in host infection through the deposition of adhesives, generation of cyst walls and storage of proteins for use during cyst germination (Gubler and Hardham, 1990; Dearnaley *et al.*, 1996). The presence of Vsv and Lpv proteins in *P. cinnamomi* and *P. parasitica* hyphae can be detected within hours after the induction of sporulation (Dearnaley *et al.,* 1996; Marshall

et al., 2001; Blackman & Hardham unpublished results). The appearance of these proteins is preceded by an induction of Vsv and Lpv gene expression (Marshall *et al*., 2001, Zhang *et al.*, 2013, Blackman & Hardham unpublished results). The percentage of immunolabelled vesicles was significantly reduced by the addition of 50 µg/ml phosphite to cultures growing in V8 broth, suggesting that phosphite may delay development or it may inhibit gene expression or production of these vesicle proteins.

RNA-Seq analysis was used to examine the effects of phosphite on expression of genes encoding two vesicle proteins and other developmentally regulated genes. The *Vsv* gene (PPTG_16264) was not expressed under *in vitro* culture conditions used for the RNA-Seq experiment and was only expressed at low levels in infected lupin roots in which situation its expression was down-regulated by phosphite treatment. Expression of two of the *Lpv* genes (PPTG_11464, PPTG_11465) was significantly induced, albeit at low levels, in the presence of phosphite *in vitro* but their expression was unchanged *in planta*. It may be possible that the *in vitro* culture conditions used for RNA-Seq, i.e. minimal medium rather than nutrient-rich V8 broth, did not induce sporulation and hence expression of these genes was low. Immunoblot analysis has shown that three Lpv proteins exist in *P. cinnamoni* (Marshall *et al.*, 2001) and two in *P. parasitica* (Blackman and Hardham, unpublished results). The *Lpv* genes are very large (11-14 kb) and contain 12-18 copies of a 534bp domain (Marshall *et al.*, 2001). This gene structure has contributed to the fact that the *Lpv* genes have not been fully assembled or sequenced in the genome of any *Phytophthora* species. Thus, in the RNA-Seq experiment, many of the reads originating from *Lpv* genes may not be assigned correctly to the appropriate *Lpv* gene. PcVsv1 protein is a putative adhesin that plays a vital role in the adhesion of *Phytophthora* spores to the plant surface during zoospore encystment (Hardham and Gubler, 1990; Robold and Hardham, 2005). Immunolabelling with antibodies specific for Vsv in *Pythium*, *Albugo* and *Plasmopara* shows that Vsv adhesins are present in all Oomycete species tested, suggesting that they occur throughout the Oomycetes and could be an elicitor of plant defence (Mateos *et al.*, 1997; Gaulin *et al.*, 2002; Hardham, 2005). Phosphite interference with other metabolic processes has been

reported, for example, the inhibition dehydroabietic acid production in *P. palmivora* mycelia (Dunstan et al., 1990).

The gene for another protein found in large peripheral vesicles, the PnCcp complement control protein (PPTG_01661) (Škalamera and Hardham, 2006; Zhang *et al.*, 2013) was not expressed under any conditions tested in the current study. This result was not surprising because *PnCcp* is most highly expressed in zoospores and is not expressed in vegetative hyphae (Zhang *et al*., 2013). Four *P. parasitica* genes that are up-regulated during sporulation (Attard *et al.*, 2014) were expressed *in vitro* and *in planta* in the current study. One of these, a sporangia-induced phosphatidyl inositol kinase (PPTG_01439), was more highly expressed *in vitro* than *in planta,* suggesting that the mycelia may have been undergoing sporulation *in vitro*. Phosphite treatment did not change the levels of expression of any of these four genes suggesting that, perhaps, phosphite is not causing a delay in development.

5.4.4. Expression analysis of normalising genes used in RNA-Seq

The normalising genes, PPTG_07764, PPTG_08273, PPTG_08636, PPTG_02092 and PPTG_09948, showed no difference in expression between control and phosphite treatments, giving an initial validation of the RNA-Seq methodology. Earlier reports found that these genes were suitable qPCR standards in the *P. parasitica*-tomato interaction (Yan and Liou, 2006) and these genes were constitutively expressed in a time-course of *P. parasitica*-lupin interaction as seen by RNA-Seq analysis (Blackman *et al.,* 2015). However, three of these genes (PPTG_07764, PPTG_02092, PPTG_09948) were more highly expressed in *P. parasitica*-inoculated lupins than *in vitro* (fold change >2). Other genes such as *elongation factor 1* (*EF-1*), have been used as normalising genes in other systems, including a study on the effects of phosphite on *P. cinnamoni* (Wong *et al.*, 2009; King *et al.,* 2010). *EF1* and another commonly used normalising gene, actin, could not be used in the current study since reads for these conserved genes also mapped to mock inoculated lupins (Blackman *et al*., 2015). In addition, a *P. parasitica EF1* gene showed variability in expression and other genes such as ubiquitin-conjugating enzyme (PPTG_08273) and *WS021* (PPTG_07764) were

better controls during sexual reproduction stage and pathogenesis (Yan and Liou, 2006). Another study found a number of genes including *GAPDH* and *ubiquitin protein ligase 7*, to be superior control genes during the infection of citrus plants by *P. parasitica* and these genes may prove useful for future analysis of gene expression during lupin infection (Mafra *et al.*, 2012). Because there are no reference genes that will meet all required standards in an experiment, gene expression stability must be first systematically validated for their quality as normalising genes in qPCR (Gutierrez *et al.*, 2008). However, the fact that phosphite did not alter the gene expression of the five genes analysed within each experiment did indicate that phosphite does not have a general effect on all gene expression.

5.4.5. The use of GO terms to predict changes in gene expressions

The REVIGO analysis results shown in Figures 5.23-5.25 were not conclusive and it was clear that the functions affected by phosphite were too diverse to highlight any specific GO term that was enriched in any one of the different treatments. Many RNA-Seq studies have used the distribution of GO terms to gain an overview of changes in gene expression in plants (Jupe *et al.*, 2013; Asai *et al.*, 2014; Chand *et al.*, 2016) and pathogens (Jupe *et al.*, 2013; Zheng *et al.*, 2013; Reitmann *et al.*, 2017). Although REVIGO is a useful tool to summarise GO analysis (Rhee *et al.*, 2008; Supek *et al.*, 2011), problems have been encountered with it. For example, (a) REVIGO can only analyse 200 GO terms in one run thus excluding other GO terms that might be of importance in the analysis, (b) while some genes may be annotated with six to eight GO terms, there are genes that have no GO terms including some that have high homology to known proteins, and (c) GO relies upon picking the right hierarchy terms. To avoid drawbacks and false positives using GO terms, genes should be manually checked and analysed (Rhee *et al.*, 2008). There are also limitations to GO analysis. The distribution of GO terms is hampered by incomplete annotation often associated with computer generated analysis, imprecise or incorrect annotation, bias in the weight of a particular GO category, proteins being assigned multiple terms, the fact that some categories have been studied more intensively than others and a

lack of coverage of all predicted proteins in any one genome (Khatri and Drăghici, 2005; Schnoes *et al.*, 2013; Laukens *et al.*, 2015). Other approaches have used pathway-orientated analysis to identify functional important pathways (Fung *et al.*, 2008; Weltmeier *et al.*, 2011; Etalo *et al.*, 2013; Rudd *et al.*, 2015). In the current study, alternative strategies were also employed to gain an understanding of specific pathways which may be important in understanding the mechanism of phosphite-induced pathogen growth inhibition and increased resistance in infected plants.

5.4.6. Metabolic pathways affected by phosphite *in planta* and *in vitro*

One aspect of the analysis focused on genes whose expression was altered both *in planta* and *in vitro*. These included 66 genes that were down-regulated and 54 genes that were up-regulated following phosphite treatment both *in planta* and *in vitro*. These data were also assessed in order to determine if certain functional categories occurred only among the down-regulated or among the up-regulated genes following phosphite treatment. It emerged, for example, that adhesion, phenylalanine metabolism and transcription/translation regulation were functions that were only found in down-regulated genes (Tables 5.8, 5.10, 5.13, 5.14). On the other hand, genes for oxidative stress-associated proteins, cytoskeleton-associated proteins, proteins from the lipoxygenase pathway and proteins involved in turgor pressure regulation were in general up-regulated in the presence of phosphite. Six genes involved in pathogenesis were down-regulated but two were up-regulated.

5.4.7. Pathogenicity genes in phosphite-mediated *P. parasitica*

The addition of 50 µg/ml phosphite led to a delay or inhibition in the infection of the lupin roots by *P. parasitica* and analysis of the RNA-Seq gene expression data also focused on genes for which there is evidence of an involvement in pathogenicity, such as CWDEs and effectors.

5.4.7.1. CWDEs

Pathogen-encoded CWDEs have a prominent role in plant pathogenesis (Wanjiru *et al.*, 2002; Reignault *et al.*, 2008) and some families are essential for a successful infection (Nguyen *et al.*, 2011; Sella *et al.*, 2016). Analysis of the expression of genes encoding CWDEs during the infection of lupin roots by *P. parasitica* has been described by Blackman *et al.* (2015) and other RNA-Seq studies have characterised CWDE expression in other host-*Phytophthora* interactions (Ospina-Giraldo *et al.*, 2010; Brouwer *et al.*, 2014; Horowitz and Ospina-Giraldo, 2015). The aim of the current study was to determine the effects of phosphite on *P. parasitica* CWDE gene expression *in planta* and *in vitro*. The approach followed was to view the results in terms of the carbohydrate substrates upon which the CWDEs acted.

The most highly expressed CWDEs during infection of lupin included the CBM1s, PPTG_06045 (rank 1) and PPTG_13482 (rank 5). These genes have a similar expression profile during the infection time-course (Blackman *et al.*, 2014). Phosphite treatment causes a small decrease in expression of these genes *in planta* and *in vitro*. PPTG_06045 is highly expressed *in planta* and PPTG_13482 is highly expressed *in vitro*. The level of expression may be due to the different carbon sources, glucose versus plant cell walls, affecting gene regulation (Aro *et al.*, 2005; dos Santos Castro *et al.*, 2014; van Munster *et al.*, 2014). Out of the 11 differentially expressed CBMs in infected lupins, only two are up-regulated in phosphite-treated seedlings. These are from the CBM63 family, members of which contain a cellulose-binding domain, and were most highly expressed during early/mid infection in lupin (Blackman *et al*., 2015). The other nine CBMs were expressed during late infection. Expression during late infection is also true for many other CWDEs acting on cellulose, and includes 24 members in the GH1, GH3, GH5, GH6, GH7, GH12 and GH30 families. Seven of the seven cellulase genes in these families that were expressed early in infection (30-36 hpi) were up-regulated in phosphite-treated roots, and 17 of 17 cellulase genes that were expressed late in infection (54-60 hpi) were down-regulated following phosphite treatment. The exceptions to this rule were a number of genes which were differentially expressed in the current study but not expressed or expressed at

very low levels in the study of Blackman *et al.* (2015). This result could be explained by the difference in the number of mapped reads in the two studies or the mapping methodology.

Pectinases play an important function in pathogenesis as they are often the first CWDEs that are expressed during pathogen invasion (Cooper, 1983; Benhamou and Côté, 1992; Blackman *et al.*, 2015). The results of the qPCR experiments described in Chapter 4 support the idea of a cascade of expression of the three main types of cell wall polysaccharides. In general pectinases, including pectin methyl esterases from the CE8 family and GH28 family polygalacturonases, are expressed early during the onset of disease infection (Section 4.4.1); this is followed by the expression of hemicellulases and then the cellulases. Analysis of the expression of pectinases in the RNA-Seq data showed that all pectinases acting on homogalacturonan (CE8, CE13, GH28, PL1, PL3), on RG1 (GH53, GH78, GH105, PL4) or on both substrates (CE12) that were expressed early in infection were up-regulated in phosphite-treated roots. The one exception was CE12 (PPTG_10440) which peaks in expression during late infection (60 hpi) but which was up-regulated in phosphite-treated roots. This phenomenon was also seen for differentially expressed genes in GH3, GH30, GH43 and GH53 families that have activity against multiple substrates.

The up-regulation of pectinases during infection following phosphite treatment is consistent with observations reported in the literature. For example, in *P. infestans* expression of a CE8 gene increased 48 h after phosphite treatment (Burra *et al.*, 2014). Degradation of plant cell wall pectin by pathogen pectinases facilitates access to other plant cell wall components CWDE and is essential for successful infection (Benhamou and Côté, 1992; Horowitz and Ospina-Giraldo, 2015).

Callose (β-1,3-glucan) deposition, in particular during papilla formation, is often triggered by pathogen-associated molecular patterns (PAMPs) (Gómez-Gómez *et al.*, 1999; Hardham *et al.*, 2007; Halim *et al.*, 2009; Luna *et al.*, 2011) and is an important part of plant defence. Callose and other molecules reinforce the plant cell wall and constitute an effective barrier at sites of attack during pathogen invasion (Hinch and Clarke, 1982; Škalamera and Heath, 1996; Brown *et al.*,

1998; You *et al.*, 2010; Eshraghi *et al.*, 2011a). In addition, *Phytophthora* cell walls contain highly branched β-1,3-glucans which can elicit a plant defence response (Fabre *et al.*, 1984; Perret *et al.*, 1992; Klarzynski *et al.*, 2000). In the current study, one callase in the GH81 family (PPTG_16828) was up-regulated following phosphite treatment both *in vitro* and *in planta*. *In planta*, PPTG_16828 was up-regulated 39-fold after phosphite treatment and is the third most highly expressed CWDE in phosphite-treated roots. In an infection time-course, expression of PPTG_16828 peaked 42-48 hpi (Blackman *et al.*, 2015). The analysis of differentially expressed β-1,3-glucanases from GH5, GH16, GH17 and GH81 families revealed that the majority were down-regulated in the presence of phosphite *in vitro* and *in planta* and again there was a correlation between phosphite-induced down-regulation and expression in late infection (Blackman *et al.*, 2015).

5.4.7.2. Cytoplasmic effectors

P. parasitica, like other *Phytophthora* and Oomycetes species, secretes proteins known as effectors, some of which are taken up into plant cells (Kamoun, 2006; Kebdani *et al.*, 2010; Bozkurt *et al.*, 2011; Liu *et al.*, 2011; Evangelisti *et al.*, 2013). These so-called cytoplasmic effectors facilitate pathogen colonisation and successful infection by disabling plant host immunity and altering plant cell structure and metabolism (Kamoun, 2006; Kebdani *et al.*, 2010). RxLR and CRN-type effectors are the most studied cytoplasmic effectors in Oomycete pathogens particularly in *Phytophthora* species (Jupe *et al.*, 2013; Wang *et al.*, 2015; Gascuel *et al.*, 2016). During a lupin-*P. parasitica* infection time series (Blackman *et al.*, 2015), the two genes (PPTG_20214 and PPTG_00121) were the most highly expressed RxLRs and reached a peak at 30 hpi (Blackman and Hardham, unpublished results).

Over 500 RxLR and 300 CRN effectors have been predicted in the *P. infestans* genome, but only a few have been characterised and their role in pathogenicity determined (Wang *et al.*, 2015). RxLR effectors, such as Avrblb2 and Avr3c, are usually expressed at early stages of infection (Dong *et al.*, 2009; Bozkurt *et al.*, 2011; Jupe *et al.*, 2013) while CRN-type effectors are expressed during late infection (Qutob *et al.*, 2002; Liu *et al.*, 2011; Stam *et al.*, 2013). For example, a

high level of expression of the *P. sojae* CRN effectors, PsCRN63 and PsojNIP, occurs in the late stages of compatible interactions in soybeans (Qutob *et al.*, 2002; Liu *et al.*, 2011; Stam *et al.*, 2013; Li *et al.*, 2016). In the present study, of the 48 putative *P. parasitica* CRNs identified, 73% were expressed *in planta* and 69% *in vitro,* suggesting that expression of CRNs did not require the presence of the plant. Only two *P. parasitica* CRN genes were differentially expressed *in planta* or *in vitro*. PPTG_11786, which has significant homology to PsCRN63 and PsCRN115, was more highly expressed *in vitro* than *in planta* and its expression was not affected by phosphite treatment. PsCRN63 triggers programmed cell death (PCD) whereas PsCRN115 prevents PCD, however, both effectors are required in tandem to induce disease development (Liu *et al.*, 2011; Zhang *et al.*, 2015; Li *et al.*, 2016). Most CRN effector genes expressed *in planta* were down-regulated by phosphite treatment and this effect of phosphite is likely to contribute to a decrease in pathogen virulence.

In contrast to CRN effectors, in the current study, three times more RxLR effectors were expressed *in planta* than *in vitro*, suggesting that the expression of many RxLR genes is dependent upon the presence of plant tissue as previously reported (Morgan and Kamoun, 2007; Whisson *et al.*, 2007; Oh *et al.*, 2009). *In planta*, most of the differentially expressed RxLR effectors were up-regulated after phosphite treatment, again correlating with early expression in *P. parasitica*-infected lupin.

5.4.7.3. Non-CWDE apoplastic effectors

In addition to CWDE, apoplastic effectors include enzyme inhibitors, elicitins, toxins and necrosis-inducing factors (NPPs) (Hardham and Cahill, 2010). In the current study, genes encoding 67 elicitins and NPPs were expressed in either or both phosphite-treated mycelia or infected lupins. Elicitins belong to a family of small (typically 98 amino acids in length), highly conserved proteins and have an important role in host-pathogen interactions (Horta *et al.*, 2008). Elicitin genes are highly expressed *in vitro* by *Phytophthora* and some *Pythium* species (Horta *et al.,* 2008; Wong *et al.*, 2009). In the present study, the expression of many elicitin and NPP genes was affected *in vitro* and/or *in planta* by phosphite

treatment. For example, *in planta* 10 of the 18 NPP1 genes that were expressed were up-regulated by phosphite treatment. Only six NPP1-like genes were expressed *in vitro* and their expression was not affected by phosphite treatment.

The gene encoding an INF1-like protein, PPTG_09075, was the second most highly expressed gene *in vitro;* expression *in planta* was 2-fold lower. Expression of this gene was down-regulated both *in vitro* and in infected lupins by phosphite treatment. PPTG_09075 has 99% identity with *P. boemeria* Boe2 elicitin and 89% similarity to *P. infestans* INF1, PITG_12551.

PPTG_01904 (now called PPTG_21148 in version 3 of the *P. parasitica* genome) and PPTG_12252 encode suppressor-necrosis 1-like proteins (SNE1) and were induced in infected lupins. Both genes were highly expressed during early infection of lupin (30-36 hpi, Blackman and Hardham unpublished results) and an SNE1 from *P. infestans* is expressed during the biotrophic phase of infected tomato (Kelley *et al*., 2010). Pre-treatment with phosphite increased expression of PPTG_21148 and PPTG_12252. Thus, once again, there is a correlation between early expression and up-regulation by phosphite.

Phosphite treatment had different effects on the expression of genes encoding transglutaminase (TGase) elicitors *in vitro* and in infected lupin roots. For instance, genes encoding two TGase elicitors, PPTG_16236 and PPTG_19674, were down-regulated *in vitro* but up-regulated *in planta* whereas PPTG_16233 and PPTG_16234 were down-regulated both *in vitro* and *in planta*. PPTG_16234 was highly expressed *in planta* and showed a 27-fold decrease in expression in phosphite-treated roots (3230 to 121 RPKM). During the infection of lupin this gene reaches a peak in expression at 48-54 hpi (Blackman and Hardham, unpublished results). Pep-13, an elicitor of defence responses in parsley, is part of an abundant cell wall transglutaminase in *P. sojae* (Brunner *et al.*, 2002) and shares 66% amino acid identity over the N-terminal 587 residues with PPTG_16234. Pep-13 prompts defence responses including ROS production and transcriptional activation of pathogenesis-related genes associated with antimicrobial phytoalexin production (Kroj *et al.*, 2003).

OPEL is a novel elicitor of *P. parasitica* with homologs only in Oomycete pathogens (Chang *et al.*, 2015). In the current study, the PPTG_03836 gene, which encodes a secreted OPEL, was down-regulated by phosphite treatment *in vitro* but there was no difference in expression level *in planta*. PPTG_03836 was highly expressed throughout the *P. parasitica*-lupin infection and peaked in expression during late infection (Blackman and Hardham, unpublished results). OPEL gene expression was also highly induced during *P. parasitica* infection of tobacco (Chang *et al.*, 2015). The infiltration of an OPEL recombinant protein into tobacco leaves resulted in defence responses such as cell death, callose formation, ROS production and induced PAMP-triggered immunity and systemic resistance (Chang *et al.,* 2015). In the current study, the combination of the large down-regulation of the TGase PPTG_16234 by phosphite, suggests that down regulation of apoplastic elicitors may be a key step in the inhibition of plant infection by phosphite.

Pathogen protease and glucanase inhibitors are apoplastic effectors that suppress host enzymes involved in defence (Tian *et al.*, 2005; Hardham and Cahill, 2010; King *et al.*, 2010). During plant-pathogen interactions, *Phytophthora* species secrete glucanase inhibitor proteins (GIPs) which inhibit endo-β-1,3-glucanase (EGases) activity (Damasceno *et al.*, 2008). In the current study, the GIPs were only expressed at low levels if at all and their expression was not affected by phosphite treatment *in vitro*. However, *in planta*, five of the seven GIPs in the *P. parasitica* genome were expressed and were up-regulated following phosphite treatment. Previous studies have shown that *P. sojae* GIPs inhibit up to 85% of the EGases activity in soybean (Bishop *et al.*, 2005) and that *P. infestans* GIPs interact with tomato EGases in the plant apoplast (Damasceno *et al.*, 2008).

Genes encoding *P. parasitica* Epi-type serine protease inhibitors were highly expressed *in planta* and were down-regulated by phosphite treatment. Kazal-type serine protease inhibitors were in general up-regulated *in planta*. Given that both of these classes of inhibitors target P69B-type tomato proteases (Tian *et al.*, 2004; Tian *et al.*, 2005), it is difficult to explain the different effects of phosphite in the context of the inhibition of pathogenesis. EpiC-type proteins inhibit cysteine proteases (Song *et al.*, 2009). In the compatible interaction between *P.*

parasitica and lupin, *P. parasitica* cysteine and serine proteases were expressed during late infection (Blackman and Hardham, unpublished results). *In planta*, strong expression of three secreted cysteine proteases (PPTG_11311, PPTG_11313, PPTG_13332) was inhibited by phosphite treatment. In contrast, serine proteases were not highly expressed, and only a few where down-regulated in the presence of phosphite.

5.4.7.4. Kinases

The mitogen-activated protein (MAP) kinases have a fundamental role in the regulation of plant defence responses (Andreasson *et al.*, 2005; Cakir and Kılıçkaya, 2015). The *P. parasitica* genome contains at least 580 kinases (L. M. Blackman, pers. comm.) and to gain a preliminary indication of the effect of phosphite, the expression of 89 genes was analysed. Of the 89, the expression of 70 (DE>2-fold change) was either up-regulated or down-regulated by phosphite treatment (results not shown).

Pyruvate, phosphate dikinase (PPDK) is an enzyme that catalyses the chemical reaction of pyruvate, ATP, and phosphate to phosphoenolpyruvate, AMP and pyrophosphate and assays of PPDK activity in *P. cinnamomi* suggest that PPDKs are essential for *Phytophthora* growth and sporulation (Marshall *et al.,* 2001). Expression of the PPDK gene, PPTG_13569, was down-regulated by phosphite *in vitro* (3.2–fold change) and in infected lupins (69-fold change). Of the five pyruvate kinases in the *P. parasitica* genome, only PPTG_03708 is affected by phosphite treatment: its expression is up-regulated *in planta* and down-regulated *in vitro*. In *P. cinnamomi,* phosphite treatment *in vitro* leads to down-regulation of gene expression of pyruvate kinase and pyruvate phosphate dikinase *Pdk2* (King *et al.*, 2010).

5.4.7.5. Response to oxidative stress

Oxidative stress is defined as the imbalance between the production of ROS and the ability to detoxify their reactive intermediates (Betteridge, 2000; Budachetri and Karim, 2015). Stressful abiotic conditions can lead to the excessive

production of ROS in plants, causing damage to carbohydrates, proteins, lipids, and nucleic acids (Mittler, 2002; Gill and Tuteja, 2010). To fight the threat of ROS, plants use scavenging enzymes and metabolites (Mittler, 2002). Among the major ROS-scavenging enzymes that were differentially expressed *in vitro* and *in planta* were enzymes involved in the production and scavenging of ROS, and proteins that provide protection by other methods.

SODs convert reactive oxygen into H_2O_2 which is then removed by the action of a number of proteins including catalase, peroxiredoxin, and glutathione S-transferases (GSTs) (Willekens *et al.*, 1995; Noctor and Foyer, 1998). The oxidative stress pathway also includes amine oxidase, thioredoxin, glutaredoxin, copper amine oxidase, glutathione peroxidase and other peroxidases, and glutathione reductases (Noctor and Foyer, 1998; Mittler *et al.*, 2004). In the present study, of the 55 *P. parasitica* genes examined *in vitro* and *in planta*, the expression of 24 was affected by phosphite treatment and in most cases expression was up-regulated. *In vitro*, *P. parasitica* catalase activity is highest in sporulating hyphae and during tobacco infection, it increases dramatically 8 hpi (Blackman and Hardham, 2008). Phosphite treatment increases the expression of two *P. parasitica* catalase genes (PPTG_06664, PPTG_06866) *in vitro* and in infected lupin roots.

GSTs are multifunctional proteins encoded by members of a divergent gene family with the main function being the detoxification of xenobiotics and removal of H_2O_2 (Marrs, 1996; Edwards *et al.*, 2000; Liu *et al.*, 2013). In plants, they have been implicated in abiotic and biotic stress responses, including to *Phytophthora* (Roxas *et al.*, 2000; Hernández *et al.*, 2009). The current study found that phosphite treatment led to an up-regulation in the expression of four of 13 *P. parasitica* GSTs *in vitro* but of only two GST genes *in planta*.

Two other proteins involved in the protection against oxidative stress, and whose expression was up-regulated by phosphite treatment in the infected lupin roots, are mannitol dehydrogenase (MTD) and alternative oxidase (AOX) (Mittler, 2002; Patel and Williamson, 2016). In *P. infestans*, the expression of a putative MTD gene (PITG_08846) is up-regulated as affected by mefenoxam treatment (Childers *et al.*, 2015). This *P. infestans* MTD gene has homology to the

differentially expressed up-regulated *P. parasitica* MTD transcripts, PPTG_06299 and PPTG_10399. AOXs function in metabolic and signalling homeostasis and their expression is influenced by biotic (e. g. pathogen infection) and abiotic stresses such as nutrient deficiency, drought and saline stress (Tsuji *et al.*, 2000; Rhoads *et al.*, 2006; Vanlerberghe, 2013). The expression of two AOX genes, PPTG_18782 and PPTG_18784, was up-regulated by phosphite treatment *in vitro* and *in planta*. The predicted protein of PPTG_18784 is closely related to a partial *P. cinnamomi* AOX (NCBI No: ACL11877.1, with 74% amino acid identity in overlapping regions). The gene encoding the *P. cinnamomi* AOX was down-regulated by treatment with 40 μg/ml phosphite (King *et al.*, 2010). Both *P. parasitica* AOX genes were more highly expressed *in vitro* than during the infection time-course conducted previously (Blackman and Hardham, unpublished results), suggesting that *P. parasitica* grown in minimal media in the current study was experiencing oxidative stress and the addition of phosphite compounded this stress.

Other proteins implicated in responses to oxidation stress, and which were up-regulated or down-regulated following phosphite treatment *in vitro* and *in planta* included a pyridine nucleotide-disulphide oxidoreductase (PPTG_04800), an S-adenosylmethionine (SAM)-dependent O-methyltransferase (PPTG_18786), and a nitrite reductase (PPTG_16900) (Tables 5.15, 5.16). An O-methyltransferase defends *Podospora anserina* from oxidative stress during senescence and also functions as a longevity assurance factor (Kunstmann and Osiewacz, 2009). A NADP-malic enzyme (NADP-ME) is an abundant enzyme involved in metabolic pathways that catalyse the oxidative decarboxylation of L-malate (Drincovich *et al.*, 2001). In the current study, NADP-ME (PPTG_19369) was down-regulated in the presence of phosphite *in vitro* and *in planta*. By contrast, phosphite treatment led to an up-regulation of the expression of the gene encoding a *P. infestans* malic enzyme (DMP400004672) during potato-infection (Burra *et al.,* 2014). One gene involved in response to oxidative stress whose expression was down-regulated gene by phosphite treatment was a ribonuclease inhibitor (RI)-like protein (PPTG_13951). Ribonuclease activity has been observed during stress (Thompson *et al.*, 2008) and it is possible that RIs may be produced to counter this activity. Expression of a pyridine nucleotide-disulphide oxidoreductase was

up-regulated by phosphite treatments *in vitro* and *in planta*. A homolog associated with antioxidant activity has been identified in ticks (Budachetri and Karim, 2015).

5.4.7.6. Transmembrane transport

The adenosine triphosphate (ATP)-binding-cassette (ABC) transporter superfamily includes a large group of proteins which link the hydrolysis of ATP to the movement of solutes across cellular membranes (Schneider and Hunke, 1998). Phosphite treatment led to the up-regulation or down-regulation of *P. parasitica* ABC transporter genes *in vitro* and *in planta*. Similar results were obtained in a microarray analysis of gene expression in *P. cinnamomi* mycelium in the presence of phosphite (40 µg/ml) *in vitro* (King *et al.*, 2010).

Three of eight amino acid/auxin permeases (AAAP), which also function in transmembrane transport, were down-regulated by phosphite treatment *in vitro* and *in planta*. Their expression was high in the infected lupin roots. A recent RNA-Seq analysis found that members of the AAAP family in *P. infestans* were among the mostly induced genes during the early infection in tomato and potato and they may encode haustoria-associated transporters (Abrahamian *et al*., 2016). Some, like those from *P. parasitica,* were more highly expressed *in planta* than *in vitro*. In *P. cactorum,* an AAAP gene is up-regulated during cyst germination and strawberry infection (Chen *et al.*, 2011) The *P. cactorum* gene (Accession no. GW874435) has 100% homology to *P. infestans* (PITG_17804) and 90% homology to an AAAP *P. parasitica* gene (PPTG_00017) (Chen *et al.*, 2011; www.ncbi.nlm.nih.gov). Phosphite treatment led to a decrease in expression of PPTG_00017 *in vitro* but an increase in expression in infected lupins.

Two transmembrane transporter proteins in the major facilitator superfamily (MFS) were highly expressed *in vitro* and *in planta* after the addition of phosphite. One gene (PPTG_15061) was up-regulated while the other gene (PPTG_13312) was down-regulated. Two recent publications have identified the *P. infestans* MFS family as the largest group of transporters with 111 proteins (Abrahamian *et al.*, 2016; Ah-Fong *et al.*, 2017). Most of these MFSs were

annotated as sugar transporters while others are believed to transport carboxylic acids, lipids and nitrate. A *P. infestans* nitrate transporter (PITG_13011) in the MFS family was expressed at a 70-100-fold higher level in potato leaves than *in vitro* (Abrahamian *et al*., 2016). Phosphite increased the expression of two *P. parasitica* mitochondrial carrier genes (PPTG_19128 and PPTG_08198) *in vitro* and in infected lupins. Mitochondrial carrier proteins function in the metabolic communication between the plant mitochondria and the cell cytoplasm (Picault *et al.*, 2004), and in *P. infestans* play an important role in intracellular trafficking or efflux (Abrahamian et al., 2016). In contrast, the gene encoding another mitochondrial carrier (CD051680: PPTG_11868) that was identified in a *P. parasitica* zoospore cDNA library (Škalamera *et al.*, 2004) was up-regulated but was not differentially expressed (fold change <2) in phosphite-treated infected lupins and *in vitro* in the current study.

A placenta-specific gene 8 protein (PLAC8), PPTG_08423 was up-regulated in the presence of phosphite in the current study. In plants, PLAC8 motif-containing proteins form a large family and are involved in transport of heavy metals and determination of fruit size and cell number (Song *et al.*, 2011). RNA-Seq analysis of *Saprolegnia parasitica,* an Oomycete fish pathogen, detected a differentially expressed PLAC8 gene in vegetative and infection tissues (Jiang *et al.*, 2013).

5.4.7.7. Cytoskeleton-associated proteins and intracellular transport

An ADP-ribosylation factor (ARF) family protein (PPTG_03018) which is a GTPase with a role in Golgi vesicle-mediated transport, is up-regulated in the presence of phosphite. Genes encoding ARFs were the most strongly up-regulated group of genes in phosphite-treated *P. cinnamomi* mycelium in the study of King *et al.* (2010). These ARF genes showed between 47- and 399-fold induction using qPCR. One of these *P. cinnamomi* ARF genes (FJ492976) has significant homolog to PPTG_03018. ARFs play a major role in the regulation of organelle structure and vesicular trafficking (D'Souza-Schorey and Chavrier, 2006). ARF proteins regulate the remodelling of the cell membrane and also interact with the actin cytoskeleton (King *et al*., 2010). The cytoskeleton plays an important role in diverse processes in eukaryotic cells and tissues, and

cytoskeleton reorganisation facilitates resistance to pathogen penetration (Hardham *et al.*, 2007; Ketelaar *et al.*, 2012). The addition of inhibitors of cytoskeleton function can cause changes in cell morphology. For example, addition of the actin depolymerising drug latrunculin B (latB) to *P. infestans* cultures caused increased hyphal branching, irregular hyphal diameters, and radial swelling of hyphal tips, and altered the position of the nuclei (Ketelaar *et al.*, 2012). The effects of phosphite-induced up-regulation of *Phytophthora* ARFs are unknown ARF knockout lines in *Candida albicans* had altered cell walls and decreased hyphal growth (Labbaoui *et al.*, 2017).

Phosphite treatment led to down-regulation of the expression of two annexins genes (PPTG_17883, PPTG_17884) *in vitro* and *in planta*. Annexins regulate the interaction between membranes and the cytoskeleton and some are known to be actin-binding proteins (Konopka-Postupolska, 2007). Of the eight *P. parasitica* annexin genes, six were more highly expressed *in planta* than *in vitro* and this included PPTG_03934 which is a homolog to a *P. cinnamomi* annexin that is down-regulated in phosphite media (King *et al.*, 2010). King et al. (2010) suggest the inhibitory effect of phosphite on *Phytophthora* species was a result of disrupted synthesis of cell walls and changed expression of cytoskeleton genes. In phosphite-treated *P. cinnamomi* mycelia, PHYCI_82113, the homolog of PPTG_03934, is down-regulated (King *et al.*, 2010). Phosphite caused a small (1.9 fold) down-regulation in the expression of PPTG_03934 but this was below the 2-fold cut-off applied in the analysis. Nevertheless, down-regulation of annexin genes makes this family of proteins prime candidates for the phosphite-induced wall changes.

Ankyrin (ANK) repeats are found in a large number of proteins and are one of the most detected amino acid motif in proteins database (Mosavi *et al.,* 2004). In the present study, the expression of two genes encoding proteins with variable numbers of ANK repeat domains (PPTG_12957, PPTG_10026) was down-regulated in phosphite-containing media. The function of these proteins is unknown and analysis of PPTG_12957 was made difficult by multiple variants. PPTG_10026 has one ankyrin repeat domain, is associated with the membrane according to GO analysis and contains a putative GPCR-chaperone domain acting.

These latter proteins are molecular chaperones for G protein-coupled receptors and may be involved in trafficking in biosynthetic pathways (Parent *et al.*, 2010). PPTG_12957 contains two ANK repeat domains but there are no other clues to its function. Ankyrin repeats are found in many proteins where they are involved in protein-protein interactions (Al-Khodor *et al.*, 2010) and have been identified in some fungal effectors (Mesarich *et al.*, 2015) but the two *P. parasitica* genes did not contain secretion signals and are unlikely to act as effectors.

5.4.7.8. Turgor pressure regulation

Turgor pressure drives the growth and expansion of plant cells (Kroeger *et al.*, 2011; Chen *et al.*, 2015). In *Arabidopsis*, an alkaline ceramidase gene *Turgor Regulation Defect 1*, is a key turgor pressure regulator specifically induced in silique guard cells and pollen tubes (Chen *et al.*, 2015). Phosphite treatment led to an increase in the expression of a *P. parasitica* alkaline phytoceramidase gene (PPTG_11865) *in vitro* and in infected lupin roots. It is possible that this potential interference in the regulation of turgor pressure contributes to the effects of phosphite on *P. parasitica* growth form and hypha morphology.

5.4.7.9. Signal transduction

The expression of four genes thought to function in signal transduction was up-regulated following phosphite treatment *in vitro* and in infected lupin roots. Two genes (PPTG_13492 and PPTG_03299) encoded phosphatidylinositol-binding proteins (pleckstrin). In a recent study, a phosphatidylinositol 3,4,5-trisphosphate, a pleckstrin-homology-domain-containing protein was shown to have phosphoinositide-binding specificities (Dowler et al., 2000). A gene (PPTG_04043) whose expression was down-regulated by phosphite treatment *in vitro* and *in planta* was copine. Copines are conserved calcium-dependent membrane-binding proteins which play roles in development and disease resistance (Zou et al., 2016). There is evidence that copines may influence calcium signalling because of their ability to interact with protein phosphatases and kinases (Tomsig *et al.*, 2003). Phosphite caused the down-regulation of

expression of a gene (PPTG_05917) encoding a protein-binding protein containing WD40 motifs *in vitro* and *in planta*.

5.4.7.10. Transcription and translation activity

In vitro, the gene (PPTG_14660) that encodes a Myb-like DNA-binding protein (according to the GO analysis) was down-regulated to the second highest degree by phosphite treatment. In the absence of phosphite treatment, this gene was 20-fold more highly expressed *in vitro* than in infected lupin roots. Two other Myb domain proteins were down-regulated following phosphite treatment *in vitro* and *in planta* (PPTG_05959, PPTG_05960). These three Myb proteins had no homology to characterised Myb proteins from *P. infestans* (Xiang and Judelson, 2010; Xiang and Judelson, 2014). Homologs for four stage-specific Myb proteins from *P. infestans* (Xiang and Judelson, 2014) were identified in the *P. parasitica* genome. These were three sporulation-specific Mybs: PPTG_06427 (83% with PITG_08755: Myb2R4); PPTG_10304 (84% with PITG_01056: Myb2R1) and PPTG_11022 (79% with PITG_06748: Myb2R3) and a mycelial-expressed Myb homolog PPTG_10384 (82% with PITG_00988: Myb2R5). All but one of these genes were expressed *in vitro* and *in planta* in the presence or absence of phosphite treatment. The exception was PPTG_06427 which was not expressed in phosphite-treated infected roots. Importantly, the expression of the sporulation-specific Myb domain proteins indicate that phosphite did not cause a delay in *P. parasitica* development in the current study. This contrasts with the situation in *P. infestans*, where Myb transcription factors delay sporulation (Xiang and Judelson, 2014). Signaling pathways involving Myb proteins may be useful targets for chemically-based or other strategies to control devastating pathogens. In the current study, the down-regulation of the expression of two Myb genes by phosphite treatment *in vitro* and *in planta* indicates that identification of their targets may make a valuable contribution to understanding the mechanisms of phosphite action.

Phosphite treatment led to down-regulation of the expression of an RNA helicase-like protein (PPTG_01239) *in vitro* and in infected lupins. This protein has a fundamental role on the rearrangement of RNAs and remodelling of

ribonucleoprotein complexes (Jarmoskaite and Russell, 2014). A gene (PPTG_04387) encoding a zinc-finger protein (CCCH-type) was also down-regulated by phosphite treatment. Zinc-finger proteins form a large family with many diverse functions (Hall, 2005). Proteins from the *Arabidopsis* CCCH family have been implicated in the response to abiotic and biotic stress (Wang *et al.*, 2008). PPTG_01239 appears to be an Oomycete-specific CCCH protein and no proteins of this type have been characterised in *Phytophthora*. Interestingly, another Oomycete-specific zinc-finger protein from *P. sojae* (C2H2-type, NCBI no. ACG80380.1) was necessary for growth, development and pathogenesis (Wang *et al.*, 2009a).

5.4.8. Concluding Remarks

Phosphite has been used for several decades in the management of *Phytophthora* diseases in different ecosystems. One of the reasons for its frequent usage is its low toxicity (LD50 > 5 g/kg) to the environment as assessed by the European Food Safety Authority in 2012 (Liljeroth *et al.*, 2016). Several studies show that phosphite application stimulates plant defence (Smillie *et al.*, 1989; Guest and Bompeix, 1990; Massoud *et al.*, 2012; Lim *et al.*, 2013; Burra *et al.*, 2014), but the molecular mechanisms underlying phosphite inhibition of *Phytophthora* growth and development have not been elucidated (Massoud *et al.*, 2012; Dalio *et al.*, 2014).

The current study is the first investigation of the effects of phosphite on the *P. parasitica* transcriptome during a compatible infection of lupin plants. The results show that phosphite causes extensive changes in pathogen gene expression and provide insights into the effects of phosphite on *Phytophthora* pathogenesis at a cellular and molecular level. In combination with the data from the draft genome sequence for lupin which has recently become available (Hane *et al.*, 2016), the data presented in this thesis chapter will provide a framework for future studies aimed at determining the mechanisms by which phosphite inhibits the development of *Phytophthora* diseases.

CHAPTER 6
General Discussion

6.1. Overview

Oomycetes such as *Phytophthora* species are among the most notorious pathogens that cause extensive economic losses and ecological damage. Globally, *Phytophthora* species have been and remain the cause of extremely damaging plant diseases (Drenth and Guest, 2004; Dunstan *et al.*, 2016). Despite the significant economic losses these *Phytophthora* species cause in agriculture and the large amounts of time and resources devoted to their research, their control remains elusive.

The project reported in this thesis focused on *P. parasitica* and its infection of young lupin seedlings. The main achievements of the research have been the development of a new host-pathogen infection assay system for studies of *Phytophthora*-plant interactions, the analysis of the expression of selected *P. parasitica* pathogenicity genes during plant infection and the elucidation of new information on the effects of the *Phytophthora*-active inhibitor, phosphite, on *P. parasitica* transcriptomes *in vitro* and *in planta*.

The new model infection assay that was developed is based on the inoculation of roots of young lupin seedlings. This new assay has a number of advantages over previously reported systems, including the facts that (i) preparation of host material takes less than 2 days, (ii) large numbers of plant replicates can be inoculated simultaneously, (iii) pathogen inoculum levels that are used are similar to those typical of field conditions, and (iv) measurement of the extent of plant colonisation using qPCR is rapid and robust. The efficacy of the newly developed assay was demonstrated through the screening of four lupin cultivars (Gungurru, Jenabillup, Jindalee, and Wonga) for their susceptibility to *P. parasitica*. The assays showed that these cultivars displayed a range of susceptibilities and that none was truly resistant. The value of the new assay was also established through its utilisation for a series of infection transcriptome studies.

The most susceptible of the four lupin cultivars, Gungurru, was selected for investigations of the expression of a number of *P. parasitica* pathogenicity genes, namely genes encoding key CWDEs, over the period 24-60 h following root inoculation. The lupin infection assay was also exploited to investigate cellular and molecular aspects of the effects of phosphite treatment. This component of the project obtained new information on *P. parasitica* transcriptomes 48 hpi. The data enabled the identification of genes whose expression changed following phosphite treatment *in vitro* and *in planta*.

6.2. Lupin as a model plant in the study of *P. parasitica* interaction

The current study established parameters for a *P. parasitica* infection system using narrow-leafed lupins as a model plant as described in Chapter 2. Early work on interactions of *Phytophthora* species and plants used narrow-leafed lupins (*L. angustifolius*) and *P. cinnamomi* (Weste *et al.*, 1973; Weste, 1975; Hinch and Clarke, 1982; Grose and Hainsworth, 1992; Rookes *et al.*, 2008). For *P. parasitica*, tobacco has been often used in disease development studies (McIntyre and Taylor, 1976; Tedford *et al.*, 1990; Van Jaarsveld *et al.*, 2003) but use of this host plant has a number of drawbacks ans discussed below. During development of the model system using lupin, a series of experiments was conducted to establish a protocol that produced reproducible results.

The current study demonstrated that use of young lupin seedlings was superior to tobacco or Arabidopsis material for a number of reasons. Lupin seeds are large and germinate quickly (in less than 48 h after imbibition); the roots and young seedlings are robust, simplifying their individual inoculation and handling as compared to infecting a cluster of about 50 young tobacco or Arabidopsis seedlings (Blackman and Hardham, 2008; Larroque *et al.*, 2013). As in other disease screening studies, the success of the lupin-*P. parasitica* infection assay relied on careful consideration and control of the experimental conditions. Parameters that were shown to be important for the establishment of a rapid, sensitive and reproducible laboratory-based lupin infection assay included: a) the age of the lupin seedlings (40-46 h after imbibition and sowing), b) the

inoculum concentration (1000 zoospores/ml in 50 ml of water), c) the sampling times (a 6-h interval was suitable for observation of the gradual response of lupin to *P. parasitica* infection), d) sufficient numbers of replicates, and e) maintenance of moisture levels during and after inoculation. As in previous studies, the aim was to develop an improved, rapid and easy infection assay techniques (McIntyre and Taylor, 1976; Tedford *et al.*, 1990; Van Jaarsveld *et al.*, 2003).

The lupin assay was used to evaluate levels of susceptibility or resistance of four lupin cultivars (Gungurru, Jenabillup, Jindalee and Wonga) a number of which are currently employed in agriculture (Chapter 3). Cultivar Gungurru was found to be the most susceptible cultivar and was used in subsequent experiments for investigations of cellular and molecular events that occur during plant infection (Chapters 4 and 5). The performance of the lupin infection assay indicated that it would be of considerable value to use it to screen newly-released lupin cultivars such as PBA Barlock, PBA Gunyidi, PBA Jurien (http://pir.sa.gov.au) in order to assess their levels of resistance or susceptibility to PRR. The work also demonstrated that the lupin assay was likely to be an excellent tool for studies of host-pathogen interactions in other *Phytophthora* species.

After the establishment and testing of the infection assay, it was used to study changes in pathogen gene expression and the effects of phosphite on *Phytophthora* growth, development and pathogenicity at cellular and molecular levels (Chapters 4 and 5). In the first set of experiments, changes in the expression of selected CWDE genes were determined using qPCR during the period 24-60 hpi. In the second set of experiments, the effects of phosphite treatment on host and pathogen transcriptomes were investigated using RNA-Seq in material collected 48 hpi. The results of these studies have provided new and valuable information on the process of plant infection by this destructive *Phytophthora* species and the effects of phosphite on pathogen gene expression.

6.3. The production and secretion of CWDEs during plant infection

CWDEs are key pathogenicity factors required by plant pathogens, including prokaryotic and eukaryotic organisms, for successful disease establishment (Kubicek *et al*., 2014). The plant cell wall is a strong and effective barrier that inhibits the ingress of the vast majority of microorganisms and potential pathogens. Pathogen CWDEs are required for the pathogen to be able to penetrate the outer plant surface and to subsequently colonise the plant, either by growing along cell walls within the apoplast or by breaching the cell wall and growing into the plant cell. As detailed in Chapter 4, plant cell walls are highly complex forms of extracellular matrix. Although only three main polysaccharide components are recognised, namely cellulose microfibrils, hemicelluloses and pectins, these broad categories encompass an immense diversity of polysaccharide molecular structures in terms of the sugar residues that comprise the carbohydrate chains, the nature of the bonds that link adjacent residues, the nature and extent of chain branching and details of their modification by side groups. Plant cell walls also contain proteins and glycoproteins, and wall strength and rigidity may be increased through impregnation with lignins and other polyphenolics (Keegstra, 2010; Wang *et al.*, 2013). In order to be able to degrade plant cell walls, pathogens must synthesise and secrete a plethora of different and often highly specialised CWDEs. Fungal and Oomycete hyphae extend through the fusion of small vesicles containing wall material and secrete material with the plasma membrane at the hyphal tip (Bartnicki-Garcia *et al*., 1989). It is also accepted, although there is little proof, that CWDEs that will function in host cell wall degradation are also secreted at the hyphal tip. The immunofluorescence labelling with anti-polygalacturonase antibodies provided evidence that is indeed the case.

In the experiments reported in Chapter 4, the lupin infection assay was used for a qPCR analysis of the expression of selected *P. parasitica* CWDEs. The results provided evidence of a distinct temporal sequence in the up-regulation of the CWDE genes. As infection proceeded from 24 hpi to 60 hpi, pectinase, then hemicellulase and then cellulase genes were expressed. This order of CWDE gene expression was similar to that reported from studies of some other pathogens

(Cooper and Wood, 1975; Martinez *et al*., 1991). It has been suggested that enzymes that act early may expose wall components to other CWDEs (Hückelhoven, 2007; Blackman *et al.*, 2015). A possible example of this observed in the lupin infection time course was the early production of pectin methylesterases which de-esterify pectins and which may facilitate subsequent attack by polygalacturonases (Blackman *et al*., 2015). The use of qPCR in this study limited the number of enzymes whose expression patterns could be monitored. A much better understanding of details and implications of the CWDE cascade during plant infection required a more global analysis, such as that provided by the RNA-Seq technique. In fact, such an RNA-Seq study using the lupin infection assay was subsequently conducted (Blackman *et al.,* 2015), with the experimental design being based on the preliminary qPCR study reported in Chapter 4 of this thesis.

6.4. Phosphite use against *Phytophthora*

The chemical phosphite has been recognised as an effective fungicide against Oomycete phytopathogens, particularly *Phytophthora* species (Smillie *et al.*, 1989; Guest and Grant, 1991; Jackson *et al.*, 2000; Thao and Yamakawa, 2009). Differences in the sensitivity of different *Phytophthora* species, and even of different isolates within a species, have been reported, as was shown in the experiments described in Chapter 5 and where possible factors underlying this variability have been discussed.

In addition, the sensitivity of a *Phytophthora* species or isolate to phosphite *in vitro* may not be the same as its sensitivity *in planta*. The effectiveness of treatments *in planta* may, for example, be influenced by production and/or activation of plant antimicrobial secondary metabolites (Guest and Grant, 1991). It is also believed that phosphite can trigger *Phytophthora* to increase production of elicitins and/or decrease the production of suppressors. These effects will augment the capability of the host plant to recognise the presence of the pathogen, leading to the induction of defence responses (Dunstan *et al.*, 1990; Saindrenan *et al.*, 1990). In addition, *Phytophthora* isolates that are more

sensitive to phosphite *in vitro* may grow more slowly *in planta* than those that are less sensitive. This may mean that the plant is able to mount a defence response more rapidly relative to the stage of pathogen colonisation than if could be a less inhibited (Guest and Bompeix, 1990; Guest and Grant, 1991).

One aspect of the effect of phosphite on *P. parasitica* that was not investigated in the current study was that of possible effects on chlamydospores production and dormancy *in vitro* as reported by McCarren *et al.* (2009). If the application of phosphite triggers the production of dormant chlamydospospores, this will have implications for the survival of the pathogen in the environment even in adverse conditions. This is of fundamental importance and warrants further assessment *in planta*. Proper detection of dormant pathogens in the environment will be a quarantine concern as it could increase the accidental movement of *Phytophthora*-infested soils (McCarren, 2006).

6.5. Does phosphite induce a developmental delay?

Quantification of the abundance of immunolabelled zoospore peripheral vesicles in *Phytophthora* mycelia *in vitro* showed that there were fewer vesicles in samples treated with phosphite than in untreated samples. This situation could result from a delay in the progress of sporulation. *In planta*, treatment with 50 µg/ml phosphite resulted in the delay and/or inhibition of symptom development in *P. parasitica*-infected lupins. These observations led to the question, is this delay due to a general inhibition of the rate of *P. parasitica* growth or to the inhibition of specific aspects of *P. parasitica* differentiation, such as asexual sporulation? This question was addressed by examining levels of transcripts encoding various stage-specific proteins. It was subsequently found that phosphite treatment did not change the transcript levels of four genes whose expression has been reported to be up-regulated during sporulation (Attard *et al.*, 2014). The results suggested that phosphite was not causing a general delay in the expression *P. parasitica* genes encoding stage-specific proteins.

6.6. Phosphite effects on the infection transcriptome

One of the most interesting results to emerge from the RNA-Seq analysis of the effect of phosphite on the *P. parasitica* transcriptome is that phosphite treatment led to an increase in transcript abundance of many genes that are normally expressed early in infection but not of genes that are normally expressed late in infection. Evidence for this included the following observations. (1) All *P. parasitica* pectinase genes that were up-regulated in phosphite-treated roots are expressed early during infection. Pectinases are often the first CWDEs expressed during infection and play crucial roles in successful pathogenesis (Cooper, 1983; Benhamou and Côté, 1992; Blackman *et al.*, 2015). The RNA-Seq analysis of the 60-h time-course of lupin infection by *P. parasitica* revealed that pectinase genes could be divided into two cohorts in terms of the timing of their expression, with one cohort being expressed early (30-36 hpi) and the other being expressed during mid or late infection (42-60 hpi) (Blackman *et al.*, 2015). (2) Seven cellulase genes that are expressed early in infection (30-36 hpi) were up-regulated in phosphite-treated lupin roots. (3) Certain RxLR effectors are expressed early (zoospore to appressorium stages) during *P. parasitica* infection in onions (Kebdani *et al.*, 2010) and the genes encoding most of these were up-regulated in phosphite-treated lupins. How this up-regulation of early pathogenicity genes by phosphite might be involved in the inhibition of *Phytophthora* growth and virulence requires further experimentation to determine.

Advances in NGS have opened up new possibilities for research aimed at understanding the mode of action of phosphite in controlling *Phytophthora* diseases. NGS has revolutionised genome sequencing and transcriptome profiling and, although methodologies such as qPCR and microarrays have their own merits, RNA-Seq has been deemed to be the best system presently available for transcriptome analysis (Wang *et al.*, 2009b). In addition, the RNA-Seq technology continues to improve. For example, the recently developed RNA-Seq analysis pipeline PANDORA (PerformANce Driven scOring of RNA-Seq stAtistics) allows enhanced comparisons of multiple algorithms (Moulos and Hatzis, 2015; Manga *et al.*, 2016).

These technical developments mean that it is an exciting time for research into plant diseases, in particular for research that aims to elucidate the molecular basis of pathogenicity and plant infection. One of the future challenges will be to continue to adapt the new methods that become available and to devise ways of applying them to both *in vitro* and *in planta* studies of plant-pathogen interactions. The new model infection assay utilising young lupin seedlings that I developed and the results from my qPCR analysis of the expression of selected pathogen CWDE genes have already made a major contribution in this regard. They have formed the basis for an in-depth analysis of the expression of *P. parasitica* CWDE genes in a detailed time-course of infection transcriptomes (Blackman *et al.,* 2015). In addition, to the best of my knowledge, my RNA-Seq study is the first to describe in detail the expression of genes in phosphite-treated *P. parasitica* mycelia and infected lupins. The results that have been obtained have increased our understanding of *Phytophthora* pathogenicity mechanisms and of the effects of phosphite on gene expression and they should aid in the development of improved strategies for managing *Phytophthora* diseases.

BIBLIOGRAPHY

Phytophthora parasitica INRA-310 Sequencing Project, Broad Institute of Harvard and MIT [Online]. Available: (http://www.broadinstitute.org/) [Accessed 12 March 2015].

Abrahamian, M., Ah-Fong, A. M., Davis, C., Andreeva, K. & Judelson, H. S. (2016). Gene expression and silencing studies in *Phytophthora infestans* reveal infection-specific nutrient transporters and a role for the nitrate reductase pathway in plant pathogenesis. *PLoS Pathogens,* 12, e1006097.

Agrios, G. N. (1997). *Plant Pathology,* San Diego California, USA, Academic Press.

Ah-Fong, A. & Judelson, H. S. (2003). Cell cycle regulator Cdc14 is expressed during sporulation but not hyphal growth in the fungus-like oomycete *Phytophthora infestans*. *Molecular Microbiology,* 50, 487-494.

Ah-Fong, A. M., Kim, K. S. & Judelson, H. S. (2017). RNA-seq of life stages of the oomycete *Phytophthora infestans* reveals dynamic changes in metabolic, signal transduction, and pathogenesis genes and a major role for calcium signaling in development. *BMC Genomics,* 18, 198.

Ailloud, F., Lowe, T. M., Robène, I., Cruveiller, S., Allen, C. & Prior, P. (2016). *In planta* comparative transcriptomics of host-adapted strains of *Ralstonia solanacearum*. *PeerJ,* 4, e1549.

Akinsanmi, O. A. & Drenth, A. (2013). Phosphite and metalaxyl rejuvenate macadamia trees in decline caused by *Phytophthora cinnamomi*. *Crop Protection,* 53, 29-36.

Al-Khodor, S., Price, C. T., Kalia, A. & Kwaik, Y. A. (2010). Functional diversity of ankyrin repeats in microbial proteins. *Trends in Microbiology,* 18, 132-139.

Ali-Shtayeh, M., Macdonald, J. & Kabashima, J. (1991). A method for using commercial ELISA tests to detect zoospores of *Phytophthora* and *Pythium* species in irrigation water. *Plant Disease,* 75, 305-311.

Ali, A., Alexandersson, E., Sandin, M., Resjö, S., Lenman, M., Hedley, P., Levander, F. & Andreasson, E. (2014). Quantitative proteomics and transcriptomics of potato in response to *Phytophthora infestans* in compatible and incompatible interactions. *BMC Genomics,* 15, 497.

Allardyce, J. A., Rookes, J. E. & Cahill, D. M. (2012). Defining plant resistance to *Phytophthora cinnamomi*: a standardized approach to assessment. *Journal of Phytopathology* 160, 269-276.

Allen, F. H. & Friend, J. (1983). Resistance of potato tubers to infection by *Phytophthora infestans*: a structural study of haustorial encasement. *Physiological Plant Pathology,* 22, 285-292.

Altschul, S. F., Madden, T. L., Schäffer, A. A., Zhang, J., Zhang, Z., Miller, W. & Lipman, D. J. (1997). Gapped BLAST and PSI-BLAST: a new generation of protein database search programs. *Nucleic Acids Research,* 25, 3389-3402.

An, Y., Kang, S., Kim, K.-D., Hwang, B. K. & Jeun, Y. (2010). Enhanced defense responses of tomato plants against late blight pathogen *Phytophthora infestans* by pre-inoculation with rhizobacteria. *Crop Protection,* 29, 1406-1412.

Anderson, J., Pegg, K., Scott, C. & Drenth, A. (2012). Phosphonate applied as a pre-plant dip controls *Phytophthora cinnamomi* root and heart rot in susceptible pineapple hybrids. *Australasian Plant Pathology,* 41, 59-68.

Andreasson, E., Jenkins, T., Brodersen, P., Thorgrimsen, S., Petersen, N. H., Zhu, S., Qiu, J. L., Micheelsen, P., Rocher, A. & Petersen, M. (2005). The MAP kinase substrate MKS1 is a regulator of plant defense responses. *EMBO Journal,* 24, 2579-2589.

Aro, N., Pakula, T. & Penttilä, M. (2005). Transcriptional regulation of plant cell wall degradation by filamentous fungi. *FEMS Microbiology Reviews,* 29, 719-739.

Aryantha, I. N. P. & Guest, D. I. (2006). Mycoparasitic and antagonistic inhibition on *Phytophthora cinnamomi* Rands by microbial agents isolated from manure composts. *Plant Pathology Journal,* 5, 291-298.

Asai, S., Rallapalli, G., Piquerez, S. J., Caillaud, M.-C., Furzer, O. J., Ishaque, N., Wirthmueller, L., Fabro, G., Shirasu, K. & Jones, J. D. (2014). Expression profiling during Arabidopsis/downy mildew interaction reveals a highly-expressed effector that attenuates responses to salicylic acid. *PLoS Pathogens,* 10, e1004443.

Aspeborg, H., Coutinho, P. M., Wang, Y., Brumer, H. & Henrissat, B. (2012). Evolution, substrate specificity and subfamily classification of glycoside hydrolase family 5 (GH5). *BMC Evolutionary Biology,* 12, 186.

Attard, A., Evangelisti, E., Kebdani-Minet, N., Panabières, F., Deleury, E., Maggio, C., Ponchet, M. & Gourgues, M. (2014). Transcriptome dynamics of *Arabidopsis thaliana* root penetration by the oomycete pathogen *Phytophthora parasitica*. *BMC Genomics,* 15, 538.

Attard, A., Gourgues, M., Callemeyn-Torre, N. & Keller, H. (2010). The immediate activation of defense responses in Arabidopsis roots is not sufficient to prevent *Phytophthora parasitica* infection. *New Phytologist,* 187, 449-460.

Avci, U., Pattathil, S. & Hahn, M. G. (2012). Immunological approaches to plant cell wall and biomass characterization: Immunolocalization of glycan epitopes. *Biomass Conversion.* Humana Press. 73-82.

Baker, K. F. (1987). Evolving concepts of biological control of plant pathogens. *Annual Review of Phytopathology,* 25, 67-85.

Barampuram, S., Allen, G. & Krasnyanski, S. (2014). Effect of various sterilization procedures on the *in vitro* germination of cotton seeds. *Plant Cell, Tissue and Organ Culture (PCTOC)*, 1-7.

Barrett, S., Shearer, B. & Hardy, G. E. S. J. (2004). Phytotoxicity in relation to *in planta* concentration of the fungicide phosphite in nine Western Australian native species. *Australasian Plant Pathology,* 33, 521-528.

Bartnicki-Garcia, S., Hergert, F. & Gierz, G. (1989). Computer simulation of fungal morphogenesis and the mathematical basis for hyphal (tip) growth. *Protoplasma,* 153, 46-57.

Battaglia, E., Benoit, I., Van Den Brink, J., Wiebenga, A., Coutinho, P. M., Henrissat, B. & De Vries, R. P. (2011). Carbohydrate-active enzymes from the zygomycete fungus *Rhizopus oryzae*: a highly specialised approach to carbohydrate degradation depicted at genome level. *BMC Genomics,* 12, 38.

Beffa, R. & Meins Jr, F. (1996). Pathogenesis-related functions of plant β-1, 3-glucanases investigated by antisense transformation—a review. *Gene,* 179, 97-103.

Bellincampi, D., Cervone, F. & Lionetti, V. (2014). Plant cell wall dynamics and wall-related susceptibility in plant–pathogen interactions. *Frontiers in Plant Science,* 5, 1-8.

Benhamou, N. & Côté, F. (1992). Ultrastructure and cytochemistry of pectin and cellulose degradation in tobacco roots infected by *Phytophthora parasitica* var. *nicotianae*. *Phytopathology,* 82, 468-478.

Bennett, J. C., Diggle, A., Evans, F. & Renton, M. (2013). Assessing eradication strategies for rain-splashed and wind-dispersed crop diseases. *Pest Management Science,* 69, 955-963.

Benson, D. (1991). Detection of *Phytophthora cinnamomi* in azalea with commercial serological assay kits. *Plant disease,* 75, 478-482.

Betteridge, D. J. (2000). What is oxidative stress? *Metabolism,* 49, 3-8.

Bienapfl, J. C., Malvick, D. K. & Percich, J. A. (2011). Specific molecular detection of *Phytophthora sojae* using conventional and real-time PCR. *Fungal Biology,* 115, 733-740.

Bilodeau, G. J., Martin, F. N., Coffey, M. D. & Blomquist, C. L. (2014). Development of a multiplex assay for genus-and species-specific detection of *Phytophthora* based on differences in mitochondrial gene order. *Phytopathology,* 104, 733-748.

Birch, P. R. J. & Whisson, S. C. (2001). *Phytophthora infestans* enters the genomics era. *Molecular Plant Pathology,* 2, 257-263.

Bircher, U. & Hohl, H. R. (1997). Surface glycoproteins associated with appressorium formation and adhesion in *Phytophthora palmivora*. *Mycological Research,* 101, 769-775.

Bishop, J. G., Ripoll, D. R., Bashir, S., Damasceno, C. M., Seeds, J. D. & Rose, J. K. (2005). Selection on glycine β-1, 3-endoglucanase genes differentially inhibited by a *Phytophthora* glucanase inhibitor protein. *Genetics,* 169, 1009-1019.

Bishop, T., Daniel, R., Guest, D., Nelson, M. & Chang, C. (2012). A digital soil map of *Phytophthora cinnamomi* in the Gondwana Rainforests of eastern Australia. *In:* Minasny, B., Malone, B. P. & Mcbratney, A. B. (eds.) *Digital soil assessments and beyond.* Leiden: CRC Press. 65-68.

Bittner, R. & Mila, A. Managing black shank of tobacco with a novel fungicide in on-farm studies. Phytopathology, 2014 3340 Pilot Knob Road, St Paul, MN 55121 USA. American Phytopathological Society 15.

Blackman, L. M., Arikawa, M., Yamada, S., Suzaki, T. & Hardham, A. R. (2011). Identification of a mastigoneme protein from *Phytophthora nicotianae*. *Protist,* 162, 100-114.

Blackman, L. M., Cullerne, D. P. & Hardham, A. R. (2014). Bioinformatic characterisation of genes encoding cell wall degrading enzymes in the *Phytophthora parasitica* genome. *BMC Genomics,* 15, 785.

Blackman, L. M., Cullerne, D. P., Torreña, P., Taylor, J. & Hardham, A. R. (2015). RNA-Seq analysis of the expression of genes encoding cell wall degrading enzymes during infection of lupin (*Lupinus angustifolius*) by *Phytophthora parasitica*. *PLoS ONE,* 10, e0136899.

Blackman, L. M. & Hardham, A. R. (2008). Regulation of catalase activity and gene expression during *Phytophthora nicotianae* development and infection of tobacco. *Molecular Plant Pathology,* 9, 495-510.

Blaker, N. & Hewitt, J. (1987). A comparison of resistance to *Phytophthora parasitica* in tomato. *Phytopathology,* 77, 1113-1116.

Block, A., Schmelz, E., O'donnell, P. J., Jones, J. B. & Klee, H. J. (2005). Systemic acquired tolerance to virulent bacterial pathogens in tomato. *Plant Physiology,* 138, 1481-1490.

Blowes, W., Heather, W., Malajczuk, N. & Shea, S. (1982). The distribution of *Phytophthora cinnamomi* Rands at two sites in Southern Western Australia and at Durras in South-Eastern New South Wales. *Australian Journal of Botany,* 30, 139-145.

Bnejdi, F., Saadoun, M., Allagui, M. B. & El Gazzah, M. (2009). Epistasis and heritability of resistance to *Phytophthora nicotianae* in pepper (*Capsicum annuum* L.). *Euphytica,* 167, 39-44.

Boccas, B. (1981). Interspecific crosses between closely related heterothallic Phytophthora species. *Phytopathology,* 71, 60-65.

Boraston, A., Bolam, D., Gilbert, H. & Davies, G. (2004). Carbohydrate-binding modules: fine-tuning polysaccharide recognition. *Biochemistry Journal,* 382, 769-781.

Bos, J. I., Kanneganti, T. D., Young, C., Cakir, C., Huitema, E., Win, J., Armstrong, M. R., Birch, P. R. & Kamoun, S. (2006). The C-terminal half of *Phytophthora infestans* RXLR effector AVR3a is sufficient to trigger R3a-mediated hypersensitivity and suppress INF1-induced cell death in *Nicotiana benthamiana*. *Plant Journal,* 48, 165-176.

Boudart, G., Charpentier, M., Lafitte, C., Martinez, Y., Jauneau, A., Gaulin, E., Esquerré-Tugayé, M.-T. & Dumas, B. (2003). Elicitor activity of a fungal endopolygalacturonase in tobacco requires a functional catalytic site and cell wall localization. *Plant Physiology,* 131, 93-101.

Bourke, A. (1991). Potato blight in Europe in 1845: The scientific controversy. *In:* Lucas, J., Shuttock, D., Shaw, D. & Cooke, L. (eds.) *Phytophthora.* Cambridge, UK: Cambridge University Press. 447.

Bowles, D. J. (1990). Defense-related proteins in higher plants. *Annual Review of Biochemistry,* 59, 873-907.

Bozkurt, T. O., Schornack, S., Win, J., Shindo, T., Ilyas, M., Oliva, R., Cano, L. M., Jones, A. M., Huitema, E. & Van Der Hoorn, R. A. (2011). *Phytophthora infestans* effector AVRblb2 prevents secretion of a plant immune protease at the haustorial interface. *Proceedings of the National Academy of Sciences, United States of America,* 108, 20832-20837.

Brasier, C., Denman, S., Brown, A. & Webber, J. (2004). Sudden oak death (*Phytophthora ramorum*) discovered on trees in Europe. *Mycological Research,* 108, 1108-1110.

Brasier, C. M. (1996). *Phytophthora cinnamomi* and oak decline in southern Europe: environmental constraints including climate change. *Annales des Sciences Forestieres,* 53, 347-358.

Bringmann, M., Landrein, B., Schudoma, C., Hamant, O., Hauser, M.-T. & Persson, S. (2012). Cracking the elusive alignment hypothesis: the microtubule–cellulose synthase nexus unraveled. *Trends in Plant Science,* 17, 666-674.

Brooks, F. (2008). Detached-leaf bioassay for evaluating taro resistance to *Phytophthora colocasiae*. *Plant Disease,* 92, 126-131.

Brouwer, H., Coutinho, P. M., Henrissat, B. & De Vries, R. P. (2014). Carbohydrate-related enzymes of important *Phytophthora* plant pathogens. *Fungal Genetics and Biology,* 72, 192-200.

Brown, I., Trethowan, J., Kerry, M., Mansfield, J. & Bolwell, G. P. (1998). Localization of components of the oxidative cross-linking of glycoproteins and of callose synthesis in papillae formed during the interaction between non-pathogenic strains of *Xanthomonas campestris* and French bean mesophyll cells. *Plant Journal,* 15, 333-343.

Brown, J. & Caligari, P. (2008). *An introduction to plant breeding,* 9600 Garsington Road, Oxford Ox4 2DQ, UK, Blackwell Publishing Ltd and Wiley & Sons. 2-5.

Brown, R. C. & Lemmon, B. E. (2009). Callose in cell division. *In:* Bacic, A., Fincher, G. & Stone, B. (eds.) *Chemistry, Biochemistry and Biology of (1→ 3)-β-Glucans and Related Polysaccharides* Burlington, USA: Elsevier Academic Press. 425-437.

Brunner, F., Rosahl, S., Lee, J., Rudd, J. J., Geiler, C., Kauppinen, S., Rasmussen, G., Scheel, D. & Nürnberger, T. (2002). Pep-13, a plant defense-inducing pathogen-associated pattern from *Phytophthora* transglutaminases. *EMBO Journal,* 21, 6681-6688.

Budachetri, K. & Karim, S. (2015). An insight into the functional role of thioredoxin reductase, a selenoprotein, in maintaining normal native microbiota in the Gulf Coast tick (*Amblyomma maculatum*). *Insect Molecular Biology,* 24, 570-581.

Buirchell, B. Narrow-leafed lupin breeding in Australia–Where to from here. Proceedings of the 12th International Lupin Conference 14-18 September 2008 2008 Fremantle, Western Australia. 226-230.

Buirchell, B. & Sweetingham, M. Lupin genetic improvement for targeted environments and markets. *In:* Turner, N. & Acuna, T., eds. 13th Australian Society of Agronomy Conference 10-14 September 2006 2006 Perth, Western Australia Australian Society of Agronomy.

Bunyanupappong, K. (1990). *Efficacy of mono-dipotassium phosphite against Phytophthora palmivora (Butl.) Butl. on durian.* MS Thesis, Kasetsart University, Bangkok, Thailand.

Burgess, T. I., Scott, J. K., Mcdougall, K. L., Stukely, M. J., Crane, C., Dunstan, W. A., Brigg, F., Andjic, V., White, D. & Rudman, T. (2016). Current and projected global distribution of *Phytophthora cinnamomi*, one of the world's worst plant pathogens. *Global Change Biology*.

Burra, D. D., Berkowitz, O., Hedley, P. E., Morris, J., Resjö, S., Levander, F., Liljeroth, E., Andreasson, E. & Alexandersson, E. (2014). Phosphite-induced changes of the transcriptome and secretome in *Solanum tuberosum* leading to resistance against *Phytophthora infestans*. *BMC Plant Biology,* 14, 254.

Butcher, T., Stukely, M. & Chester, G. (1984). Genetic variation in resistance of *Pinus radiata* to *Phytophthora cinnamomi*. *Forest Ecology and Management,* 8, 197-220.

Caffall, K. H. & Mohnen, D. (2009). The structure, function, and biosynthesis of plant cell wall pectic polysaccharides. *Carbohydrate Research,* 344, 1879-1900.

Cahill, D., Bennett, I. & Mccomb, J. (1993). Mechanisms of resistance to *Phytophthora cinnamomi* in clonal, micropropagated *Eucalyptus marginata*. *Plant Pathology,* 42, 865-872.

Cahill, D. M., Cope, M. & Hardham, A. R. (1996). Thrust reversal by tubular mastigonemes: immunological evidence for a role of mastigonemes in forward motion of zoospores of *Phytophthora cinnamomi*. *Protoplasma,* 194, 18-28.

Cahill, D. M., Rookes, J. E., Wilson, B. A., Gibson, L. & Mcdougall, K. L. (2008). *Phytophthora cinnamomi* and Australia's biodiversity: impacts, predictions and progress towards control. *Australian Journal of Botany,* 56, 279-310.

Cakir, B. & Kılıçkaya, O. (2015). Mitogen-activated protein kinase cascades in *Vitis vinifera*. *Frontiers in plant science,* 6, 556.

Cannon, M. C., Terneus, K., Hall, Q., Tan, L., Wang, Y., Wegenhart, B. L., Chen, L., Lamport, D. T., Chen, Y. & Kieliszewski, M. J. (2008). Self-assembly of the plant cell wall requires an extensin scaffold. *Proceedings of the National Academy of Sciences, United States of America,* 105, 2226-2231.

Cantarel, B. L., Coutinho, P. M., Rancurel, C., Bernard, T., Lombard, V. & Henrissat, B. (2009). The Carbohydrate-Active EnZymes database (CAZy): an expert resource for glycogenomics. *Nucleic Acids Research,* 37, 233-238.

Cantu, D., Vicente, A. R., Labavitch, J. M., Bennett, A. B. & Powell, A. L. (2008). Strangers in the matrix: plant cell walls and pathogen susceptibility. *Trends in Plant Science,* 13, 610-617.

Cao, K.-Q. & Forrer, H. (2001). Current status and prosperity on biological control of potato late blight (*Phytophthora infestans*). *Journal of Agricultural University of Hebei*, 1-10.

Carbon, S., Ireland, A., Mungall, C. J., Shu, S., Marshall, B., Lewis, S. & Group, W. P. W. (2009). AmiGO: online access to ontology and annotation data. *Bioinformatics,* 25, 288-289.

Carlile, M. J. (1983). Motility, taxis, and tropism in *Phytophthora.* In: *Phytophthora*, It's Biology Taxonomy, Ecology and Pathology. *American Phytopathological Society*, 95-107.

Carpita, N. C. & Gibeaut, D. M. (1993). Structural models of primary cell walls in flowering plants: consistency of molecular structure with the physical properties of the walls during growth. *Plant Journal,* 3, 1-30.

Cartwright, D. K. & Spurr, H. (1998). Biological control of *Phytophthora parasitica* var. *nicotianae* on tobacco seedlings with non-pathogenic binucleate *Rhizoctonia* fungi. *Soil Biology and Biochemistry,* 30, 1879-1884.

Catal, M., Erler, F., Fulbright, D. W. & Adams, G. C. (2013). Real-time quantitative PCR assays for evaluation of soybean varieties for resistance to the stem and root rot pathogen *Phytophthora sojae*. *European Journal of Plant Pathology,* 137, 859-869.

Catanzariti, A.-M., Mago, R., Ellis, J. & Dodds, P. (2011). Constructing haustorium-specific cDNA libraries from rust fungi. *In:* Mcdowell, J. M. (ed.) *Plant immunity: methods and protocols.* NY, USA: Humana Press. 79-87.

Chand, S. K., Nanda, S., Rout, E., Mohanty, J. N., Mishra, R. & Joshi, R. K. (2016). De novo sequencing and characterization of defense transcriptome

responsive to *Pythium aphanidermatum* infection in *Curcuma longa* L. *Physiological and Molecular Plant Pathology,* 94, 27-37.

Chang, Y. H., Yan, H. Z. & Liou, R. F. (2015). A novel elicitor protein from *Phytophthora parasitica* induces plant basal immunity and systemic acquired resistance. *Molecular Plant Pathology,* 16, 123-136.

Chatterjee, D., Kudlinzki, D., Linhard, V., Saxena, K., Schieborr, U., Gande, S. L., Wurm, J. P., Wöhnert, J., Abele, R. & Rogov, V. V. (2015). Structure and biophysical characterization of the S-adenosylmethionine-dependent O-methyltransferase PaMTH1, a putative enzyme accumulating during senescence of P*odospora anserina*. *Journal of Biological Chemistry,* 290, 16415-16430.

Chee, K.-H. & Newhook, F. J. (1965). Improved methods for use in studies on *Phytophtohora cinnamomi* Rands and other *Phytophthora* species. *New Zealand Journal of Agricultural Research,* 8, 88-95.

Chen, L.-Y., Shi, D.-Q., Zhang, W.-J., Tang, Z.-S., Liu, J. & Yang, W.-C. (2015). The Arabidopsis alkaline ceramidase TOD1 is a key turgor pressure regulator in plant cells. *Nature Communications,* 6, 6030.

Chen, L., Shen, D., Sun, N., Xu, J., Wang, W. & Dou, D. (2014). *Phytophthora sojae* TatD nuclease positively regulates sporulation and negatively regulates pathogenesis. *Molecular Plant-Microbe Interactions,* 27, 1070-1080.

Chen, X.-R., Xing, Y.-P., Li, Y.-P., Tong, Y.-H. & Xu, J.-Y. (2013a). RNA-Seq reveals infection-related gene expression changes in *Phytophthora capsici*. *PLoS ONE,* 8, e74588.

Chen, X., Klemsdal, S. S. & Brurberg, M. B. (2011). Identification and analysis of *Phytophthora cactorum* genes up-regulated during cyst germination and strawberry infection. *Current Genetics,* 57, 297.

Chen, Y., Conner, R., Gillard, C., Mclaren, D., Boland, G., Balasubramanian, P., Stasolla, C., Zhou, Q., Hwang, S. & Chang, K. (2012). A quantitative real-time PCR assay for detection of *Colletotrichum lindemuthianum* in navy bean seeds. *Plant Pathology,* 62, 900-907.

Chen, Y., Dunbabin, V., Diggle, A., Siddique, K. & Rengel, Z. (2013b). Phosphorus starvation boosts carboxylate secretion in P-deficient genotypes of *Lupinus angustifolius* with contrasting root structure. *Crop and Pasture Science,* 64, 588-599.

Childers, R., Danies, G., Myers, K., Fei, Z., Small, I. M. & Fry, W. E. (2015). Acquired resistance to mefenoxam in sensitive isolates of *Phytophthora infestans*. *Phytopathology,* 105, 342-349.

Cho, K., Kim, Y., Wi, S. J., Seo, J. B., Kwon, J., Chung, J. H., Park, K. Y. & Nam, M. H. (2013). Metabolic survey of defense responses to a compatible hemibiotroph, *Phytophthora parasitica* var. *nicotianae*, in ethylene signaling-impaired tobacco. *Journal of Agricultural and Food Chemistry,* 61, 8477-8489.

Chung, P. L. & Trevithick, J. R. (1970). Biochemical and histochemical localization of invertase in *Neurospora crassa* during conidial germination and hyphal growth. *Journal of Bacteriology,* 102, 423-429.

Clavaud, C., Aimanianda, V. & Latge, J. (2009). Organization of fungal, oomycete and lichen (1, 3)-β-glucans. *In:* Bacic, A., Fincher, G. B. & Stone, B. A. (eds.) *Chemistry, biochemistry, and biology of 1-3 beta glucans and related polysaccharides.* Amsterdam: Academic Press. 387-424.

Cline, E. T., Farr, D. F. & Rossman, A. Y. (2008). A synopsis of *Phytophthora* with accurate scientific names, host range, and geographic distribution. *Plant Health Progress*, doi: 10.1094/PHP-2008-0318-01.

Coffey, M. & Bower, L. (1984). *In vitro* variability among isolates of eight *Phytophthora* species in response to phosphorous acid. *Phytopathology,* 74, 738-742.

Coffey, M. & Joseph, M. (1985). Effects of phosphorous acid and fosetyl-Al on the life cycle of *Phytophthora cinnamomi* and *Phytophthora citricola*. *Phytopathology,* 75, 1042-1046.

Coffey, M. D. (1987). Phytophthora root rot of avocado. *Plant Disease,* 71, 1046-1052.

Colas, V., Lacourt, I., Ricci, P., Vanlerberghe-Masutti, F., Poupet, A. & Panabières, F. (1998). Diversity of virulence in *Phytophthora parasitica* on tobacco, as reflected by nuclear RFLPs. *Phytopathology,* 88, 205-212.

Conesa, A., Götz, S., García-Gómez, J. M., Terol, J., Talón, M. & Robles, M. (2005). Blast2GO: a universal tool for annotation, visualization and analysis in functional genomics research. *Bioinformatics,* 21, 3674-3676.

Cook, B., Clay, R., Bergmann, C., Albersheim, P. & Darvill, A. (1999). Fungal polygalacturonases exhibit different substrate degradation patterns and differ in their susceptibilities to polygalacturonase-inhibiting proteins. *Molecular plant-microbe interactions,* 12, 703-711.

Cook, R. J. & Baker, K. F. (1983). *The nature and practice of biological control of plant pathogens*, American Phytopathological Society.

Cooke, D. E. & Andersson, B. (2013). *Phytophthora infestans* and potato late blight in Europe. *In:* Lamour, K. (ed.) *Phytophthora: a global perspective.* London, UK: CAB International. 59-67.

Cooper, R. M. (1983). The mechanisms and significance of enzymatic degradation of host cell walls by parasites. *In:* Callow, J. A. (ed.) *Biochemical Plant Pathology.* New York.: John Wiley & Sons Ltd. 101-135.

Cooper, R. M. & Wood, R. (1975). Regulation of synthesis of cell wall degrading enzymes by *Verticillium albo-atrum* and *Fusarium oxysporum* f. sp. *lycopersici*. *Physiological Plant Pathology,* 5, 135-156.

Copes, W., Yang, X. & Hong, C. (2015). *Phytophthora* species recovered from irrigation reservoirs in Mississippi and Alabama nurseries and pathogenicity of three new species. *Plant Disease,* 99, 1390-1395.

Cordier, C., Pozo, M. J., Barea, J.-M., Gianinazzi, S. & Gianinazzi-Pearson, V. (1998). Cell defense responses associated with localized and systemic resistance to *Phytophthora parasitica* induced in tomato by an arbuscular mycorrhizal fungus. *Molecular Plant-Microbe Interactions,* 11, 1017-1028.

Corpas, F. J., Begara-Morales, J. C., Sánchez-Calvo, B., Chaki, M. & Barroso, J. B. (2015). Nitration and S-nitrosylation: two post-translational modifications (PTMs) mediated by reactive nitrogen species (RNS) and their role in signalling processes of plant cells. *In: Reactive oxygen and nitrogen species signaling and communication in plants.* Springer International Publishing. 267-281.

Cosgrove, D. J. (2005). Growth of the plant cell wall. *Nature Reviews Molecular Cell Biology,* 6, 850-861.

Costa, J. L. S., Menge, J. A. & Casale, W. L. (2000). Biological control of *Phytophthora* root rot of avocado with microorganisms grown in organic mulches. *Brazilian Journal of Microbiology,* 31, 239-246.

Cowley, R. B., Ash, G. J., Harper, J. D., Orchard, B. A. & Luckett, D. J. Using detached leaves and pods to screen resistance to Phomopsis (*Diaporthe toxica*) in *Lupinus albus*. *In:* Berger, J. a. P. a. J. B., ed. 12th International Lupin Conference, 14-18 September 2008 2008 Fremantle, Western Australia. International Lupin Association, Canterbury, New Zealand. 308-311.

Cowling, W., Buirchell, B., Frencel, I., Koch, S., Martins, J. N., Römer, P., Sweetingham, M., Talhinhas, P., Santen, E. V. & Baer, E. V. International evaluation of resistance to anthracnose in lupin. In: Proceedings of the 9th International Lupin Conference Lupin, an ancient crop for the new millennium, 1999 Klink/Muritz, Germany, 20-24 June, 1999. International Lupin Association, 16-22.

Cowling, W., Hamblin, J., Wood, P. M. & Gladstones, J. (1987). Resistance to Phomopsis stem blight in *Lupinus angustifolius* L. *Crop Science,* 27, 648-652.

Cowling, W., Sweetingham, M., Diepeveen, D. & Cullis, B. (1997). Heritability of resistance to brown spot and root rot of narrow-leafed lupins caused by *Pleiochaeta setosa* (Kirchn.) Hughes in field experiments. *Plant Breeding,* 116, 341-345.

Crane, C. & Shearer, B. (2014). Comparison of phosphite application methods for control of *Phytophthora cinnamomi* in threatened communities. *Australasian Plant Pathology,* 43, 143-149.

Crone, M., Mccomb, J. A., O'brien, P. A. & Hardy, G. E. S. J. (2013). Survival of *Phytophthora cinnamomi* as oospores, stromata, and thick-walled chlamydospores in roots of symptomatic and asymptomatic annual and herbaceous perennial plant species. *Fungal Biology,* 117, 112-123.

Cvitanich, C. & Judelson, H. S. (2003). A gene expressed during sexual and asexual sporulation in *Phytophthora infestans* is a member of the Puf family of translational regulators. *Eukaryotic Cell,* 2, 465-473.

D'souza-Schorey, C. & Chavrier, P. (2006). ARF proteins: roles in membrane traffic and beyond. *Nature Reviews Molecular Cell Biology,* 7, 347-358.

Daayf, F., Adam, L. & Fernando, W. (2003). Comparative screening of bacteria for biological control of potato late blight (strain US-8), using *in vitro*, detached-leaves, and whole-plant testing systems. *Canadian Journal of Plant Pathology,* 25, 276-284.

Dai, Y., Liu, T., Zhang, L., Li, Z., Guo, W., Cao, S., Pan, Y., Chen, F. & Gao, Z. (2015). First report of Phytophthora root and stem rot caused by *Phytophthora sojae* on soybean in Taihe of China. *Plant Disease,* 99, 1861.

Dalio, R. J., Fleischmann, F., Humez, M. & Osswald, W. (2014). Phosphite protects *Fagus sylvatica* seedlings towards *Phytophthora plurivora* via local toxicity, priming and facilitation of pathogen recognition. *PLoS ONE,* 9, e87860.

Damasceno, C. M., Bishop, J. G., Ripoll, D. R., Win, J., Kamoun, S. & Rose, J. K. (2008). Structure of the glucanase inhibitor protein (GIP) family from *Phytophthora* species suggests coevolution with plant endo-β-1, 3-glucanases. *Molecular Plant-Microbe Interactions,* 21, 820-830.

Dandurand, L. & Menge, J. (1994). Influence of *Fusarium solani* on chemotaxis of zoospores of *Phytophthora parasitica* and *Phytophthora citrophthora* and

on distribution of ^{14}C in citrus tissues and root exudate. *Soil Biology and Biochemistry,* 26, 75-79.

Darakis, G., Bourbos, V. & Skoudridakis, M. (1997). Phosphonate transport in *Phytophthora capsici*. *Plant Pathology,* 46, 762-772.

Dart, N. L. & Chastagner, G. A. (2007). Estimated economic losses associated with the destruction of plants due to *Phytophthora ramorum* quarantine efforts in Washington State. *Plant Health Progress*, doi:10.1094/PHP-2007-0508-02-RS.

Davidson, J., Werres, S., Garbelotto, M., Hansen, E. & Rizzo, D. (2003). Sudden oak death and associated diseases caused by *Phytophthora ramorum Plant Health Progress*, doi:10.1094/PHP-2003-0707-01-DG.

De Vries, R. P. & Visser, J. (2001). *Aspergillus* enzymes involved in degradation of plant cell wall polysaccharides. *Microbiology and Molecular Biology Reviews,* 65, 497-522.

Dearnaley, J. D. W., Maleszka, J. & Hardham, A. R. (1996). Synthesis of zoospore peripheral vesicles during sporulation of *Phytophthora cinnamomi*. *Mycological Research,* 100, 39-48.

Deising, H., Frittrang, A. K., Kunz, S. & Mendgen, K. (1995). Regulation of pectin methylesterase and polygalacturonate lyase activity during differentiation of infection structures in *Uromyces viciae-fabae*. *Microbiology,* 141, 561-571.

Demmel, A., Hupfer, C., Busch, U. & Engel, K.-H. (2012). Quantification of lupine (*Lupinus angustifolius*) in wheat flour using real-time PCR and an internal standard material. *European Food Research and Technology,* 235, 61-66.

Dickson, K. A., Haigis, M. C. & Raines, R. T. (2005). Ribonuclease inhibitor: structure and function. *Progress in Nucleic Acid Research and Molecular Biology,* 80, 349-374.

Dodds, P. N., Rafiqi, M., Gan, P. H. P., Hardham, A. R., Jones, D. A. & Ellis, J. G. (2009). Effectors of biotrophic fungi and oomycetes: pathogenicity factors and triggers of host resistance. *New Phytologist,* 183, 993-1000.

Dolan, T., Cohen, Y. & Coffey, M. (1986). Protection of *Persea* species against *Phytophthora cinnamomi* and *P. citricola* by prior inoculation with a citrus isolate of *P. parasitica*. *Phytopathology,* 76, 194-198.

Dong, S., Qutob, D., Tedman-Jones, J., Kuflu, K., Wang, Y., Tyler, B. M. & Gijzen, M. (2009). The *Phytophthora sojae* avirulence locus Avr3c encodes a multi-copy RXLR effector with sequence polymorphisms among pathogen strains. *PLoS ONE,* 4, e5556.

Donofrio, N. M. & Delaney, T. P. (2001). Abnormal callose response phenotype and hypersusceptibility to *Peronospora parasitica* in defense-compromised Arabidopsis nim1-1 and salicylate hydroxylase-expressing plants. *Molecular Plant-Microbe Interactions,* 14, 439-450.

Dorrance, A. E. (2013). *Phytophthora sojae* in soybean. *In:* Lamour, K. (ed.) *Phytophthora: a global perspective.* London, UK: CAB International. 79-86.

Dos Santos, Á. F., Tessmann, D. J., Alves, T. C. A., Vida, J. B. & Harakava, R. (2011). Root and crown rot of Brazilian pine (*Araucaria angustifolia*) caused by *Phytophthora cinnamomi*. *Journal of Phytopathology,* 159, 194-196.

Dos Santos Castro, L., Pedersoli, W. R., Antoniêto, A. C. C., Steindorff, A. S., Silva-Rocha, R., Martinez-Rossi, N. M., Rossi, A., Brown, N. A., Goldman,

G. H. & Faça, V. M. (2014). Comparative metabolism of cellulose, sophorose and glucose in *Trichoderma reesei* using high-throughput genomic and proteomic analyses. *Biotechnology for Biofuels,* 7, 1.

Douaiher, M. N., Nowak, E., Durand, R., Halama, P. & Reignault, P. (2007). Correlative analysis of *Mycosphaerella graminicola* pathogenicity and cell wall-degrading enzymes produced in vitro: the importance of xylanase and polygalacturonase. *Plant Pathology,* 56, 79-86.

Douhan, G., Fuller, E., Mckee, B. & Pond, E. (2004). Genetic diversity analysis of avocado (*Persea americana* Miller) rootstocks selected under greenhouse conditions for tolerance to *Phytophthora* root rot caused by *Phytophthora cinnamomi*. *Euphytica,* 182, 209-217.

Dowler, S., Currie, R. A., Campbell, D. G., Maria, D., Kular, G., Downes, C. P. & Alessi, D. R. (2000). Identification of pleckstrin-homology-domain-containing proteins with novel phosphoinositide-binding specificities. *Biochemical Journal,* 351, 19-31.

Drenth, A. & Guest, D. I. (2004). *Phytophthora* in the tropics. *In:* Drenth, A. & Guest, D. I. (eds.) *Diversity and Management of Phytophthora in Southeast Asia.* Canberra, Australia: Australian Centre for International Agricultural Research. 30-41.

Drincovich, M. a. F., Casati, P. & Andreo, C. S. (2001). NADP-malic enzyme from plants: a ubiquitous enzyme involved in different metabolic pathways. *FEBS Letters,* 490, 1-6.

Dudler, R. (1990). The single-copy actin gene of *Phytophthora megasperma* encodes a protein considerably diverged from any other known actin. *Plant Molecular Biology,* 14, 415-422.

Dunstan, R., Smillie, R. & Grant, B. (1990). The effects of sub-toxic levels of phosphonate on the metabolism and potential virulence factors of *Phytophthora palmivora*. *Physiological and Molecular Plant Pathology,* 36, 205-220.

Dunstan, W. A., Howard, K., Hardy, G. E. S. & Burgess, T. I. (2016). An overview of Australia's *Phytophthora* species assemblage in natural ecosystems recovered from a survey in Victoria. *IMA Fungus,* 7, 47-58.

Dunstan, W. A., Rudman, T., Shearer, B. L., Moore, N. A., Paap, T., Calver, M. C., Dell, B. & Hardy, G. E. S. J. (2010). Containment and spot eradication of a highly destructive, invasive plant pathogen (*Phytophthora cinnamomi*) in natural ecosystems. *Biological Invasions,* 12, 913-925.

Edwards, R., Dixon, D. P. & Walbot, V. (2000). Plant glutathione S-transferases: enzymes with multiple functions in sickness and in health. *Trends in Plant Science,* 5, 193-198.

Elad, Y. (1996). Mechanisms involved in the biological control of *Botrytis cinerea* incited diseases. *European Journal of Plant Pathology,* 102, 719-732.

Ellinger, D., Naumann, M., Falter, C., Zwikowics, C., Jamrow, T., Manisseri, C., Somerville, S. C. & Voigt, C. A. (2013). Elevated early callose deposition results in complete penetration resistance to powdery mildew in Arabidopsis. *Plant Physiology,* 161, 1433-1444.

Ellinger, D. & Voigt, C. A. (2014). Callose biosynthesis in arabidopsis with a focus on pathogen response: what we have learned within the last decade. *Annals of Botany,* 114, 1-10.

Elliott, M., Shamoun, S., Sumampong, G., James, D., Masri, S. & Varga, A. (2009). Evaluation of several commercial biocontrol products on European and North American populations of *Phytophthora ramorum*. *Biocontrol Science and Technology,* 19, 1007-1021.

Engelbrecht, J., Duong, T. A. & Van Den Berg, N. (2013). Development of a nested quantitative real time PCR for detecting *Phytophthora cinnamomi* in *Persea americana* rootstocks. *Plant Disease,* 97, 1012-1017.

Enkerli, K., Mims, C. & Hahn, M. (1997a). Immunogold localization of callose and other plant cell wall components in soybean roots infected with the oomycete *Phytophthora sojae*. *Canadian Journal of Botany,* 75, 1509-1517.

Enkerli, K., Mims, C. & Hahn, M. (1997b). Ultrastructure of compatible and incompatible interactions of soybean roots infected with the plant pathogenic oomycete *Phytophthora sojae*. *Canadian Journal of Botany,* 75, 1493-1508.

Erwin, D. C. & Ribeiro, O. K. (1996). *Phytophthora diseases worldwide,* St. Paul, Minnesota, USA, American Phytopathological Society (APS Press).

Eschen-Lippold, L., Landgraf, R., Smolka, U., Schulze, S., Heilmann, M., Heilmann, I., Hause, G. & Rosahl, S. (2012). Activation of defense against *Phytophthora infestans* in potato by down-regulation of syntaxin gene expression. *New Phytologist,* 193, 985-996.

Eshraghi, L., Anderson, J., Aryamanesh, N., Shearer, B., Mccomb, J., Hardy, G. E. S. & O'brien, P. A. (2011a). Phosphite primed defence responses and enhanced expression of defence genes in *Arabidopsis thaliana* infected with *Phytophthora cinnamomi*. *Plant Pathology,* 60, 1086-1095.

Eshraghi, L., Aryamanesh, N., Anderson, J. P., Shearer, B., Mccomb, J. A., Hardy, G. E. S. J. & O'brien, P. A. (2011b). A quantitative PCR assay for accurate in planta quantification of the necrotrophic pathogen *Phytophthora cinnamomi*. *European Journal of Plant Pathology,* 131, 419-430.

Esquerré-Tugayé, M.-T., Boudart, G. & Dumas, B. (2000). Cell wall degrading enzymes, inhibitory proteins, and oligosaccharides participate in the molecular dialogue between plants and pathogens. *Plant Physiology and Biochemistry,* 38, 157-163.

Etalo, D. W., Stulemeijer, I. J., Van Esse, H. P., De Vos, R. C., Bouwmeester, H. J. & Joosten, M. H. (2013). System-wide hypersensitive response-associated transcriptome and metabolome reprogramming in tomato. *Plant Physiology,* 162, 1599-1617.

Evangelisti, E., Govetto, B., Minet-Kebdani, N., Kuhn, M. L., Attard, A., Ponchet, M., Panabières, F. & Gourgues, M. (2013). The *Phytophthora parasitica* RXLR effector penetration-specific effector 1 favours *Arabidopsis thaliana* infection by interfering with auxin physiology. *New Phytologist,* 199, 476-489.

Evers, D., Ghislain, M., Hoffmann, L., Hausman, J.-F. & Dommes, J. (2006). A late blight resistant potato plant overexpresses a gene coding for α-galactosidase upon infection by *Phytophthora infestans*. *Biologia Plantarum,* 50, 265-271.

Eye, L. L., Sneh, B. & Lockwood, J. (1978). Inoculation of soybean seedlings with zoospores of *Phytophthora megasperma* var. *sojae* for pathogenicity and race determination. *Phytopathology,* 68, 1769-1773.

Fabre, I., Bruneteau, M., Ricci, P. & Michel, G. (1984). Isolation and structural studies of glucans from *Phytophthora parasitica*. *European Journal of Biochemistry,* 142, 99-103.

Fang, J. & Tsao, P. (1995a). Efficacy of *Penicillium funiculosum* as a biological control agent against Phytophthora root rots of azalea and citrus. *Phytopathology,* 85, 871-878.

Fang, J. & Tsao, P. (1995b). Evaluation of *Pythium nunn* as a potential biocontrol agent against Phytophthora root rots of azalea and sweet orange. *Phytopathology,* 85, 29-36.

Farih, A., Tsao, P. H. & Menge, J. A. (1981). Fungitoxic activity of efosite aluminum on growth, sporulation, and germination of *Phytophthora parasitica* and *P. citrophthora*. *Phytopathology,* 71, 934-936.

Fenn, M. & Coffey, M. (1984). Studies on the *in vitro* and *in vivo* antifungal activity of fosetyl-Al and phosphorous acid. *Phytopathology,* 74, 606-611.

Fenn, M. & Coffey, M. (1985). Further evidence for the direct mode of action of fosetyl-Al and phosphorous acid. *Phytopathology* 75, 1064-1068.

Filonow, A. & Lockwood, J. (1985). Evaluation of several actinomycetes and the fungus *Hyphochytrium catenoides* as biocontrol agents for Phytophthora root rot of soybean. *Plant Disease,* 69, 1033-1036.

Forbes, G., Morales, J., Restrepo, S., Perez, W., Gamboa, S., Ruiz, R., Cedeño, L., Fermin, G., Andreu, A., Acuña, I. & Oliva, R. (2013). *Phytophthora infestans* and *Phytophthora andina* on solanaceous hosts in South America. *In:* Lamour, K. (ed.) *Phytophthora: a global perspective.* London, UK: CAB International. 48-58.

Frankel, S. J. (2008). Sudden oak death and *Phytophthora ramorum* in the USA: a management challenge. *Australasian Plant Pathology,* 37, 19-25.

French, B., Shea, G. And Buirchell, B (2008). Introduction and history. *In:* White, P., French, B. & Mclarty, A. (eds.) *Producing lupins.* 2nd ed. South Perth, WA: Department of Agriculture and Food. 168.

Fry, S. C. (1989). Cellulases, hemicelluloses and auxin-stimulated growth: a possible relationship. *Physiologia Plantarum,* 75, 532-536.

Fry, W. (2008). *Phytophthora infestans*: the plant (and R gene) destroyer. *Molecular Plant Pathology,* 9, 385-402.

Fu, Y., Yin, H., Wang, W., Wang, M., Zhang, H., Zhao, X. & Du, Y. (2011). β-1, 3-Glucan with different degree of polymerization induced different defense responses in tobacco. *Carbohydrate Polymers,* 86, 774-782.

Fujii, T., Shimizu, M., Doi, Y., Fujita, T., Ito, T., Miura, D., Wariishi, H. & Takaya, N. (2011). Novel fungal phenylpyruvate reductase belongs to d-isomer-specific 2-hydroxyacid dehydrogenase family. *Biochimica et Biophysica Acta (BBA)-Proteins and Proteomics,* 1814, 1669-1676.

Fung, R. W., Gonzalo, M., Fekete, C., Kovacs, L. G., He, Y., Marsh, E., Mcintyre, L. M., Schachtman, D. P. & Qiu, W. (2008). Powdery mildew induces defense-oriented reprogramming of the transcriptome in a susceptible but not in a resistant grapevine. *Plant Physiology,* 146, 236-249.

Furuichi, N. & Suzuki, J. (1990). Purification and properties of suppressor glucan isolated from *Phytophthora infestans*. *Annals of the Phytopathological Society of Japan,* 56, 457-467.

Furuichi, N., Yokokawa, K., Okamura, H. & Ohta, M. (2014). PiPE, a Phytophthora-associated PAMPS from *P. infestans*, binds to a Ca2+-

dependent protein kinase (CDPK) in potato for the induction of hypersensitive reaction. *Journal of Clinical & Experimental Pathology,* 4, 2161-0681.

Gabor, B., O'gara, E., Philip, B., Horan, D. & Hardham, A. (1993). Specificities of monoclonal antibodies to *Phytophthora cinnamomi* in two rapid diagnostic assays. *Plant Disease,* 77, 1189-1197.

Gachon, C., Mingam, A. & Charrier, B. (2004). Real-time PCR: what relevance to plant studies? *Journal of Experimental Botany,* 55, 1445-1454.

Gagnon, M.-C., Bergeron, M.-J., Hamelin, R. C., Grünwald, N. J. & Bilodeau, G. J. (2014). Real-time PCR assay to distinguish *Phytophthora ramorum* lineages using the cellulose binding elicitor lectin (CBEL) locus. *Canadian Journal of Plant Pathology,* 36, 367-376.

Galan, A. M. G., Brohée, M., Scaravelli, E., Van Hengel, A. J. & Chassaigne, H. (2010). Development of real-time PCR assays for the detection of lupin residues in food products. *European Food Research and Technology,* 230, 597-608.

Galiana, E., Fourré, S. & Engler, G. (2008). *Phytophthora parasitica* biofilm formation: installation and organization of microcolonies on the surface of a host plant. *Environmental Microbiology,* 10, 2164-2171.

Gallup, C., Sullivan, M. & Shew, H. (2006). Black shank of tobacco. *Plant Health Instructor*, doi: 10.1094/PHI-I-2006-0717-01.

Gangneux, C., Cannesan, M.-A., Bressan, M., Castel, L., Moussart, A., Vicré-Gibouin, M., Driouich, A., Trinsoutrot-Gattin, I. & Laval, K. (2014). A sensitive assay for rapid detection and quantification of *Aphanomyces euteiches* in soil. *Phytopathology,* 104, 1138-1147.

Gao, L., Tu, Z. J., Millett, B. P. & Bradeen, J. M. (2013). Insights into organ-specific pathogen defense responses in plants: RNA-seq analysis of potato tuber-*Phytophthora infestans* interactions. *BMC Genomics,* 14, 340.

Garbe, J. & Collin, M. (2012). Bacterial hydrolysis of host glycoproteins-powerful protein modification and efficient nutrient acquisition. *Journal of Innate Immunity,* 4, 121-131.

Garbelotto, M., Harnik, T. Y. & Schmidt, D. J. (2009). Efficacy of phosphonic acid, metalaxyl-M and copper hydroxide against *Phytophthora ramorum in vitro* and *in planta*. *Plant Pathology,* 58, 111-119.

Garibaldi, A., Bertetti, D., Pensa, P., Ortu, G. & Gullino, M. (2015). *Phytophthora cryptoea* on common sage (*Salvia officinalis* L.) in Italy. *Plant Disease,* 99, 161-161.

Gascuel, Q., Buendia, L., Pecrix, Y., Blanchet, N., Muños, S., Vear, F. & Godiard, L. (2016). RXLR and CRN effectors from the sunflower downy mildew pathogen *Plasmopara halstedii* induce hypersensitive-like responses in resistant sunflower lines. *Frontiers in Plant Science,* 7, doi: 10.3389/fpls.2016.01887.

Gaulin, E., Jauneau, A., Villalba, F., Rickauer, M., Esquerré-Tugayé, M.-T. & Bottin, A. (2002). The CBEL glycoprotein of *Phytophthora parasitica* var. *nicotianae* is involved in cell wall deposition and adhesion to cellulosic substrates. *Journal of Cell Science,* 115, 4565-4575.

Gautam, Y., Cahill, D. & Hardham, A. (1999). Development of a quantitative immunodipstick assay for *Phytophthora nicotianae*. *Food and Agricultural Immunology,* 11, 229-242.

Gavery, M. R. & Roberts, S. B. (2012). Characterizing short read sequencing for gene discovery and RNA-Seq analysis in *Crassostrea gigas*. *Comparative Biochemistry and Physiology Part D: Genomics and Proteomics,* 7, 94-99.

Gees, R. & Coffey, M. (1989). Evaluation of a strain of *Myrothecium roridum* as a potential biocontrol agent against *Phytophthora cinnamomi*. *Phytopathology,* 79, 1079-1084.

Gentile, S., Valentino, D. & Tamietti, G. (2009). Control of ink disease by trunk injection of potassium phosphite. *Journal of Plant Pathology,* 91, 565-571.

Giannakis, C., Bucheli, C., Skene, K., Robinson, S. & Scott, N. S. (1998). Chitinase and β-1, 3-glucanase in grapevine leaves: a possible defence against powdery mildew infection. *Australian Journal of Grape and Wine Research,* 4, 14-22.

Gill, S. S. & Tuteja, N. (2010). Reactive oxygen species and antioxidant machinery in abiotic stress tolerance in crop plants. *Plant Physiology and Biochemistry,* 48, 909-930.

Gille, S. & Pauly, M. (2012). O-acetylation of plant cell wall polysaccharides. *Frontiers in Plant Science,* 3, 12.

Gladstones, J. (1989). *Lupinus angustifolius* L. (narrow-leafed lupin) cv. Gungurru. *Animal Production Science,* 29, 913-914.

Gladstones, J. An historical review of lupins in Australia *In:* Dracup, M. & Palta, J., eds. Proceedings of the 1st Australian Lupin Technical Symposium, 17–21 October 1994 1994 South Perth, WA Department of Agriculture, 1-38.

Godfrey, S. a. C., Silby, M. W., Falloon, P. G. & Mahanty, H. K. (2000). Biological control of *Phytophthora megasperma* var. *sojae*, causal agent of Phytophthora rot of asparagus, by *Pseudomonas aureofaciens* PA147–2: A preliminary field trial. *New Zealand Journal of Crop and Horticultural Science,* 28, 97-103.

Gómez-Gómez, L., Felix, G. & Boller, T. (1999). A single locus determines sensitivity to bacterial flagellin in *Arabidopsis thaliana*. *Plant Journal,* 18, 277-284.

Gooday, G. & Hunsley, D. (1971). Cellulose wall ingrowths in *Phytophthora parasitica*. *Transactions of the British Mycological Society,* 57, 178-179.

Goodwin, P., English, J., Neher, D., Duniway, J. & Kirkpatrick, B. (1990). Detection of *Phytophthora parasitica* from soil and host tissue with a species-specific DNA probe. *Phytopathology,* 80, 277-281.

Gordon, S., Berry, S., St. Martin, S. & Dorrance, A. (2007a). Genetic analysis of soybean plant introductions with resistance to *Phytophthora sojae*. *Phytopathology,* 97, 106-112.

Gordon, S., Kowitwanich, K., Pipatpongpinyo, W., St. Martin, S. & Dorrance, A. (2007b). Molecular marker analysis of soybean plant introductions with resistance to *Phytophthora sojae*. *Phytopathology,* 97, 113-118.

Görnhardt, B., Rouhara, I. & Schmelzer, E. (2000). Cyst germination proteins of the potato pathogen *Phytophthora infestans* share homology with human mucins. *Molecular Plant-Microbe Interactions,* 13, 32-42.

Goss, E. M., Larsen, M., Vercauteren, A., Werres, S., Heungens, K. & Grünwald, N. J. (2011). *Phytophthora ramorum* in Canada: evidence for migration within North America and from Europe. *Phytopathology,* 101, 166-171.

Götesson, A., Marshall, J. S., Jones, D. A. & Hardham, A. R. (2002). Characterization and evolutionary analysis of a large polygalacturonase

gene family in the oomycete plant pathogen *Phytophthora cinnamomi*. *Molecular Plant-Microbe Interactions,* 15, 907-921.

Govers, F. & Gijzen, M. (2006). *Phytophthora* genomics: the plant destroyers' genome decoded. *Molecular Plant-Microbe Interactions,* 19, 1295-1301.

Gracey, A. Y., Troll, J. V. & Somero, G. N. (2001). Hypoxia-induced gene expression profiling in the euryoxic fish *Gillichthys mirabilis*. *Proceedings of the National Academy of Sciences, United States of America,* 98, 1993-1998.

Graham, J. (1995). Root regeneration and tolerance of citrus rootstocks to root rot caused by *Phytophthora nicotianae*. *Phytopathology,* 85, 111-117.

Granke, L. & Hausbeck, M. (2010). Effects of temperature, concentration, age, and algaecides on *Phytophthora capsici* zoospore infectivity. *Plant Disease,* 94, 54-60.

Greenhalgh, F. (1978). Evaluation of techniques for quantitative detection of *Phytophthora cinnamomi*. *Soil Biology and Biochemistry,* 10, 257-259.

Grenville-Briggs, L. J., Anderson, V. L., Fugelstad, J., Avrova, A. O., Bouzenzana, J., Williams, A., Wawra, S., Whisson, S. C., Birch, P. R. & Bulone, V. (2008). Cellulose synthesis in *Phytophthora infestans* is required for normal appressorium formation and successful infection of potato. *Plant Cell* 20, 720-738.

Grenville-Briggs, L. J., Van West, P (2005). *The biotrophic stages of oomycete-plant interactions*, Elsevier Academic Press, USA.

Griffith, J. M., Coffey, M. D. & Grant, B. R. (1993). Phosphonate inhibition as a function of phosphate concentration in isolates of *Phytophthora palmivora*. *Microbiology,* 139, 2109-2116.

Grose, M. & Hainsworth, J. (1992). Soil water extraction, measured by computer-assisted tomography, in seedling *Lupinus angustifolius* cv. Yandee when healthy and infected with *Phytophthora cinnamomi*. *Journal of Experimental Botany,* 43, 121-127.

Grote, D., Olmos, A., Kofoet, A., Tuset, J., Bertolini, E. & Cambra, M. (2002). Specific and sensitive detection of *Phytophthora nicotianae* by simple and nested-PCR. *European Journal of Plant Pathology,* 108, 197-207.

Grünwald, N. J., Garbelotto, M., Goss, E. M., Heungens, K. & Prospero, S. (2012). Emergence of the sudden oak death pathogen *Phytophthora ramorum*. *Trends in Microbiology,* 20, 131-138.

Grünwald, N. J., Goss, E. M. & Press, C. M. (2008). *Phytophthora ramorum*: a pathogen with a remarkably wide host range causing sudden oak death on oaks and ramorum blight on woody ornamentals. *Molecular Plant Pathology,* 9, 729-740.

Gubler, F. & Hardham, A. R. (1990). Protein storage in large peripheral vesicles in *Phytophthora* zoospores and its breakdown after cyst germination. *Experimental Mycology,* 14, 393-404.

Gubler, W., Rolshausen, P., Trouillas, F., Úrbez-Torres, J., Voegel, T., Leavitt, G. & Weber, E. (2005). Grapevine trunk diseases in California. *Practical Winery Vineyard Magazine,* January/February 2005, 6-25.

Guenthner, J., Michael, K. & Nolte, P. (2001). The economic impact of potato late blight on US growers. *Potato Research,* 44, 121-125.

Guest, D. (1984). Modification of defense responses in tobacco and capsicum following treatment with Fosetyl-Al [Aluminium tris (o-ethyl phosphonate)]. *Physiological Plant Pathology,* 25, 125-134.

Guest, D. & Bompeix, G. (1990). The complex mode of action of phosphonates. *Australasian Plant Pathology,* 19, 113-115.

Guest, D. & Grant, B. (1991). The complex action of phosphonates as antifungal agents. *Biological Reviews,* 66, 159-187.

Gutierrez, L., Mauriat, M., Guénin, S., Pelloux, J., Lefebvre, J. F., Louvet, R., Rusterucci, C., Moritz, T., Guerineau, F. & Bellini, C. (2008). The lack of a systematic validation of reference genes: a serious pitfall undervalued in reverse transcription-polymerase chain reaction (RT-PCR) analysis in plants. *Plant Biotechnology Journal,* 6, 609-618.

Haas, B. J., Kamoun, S., Zody, M. C., Jiang, R. H., Handsaker, R. E., Cano, L. M., Grabherr, M., Kodira, C. D., Raffaele, S., Torto-Alalibo, T., Bozkurt, T. O., Ah-Fong, A. M. V., Alvarado, L., Anderson, V. L., Armstrong, M. R., Avrova, A., Baxter, L., Beynon, J., Boevink, P. C., Bollmann, S. R., Bos, J. I. B., Bulone, V., Cai, G., Cakir, C., Carrington, J. C., Chawner, M., Conti, L., Costanzo, S., Ewan, R., Fahlgren, N., Fischbach, M. A., Fugelstad, J., Gilroy, E. M., Gnerre, S., Green, P. J., Grenville-Briggs, L. J., Griffith, J., Grünwald, N. J., Horn, K., Horner, N. R., Hu, C.-H., Huitema, E., Jeong, D.-H., Jones, A. M. E., Jones, J. D. G., Jones, R. W., Karlsson, E. K., Kunjeti, S. G., Lamour, K., Liu, Z., Ma, L., Maclean, D., Chibucos, M. C., Mcdonald, H., Mcwalters, J., Meijer, H. J. G., Morgan, W., Morris, P. F., Munro, C. A., O'neill, K., Ospina-Giraldo, M., Pinzón, A., Pritchard, L., Ramsahoye, B., Ren, Q., Restrepo, S., Roy, S., Sadanandom, A., Savidor, A., Schornack, S., Schwartz, D. C., Schumann, U. D., Schwessinger, B., Seyer, L., Sharpe, T., Silvar, C., Song, J., Studholme, D. J., Sykes, S., Thines, M., Phuntumart, P. J. I. V. D. V. V., Wawra, S., Weide, R., Win, J., Young, C., Zhou, S., Fry, W., Meyers, B. C., West, P. V., Ristaino, J., Govers, F., Birch, P. R. J., Whisson, S. C., Judelson, H. S. & Nusbaum, C. (2009). Genome sequence and analysis of the Irish potato famine pathogen *Phytophthora infestans*. *Nature,* 461, 393-398.

Hächler, H. & Hohl, H. (1984). Temporal and spatial distribution patterns of collar and papillae wall appositions in resistant and susceptible tuber tissue of *Solanum tuberosum* infected by *Phytophthora infestans*. *Physiological Plant Pathology,* 24, 107-118.

Haddadi, P., Ma, L., Wang, H. & Borhan, M. H. (2016). Genome-wide transcriptomic analyses provide insights into the lifestyle transition and effector repertoire of *Leptosphaeria maculans* during the colonization of *Brassica napus* seedlings. *Molecular Plant Pathology,* 17, 1196-1210.

Hafez, M., Burger, G., Steinberg, S. V. & Lang, F. (2013). A second eukaryotic group with mitochondrion-encoded tmRNA: *in silico* identification and experimental confirmation. *RNA Biology,* 10, 1117-1124.

Haldar, K., Kamoun, S., Hiller, N. L., Bhattacharje, S. & Van Ooij, C. (2006). Common infection strategies of pathogenic eukaryotes. *Nature Reviews Microbiology,* 4, 922-931.

Halim, V. A., Altmann, S., Ellinger, D., Eschen-Lippold, L., Miersch, O., Scheel, D. & Rosahl, S. (2009). PAMP-induced defense responses in potato require both salicylic acid and jasmonic acid. *Plant Journal,* 57, 230-242.

Hall, T. M. T. (2005). Multiple modes of RNA recognition by zinc finger proteins. *Current Opinion in Structural Biology,* 15, 367-373.

Halterman, D. & Gevens, A. J. (2013). *Phytophthora infestans* in the USA. *In:* Lamour, K. (ed.) *Phytophthora: A Global Perspective.* London, UK: CAB International. 68-78.

Hanchey, P. & Wheeler, H. (1971). Pathological changes in ultrastructure: tobacco roots infected with *Phytophthora parasitica* var. *nicotianae*. *Phytopathology,* 61, 33-39.

Handelsman, J., Nesmith, W. C. & Raffel, S. J. (1991). Microassay for biological and chemical control of infection of tobacco by *Phytophthora parasitica* var. *nicotianae*. *Current Microbiology,* 22, 317-319.

Hane, J. K., Ming, Y., Kamphuis, L. G., Nelson, M. N., Garg, G., Atkins, C. A., Bayer, P. E., Bravo, A., Bringans, S. & Cannon, S. (2016). A comprehensive draft genome sequence for lupin (*Lupinus angustifolius*), an emerging health food: insights into plant–microbe interactions and legume evolution. *Plant Biotechnology Journal,* 15, 318-330.

Hansen, E. M., Reeser, P. W. & Sutton, W. (2012). *Phytophthora* beyond agriculture. *Annual Review of Phytopathology,* 50, 359-378.

Hardham, A. (1989). Lectin and antibody labelling of surface components of spores of *Phytophthora cinnamomi*. *Functional Plant Biology,* 16, 19-32.

Hardham, A. R. (2001). The cell biology behind *Phytophthora* pathogenicity. *Australasian Plant Pathology,* 30, 91-98.

Hardham, A. R. (2005). *Phytophthora cinnamomi*. *Molecular Plant Pathology,* 6, 589-604.

Hardham, A. R. (2007). Cell biology of plant–oomycete interactions. *Cellular Microbiology,* 9, 31-39.

Hardham, A. R. & Blackman, L. M. (2010). Molecular cytology of *Phytophthora*-plant interactions. *Australasian Plant Pathology,* 39, 29-35.

Hardham, A. R. & Cahill, D. M. (2010). The role of oomycete effectors in plant–pathogen interactions. *Functional plant biology,* 37, 919-925.

Hardham, A. R. & Gubler, F. (1990). Polarity of attachment of zoospores of a root pathogen and pre-alignment of the emerging germ tube. *Cell Biology International Reports,* 14, 947-956.

Hardham, A. R., Jones, D. A. & Takemoto, D. (2007). Cytoskeleton and cell wall function in penetration resistance. *Current Opinion in Plant Biology,* 10, 342-348.

Hardham, A. R. & Mitchell, H. J. (1998). Use of molecular cytology to study the structure and biology of phytopathogenic and mycorrhizal fungi. *Fungal Genetics and Biology,* 24, 252-284.

Hardham, A. R. & Shan, W. (2009). Cellular and molecular biology of *Phytophthora*–plant interactions. *In:* Esser, K. (ed.) *Plant Relationships, 2nd Edition.* Verlag Berlin Heidelberg: Springer. 3-27.

Hardham, A. R., Suzaki, E. & Perkin, J. L. (1986). Monoclonal antibodies to isolate-, species-, and genus-specific components on the surface of zoospores and cysts of the fungus *Phytophthora cinnamomi*. *Canadian Journal of Botany,* 64, 311-321.

Hardy, G. E. S. J., Barrett, S. & Shearer, B. L. (2001a). The future of phosphite as a fungicide to control the soilborne plant pathogen *Phytophthora cinnamomi* in natural ecosystems. *Australasian Plant Pathology,* 30, 133-139.

Hardy, G. S. J., Colquhoun, I. J., Shearer, B. L. & Tommerup, I. (2001b). The impact and control of *Phytophthora cinnamomi* in native and rehabilitated forest ecosystems in Western Australia. *Forest Snow and Landscape Research,* 76, 337-343.

Hargreaves, A. & Duncan, J. (1978). Detection of *Phytophthora* species in field soils by simple baiting procedures. *Soil Biology and Biochemistry,* 10, 343-345.

Harlow, E. & Lane, D. (1988). *Antibodies: a laboratory manual*, Cold Spring Harbor Laboratory. 825.

Hart, T., Komori, H. K., Lamere, S., Podshivalova, K. & Salomon, D. R. (2013). Finding the active genes in deep RNA-Seq gene expression studies. *BMC Genomics,* 14, 778.

Hartmann, E. & Hartmann, R. K. (2003). The enigma of ribonuclease P evolution. *TRENDS in Genetics,* 19, 561-569.

Hayden, K. J., Garbelotto, M., Knaus, B. J., Cronn, R. C., Rai, H. & Wright, J. W. (2014). Dual RNA-seq of the plant pathogen *Phytophthora ramorum* and its tanoak host. *Tree Genetics & Genomes,* 10, 489-502.

Hee, W. Y., Torreña, P. S., Blackman, L. M. & Hardham, A. R. (2013). *Phytophthora cinnamomi* in Australia. *In:* Lamour, K. (ed.) *Phytophthora: A Global Perspective.* London, UK: CAB International. 124-134.

Hématy, K., Cherk, C. & Somerville, S. (2009). Host–pathogen warfare at the plant cell wall. *Current Opinion in Plant Biology,* 12, 406-413.

Henrissat, B. & Davies, G. J. (2000). Glycoside hydrolases and glycosyltransferases. Families, modules, and implications for genomics. *Plant Physiology,* 124, 1515-1519.

Hernández, I., Chacón, O., Rodriguez, R., Portieles, R., López, Y., Pujol, M. & Borrás-Hidalgo, O. (2009). Black shank resistant tobacco by silencing of glutathione S-transferase. *Biochemical and Biophysical Research Communications,* 387, 300-304.

Hervé, C., Rogowski, A., Blake, A. W., Marcus, S. E., Gilbert, H. J. & Knox, J. P. Carbohydrate-binding modules promote the enzymatic deconstruction of intact plant cell walls by targeting and proximity effects. Proceedings of the National Academy of Sciences, United States of America, 2010 USA. 15293-15298.

Hinch, J. & Clarke, A. E. (1982). Callose formation in *Zea mays* as a response to infection with *Phytophthora cinnamomi*. *Physiological Plant Pathology,* 21, 113-124.

Hinch, J., Wetherbee, R., Mallett, J. & Clarke, A. (1985). Response of *Zea mays* roots to infection with *Phytophthora cinnamomi*. *Protoplasma,* 126, 178-187.

Ho, H. & Zentmyer, G. (1977). Morphology of *Phytophthora cinnamomi*. *Mycologia,* 69, 701-713.

Hohl, H. R. & Suter, E. (1976). Host-parasite interfaces in a resistant and a susceptible cultivar of *Solanum tuberosum* inoculated with *Phytophthora infestans*: leaf tissue. *Canadian Journal of Botany,* 54, 1956-1970.

Holmes, K. & Benson, D. (1994). Evaluation of *Phytophthora parasitica* var. *nicotianae* for biocontrol of *Phytophthora parasitica* on *Catharanthus roseus*. *Plant Disease,* 78, 193-199.

Horn, S. J., Vaaje-Kolstad, G., Westereng, B. & Eijsink, V. G. (2012). Novel enzymes for the degradation of cellulose. *Biotechnology for Biofuels,* 5, 1-13.

Horowitz, B. B. & Ospina-Giraldo, M. D. (2015). The pectin methylesterase gene complement of *Phytophthora sojae*: Structural and functional analyses, and the evolutionary relationships with its oomycete homologs. *PLoS ONE,* 10, e0142096.

Horta, M., Sousa, N., Coelho, A. C., Neves, D. & Cravador, A. (2008). *In vitro* and *in vivo* quantification of elicitin expression in *Phytophthora cinnamomi*. *Physiological and Molecular Plant Pathology,* 73, 48-57.

Hosseini, S., Karlsson, M., Jensen, D. F. & Heyman, F. (2012). Quantification of *Phytophthora pisi* DNA and RNA transcripts during in planta infection of pea. *European Journal of Plant Pathology,* 132, 455-468.

Hosseini, S., Resjö, S., Liu, Y., Durling, M., Heyman, F., Levander, F., Liu, Y., Elfstrand, M., Jensen, D. F. & Andreasson, E. (2015). Comparative proteomic analysis of hyphae and germinating cysts of *Phytophthora pisi* and *Phytophthora sojae*. *Journal of Proteomics,* 117, 24-40.

Hua, C., Wang, Y., Zheng, X., Dou, D., Zhang, Z. & Govers, F. (2008). A *Phytophthora sojae* G-protein α subunit is involved in chemotaxis to soybean isoflavones. *Eukaryotic Cell,* 7, 2133-2140.

Huang, P., Ju, H.-W., Min, J.-H., Zhang, X., Kim, S.-H., Yang, K.-Y. & Kim, C. S. (2013). Overexpression of L-type lectin-like protein kinase 1 confers pathogen resistance and regulates salinity response in *Arabidopsis thaliana*. *Plant science,* 203, 98-106.

Hüberli, D., Hardy, G. S. J., White, D., Williams, N. & Burgess, T. (2013). Fishing for *Phytophthora* from Western Australia's waterways: a distribution and diversity survey. *Australasian Plant Pathology,* 42, 251-260.

Hückelhoven, R. (2005). Powdery mildew susceptibility and biotrophic infection strategies. *FEMS Microbiology Letters,* 245, 9-17.

Hückelhoven, R. (2007). Cell wall-associated mechanisms of disease resistance and susceptibility. *Annual Review of Phytopathology,* 45, 101-127.

Hultberg, M., Bengtsson, T. & Liljeroth, E. (2010). Late blight on potato is suppressed by the biosurfactant-producing strain *Pseudomonas koreensis* 2.74 and its biosurfactant. *BioControl,* 55, 543-550.

Hwang, S. & Ko, W. (1978). Biology of chlamydospores, sporangia, and zoospores of *Phytophthora cinnamomi* in soil. *Phytopathology,* 68, 726-731.

Ibáñez, A. J., Scharte, J., Bones, P., Pirkl, A., Meldau, S., Baldwin, I. T., Hillenkamp, F., Weis, E. & Dreisewerd, K. (2010). Rapid metabolic profiling of *Nicotiana tabacum* defence responses against *Phytophthora nicotianae* using direct infrared laser desorption ionization mass spectrometry and principal component analysis. *Plant Methods,* 6, 14.

Infantino, A., Kharrat, M., Riccioni, L., Coyne, C. J., Mcphee, K. E. & Grünwald, N. J. (2006). Screening techniques and sources of resistance to root diseases in cool season food legumes. *Euphytica,* 147, 201-221.

Ireland, K., Hüberli, D., Dell, B., Smith, I., Rizzo, D. & Hardy, G. Susceptibility of Australian plant species to *Phytophthora ramorum*. Sudden Oak Death Fourth Science Symposium, 2010 Albany, CA. U.S. Department of Agriculture, Forest Service, Pacific Southwest Research 202-205.

Ireland, K. B., Hüberli, D., Dell, B., Smithe, I. W., Rizzof, D. M. & Hardy, G. E. S. J. (2012). Potential susceptibility of Australian native plant species to

branch dieback and bole canker diseases caused by *Phytophthora ramorum*. *Plant Pathology* 61, 234–246.

Irwin, J. & Langdon, P. (1982). A laboratory procedure for determining relative levels of field resistance in soybeans to *Phytophthora megasperma* f. sp. *glycinea*. *Crop and Pasture Science,* 33, 33-39.

Irwin, J. a. G., Cahill, D. M. & Drenth, A. (1995). *Phytophthora* in Australia. *Australian Journal of Agricultural Research,* 46, 1311-1338.

Jackson, T. J., Burgess, T., Colquhoun, I. & Hardy, G. E. S. (2000). Action of the fungicide phosphite on *Eucalyptus marginata* inoculated with *Phytophthora cinnamomi*. *Plant pathology,* 49, 147-154.

James, W. C. (1974). Assessment of plant diseases and losses. *Annual Review of Phytopathology,* 12, 27-48.

Jamet, E., Canut, H., Boudart, G. & Pont-Lezica, R. F. (2006). Cell wall proteins: a new insight through proteomics. *Trends in plant science,* 11, 33-39.

Jarmoskaite, I. & Russell, R. (2014). RNA helicase proteins as chaperones and remodelers. *Annual Review of Biochemistry,* 83, 697-725.

Jeisman, C. (2014). Lupin variety sowing guide 2015. [Accessed 10 December 2014].

Jiang, R. H. Y., De Bruijn, I., Haas, B. J., Belmonte, R., Löbach, L., Christie, J., Van Den Ackerveken, G., Bottin, A., Bulone, V., Díaz-Moreno, S. M., Dumas, B., Fan, L., Gaulin, E. & Van West, P. (2013). Distinctive expansion of potential virulence genes in the genome of the oomycete. *PloS Genetics,* 9, 6.

Johnson, E., Wolff, M., Wernsman, E. & Rufty, R. (2002). Marker-assisted selection for resistance to black shank disease in tobacco. *Plant Disease,* 86, 1303-1309.

Johnson, R. (1992). Past, present and future opportunities in breeding for disease resistance, with examples from wheat. *Euphytica,* 63, 3-22.

Jones, J. P. & Johnson, H. W. (1960). *Phytophthora* root and stem rot of Lupines. *Phytopathology,* 50.

Jones, R. A. (2001). Developing integrated disease management strategies against non-persistently aphid-borne viruses: a model programme. *Integrated Pest Management Reviews,* 6, 15-46.

Jones, T. M., Anderson, A. J. & Albersheim, P. (1972). Host-pathogen interactions IV. Studies on the polysaccharide-degrading enzymes secreted by *Fusarium oxysporum* f. sp. *lycopersici*. *Physiological Plant Pathology,* 2, 153-166.

Jongedijk, E., Tigelaar, H., Van Roekel, J. S., Bres-Vloemans, S. A., Dekker, I., Van Den Elzen, P. J., Cornelissen, B. J. & Melchers, L. S. (1995). Synergistic activity of chitinases and β-1, 3-glucanases enhances fungal resistance in transgenic tomato plants. *Euphytica,* 85, 173-180.

Judelson, H. S., Ah-Fong, A. M., Aux, G., Avrova, A. O., Bruce, C., Cakir, C. & Windass, J. (2008). Gene expression profiling during asexual development of the late blight pathogen *Phytophthora infestans* reveals a highly dynamic transcriptome. *Molecular Plant-Microbe Interactions,* 21, 433-447.

Judelson, H. S. & Blanco, F. A. (2005). The spores of *Phytophthora*: weapons of the plant destroyer. *Nature Reviews Microbiology,* 3, 47-58.

Jung, T. & Blaschke, M. (2004). Phytophthora root and collar rot of alders in Bavaria: distribution, modes of spread and possible management strategies. *Plant Pathology,* 53, 197-208.

Jung, T., Colquhoun, I. & Hardy, G. S. J. (2013). New insights into the survival strategy of the invasive soilborne pathogen *Phytophthora cinnamomi* in different natural ecosystems in Western Australia. *Forest Pathology,* 43, 266-288.

Jupe, J., Stam, R., Howden, A. J., Morris, J. A., Zhang, R., Hedley, P. E. & Huitema, E. (2013). *Phytophthora capsici*-tomato interaction features dramatic shifts in gene expression associated with a hemi-biotrophic lifestyle. *Genome Biology,* 14, R63.

Kaiser, W., Ramsey, M., Makkouk, K., Bretag, T., Açikgöz, N., Kumar, J. & Nutter Jr, F. (2000). Foliar diseases of cool season food legumes and their control. *In:* Knight, R. (ed.) *Linking research and marketing opportunities for pulses in the 21st century.* Kluwer Academic Publishers. 437-455.

Kamoun, S. (2006). A catalogue of the effector secretome of plant pathogenic oomycetes. *Annual Review Phytopathology,* 44, 41-60.

Kamoun, S., Furzer, O., Jones, J. D., Judelson, H. S., Ali, G. S., Dalio, R. J., Roy, S. G., Schena, L., Zambounis, A., Panabières, F., Cahill, D., Ruocco, M., Figueiredo, A., Chen, X.-R., Hulvey, J., Stam, R., Lamour, K., Gijzen, M., Tyler, B. M., Grünwald, N. J., Mukhtar, M. S., Tome, D. F. A., Tor, M., Ackerveken, G. V. D., Mcdowell, J., Daayf, F., Fry, W. E., Lindqvist-Kreuze, H., Meijer, H. J. G., Petre, B., Ristaino, J., Yoshida, K., Birch, P. R. J. & Govers, F. (2014). The top 10 oomycete pathogens in molecular plant pathology. *Molecular Plant Pathology*, doi: 10.1111/mpp.12190, 1-22.

Kamoun, S., Huitema, E. & Vleeshouwers, V. G. (1999). Resistance to oomycetes: a general role for the hypersensitive response? *Trends in Plant Science,* 4, 196-200.

Kamoun, S., Van West, P., Vleeshouwers, V. G. a. A., De Groot, K. E. & Govers, F. (1998). Resistance of *Nicotiana benthamiana* to *Phytophthora infestans* is mediated by the recognition of the elicitor protein INF1. *Plant Cell,* 10, 1413-1426.

Kannwischer, M. & Mitchell, D. (1981). Relationships of numbers of spores of *Phytophthora parasitica* var. *nicotianae* to infection and mortality of tobacco. *Phytopathology,* 71, 69-73.

Kavanagh, K., Jörnvall, H., Persson, B. & Oppermann, U. (2008). Medium-and short-chain dehydrogenase/reductase gene and protein families. *Cellular and Molecular Life Sciences,* 65, 3895.

Kebdani, N., Pieuchot, L., Deleury, E., Panabieres, F., Le Berre, J. Y. & Gourgues, M. (2010). Cellular and molecular characterization of *Phytophthora parasitica* appressorium-mediated penetration. *New Phytologist,* 185, 248-257.

Keegstra, K. (2010). Plant cell walls. *Plant Physiology,* 154, 483-486.

Kehoe, M., Buirchell, B., Coutts, B. & Jones, R. (2014). Black pod syndrome of *Lupinus angustifolius* is caused by late infection with bean yellow mosaic virus. *Plant Disease,* 98, 739-745.

Kellam, M. & Coffey, M. (1985). Quantitative comparison of the resistance to Phytophthora root rot in three avocado rootstocks. *Phytopathology,* 75, 230-234.

Kemen, E., Gardiner, A., Schultz-Larsen, T., Kemen, A. C., Balmuth, A. L., Robert-Seilaniantz, A., Bailey, K., Holub, E., Studholme, D. J. & Maclean, D. (2011). Gene gain and loss during evolution of obligate parasitism in the white rust pathogen of *Arabidopsis thaliana*. *PLoS Biology,* 9, e1001094.

Kemen, E. & Jones, J. D. G. (2012). Obligate biotroph parasitism: can we link genomes to lifestyles? *Trends in Plant Science,* 17, 448-457.

Kenerly, C., Papke, K. & Bruck, R. (1984). Effect of flooding on development of Phytophthora root rot in fraser fir seedlings. *Phytopathology,* 74, 401-404.

Ketelaar, T., Meijer, H. J., Spiekerman, M., Weide, R. & Govers, F. (2012). Effects of latrunculin B on the actin cytoskeleton and hyphal growth in *Phytophthora infestans*. *Fungal Genetics and Biology,* 49, 1014-1022.

Kettel, K. F., Tuck, B., Payne, W., Chen, C., Machado, S. & Karow, R. (2003). Narrow-leaf lupin. *Dryland Cropping Systems.* Corvallis, Oregon, USA: Oregon State University Extension Service. 1-11.

Khatib, M., Lafitte, C., Esquerré-Tugayé, M. T., Bottin, A. & Rickauer, M. (2004). The CBEL elicitor of *Phytophthora parasitica* var. *nicotianae* activates defence in *Arabidopsis thaliana* via three different signalling pathways. *New Phytologist,* 162, 501-510.

Khatri, P. & Drăghici, S. (2005). Ontological analysis of gene expression data: current tools, limitations, and open problems. *Bioinformatics,* 21, 3587-3595.

Khokhar, M. & Gupta, R. (2014). Integrated disease management. *Popular Kheti,* 2, 87-91.

Kim, J. S. & Daniel, G. (2012a). Immunolocalization of hemicelluloses in *Arabidopsis thaliana* stem. Part I: temporal and spatial distribution of xylans. *Planta,* 236, 1275-1288.

Kim, J. S. & Daniel, G. (2012b). Immunolocalization of hemicelluloses in *Arabidopsis thaliana* stem. Part II: Mannan deposition is regulated by phase of development and its patterns of temporal and spatial distribution differ between cell types. *Planta,* 236, 1367-1379.

King, M., Reeve, W., Van Der Hoek, M. B., Williams, N., Mccomb, J., O'brien, P. A. & Hardy, G. E. S. J. (2010). Defining the phosphite-regulated transcriptome of the plant pathogen *Phytophthora cinnamomi*. *Molecular Genetics and Genomics,* 284, 425-435.

Kirk, W., Wharton, P., Hammerschmidt, R., Samen, F. & Douches, D. (2004). Michigan potato diseases. Available: www.potatodiseases.org/ [Accessed 21 October 2015].

Klarzynski, O., Plesse, B., Joubert, J.-M., Yvin, J.-C., Kopp, M., Kloareg, B. & Fritig, B. (2000). Linear β-1, 3 glucans are elicitors of defense responses in tobacco. *Plant Physiology,* 124, 1027-1038.

Knight, N. L., Sutherland, M. W., Martin, A. & Herde, D. J. (2012). Assessment of infection by *Fusarium pseudograminearum* in wheat seedling tissues using quantitative PCR and a visual discoloration scale. *Plant Disease,* 96, 1661-1669.

Konopka-Postupolska, D. (2007). Annexins: putative linkers in dynamic membrane–cytoskeleton interactions in plant cells. *Protoplasma,* 230, 203-215.

Kortekamp, A. (2005). Growth, occurrence and development of septa in *Plasmopara viticola* and other members of the Peronosporaceae using light- and epifluorescence-microscopy. *Mycological Research,* 109, 640-648.

Kotze, J., Moll, J. & Darvas, J. (1987). Root rot control in South Africa: Past, present and future. *South African Avocado Growers' Association Yearbook,* 10, 89-91.

Kováts, K., Binder, A. & Hohl, H. R. (1991). Cytology of induced systemic resistance of cucumber to *Colletotrichum lagenarium*. *Planta,* 183, 484-490.

Kroeger, J. H., Zerzour, R. & Geitmann, A. (2011). Regulator or driving force? The role of turgor pressure in oscillatory plant cell growth. *PLoS ONE,* 6, e18549.

Kroj, T., Rudd, J. J., Nürnberger, T., Gäbler, Y., Lee, J. & Scheel, D. (2003). Mitogen-activated protein kinases play an essential role in oxidative burst-independent expression of pathogenesis-related genes in parsley. *Journal of Biological Chemistry,* 278, 2256-2264.

Kroon, L. P., Brouwer, H., De Cock, A. W. & Govers, F. (2012). The genus *Phytophthora* anno 2012. *Phytopathology,* 102, 348-364.

Kubicek, C. P., Starr, T. L. & Glass, L. (2014). Plant cell wall-degrading enzymes and their secretion in plant pathogenic fungi. *Annual Review of Phytopathology,* 52, 427-451.

Kunjeti, S. G., Evans, T. A., Marsh, A. G., Gregory, N. F., Kunjeti, S., Meyers, B. C., Kalavacharla, V. S. & Donofrio, N. M. (2012). RNA-Seq reveals infection-related global gene changes in *Phytophthora phaseoli*, the causal agent of lima bean downy mildew. *Molecular Plant Pathology,* 13, 454-466.

Kunstmann, B. & Osiewacz, H. D. (2009). The S-adenosylmethionine dependent O-methyltransferase PaMTH1: a longevity assurance factor protecting *Podospora anserina* against oxidative stress. *Aging,* 1, 328-334.

Labbaoui, H., Bogliolo, S., Ghugtyal, V., Solis, N. V., Filler, S. G., Arkowitz, R. A. & Bassilana, M. (2017). Role of Arf GTPases in fungal morphogenesis and virulence. *PLoS Pathogens,* 13, e1006205.

Lamour, K. (2013). *Phytophthora: a global perpective,* London, UK, CAB International. 256.

Lan, C., Liu, P., Li, B., Chen, Q. & Weng, Q. (2013). Development of a specific PCR assay for the rapid and sensitive detection of *Phytophthora capsici*. *Australasian Plant Pathology,* 42, 379-384.

Larroque, M., Belmas, E., Martinez, T., Vergnes, S., Ladouce, N., Lafitte, C., Gaulin, E. & Dumas, B. (2013). Pathogen-associated molecular pattern-triggered immunity and resistance to the root pathogen *Phytophthora parasitica* in *Arabidopsis*. *Journal of Experimental Botany,* 64, 3615-3625.

Latijnhouwers, M., De Wit, P. J. & Govers, F. (2003). Oomycetes and fungi: similar weaponry to attack plants. *Trends in Microbiology,* 11, 462-469.

Laukens, K., Naulaerts, S. & Berghe, W. V. (2015). Bioinformatics approaches for the functional interpretation of protein lists: from ontology term enrichment to network analysis. *Proteomics,* 15, 981-996.

Le Berre, J.-Y., Engler, G. & Panabières, F. (2008). Exploration of the late stages of the tomato–*Phytophthora parasitica* interactions through histological analysis and generation of expressed sequence tags. *New Phytologist,* 177, 480-492.

Lee, S.-J. & Rose, J. K. (2010). Mediation of the transition from biotrophy to necrotrophy in hemibiotrophic plant pathogens by secreted effector proteins. *Plant Signaling & Behavior,* 5, 769-772.

Lees, A., Sullivan, L., Lynott, J. & Cullen, D. (2012). Development of a quantitative real-time PCR assay for *Phytophthora infestans* and its applicability to leaf, tuber and soil samples. *Plant Pathology,* 61, 867-876.

Legavre, T., Ducamp, M., Sabau, X., Argout, X., Fouet, O., Dedieu, F., Surujdeo-Maharaj, S., Garcia, D., Paulin, D. & Lanaud, C. (2015). Identification of *Theobroma cacao* genes differentially expressed during *Phytophthora megakarya* infection. *Physiological and Molecular Plant Pathology,* 92, 1-13.

Levasseur, A., Drula, E., Lombard, V., Coutinho, P. M. & Henrissat, B. (2013). Expansion of the enzymatic repertoire of the CAZy database to integrate auxiliary redox enzymes. *Biotechnology Biofuels,* 6, 41.

Levina, N., Heath, I. & Lew, R. (2000). Rapid wound responses of *Saprolegnia ferax* hyphae depend upon actin and Ca2+-involving deposition of callose plugs. *Protoplasma,* 214, 199-209.

Levy, A. & Epel, B. L. (2009). Cytology of the (1–3)-beta-glucan (callose) in plasmodesmata and sieve plate pores. *In:* Bacic, A., Fincher, G. & Stone, B. (eds.) *Chemistry, biochemistry and biology of (1, 3)-beta glucans and related polysaccharides.* St. Louis, MO: Elsevier Inc. 439-463.

Li, M., Asano, T., Suga, H. & Kageyama, K. (2011). A multiplex PCR for the detection of *Phytophthora nicotianae* and *P. cactorum*, and a survey of their occurrence in strawberry production areas of Japan. *Plant Disease,* 95, 1270-1278.

Li, Q., Zhang, M., Shen, D., Liu, T., Chen, Y., Zhou, J.-M. & Dou, D. (2016). A *Phytophthora sojae* effector PsCRN63 forms homo-/hetero-dimers to suppress plant immunity via an inverted association manner. *Scientific Reports,* 6, DOI: 10.1038/srep26951.

Liljeroth, E., Lankinen, Å., Wiik, L., Burra, D. D., Alexandersson, E. & Andreasson, E. (2016). Potassium phosphite combined with reduced doses of fungicides provides efficient protection against potato late blight in large-scale field trials. *Crop Protection,* 86, 42-55.

Lim, S., Borza, T., Peters, R. D., Coffin, R. H., Al-Mughrabi, K. I., Pinto, D. M. & Wang-Pruski, G. (2013). Proteomics analysis suggests broad functional changes in potato leaves triggered by phosphites and a complex indirect mode of action against *Phytophthora infestans*. *Journal of Proteomics,* 96, 207-223.

Lindbeck, K., Marcroft, S., Van De Wouw, A., Elliott, V. & Howlett, B. Canola and pulse disease management –maintaining the vigilance in 2014. *In:* Crane, J., ed. 2014 Update New South Wales: Share knowledge – accelerate adoption, 2014 Temora Ex-Services Memorial Club, 130 Baker Street, Temora, NSW. Grains Research and Development Corporation, 228.

Lindbeck, K. & Nikandrow, A. (2002). Phytophthora root rot of lupins. [Accessed 09 December 2014].

Lionetti, V. (2015). PECTOPLATE: the simultaneous phenotyping of pectin methylesterases, pectinases, and oligogalacturonides in plants during biotic stresses. *Frontiers in Plant Science,* 6, 331.

Lionetti, V., Cervone, F. & Bellincampi, D. (2012). Methyl esterification of pectin plays a role during plant–pathogen interactions and affects plant resistance to diseases. *Journal of Plant Physiology,* 169, 1623-1630.

Liu, T., Ye, W., Ru, Y., Yang, X., Gu, B., Tao, K., Lu, S., Dong, S., Zheng, X. & Shan, W. (2011). Two host cytoplasmic effectors are required for pathogenesis of *Phytophthora sojae* by suppression of host defenses. *Plant Physiology,* 155, 490-501.

Liu, Y.-J., Han, X.-M., Ren, L.-L., Yang, H.-L. & Zeng, Q.-Y. (2013). Functional divergence of the glutathione S-transferase supergene family in *Physcomitrella patens* reveals complex patterns of large gene family evolution in land plants. *Plant Physiology,* 161, 773-786.

Liu, Y., Zhou, J. & White, K. P. (2014). RNA-seq differential expression studies: more sequence or more replication? *Bioinformatics,* 30, 301-304.

Llorente, B., Bravo-Almonacid, F., Cvitanich, C., Orlowska, E., Torres, H., Flawia, M. & Alonso, G. (2010). A quantitative real-time PCR method for in planta monitoring of *Phytophthora infestans* growth. *Letters in Applied Microbiology,* 51, 603-610.

Lo, C. (1998). General mechanisms of action of microbial biocontrol agents. *Plant Pathology Bulletin,* 7, 155-166.

Lombard, V., Bernard, T., Rancurel, C., Brumer, H., Coutinho, P. & Henrissat, B. (2010). A hierarchical classification of polysaccharide lyases for glycogenomics. *Biochemistry Journal,* 432, 437-444.

Lowe, S., Browne, M. & Boudjelas, S. (2000). *100 of the world's worst invasive alien species: a selection from the global invasive species database,* Auckland, New Zealand, Invasive Species Specialist Group. 1-12.

Lu, Y. J., Schornack, S., Spallek, T., Geldner, N., Chory, J., Schellmann, S., Schumacher, K., Kamoun, S. & Robatzek, S. (2012). Patterns of plant subcellular responses to successful oomycete infections reveal differences in host cell reprogramming and endocytic trafficking. *Cellular Microbiology,* 14, 682-697.

Ludowici, V., Zhang, W., Blackman, L. & Hardham, A. (2013). *Phytophthora nicotianae*. *In:* Lamour, K. (ed.) *Phytophthora: A Global Perspective.* London, UK: CAB International. 113-123.

Ludowici, V. A. (2013). *The Phytophthora nicotianae zoospore secretome.* PhD thesis, Research School of Biology, The Australian National University, Australia. 313.

Luna, E., Pastor, V., Robert, J., Flors, V., Mauch-Mani, B. & Ton, J. (2011). Callose deposition: a multifaceted plant defense response. *Molecular Plant-Microbe Interactions,* 24, 183-193.

Luongo, L., Haegi, A., Galli, M., Berti, S., Vitale, S. & Belisario, A. (2015). First report of *Phytophthora megasperma* causing decline and death on *Celtis australis* in Italy. *Plant Disease,* 99, 155-155.

Macdonald, J., Stites, J. & Kabashima, J. (1990). Comparison of serological and culture plate methods for detecting species of *Phytophthora*, *Pythium*, and *Rhizoctonia* in ornamental plants. *Plant Disease,* 74, 655-659.

Machinandiarena, M. F., Lobato, M. C., Feldman, M. L., Daleo, G. R. & Andreu, A. B. (2012). Potassium phosphite primes defense responses in potato against *Phytophthora infestans*. *Journal of Plant Physiology,* 169, 1417-1424.

Mafra, V., Kubo, K. S., Alves-Ferreira, M., Ribeiro-Alves, M., Stuart, R. M., Boava, L. P., Rodrigues, C. M. & Machado, M. A. (2012). Reference genes for accurate transcript normalization in citrus genotypes under different experimental conditions. *PLoS ONE,* 7, e31263.

Malajczuk, N., Mccomb, A. & Loneragan, J. (1975). Phosphorus uptake and growth of mycorrhizal and uninfected seedlings of *Eucalyptus calophylla* R. Br. *Australian Journal of Botany,* 23, 231-238.

Malajczuk, N., Mccomb, A. & Parker, C. (1977). Infection by *Phytophthora cinnamomi* Rands of roots of *Eucalyptus calophylla* R. Br. and *Eucalyptus marginata* Donn. ex Sm. *Australian Journal of Botany,* 25, 483-500.

Maloy, O. C. (2005). Plant disease management. The Plant Health Instructor.

Mammellaa, M. A., Cacciolab, S. O., Martinc, F. & Schenaa, L. (2011). Genetic characterization of *Phytophthora nicotianae* by the analysis of polymorphic regions of the mitochondrial DNA. *Fungal Biology,* 115, 432–442.

Manga, P., Klingeman, D. M., Lu, T.-Y. S., Mehlhorn, T. L., Pelletier, D. A., Hauser, L. J., Wilson, C. M. & Brown, S. D. (2016). Replicates, read numbers, and other important experimental design considerations for microbial RNA-seq identified using *Bacillus thuringiensis* datasets. *Frontiers in Microbiology,* 7, doi: 10.3389/fmicb.2016.00794.

Marcus, S. E., Verhertbruggen, Y., Hervé, C., Ordaz-Ortiz, J. J., Farkas, V., Pedersen, H. L., Willats, W. G. & Knox, J. P. (2008). Pectic homogalacturonan masks abundant sets of xyloglucan epitopes in plant cell walls. *BMC Plant Biology,* 8, 60.

Marks, G. & Smith, I. (1992). Metalaxyl and phosphonate as prophylactic and curative agents against stem infection of Leucadendron caused by *Phytophthora cinnamomi*. *Animal Production Science,* 32, 255-259.

Marrs, K. A. (1996). The functions and regulation of glutathione S-transferases in plants. *Annual Review of Plant Biology,* 47, 127-158.

Marshall, J., Wilkinson, J., Moore, T. & Hardham, A. (2001). Structure and expression of the genes encoding proteins resident in large peripheral vesicles of *Phytophthora cinnamomi* zoospores. *Protoplasma,* 215, 226-239.

Martin, F., Kohler, A., Murat, C., Balestrini, R., Coutinho, P. M., Jaillon, O., Montanini, B., Morin, E., Noel, B. & Percudani, R. (2010). Périgord black truffle genome uncovers evolutionary origins and mechanisms of symbiosis. *Nature,* 464, 1033-1038.

Martinez, M., Alconada, M., Guillén, F., Vázquez, C. & Reyes, F. (1991). Pectic activities from *Fusarium oxysporum* f. sp. *melonis*: purification and characterization of an exopolygalacturonase. *FEMS Microbiology Letters,* 81, 145-149.

Martins, I. M., Martins, F., Belo, H., Vaz, M., Carvalho, M., Cravador, A. & Choupina, A. (2014). Cloning, characterization and in vitro and in planta expression of a glucanase inhibitor protein (GIP) of *Phytophthora cinnamomi*. *Molecular Biology Reports,* 41, 2453-2462.

Massa, A. N., Childs, K. L. & Buell, C. R. (2013). Abiotic and biotic stress responses in group Phureja DM1-3 516 R44 as measured through whole transcriptome sequencing. *The Plant Genome,* 6, doi:10.3835/plantgenome2013.05.0014.

Massoud, K., Barchietto, T., Le Rudulier, T., Pallandre, L., Didierlaurent, L., Garmier, M., Ambard-Bretteville, F., Seng, J.-M. & Saindrenan, P. (2012).

Dissecting phosphite-induced priming in Arabidopsis infected with *Hyaloperonospora arabidopsidis*. *Plant Physiology,* 159, 286-298.

Mateos, F. V., Rickauer, M. & Esquerré-Tugayé, M.-T. (1997). Cloning and characterization of a cDNA encoding an elicitor of *Phytophthora parasitica* var. *nicotianae* that shows cellulose-binding and lectin-like activities. *Molecular Plant-Microbe Interactions,* 10, 1045-1053.

Matheron, M. & Matejka, J. (1990). Differential virulence of *Phytophthora parasitica* recovered from citrus and other plants to rough lemon and tomato. *Plant Disease,* 74, 138-140.

Matheron, M., Wright, G. & Porchas, M. (1998). Resistance to *Phytophthora citrophthora* and *P. parasitica* and nursery characteristics of several citrus rootstocks. *Plant Disease,* 82, 1217-1225.

Matthews, P., Mccaffery, D. & Jenkins, L. (2014). Winter Crop Variety Sowing Guide 2014. *NSW DPI Management guide* [Online]. Available: www.dpi.nsw.gov.au [Accessed 10 December 2014].

Mccarren, K. (2006). *Saprophytic ability and the contribution of chlamydospores and oospores to the survival of Phytophthora cinnamomi.* PhD, Murdoch University. 201.

Mccarren, K. L., Mccomb, J. A., Shearer, B. L. & Hardy, G. E. S. J. (2009). Phosphite impact on the in vitro production and viability of selfed oospores by *Phytophthora cinnamomi*. *Forest Pathology,* 39, 124-132.

Mccorkle, K., Lewis, R. & Shew, D. (2013). Resistance to *Phytophthora nicotianae* in tobacco breeding lines derived from variety Beinhart 1000. *Plant Disease,* 97, 252-258.

Mcdonald, B. A. & Linde, C. (2002). Pathogen population genetics, evolutionary potential, and durable resistance. *Annual Review of Phytopathology,* 40, 349-379.

Mcintyre, J. & Taylor, G. (1976). Screening tobacco seedlings for resistance to *Phytophthora parasitica* var. *nicotianae*. *Phytopathology,* 66, 70-73.

Meena, M., Prasad, V., Zehra, A., Gupta, V. K. & Upadhyay, R. S. (2015). Mannitol metabolism during pathogenic fungal–host interactions under stressed conditions. *Frontiers in Microbiology,* 6, 1019.

Meins, F. & Ahl, P. (1989). Induction of chitinase and β-1, 3-glucanase in tobacco plants infected with *Pseudomonas tabaci* and *Phytophthora parasitica* var. *nicotianae*. *Plant Science,* 61, 155-161.

Mélida, H., Sandoval-Sierra, J. V., Diéguez-Uribeondo, J. & Bulone, V. (2013). Analyses of extracellular carbohydrates in oomycetes unveil the existence of three different cell wall types. *Eukaryotic Cell,* 12, 194-203.

Meng, Y., Zhang, Q., Ding, W. & Shan, W. (2014). *Phytophthora parasitica*: a model oomycete plant pathogen. *Mycology: An International Journal of Fungal Biology,* 5, 43-51.

Mesarich, C. H., Bowen, J. K., Hamiaux, C. & Templeton, M. D. (2015). Repeat-containing protein effectors of plant-associated organisms. *Frontiers in Plant Science,* 6.

Messenger, B., Menge, J. & Pond, E. (2000). Effects of gypsum soil amendments on avocado growth, soil drainage, and resistance to *Phytophthora cinnamomi*. *Plant disease,* 84, 612-616.

Meyer, F. E., Shuey, L. S., Naidoo, S., Mamni, T., Berger, D. K., Myburg, A. A., Van Den Berg, N. & Naidoo, S. (2016). Dual RNA-sequencing of *Eucalyptus*

nitens during *Phytophthora cinnamomi* challenge reveals pathogen and host factors influencing compatibility. *Frontiers in Plant Science,* 7, doi: 10.3389/fpls.2016.00191.

Mitchell, J. (1973). The mechanisms of biological control of plant diseases. *Soil Biology and Biochemistry,* 5, 721-728.

Mittler, R. (2002). Oxidative stress, antioxidants and stress tolerance. *Trends in Plant Science,* 7, 405-410.

Mittler, R., Vanderauwera, S., Gollery, M. & Van Breusegem, F. (2004). Reactive oxygen gene network of plants. *Trends in Plant Science,* 9, 490-498.

Mohamed, H. & Mazen, M. (2012). Influence of some biotic and abiotic inducers on Fusarium wilt disease incidence of lupin (*Lupinus albus*) on disease resistance and protein pattern. *Plant Pathology & Quarantine,* 2, 179–188.

Montánchez, I., Arana, I., Parada, C., Garaizabal, I., Orruño, M., Barcina, I. & Kaberdin, V. R. (2014). Reprogramming of *Vibrio harveyi* gene expression during adaptation in cold seawater. *FEMS Microbiology Ecology,* 87, 193-203.

Morgan, W. & Kamoun, S. (2007). RXLR effectors of plant pathogenic oomycetes. *Current Opinion in Microbiology,* 10, 332-338.

Mortazavi, A., Williams, B. A., Mccue, K., Schaeffer, L. & Wold, B. (2008). Mapping and quantifying mammalian transcriptomes by RNA-Seq. *Nature Methods,* 5, 621-628.

Mosavi, L. K., Cammett, T. J., Desrosiers, D. C. & Peng, Z. Y. (2004). The ankyrin repeat as molecular architecture for protein recognition. *Protein Science,* 13, 1435-1448.

Moulos, P. & Hatzis, P. (2015). Systematic integration of RNA-Seq statistical algorithms for accurate detection of differential gene expression patterns. *Nucleic Acids Research,* 43, e25.

Nagalakshmi, U., Wang, Z., Waern, K., Shou, C., Raha, D., Gerstein, M. & Snyder, M. (2008). The transcriptional landscape of the yeast genome defined by RNA sequencing. *Science,* 320, 1344-1349.

Nagle, A. M., Long, R. P., Madden, L. V. & Bonello, P. (2010). Association of *Phytophthora cinnamomi* with white oak decline in southern Ohio. *Plant Disease,* 94, 1026-1034.

Narayan, R. D., Blackman, L. M., Shan, W. & Hardham, A. R. (2010). *Phytophthora nicotianae* transformants lacking dynein light chain 1 produce non-flagellate zoospores. *Fungal Genetics and Biology,* 47, 663-671.

Nath, V. S., Hegde, V. M., Jeeva, M. L., Misra, R. S., Veena, S. S., Raj, M., Unnikrishnan, S. K. & Darveekaran, S. S. (2014). Rapid and sensitive detection of *Phytophthora colocasiae* responsible for the taro leaf blight using conventional and real-time PCR assay. *FEMS Microbiology Letters,* 352, 174-183.

Nath, V. S., Senthil, M., Hegde, V. M., Jeeva, M. L., Misra, R. S., Veena, S. S. & Raj, M. (2013). Molecular evidence supports hypervariability in *Phytophthora colocasiae* associated with leaf blight of taro. *European Journal of Plant Pathology,* 136, 483-494.

Neher, D. & Duniway, J. (1992). Dispersal of *Phytophthora parasitica* in tomato fields by furrow irrigation. *Plant Disease,* 76, 582-586.

Nemestothy, G. & Guest, D. (1990). Phytoalexin accumulation, phenylalanine ammonia lyase activity and ethylene biosynthesis in fosetyl-Al treated

resistant and susceptible tobacco cultivars infected with *Phytophthora nicotianae* var. *nicotianae*. *Physiological and Molecular Plant Pathology,* 37, 207-219.

Newhook, F. (1959). The association of *Phytophthora* spp. with mortality of *Pinus radiata* and other conifers: I. Symptoms and epidemiology in shelterbelts. *New Zealand Journal of Agricultural Research,* 2, 808-843.

Nguema-Ona, E., Vicré-Gibouin, M., Cannesan, M.-A. & Driouich, A. (2013). Arabinogalactan proteins in root–microbe interactions. *Trends in plant science,* 18, 440-449.

Nguyen, Q. B., Itoh, K., Van Vu, B., Tosa, Y. & Nakayashiki, H. (2011). Simultaneous silencing of endo-β-1, 4 xylanase genes reveals their roles in the virulence of *Magnaporthe oryzae*. *Molecular Biology*, doi: 10.1111/j.1365-2958.2011.07746.x.

Nicolaisen, M., Supronienė, S., Nielsen, L. K., Lazzaro, I., Spliid, N. H. & Justesen, A. F. (2009). Real-time PCR for quantification of eleven individual *Fusarium* species in cereals. *Journal of Microbiological Methods,* 76, 234-240.

Niere, J., Deangelis, G. & Grant, B. (1994). The effect of phosphonate on the acid-soluble phosphorus components in the genus *Phytophthora*. *Microbiology,* 140, 1661-1670.

Nikandrow, A., Gilbert, R., Gunning, D., Lawler, M., Lindbeck, K. & Murray, G. (2001). First report of *Phytophthora* sp. causing a root and basal stem rot of narrow-leaf lupin in Australia. *Plant Pathology,* 50, 811-811.

Noctor, G. & Foyer, C. H. (1998). Ascorbate and glutathione: keeping active oxygen under control. *Annual Review of Plant Biology,* 49, 249-279.

Nolan, T., Hands, R. E. & Bustin, S. A. (2006). Quantification of mRNA using real-time RT-PCR. *Nature Protocols,* 1, 1559-1582.

Nowicki, M., Foolad, M. R., Nowakowska, M. & Kozik, E. U. (2012). Potato and tomato late blight caused by *Phytophthora infestans*: An overview of pathology and resistance breeding. *Plant Disease,* 96, 4-17.

O'connell, R. J., Thon, M. R., Hacquard, S., Amyotte, S. G., Kleemann, J., Torres, M. F., Damm, U., Buiate, E. A., Epstein, L. & Alkan, N. (2012). Lifestyle transitions in plant pathogenic *Colletotrichum* fungi deciphered by genome and transcriptome analyses. *Nature Genetics,* 44, 1060-1065.

O'neill, M. A., Eberhard, S., Albersheim, P. & Darvill, A. G. (2001). Requirement of borate cross-linking of cell wall rhamnogalacturonan II for Arabidopsis growth. *Science,* 294, 846-849.

O'sullivan, A. C. (1997). Cellulose: the structure slowly unravels. *Cellulose,* 4, 173-207.

O'connell, R. J. & Panstruga, R. (2006). Tête à tête inside a plant cell: establishing compatibility between plants and biotrophic fungi and oomycetes. *New Phytologist,* 171, 699-718.

O'herlihy, E. A., Duffy, E. M. & Cassells, A. C. (2003). The effects of arbuscular mycorrhizal fungi and chitosan sprays on yield and late blight resistance in potato crops from microplants. *Folia Geobotanica,* 38, 201-207.

Ogle, H. & Dale, M. (1997). Disease management: cultural practices. *In:* Brown, J. & Ogle, H. (eds.) *Plant pathogens and plant diseases.* Armidale, Australia: Rockvale Publications. 390-404.

Oh, S.-K., Young, C., Lee, M., Oliva, R., Bozkurt, T. O., Cano, L. M., Win, J., Bos, J. I., Liu, H.-Y. & Van Damme, M. (2009). *In planta* expression screens of *Phytophthora infestan*s RXLR effectors reveal diverse phenotypes, including activation of the *Solanum bulbocastanum* disease resistance protein Rpi-blb2. *Plant Cell,* 21, 2928-2947.

Oliver, R. P. & Ipcho, S. V. (2004). *Arabidopsis* pathology breathes new life into the necrotrophs-vs.-biotrophs classification of fungal pathogens. *Molecular Plant Pathology,* 5, 347-352.

Ospina-Giraldo, M. D., Mcwalters, J. & Seyer, L. (2010). Structural and functional profile of the carbohydrate esterase gene complement in *Phytophthora infestans*. *Current Genetics,* 56, 495-506.

Østergaard, L., Petersen, M., Mattsson, O. & Mundy, J. (2002). An Arabidopsis callose synthase. *Plant Molecular Biology,* 49, 559-566.

Ozsolak, F. & Milos, P. M. (2010). RNA sequencing: advances, challenges and opportunities. *Nature Reviews Genetics,* 12, 87-98.

Pabst, M., Fischl, R. M., Brecker, L., Morelle, W., Fauland, A., Köfeler, H., Altmann, F. & Léonard, R. (2013). Rhamnogalacturonan II structure shows variation in the side chains monosaccharide composition and methylation status within and across different plant species. *Plant Journal,* 76, 61-72.

Pais, M., Win, J., Yoshida, K., Etherington, G. J., Cano, L. M., Raffaele, S., Banfield, M. J., Jones, A., Kamoun, S. & Saunders, D. G. (2013). From pathogen genomes to host plant processes: the power of plant parasitic oomycetes. *Genome Biology,* 14, 211.

Panabières, F., Amselem, J., Galiana, E. & Le Berre, J.-Y. (2005). Gene identification in the oomycete pathogen *Phytophthora parasitica* during *in vitro* vegetative growth through expressed sequence tags. *Fungal Genetics and Biology,* 42, 611-623.

Pang, Z., Chen, L., Miao, J., Wang, Z., Bulone, V. & Liu, X. (2015). Proteomic profile of the plant-pathogenic oomycete *Phytophthora capsici* in response to the fungicide pyrimorph. *Proteomics,* 15, 2972-2982.

Parent, A., Roy, S. J., Iorio-Morin, C., Lépine, M.-C., Labrecque, P., Gallant, M. A., Slipetz, D. & Parent, J.-L. (2010). ANKRD13C acts as a molecular chaperone for G protein-coupled receptors. *Journal of Biological Chemistry,* 285, 40838-40851.

Patel, T. K. & Williamson, J. D. (2016). Mannitol in plants, fungi, and plant–fungal interactions. *Trends in Plant Science,* 21, 486-497.

Pauly, M. & Keegstra, K. (2008). Cell-wall carbohydrates and their modification as a resource for biofuels. *Plant Journal,* 54, 559-568.

Pearson, D. E. & Callaway, R. M. (2003). Indirect effects of host-specific biological control agents. *Trends in Ecology & Evolution,* 18, 456-461.

Perret, J., Bruneteau, M., Michel, G., Marais, M., Joseleau, J. & Ricci, P. (1992). Effect of growth conditions on the structure of β-d-glucans from *Phytophthora parasitica* Dastur, a phytopathogenic fungus. *Carbohydrate Polymers,* 17, 231-236.

Petersen, T. N., Kauppinen, S. & Larsen, S. (1997). The crystal structure of rhamnogalacturonase A from *Aspergillus aculeatus*: a right-handed parallel β helix. *Structure,* 5, 533-544.

Picault, N., Hodges, M., Palmieri, L. & Palmieri, F. (2004). The growing family of mitochondrial carriers in Arabidopsis. *Trends in Plant Science,* 9, 138-146.

Pilbeam, R., Howard, K., Shearer, B. & Hardy, G. (2011). Phosphite stimulated histological responses of *Eucalyptus marginata* to infection by *Phytophthora cinnamomi*. *Trees - Structure and Function,* 25, 1121-1131.

Pirrung, M. C. & Southern, E. M. (2014). The genesis of microarrays. *Biochemistry and Molecular Biology Education,* 42, 106-113.

Pogorelko, G., Lionetti, V., Bellincampi, D. & Zabotina, O. (2013). Cell wall integrity: targeted post-synthetic modifications to reveal its role in plant growth and defense against pathogens. *Plant Signaling & Behavior,* 8, e25435.

Popper, Z. A. & Fry, S. C. (2008). Xyloglucan– pectin linkages are formed intra-protoplasmically, contribute to wall-assembly, and remain stable in the cell wall. *Planta,* 227, 781-794.

Pozo, M. J., Azcón-Aguilar, C., Dumas-Gaudot, E. & Barea, J. M. (1999). β-1, 3-glucanase activities in tomato roots inoculated with arbuscular mycorrhizal fungi and/or *Phytophthora parasitica* and their possible involvement in bioprotection. *Plant Science,* 141, 149-157.

Prade, R. A., Zhan, D., Ayoubi, P. & Mort, A. J. (1999). Pectins, pectinases and plant-microbe interactions. *Biotechnology and Genetic Engineering Reviews,* 16, 361-392.

Pratt, B. & Heather, W. (1972). Method for rapid differentiation of *Phytophthora cinnamomi* from other *Phytophthora* species isolated from soil by lupin baiting. *Transactions of the British Mycological Society,* 59, 87-96.

Pratt, B., Heather, W. & Shepherd, C. (1973). Recovery of *Phytophthora cinnamomi* from native vegetation in a remote area of New South Wales. *Transactions of the British Mycological Society,* 60, 197-204.

Pritchard, I. (2014). *Lupin varieties for Western Australia: 2014* [Online]. DAFWA. Available: https://agric.wa.gov.au/n/2941 [Accessed 31 October 2014].

Pscheidt, J., Burket, J., Fischer, S. & Hamm, P. (1992). Sensitivity and clinical use of Phytophthora-specific immunoassay kits. *Plant Disease,* 76, 928-932.

Qutob, D., Kamoun, S. & Gijzen, M. (2002). Expression of a *Phytophthora sojae* necrosis-inducing protein occurs during transition from biotrophy to necrotrophy. *Plant Journal,* 32, 361-373.

Raffaele, S., Win, J., Cano, L. M. & Kamoun, S. (2010). Analyses of genome architecture and gene expression reveal novel candidate virulence factors in the secretome of *Phytophthora infestans*. *BMC Genomics,* 11, 637.

Rahman, M. Z., Uematsu, S., Kimishima, E., Kanto, T., Kusunoki, M., Motohashi, K., Ishiguro, Y., Suga, H. & Kageyama, K. (2015). Two plant pathogenic species of *Phytophthora* associated with stem blight of Easter lily and crown rot of lettuce in Japan. *Mycoscience,* 56, 419–433.

Ramos-Molina, B., Lambertos, A., López-Contreras, A. J. & Peñafiel, R. (2013). Mutational analysis of the antizyme-binding element reveals critical residues for the function of ornithine decarboxylase. *Biochimica et Biophysica Acta (BBA)-General Subjects,* 1830, 5157-5165.

Randall, T. A., Dwyer, R. A., Huitema, E., Beyer, K., Cvitanich, C., Kelkar, H., Ah Fong, A. M., Gates, K., Roberts, S. & Yatzkan, E. (2005). Large-scale

gene discovery in the oomycete *Phytophthora infestans* reveals likely components of phytopathogenicity shared with true fungi. *Molecular Plant-Microbe Interactions,* 18, 229-243.

Reeser, M. P. W., Sutton, W., Hansen, E., Goheen, E. M., Fieland, V. & Grünwald, N. J. (2015). First report of *Phytophthora occultans* causing root and collar rot on Ceanothus, boxwood, rhododendron, and other hosts in horticultural nurseries in Oregon, USA. *Plant Disease,* 99, 1282.

Reeves, T., Ellington, A. & Brooke, H. (1984). Effects of lupin-wheat rotations on soil fertility, crop disease and crop yields. *Australian Journal of Experimental Agriculture,* 24, 595-600.

Reid, A. (2006). Sampling and testing for plant pathogens. Available: http://archive.agric.wa.gov.au/objtwr/imported_assets/content/pw/ph/bulletin2006_sampling_areid.pdf [Accessed 28 January 2015].

Reignault, P., Valette-Collet, O. & Boccara, M. (2008). The importance of fungal pectinolytic enzymes in plant invasion, host adaptability and symptom type. *European Journal of Plant Pathology,* 120, 1-11.

Reiter, W.-D. (2002). Biosynthesis and properties of the plant cell wall. *Current Opinion in Plant Biology,* 5, 536-542.

Reitmann, A., Berger, D. K. & Van Den Berg, N. (2017). Putative pathogenicity genes of *Phytophthora cinnamomi* identified via RNA-Seq analysis of pre-infection structures. *European Journal of Plant Pathology,* 147, 211-228.

Ren, X., Zhang, N., Cao, M., Wu, K., Shen, Q. & Huang, Q. (2012). Biological control of tobacco black shank and colonization of tobacco roots by a *Paenibacillus polymyxa* strain C5. *Biology and Fertility of Soils,* 48, 613-620.

Rhee, S. Y., Wood, V., Dolinski, K. & Draghici, S. (2008). Use and misuse of the gene ontology annotations. *Nature Reviews Genetics,* 9, 509-515.

Rhoads, D. M., Umbach, A. L., Subbaiah, C. C. & Siedow, J. N. (2006). Mitochondrial reactive oxygen species. Contribution to oxidative stress and interorganellar signaling. *Plant Physiology,* 141, 357-366.

Ribeiro, O., Erwin, D. & Zentmyer, G. (1975). An improved synthetic medium for oospore production and germination of several *Phytophthora* species. *Mycologia,* 67, 1012-1019.

Ribeiro, O. K. (2013). A historical perspective of *Phytophthora*. *In:* Lamour, K. (ed.) *Phytophthora: A Global Perspective.* London, UK: CAB International. 1-10.

Ridley, B. L., O'neill, M. A. & Mohnen, D. (2001). Pectins: structure, biosynthesis, and oligogalacturonide-related signaling. *Phytochemistry,* 57, 929-967.

Robles, J. A., Qureshi, S. E., Stephen, S. J., Wilson, S. R., Burden, C. J. & Taylor, J. M. (2012). Efficient experimental design and analysis strategies for the detection of differential expression using RNA-Sequencing. *BMC Genomics,* 13, 1.

Robold, A. & Hardham, A. (1998). Production of species-specific monoclonal antibodies that react with surface components on zoospores and cysts of *Phytophthora nicotianae*. *Canadian Journal of Microbiology,* 44, 1161-1170.

Robold, A. V. & Hardham, A. R. (2005). During attachment *Phytophthora* spores secrete proteins containing thrombospondin type 1 repeats. *Current Genetics,* 47, 307-315.

Rookes, J. E., Wright, M. L. & Cahill, D. M. (2008). Elucidation of defence responses and signalling pathways induced in *Arabidopsis thaliana* following challenge with *Phytophthora cinnamomi*. *Physiological and Molecular Plant Pathology,* 72, 151-161.

Rossman, A. Y. & Palm, M. E. (2006). Why are *Phytophthora* and other Oomycota not true fungi? *Outlooks on Pest Management,* 17, 217.

Roxas, V. P., Lodhi, S. A., Garrett, D. K., Mahan, J. R. & Allen, R. D. (2000). Stress tolerance in transgenic tobacco seedlings that overexpress glutathione S-transferase/glutathione peroxidase. *Plant and Cell Physiology,* 41, 1229-1234.

Rudd, J. J., Kanyuka, K., Hassani-Pak, K., Derbyshire, M., Andongabo, A., Devonshire, J., Lysenko, A., Saqi, M., Desai, N. M. & Powers, S. J. (2015). Transcriptome and metabolite profiling of the infection cycle of *Zymoseptoria tritici* on wheat reveals a biphasic interaction with plant immunity involving differential pathogen chromosomal contributions and a variation on the hemibiotrophic lifestyle definition. *Plant Physiology,* 167, 1158-1185.

Sacco, M. A., Koropacka, K., Grenier, E., Jaubert, M. J., Blanchard, A., Goverse, A., Smant, G. & Moffett, P. (2009). The cyst nematode SPRYSEC protein RBP-1 elicits Gpa2-and RanGAP2-dependent plant cell death. *PLoS Pathogens,* 5, e1000564.

Saindrenan, P., Barchietto, T. & Bompeix, G. (1990). Effects of phosphonate on the elicitor activity of culture filtrates of *Phytophthora cryptogea* in *Vigna unguiculata*. *Plant Science,* 67, 245-251.

Sambrook, J. & Russell, D. (2001). *Molecular Cloning: A Laboratory Manual (Vol 3)* Cold Spring Harbor, New York, N. Y., USA., Cold Spring Harbor Laboratory Press.

Sanzani, S. M., Schena, L., De Cicco, V. & Ippolito, A. (2012). Early detection of *Botrytis cinerea* latent infections as a tool to improve postharvest quality of table grapes. *Postharvest Biology and Technology,* 68, 64-71.

Saurat, M. C., Schenck, M. N., Fourrier, M. C., Cerf, M. I., Casset, M. C. & Ioos, R. (2015). First report of *Phytophthora niederhauserii* causing wilt of *Begonia elatior* in France. *Plant Disease,* 99, 1277.

Savage, E., Clayton, C., Hunter, J., Brenneman, J., Laviola, C. & Gallegly, M. (1968). Homothallism, heterothallism, and interspecific hybridization in the genus *Phytophthora*. *Phytopathology,* 58, 1004-1021.

Scheller, H. V. & Ulvskov, P. (2010). Hemicelluloses. *Plant Biology,* 61, 263-289.

Schneider, E. & Hunke, S. (1998). ATP-binding-cassette (ABC) transport systems: functional and structural aspects of the ATP-hydrolyzing subunits/domains. *FEMS Microbiology Reviews,* 22, 1-20.

Schnoes, A. M., Ream, D. C., Thorman, A. W., Babbitt, P. C. & Friedberg, I. (2013). Biases in the experimental annotations of protein function and their effect on our understanding of protein function space. *PLoS Computational Biology,* 9, e1003063.

Schoonhoven, A. V. & Pastor-Corrales, M. A. (1987). *Standard system for the evaluation of bean germplasm,* Cali, Colombia, Centro Internacional de Agricultura Tropical (CIAT). 54.

Seem, R. (1984). Disease incidence and severity relationships. *Annual Review of Phytopathology,* 22, 133-150.

Séjalon-Delmas, N., Mateos, F. V., Bottin, A., Rickauer, M., Dargent, R. & Esquerré-Tugayé, M. (1997). Purification, elicitor activity, and cell wall localization of a glycoprotein from *Phytophthora parasitica* var. *nicotianae*, a fungal pathogen of tobacco. *Phytopathology,* 87, 899-909.

Sella, L., Castiglioni, C., Paccanaro, M. C., Janni, M., Schäfer, W., D'ovidio, R. & Favaron, F. (2016). Involvement of fungal pectin methylesterase activity in the interaction between *Fusarium graminearum* and wheat. *Molecular Plant-Microbe Interactions,* 29, 258-267.

Serrano, M. S., Fernández-Rebollo, P., De Vita, P. & Sánchez, M. E. (2013). Calcium mineral nutrition increases the tolerance of *Quercus ilex* to Phytophthora root disease affecting oak rangeland ecosystems in Spain. *Agroforestry Systems,* 87, 173-179.

Serrazina, S., Santos, C., Machado, H., Pesquita, C., Vicentini, R., Pais, M. S., Sebastiana, M. & Costa, R. (2015). Castanea root transcriptome in response to *Phytophthora cinnamomi* challenge. *Tree Genetics & Genomes,* 11, 1-19.

Shan, W. & Hardham, A. R. (2004). Construction of a bacterial artificial chromosome library, determination of genome size, and characterization of an Hsp70 gene family in *Phytophthora nicotianae*. *Fungal Genetics and Biology,* 41, 369-380.

Shan, W., Marshall, J. S. & Hardham, A. R. (2004). Gene expression in germinated cysts of *Phytophthora nicotianae*. *Molecular Plant Pathology,* 5, 317-330.

Shao, M., Du, W., Yu, D., Du, P., Ni, S., Xu, Y. & Zhang, H. (2015). First report of stem rot of konjac caused by *Phytophthora nicotianae* in China. *Plant Disease,* 99, 283-283.

Shearer, B. & Crane, C. (2009). Influence of site and rate of low-volume aerial phosphite spray on lesion development of *Phytophthora cinnamomi* and phosphite persistence in *Lambertia inermis* var. *inermis* and *Banksia grandis*. *Australasian Plant Pathology,* 38, 288-304.

Shearer, B., Crane, C. & Cochrane, A. (2004). Quantification of the susceptibility of the native flora of the South-West Botanical Province, Western Australia, to *Phytophthora cinnamomi*. *Australian Journal of Botany,* 52, 435-443.

Shearer, B. L., Fairman, R. G. & Grant, M. J. (2006). Effective concentration of phosphite in controlling *Phytophthora cinnamomi* following stem injection of *Banksia* species and *Eucalyptus marginata*. *Forest Pathology,* 36, 119-135.

Shen, D., Chai, C., Ma, L., Zhang, M. & Dou, D. (2016). Comparative RNA-Seq analysis of *Nicotiana benthamiana* in response to *Phytophthora parasitica* infection. *Plant Growth Regulation,* 80, 59-67.

Showalter, A. M. (1993). Structure and function of plant cell wall proteins. *Plant Cell,* 5, 9-23.

Simon, U. K., Bauer, R., Rioux, D., Simard, M. & Oberwinkler, F. (2005). The intercellular biotrophic leaf pathogen *Cymadothea trifolii* locally degrades pectins, but not cellulose or xyloglucan in cell walls of *Trifolium repens*. *New Phytologist,* 165, 243-260.

Singh, U. & Chand, R. (1982). Effect of *Alternaria carthami* inoculum density on disease development in safflower. *Transactions of the British Mycological Society,* 78, 178-180.

Škalamera, D. & Hardham, A. (2006). PnCcp, a *Phytophthora nicotianae* protein containing a single complement control protein module, is sorted into large peripheral vesicles in zoospores. *Australasian Plant Pathology,* 35, 593-603.

Škalamera, D. & Heath, M. C. (1996). Cellular mechanisms of callose deposition in response to fungal infection or chemical damage. *Canadian journal of botany,* 74, 1236-1242.

Škalamera, D., Wasson, A. & Hardham, A. R. (2004). Genes expressed in zoospores of *Phytophthora nicotianae*. *Molecular Genetics and Genomics,* 270, 549-557.

Smillie, R., Grant, B. & Guest, D. (1989). The mode of action of phosphite: evidence for both direct and indirect modes of action on three *Phytophthora* spp. in plants. *Phytopathology,* 79, 921-926.

Smith, C. G., Rodgers, M. W., Zimmerlin, A., Ferdinando, D. & Bolwell, G. P. (1994). Tissue and subcellular immunolocalisation of enzymes of lignin synthesis in differentiating and wounded hypocotyl tissue of French bean (*Phaseolus vulgaris* L.). *Planta,* 192, 155-164.

Smith, L. A., Dann, E. K., Pegg, K. G. & Whiley, A. W. Management of *Phytophthora cinnamomi* in Australian avocado orchards. *In:* Stirling, G. R., ed. 6th Australasian Soilborne Diseases Symposium, 9-11 August 2010 Twin Waters, Queensland. 107.

Smith, P. M. (1979). A study of the effects of fungitoxic compounds on *Phytophthora cinnamomi* in water. *Annals of Applied Biology,* 93, 149-157.

Solla, A., García, L., Pérez, A., Cordero, A., Cubera, E. & Moreno, G. (2009). Evaluating potassium phosphonate injections for the control of *Quercus ilex decline* in SW Spain: Implications of low soil contamination by *Phytophthora cinnamomi* and low soil water content on the effectiveness of treatments. *Phytoparasitica,* 37, 303-316.

Somerville, C., Bauer, S., Brininstool, G., Facette, M., Hamann, T., Milne, J., Osborne, E., Paredez, A., Persson, S. & Raab, T. (2004). Toward a systems approach to understanding plant cell walls. *Science,* 306, 2206-2211.

Song, J., Win, J., Tian, M., Schornack, S., Kaschani, F., Ilyas, M., Van Der Hoorn, R. A. & Kamoun, S. (2009). Apoplastic effectors secreted by two unrelated eukaryotic plant pathogens target the tomato defense protease Rcr3. *Proceedings of the National Academy of Sciences, United States of America,* 106, 1654-1659.

Song, W.-Y., Hörtensteiner, S., Tomioka, R., Lee, Y. & Martinoia, E. (2011). Common functions or only phylogenetically related? The large family of PLAC8 motif-containing/PCR genes. *Molecules and Cells,* 31, 1-7.

Spanu, P. D. (2012). The genomics of obligate (and nonobligate) biotrophs. *Annual Review of Phytopathology,* 50, 91-109.

Sprockett, D. D. (2009). *The evolution of fungal pectinases in Glycosyl Hydrolase Family 28 and their association with ecological strategy.* MS Thesis, Kent State University. 111.

Stam, R., Jupe, J., Howden, A. J., Morris, J. A., Boevink, P. C., Hedley, P. E. & Huitema, E. (2013). Identification and characterisation CRN effectors in *Phytophthora capsici* shows modularity and functional diversity. *PLoS ONE,* 8, e59517.

Stasikowski, P., Mccomb, J., Scott, P., Paap, T., O'brien, P. & Hardy, G. S. J. (2014). Calcium sulphate soil treatments augment the survival of phosphite-sprayed *Banksia leptophylla* infected with *Phytophthora cinnamomi*. *Australasian Plant Pathology,* 43, 369-379.

Sullivan, M., Melton, T. & Shew, H. (2005). Managing the race structure of *Phytophthora parasitica* var. *nicotianae* with cultivar rotation. *Plant disease,* 89, 1285-1294.

Sun, D., Hussain, H. I., Yi, Z., Siegele, R., Cresswell, T., Kong, L. & Cahill, D. M. (2014). Uptake and cellular distribution, in four plant species, of fluorescently labeled mesoporous silica nanoparticles. *Plant Cell Reports*, 1-14.

Sun, J., Tian, C., Diamond, S. & Glass, N. L. (2012). Deciphering transcriptional regulatory mechanisms associated with hemicellulose degradation in *Neurospora crassa*. *Eukaryotic Cell,* 11, 482-493.

Supek, F., Bošnjak, M., Škunca, N. & Šmuc, T. (2011). REVIGO summarizes and visualizes long lists of gene ontology terms. *PLoS ONE,* 6, e21800.

Takemoto, D., Jones, D. A. & Hardham, A. R. (2003). GFP-tagging of cell components reveals the dynamics of subcellular re-organization in response to infection of Arabidopsis by oomycete pathogens. *Plant Journal,* 33, 775-792.

Taylor, R. J., Pasche, J. S., Shew, H. D., Lannon, K. & Gudmestad, N. C. (2012). Tuber rot of potato caused by *Phytophthora nicotianae*: isolate aggressiveness and cultivar susceptibility. *Plant Disease,* 96, 693-704.

Tedford, E., Miller, T. & Nielsen, M. (1990). A detached-leaf technique for detecting resistance to *Phytophthora parasitica* var. *nicotianae* in tobacco. *Plant Disease,* 74, 313-316.

Thao, H. T. B. & Yamakawa, T. (2009). Phosphite (phosphorous acid): fungicide, fertilizer or bio-stimulator? *Soil Science and Plant Nutrition,* 55, 228-234.

Thines, M. (2013). Taxonomy and phylogeny of *Phytophthora* and related oomycetes. *In:* Lamour, K. (ed.) *Phytophthora: A Global Perspective.* London, UK: CAB International. 11-18.

Thomas, G., Jones, R and Vanstone, V (2008). Diseases of lupin. *In:* White, P., French, B. And Mclarty, A. (ed.) *Producing lupins.* South Perth, WA: Department of Agriculture and Food. 168.

Thomas, G., Macleod, B. & Vanstone, V. (2010). Lupin root diseases. Available: http://www.agric.wa.gov.au/ [Accessed 11 December 2014].

Thomas, G. & Sweetingham, M. (2004). Cultivar and environment influence the development of lupin anthracnose caused by *Colletotrichum lupini*. *Australasian Plant Pathology,* 33, 571-577.

Thompson, D. M., Lu, C., Green, P. J. & Parker, R. (2008). tRNA cleavage is a conserved response to oxidative stress in eukaryotes. *RNA,* 14, 2095-2103.

Thurston, H. (1990). Plant disease management practices of traditional farmers. *Plant Disease,* 74, 96-101.

Tian, M., Benedetti, B. & Kamoun, S. (2005). A second Kazal-like protease inhibitor from Phytophthora infestans inhibits and interacts with the apoplastic pathogenesis-related protease P69B of tomato. *Plant physiology,* 138, 1785-1793.

Tian, M., Huitema, E., Da Cunha, L., Torto-Alalibo, T. & Kamoun, S. (2004). A Kazal-like extracellular serine protease inhibitor from *Phytophthora*

infestans targets the tomato pathogenesis-related protease P69B. *Journal of Biological Chemistry,* 279, 26370-26377.

Tian, M., Win, J., Song, J., Van Der Hoorn, R., Van Der Knaap, E. & Kamoun, S. (2007). A *Phytophthora infestans* cystatin-like protein targets a novel tomato papain-like apoplastic protease. *Plant Physiology,* 143, 364-377.

Tippett, J. T., Holland, A., Marks, G. & O'brien, T. (1976). Penetration of *Phytophthora cinnamomi* into disease tolerant and susceptible eucalypts. *Archives of Microbiology,* 108, 231-242.

Tivoli, B., Baranger, A., Avila, C. M., Banniza, S., Barbetti, M., Chen, W., Davidson, J., Lindeck, K., Kharrat, M. & Rubiales, D. (2006). Screening techniques and sources of resistance to foliar diseases caused by major necrotrophic fungi in grain legumes. *Euphytica,* 147, 223-253.

Tomsig, J. L., Snyder, S. L. & Creutz, C. E. (2003). Identification of targets for calcium signaling through the copine family of proteins characterization of a coiled-coil copine-binding motif. *Journal of Biological Chemistry,* 278, 10048-10054.

Tooley, P., Bunyard, B., Carras, M. & Hatziloukas, E. (1997). Development of PCR primers from internal transcribed spacer region 2 for detection of *Phytophthora* species infecting potatoes. *Applied and Environmental Microbiology,* 63, 1467-1475.

Torto-Alalibo, T., Li, S., Styer, A., Huitema, E., Testa, A., Gow, N. A., Van West, P. & Kamoun, S. (2003). EST mining and functional expression assays identify extracellular effector proteins from the plant pathogen *Phytophthora*. *Genome Research,* 13, 1675-1685.

Torto-Alalibo, T., Rauser, L. & Kamoun, S. (2002). The pipg1 gene of the oomycete *Phytophthora infestans* encodes a fungal-like endopolygalaturonase. *Current Genetics,* 40, 385-390.

Trapero-Casas, A., Rodriguez-Tello, A. & Kaiser, W. (2000). Lupins, a new host of *Phytophthora erythroseptica*. *Plant Disease,* 84, 488-488.

Trotta, A., Varese, G., Gnavi, E., Fusconi, A., Sampo, S. & Berta, G. (1996). Interactions between the soilborne root pathogen *Phytophthora nicotianae* var. *parasitica* and the arbuscular mycorrhizal fungus *Glomus mosseae* in tomato plants. *Plant and Soil,* 185, 199-209.

Tsuji, H., Nakazono, M., Saisho, D., Tsutsumi, N. & Hirai, A. (2000). Transcript levels of the nuclear-encoded respiratory genes in rice decrease by oxygen deprivation: evidence for involvement of calcium in expression of the alternative oxidase 1a gene. *FEBS Letters,* 471, 201-204.

Türkölmez, Ş., Çiftçi, O., Ulubaş Serçe, Ç. & Derviş, S. (2015). First report of Phytophthora crown and root rot of cherry caused by *Phytophthora palmivora* in eastern Turkey. *Canadian Journal of Plant Pathology,* 37, 390-396.

Tyagi, R., Lee, Y. T., Guddat, L. W. & Duggleby, R. G. (2005). Probing the mechanism of the bifunctional enzyme ketol-acid reductoisomerase by site-directed mutagenesis of the active site. *FEBS Journal,* 272, 593-602.

Tyler, B. M. (2002). Molecular basis of recognition between Phytophthora pathogens and their hosts. *Annual Review of Phytopathology,* 40, 137-167.

Tyler, B. M. (2007). *Phytophthora sojae*: root rot pathogen of soybean and model oomycete. *Molecular Plant Pathology,* 8, 1-8.

Tynan, K., Wilkinson, C., Holmes, J., Dell, B., Colquhoun, I., Mccomb, J. & Hardy, G. E. S. J. (2001). The long-term ability of phosphite to control *Phytophthora cinnamomi* in two native plant communities of Western Australia. *Australian Journal of Botany,* 49, 761-770.

Underwood, W. (2012). The plant cell wall: a dynamic barrier against pathogen invasion. *Frontiers in Plant Science,* 3, 1-6.

Ünligil, U. M. & Rini, J. M. (2000). Glycosyltransferase structure and mechanism. *Current Opinion in Structural Biology,* 10, 510-517.

Utkhede, R. (1986). In vitro screening of the world apple germplasm collection for resistance to *Phytophthora cactorum* crown rot. *Scientia Horticulturae,* 29, 205-210.

Valderrama, R., Corpas, F. J., Carreras, A., Gomez-Rodriguez, M. V., Chaki, M., Pedrajas, J. R., Fernandez-Ocaña, A., Del Rio, L. A. & Barroso, J. B. (2006). The dehydrogenase-mediated recycling of NADPH is a key antioxidant system against salt-induced oxidative stress in olive plants. *Plant, Cell & Environment,* 29, 1449-1459.

Van Jaarsveld, E., Wingfield, M. & Drenth, A. (2003). A rapid seedling based screening technique to assay tobacco for resistance to *Phytophthora nicotianae*. *Journal of Phytopathology,* 151, 389-394.

Van Kan, J. A. (2006). Licensed to kill: the lifestyle of a necrotrophic plant pathogen. *Trends in Plant Science,* 11, 247-253.

Van Munster, J. M., Daly, P., Delmas, S., Pullan, S. T., Blythe, M. J., Malla, S., Kokolski, M., Noltorp, E. C., Wennberg, K. & Fetherston, R. (2014). The role of carbon starvation in the induction of enzymes that degrade plant-derived carbohydrates in *Aspergillus niger*. *Fungal Genetics and Biology,* 72, 34-47.

Vanlerberghe, G. C. (2013). Alternative oxidase: a mitochondrial respiratory pathway to maintain metabolic and signaling homeostasis during abiotic and biotic stress in plants. *International Journal of Molecular Sciences,* 14, 6805-6847.

Varner, J. E. & Lin, L.-S. (1989). Plant cell wall architecture. *Cell,* 56, 231-239.

Vasudevan, K., Cruz, C. M. V., Gruissem, W. & Bhullar, N. K. (2014). Large scale germplasm screening for identification of novel rice blast resistance sources. *Frontiers in Plant Science,* 5, doi:10.3389/fpls.2014.00505.

Velasquez, S. M., Ricardi, M. M., Dorosz, J. G., Fernandez, P. V., Nadra, A. D., Pol-Fachin, L., Egelund, J., Gille, S., Harholt, J. & Ciancia, M. (2011). O-glycosylated cell wall proteins are essential in root hair growth. *Science,* 332, 1401-1403.

Veneault-Fourrey, C., Kohler, A., Morin, E., Balestrini, R., Plett, J., Danchin, E., Coutinho, P., Wiebenga, A., De Vries, R. P. & Henrissat, B. (2014). Genomic and transcriptomic analysis of *Laccaria bicolor* CAZome reveals insights into polysaccharides remodelling during symbiosis establishment. *Fungal Genetics and Biology,* 72, 168-181.

Vigo, C., Norman, J. & Hooker, J. (2000). Biocontrol of the pathogen *Phytophthora parasitica* by arbuscular mycorrhizal fungi is a consequence of effects on infection loci. *Plant Pathology,* 49, 509-514.

Vincken, J.-P., Schols, H. A., Oomen, R. J., Mccann, M. C., Ulvskov, P., Voragen, A. G. & Visser, R. G. (2003). If homogalacturonan were a side chain of

rhamnogalacturonan I. Implications for cell wall architecture. *Plant Physiology,* 132, 1781-1789.

Vleeshouwers, V. G., Raffaele, S., Vossen, J. H., Champouret, N., Oliva, R., Segretin, M. E., Rietman, H., Cano, L. M., Lokossou, A. & Kessel, G. (2011). Understanding and exploiting late blight resistance in the age of effectors. *Annual Review of Phytopathology,* 49, 507-531.

Vleeshouwers, V. G., Van Dooijeweert, W., Keizer, L. P., Sijpkes, L., Govers, F. & Colon, L. T. (1999). A laboratory assay for *Phytophthora infestans* resistance in various *Solanum* species reflects the field situation. *European Journal of Plant Pathology,* 105, 241-250.

Vogel, J. (2008). Unique aspects of the grass cell wall. *Current Opinion in Plant Biology,* 11, 301-307.

Voigt, C. A. (2014). Callose-mediated resistance to pathogenic intruders in plant defense-related papillae. *Frontiers in Plant Science,* 5, 168.

Vorwerk, S., Somerville, S. & Somerville, C. (2004). The role of plant cell wall polysaccharide composition in disease resistance. *Trends in Plant Science,* 9, 203-209.

Walker, C. A. & Van West, P. (2007). Zoospore development in the oomycetes. *Fungal Biology Reviews,* 21, 10-18.

Wan, J., Dunning, M. F. & Bent, A. F. (2002). Probing plant-pathogen interactions and downstream defense signaling using DNA microarrays. *Functional & Integrative Genomics,* 2, 259-273.

Wang, D., Guo, Y., Wu, C., Yang, G., Li, Y. & Zheng, C. (2008). Genome-wide analysis of CCCH zinc finger family in Arabidopsis and rice. *BMC Genomics,* 9, 44.

Wang, M., Weiberg, A. & Jin, H. (2015). Pathogen small RNAs: a new class of effectors for pathogen attacks. *Molecular Plant Pathology,* 16, 219-223.

Wang, Y., Chantreau, M., Sibout, R. & Hawkins, S. (2013). Plant cell wall lignification and monolignol metabolism. *Frontiers in Plant Science,* 4, 220.

Wang, Y., Dou, D., Wang, X., Li, A., Sheng, Y., Hua, C., Cheng, B., Chen, X., Zheng, X. & Wang, Y. (2009a). The PsCZF1 gene encoding a C 2 H 2 zinc finger protein is required for growth, development and pathogenesis in *Phytophthora sojae*. *Microbial Pathogenesis,* 47, 78-86.

Wang, Y., Li, A., Wang, X., Zhang, X., Zhao, W., Dou, D., Zheng, X. & Wang, Y. (2010). GPR11, a putative seven-transmembrane G protein-coupled receptor, controls zoospore development and virulence of *Phytophthora sojae*. *Eukaryotic Cell,* 9, 242-250.

Wang, Y., Meng, Y., Zhang, M., Tong, X., Wang, Q., Sun, Y., Quan, J., Govers, F. & Shan, W. (2011). Infection of *Arabidopsis thaliana* by *Phytophthora parasitica* and identification of variation in host specificity. *Molecular Plant Pathology,* 12, 187-201.

Wang, Z., Gerstein, M. & Snyder, M. (2009b). RNA-Seq: a revolutionary tool for transcriptomics. *Nature Reviews Genetics,* 10, 57-63.

Wanjiru, W. M., Zhensheng, K. & Buchenauer, H. (2002). Importance of cell wall degrading enzymes produced by *Fusarium graminearum* during infection of wheat heads. *European Journal of Plant Pathology,* 108, 803-810.

Ward, J. A., Ponnala, L. & Weber, C. A. (2012). Strategies for transcriptome analysis in nonmodel plants. *American Journal of Botany,* 99, 267-276.

Ware, A. (2014). Lupin variety sowing guide 2014. [Accessed 03 July 2014].

Way, H. M., Kazan, K., Goulter, K. C., Birch, R. G. & Manners, J. M. (2000). Expression of the Shpx2 peroxidase gene of *Stylosanthes humilis* in transgenic tobacco leads to enhanced resistance to *Phytophthora parasitica* pv. *nicotianae* and *Cercospora nicotianae*. *Molecular Plant Pathology,* 1, 223-232.

Weiland, J. (2015). First report of *Phytophthora cactorum* and *P. citrophthora* causing root rot of *Ribes lobbii* in Oregon. *Plant Disease,* 99, 157-157.

Weir, B. S., Paderes, E. P., Anand, N., Uchida, J. Y., Pennycook, S. R., Bellgard, S. E. & Beever, R. E. (2015). A taxonomic revision of *Phytophthora* Clade 5 including two new species, *Phytophthora agathidicida* and *P. cocois*. *Phytotaxa,* 205, 21-38.

Weltmeier, F., Mäser, A., Menze, A., Hennig, S., Schad, M., Breuer, F., Schulz, B., Holtschulte, B., Nehls, R. & Stahl, D. J. (2011). Transcript profiles in sugar beet genotypes uncover timing and strength of defense reactions to *Cercospora beticola* infection. *Molecular Plant-Microbe Interactions,* 24, 758-772.

Werres, S., Hahn, R. & Themann, K. (1997). Application of different techniques to detect *Phytophthora* spp. in roots of commercially produced *Chamaecyparis lawsoniana*. *Journal of Plant Disease Protection,* 104, 474-482.

Weste, G. (1975). The distribution of *Phytophthora cinnamomi* within the National Park, Wilson's Promontory, Victoria. *Australian Journal of Botany,* 23, 67-76.

Weste, G. Disease caused by *Phytophthora* in Australia and its impact on native forests, woodlands and heathlands. *In:* Cohen, S. D. & Juzwik, J., eds. Sudden Oak Death Symposium, 2003 April 21-May 12 2003 St. Paul, MN. U.S. Department of Agriculture, Forest Service, North Central Research Station, 108.

Weste, G., Cooke, D. & Taylor, P. (1973). The invasion of native forest by *Phytophthora cinnamomi.* II. Post-infection vegetation patterns, regeneration, decline in inoculum and attempted control. *Australian Journal of Botany,* 21, 13-29.

Weste, G. & Marks, G. (1987). The biology of *Phytophthora cinnamomi* in Australasian forests. *Annual Review of Phytopathology,* 25, 207-229.

Whisson, S. C., Boevink, P. C., Moleleki, L., Avrova, A. O., Morales, J. G., Gilroy, E. M., Armstrong, M. R., Grouffaud, S., Van West, P. & Chapman, S. (2007). A translocation signal for delivery of oomycete effector proteins into host plant cells. *Nature,* 450, 115-118.

Wi, S. J., Ji, N. R. & Park, K. Y. (2012). Synergistic biosynthesis of biphasic ethylene and reactive oxygen species in response to hemibiotrophic *Phytophthora parasitica* in tobacco plants. *Plant Physiology,* 159, 251-265.

Wicks, T. & Hall, B. (1990). Control of *Phytophthora* canker with phosphonate in artificially inoculated almond and cherry trees. *Animal Production Science,* 30, 413-420.

Widmer, T. L. (2014). Screening *Trichoderma* species for biological control activity against *Phytophthora ramorum* in soil. *Biological Control,* 79, 43-48.

Wilhelm, J., Pingoud, A. & Hahn, M. (2003). Real-time PCR-based method for the estimation of genome sizes. *Nucleic Acids Research,* 31, e56-e56.

Wilkinson, C., Holmes, J., Dell, B., Tynan, K., Mccomb, J., Shearer, B., Colquhoun, I. & Hardy, G. S. J. (2001a). Effect of phosphite on in planta zoospore production of *Phytophthora cinnamomi*. *Plant Pathology,* 50, 587-593.

Wilkinson, C., Holmes, J., Tynan, K., Colquhoun, I., Mccomb, J., Hardy, G. E. S. J. & Dell, B. (2001b). Ability of phosphite applied in a glasshouse trial to control *Phytophthora cinnamomi* in five plant species native to Western Australia. *Australasian Plant Pathology,* 30, 343-351.

Wilkinson, C., Shearer, B., Jackson, T. & Hardy, G. S. J. (2001c). Variation in sensitivity of Western Australian isolates of *Phytophthora cinnamomi* to phosphite *in vitro*. *Plant Pathology,* 50, 83-89.

Willats, W. G., Gilmartin, P. M., Mikkelsen, J. D. & Knox, J. P. (1999). Cell wall antibodies without immunization: generation and use of de-esterified homogalacturonan block-specific antibodies from a naive phage display library. *Plant Journal,* 18, 57-65.

Willats, W. G., Mccartney, L., Mackie, W. & Knox, J. P. (2001). Pectin: cell biology and prospects for functional analysis. *Plant Molecular Biology,* 47, 9-27.

Willekens, H., Inzé, D., Van Montagu, M. & Van Camp, W. (1995). Catalases in plants. *Molecular Breeding,* 1, 207-228.

Williamson, P., Sivasithamparam, K. & Cowling, W. (1991). Formation of subcuticular coralloid hyphae by *Phomopsis leptostromiformis* upon latent infection of narrow-leafed lupins. *Plant Disease,* 75, 1023-1026.

Wong, M.-H. (2006). *Phosphite induces morphological and molecular changes in Phytophthora species.* MPhil Thesis, Murdoch University, Perth. 129.

Wong, M. H., Mccomb, J., Hardy, G. E. S. J. & Brien, P. a. O. (2009). Phosphite induces expression of a putative proteophosphoglycan gene in *Phytophthora cinnamomi*. *Australasian Plant Pathology,* 38, 235-241.

Wösten, H. A., Moukha, S. M., Sietsma, J. H. & Wessels, J. G. (1991). Localization of growth and secretion of proteins in *Aspergillus niger*. *Journal of General Microbiology,* 137, 2017-2023.

Xiang, Q. & Judelson, H. S. (2010). Myb transcription factors in the oomycete *Phytophthora* with novel diversified DNA-binding domains and developmental stage-specific expression. *Gene,* 453, 1-8.

Xiang, Q. & Judelson, H. S. (2014). Myb transcription factors and light regulate sporulation in the oomycete *Phytophthora infestans*. *PLoS ONE,* 9, e92086.

Xiao, K., Kinkel, L. L. & Samac, D. A. (2002). Biological control of Phytophthora root rots on alfalfa and soybean with Streptomyces. *Biological Control,* 23, 285-295.

Yan, H.-Z. & Liou, R.-F. (2005). Cloning and analysis of pppg1, an inducible endopolygalacturonase gene from the oomycete plant pathogen *Phytophthora parasitica*. *Fungal Genetics and Biology,* 42, 339-350.

Yan, H. Z. & Liou, R. F. (2006). Selection of internal control genes for real-time quantitative RT-PCR assays in the oomycete plant pathogen *Phytophthora parasitica*. *Fungal Genetics and Biology,* 43, 430-438.

Yang, Zhao, W., Hua, C., Zheng, X., Jing, M., Li, D., Govers, F., Meijer, H. & Wang, Y. (2013a). Chemotaxis and oospore formation in *Phytophthora sojae* are controlled by G-protein-coupled receptors with a phosphatidylinositol phosphate kinase domain. *Molecular Microbiology,* 88, 382-394.

Yang, H., Boersma, J. G., You, M., Buirchell, B. J. & Sweetingham, M. W. (2004). Development and implementation of a sequence-specific PCR marker linked to a gene conferring resistance to anthracnose disease in narrow-leafed lupin (*Lupinus angustifolius* L.). *Molecular Breeding,* 14, 145-151.

Yang, H. & Sweetingham, M. (1998). Taxonomy of *Colletotrichum* isolates associated with lupin anthracnose. *Australian Journal of Agricultural Research,* 49, 1213-1224.

Yang, H., Sweetingham, M. & Cowling, W. (1996). The leaf infection process and resistance to *Pleiochaeta setosa* in three lupin species. *Crop and Pasture Science,* 47, 787-799.

Yang, H., Tao, Y., Zheng, Z., Shao, D., Li, Z., Sweetingham, M. W., Buirchell, B. J. & Li, C. (2013b). Rapid development of molecular markers by next-generation sequencing linked to a gene conferring phomopsis stem blight disease resistance for marker-assisted selection in lupin (*Lupinus angustifolius* L.) breeding. *Theoretical and Applied Genetics,* 126, 511-522.

Yang, X., Tyler, B. M. & Hong, C. (2017). An expanded phylogeny for the genus *Phytophthora*. *IMA Fungus,* 8, 355-398.

You, M. K., Shin, H. Y., Kim, Y. J., Ok, S. H., Cho, S. K., Jeung, J. U., Yoo, S. D., Kim, J. K. & Shin, J. S. (2010). Novel bifunctional nucleases, OmBBD and AtBBD1, are involved in abscisic acid-mediated callose deposition in Arabidopsis. *Plant Physiology,* 152, 1015-1029.

Yu, X., Liu, X., Wang, P. & Wang, Y. (2015). First report of cherry stem rot and leaf necrosis disease caused by *Phytophthora nicotianae* in Yantai, China. *Plant Disease,* 99, 284-284.

Zenoni, S., Ferrarini, A., Giacomelli, E., Xumerle, L., Fasoli, M., Malerba, G., Bellin, D., Pezzotti, M. & Delledonne, M. (2010). Characterization of transcriptional complexity during berry development in *Vitis vinifera* using RNA-Seq. *Plant Physiology,* 152, 1787-1795.

Zentmyer, G. (1979). Report on Phytophthora root rot of Avocado in South Africa. *South African Avocado Growers' Association Yearbook* 3, 7-9.

Zerillo, M. M., Adhikari, B. N., Hamilton, J. P., Buell, C. R., Lévesque, C. A. & Tisserat, N. (2013). Carbohydrate-active enzymes in *Pythium* and their role in plant cell wall and storage polysaccharide degradation. *PLoS ONE,* 8, e72572.

Zhang, L. & Kan, J. A. (2013). *Botrytis cinerea* mutants deficient in d-galacturonic acid catabolism have a perturbed virulence on *Nicotiana benthamiana* and Arabidopsis, but not on tomato. *Molecular Plant Pathology,* 14, 19-29.

Zhang, M., Li, Q., Liu, T., Liu, L., Shen, D., Zhu, Y., Liu, P., Zhou, J.-M. & Dou, D. (2015). Two cytoplasmic effectors of *Phytophthora sojae* regulate plant cell death via interactions with plant catalases. *Plant Physiology,* 167, 164-175.

Zhang, W., Blackman, L. M. & Hardham, A. R. (2013). Transient fusion and selective secretion of vesicle proteins in *Phytophthora nicotianae* zoospores. *PeerJ,* 1, e221.

Zhao, Q. & Dixon, R. A. (2011). Transcriptional networks for lignin biosynthesis: more complex than we thought? *Trends in Plant Science,* 16, 227-233.

Zhao, Q. & Dixon, R. A. (2014). Altering the cell wall and its impact on plant disease: from forage to bioenergy. *Annual Review of Phytopathology,* 52, 69-91.

Zhao, Z., Liu, H., Wang, C. & Xu, J.-R. (2013). Comparative analysis of fungal genomes reveals different plant cell wall degrading capacity in fungi. *BMC Genomics,* 14, 274.

Zheng, A., Lin, R., Zhang, D., Qin, P., Xu, L., Ai, P., Ding, L., Wang, Y., Chen, Y. & Liu, Y. (2013). The evolution and pathogenic mechanisms of the rice sheath blight pathogen. *Nature Communications,* 4, 1424.

Ziegler, E. & Pontzen, R. (1982). Specific inhibition of glucan-elicited glyceollin accumulation in soybeans by an extracellular mannan-glycoprotein of *Phytophthora megasperma* f. sp. *glycinea*. *Physiological Plant Pathology,* 20, 321-331.

Zimnoch-Guzowska, E., Lebecka, R., Kryszczuk, A., Maciejewska, U., Szczerbakowa, A. & Wielgat, B. (2003). Resistance to *Phytophthora infestans* in somatic hybrids of *Solanum nigrum* L. and diploid potato. *Theoretical and Applied Genetics,* 107, 43-48.

Zinati, G. M. (2015). Compost in the 20th century: a tool to control plant diseases in nursery and vegetable crops. *HortTechnology,* 15, 61-66.

Zou, B., Hong, X., Ding, Y., Wang, X., Liu, H. & Hua, J. (2016). Identification and analysis of copine/BONZAI proteins among evolutionarily diverse plant species. *Genome,* 59, 565-573.

Zuluaga, A. P., Vega-Arreguín, J. C., Fei, Z., Ponnala, L., Lee, S. J., Matas, A. J., Patev, S., Fry, W. E. & Rose, J. K. (2016). Transcriptional dynamics of *Phytophthora infestans* during sequential stages of hemibiotrophic infection of tomato. *Molecular Plant Pathology,* 17, 29-41.

APPENDICES

Appendix I

Media and buffers preparation

a) Media for *Phytophthora* growth

Clarified V8 Juice

V8 vegetable juice (Campbell Soup Co., Camden, NJ, USA) was centrifuged at 8,000 g for 10 min at 4˚C and then filtered through GFA filter paper (Millipore). The cleared V8 juice was stored in -20˚C until use.

10% V8 Agar

Reagent	Quantity	Manufacturer
Clarified V8 Juice (above)	100 ml	Campbell Soup Co.
β-sitosterol	0.02 g	MP Biomedicals Inc.
$CaCO_3$	0.1 g	Univar
Bacto agar	17 g	Bacto
Distilled water	~900 ml	

The pH was adjusted to 6.3 with 10 M sodium hydroxide. Agar was sterilised by autoclaving at 121˚C for 20 min and poured into 90 mm diameter Petri dishes. The plates were stored at 4˚C in plastic bags until use.

5% V8 Broth

Reagent	Quantity	Manufacturer
Clarified V8 Juice (above)	50 ml	Campbell Soup Co.
$CaCO_3$	0.1 g	Univar
β-sitosterol	0.02 g	MP Biomedicals Inc.
Distilled water	~950 ml	

The pH was adjusted to 6.3 with 10 M sodium hydroxide. Broth was sterilised by autoclaving at 121˚C for 20 min.

Mineral Salts Solution

Stock Solution A

Reagent	Quantity	Manufacturer
1 M KNO_3	101.10 g	Sigma-Aldrich
2 M $Ca(NO_3)_2$	328.18 g	Sigma-Aldrich
Distilled water	1000 ml	

Stock Solution B

Reagent	Quantity	Manufacturer

0.8M $MgSO_4$	240.73 g	Sigma-Aldrich
Distilled water	1000 ml	

7.5 ml of each stock (A and B) was added to 1.5 l distilled water, autoclaved at 121˚C for 20 min and stored at 4˚C until use. Stock solutions were brought to room temperature before using and added with 3 ml of filter-sterilised chelated iron solutions in sterile condition.

Chelated Iron Solution

Reagent	Quantity	Manufacturer
10mM $FeSO_4 \cdot 7H_2O$	1.39 g	Sigma-Aldrich
10mM Na_2EDTA	1.86 g	Sigma-Aldrich
Distilled water	1000 ml	

$FeSO_4$ and Na_2EDTA were added to distilled water gently stirring on a hot plate until colour has turned yellow. Solution was stored at 4°C until use.

b) Modified Ribeiro's Medium

9% Glucose Stock Solution (Carbon Source)

Reagent	Quantity	Manufacturer
D-Glucose	90 g	Sigma-Aldrich
Distilled water	1000 ml	

Glucose stock solution (9%) was prepared and autoclaved at 121°C for 20 mins and stored at room temperature until use.

Micronutrient Stock Solution

Reagent	Quantity	Manufacturer
$Na_2MoO_4.2H_2O$	41.1 mg	BDH Chemicals
$ZnSO_4.7H_2O$	87.8 mg	BDH Chemicals
$CuSO_4.5H_2O$	7.85 mg	BDH Chemicals
$MnSO_4.H_2O$	15.4 mg	APS
$Na_2B_4O_7$	0.5 mg	BDH
Distilled water	100 ml	

Micronutrient stock solution was prepared and autoclaved at 121°C for 20 mins and stored at room temperature until use.

Thiamine Stock Solution

Reagent	Quantity	Manufacturer
Thiamine-HCl	100 mg	Sigma-Aldrich
Distilled water	100 ml	

Thiamine stock solution was filter sterilised through a 0.22 µm filter before adding to final medium.

Ferric Stock Solution

Reagent	Quantity	Manufacturer
$FeCl_3.6H_2O$	50 mg	Sigma-Aldrich
EDTA	2.6 g	Sigma-Aldrich
KOH	1.5 g	Sigma-Aldrich

Distilled water	100 ml

Iron chelate stock solution was filter sterilised through a 0.22 µm filter before adding to final medium.

Basal Media

Reagent	Quantity	Manufacturer
L-Asparagine	0.1 g	Sigma-Aldrich
KNO_3	0.15 g	Sigma-Aldrich
KH_2PO_4	0.034 g	Sigma-Aldrich
$MgSO_4.7H_2O$	0.5 g	Sigma-Aldrich
$CaCl_2.2H_2O$	0.13 g	Sigma-Aldrich
HEPES	2.38 g	Sigma-Aldrich
Micronutrient stock solution	1 ml	
Ferric stock solution	1 ml	
Distilled water to final volume	950 ml	

The pH was adjusted to 6.3. Agar was sterilised by autoclaving at 121˚C for 20 min and poured into 90 mm diameter Petri dishes.

Final growth medium

Basal medium was dispensed into 180 ml aliquots in 500 ml flasks. Each flask was added with 3.4 g agar. Filter-sterilised thiamine stock solution (0.2 ml) was added to each flask and autoclaved at 121˚C for 20 min. The 9% glucose stock solution (20 ml) was added to each flask.

Phosphite treatments

10% (10 g/100 ml) Phosphite Stock Solution

Reagent	Quantity	Manufacturer
Phosphorous acid (H_3PO_3) 99%	10.1 g	Sigma-Aldrich
Distilled water	70 ml	

The pH was adjusted to 6.3 with KOH. 100 ml solution was made up and filter sterilised through a 0.22 µm filter. The solution was stored in the dark at 4°C.

For growth experiments on solid media

- Appropriate amount of phosphite stock solution was added to each 180 ml aliquot.

For RNA extractions

- *Phytophthora* mycelia were grown in liquid culture media
- Final growth medium was prepared as above but lacking agar
- Glucose stock solution and appropriate amount of phosphite stock solution was added to each aliquot.

c) Staining solutions and buffer

Iodine-Potassium Iodide Solution (IKI)

Reagent	Quantity	Manufacturer
Potassium iodide	2 g	Sigma-Aldrich
Iodine	0.2 g	Sigma-Aldrich
Distilled water	100 ml	

2 g of potassium iodide was dissolved in 100 ml water. Once dissolved, 0.2 g of iodine was added and dissolved. IKI solution stains starch.

Jensen, W. A. 1962. Botanical histochemistry: principles and practice. W.H. Freeman and Co. San Francisco, USA.

Trypan blue stain

Reagent	Quantity	Manufacturer
Lactic acid	10 ml	Sigma-Aldrich
Glycerol	10 ml	Sigma-Aldrich
Phenol	10 g	Sigma-Aldrich
Trypan blue	10 mg	Sigma-Aldrich
Distilled water	10 ml	

Phosphate-Buffered Saline (PBS)

Reagent	Quantity	Manufacturer
Na_2HPO_4	11.44 g	Sigma-Aldrich
NaH_2PO_4	1.25 g	Sigma-Aldrich
NaCl	17.53 g	Sigma-Aldrich
Distilled water	1000 ml	

Appendix II

Primer Sequences

WS021 pair

WS21F Sequence	5’ TGGTGCGTCTGATGGAAC
WS21R Sequence	5’ GCCTTTATTCTGCGTCGTC
NCBI Accession number	CF891675

WS041 pair qPCR

WS41qF Sequence	5’ CACGTACACATGCCCGAGAC
WS41qR Sequence	5’ TTCCCATGTAGGCCGAGTATTC
NCBI Accession number	CF891677

LaNIT4 pair qPCR

LaNIT4qF Sequence	5’ TCCAGACTCCAGAAGCAGA
LaNIT4qR Sequence	5’ AAGCACCACACCAAAACTACA
NCBI Accession number	AAT36331

PnPG1 (PPTG_15162.1) pair qPCR

PnPG1qF Sequence	5’ TGAGCAGAAACAACCACG
PnPG1qR Sequence	5’ TGACCAGCAGACCAGAGAC

PnPG5 (PPTG_15173.1) pair qPCR

PnPG5qF Sequence	5’ GTTACCATCACGGACATCACC
PnPG5qR Sequence	5’ TTGCTGCTTTACGCTACTCTC

PnPG6 (PPTG_17704.1) pair qPCR

PnPG6qF Sequence	5’ TGGCGGTCACGGTATCTC

PnPG6qR Sequence	5’ CCTCCTTTTTCCTTGCTGTAGTC

PnPG8 (PPTG_15179.1) pair qPCR

PnPG8qF Sequence	5’ TCAGTCGTCCCGTCTTCTTC
PnPG8qR Sequence	5’ AGCCGTCCGTTCTTGG

PME26a (PPTG_05287.1) pair qPCR

PME26a F Sequence	5’ CGCACCGATAACTCAAACC
PME26a R Sequence	5’ TGTCACCGTTCCACTTCTG

PME45 (PPTG_10338.1) pair qPCR

PME45 F Sequence	5’ GCTGTGGATTTCGTCTTTGG
PME45 R Sequence	5’ GGTTAGCCGTGTTGTTGTCTC

Xy2.75 (PPTG_17851.1) pair qPCR

Xy2.75 F Sequence	5’ TGTCCAACCACATTACCAAGG
Xy2.75 R Sequence	5’ ACGCCTTCAACCCAAATC

Cel2.6 (PPTG_19337.1) pair qPCR

Cel2.6 F Sequence	5’ CACTTCGGACCCTAATACTGC
Cel2.6 R Sequence	5’ CCTGCCTTGACCATAACCTC

Appendix Tables

Appendix Table 2.1. Parameters used in infection assays for *P. parasitica*

Host plant species	Plant organ	Inoculation method	Detection system	Purpose of assay	Results/Problems	Reference
Arabidopsis	seedlings	Arabidopsis seeds were sterilised and deposited in 6-well multiplates and (Larroque *et al.*, 2013)were inoculated with 4 ml of *P. parasitica* zoospores (1000 cells/ml)	qPCR, symptom-index, Luminescence was measured using a digital luminometer	Investigated the role of cellulose binding elicitor lectin (CBEL) - triggered immunity in the *P. parasitica*–*Arabidopsis* interaction	Results show that CBEL-triggered immunity required BAK1 and RBOH (respiratory burst oxidase homologue), which also control resistance to the non-adapted *P. parasitica* Ppn0 strain	(Larroque *et al.*, 2013)
Arabidopsis	roots	Live root tissues were inoculated by dipping into a zoospore suspension (10^5 spores/ml) for 5 s	Scanning electron microscopy and interference contrast microscopy	Investigated the infection process of *A. thaliana* by *P. parasitica*	Water-soaked lesions developed on leaves 3 dpi and sporangia formed within 5 dpi. *P. parasitica* developed appressoria-like swellings and penetrated epidermal cells directly and preferably at the junction between anticlinal host cell walls.	(Wang *et al.*, 2011)
Citrus cvs (orange, citrange, citrumelo, mandarin, and lemon)	roots	Root pruning and soil sampling (greenhouse and field evaluation)	Plating method and ELISA	Determined the varying tolerance of citrus rootstocks to Phytophthora root rot	Tolerance of citrus cvs to root rot is expressed on its capability to generate roots (e.g. lemon) or the limitation of conversion of infection to propagules (e.g. orange)	(Graham, 1995)

Appendix Table 2.1. Cont.

Tobacco	shoots	Tobacco shoots with four to five leaves were inoculated directly with a pathogen plug (1 cm in diameter)	qPCR, Ultra performance liquid chromato-graphy quadrupole time-of-flight mass spectrometry (UPLC-QTOF-MS) analysis	Investigated the interactive effect of ROS and ethylene signalling on the metabolic responses associated with defence and/or susceptible responses of tobacco to *Ppn*	Nicotine and phenylpropanoid−polyamin e conjugates and two bis(dihydrocaffeoyl)−spermine isomers, and their intermediates were present at lower levels in *Ein3-AS* transgenic plants during *Ppn* interaction than in WT, whereas galactolipid and oxidized free fatty acid levels were higher in *Ein3-AS* transgenic plants	(Cho *et al.*, 2013)
Tobacco	roots, stem, leaves	**Roots** -single oat grain was placed into each of four separate 5-cm-deep holes **Stem**-inoculated with pathogen-infested toothpicks 5 to 6 WAT **Leaf**- inoculated at two or four locations with 40 µl aliquot of suspension containing 100 zoospores/µl	Disease severity index and percent root rot	Quantified the components of resistance in roots of double haploid (DH) lines derived from resistant parent Beinhart 1000 (BH) and determined if resistance, conferred by quantitative trait loci (QTL) on linkage groups (LGs) is expressed in stem and leaf tissues	**Root resistance-** Moderate to high levels of disease developed in all DH groups and parental lines (high level of resistance) **Stem resistance-** All genotypes developed stem lesions, which were first observed 2 days after inoculation (low resistance) **Leaf resistance**- Leaf lesions developed in all DH groups and parental lines (no resistance)	(McCorkle *et al.*, 2013)

Appendix Table 2.1. Cont.

Tobacco	leaves	Tobacco shoots with four to five leaves were inoculated directly with a pathogen plug (1 cm in diameter)	fluorescence was detected by spectrofluoro-photometer -ethylene content was determined by gas chromate-graphy - transcripts analysis by qPCR	Investigated the biphasic ROS and ethylene production during the defence response against *Ppn* in susceptible tobacco	The initial transient increase in ROS and ethylene at 1 and 3 h (phase I), respectively, followed by a second massive increase at 48 and 72 h (phase II), respectively, after pathogen inoculation. Ethylene and ROS levels relates with compatible *Ppn* spread in susceptible plants	(Wi *et al.*, 2012)
Tobacco	**seedlings**-3-week-old **adult plants**-8-week-old	**Seedlings** – root immersion in 60ml sdH_2O with 7.2×10^4 zoospores/ml **Adult plants**-inoculated by removing the cambium from the stems and a *P. parasitica* disc of agar was placed into the wound	Disease severity	Developed an improved and rapid technique that could also be used to characterize races of *P. parasitica*	A strong positive correlation was found between results of the seedling assay and adult plant trials for all isolates and cvs tested	(Van Jaarsveld *et al.*, 2003)
Tobacco	leaf	Mycelial plugs (detached-leaf technique)	Lesion development; Percent infection	Developed a screening technique for the evaluation of black shank resistance at an early growth stage	The technique is quick, repeatable, and non-destructive, and can be used in combination with other pathogens but was not effective in detecting race-specific resistance derived from *Nicotiana longiflora*	(Tedford *et al.*, 1990)

Appendix Table 2.1. Cont.

Tobacco	seedling	Spraying with 10^4-10^5 zoospores/ml	Percent infection; Disease severity	Developed a rapid means of evaluating young tobacco seedlings for black shank resistance	The concentration of 10^4 zoospores/ml gave a resistance index for all cvs and places about eight viable zoospores on or near each seedling	(McIntyre and Taylor, 1976)
Tobacco	roots	Root-dipping in zoospore suspension	Electron microscopy	Examined the significance of cell wall modifications in in tobacco roots infected with *P. parasitica*	Resistant tobacco lines showed a HR response evident in epidermal and cortical cells. Susceptible lines showed changes in advance of the pathogen; swelling of ER, formation of structures on cell wall, increased vesicular activity by the golgi apparatus, and decreased electron density of the vacuoles	(Hanchey and Wheeler, 1971)
Tobacco	stem, leaves	4 mm agar mycelial plug placed on the cut site of decapitated stems and on detached leaves	Peroxidase assays and isozyme analysis, Southern and Northern blot analysis	Established the role of *Shpx2* peroxidase gene in plant defence	The expression of *Shpx2* peroxidase gene in transgenic tobacco leads to increased protection to *Ppn* and *Cercospora nicotianae*	(Way *et al.*, 2000)
Tobacco	seedlings	Each seedling (7-day-old) placed in 96-well microtiter plate was inoculated with 25 µl of 2×10^4 *Ppn* zoospores/ml	Microscopic examination	Developed a rapid microassay for testing potential agents for the control of *Ppn* under hydroponic conditions	Inoculated seedlings of susceptible cv KY14 were infected 72 hpi and *Ppn* produced sporangia on the surfaces of the seedlings. Sporangia did not develop in seedlings added with Metalaxyl or the biocontrol agent, *Bacillus cereus* UW85	(Handelsman *et al.*, 1991)

Appendix Table 2.1. Cont.

Tomato	Roots and shoots	Inoculated at the fourth leaf stage with a nutrient solution containing 5×10^4 propagules of the pathogen per ml	Microscopy, simple PCR, Conventional nested-PCR, One closed tube nested-PCR	Developed conventional and single closed tube nested-PCRs for the specific and sensitive detection of *P. parasitica*	A positive reaction, characterized by an amplification product of 737 bp, was shown by all *P. parasitica* isolates and two *P. parasitica/cactorum* hybrids and no amplification product was observed in other *Phytophthora* spp. and genera	(Grote *et al.*, 2002)
Tomato	roots	Seedlings were grown hydroponically and inoculated with 2×10^6 zoospores	Microscopic examination, dilution plating method; grid intersect method	Determined quantitatively the basis of resistance in one commercial tomato cv and two accessions of *L. esculentum* var. *cerasiforme*	Different types of resistance to *P. parasitica* exist in tomato; less colonisation of roots by *P. parasitica* and inhibition of lesion extension and hyphal growth.	(Blaker and Hewitt, 1987)
Tobacco and Tomato	**tobacco** – stem and roots **tomato** – roots	Tobacco- **Stem -** two mycelial plugs placed to the cut surfaces of decapitated stems **Roots** - Inocation was done by replacing the growth medium with 20 ml of sH_2O added with 100 zoospores Tomato - a mycelium plug (1 cm dia) was placed on the cut extremity of the root system	Restriction fragment length polymorphisms (RFLPs) of both nuclear and mitochondrial DNA (mtDNA)	Investigated the ability *P. parasitica* isolates to infect tobacco and tomato, as related to elicitin production	Black shank isolates can be distinguished from other *P. parasitica* isolates based on genetic criteria. Severe black shank is caused by a limited number of TE– strains. Unexpected absence of elicitin production has precluded population replacements in areas of intensive tobacco cultivation	(Colas *et al.*, 1998)

Appendix Table 2.2. Parameters used in infection assays for *Phytophthora* species apart from *P. parasitica*

Host plant species	*Phytophthora* species	Plant organ	Inoculation method	Detection system	Purpose of assay	Results/Problems	Reference
Avocado	*P. cinnamomi*	Roots	1 h inoculation with 7.2×10^4 zoospores/ml	Nested qPCR	Developed an accurate, low cost assay for *in planta* quantification of *P. cinnamomi* to evaluate disease tolerance	The amount of *P. cinnamomi* quantified in roots was higher in the less-tolerant R0.12 plants than the highly tolerant Dusa plants at all time points	(Engelbrecht *et al.*, 2013)
Lupin and Arabidopsis	*P. cinnamomi*	Lupin - roots Arabidopsis - leaves	**Lupin** - inoculated with 2 mm dia plug of mycelium at roots tips **Arabidopsis**- inoculated with 5 µl of 1×10^5 zoospores/ml on the abaxial surface	qPCR	Developed a sensitive qPCR assay to quantify *P. cinnamomi* at all stages of the necrotrophic pathogen–host interaction	qPCR assay enables quantitative measurement of in planta DNA of *P. cinnamomi*, that avoids problems caused by variation in DNA extraction efficiency and degradation of host DNA during host tissue necrosis	(Eshraghi *et al.*, 2011b)
Lupin and corn/maize	*P. cinnamomi*	Roots	Inoculated with a 20 µl drop of zoospore suspension (1×10^5 spores/ml), placed 5 mm behind the root tip	Plant fresh weight, root length, root lesion length, relative chlorophyll concentra-tion	Used a set of parameters based on measurable, macroscopic observations that are commonly used for disease assessment that would enable characterization of resistance to *P. cinnamomi* under controlled conditions	**Corn** - no significant difference in fresh weight, root length, chlorophyll content and lesion size; pathogen colonisation was limited to the inoculation site **Lupin**- a significant reduction in plant fresh weight and leaf chlorophyll content, root growth cessation, increased lesion lengths and pathogen colonisation	(Allardyce *et al.*, 2012)

Appendix Table 2.2. Cont.

Lupin and corn/maize	*P. cinnamomi*	Roots	Inoculated with 10^4 zoospores/ml	Scanning microscopy	Compared callose production in roots of resistant and susceptible plant in response to *P. cinnamomi.*	Invasion of *P. cinnamomi* resulted in papillae production that contains callose in the resistant maize but not in the susceptible lupin	(Hinch and Clarke, 1982)
Oak trees	*P. ramorum*	Leaves	*Camellia japonica* and *Rhododendron* sp. were infected with two isolates of *P. ramorum* EU2 lineage and one isolate of *P. ramorum* NA2 lineage	RT-PCR	Developed ASOPCR assays for the identification of *P. ramorum* EU2 lineage and validated a combination of ASO-PCR assays for the identification of the four *P. ramorum* lineages	Amplification of the CBEL locus produced a PCR fragment of 650 bp. Sequencing of this fragment produced a 616 bp sequence for all EU2, EU1, NA1 and NA2 isolates. Blind tests revealed diagnostic profiles unique to each lineage.	(Gagnon *et al.*, 2014)
Pea	*P. pisi*	Roots	Root dipping in *P. pisi* (1.2×10^5 zoospores/ml) for 30 min	Microscopic examination, RT-PCR	Established an *in planta* infection system of *P. pisi* on pea and to developed a qPCR method to measure *P. pisi* and pea DNA	Zoospores were attracted to the root tips and encysted within 30 min. At 6 h, *P. pisi* reached five cortical cell layers. RT-PCR showed induction of genes encoding putative enzyme inhibitors at 2 hpi and 6 hpi. Genes encoding putative cysteine protease, glucanase, pleiotropic drug transporter and crinkler proteins were induced during the late phase of infection	(Hosseini *et al.*, 2012)

Appendix Table 2.2. Cont.

Pepper	*P. capsici*	Diseased tissues (stem or leaf)	Inoculated by placing a 50 ml drop of sporangial suspension (10,000 sporangia per ml)	Multiplex PCR and Nested qPCR	Developed a species-specific PCR assay for the detection of *P. capsici* based on the Ras-related protein gene Ypt1	PCR amplification with the species-specific primer pair resulted in products of 364 bp solely from all isolates of *P. capsici*. The detection sensitivity of the species-specific primer pair Pc1F/Pc1R was 10 pg of gDNA	(Lan *et al.*, 2013) and (Tooley *et al.*, 1997) for inoculation method
Potato	*P. infestans*	Potato tissues	Inoculated with 5×10^4 zoospores/ml	ELISA	Investigated the interaction of PiPE, Mycelical Wall Component (MWC) and the Mycelical Homogenate (MH) from *P. infestans* with the His-tagged protein of Ca2+-Dependent Protein Kinase (RiCDPK2) from potato cv. Rishiri (R1-gene)	PiPE, a Phytophthora-associated PAMPS (Pathogen Associated Molecular Patterns), induced generation of active oxygen species and HR by treatment of potato tuber tissues	(Furuichi *et al.*, 2014) and (Furuichi and Suzuki, 1990) for inoculation method
Soybean	*P. sojae*	Seedlings	inoculated with *P. sojae* isolates using an inoculum layer method that involves placing an agar culture below the seed at planting time	qPCR	Developed qPCR assays for the quantifications *of P. sojae* and determined the pathogen load in infected roots using the assays, and evaluated soybean varieties for resistance	*P. sojae* DNA quantities detected in both qPCR assays had high correlations with disease severity index (DSI) ratings of soybean varieties	(Catal *et al.*, 2013)

Appendix Table 2.2. Cont.

Strawberry	*P. cactorum* and *P. nicotianae*	Soil from strawberry production areas of Japan		Simplex PCR, Multiplex PCR	Developed a multiplex PCR assay for the simultaneous detection of *P. cactorum* and *P. nicotianae* that infect strawberry plants in Japan	Multiplex PCR differentiated between *P. cactorum* and *P. nicotianae* in DNA mixtures of the two species mycelia. Both species were detected in artificially and naturally infested soils.	(Li *et al.*, 2011)
Potato	*P. infestans*	Leaf, tuber, and (soil)	Detached leaflets were inoculated by placing a 20 µl droplet of *P. infestans* inoculum (1.4×10^4 sporangia/ml) on the abaxial side of each leaflet	qPCR	Developed a qPCR assay that can be used in conjunction with other potato pathogen assays for epidemiological investigations	The assay was specific to *P. infestans* and related non-potato pathogens, *P. mirabilis*, *P. phaseoli* and *P. ipomoea*, but was not detected in potato pathogens *P. erythroseptica* and *P. nicotianae*. The assay could reliably detect *P. infestans* DNA at 100 fg per reaction and effective in quantifying *P. infestans* in leaf tissue from 24 hpi infected symptomless tubers and diseased tubers	(Lees *et al.*, 2012)
Potato	*P. infestans*	Leaflets and tuber	Leaflets/Tubers were inoculated on the abaxial side with equidistant droplets of 10 µl of water containing 250 sporangia	qPCR	Established a reliable and rapid protocol for a high quality DNA from infected host and pathogen; developed an assay for *in planta* monitoring of *P. infestans*	qPCR assay able to detect *P. infestans* in potato leaf and tuber tissue before the first symptoms of the disease were observed and to monitor the *in planta* growth of the pathogen for 6 days	(Llorente *et al.*, 2010)

Appendix Table 2.2. Cont.

Potato	*P. infestans*	Tuber	Potato slices were evenly inoculated with from 40 to 4000 sporelings cm^{-2}.	Microscopic examination	Investigated the number and distribution of collars and papillae in both susceptible and resistant potato cvs .	In Bintje (susceptible) 0-12% and in Eba (resistant) 40-90% of the wall appositions were papillae. Eight times more papillae in the resistant than in the susceptible cv	(Hächler and Hohl, 1984)
Soybean	*P. sojae*	Seedlings	Agar cultures were placed on the base layer of vermiculite in each pot then planted with soybean seeds	Microscopic examination; conventional PCR, and qPCR	Evaluated PCR methods for specific, rapid, and sensitive detection of *P. sojae*.	PS primers were not specific for *P. sojae* in conventional PCR but PSOJ primers were specific for detection of *P. sojae* with qPCR and yielded positive results on *P. sojae* gDNA. Oospores were observed in rotted roots	(Bienapfl *et al.*, 2011)
Taro	*P. colocasiae*	Leaves	Used a modified floating disc for five taro leaf disks (5×5 cm) floated in sdH_2O in 200-mm Petri plates and inoculated with a mycelial disc (5 mm)	Conventional PCR, qPCR	Developed a conventional and real-time PCR assay for faster, sensitive and efficient detection of *P. colocasiae*	In conventional PCR, the lower limit of detection was 50 pg DNA, in qPCR, the detection limit was 12.5 fg for the primer based on *Ypt1* gene. *P. colocasiae* was detected from artificially infested samples 18 and 15 hpi in RT-PCR and qPCR	(Nath *et al.*, 2014) and inoculation methods in (Nath *et al.*, 2013)

Legend:
cv(s) – cultivar(s)
dpi – days post inoculation
ELISA – Enzyme-Linked Immunosorbent Assay
ER – endoplasmic reticulum
HR – hypersensitive response
hpi – hours post inoculation
qPCR – quantitative real time PCR
Ppn – *P. parasitica* pv *nicotianae*
ROS – reactive oxygen species
sdH_2O – sterile distilled water
WAT - weeks after transplanting
WT – wild type

Appendix GraphPad Output 3.1. Two-way ANOVA and Bonferroni post-tests of the disease incidence of Gungurru cultivar inoculated with different zoospore concentrations for 10 min (n=24).

Two-way ANOVA				
Source of Variation	% of total variation	P value		
Interaction	22.87	< 0.0001		
Column Factor	47.83	< 0.0001		
hpi	27.26	< 0.0001		
Source of Variation	P value summary	Significant?		
Interaction	***	Yes		
Column Factor	***	Yes		
hpi	***	Yes		
Source of Variation	Df	Sum-of-squares	Mean square	F
Interaction	24	28560	1190	16.33
Column Factor	4	59720	14930	204.9
hpi	6	34040	5673	77.87
Residual	35	2550	72.86	

Bonferroni posttests

125 vs 250

hpi	Difference	t	P value	Summary
0.0	0.0	0.0	P > 0.05	ns
8.000	0.0	0.0	P > 0.05	ns
24.00	0.0	0.0	P > 0.05	ns
30.00	0.0	0.0	P > 0.05	ns
48.00	0.0	0.0	P > 0.05	ns
54.00	0.0	0.0	P > 0.05	ns
72.00	10.00	1.172	P > 0.05	ns

125 vs 500

hpi	Difference	t	P value	Summary
0.0	0.0	0.0	P > 0.05	ns
8.000	0.0	0.0	P > 0.05	ns
24.00	5.000	0.5858	P > 0.05	ns
30.00	10.00	1.172	P > 0.05	ns
48.00	45.00	5.272	P<0.001	***
54.00	55.00	6.444	P<0.001	***
72.00	65.00	7.615	P<0.001	***

125 vs 1000

hpi	Difference	t	P value	Summary
0.0	0.0	0.0	P > 0.05	ns
8.000	0.0	0.0	P > 0.05	ns
24.00	75.00	8.787	P<0.001	***
30.00	75.00	8.787	P<0.001	***
48.00	95.00	11.13	P<0.001	***
54.00	90.00	10.54	P<0.001	***
72.00	90.00	10.54	P<0.001	***

Appendix GraphPad Output 3.1. Cont.

125 vs 2000

hpi	Difference	t	P value	Summary
0.0	0.0	0.0	P > 0.05	ns
8.000	0.0	0.0	P > 0.05	ns
24.00	100.0	11.72	P<0.001	***
30.00	100.0	11.72	P<0.001	***
48.00	100.0	11.72	P<0.001	***
54.00	95.00	11.13	P<0.001	***
72.00	95.00	11.13	P<0.001	***

250 vs 500

hpi	Difference	t	P value	Summary
0.0	0.0	0.0	P > 0.05	ns
8.000	0.0	0.0	P > 0.05	ns
24.00	5.000	0.5858	P > 0.05	ns
30.00	10.00	1.172	P > 0.05	ns
48.00	45.00	5.272	P<0.001	***
54.00	55.00	6.444	P<0.001	***
72.00	55.00	6.444	P<0.001	***

250 vs 1000

hpi	Difference	t	P value	Summary
0.0	0.0	0.0	P > 0.05	ns
8.000	0.0	0.0	P > 0.05	ns
24.00	75.00	8.787	P<0.001	***
30.00	75.00	8.787	P<0.001	***
48.00	95.00	11.13	P<0.001	***
54.00	90.00	10.54	P<0.001	***
72.00	80.00	9.372	P<0.001	***

250 vs 2000

hpi	Difference	t	P value	Summary
0.0	0.0	0.0	P > 0.05	ns
8.000	0.0	0.0	P > 0.05	ns
24.00	100.0	11.72	P<0.001	***
30.00	100.0	11.72	P<0.001	***
48.00	100.0	11.72	P<0.001	***
54.00	95.00	11.13	P<0.001	***
72.00	85.00	9.958	P<0.001	***

500 vs 1000

hpi	Difference	t	P value	Summary
0.0	0.0	0.0	P > 0.05	ns
8.000	0.0	0.0	P > 0.05	ns
24.00	70.00	8.201	P<0.001	***
30.00	65.00	7.615	P<0.001	***
48.00	50.00	5.858	P<0.001	***
54.00	35.00	4.100	P<0.01	**
72.00	25.00	2.929	P <0.05	*

Appendix GraphPad Output 3.1. Cont.

500 vs 2000

hpi	Difference	t	P value	Summary
0.0	0.0	0.0	P > 0.05	ns
8.000	0.0	0.0	P > 0.05	ns
24.00	95.00	11.13	P<0.001	***
30.00	90.00	10.54	P<0.001	***
48.00	55.00	6.444	P<0.001	***
54.00	40.00	4.686	P<0.001	***
72.00	30.00	3.515	P<0.01	**

1000 vs 2000

hpi	Difference	t	P value	Summary
0.0	0.0	0.0	P > 0.05	ns
8.000	0.0	0.0	P > 0.05	ns
24.00	25.00	2.929	P <0.05	*
30.00	25.00	2.929	P <0.05	*
48.00	5.000	0.5858	P > 0.05	ns
54.00	5.000	0.5858	P > 0.05	ns
72.00	5.000	0.5858	P > 0.05	ns

Asterisks indicate statistically significant differences between pairwise comparisons.
*, p = 0.01-0.05; **, p = 0.001-0.01; ***, p = <0.001

Appendix GraphPad Output 3.2. Two-way ANOVA and Newman-Keuls Multiple Comparison Test of the disease severity of Gungurru cultivar inoculated with different zoospore concentrations for 10 min (n=24).

ANOVA Table	SS	df	MS
Treatment (between columns)	143.9	4	35.97
Individual (between rows)	124.7	6	20.78
Residual (random)	98.31	24	4.096
Total	366.9	34	

Newman-Keuls Multiple Comparison Test	Mean Diff.	q	Significant? P <0.05?	Summary
125 vs 2000	-5.071	6.629	Yes	***
125 vs 1000	-3.786	4.949	Yes	**
125 vs 500	-1.500	1.961	No	ns
125 vs 250	-0.07143	---	No	ns
250 vs 2000	-5.000	6.536	Yes	***
250 vs 1000	-3.714	4.855	Yes	**
250 vs 500	-1.429	---	No	ns
500 vs 2000	-3.571	4.669	Yes	**
500 vs 1000	-2.286	2.988	Yes	*
1000 vs 2000	-1.286	1.681	No	ns

Asterisks indicate statistically significant differences between pairwise comparisons.
*, p = 0.01-0.05; **, p = 0.001-0.01; ***, p = <0.001

Appendix GraphPad Output 3.3. Two-way ANOVA and Bonferroni post-test of the disease incidence of Gungurru and Jenabillup cultivars inoculated with 1000 zoospores/ml for 10 min.

Two-way ANOVA				
Source of Variation	% of total variation	P value		
Interaction	3.36	< 0.0001		
Column Factor	1.45	< 0.0001		
hpi	88.07	< 0.0001		
Source of Variation	P value summary	Significant?		
Interaction	***	Yes		
Column Factor	***	Yes		
hpi	***	Yes		
Source of Variation	Df	Sum-of-squares	Mean square	F
Interaction	9	7689	854.3	8.121
Column Factor	1	3324	3324	31.59
hpi	9	201724	22414	213.1
Residual	114	11992	105.2	

Bonferroni post-tests

Gungurru vs Jenabillup				
hpi	Difference	t	P value	Summary
0.0	0.0	0.0	P > 0.05	ns
12.00	0.0	0.0	P > 0.05	ns
18.00	-5.556	1.149	P > 0.05	ns
24.00	-20.17	4.046	P<0.001	***
30.00	-40.80	7.687	P<0.001	***
36.00	-37.33	6.305	P<0.001	***
42.00	-9.400	1.514	P > 0.05	ns
48.00	0.0	0.0	P > 0.05	ns
54.00	0.0	0.0	P > 0.05	ns
60.00	0.0	0.0	P > 0.05	ns

Asterisks indicate statistically significant differences between pairwise comparisons. *, p = 0.01-0.05; **, p = 0.001-0.01; ***, p = <0.001

Appendix GraphPad Output 3.4. Two-way ANOVA and Bonferroni post-tests of the disease severity of Gungurru and Jenabillup cultivars inoculated with 1000 zoospores/ml for 10 min.

Two-way ANOVA

Source of Variation	% of total variation	P value
Interaction	1.77	< 0.0001
Column Factor	1.37	< 0.0001
hpi	90.58	< 0.0001

Source of Variation	P value summary	Significant?
Interaction	***	Yes
Column Factor	***	Yes
hpi	***	Yes

Source of Variation	Df	Sum-of-squares	Mean square	F
Interaction	9	24.62	2.735	6.948
Column Factor	1	18.97	18.97	48.18
hpi	9	1257	139.6	354.7
Residual	114	44.88	0.3937	

Bonferroni post-test

Gungurru vs Jenabillup

hpi	Difference	t	P value	Summary
0.0	0.0	0.0	P > 0.05	ns
12.00	0.0	0.0	P > 0.05	ns
18.00	-0.1111	0.3756	P > 0.05	ns
24.00	-0.5556	1.822	P > 0.05	ns
30.00	-1.089	3.354	P <0.05	*
36.00	-2.333	6.441	P<0.001	***
42.00	-1.967	5.176	P<0.001	***
48.00	-2.000	5.264	P<0.001	***
54.00	-0.5000	0.8729	P > 0.05	ns
60.00	0.0	0.0	P > 0.05	ns

Appendix Table 5.1. *P. parasitica* predicted transcripts removed from infected lupin RNA-Seq analysis. These reads were removed as *P. parasitica* reads mapped to the homologous genes from lupin (Blackman *et al.* 2015).

Gene ID	Putative gene function
PPTG_00150	succinate dehydrogenase [ubiquinone] flavoprotein subunit, mitochondrial
PPTG_00784	hypothetical protein
PPTG_01678	ubiquitin-60S ribosomal protein L40
PPTG_01812	hypothetical protein
PPTG_01949	adenosylhomocysteinase
PPTG_01954	ubiquitin-40S ribosomal protein S27a
PPTG_02042	40S ribosomal protein S16
PPTG_02122	hsp70-like protein
PPTG_02403	pre-mRNA-processing-splicing factor 8
PPTG_02460	hypothetical protein
PPTG_02785	V-type H(+)-translocating pyrophosphatase
PPTG_03355	hypothetical protein
PPTG_03356	thioredoxin-like protein 4A
PPTG_03708	pyruvate kinase
PPTG_03960	26S proteasome regulatory subunit 4 like B
PPTG_04035	ADP-ribosylation factor
PPTG_04484	14-3-3-like protein
PPTG_04831	methylcrotonoyl-CoA carboxylase subunit alpha
PPTG_05308	GT20 alpha,alpha-trehalose-phosphate synthase [UDP-forming]
PPTG_05654	actin-1
PPTG_08107	deoxyhypusine synthase
PPTG_08453	tubulin alpha chain
PPTG_08465	tubulin alpha chain
PPTG_08466	tubulin alpha chain
PPTG_08498	tubulin alpha chain
PPTG_08506	tubulin alpha chain
PPTG_09226	S-adenosylmethionine synthase 2
PPTG_09645	triosephosphate isomerase/glyceraldehyde-3-phosphate dehydrogenase
PPTG_10117	histone H3
PPTG_11052	elongation factor 1-alpha
PPTG_11158	elongation factor 1-alpha
PPTG_12134	V-type proton ATPase subunit B, isoform
PPTG_12264	hypothetical protein
PPTG_13130	calmodulin
PPTG_13414	60S ribosomal protein L3
PPTG_13452	histone H2B
PPTG_13841	ATP synthase subunit beta, mitochondrial
PPTG_14209	hypothetical protein
PPTG_14263	DNA-directed RNA polymerase III subunit polypeptide
PPTG_14388	HECT E3 ubiquitin ligase
PPTG_14402	hypothetical protein
PPTG_14761	transmembrane protein
PPTG_14842	endomembrane protein 70-like protein
PPTG_15082	phosphoglycerate kinase, chloroplastic
PPTG_15113	tubulin beta chain
PPTG_15164	GH28

Appendix Table 5.1. Cont.

PPTG_15348	actin-1
PPTG_16002	actin-1
PPTG_16038	anaphase-promoting complex subunit
PPTG_16493	serine/threonine-protein phosphatase 6 catalytic subunit
PPTG_17946	ATP-dependent RNA helicase eIF4A
PPTG_18195	60S ribosomal protein L44
PPTG_18475	hypothetical protein
PPTG_18599	60S ribosomal protein L27a
PPTG_19143	pre-mRNA-splicing factor ATP-dependent RNA helicase
PPTG_19188	heat shock protein 90-4
PPTG_19399	peptidyl-prolyl cis-trans isomerase
PPTG_20306	S-adenosylmethionine synthase 2
PPTG_20358	hypothetical protein
PPTG_20417	hypothetical protein
PPTG_20464	hypothetical protein

Appendix Table 5.2. *In vitro* culture specific gene expression. Genes that were considered to be specific if they had RPKM >1 in one culture condition and <1 RPKM in the other and providing they were significantly different (FDR <0.05). SP: Signal peptide for classical secretion pathway.

Gene ID	Putative gene function	RPKM Pp	RPKM Pp+Phi	Fold change	FDR
PPTG_00019	amino Acid/Auxin Permease (AAAP) family	3.6	1.0	-1.9	0.000
PPTG_00249	hypothetical protein	4.0	1.0	-2.0	0.000
PPTG_00395	lipase	1.3	0.5	-1.5	0.000
PPTG_00453	hypothetical protein	4.2	0.9	-2.2	0.001
PPTG_00806	CE1 (feruloyl esterase)	1.3	0.7	-0.8	0.003
PPTG_00932	hypothetical protein	1.1	0.6	-0.9	0.000
PPTG_01190	hypothetical protein	2.7	0.4	-2.8	0.000
PPTG_01626	hypothetical protein	2.0	0.1	-4.1	0.031
PPTG_01630	hypothetical protein	4.6	0.5	-3.2	0.000
PPTG_01746	protein kinase	1.0	0.7	-0.6	0.040
PPTG_01988	protein kinase	1.1	0.7	-0.6	0.048
PPTG_02335	hypothetical protein	1.4	0.7	-1.0	0.032
PPTG_02531	hypothetical protein	1.3	0.7	-0.9	0.000
PPTG_02738	catalase/peroxidase HPI	15.3	0.8	-4.3	0.000
PPTG_02783	hypothetical protein	2.2	0.9	-1.2	0.000
PPTG_02965	cysteine desulfurase	2.1	1.0	-1.1	0.000
PPTG_03150	secreted RxLR effector peptide	1.6	0.4	-1.9	0.002
PPTG_03151	hypothetical protein	2.0	0.6	-1.8	0.001
PPTG_03425	hypothetical protein	1.7	0.6	-1.6	0.050
PPTG_03562	PL3 (pectate lyase)	3.0	0.8	-1.9	0.000
PPTG_03734	GT1 sterol 3-beta-glucosyltransferase	2.3	0.6	-1.9	0.000
PPTG_03762	crinkler-like protein	1.5	0.8	-1.0	0.001
PPTG_03985	hypothetical protein	1.8	0.8	-1.2	0.000
PPTG_04148	AA8 (iron reductase)	1.7	0.9	-0.9	0.000
PPTG_04510	MtN3-like protein	4.7	0.7	-2.8	0.000
PPTG_04552	hypothetical protein	1.3	0.3	-2.3	0.004
PPTG_04619	hypothetical protein	1.7	0.6	-1.4	0.000
PPTG_04796	pyridine nucleotide-disulphide oxidoreductase	1.1	0.4	-1.6	0.001
PPTG_04854	bardet-Biedl syndrome 1 family protein	1.2	0.6	-0.9	0.000
PPTG_05747	hypothetical protein	1.3	0.9	-0.5	0.011
PPTG_05877	GH3 (b-1,4-glucanase, b-1,4-xylanase, b-1,3-/-1,5-arabinanase)	1.6	0.6	-1.5	0.000
PPTG_05962	Myb-like DNA-binding protein	1.1	0.6	-1.0	0.048
PPTG_06003	hypothetical protein	1.7	0.6	-1.4	0.000
PPTG_06121	hypothetical protein	1.8	0.8	-1.2	0.000
PPTG_06189	hypothetical protein	1.3	0.7	-0.9	0.015
PPTG_06212	calcium/calmodulin-dependent 3',5'-cyclic nucleotide phosphodiesterase	1.3	0.4	-1.7	0.016
PPTG_06395	hypothetical protein	2.3	0.3	-2.9	0.000

Appendix Table 5.2. Cont.

PPTG_06657	ATP-binding Cassette (ABC) superfamily	1.2	0.7	-0.9	0.001
PPTG_06793	hypothetical protein	1.1	0.7	-0.8	0.033
PPTG_06958	bZIP transcription factor	1.7	0.2	-3.1	0.001
PPTG_07127	short chain dehydrogenase	1.3	0.7	-0.9	0.036
PPTG_07360	GT31	1.6	0.7	-1.3	0.000
PPTG_07408	hypothetical protein	1.8	0.5	-1.7	0.000
PPTG_07418	hypothetical protein	2.3	0.8	-1.4	0.000
PPTG_07619	hypothetical protein	1.2	0.5	-1.4	0.015
PPTG_07714	hypothetical protein	1.3	0.7	-1.0	0.022
PPTG_07837	hypothetical protein	1.7	0.2	-3.0	0.029
PPTG_08340	hypothetical protein	1.7	0.9	-0.9	0.001
PPTG_08849	transmembrane protein	1.3	0.7	-0.9	0.000
PPTG_08908	hypothetical protein	1.5	0.9	-0.8	0.009
PPTG_09078	GT4	1.4	0.9	-0.8	0.004
PPTG_09228	hypothetical protein	1.1	0.7	-0.6	0.015
PPTG_09377	hypothetical protein	1.8	0.5	-1.9	0.000
PPTG_09411	protein kinase	2.1	0.9	-1.2	0.000
PPTG_10224	hypothetical protein	1.5	0.8	-0.8	0.012
PPTG_10357	hypothetical protein	1.5	0.4	-2.0	0.000
PPTG_10405	hypothetical protein	2.0	0.7	-1.5	0.000
PPTG_10916	hypothetical protein	1.2	0.8	-0.7	0.003
PPTG_11495	hypothetical protein	1.7	0.7	-1.3	0.000
PPTG_11536	hypothetical protein	1.6	0.9	-0.9	0.040
PPTG_11567	hypothetical protein	1.7	0.3	-2.3	0.000
PPTG_11651	hypothetical protein	1.2	0.3	-2.0	0.000
PPTG_12067	protein kinase	1.1	0.2	-2.1	0.000
PPTG_12106	hypothetical protein	1.5	0.6	-1.3	0.000
PPTG_12246	hypothetical protein	2.3	0.7	-1.8	0.049
PPTG_12285	hypothetical protein	2.3	0.5	-2.2	0.000
PPTG_12415	hypothetical protein	1.8	0.8	-1.1	0.002
PPTG_12623	hypothetical protein	3.7	0.8	-2.3	0.019
PPTG_12762	hypothetical protein	3.1	0.7	-2.2	0.000
PPTG_12791	hypothetical protein	1.0	0.5	-1.1	0.049
PPTG_12877	hypothetical protein	1.3	0.9	-0.6	0.010
PPTG_12896	PL1 (pectate/pectin lyase)	1.3	0.8	-0.7	0.005
PPTG_12958	hypothetical protein	3.7	0.4	-3.3	0.000
PPTG_13026	hypothetical protein	2.8	0.8	-1.9	0.000
PPTG_13186	hypothetical protein	4.7	0.9	-2.4	0.000
PPTG_13200	hypothetical protein	1.0	0.6	-0.7	0.014
PPTG_13229	ATP-binding Cassette (ABC) superfamily	1.3	0.3	-2.2	0.000
PPTG_13291	amino Acid-Polyamine-Organocation (APC) family	1.3	0.8	-0.7	0.030
PPTG_13568	hypothetical protein	3.7	1.0	-1.9	0.000
PPTG_13988	cytochrome P450	1.6	0.6	-1.4	0.000
PPTG_14184	serine protease family S33	2.0	1.0	-1.0	0.000
PPTG_14291	hypothetical protein	1.0	0.3	-1.6	0.003
PPTG_14354	hypothetical protein	6.9	0.7	-3.4	0.000
PPTG_14483	GH3 (b-1,4-glucanase, b-1,4-xylanase, b-1,3-/-1,5-arabinanase)	5.6	0.8	-2.9	0.000
PPTG_14820	hypothetical protein	2.4	0.9	-1.4	0.000

Appendix Table 5.2. Cont.

PPTG_14859	GH30 (b-1,6-galactanase)	1.4	0.8	-0.7	0.017
PPTG_14946	hypothetical protein	1.3	0.6	-1.1	0.001
PPTG_15049	hypothetical protein	1.8	0.9	-1.0	0.006
PPTG_15246	hypothetical protein	2.4	0.6	-2.0	0.000
PPTG_15298	extracellular dioxygenase	1.0	0.5	-1.1	0.039
PPTG_15412	hypothetical protein	1.1	0.2	-2.3	0.000
PPTG_15504	hypothetical protein	2.3	0.6	-1.9	0.003
PPTG_15940	hypothetical protein	1.9	0.5	-2.1	0.000
PPTG_16085	hypothetical protein	1.4	0.7	-0.9	0.003
PPTG_16189	protein kinase	1.3	0.9	-0.7	0.023
PPTG_16238	hypothetical protein	1.4	0.3	-2.4	0.004
PPTG_17122	hypothetical protein	2.4	0.7	-1.8	0.001
PPTG_17185	GH17 (endo-b-1,3-glucanase)	1.3	0.7	-0.9	0.035
PPTG_17505	PL1 (pectate/pectin lyase)	1.8	0.5	-1.9	0.000
PPTG_17525	hypothetical protein	1.2	0.1	-3.3	0.003
PPTG_17795	hypothetical protein	3.6	0.9	-2.1	0.014
PPTG_17904	hypothetical protein	1.3	0.5	-1.3	0.001
PPTG_17960	hypothetical protein	12.5	0.8	-3.9	0.000
PPTG_18154	hypothetical protein	1.3	0.8	-0.7	0.031
PPTG_18371	hypothetical protein	4.9	0.7	-2.8	0.000
PPTG_18452	hypothetical protein	2.2	0.5	-2.1	0.000
PPTG_18510	hypothetical protein	1.5	0.7	-1.1	0.000
PPTG_18634	hypothetical protein	1.2	0.4	-1.5	0.002
PPTG_18661	hypothetical protein	1.0	0.3	-1.7	0.022
PPTG_18664	hypothetical protein	1.2	0.3	-1.8	0.002
PPTG_18850	hypothetical protein	1.2	0.7	-0.6	0.045
PPTG_19164	GH53 (b-1,4-galactanase)	1.1	0.4	-1.5	0.000
PPTG_19544	hypothetical protein	1.9	0.3	-2.5	0.021
PPTG_19554	hypothetical protein	1.1	0.6	-0.8	0.001
PPTG_19828	hypothetical protein	2.8	0.4	-2.9	0.006
PPTG_20058	hypothetical protein	2.0	1.0	-1.0	0.000
PPTG_20318	hypothetical protein	1.5	0.5	-1.6	0.001
PPTG_20376	hypothetical protein	2.4	0.5	-2.2	0.011
PPTG_00055	carbonic anhydrase	0.5	1.5	1.5	0.007
PPTG_00440	hypothetical protein	0.3	1.3	1.9	0.010
PPTG_00568	hypothetical protein	0.6	1.3	1.1	0.016
PPTG_00859	hypothetical protein	0.3	1.4	2.3	0.000
PPTG_01020	hypothetical protein	0.8	1.2	0.6	0.049
PPTG_01067	succinate semialdehyde dehydrogenase	0.8	2.3	1.5	0.000
PPTG_01686	hypothetical protein	1.0	2.1	1.2	0.003
PPTG_02382	hypothetical protein	1.0	1.4	0.5	0.050
PPTG_02825	hypothetical protein	0.8	2.0	1.3	0.000
PPTG_02901	hypothetical protein	0.2	6.2	4.7	0.000
PPTG_02989	hypothetical protein	0.9	2.7	1.6	0.000
PPTG_02382	hypothetical protein	1.0	1.4	0.5	0.050
PPTG_03396	hypothetical protein	0.9	3.1	1.8	0.000
PPTG_03679	aquaporin	0.8	2.8	1.8	0.000
PPTG_04166	sporangia induced protein	0.5	1.1	1.0	0.005
PPTG_04298	hypothetical protein	0.2	1.3	2.5	0.007
PPTG_04738	hypothetical protein	0.4	1.3	1.7	0.000

Appendix Table 5.2. Cont.

PPTG_05094	hypothetical protein	0.5	1.0	1.1	0.008
PPTG_05739	hypothetical protein	0.9	1.3	0.5	0.048
PPTG_05764	hypothetical protein	0.6	2.2	1.9	0.007
PPTG_06866	catalase	0.7	2.3	1.8	0.000
PPTG_06993	mitochondrial Carrier (MC) family	0.8	1.4	0.7	0.020
PPTG_08864	hypothetical protein	0.9	1.5	0.7	0.031
PPTG_09443	hypothetical protein	0.5	1.2	1.4	0.000
PPTG_09447	hypothetical protein	0.8	1.3	0.7	0.009
PPTG_09460	PL1 (pectate/pectin lyase)	0.8	1.6	1.0	0.002
PPTG_09925	hypothetical protein	0.9	1.6	0.8	0.033
PPTG_10140	GH81 (endo-b-1,3-glucanase)	0.8	1.2	0.5	0.049
PPTG_10161	GH81 (endo-b-1,3-glucanase)	0.9	2.0	1.1	0.000
PPTG_10490	trypsin protease GIP	1.0	1.8	0.9	0.010
PPTG_10658	hypothetical protein	0.2	2.1	3.2	0.024
PPTG_10688	hypothetical protein	0.9	1.6	0.8	0.004
PPTG_11445	hypothetical protein	0.6	1.1	0.9	0.001
PPTG_11448	12-oxophytodienoate reductase	0.4	1.2	1.7	0.001
PPTG_11464	hypothetical protein	0.8	3.0	1.9	0.000
PPTG_13184	hypothetical protein	0.9	3.0	1.7	0.000
PPTG_14138	hypothetical protein	0.5	1.1	1.1	0.000
PPTG_14368	hypothetical protein	0.5	1.2	1.2	0.000
PPTG_15173	GH28 (polygalacturonase)	0.6	1.8	1.5	0.000
PPTG_15644	hypothetical protein	0.9	1.8	0.9	0.006
PPTG_16203	protein kinase	0.9	1.7	0.9	0.003
PPTG_16829	hypothetical protein	0.5	4.1	2.9	0.000
PPTG_16833	hypothetical protein	0.4	1.8	2.3	0.003
PPTG_17003	hypothetical protein	0.5	2.3	2.3	0.000
PPTG_17189	cobalamin synthesis protein	0.4	1.4	1.7	0.000
PPTG_17396	hypothetical protein	0.8	1.1	0.5	0.034
PPTG_17432	MtN3-like protein	0.8	3.7	2.2	0.000
PPTG_18025	hypothetical protein	0.5	2.3	2.2	0.003
PPTG_18398	hypothetical protein	0.4	1.1	1.4	0.042
PPTG_18785	hypothetical protein	0.4	2.1	2.4	0.000

Appendix Table 5.3. Infected lupin specific gene expression. Genes that were considered to be specific if they had RPKM >1 in one culture condition and <1 RPKM in the other and providing they were significantly different (FDR <0.05). SP: Signal peptide for classical secretion pathway.

Gene ID	Putative gene function	Lupin +Pp mean RPKM	Lupin+ Pp+Pi RPKM	Fold change	FDR p-value	SP
PPTG_17678	croquemort-like mating protein M82	29.18	0.11	-249.71	0.00	
PPTG_05358	centrin (PnCen1) caltractin	3.53	0.00	-214.27	0.00	
PPTG_09880	hypothetical protein	3.40	0.00	-183.11	0.00	SP
PPTG_00012	amino Acid/Auxin Permease (AAAP) family	1.27	0.00	-181.51	0.00	
PPTG_08738	SCP-like extracellular protein	2.10	0.00	-115.85	0.00	SP
PPTG_01512	hypothetical protein	1.56	0.00	-108.41	0.01	
PPTG_11396	hypothetical protein	7.73	0.06	-80.95	0.00	
PPTG_13569	pyruvate, phosphate dikinase	50.73	0.68	-69.36	0.00	
PPTG_00015	amino Acid/Auxin Permease (AAAP) family	6.50	0.08	-69.12	0.00	
PPTG_10334	hypothetical protein	30.91	0.59	-51.24	0.00	
PPTG_08684	folate-Biopterin transporter (FBT) family	20.76	0.42	-46.28	0.00	
PPTG_04507	hypothetical protein	1.52	0.00	-41.48	0.04	SP
PPTG_11489	hypothetical protein	4.69	0.13	-35.41	0.00	
PPTG_05975	carbonic anhydrase	4.86	0.10	-34.14	0.00	SP
PPTG_13068	hypothetical protein	23.67	0.75	-32.83	0.00	SP
PPTG_03572	hypothetical protein	6.01	0.12	-31.35	0.00	
PPTG_17213	hypothetical protein	9.84	0.36	-26.88	0.00	
PPTG_11096	PL3	14.31	0.51	-25.05	0.00	SP
PPTG_08842	hypothetical protein	10.83	0.39	-24.67	0.00	SP
PPTG_02225	sodium-dependent phosphate transporter	2.14	0.08	-23.76	0.00	
PPTG_13736	hypothetical protein	3.97	0.18	-21.13	0.00	SP
PPTG_11095	PL3	6.01	0.30	-19.16	0.00	SP
PPTG_09488	hypothetical protein	6.57	0.33	-18.36	0.00	
PPTG_13158	hypothetical protein	2.87	0.14	-17.64	0.00	
PPTG_20350	hypothetical protein	4.92	0.26	-17.05	0.00	
PPTG_10448	hypothetical protein	3.32	0.18	-17.02	0.00	
PPTG_01315	hypothetical protein	6.30	0.39	-16.39	0.00	
PPTG_17003	hypothetical protein	1.16	0.05	-15.91	0.00	
PPTG_16475	hypothetical protein	13.19	0.81	-15.45	0.00	
PPTG_06718	hypothetical protein	1.96	0.13	-15.27	0.00	
PPTG_09411	protein kinase	1.49	0.09	-14.86	0.00	SP
PPTG_13013	hypothetical protein	1.32	0.07	-14.85	0.00	SP
PPTG_20351	CBM13	4.55	0.31	-14.50	0.00	
PPTG_01172	hypothetical protein	2.67	0.16	-14.32	0.01	SP
PPTG_00885	transmembrane protein	5.97	0.43	-13.92	0.00	
PPTG_13075	hypothetical protein	2.28	0.17	-13.75	0.00	
PPTG_05037	SCP-like extracellular protein	1.10	0.07	-13.59	0.00	SP
PPTG_06389	hypothetical protein	3.35	0.22	-13.57	0.00	SP
PPTG_00601	serine protease family S33	13.30	0.91	-13.42	0.00	SP
PPTG_09670	hypothetical protein	6.65	0.45	-13.21	0.00	
PPTG_06366	hypothetical protein	5.32	0.36	-13.21	0.00	SP
PPTG_06290	small cysteine rich protein SCR108	1.27	0.09	-12.59	0.03	SP
PPTG_04395	serine protease family S33	6.50	0.52	-12.51	0.00	SP
PPTG_00479	CBM1	4.74	0.39	-12.50	0.00	SP

Appendix Table 5.3 Cont.

PPTG_01511	hypothetical protein	3.21	0.21	-11.80	0.03	
PPTG_01314	hypothetical protein	5.26	0.46	-11.31	0.00	
PPTG_05175	hypothetical protein	1.31	0.11	-11.28	0.01	
PPTG_13442	bardet-Biedl syndrome 2 protein	6.06	0.51	-11.26	0.00	
PPTG_02544	zinc (Zn2)-Iron (Fe2) Permease (ZIP) family	3.66	0.31	-11.04	0.00	SP
PPTG_05250	elicitin-like mating protein M25	1.79	0.15	-11.01	0.00	SP
PPTG_03640	dicarboxylate/Amino Acid:Cation (Na or H) Symporter (DAACS) family	2.54	0.22	-10.91	0.01	
PPTG_12435	hypothetical protein	4.50	0.43	-10.48	0.00	
PPTG_12518	hypothetical protein	5.90	0.53	-10.30	0.00	SP
PPTG_13404	hypothetical protein	3.52	0.33	-10.29	0.00	
PPTG_04184	hypothetical protein	6.01	0.55	-10.11	0.00	
PPTG_16051	intraflagellar transporter 140	3.50	0.34	-9.99	0.00	
PPTG_03161	hypothetical protein	6.31	0.64	-9.98	0.00	SP
PPTG_13584	hypothetical protein	1.26	0.12	-9.91	0.02	
PPTG_11385	sodium-dependent phosphate transporter	8.45	0.77	-9.77	0.00	
PPTG_18660	hypothetical protein	3.47	0.34	-9.76	0.00	
PPTG_05023	hypothetical protein	3.30	0.33	-9.74	0.00	
PPTG_10099	hypothetical protein	5.71	0.58	-9.59	0.00	
PPTG_01068	choline dehydrogenase	9.46	0.98	-9.47	0.00	
PPTG_11310	hypothetical protein	2.70	0.28	-9.35	0.00	SP
PPTG_14419	hypothetical protein	8.16	0.87	-9.32	0.00	
PPTG_12104	hypothetical protein	1.41	0.15	-9.23	0.00	
PPTG_18666	hypothetical protein	4.26	0.51	-9.22	0.00	
PPTG_19725	hypothetical protein	3.19	0.28	-9.21	0.00	
PPTG_05517	hypothetical protein	2.46	0.19	-8.96	0.00	SP
PPTG_12695	hypothetical protein	1.23	0.13	-8.90	0.00	SP
PPTG_09947	hypothetical protein	1.69	0.18	-8.76	0.00	
PPTG_13031	hypothetical protein	2.12	0.24	-8.68	0.00	SP
PPTG_01222	hypothetical protein	4.28	0.42	-8.65	0.00	
PPTG_05526	cysteine dioxygenase	7.97	0.85	-8.65	0.00	
PPTG_15657	hypothetical protein	4.93	0.48	-8.57	0.00	
PPTG_12639	hypothetical protein	1.15	0.12	-8.52	0.04	
PPTG_18705	outer Dynein Arm Light Chain 2	4.14	0.46	-8.52	0.00	
PPTG_00223	neutral ceramidase	4.66	0.51	-8.25	0.00	SP
PPTG_16244	GH5	7.48	0.85	-8.25	0.00	SP
PPTG_05203	hypothetical protein	7.36	0.87	-8.16	0.01	
PPTG_14726	hypothetical protein	3.97	0.49	-8.09	0.00	
PPTG_08079	hypothetical protein	3.00	0.38	-8.08	0.00	SP
PPTG_17320	hypothetical protein	1.19	0.11	-7.99	0.04	SP
PPTG_03571	hypothetical protein	3.57	0.50	-7.98	0.00	
PPTG_07132	hypothetical protein	1.94	0.17	-7.97	0.04	
PPTG_00399	lipase	3.21	0.42	-7.74	0.00	SP
PPTG_04611	AP-2 complex subunit sigma	7.14	0.90	-7.70	0.00	
PPTG_03195	secreted effector peptide	3.64	0.48	-7.47	0.00	SP
PPTG_02178	hypothetical protein	2.88	0.37	-7.40	0.00	
PPTG_08439	phospholipid-transporting ATPase	3.23	0.44	-7.36	0.00	
PPTG_11019	hypothetical protein	4.16	0.51	-7.34	0.00	
PPTG_16207	protein kinase	1.57	0.21	-7.16	0.00	
PPTG_04689	copine-like protein	5.35	0.76	-7.10	0.00	
PPTG_08149	hypothetical protein	1.48	0.16	-6.97	0.01	
PPTG_10672	hypothetical protein	5.55	0.77	-6.88	0.00	
PPTG_10975	hypothetical protein	6.13	0.81	-6.88	0.00	
PPTG_12246	hypothetical protein	2.33	0.33	-6.88	0.00	
PPTG_19256	adenylate kinase	1.00	0.12	-6.76	0.00	

Appendix Table 5.3 Cont.

PPTG_08852	secreted RxLR effector peptide	2.49	0.36	-6.76	0.00	SP
PPTG_20175	GH72	1.37	0.18	-6.73	0.00	SP
PPTG_13889	hypothetical protein	1.63	0.23	-6.66	0.00	
PPTG_09114	hypothetical protein	2.04	0.30	-6.65	0.00	
PPTG_00395	lipase	2.44	0.37	-6.47	0.00	SP
PPTG_12820	hypothetical protein	2.50	0.36	-6.42	0.00	
PPTG_19508	serine protease family S33	5.56	0.85	-6.34	0.00	
PPTG_14291	hypothetical protein	1.17	0.15	-6.21	0.00	
PPTG_04817	hypothetical protein	1.45	0.22	-6.20	0.00	
PPTG_16223	Myb-like DNA-binding protein	2.57	0.41	-6.16	0.00	
PPTG_16086	hypothetical protein	1.52	0.24	-6.15	0.00	SP
PPTG_14391	GH3	6.17	0.95	-6.13	0.00	SP
PPTG_04066	hypothetical protein	4.64	0.71	-6.06	0.00	
PPTG_10320	Ras family GTPase	1.60	0.23	-6.00	0.00	
PPTG_12430	hypothetical protein	5.88	0.98	-5.84	0.00	
PPTG_05310	Rab11 family GTPase	4.43	0.77	-5.75	0.00	
PPTG_14539	hypothetical protein	1.94	0.29	-5.72	0.00	
PPTG_15107	CBM13	2.97	0.49	-5.72	0.00	
PPTG_11162	hypothetical protein	2.58	0.44	-5.70	0.00	
PPTG_16971	hypothetical protein	1.27	0.17	-5.70	0.03	
PPTG_18867	hypothetical protein	2.26	0.38	-5.66	0.00	
PPTG_14562	cytochrome P450	4.91	0.83	-5.65	0.00	SP
PPTG_14628	dynein light chain-like protein	1.86	0.24	-5.61	0.02	
PPTG_08215	hypothetical protein	1.75	0.31	-5.59	0.00	
PPTG_04615	hypothetical protein	4.15	0.71	-5.54	0.00	
PPTG_07037	hypothetical protein	4.39	0.81	-5.48	0.00	
PPTG_04227	protein kinase	3.67	0.61	-5.45	0.00	
PPTG_17353	hypothetical protein	2.23	0.40	-5.42	0.00	
PPTG_19148	tubulin-tyrosine ligase family protein	4.20	0.77	-5.42	0.00	
PPTG_17445	hypothetical protein	1.77	0.32	-5.37	0.00	SP
PPTG_10411	hypothetical protein	5.49	0.99	-5.37	0.00	
PPTG_07196	hypothetical protein	3.37	0.55	-5.34	0.00	SP
PPTG_06270	ADP-ribosylation factor-like protein 3	3.93	0.70	-5.26	0.00	
PPTG_08524	dynein 1b Light Intermediate Chain	1.54	0.31	-5.25	0.01	
PPTG_06971	hypothetical protein	3.96	0.65	-5.25	0.00	
PPTG_00379	hypothetical protein	2.77	0.50	-5.21	0.00	
PPTG_15548	hypothetical protein	2.30	0.43	-5.18	0.00	
PPTG_19858	hypothetical protein	1.63	0.30	-5.17	0.01	SP
PPTG_09310	hypothetical protein	4.09	0.72	-5.16	0.00	
PPTG_04933	GH1	5.30	0.98	-5.14	0.00	
PPTG_02788	hypothetical protein	2.77	0.56	-5.07	0.00	
PPTG_00289	hypothetical protein	2.86	0.57	-5.06	0.00	
PPTG_03552	hypothetical protein	2.08	0.39	-5.06	0.00	
PPTG_10405	hypothetical protein	2.67	0.52	-5.03	0.00	
PPTG_15644	hypothetical protein	3.52	0.65	-5.02	0.00	
PPTG_04083	hypothetical protein	2.58	0.46	-5.01	0.00	SP
PPTG_13016	GT60	4.09	0.77	-4.91	0.00	SP
PPTG_13294	hypothetical protein	5.50	0.96	-4.86	0.00	
PPTG_07262	hypothetical protein	4.32	0.82	-4.86	0.00	
PPTG_12818	hypothetical protein	3.26	0.62	-4.84	0.00	
PPTG_17337	hypothetical protein	3.40	0.70	-4.83	0.01	
PPTG_11925	hypothetical protein	1.91	0.38	-4.83	0.00	
PPTG_00482	hypothetical protein	2.24	0.53	-4.76	0.03	SP
PPTG_18620	hypothetical protein	4.64	0.87	-4.76	0.00	SP
PPTG_05530	hypothetical protein	1.41	0.31	-4.76	0.00	
PPTG_06797	hypothetical protein	2.40	0.48	-4.75	0.01	
PPTG_11931	hypothetical protein	4.64	0.93	-4.74	0.01	
PPTG_06967	hypothetical protein	4.06	0.75	-4.73	0.02	
PPTG_00746	cGMP 3',5'-cyclic phosphodiesterase subunit delta	1.81	0.37	-4.72	0.03	

Appendix Table 5.3 Cont.

PPTG_10323	hypothetical protein	2.82	0.56	-4.67	0.00	
PPTG_00655	hypothetical protein	2.86	0.59	-4.67	0.00	SP
PPTG_06256	hypothetical protein	3.37	0.76	-4.65	0.00	SP
PPTG_06216	hypothetical protein	3.96	0.82	-4.61	0.00	
PPTG_03208	hypothetical protein	2.97	0.63	-4.60	0.02	
PPTG_12438	hypothetical protein	3.33	0.71	-4.58	0.00	
PPTG_08239	hypothetical protein	2.04	0.41	-4.57	0.02	
PPTG_06493	hypothetical protein	1.49	0.31	-4.56	0.02	
PPTG_06122	hypothetical protein	1.52	0.27	-4.56	0.03	
PPTG_10596	CBM40	2.13	0.42	-4.54	0.00	
PPTG_07726	hypothetical protein	3.13	0.60	-4.52	0.02	SP
PPTG_12263	hypothetical protein	3.51	0.77	-4.51	0.00	
PPTG_13204	GPI-anchored serine-glycine rich elicitin INL3a-like protein	1.17	0.24	-4.50	0.01	SP
PPTG_03241	hypothetical protein	3.40	0.71	-4.50	0.00	
PPTG_08440	hypothetical protein	1.42	0.29	-4.45	0.01	
PPTG_00193	hypothetical protein	1.38	0.30	-4.44	0.03	SP
PPTG_10333	hypothetical protein	4.20	0.96	-4.42	0.00	
PPTG_18850	hypothetical protein	3.62	0.77	-4.41	0.00	SP
PPTG_04913	hypothetical protein	1.94	0.41	-4.36	0.05	
PPTG_11688	hypothetical protein	1.38	0.30	-4.34	0.00	
PPTG_02603	hypothetical protein	2.02	0.39	-4.33	0.02	
PPTG_16622	hypothetical protein	1.85	0.43	-4.30	0.01	
PPTG_10233	hypothetical protein	2.20	0.48	-4.26	0.01	SP
PPTG_12838	hypothetical protein	2.07	0.47	-4.26	0.01	SP
PPTG_17418	hypothetical protein	3.71	0.85	-4.19	0.00	
PPTG_11689	hypothetical protein	1.09	0.22	-4.17	0.00	
PPTG_00140	GH6	1.74	0.40	-4.14	0.00	SP
PPTG_09879	kinesin-like protein KIF6	1.12	0.25	-4.09	0.00	
PPTG_04854	bardet-Biedl syndrome 1 family protein	2.27	0.53	-4.08	0.00	
PPTG_02086	carbohydrate-binding protein	2.13	0.46	-4.07	0.01	SP
PPTG_10361	protein kinase	1.68	0.40	-4.06	0.00	SP
PPTG_15912	hypothetical protein	1.19	0.27	-4.01	0.04	
PPTG_09555	hypothetical protein	2.80	0.68	-4.00	0.00	
PPTG_04151	hypothetical protein	2.97	0.66	-3.96	0.00	
PPTG_04152	hypothetical protein	1.88	0.47	-3.94	0.00	
PPTG_14169	protein kinase	1.93	0.47	-3.94	0.00	SP
PPTG_18693	hypothetical protein	2.23	0.58	-3.93	0.03	
PPTG_19562	hypothetical protein	1.26	0.30	-3.91	0.00	
PPTG_02575	sodium-dependent phosphate transporter	2.54	0.57	-3.91	0.00	
PPTG_00080	carbonic anhydrase	2.24	0.47	-3.86	0.04	SP
PPTG_16213	Myb-like DNA-binding protein	3.81	0.91	-3.86	0.01	
PPTG_07599	hypothetical protein	1.91	0.51	-3.83	0.04	
PPTG_12054	hypothetical protein	1.74	0.44	-3.78	0.00	
PPTG_00397	GH3	3.74	0.95	-3.77	0.00	SP
PPTG_14723	hypothetical protein	1.71	0.43	-3.77	0.00	
PPTG_07360	GT31	2.52	0.65	-3.76	0.00	SP
PPTG_02973	hypothetical protein	3.37	0.82	-3.76	0.00	
PPTG_01166	hypothetical protein	2.18	0.57	-3.69	0.00	
PPTG_09423	hypothetical protein	2.86	0.73	-3.68	0.01	
PPTG_13142	hypothetical protein	2.32	0.63	-3.66	0.00	SP
PPTG_01223	hypothetical protein	1.98	0.51	-3.65	0.00	SP
PPTG_11044	transmembrane protein	1.62	0.45	-3.61	0.00	SP
PPTG_05153	hypothetical protein	1.32	0.36	-3.59	0.03	
PPTG_10746	hypothetical protein	2.55	0.72	-3.58	0.01	
PPTG_12458	transmembrane protein	2.41	0.64	-3.56	0.00	
PPTG_04246	hypothetical protein	2.29	0.59	-3.55	0.05	
PPTG_18566	dynein heavy chain	1.85	0.50	-3.54	0.00	
PPTG_07908	hypothetical protein	2.54	0.72	-3.51	0.00	
PPTG_08141	hypothetical protein	1.45	0.41	-3.51	0.03	

Appendix Table 5.3 Cont.

PPTG_01318	cytochrome P450	3.48	0.93	-3.50	0.00	SP
PPTG_05017	hypothetical protein	1.83	0.51	-3.48	0.00	
PPTG_09655	hypothetical protein	3.18	0.88	-3.43	0.00	
PPTG_11581	hypothetical protein	2.06	0.57	-3.41	0.00	
PPTG_04648	hypothetical protein	2.99	0.81	-3.41	0.01	SP
PPTG_05165	cysteine protease family C02	1.03	0.30	-3.37	0.00	
PPTG_10617	hypothetical protein	2.57	0.73	-3.37	0.00	SP
PPTG_11495	hypothetical protein	2.03	0.56	-3.35	0.01	
PPTG_19816	hypothetical protein	3.30	0.94	-3.33	0.00	
PPTG_06719	hypothetical protein	3.09	0.87	-3.33	0.00	
PPTG_13534	voltage-gated Ion Channel (VIC) superfamily	2.11	0.62	-3.32	0.00	
PPTG_03156	hypothetical protein	3.08	0.91	-3.31	0.00	SP
PPTG_05176	hypothetical protein	2.03	0.63	-3.30	0.02	SP
PPTG_11446	hypothetical protein	2.13	0.58	-3.29	0.00	
PPTG_02207	hypothetical protein	2.32	0.67	-3.22	0.00	
PPTG_17927	hypothetical protein	1.04	0.33	-3.18	0.00	SP
PPTG_11451	GAF domain-containing protein	2.37	0.72	-3.15	0.00	
PPTG_14390	hypothetical protein	2.85	0.87	-3.14	0.00	
PPTG_15430	hypothetical protein	2.23	0.70	-3.14	0.04	
PPTG_13123	hypothetical protein	3.14	0.97	-3.09	0.00	SP
PPTG_05681	hypothetical protein	2.82	0.89	-3.08	0.00	
PPTG_13813	hypothetical protein	2.48	0.74	-3.04	0.01	
PPTG_19543	hypothetical protein	1.72	0.55	-3.03	0.04	
PPTG_03415	hypothetical protein	3.07	0.99	-3.01	0.01	
PPTG_07193	hypothetical protein	2.91	0.94	-3.01	0.00	
PPTG_11937	dysferlin-like protein	1.49	0.47	-3.01	0.00	
PPTG_16788	hypothetical protein	1.61	0.42	-2.98	0.05	SP
PPTG_02144	hypothetical protein	2.34	0.73	-2.95	0.00	
PPTG_20387	hypothetical protein	1.34	0.42	-2.91	0.02	
PPTG_02366	hypothetical protein	2.25	0.76	-2.90	0.00	
PPTG_12758	dynein heavy chain, outer arm	2.25	0.74	-2.89	0.00	
PPTG_12474	GH16	2.74	0.92	-2.88	0.00	SP
PPTG_11288	sporangia Induced Dynein Regulatory Complex protein	1.92	0.68	-2.86	0.05	
PPTG_16417	hypothetical protein	1.74	0.59	-2.80	0.02	
PPTG_19413	hypothetical protein	1.25	0.43	-2.79	0.04	
PPTG_13575	hypothetical protein	2.06	0.70	-2.78	0.00	
PPTG_11289	presenilin-like protein	1.74	0.61	-2.76	0.02	
PPTG_19440	hypothetical protein	1.74	0.59	-2.74	0.01	
PPTG_19597	hypothetical protein	1.21	0.43	-2.73	0.03	
PPTG_17597	hypothetical protein	2.29	0.74	-2.73	0.01	
PPTG_00718	hypothetical protein	2.93	0.97	-2.73	0.00	
PPTG_00649	hypothetical protein	2.57	0.91	-2.70	0.00	
PPTG_11440	hypothetical protein	2.20	0.79	-2.68	0.00	
PPTG_08102	kinesin-like protein	1.96	0.71	-2.67	0.00	
PPTG_19222	hypothetical protein	1.98	0.68	-2.67	0.04	SP
PPTG_10877	protein kinase	2.71	0.98	-2.65	0.00	
PPTG_05188	actin-like protein	1.46	0.50	-2.64	0.04	
PPTG_12055	hypothetical protein	1.51	0.51	-2.63	0.04	
PPTG_05309	hypothetical protein	2.41	0.86	-2.63	0.03	
PPTG_09265	hypothetical protein	1.57	0.58	-2.60	0.02	
PPTG_02082	hypothetical protein	1.95	0.68	-2.59	0.03	
PPTG_13298	drug/Metabolite transporter (DMT) superfamily	2.02	0.76	-2.55	0.01	
PPTG_19154	hypothetical protein	1.12	0.43	-2.45	0.03	
PPTG_03686	hypothetical protein	1.10	0.44	-2.41	0.02	
PPTG_05500	hypothetical protein	1.46	0.60	-2.38	0.05	
PPTG_11435	phosphatidylinositol-4-phosphate-5-kinase (Pi-PIPK-D8/GPCR-PIPK)	1.93	0.80	-2.38	0.01	

Appendix Table 5.3 Cont.

PPTG_06000	hypothetical protein	2.03	0.83	-2.37	0.05	
PPTG_17977	hypothetical protein	1.00	0.42	-2.33	0.02	
PPTG_18426	hypothetical protein	2.31	0.90	-2.31	0.03	SP
PPTG_14634	hypothetical protein	1.76	0.74	-2.28	0.02	
PPTG_12245	hypothetical protein	1.75	0.74	-2.24	0.00	
PPTG_06670	hypothetical protein	2.13	0.94	-2.22	0.04	
PPTG_14555	hsp70-like protein	1.84	0.80	-2.22	0.02	
PPTG_01034	ATP-binding Cassette (ABC) superfamily	1.40	0.60	-2.19	0.01	
PPTG_15185	hypothetical protein	1.56	0.67	-2.15	0.02	
PPTG_06374	hypothetical protein	1.77	0.81	-2.13	0.01	
PPTG_06293	ATP-binding Cassette (ABC) superfamily	1.34	0.59	-2.13	0.02	
PPTG_13621	hypothetical protein	1.75	0.82	-2.11	0.01	
PPTG_13428	hypothetical protein	1.13	0.52	-2.11	0.01	
PPTG_14154	ATP-binding Cassette (ABC) superfamily	1.69	0.76	-2.10	0.00	
PPTG_06121	hypothetical protein	1.84	0.80	-2.10	0.04	
PPTG_18685	hypothetical protein	1.09	0.51	-2.05	0.03	
PPTG_05747	hypothetical protein	1.34	0.64	-1.99	0.01	
PPTG_01653	dynein heavy chain	1.85	0.91	-1.94	0.00	
PPTG_04252	hypothetical protein	1.11	0.55	-1.92	0.03	
PPTG_11964	hypothetical protein	1.62	0.87	-1.78	0.05	SP
PPTG_14586	hypothetical protein	1.44	0.91	-1.50	0.02	
PPTG_17116	hypothetical protein	0.73	1.49	1.97	0.05	
PPTG_16597	cysteine protease family C01A	0.94	1.86	1.97	0.04	SP
PPTG_16075	phospholipid-transporting ATPase	0.51	1.02	1.98	0.03	
PPTG_11833	canalicular multispecific organic anion transporter	0.67	1.29	1.99	0.04	
PPTG_05607	WD repeat-containing protein srw1	0.87	1.72	2.01	0.03	
PPTG_12784	hypothetical protein	0.73	1.39	2.01	0.04	
PPTG_06382	hypothetical protein	0.79	1.47	2.02	0.02	SP
PPTG_08884	RNA pseudouridylate synthase	0.90	1.84	2.04	0.03	
PPTG_09228	hypothetical protein	0.56	1.14	2.06	0.04	
PPTG_16170	hypothetical protein	0.82	1.64	2.10	0.03	
PPTG_01311	cytochrome P450	0.65	1.44	2.22	0.03	SP
PPTG_10142	hypothetical protein	0.81	1.76	2.25	0.00	
PPTG_08663	hypothetical protein	0.70	1.52	2.27	0.03	SP
PPTG_14681	ammonium transporter (Amt) family	0.99	2.31	2.30	0.04	SP
PPTG_07925	ammonium transporter (Amt) family	0.90	2.05	2.30	0.04	SP
PPTG_15408	hypothetical protein	0.92	2.13	2.31	0.02	
PPTG_14420	hypothetical protein	0.80	1.80	2.33	0.01	
PPTG_08155	hypothetical protein	0.76	1.64	2.36	0.03	
PPTG_04683	kinesin-like protein	0.45	1.08	2.39	0.02	
PPTG_16901	nitrate reductase [NADPH]	0.93	2.14	2.40	0.00	
PPTG_06925	bzip transcription factor	0.96	2.26	2.45	0.03	
PPTG_16533	phospholipase D, Pi-sPLD-like-7	0.99	2.19	2.46	0.01	SP
PPTG_10750	hypothetical protein	0.51	1.33	2.52	0.05	
PPTG_01459	hypothetical protein	0.75	1.83	2.52	0.00	
PPTG_04499	MtN3-like protein	0.82	2.14	2.57	0.03	SP
PPTG_04299	ATP-binding Cassette (ABC) superfamily	0.57	1.38	2.57	0.01	
PPTG_10750	hypothetical protein	0.51	1.33	2.52	0.05	
PPTG_08806	axin interactor	0.64	1.62	2.58	0.04	
PPTG_03418	hypothetical protein	0.72	1.78	2.59	0.01	
PPTG_00990	hypothetical protein	0.48	1.31	2.61	0.02	

Appendix Table 5.3 Cont.

PPTG_07520	hypothetical protein	0.95	2.42	2.64	0.02	SP
PPTG_04673	hypothetical protein	0.68	1.81	2.65	0.00	SP
PPTG_06288	CE8	0.60	1.46	2.65	0.03	SP
PPTG_09422	ATP-binding Cassette (ABC) superfamily	0.63	1.65	2.68	0.00	
PPTG_03142	AA10	0.94	2.53	2.68	0.03	SP
PPTG_11415	threonine aspartase	0.36	1.01	2.78	0.05	
PPTG_16965	hypothetical protein	0.46	1.32	2.81	0.01	SP
PPTG_11048	voltage-gated Ion Channel (VIC) superfamily	0.42	1.14	2.84	0.00	
PPTG_16695	hypothetical protein	0.37	1.11	2.85	0.00	SP
PPTG_12467	GH16	0.59	1.53	2.85	0.00	SP
PPTG_00205	hypothetical protein	1.00	2.85	2.86	0.01	
PPTG_09813	hypothetical protein	0.67	2.02	2.87	0.01	
PPTG_09231	CBM50 (09231+09232)	0.67	1.59	2.89	0.05	
PPTG_16426	transmembrane protein	0.39	1.17	2.99	0.01	
PPTG_17706	hypothetical protein	0.75	2.25	3.02	0.04	
PPTG_00341	secreted effector peptide	0.74	2.45	3.06	0.02	
PPTG_10161	GH81	0.80	2.30	3.07	0.00	SP
PPTG_17179	hypothetical protein	0.62	1.72	3.09	0.00	SP
PPTG_03782	GT4	0.97	2.94	3.12	0.00	SP
PPTG_06685	ATP-binding Cassette (ABC) superfamily	0.71	2.14	3.14	0.00	
PPTG_15174	GH28	0.64	1.99	3.17	0.00	SP
PPTG_07508	hypothetical protein	0.57	1.63	3.21	0.04	
PPTG_16720	hypothetical protein	0.86	2.53	3.23	0.02	
PPTG_02574	hypothetical protein	0.60	1.99	3.26	0.00	
PPTG_07098	secreted RxLR effector peptide	0.26	1.03	3.27	0.02	SP
PPTG_19923	acyltransferase family protein	0.89	2.74	3.28	0.01	
PPTG_11317	hypothetical protein	0.43	1.41	3.32	0.01	SP
PPTG_06715	hypothetical protein	0.92	3.19	3.34	0.02	
PPTG_13640	hypothetical protein	0.38	1.13	3.34	0.02	
PPTG_12496	transmembrane protein	0.33	1.07	3.35	0.00	
PPTG_16188	protein kinase	0.31	1.08	3.37	0.00	SP
PPTG_03413	hypothetical protein	0.33	1.07	3.38	0.01	
PPTG_10927	O-methyltransferase	0.32	1.19	3.39	0.02	
PPTG_12902	PL1	0.72	2.45	3.43	0.02	SP
PPTG_11056	tenascin-like protein	0.89	2.90	3.45	0.00	SP
PPTG_13226	molybdenum cofactor biosynthesis protein C	0.68	2.12	3.46	0.02	
PPTG_01766	hypothetical protein	0.91	2.94	3.50	0.00	SP
PPTG_12399	secreted RxLR effector peptide	0.80	2.87	3.53	0.00	SP
PPTG_09618	D-isomer specific 2-hydroxyacid dehydrogenase	0.60	2.21	3.57	0.00	
PPTG_02953	hypothetical protein	0.34	1.21	3.57	0.00	
PPTG_01133	P-type ATPase (P-ATPase) superfamily	0.29	1.02	3.59	0.00	
PPTG_00075	carbonic anhydrase	0.65	2.12	3.65	0.01	SP
PPTG_06637	hypothetical protein	0.64	2.21	3.66	0.00	SP
PPTG_10565	hypothetical protein	0.40	1.35	3.68	0.03	
PPTG_09178	hypothetical protein	0.55	1.77	3.69	0.04	
PPTG_06174	hypothetical protein	0.32	1.29	3.73	0.05	
PPTG_19035	hypothetical protein	0.97	3.67	3.75	0.02	
PPTG_08516	protein kinase	0.43	1.53	3.82	0.00	
PPTG_07090	hypothetical protein	0.48	2.00	3.84	0.02	SP
PPTG_05101	hypothetical protein	0.38	1.59	3.85	0.00	
PPTG_19694	hypothetical protein	0.59	2.45	3.86	0.01	
PPTG_13278	hypothetical protein	0.40	1.34	3.88	0.00	
PPTG_14776	protein kinase	0.33	1.32	3.89	0.00	
PPTG_06066	kinesin-like protein	0.49	1.71	3.92	0.00	
PPTG_18780	ATP-binding Cassette (ABC) superfamily	0.32	1.11	3.93	0.00	

Appendix Table 5.3 Cont.

PPTG_01966	protein-L-isoaspartate O-methyltransferase	0.25	1.17	4.02	0.03	
PPTG_03429	ATP-binding Cassette (ABC) superfamily	0.56	2.21	4.08	0.00	
PPTG_19501	hypothetical protein	0.53	2.68	4.08	0.02	
PPTG_02870	hypothetical protein	0.74	3.34	4.09	0.01	
PPTG_08677	transmembrane protein	0.64	2.53	4.09	0.00	
PPTG_12209	hypothetical protein	0.81	3.20	4.10	0.00	
PPTG_10924	hypothetical protein	0.35	1.54	4.11	0.00	
PPTG_11305	multicopper oxidase	0.53	1.96	4.11	0.00	SP
PPTG_17563	hypothetical protein	0.25	1.15	4.13	0.01	
PPTG_11472	hypothetical protein	0.57	2.41	4.20	0.00	
PPTG_18690	hypothetical protein	0.57	2.41	4.20	0.00	
PPTG_03115	diphthine synthase	0.98	3.52	4.21	0.01	
PPTG_16711	hypothetical protein	0.53	2.22	4.23	0.00	
PPTG_09450	hypothetical protein	0.24	1.05	4.28	0.02	
PPTG_07659	NPP1-like protein	0.38	1.56	4.30	0.02	SP
PPTG_12466	GH16	0.73	2.88	4.31	0.00	
PPTG_16724	hypothetical protein	0.23	1.19	4.45	0.00	SP
PPTG_17839	mannitol dehydrogenase	0.58	2.35	4.50	0.00	
PPTG_07121	hypothetical protein	0.70	3.35	4.52	0.00	SP
PPTG_16693	hypothetical protein	0.31	1.33	4.56	0.00	SP
PPTG_13212	secreted RxLR effector peptide	0.61	2.63	4.57	0.00	
PPTG_18628	hypothetical protein	0.99	4.36	4.59	0.00	SP
PPTG_06593	hypothetical protein	0.61	2.79	4.63	0.00	
PPTG_04290	ATP-binding Cassette (ABC) superfamily	0.62	2.91	4.67	0.00	
PPTG_16722	hypothetical protein	0.58	3.00	4.69	0.02	
PPTG_16073	Ser/Thr protein kinase	0.24	1.07	4.69	0.01	
PPTG_03845	GH5	0.36	1.49	4.72	0.00	
PPTG_11343	hypothetical protein	0.81	3.59	4.76	0.00	
PPTG_06578	hypothetical protein	0.25	1.15	4.84	0.00	SP
PPTG_05840	PL3	0.91	3.91	4.84	0.00	
PPTG_08678	folate-Biopterin transporter (FBT) family	0.89	4.49	4.86	0.00	
PPTG_12863	hypothetical protein	0.76	3.66	4.88	0.01	
PPTG_10136	CE13	0.87	3.76	4.88	0.00	SP
PPTG_18573	hypothetical protein	0.83	3.53	4.91	0.00	
PPTG_06136	hypothetical protein	0.57	2.26	4.92	0.03	
PPTG_15732	hypothetical protein	0.32	1.72	4.99	0.00	
PPTG_20439	hypothetical protein	0.27	1.39	5.01	0.03	
PPTG_10157	DNA polymerase lambda-like protein	0.35	1.77	5.03	0.00	
PPTG_12374	hypothetical protein	0.29	1.33	5.05	0.00	
PPTG_06936	hypothetical protein	0.98	4.83	5.08	0.00	
PPTG_16869	hypothetical protein	0.41	2.26	5.09	0.00	
PPTG_13550	voltage-gated potassium channel subunit beta	0.29	1.41	5.12	0.00	
PPTG_20399	hypothetical protein	0.51	3.00	5.13	0.02	
PPTG_07955	hypothetical protein	0.27	1.94	5.13	0.03	
PPTG_16710	hypothetical protein	0.42	1.96	5.14	0.00	
PPTG_14764	transmembrane protein	0.64	3.18	5.19	0.00	
PPTG_10230	GH131	0.59	3.43	5.25	0.00	SP
PPTG_01284	hypothetical protein	0.97	5.43	5.26	0.00	
PPTG_02948	hypothetical protein	0.90	4.45	5.27	0.00	SP
PPTG_20291	hypothetical protein	0.52	3.13	5.34	0.00	
PPTG_12956	hypothetical protein	0.88	3.85	5.34	0.00	
PPTG_09940	hypothetical protein	0.26	1.59	5.34	0.00	
PPTG_19586	secreted RxLR effector peptide	0.22	1.58	5.40	0.02	SP
PPTG_02511	hypothetical protein	0.84	4.23	5.42	0.00	
PPTG_10009	hypothetical protein	0.72	3.44	5.44	0.00	SP
PPTG_15582	hypothetical protein	0.96	4.43	5.45	0.00	

Appendix Table 5.3 Cont.

PPTG_06923	hypothetical protein	0.80	4.27	5.51	0.00	
PPTG_03362	hypothetical protein	0.95	5.45	5.52	0.00	
PPTG_09464	hypothetical protein	0.29	1.43	5.54	0.00	
PPTG_06657	ATP-binding Cassette (ABC) superfamily	0.24	1.28	5.55	0.00	
PPTG_19278	hypothetical protein	0.21	1.22	5.56	0.03	
PPTG_20369	hypothetical protein	0.24	1.35	5.56	0.00	
PPTG_12415	hypothetical protein	0.45	2.07	5.61	0.00	
PPTG_06606	hypothetical protein	0.30	1.83	5.61	0.00	
PPTG_11504	GH12	0.88	4.84	5.63	0.00	
PPTG_04503	MtN3-like protein	0.13	1.01	5.73	0.01	SP
PPTG_13541	hypothetical protein	0.83	4.99	5.76	0.00	
PPTG_13676	hypothetical protein	0.62	3.56	5.77	0.00	
PPTG_15549	secreted RxLR effector peptide	0.48	2.45	5.77	0.00	SP
PPTG_13746	hypothetical protein	0.24	1.34	5.78	0.00	SP
PPTG_07597	hypothetical protein	0.37	1.68	5.84	0.01	
PPTG_12335	hypothetical protein	0.45	2.24	5.88	0.01	
PPTG_00074	carbonic anhydrase	0.46	2.50	5.97	0.00	SP
PPTG_14691	hypothetical protein	0.37	1.75	6.02	0.00	
PPTG_08329	hypothetical protein	0.30	1.86	6.08	0.00	
PPTG_19584	short chain dehydrogenase	0.18	1.17	6.10	0.00	SP
PPTG_15881	hypothetical protein	0.13	1.05	6.20	0.00	
PPTG_14930	hypothetical protein	0.50	3.08	6.42	0.00	
PPTG_08935	hypothetical protein	0.21	1.29	6.50	0.00	
PPTG_11950	hypothetical protein	0.27	2.18	6.51	0.00	
PPTG_12206	effector	0.31	1.50	6.61	0.03	SP
PPTG_05540	hypothetical protein	0.63	3.98	6.63	0.00	
PPTG_20392	hypothetical protein	0.16	1.51	6.65	0.02	
PPTG_06912	hypothetical protein	0.66	4.61	6.73	0.01	
PPTG_07841	hypothetical protein	0.26	2.55	6.76	0.00	
PPTG_00388	secreted RxLR effector peptide	0.25	1.67	6.83	0.00	SP
PPTG_20119	hypothetical protein	0.84	4.93	6.86	0.00	
PPTG_03215	hypothetical protein	0.14	1.03	6.93	0.00	
PPTG_10810	hypothetical protein	0.68	5.54	6.98	0.00	
PPTG_19064	hypothetical protein	0.18	1.46	6.99	0.00	
PPTG_05993	hypothetical protein	1.00	6.38	7.02	0.00	SP
PPTG_14532	hypothetical protein	0.63	4.20	7.03	0.00	
PPTG_16696	hypothetical protein	0.21	1.84	7.06	0.00	
PPTG_08607	hypothetical protein	0.23	1.59	7.08	0.00	SP
PPTG_16821	cGMP-dependent protein kinase	0.33	2.49	7.19	0.00	
PPTG_17769	hypothetical protein	0.21	1.12	7.20	0.02	
PPTG_11474	hypothetical protein	0.16	1.18	7.25	0.00	
PPTG_00463	hypothetical protein	0.14	1.31	7.30	0.00	SP
PPTG_15165	GH28	0.17	1.27	7.31	0.00	SP
PPTG_17037	hypothetical protein	0.35	2.65	7.31	0.00	
PPTG_07181	PL3	0.29	2.06	7.33	0.00	SP
PPTG_02048	hypothetical protein	0.24	1.73	7.34	0.00	SP
PPTG_18108	hypothetical protein	0.13	1.29	7.37	0.04	SP
PPTG_13638	hypothetical protein	0.13	1.29	7.55	0.00	
PPTG_15608	secreted effector peptide	0.19	1.44	7.60	0.00	SP
PPTG_04292	hypothetical protein	0.54	3.70	7.64	0.00	
PPTG_08397	hypothetical protein	0.84	6.80	7.66	0.00	
PPTG_11839	hypothetical protein	0.12	1.28	7.71	0.00	
PPTG_19703	hypothetical protein	0.80	5.83	7.73	0.00	
PPTG_07575	protease inhibitor Epi9	0.77	4.46	7.78	0.00	SP
PPTG_15944	mitogen-activated protein kinase kinase kinase	0.25	2.05	7.78	0.00	
PPTG_18291	SCP-like extracellular protein	0.32	2.56	7.78	0.00	
PPTG_12789	hypothetical protein	0.39	3.61	7.79	0.00	
PPTG_12813	hypothetical protein	0.32	2.47	7.90	0.00	
PPTG_18571	hypothetical protein	0.13	1.02	8.05	0.00	

Appendix Table 5.3 Cont.

PPTG_19793	hypothetical protein	0.24	2.21	8.12	0.00	SP
PPTG_12413	hypothetical protein	0.36	2.59	8.14	0.00	
PPTG_07568	hypothetical protein	0.36	1.98	8.21	0.01	
PPTG_20380	hypothetical protein	0.25	2.20	8.23	0.00	SP
PPTG_09186	hypothetical protein	0.75	6.43	8.25	0.00	
PPTG_07696	hypothetical protein	0.20	1.89	8.30	0.00	SP
PPTG_18568	hypothetical protein	0.34	3.22	8.33	0.00	
PPTG_16476	hypothetical protein	0.30	2.43	8.51	0.00	
PPTG_06181	hypothetical protein	0.18	1.50	8.51	0.00	
PPTG_08645	hypothetical protein	0.65	5.30	8.57	0.00	SP
PPTG_06440	hypothetical protein	0.26	3.07	8.79	0.01	
PPTG_20031	hypothetical protein	0.66	4.73	8.80	0.00	
PPTG_08020	CE8	0.11	1.23	8.87	0.00	SP
PPTG_01857	hypothetical protein	0.76	6.69	8.89	0.00	SP
PPTG_07663	hypothetical protein	0.35	3.49	8.95	0.00	
PPTG_03379	hypothetical protein	0.31	2.13	8.99	0.00	
PPTG_04159	hypothetical protein	0.25	3.71	9.26	0.00	
PPTG_15333	secreted effector peptide	0.47	4.32	9.27	0.00	SP
PPTG_13522	hypothetical protein	0.45	4.19	9.32	0.00	
PPTG_07873	hypothetical protein	0.26	3.26	9.58	0.00	
PPTG_01649	hypothetical protein	0.83	9.40	9.63	0.00	
PPTG_01767	hypothetical protein	0.95	8.63	9.77	0.00	
PPTG_12795	hypothetical protein	0.22	2.05	10.02	0.00	
PPTG_19972	hypothetical protein	0.90	9.32	10.05	0.00	SP
PPTG_15789	thioredoxin-like protein	0.50	4.91	10.06	0.00	SP
PPTG_15444	GT71	0.08	1.02	10.10	0.00	
PPTG_15391	hypothetical protein	0.59	5.34	10.17	0.00	SP
PPTG_11025	hypothetical protein	0.53	5.55	10.20	0.00	
PPTG_12120	peptidyl-prolyl cis-trans isomerase	0.29	3.48	10.30	0.00	
PPTG_08548	hypothetical protein	0.44	3.84	10.33	0.00	
PPTG_00533	hypothetical protein	0.59	4.80	10.45	0.00	
PPTG_17749	secreted RxLR effector peptide	0.91	8.56	10.60	0.00	
PPTG_11547	hypothetical protein	0.12	1.34	10.97	0.00	
PPTG_05355	hypothetical protein	0.31	2.33	10.98	0.00	SP
PPTG_20094	hypothetical protein	0.12	1.71	11.01	0.00	
PPTG_14969	hypothetical protein	0.47	4.57	11.14	0.00	
PPTG_17042	hypothetical protein	0.12	1.73	11.68	0.00	
PPTG_20160	hypothetical protein	0.13	1.82	11.85	0.00	
PPTG_05849	hypothetical protein	0.09	1.38	11.88	0.00	
PPTG_03477	secreted effector peptide	0.13	2.17	11.97	0.00	
PPTG_15506	hypothetical protein	0.35	4.17	12.01	0.00	
PPTG_04235	secreted RxLR effector peptide	0.90	11.27	12.21	0.00	SP
PPTG_07624	major facilitator superfamily transporter (MFS)	0.27	3.51	12.44	0.00	
PPTG_04291	hypothetical protein	0.61	7.46	12.48	0.00	
PPTG_03881	hypothetical protein	0.05	1.06	12.53	0.05	
PPTG_19857	hypothetical protein	0.07	1.40	13.03	0.00	
PPTG_19047	secreted RxLR effector peptide	0.48	5.14	13.34	0.00	SP
PPTG_07391	hypothetical protein	0.18	2.27	13.38	0.00	
PPTG_14649	hypothetical protein	0.50	6.31	14.09	0.00	
PPTG_11679	hypothetical protein	0.07	1.21	14.33	0.00	
PPTG_10784	hypothetical protein	0.41	5.78	14.43	0.00	
PPTG_12412	hypothetical protein	0.28	4.06	15.09	0.00	
PPTG_00530	hypothetical protein	0.84	13.97	15.22	0.00	
PPTG_18549	hypothetical protein	0.08	1.91	15.50	0.00	
PPTG_05253	hypothetical protein	0.22	3.38	15.51	0.00	
PPTG_20207	aldo/keto reductase family protein	0.18	2.93	15.58	0.00	
PPTG_13666	hypothetical protein	0.64	10.64	15.80	0.00	
PPTG_06907	hypothetical protein	0.57	8.67	16.25	0.00	
PPTG_19641	secreted RxLR effector peptide	0.03	1.09	16.62	0.01	SP
PPTG_06988	secreted RxLR effector peptide	0.04	1.06	16.75	0.02	SP

Appendix Table 5.3 Cont.

PPTG_12771	hypothetical protein	0.03	1.31	17.99	0.02	
PPTG_05683	hypothetical protein	0.90	16.45	18.98	0.00	
PPTG_15392	hypothetical protein	0.35	5.77	19.14	0.00	SP
PPTG_05953	aldo/keto reductase family protein	0.27	5.16	19.90	0.00	
PPTG_16518	hypothetical protein	0.11	2.45	21.49	0.00	
PPTG_11671	hypothetical protein	0.11	1.68	22.58	0.00	
PPTG_03489	protease inhibitor EpiC1	0.30	5.33	23.29	0.00	
PPTG_07888	voltage-gated potassium channel subunit beta	0.05	1.20	25.36	0.00	
PPTG_20331	hypothetical protein	0.10	3.42	28.89	0.00	
PPTG_00127	hypothetical protein	0.25	7.14	31.16	0.00	
PPTG_16833	hypothetical protein	0.94	40.90	45.94	0.00	
PPTG_07106	cleavage induced protein	0.01	1.15	49.84	0.00	
PPTG_16829	hypothetical protein	0.05	4.73	62.00	0.00	
PPTG_17836	hypothetical protein	0.12	10.34	94.26	0.00	
PPTG_16305	hypothetical protein	0.22	22.83	117.39	0.00	
PPTG_17016	secreted effector peptide	0.00	1.82	135.14	0.00	SP

Appendix Table 5.4. Expression of *P. parasitica* crinkler-type effectors in vitro and in 48 hpi infected lupin roots with and without phosphite. Shaded regions indicate genes that are differentially expressed in one or both experiments (fold change >2, >2 RPKM).

Gene ID	Putative gene function	*In vitro*			*In planta*		
		RPKM MRM	RPKM MRM + Phi	Fold change	RPKM infected lupin	RPKM infected lupin+Phi	Fold change
PPTG_20436	crinkler (CRN) domain-containing protein	0	0	1.0	0	0	6.6
PPTG_17744	crinkler (CRN) family protein	0	0	-3.2	3	11	3.7
PPTG_03762	crinkler-like protein	59	55	-1.1	0	1	1.9
PPTG_07602	crinkler (CRN) family protein, pseudogene	9	8	-1.0	1	2	1.7
PPTG_03772	crinkler (CRN) family protein, pseudogene	43	42	-1.0	21	26	1.3
PPTG_06852	crinkler (CRN) family protein, pseudogene	125	129	1.0	1	1	1.2
PPTG_18375	crinkler (CRN) family protein, pseudogene	667	695	1.0	1	1	1.2
PPTG_07603	crinkler (CRN) family protein	23	25	1.0	1	1	1.1
PPTG_14816	crinkler (CRN) family protein	49	60	1.2	15	16	1.1
PPTG_09194	crinkler (CRN) family protein, pseudogene	4	5	1.3	11	12	1.1
PPTG_03580	crinkler-like protein	264	361	1.3	2	2	1.1
PPTG_07157	crinkler (CRN) family protein	20	13	-1.5	27	26	1.0
PPTG_05866	crinkler (CRN) family protein	2	2	-1.1	176	169	-1.0
PPTG_06891	crinkler (CRN) family protein	0	0	-1.1	54	51	-1.0
PPTG_11786	crinkler (CRN) family protein	18	16	-1.1	23	21	-1.1
PPTG_14697	crinkler (CRN) family protein	95	98	1.0	14	13	-1.1
PPTG_08911	crinkler (CRN) family protein	7	7	1.0	302	251	-1.2
PPTG_19223	crinkler (CRN) family protein, pseudogene	0	0	1.0	13	10	-1.2

Appendix Table 5.4 Cont.

PPTG_07152	crinkler (CRN) family protein, pseudogene	16	17	1.0	45	34	-1.3
PPTG_10698	crinkler (CRN) family protein, pseudogene	57	64	1.1	6	5	-1.3
PPTG_07145	crinkler (CRN) family protein, pseudogene	75	85	1.1	756	550	-1.3
PPTG_07745	crinkler (CRN) family protein, pseudogene	207	243	1.2	26	18	-1.3
PPTG_12683	crinkler (CRN) family protein, pseudogene	840	1002	1.2	130	93	-1.3
PPTG_00415	crinkler-like protein	90	107	1.2	13	9	-1.4
PPTG_19224	crinkler (CRN) family protein, pseudogene	75	90	1.2	55	38	-1.4
PPTG_07159	crinkler (CRN) family protein, pseudogene	2	3	1.3	54	37	-1.4
PPTG_01111	crinkler (CRN) family protein, pseudogene	1	1	-1.9	3	2	-1.4
PPTG_17734	crinkler (CRN) family protein	5	4	-1.3	21	12	-1.6
PPTG_16385	crinkler (CRN) family protein, pseudogene	9	11	1.2	4	2	-1.7
PPTG_11553	hypothetical protein	11	9	-1.3	3	1	-2.3